

Density of asteroids

B. Carry

European Space Astronomy Centre, ESA, P.O. Box 78, 28691 Villanueva de la Cañada, Madrid, Spain

Abstract

The small bodies of our solar system are the remnants of the early stages of planetary formation. A considerable amount of information regarding the processes that occurred during the accretion of the early planetesimals is still present among this population. A review of our current knowledge of the density of small bodies is presented here. Density is indeed a fundamental property for the understanding of their composition and internal structure. Intrinsic physical properties of small bodies are sought by searching for relationships between the dynamical and taxonomic classes, size, and density. Mass and volume estimates for 287 small bodies (asteroids, comets, and transneptunian objects) are collected from the literature. The accuracy and biases affecting the methods used to estimate these quantities are discussed and best-estimates are strictly selected. Bulk densities are subsequently computed and compared with meteorite density, allowing to estimate the macroporosity (*i.e.*, amount of voids) within these bodies. Dwarf-planets apparently have no macroporosity, while smaller bodies (<400 km) can have large voids. This trend is apparently correlated with size: C and S-complex asteroids tends to have larger density with increasing diameter. The average density of each Bus-DeMeo taxonomic classes is computed (DeMeo et al., 2009, Icarus 202). S-complex asteroids are more dense on average than those in the C-complex that in turn have a larger macroporosity, although both complexes partly overlap. Within the C-complex asteroids, B-types stand out in albedo, reflectance spectra, and density, indicating a unique composition and structure. Asteroids in the X-complex span a wide range of densities, suggesting that many compositions are included in the complex. Comets and TNOs have high macroporosity and low density, supporting the current models of internal structures made of icy aggregates. Although the number of density estimates sky-rocketed during last decade from a handful to 287, only a third of the estimates are more precise than 20%. Several lines of investigation to refine this statistic are contemplated, including observations of multiple systems, 3-D shape modeling, and orbital analysis from Gaia astrometry.

Keywords: Minor planets, Mass, Volume, Density, Porosity

1. Small bodies as remnants of planetesimals

The small bodies of our solar System are the left-overs of the building blocks that accreted to form the planets, some 4.6 Gyr ago. They represent the most direct witnesses of the conditions that reigned in the proto-planetary nebula (Bottke et al. 2002a). Indeed, terrestrial planets have thermally evolved and in some cases suffered erosion (*e.g.*, plate tectonic, volcanism) erasing evidence of their primitive composition. For most small bodies, however, their small diameter limited the amount of radiogenic nuclides in their interior, and thus the amount of energy for internal heating. The evolution of small bodies is therefore mainly exogenous, through eons of collisions, external heating, and bombardment by high energy particles.

A detailed study of the composition of small bodies can be achieved in the laboratory, by analyzing their terrestrial counterparts: meteorites. The distribution of elements, isotopes in meteorites, together with the level of heating and aqueous alteration they experienced tell us about the temperature, elemental abundance, and timescales during the accretion stages (*e.g.*, Halliday and Kleine 2006). The connection of this information

with specific locations in the Solar System constrains the formation scenarios of our Solar System. This requires the identification of links between the meteorites and the different populations of small bodies.

Indeed, if meteorites are samples from the Solar System, several questions are raised. Is this sampling complete? Is this sampling homogeneous? Some of the identified asteroid types (see Sect. 2) lack of a terrestrial analog. The most flagrant example are the O-type asteroids (3628) Božněmcová and (7472) Kumakiri that appear unlike any measured meteorite assemblage (Burbine et al. 2011). Coupled mineralogical and dynamical studies have shown that meteorites come from specific locations. Other regions of the Solar System may therefore be unrepresented in our meteorite collection (see the discussions in Burbine et al. 2002; Bottke et al. 2002b; Vernazza et al. 2008, for instance).

Additionally, the current orbits of small bodies may be different from the place they originally formed. For instance, it has been suggested that the giant planets migrated to their current orbits (the Nice model, see Tsiganis et al. 2005), injecting material from the Kuiper Belt into the inner Solar System (Levison et al. 2009). Similarly, gravitational interaction among planetary embryos may have caused outward migration of plan-

Email address: benoit.carry@esa.int (B. Carry)

etesimals from Earth's vicinity into the main belt (Bottke et al. 2006). Current distribution of small bodies may therefore not reflect the original distribution of material in the Solar System. It however tells us about the dynamical processes that occurred over history. Analysis of the composition of meteorites in the laboratory, of small bodies from remote-sensing, and of their distribution in the Solar System are therefore pre-requisites to understanding the formation and evolution of our Solar System.

2. Linking small bodies with meteorites

Most of our knowledge on the mineralogy of asteroids has been derived by analysis of their reflectance spectra in the visible and near-infrared (VNIR). The shape of these spectra has been used to classify the asteroids into broad groups, following several classification schemes called taxonomies. In what follows, I refer to the taxonomy by DeMeo et al. (2009), based on the largest wavelength range (0.4–2.4 μm). It encloses 15 classes grouped into three *complexes* (C, S, and X), with 9 additional classes called *end-members* (see DeMeo et al. 2009, for a detailed description of the classes). Mineralogical interpretations and links with meteorites have been proposed for several classes.

Asteroids belonging to the S complex (S, Sa, Sq, Sr, and Sv) and to the Q class have been successfully linked to the most common meteorites, the ordinary chondrites (OCs). This link had been suggested for years based on the presence of two deep absorption bands in their spectra, around 1 and 2 microns, similar to that of OCs and characteristic of a mixture of olivines and pyroxenes (see for instance Chapman 1996; Brunetto et al. 2006, among many others). The analysis of the sample from the S-type asteroid Itokawa returned by the Hayabusa spacecraft confirmed this link (Yurimoto et al. 2011). The two end-member classes A and V have a mineralogy related to the S-complex. A-types are asteroids made of almost pure olivine, which possible analogs are the achondrite meteorites of the Brachinite and Pallasite groups (see, e.g., Bell et al. 1989; de León et al. 2004). In opposition, V-types are made of pure pyroxenes and are related to the HED achondrite meteorites (e.g., McCord et al. 1970). A- and V-types are believed to correspond to the mantle and the crust of differentiated parent bodies (Burbine et al. 1996).

The link between the hydrated carbonaceous chondrites (CCs) CI and CM and the asteroids in the C-complex seems well established (Cloutis et al. 2011a,b). The anhydrous CV/CO carbonaceous chondrites have also been linked with B-types (Clark et al. 2010). The scarcity and low contrast of absorption features in the VNIR prevents a detailed description of the mineralogy and association with meteorites of these asteroid types (B, C, Cb, Cg, Cgh, Ch). Spectroscopy in the 2.5–4 μm wavelength range, however, revealed the presence of hydration features (Lebofsky 1978; Jones et al. 1990; Rivkin et al. 2002). These features were interpreted as evidences for aqueous alteration, similar to that experienced by CI/CM parent bodies (Cloutis et al. 2011a,b). Due to their similar composition to that of the solar photosphere, CI meteorites are often considered the most primitive material in the Solar System (see Weisberg et al.

2006, for an overview of meteorite classes). This has made the compositional study of these so-called *primitive asteroids* a primary goal in planetary science.

The VNIR spectra of asteroids in the X-complex are devoid of strong absorption bands. However, several weak features (e.g., around 0.9 μm) have been identified and used to discriminate sub-classes (Clark et al. 2004; Ockert-Bell et al. 2010; Fornasier et al. 2011). Proposed meteorite analogs for X, Xc, Xe, and Xk asteroids virtually cover the entire meteorite collection: the anhydrous CV/CO carbonaceous chondrites (Barucci et al. 2005, 2012), enstatite chondrites and aubrites (Vernazza et al. 2009b, 2011b; Ockert-Bell et al. 2010), mesosiderites (Vernazza et al. 2009b), stony-iron (Ockert-Bell et al. 2010), and iron meteorites (Fornasier et al. 2011). The mineralogy represented in the X-complex is therefore probably more diverse than in the S- and C-complexes, due to the limits of the taxonomy based on spectral features only. It is worth noting that in former taxonomies (e.g., Tholen and Barucci 1989), the X-complex was divided into three main groups, E, M, and P, distinguished by albedo.

L-types have been suggested to be the most ancient asteroids that currently exist. From the comparison of their VNIR spectra with laboratory material, a fraction of $30 \pm 10\%$ of Calcium- and aluminum-rich inclusions was proposed (Sunshine et al. 2008). This value is significantly higher than that of meteorites. This suggests a very early accretion together with a low degree of alteration while crossing the entire history of the Solar System. With a similar spectral shape, K-types have often been described as intermediates between S- and C-like material (DeMeo et al. 2009). Most of the K-type are associated with the Eos dynamical family in the outer Main Belt. They have been tentatively linked with the anhydrous CO, CV, and CK, and hydrated but metal-rich CR carbonaceous chondrites meteorites (Bell et al. 1989; Doressoundiram et al. 1998; Clark et al. 2009).

The mineralogy of the remaining end-members classes is more uncertain, owing to the apparent absence of strong spectral features (D and T) or to the mismatch of features with any known material (O and R). It has been suggested that T-types contain a high fraction of metallic contents, and may be related to the iron cores of differentiated asteroids, hence iron meteorites (Britt et al. 1992). D-types are among the reddest objects in the Solar System, not unlike that of comet nuclei and some transneptunian objects (Barucci et al. 2008). Their emission spectra in the mid-infrared indeed show striking similarities with that of comet nuclei (Emery et al. 2006, 2011). Both O and R classes were defined to describe the spectral shape of a single object, (3628) Božněmcová and (349) Dembowska respectively. Both types display broad absorption bands around 1 and 2 microns. These bands are however unlike those of S-types or any type of pyroxenes and olivines in our sample collection (Burbine et al. 2011).

Comets and transneptunian objects (TNOs) are volatile-rich bodies. These two populations are dynamically linked, the later being one of the reservoir of periodic comets (Jewitt 2004). Several compositional groups have been identified among TNOs: water ice dominated spectra, methane-rich

spectra, and featureless spectra similar to that of comet nuclei (Barucci et al. 2008). There is no evidence for a meteorite sample from these dynamic classes, although the delivery from Kuiper Belt material to Earth should be possible (Gounelle et al. 2008).

As seen from this short summary, asteroid-meteorites connections and detailed mineralogy remain open questions in many cases: only about half of the 24 classes defining the taxonomy by DeMeo et al. (2009) have a mineralogical interpretation. Expanding the taxonomy toward longer wavelengths (2–5 and 5–40 μm range) will help in that respect (e.g., Rivkin et al. 1995, 2002; Emery et al. 2006). Additional constraints must however be used to refine current mineralogy interpretations, especially for objects with featureless spectra. Visible and radar albedos, thermal inertia, and density provide valuable constraints on the composition of these objects (e.g., Fornasier et al. 2011). Among these, the most fundamental property to understand the composition and internal structure is perhaps the density (Britt et al. 2002; Consolmagno et al. 2008).

3. The density: a fundamental property

As described above, from the analysis of the surface properties such as reflectance spectra or albedo, it is possible to make inferences on composition. These observables however tell us about surface composition only, which may or may not be reflective of the bulk composition of the body (Elkins-Tanton et al. 2011). For instance, the surface of Earth, the *Blue Planet*, is covered by water while its overall composition is totally different. Earth’s density is indeed indicative of a rocky composition with a core of denser material. Densities of small bodies are much more subtle, but still contain critical information.

From the compilation of the density of about 20 asteroids, Britt et al. (2002) already showed that differences are visible among that population. In a more recent review including 40 small bodies, Consolmagno et al. (2008) highlighted four trends in macroporosity (hereafter \mathcal{P}). The macroporosity reflects the amount of voids larger than the typical micrometer-sized cracks of meteorites. The largest asteroids (mass above 10^{20} kg) are apparently compact bodies without any macroporosity. This contrasts strongly with all the other less massive small bodies that have 20% or more macroporosity. The fraction of voids increases dramatically for icy bodies (comets and TNOs). Finally, *primitive* C-type asteroids tends to have larger macroporosity than the *basaltic* S-type.

Macroporosity, if present to a large extent, may have strong consequences on certain physical properties such as gravity field, thermal diffusivity, seismic velocity, and of course on collisional lifetimes (see the review by Britt et al. 2002). Macroporosity can also help in understanding the collisional history: intact bodies are expected to have low-to-no macroporosity, while heavily impacted objects may have large cracks, fractures (i.e., moderate \mathcal{P}), or be gravitational re-accumulation of material (i.e., rubble-piles, characterized by high values of \mathcal{P}).

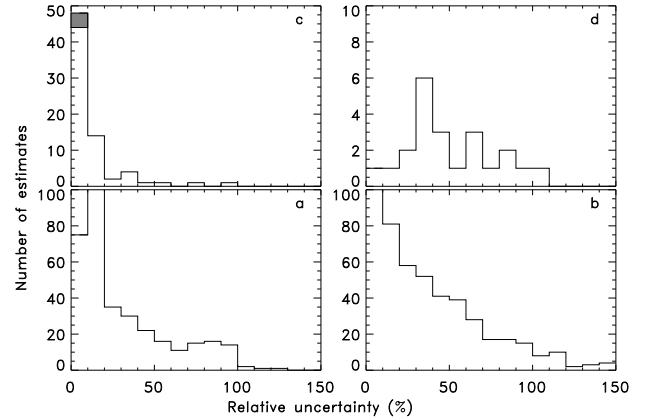


Figure 1: Distribution of the relative accuracy of mass estimates obtained with four different methods (see text): (a) orbit deflection during close encounters, (b) planetary ephemeris, (c) orbit of natural satellites or spacecrafts (gray bar), and (d) indirect determination of density (Sect. 4.3) converted into mass.

4. Determination of density

Direct measurement of the *bulk* density (ρ) involves the independent measures of the mass (M) and volume (V): $\rho = M/V$. Indirect determination of the density are also possible by modeling the mutual eclipses of a binary system (e.g., Behrend et al. 2006) or the non-gravitational forces on a comet nucleus (e.g., Davidsson et al. 2007). This study aims at deriving constraints on the intrinsic physical properties of small bodies by searching for relationships between, the dynamical and taxonomic classes, size, and density. An extensive compilation of the mass, volume, and resulting density estimates available in the literature is therefore presented here.

There are 994 published mass estimates for 267 small bodies (Sect. 4.1). For each object, the volume determinations are also compiled here, resulting in 1454 independent estimates (Sect. 4.2). Finally, the density of 24 small bodies has also been indirectly determined (Sect. 4.3). In total, 287 density estimates are available, for small bodies pertaining to all the dynamical classes: 17 near-Earth asteroids (NEAs), 230 Main-Belt (MBAs) and Trojan asteroids, 12 comets, and 28 transneptunian objects (TNOs). There is however a large spread among the independent estimates of the mass and volume estimates of these objects. Additionally, several estimates lead to obvious non-physical densities such as 0.05 or 20, the respective densities of Aerogel and Platinum. A rigorous selection of the different estimates is therefore needed. Some specifics of mass and diameter estimates are discussed below, together with selection criteria.

4.1. Mass estimates

The determination of the mass of a minor planet relies on the analysis of its gravitational effects on other objects (see the review by Hilton 2002, for instance). The 994 mass estimates for 267 small bodies listed in Appendix A can be divided in 4 categories, owing to the gravitational effects that were analyzed:

1. **Orbit deflection during close encounters:** The mass of small bodies is several order of magnitude lower than that

of planets. Asteroids can nevertheless slightly influence the orbit of other smaller asteroids (e.g., Michalak 2000, 2001) and of Mars (e.g., Pitjeva 2001; Mouret et al. 2009) during close encounters. This method has been widely used, resulting in 547 mass estimates. An accuracy of few percent can be reached for the most massive asteroids such as (1) Ceres, (2) Pallas, or (4) Vesta (e.g., Konopliv et al. 2006; Zielenbach 2011). The accuracy however drops for smaller asteroids, and about a third have uncertainties cruder than 100% (see, for instance Somenzi et al. 2010; Zielenbach 2011, and Fig. 1.a).

2. **Planetary ephemeris:** Numerical models have been developed to describe and predict the position of planets and minor planets around the Sun. In addition to the Sun and the planets, the gravitational influence of several asteroids must be taken into account to properly describe the observed position of planets, satellites, and spacecrafts (see Baer and Chesley 2008; Baer et al. 2011; Fienga et al. 2008, 2009, 2010; Folkner et al. 2009, for details). In that respect, this method is similar to the analysis of close encounters. There is however a strong philosophical difference between these two methods: analysis of close encounters consists of considering N times a 1-to-1 gravitational interaction, while planetary ephemeris are conceptually closer to a N -to-1 interaction. Similarly to the results obtained from close encounters, the best accuracy is achieved for largest asteroids and becomes cruder for smaller objects. The mean accuracy is of 45%, but values are distributed up to 100% (Fig. 1.b).
3. **Spacecraft tracking:** The Doppler shifts of the radio signals sent by spacecraft around an asteroid can be used to determine its orbit or the deflection of its trajectory during a flyby. These frequency shifts are imposed by the gravitational perturbation and are related to the mass of the asteroid (Yeomans et al. 1997, 2000; Fujiwara et al. 2006; Pätzold et al. 2011). It is by far the most precise technique with a typical accuracy of a couple of percent (Fig. 1.c). It will however remain limited to a handful of small bodies (only four to date).
4. **Orbit of a satellite:** From optical or radar images of the components of the system, their mutual orbit can be determined and the mass derived with Kepler's third law (see, for instance, Petit et al. 1997; Merline et al. 1999, 2002; Margot et al. 2002; Marchis et al. 2005b, 2008a,b; Brown et al. 2005, 2010; Carry et al. 2011; Fang et al. 2011). The 28 mass estimates available for TNOs were derived from optical imaging with the Hubble space telescope or large ground-based telescopes equipped with adaptive-optics cameras (e.g., Grundy et al. 2009; Dumas et al. 2011). Similarly, the 17 mass estimates for NEAs were all derived from radar (e.g., Ostro et al. 2006; Shepard et al. 2006), with the exception of Itokawa which was the target of the Hayabusa sample-return mission (Fujiwara et al. 2006). Additionally, the mass of 26 MBAs was determined by optical imaging. In total, 68 mass estimates have been derived by analyzing the orbit of a satellite. It is the second most-precise technique with a typical accuracy of about

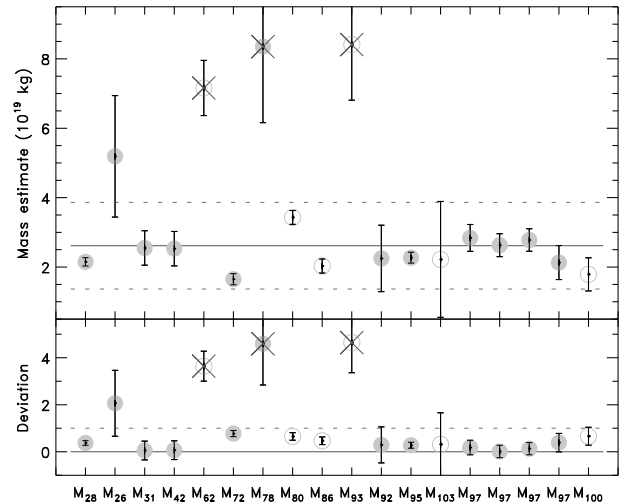


Figure 2: The 18 mass estimates for (52) Europa (see Appendix D for the references). **Top:** The different mass estimates M_i , in 10^{19} kg. Symbols indicate the method used to determine the mass: deflections (gray disk) or planetary ephemeris (open circle). Crossed estimates were discarded from the analysis (see text). Horizontal solid and dashed lines are respectively the weighted average (μ) and standard deviation (σ) of the mass estimates before selection. **Bottom:** Same as above, but plotted as a function of the distance to the average value, in units of deviation: $(M_i - \mu) / \sigma$. Similar plots for each of the 140 small bodies with multiple mass estimates are provided in Appendix A.

10–15% (Fig. 1.c). It is the most productive method of accurate mass determinations. With currently more than 200 known binaries, many mass estimates are still to come.

Based on these considerations and a close inspection of the different mass estimates available (e.g., Fig. 2), the following criteria for selecting mass estimates were applied: Mass estimates derived from either the third or the fourth method (spacecraft or satellite) prevail upon the first two methods (deflection and ephemeris). Mass estimates leading to non-physical densities are discarded. Mass estimates that do not agree within uncertainties with the range drawn by the weighted average and standard deviation are discarded. The weighted average and standard deviation are subsequently recomputed. The 994 mass estimates are provided in Appendix A together with bibliographic references and notes on selection.

A summary of the precision achieved on mass estimates is presented in Fig. 3. The contribution provided here is illustrated by the difference between the cumulative distribution of relative precision before (dashed line) and after (solid line) the selection (about 20% of the estimates were discarded). For estimates with a relative uncertainty below 50%, the selection of estimates slightly improves the final accuracy, increasing the number of accurate estimates by 5 to 10%. The apparent degradation introduced by the selection for low-precision estimates is due to rejection of about 10% of these estimates. In other words, these estimates lead to unrealistic densities and should not be considered. Furthermore, the distribution presented in Fig. 3 is based on the uncertainties reported by the different authors. The discrepancy between estimates however often reaches disconcerting levels. For instance, the estimates M_{28} (Krasinsky et al. 2001), M_{72} (Baer et al. 2008), M_{80} (Fienga

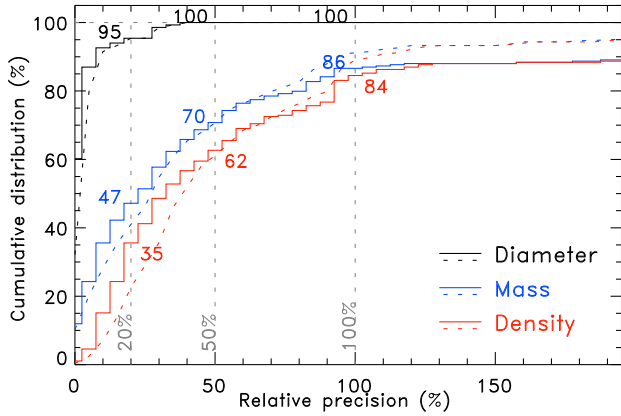


Figure 3: Cumulative distribution of the accuracy on the diameter (black), mass (blue), and density (red) estimates. Dashed and solid lines represent the distributions before and after selection of best estimates (see text for details). Three reference levels for the relative accuracy are drawn: 20%, 50% and 100%, with the fraction of targets with a better accuracy reported for each estimate (after selection only).

et al. 2009), and M_{86} (Folkner et al. 2009) of the mass of (52) Europa fall within the range drawn by the weighted mean and deviation (Fig. 2). They nevertheless strongly disagree: the different values are between 4 and 11 σ one from each other.

Such differences are indicative of underestimated uncertainties. Accuracy is often reported as the formal standard deviation (σ), which in some cases may be small compared to systematics. The uncertainties on the mass determinations should therefore be considered as lower limits, to which some systematics could be added. As a result, the cumulative distribution of the relative precision presented in Fig. 3 is optimistic and gives an upper limit to the amount of accurate estimates. Therefore, even with mass estimates available for more than 250 small bodies, our knowledge is still very limited: Only about half of the estimates are more accurate than 20%, and no more than 70% of the estimates are more accurate than 50% (higher uncertainties preventing any firm conclusion).

4.2. Volume estimates

As already noted by several authors, the most problematic part of determining the density of a small body is to measure any mass at all (e.g., Merline et al. 2002; Consolmagno et al. 2008). The number of density estimates presented here is limited by the number of mass estimates, and not by the number of volume estimates (generally reported as volume-equivalent diameter, hereafter ϕ). Many different observing techniques and methods of analysis have been used to evaluate the diameter of small bodies (see the review by Carry et al. 2012). The 1454 diameter estimates listed in Appendix B were derived with 15 different methods, that can be grouped into 4 categories:

1. **Absolute magnitude:** It could almost be considered an *absence* of size estimate. It is the crudest method to evaluate the diameter of a small body (Fig. 4.a). From the absolute magnitude H and an *assumed* geometric albedo p , the diameter is given by ϕ (km) = $1329 p^{-0.5} 10^{-0.2H}$

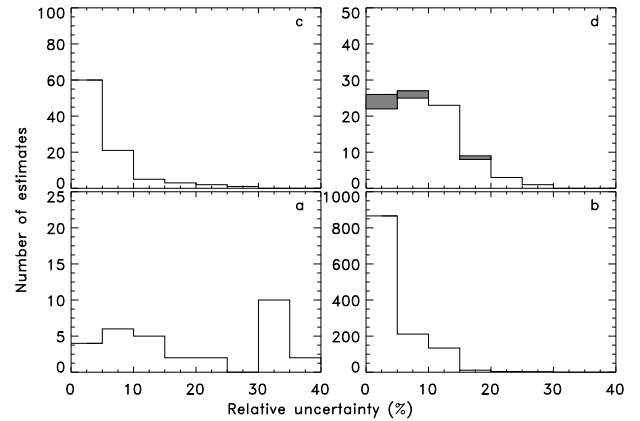


Figure 4: Distribution of the relative accuracy of diameter estimates obtained with four classes of different methods (see text): (a) crude estimates from absolute magnitude, (b) thermal radiometry, (c) direct measurement limited to a single geometry, and (d) shape modeling based on several geometries (gray bars represent the diameters derived from spacecraft encounters). Although estimates in sub-plot (d) are expected to be the most precise, it is not reflected in their relative uncertainty distribution. The possible underestimation of biases in other techniques may be the cause (see text).

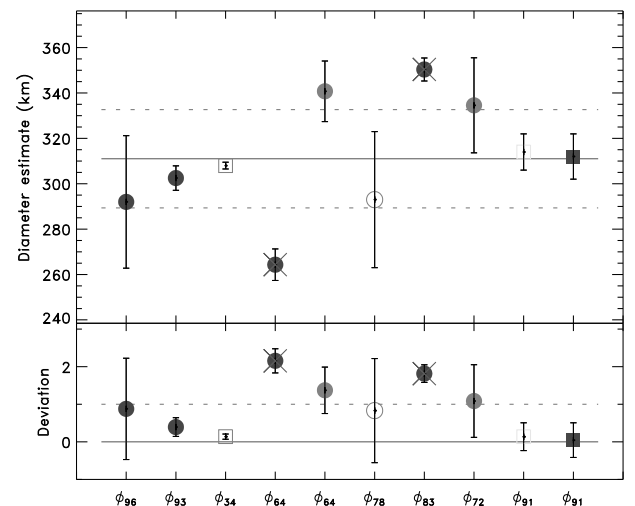


Figure 5: The 10 diameter estimates for (52) Europa (see Appendix D for the references). **Top:** The different diameter estimates ϕ_i , in km. Symbols indicate the method used to determine the diameter: mid-infrared radiometry modeled using the Standard Thermal Model (STM: ϕ_{96} , ϕ_{93} , ϕ_{64} , and ϕ_{83}) and the near-Earth asteroid thermal model (NEATM: ϕ_{64} and ϕ_{72}), disk-resolved imaging on a single epoch (ϕ_{34}), combination of lightcurves and stellar occultations (ϕ_{78}), or shape modeling (ϕ_{91}). See Appendix B for a complete description of the symbols. Crossed estimates were discarded from the analysis (see text). Horizontal solid and dashed lines are respectively the weighted average (μ) and standard deviation (σ) of the diameter estimates before selection. **Bottom:** Same as above, but plotted as a function of the distance to the average value, in units of deviation: $(\phi_i - \mu) / \sigma$. Similar plots for each of the 246 small bodies with multiple diameter estimates are provided in Appendix B.

(Pravec and Harris 2007, and references therein). The diameter of 29 small bodies presented here were derived using their absolute magnitude, in absence of any other estimates. This particularly applies to TNOs.

2. **Thermal modeling of mid-infrared radiometry:** It is by far the main provider of diameter estimates: 1233 diam-

eter estimates out of the 1454 listed in [Appendix B](#) (*i.e.*, $\approx 85\%$). Asteroids are indeed among the brightest sources in the sky at mid-infrared wavelengths (5–20 μm), so infrared satellites (IRAS, ISO, AKARI, Spitzer, and WISE) have been able to acquire observations of a vast number of these objects (see [Tedesco et al. 2002](#); [Ryan and Woodward 2010](#); [Usui et al. 2011](#); [Masiero et al. 2011](#); [Mueller et al. 2011](#)). The diameter and albedo of the colder TNOs have also been studied at longer wavelengths with Spitzer and Herschel (*e.g.*, [Stansberry et al. 2008](#); [Müller et al. 2009](#)). As visible in [Fig. 4.b](#), the typical uncertainty is of only few percent. In many case, however, the different estimates from thermal modeling disagree above their respective quoted uncertainty (see [Table 3](#) in [Delbo and Tanga 2009](#), illustrating the issue). For instance, in the case of Europa ([Fig. 5](#)), both diameter estimates ϕ_{64} ([Ryan and Woodward 2010](#)) where based on the same data, but used two different thermal modeling, and disagree at more than 6σ . Such differences are again indicative of underestimated uncertainties. Accuracy is often reported as the formal standard deviation (σ), which in some cases may be small compared to systematics. In the present case, the simplified standard thermal model ([Lebofsky et al. 1986](#)) and near-Earth asteroid thermal model ([Harris 1998](#)) widely used do not take into account the spin and shape of the small body into account, and can therefore be strongly biased. A more realistic level of accuracy is about 10% ([Lim et al. 2010](#)), at which these estimates are still highly valuable given the huge number of small bodies that have been studied that way.

3. **Direct measurements of a single geometry:** Stellar occultations or disk-resolved images can provide an extremely precise measure of the apparent size and shape of a small body (*e.g.*, [Brown and Trujillo 2004](#); [Brown et al. 2006](#); [Marchis et al. 2006b, 2008a](#); [Dunham et al. 2011](#)). When these direct measurements are limited to a single geometry, however, the evaluation of the diameter may be biased. The volume is 3-D while a single geometry only provides 2-D constraints. The typical accuracy of 5% ([Fig. 4.c](#)) may therefore be optimistic. Nevertheless, these estimates are highly valuable, being based on direct measurements.
4. **Shape modeling based on several geometries:** The least numerous but most precise diameter estimates are derived when the spin and 3-D shape of the objects are modeled, thus limiting the 2-D to 3-D related biases ([Fig. 4.d](#)). Small bodies can be modeled as smooth tri-axial ellipsoids (*e.g.*, [Thomas et al. 2005](#); [Schmidt et al. 2009](#); [Drummond et al. 2009, 2010](#)), convex shapes ([Descamps et al. 2007b](#); [Durech et al. 2011](#)), or realistic 3-D shapes ([Veverka et al. 2000](#); [Ostro et al. 2006, 2010](#); [Carry et al. 2010a,b](#); [Sierks et al. 2011](#)). In particular, spacecraft encounters with (25 143) Itokawa and (21) Lutetia have shown that multi-data approaches provide reliable and precise diameter estimates: *e.g.*, lightcurve-derived shape model with thermal radiometry ([Mueller et al. 2006](#)) or combined inversion of disk-resolved imaging and lightcurves ([Kaasalainen 2011](#);

[Carry et al. 2010b, 2012](#)).

As visible in [Figs. 3](#) and [4](#), the diameter estimates are generally intrinsically much more precise than the mass determination: all the estimates are known to better than 50% relative precision, and a large majority to better than 10%. Diameter estimates from different techniques moreover generally agree, suggesting that systematics are commensurable with formal uncertainties. The same selection criteria than for mass estimates were applied here, and about 15% of the estimates were discarded. Paradoxically, once the mass is determined, the uncertainty on the volume ($\delta V/V$) often becomes the major source of uncertainty on the density (ρ). Indeed,

$$\frac{\delta\rho}{\rho} = \sqrt{\left(\frac{\delta M}{M}\right)^2 + \left(\frac{\delta V}{V}\right)^2} = \sqrt{\left(\frac{\delta M}{M}\right)^2 + 9\left(\frac{\delta\phi}{\phi}\right)^2} \quad (1)$$

The contribution of the uncertainty on the diameter ($\delta\phi/\phi$) therefore easily overwhelms that of the mass ($\delta M/M$). In the compilation presented here, however, the mass is the limiting factor for 61% of the objects, contributing to $\approx 72\%$ of the density uncertainty. This is mainly due to the high number of non-precise mass estimates ([Fig. 3](#)). If only the density estimates with a relative precision better than 20% are considered, then the situation is reversed: the diameter is the limiting factor for 75% of the objects, contributing to $\approx 68\%$ of the density uncertainty. For these reasons, the mass should therefore be considered the limiting factor in most of the cases. As already discussed elsewhere, however, when a reliable mass estimate is available (*i.e.*, usually from the presence of a satellite), the precision on the volume generally limits the accuracy on the density ([Merline et al. 2002](#); [Britt et al. 2002](#); [Consolmagno et al. 2008](#)).

4.3. Indirect density estimates

For small bodies with diameters of a few to tens of kilometers the methods to estimate their mass listed above ([Sect. 4.1](#)) cannot be used. The gravitational influence of these very small bodies is too tiny to be measured. Even in the case of binary systems, their angular extent is generally too small to be imaged with current technology. The only exception are the small binary NEAs that can be imaged with radar during close approaches with Earth. Yet, a large fraction of the currently known binaries are small-sized systems discovered by studying their lightcurves (86 out of 207, *e.g.*, [Mottola and Lahulla 2000](#); [Pravec et al. 2002, 2006](#)). Indeed, photometric observations of the mutual eclipses of a system provide many constraints, for instance, on the ratio between the diameters of the two components or between the primary diameter and the orbit semi-major axis (see [Scheirich and Pravec 2009](#)).

Nevertheless, these parameters are dimensionless from lightcurve observations only. The *absolute* scale, hence semi-major axis and thus mass, cannot be derived. Usually, both components are *assumed* to have the same bulk density to bypass this restriction (*e.g.*, [Scheirich and Pravec 2009](#)). These estimates are indirect, being derived without measuring the mass nor the size. The accuracy reached greatly depends on

each system, and ranges from a few percent to 100% (Fig. 1.d). It is worth noting that if small-sized binaries are formed by rotational breakup (Walsh et al. 2008) as suggested by the fast rotations of the primaries (Pravec et al. 2002, 2006, 2010), the porosity, hence density, of the components may be significantly different. These density estimates may therefore be biased, in absence of an independent measure of the scale of the systems.

Measuring the mass of comets is another challenge. With diameters typically smaller than 10 km, comets have very small masses. In absence of a satellite, studying their gravitational effect on other objects is hopeless. The activity of their nucleus however provides an indirect way to estimate their mass. Indeed, the forces resulting from the gas jets slowly change the orbit of the nucleus around the Sun. Modeling this non-gravitational effect provides the mass of the nucleus (e.g., Davidsson and Gutiérrez 2004, 2005, 2006; Davidsson et al. 2007; Sosa and Fernández 2009). The masses of 11 comets have been derived using this approach. Richardson et al. (2007) have also studied the expansion of ejecta created by the Deep Impact experiment on the comet 9P/Tempell. This is the most direct measurement of the mass of a comet, independent of the non-gravitational effect.

A summary of the mass, volume-equivalent diameter and bulk density of the 287 small bodies compiled here is provided in Table 1. The values listed are the weighted average and standard deviation of all the selected estimates (see Appendix A, Appendix B, and Appendix C). The density is given normalized to that of liquid water (1000 kg m^{-3}), *i.e.*, dimensionless. The estimates have been ranked from A to E, owing to the level of relative accuracy achieved on the density: B better than 20%, C between 20 and 50%, D between 50 and 100%, and E cruder than 100%. A stands for reliable estimates (more precise than 20%), based on more than 5 mass estimates and 5 diameter estimates, or a spacecraft encounter. Irrelevant densities are tagged with a cross (X). Only about a third of the 287 density estimates have a relative precision better than 20% (Fig. 3), and two third better than 50%, above which level nothing relevant can be derived.

The fraction of volume occupied by voids, the macroporosity \mathcal{P} , is also reported, computed as:

$$\mathcal{P}(\%) = 100 \left(1 - \frac{\rho}{\rho_m} \right) \quad (2)$$

with ρ the asteroid bulk density and ρ_m the bulk density of the associated meteorite (Table 2). The macroporosity is the least constrained of all the quantities discussed here. Indeed, it is affected by the uncertainties and possible biases on the diameter and mass estimates and also from the possible ambiguous links with meteorites (Sect. 2 and Table 3). Depending on the meteorite association, the macroporosity may change by 30–40%. For instance, while (16) Psyche was the most porous asteroid listed by Britt et al. (2002) and Consolmagno et al. (2008) with a macroporosity of about 70%, it stands in the low macroporosity range (about 18%). A low macroporosity is actually more consistent with the link between Psyche and iron meteorites than the very high value of $\sim 75\%$ found previously.

Table 2: Average bulk density (ρ) measured on N_s sample of N_m meteorites used in Table 1: Ordinary chondrites (OC: H, L, and LL), Carbonaceous chondrites (CC: CI, CM, CR, CO, CV, and CK), Enstatites chondrites (EH and EL), Achondrites HED (*i.e.*, average of Howardites, Eucrites, and Diogenites), Stony-Iron (Pallasites, Mesosiderites, and Steinbach), and Iron meteorites (Ataxites and Hexahedrites). Terrestrial weathering has a strong effect on the porosity of found OCs with respect to fallen OCs (Consolmagno et al. 2008). Only measurements on falls are therefore used here. For the other meteorite classes, both finds and falls are used. The density of liquid water of 1.00 ± 0.10 is used as a proxy for the volatiles that compose icy bodies. **References:** (1) Consolmagno and Britt (1998), (2) Britt and Consolmagno (2003), (3) Consolmagno et al. (2008), (4) Macke et al. (2010), and (5) Macke et al. (2011).

Meteorite		ρ	N_s	N_m	Refs.
Ord. chondrites	H	3.42 ± 0.18	265	157	2,3
Ord. chondrites	L	3.36 ± 0.16	277	160	2,3
Ord. chondrites	LL	3.22 ± 0.22	149	39	2,3
Carb. Chondrites	CI	1.60 ± 0.03	14	4	2,3
Carb. Chondrites	CM	2.25 ± 0.08	33	18	2,3
Carb. Chondrites	CR	3.10	7	3	2
Carb. Chondrites	CO	3.03 ± 0.19	22	8	2,3
Carb. Chondrites	CV	2.79 ± 0.06	51	10	2,3
Carb. Chondrites	CK	2.85 ± 0.08	3	3	3
Enstatites	EH	3.47 ± 0.21	16	9	4
Enstatites	EL	3.46 ± 0.32	25	14	4
Achondrites	HED	3.25 ± 0.26	96	56	5
Stony-Iron	Pal	4.76 ± 0.10	10	5	2
Stony-Iron	Mes	4.35 ± 0.02	8	3	2
Stony-Iron	Ste	4.18 ± 0.10	2	1	2
Iron	Ata	4.01 ± 0.04	1	1	1
Iron	Hex	7.37 ± 0.14	2	2	1
Iron	Oct	7.14 ± 0.13	5	5	1

5. Density and macroporosity of small bodies

The density and macroporosity of small bodies and their relationships with asteroid taxonomy, dynamical class, and diameter are discussed here.

For asteroids, the distribution of density estimates over taxonomic classes is presented in Fig. 6. The taxonomy is based on a limited sample (371 objects, see DeMeo et al. 2009) and the relative part represented by each class in the whole population may be substantially different (Bus 1999) but this discussion is beyond the scope of present analysis. Density estimates are available for the three complexes: 109 for C complex, and 50 for both S and X complexes. End-members are less represented: only 15 density estimates are available, although end-members represent about 20% of the asteroids. For density estimates with relative accuracy better 20% only, the statistic is however based on low-numbers (see Table 3). The situation is particularly dramatic for end-members: only K-type and V-types have reliable estimates. The number of density estimates for comets and TNOs also drops with increasing levels of relative precision (Table 3).

The density estimates are plotted in Fig. 7, regrouped into 6 categories: TNOs, comets, and four asteroid groups: S, C, and X complexes, and end-members. Macroporosity estimates

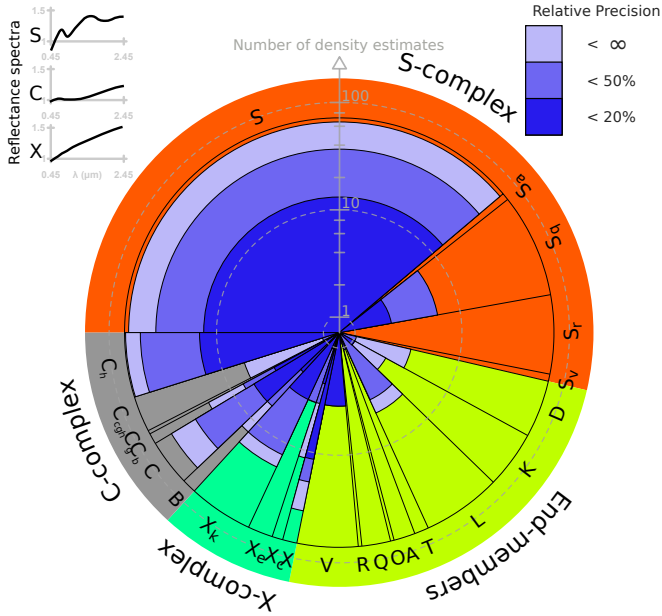


Figure 6: Pie chart showing the fraction of asteroids within each class of the taxonomy by DeMeo et al. (2009), based on 371 objects. Complexes (C, S, and X) and end-members are displayed in gray, red, green and yellow respectively. Typical reflectance spectra of the complexes are also reported (top left). For each class, the number of density estimates, with a relative precision better than 20%, 50%, and regardless to the precision (∞), are drawn in blue wedges.

(Eq. 2) are similarly plotted in Fig. 8. Several trends can be observed:

- Asteroids in the S-complex are more dense than those in the C-complex (confirming Britt et al. 2002, findings).
- Asteroids in the C-complex seem to have larger macroporosity than those in the S-complex.
- The density of asteroids from both the S-complex and the C-complex seems to increase with the mass, apparently resulting from a decreasing macroporosity.
- In both C and S-complex, NEAs seem to have a lower density than MBAs, following the trend between mass and density observed for MBAs.
- At comparable sizes, B-types appear significantly denser ($\rho \sim 2.4$) than the other types of the C-complex that gather around $\rho \sim 1.4$.
- The density of the X-complex asteroids covers a large range, from the most dense Xc-types with $\rho \sim 4.9$ to X-types with $\rho \sim 1.8$.
- Comets have very low densities ($\rho \sim 0.5$), low even considering their volatile-rich composition (in agreement with spacecraft observations, see Richardson et al. 2007).
- The density of TNOs covers a large range, from comet-like ($\rho \sim 0.5$) to the rocky (50 000) Quaoar ($\rho \sim 3.6$).
- Dwarf-planets apparently have no macroporosity, contrary to small bodies whose masses are inferior to $\approx 10^{20}$ kg.
- For each type of small body, the dispersion in density and macroporosity is huge.

These trends are discussed below. The large dispersion of values is however attributed to observational and methodological biases, rather than to genuine physical effects. Indeed, when considering different levels of accuracy, the distributions narrow with precision. In other words, biased estimates artificially spread the density distribution, hence the need for *realistic* evaluation of uncertainties.

5.1. C-complex and sub-groups

Most of the asteroids in the C-complex have densities ranging from the highly porous (253) Mathilde ($\rho \sim 1.3$) to the dense (2) Pallas ($\rho \sim 2.9$). This interval overlaps with CCs meteorites, and the structure of these asteroids ranges from large, compact, bodies ($\mathcal{P} \sim 0\%$) to rubble-piles ($\mathcal{P} \sim 40\text{--}60\%$). This trend for large bodies to present a zero macroporosity can be explained by the high pressure of their interiors. Following Britt et al. (2002, and references therein), silicate grains start to fracture when the pressure reaches $\sim 10^7$ Pa. This threshold is reached within the first few kilometers from the surface of large bodies, allowing a thin layer only to host macroporosity. Because large-scale *grains* (i.e., rubble) are expected to grind at much smaller pressures, the transition from compact to fractured bodies is expected to be smooth.

Indeed, these different structures are apparently correlated with the mass of the asteroids (Fig. 9). The correlation coefficient between density and diameter is 68% and this trend seems real although the sample is still size-limited. From this trend (the linear regression in Fig. 9), the mass of hypothetical asteroids made of each type of CCs meteorites, without macroporosity, are all within $10^{19}\text{--}10^{20}$ kg, corresponding to the observed transition between compact and fractured asteroids. This suggests that large C-complex asteroids ($\phi \geq 300$ km) have intact structures, while smaller asteroids have porous interiors because the internal pressure never reaches the threshold for silicate compaction. This is consistent with the current vision of the dynamical history of the Main Belt: large asteroids survived intact throughout the history of the Solar System, while most of the material was removed or grinded into pieces (Morbidelli et al. 2009). This is also supported by the apparent lower density of about 1.2 for the 7 NEAs, with respect to about 2 for the 53 MBAs.

Among the C-complex, B-types have distinct surface properties: negative spectral slope in the visible and higher albedo (see the compilation of albedo per taxonomic class from Ryan and Woodward 2010; Usui et al. 2011; Masiero et al. 2011). From a comprehensive comparison of 22 C-complex asteroids with laboratory spectra of meteorites, Clark et al. (2010) indeed found that spectra of C-types were best matched by aqueous-altered CI/CM carbonaceous chondrites while those of B-types by other CCs sub-groups (mainly CO, CV, but also CK and CR). This is supported by the density estimates (Table 3): B-types are significantly denser ($\rho \sim 2.4$) than the other types of the C-complex, following the trend observed in meteorites. Although only two B-types have density estimates more accurate than 20%, (2) Pallas and (704) Interamnia, this trend of a larger density is constantly found at different levels of precision (Table 3) and diameters (Table 1). B-types are thus intrinsically

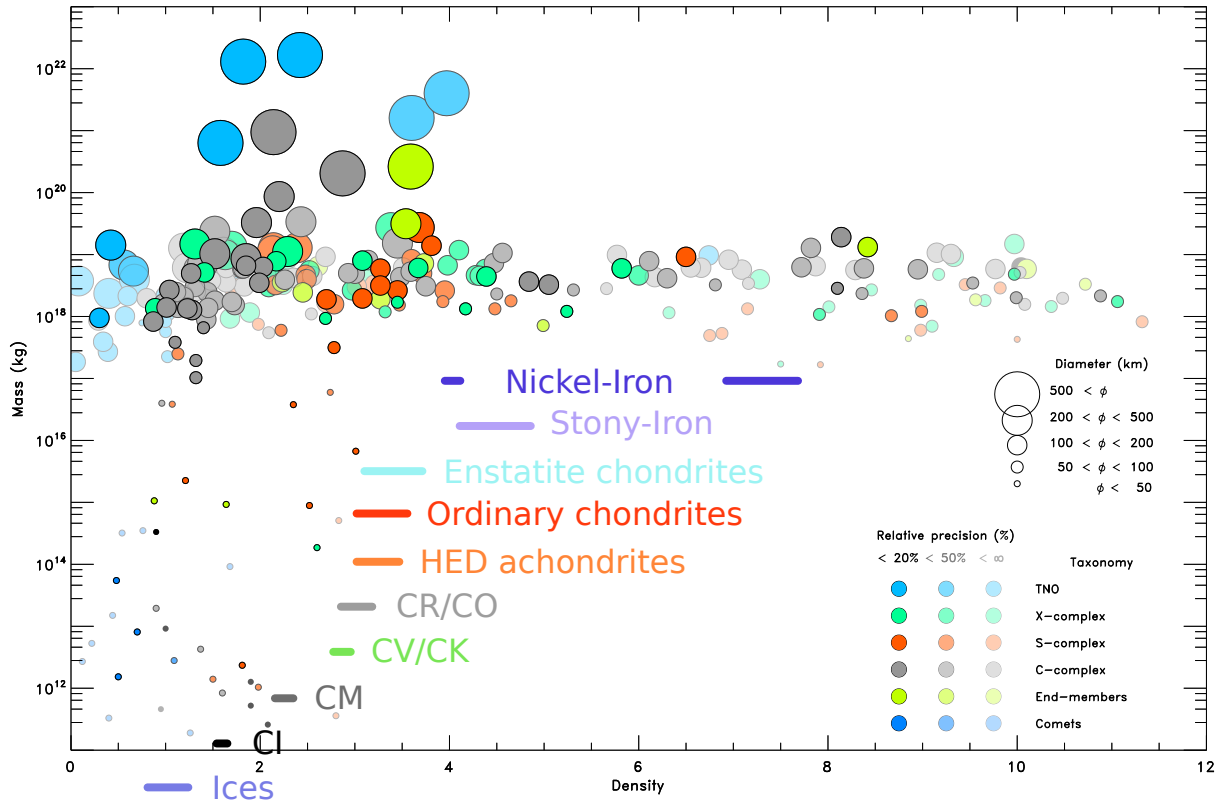


Figure 7: Density vs. Mass. Small bodies are divided into 6 categories: TNOs (light blue), comets (blue), and asteroids (all dynamic class together) divided into four taxonomic groups: S-complex in red, C-complex in grey, X-complex in green, and end-members in yellow (similar to Fig. 6). Asteroids which taxonomy is unknown are plotted in black. The size of the symbols is a function of the object diameters, and the three different levels of contrast correspond to three cuts of relative accuracy: $< 20\%$, $< 50\%$, and regardless to the precision ($< \infty$). The density of the different class of meteorites is also drawn, at arbitrary masses (Table 2).

more dense than the other C-types, independently from the mass-density trend observed among C-complex asteroids (see above). Therefore, in addition to albedo and reflectance spectra that point toward different surface properties/composition, density suggests that there are fundamental differences in the composition and internal structures of B-types. The recent recovery of the Almahata Sitta meteorite, originating from the impact of asteroid 2008 TC₃ on Earth in October 2008, indeed indicated that B-type could be associated with unusual Ureilite achondrites (Jenniskens et al. 2009). Based on a comparison of the densities of (1) Ceres and (2) Pallas (used as archetypes for the definition of C and B taxonomic classes), Carry et al. (2010a) had suggested that B-types were less hydrated than C-types; a hypothesis supported by the lack of signature of organic or icy material in their spectra (Jones et al. 1990).

Finally, the three D-types have density estimates around 9. These estimates were discarded from the analysis, as their uncertainty range does not overlap with meteorites, even the highly dense iron hexahedrites (Table 2).

5.2. S-complex and related end-members

The density of S-complex asteroids is distributed in a narrow interval (about 2 to 3), slightly below the density of their associated meteorites, the ordinary chondrites. The resulting macroporosity is generally smaller than 30%, *i.e.*, these asteroids may present cracks and fractures but are still coherent (not

rubble-piles). This highlights intrinsic differences with the C-complex. The higher density is revelatory of the difference in composition: *basaltic* ordinary chondrites vs. *primitive* CI/CM carbonaceous chondrites. The lower macroporosity suggests a difference in formation and response to shocks. S-complex asteroids are made of *igneous* rocks, *i.e.*, they experienced a stage of high temperatures and were partly or entirely melted. If S-types acquired some cohesion in the process, subsequent impacts would have either not enough energy to overpass this cohesion barrier, leaving them with cracks and fractures only, or enough energy to break their structure and destroy them (“battered to bits”: Burbine et al. 1996). The current S-complex asteroids would therefore be the few remnants of an originally much larger population (Morbidelli et al. 2009).

There are only four density estimates of asteroids belonging to the A and V classes. The only A-type, (354) Eleonora, has a density of 3.7 ± 1.4 , much higher than S-types. This value is in agreement with the density of terrestrial olivines and stony-iron Pallasites meteorites (Sect. 2 and Table 2), although the rough relative accuracy allows a wide range of possibilities. Average density of the three V-types is surprisingly low: ≈ 1.9 . A close inspection however reveals that (4) Vesta has a high density of 3.6 while the two 10 km-sized (809) Lunda and (854) Frostia have low densities of 1.6 and 0.9 respectively. These density measurement are hardly comparable. Vesta is a differ-

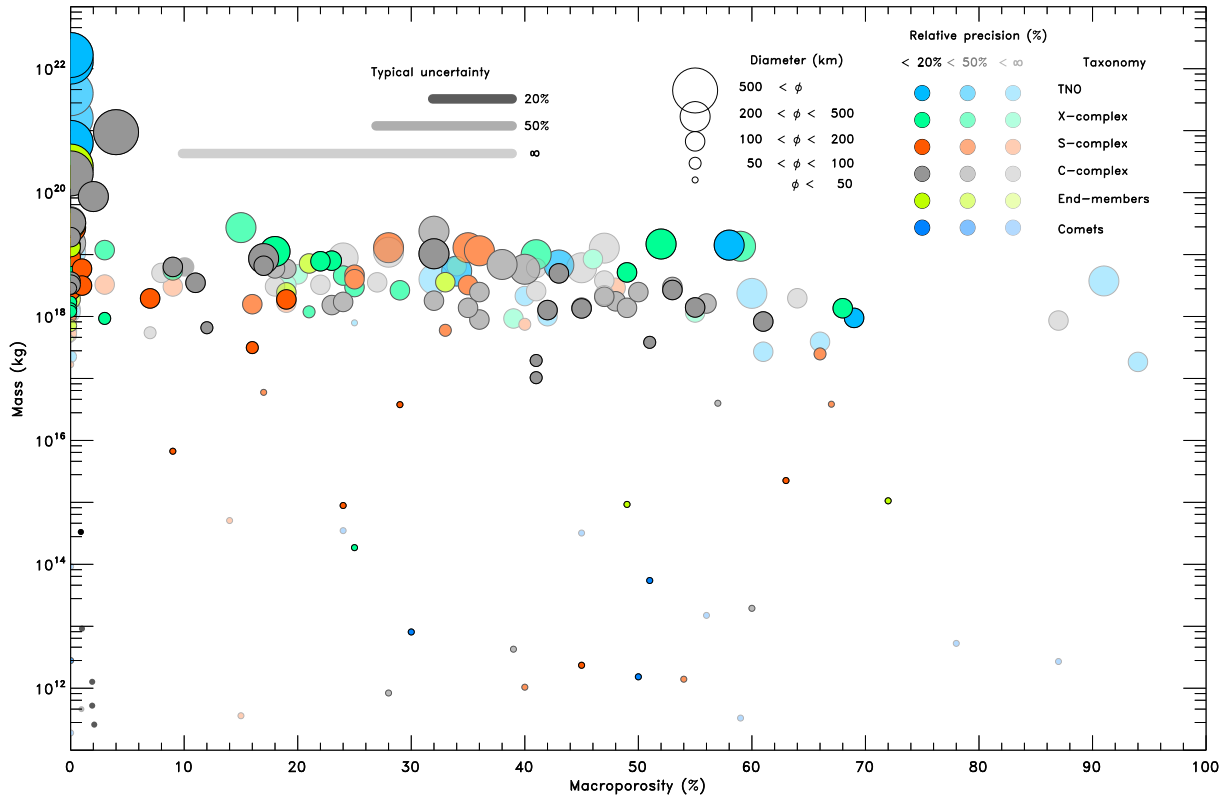


Figure 8: Macroporosity vs. Mass. The color and size of the symbols are similar to Fig. 7. Macroporosity is obtained from Eq. 2 and the asteroid-meteorite links listed in 3. The typical uncertainty in macroporosity for three precision level on density are displayed (20%, 50%, and regardless to the precision: ∞). Additionally, an erroneous asteroid-meteorite link can shift any value by 30–40%.

entiated asteroid with a pyroxene-rich crust, analog to the HED meteorites, and a denser olivine-rich mantle (e.g., McCord et al. 1970; Binzel et al. 1997). The low density of Lundia and Frostia implies a high macroporosity, above 50%, in the rubble-pile regime. Owing to their small size, they are the product of the collisional disruption of a larger parent body, and such a porous structure is not so surprising.

5.3. X complex, or X melting pot?

The large spread in density and macroporosity of asteroids in the X-complex does not reduce with increasing levels of accuracy, contrary to the other groups of small bodies. This suggests that multiple compositions are present in the complex. This is supported by the many different proposed analog meteorites (see Sect. 2) and wider distribution of albedo with respect to C and S complexes (Fig. 9 by Ryan and Woodward 2010). The current definition of the X-complex (DeMeo et al. 2009) indeed encompass the former E, M, and P groups that were distinguished owing to their albedo (Tholen and Barucci 1989).

Both Xc and Xk class have densities above 4, in the range of stony-iron and iron meteorites (Table 2). The density of X-types and Xe-types is lower, at about 1.8 and 2.6 respectively, closer to the proposed CV carbonaceous chondrites and enstatite chondrites meteorites. These asteroids have been grouped together in the taxonomy by DeMeo et al. (2009) owing to their spectra similarity. Given the low-contrast of

their reflectance spectra, however, this grouping may be artificial. Many different compositions are likely to be represented among the X-complex. Further understanding and classification of these asteroids will benefit using a larger wavelength range (e.g., Vernazza et al. 2011b) and albedo (e.g., Ockert-Bell et al. 2010; Fornasier et al. 2011).

5.4. Dwarf planets and small bodies

There are only 8 small bodies more massive than 10^{20} kg: Ceres, Pallas, Vesta, Quaoar, Orcus, Pluto, Haumea, and Eris. These objects have diameters larger than 500 km and can be considered dwarf planets. Their density is high, between 2 and 4, above that of their analog meteorites. This population particularly stands out in Fig. 8, where the dwarf planets ($M \geq 10^{20}$ kg) are all packed near the $\mathcal{P} \approx 0$ axis, and the other small bodies below 10^{20} kg are spread over the entire graph. This suggests that these bodies are differentiated, with the presence of higher density material below the surface, e.g., silicate or iron cores (Fraser and Brown 2010; Castillo-Rogez and McCord 2010).

The majority (75%) of the small bodies in the sample compiled here are main-belt and Trojan asteroids with masses between 10^{17} and 10^{20} kg. These asteroids have diameters between 50 and 400 km, densities between 0.9 and 5.8, and macroporosities up to 70%, from the highly porous (90) Antiope to the very compact asteroid (46) Hestia. The pres-

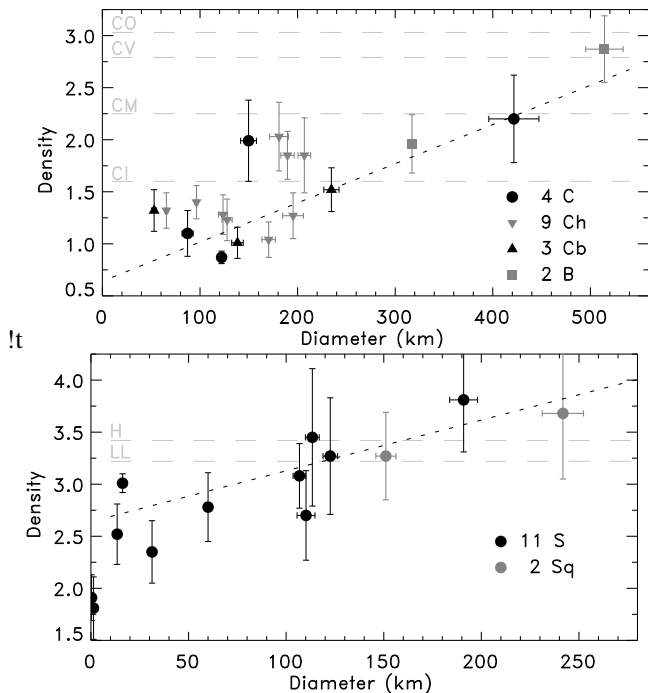


Figure 9: Density vs. diameter. **Top:** The 18 asteroids in the C-complex (20% relative precision only, without Ceres). Average density for the CI, CM, CV, and CV carbonaceous chondrites are also reported (light grey horizontal dashed lines). The oblique dotted line is a linear regression on this sample with a correlation coefficient of 68%. **Bottom:** The 13 asteroids in the S-complex (20% relative precision only). Average density for the LL and H ordinary chondrites are also reported (light grey horizontal dashed lines). The oblique dotted line is a linear regression on this sample with a correlation coefficient of 51%.

sure inside an object with a mass lower than $\approx 10^{20}$ kg never reaches 10^7 Pa (the threshold for silicate grain compaction, see Sect. 5.1, Fig. 9, and Consolmagno et al. 2008). These high levels of macroporosity are therefore not unexpected. The broad range of densities is more surprising. It is partly due to different compositions of these objects, but also to the often large biases affecting the density estimates. Indeed, the fraction of asteroids with densities lower than 4, decreases from 56% to 16% by considering the estimates more precise than 20% only. Said differently, most of the small bodies with a density larger than ≈ 4 suffer from low-precision estimates with underestimated volume and/or overestimated mass.

This is supported by the distribution of density and macroporosity among NEAs ($M \leq 10^{17}$ kg). If the macroporosity of NEA also spans a similar range up to 70%, the most dense NEA is (433) Eros, with $\rho \sim 3$ only. By opposition to MBAs, all the mass estimates available for NEA were derived from a spacecraft encounter or from the orbit of a satellite, the most-precise techniques (Fig. 1). The accuracy on their density is therefore limited by the relative precision of their volume-equivalent diameters, which is generally less affected by biases (Sect. 4). The distribution of density among NEAs may therefore be more representative of the *real* density distribution than what we now observe for main-belt asteroids. Because NEAs only represent 6% of the sample presented here, strong efforts to improve the mass estimates of MBAs must be undertaken.

5.5. Transneptunian objects

This population includes a wide range of sizes, from dwarf-planets such as Pluto with diameters above 2 000 km down to small bodies of a few tens of kilometers. All of the 28 TNOs listed in Table 1 have satellites and the main source of uncertainty is the precision on volume estimates, similarly to NEAs. The situation is however worse for TNOs. Indeed, volume estimates from thermal radiometry (e.g., Lellouch et al. 2010), stellar occultation (e.g., Sicardy et al. 2011) or direct imaging (e.g., Fraser and Brown 2010) are available for the few larger TNOs only. The diameter of 11 TNOs was roughly estimated from their apparent magnitude. Given the lack of knowledge on their albedo and the 20% uncertainty affecting albedo estimates (see Lim et al. 2010), only crude diameter estimates can be derived (Fig. 4.a). The diameters of 7 additional TNOs have been estimated from an *assumed* density of 1.0 (Parker et al. 2011; Sheppard et al. 2011). Only 10 density estimates were therefore determined from *direct* measurements. Of these, only 5 have a relative precision better than 20%: 1999 TC₃₆, Typhon, Orcus, Pluto, and Eris.

The 5 TNOs larger than $\approx 1 000$ km have densities above 1.5, indicating differentiated interiors as described before (Sect. 5.4). On the contrary, the 5 other 100 km-sized TNOs have densities around 0.5, indicative of highly porous structures ($\mathcal{P} \geq 50\%$). The increase in macroporosity for smaller objects is similar to that observed for asteroids. Current asteroid and TNO populations are the result of collisions over History and such similarities are therefore expected.

5.6. Comets

The comets are the least massive objects listed here, from 10^{14} to 10^{17} kg. With a diameter of typically a few hundreds meters to a couple of kilometers and a very bright coma with respect to the nucleus itself as soon as they are active, observations of comet nuclei are very difficult. Current knowledge of the physical properties of comet nuclei is therefore still limited (Lamy et al. 2004).

The comets have a very low density: 9 of the 12 comets listed here have a density below 1. The weighted average density of all 12 comets is 0.47 ± 0.25 only, marginally below the limit value of 0.6 inferred from rotation properties (e.g., Lamy et al. 2004; Snodgrass et al. 2006). The resulting macroporosity is generally high ($\mathcal{P} \geq 30\text{--}50\%$), consistent with our current understanding of the structure of a comet nucleus: a highly porous assemblage of ices and silicates (see Weissman et al. 2004, for a review). These values of density and macroporosity are consistent with those of the small-sized TNOs (Sect. 5.5). This is reassuring given that TNOs are thought to be the reservoir of Jupiter-family comets (Jewitt 2004).

6. Perspectives

Our knowledge on the density and macroporosity of small bodies has seen a revolution in the last 10 years, from 17 objects listed by Britt et al. (2002), to 40 by Consolmagno et al. (2008), to 287 here. If the sample has increased by about an order of magnitude, only a third of the density estimates have a relative precision better than 20%. Improving the accuracy of mass and volume estimates is therefore necessary. Several lines of investigations are still required to improve our understanding of asteroids composition and internal structure.

6.1. Asteroid-meteorite link

As briefly described in Sect. 2, only half of the 24 classes of the asteroid taxonomy have mineralogy interpretations (DeMeo et al. 2009). Together with the dynamic of asteroids, it is one of the fundamental knowledge required to constrain the models of planetary formation (e.g., Morbidelli et al. 2005; Walsh et al. 2011). Efforts to determine the surface properties must be continued. Irradiation experiments in the laboratory have allowed to understand the space weathering processes on the surfaces of olivines and pyroxenes-rich S-complex asteroids (see Chapman 1996; Strazzulla et al. 2005; Vernazza et al. 2006, 2009a, among many others), including the related end-members A and V types (Brunetto et al. 2007; Fulvio et al. 2012). The influence of the space weathering on the reflectance spectra of most meteorite types is however still unknown, apart from some experiments on enstatite chondrites and mesosiderites (Vernazza et al. 2009b).

Mid-infrared spectroscopy (2–5 and 5–40 μm range) will also help refining the mineralogy (e.g., Rivkin et al. 2002; Emery et al. 2006), providing the regolith packing can be reproduced in the laboratory (e.g., Vernazza et al. 2010, 2011a; King et al. 2011). Albedo measurements should also be used (Fornasier et al. 2011), although the typical uncertainty of about 20% that

can be expected from simple thermal models (Lim et al. 2010) may preclude strong conclusions for the time being. Density can also greatly help in that respect. The comparison of bulk density resulting from the possible composition with the asteroid bulk density may confirm or invalidate the composition (Sierks et al. 2011). Refining the asteroid-meteorite links will allow to secure the macroporosity estimates, hence our knowledge of the interior of small bodies.

6.2. Accurate mass estimates

Estimating any mass at all is the limiting factor in determining the density of small bodies (e.g., Consolmagno et al. 2008). Furthermore, in most of the cases, the density accuracy is hampered by the large uncertainty of mass estimates (Sect. 4.2). Improving the number and accuracy of mass estimates is therefore required.

The study of binary systems is highly relevant in that respect. It is the most productive method to determine accurate mass estimates (Fig. 1.c). However, only a third of the 200 known binaries have a mass estimate (Sect. 4.1). Most of the binaries were indeed discovered from lightcurves, and their angular separation is too small to be resolved. Upcoming facilities such as the ALMA interferometer or the E-ELT will provide the angular resolution required to resolve these systems, and many more accurate mass determinations should be available in few years. Additional optical and radar imaging observations, together with lightcurves of mutual events of known binaries, will also help improving the current mass estimates (e.g., Descamps et al. 2008).

In parallel, the astrometry observations by Gaia will provide additional mass determinations. Around 350 000 small bodies are expected to be observed during the 5 years mission, with an average of 50 to 60 epochs on each (Mignard et al. 2007). The micro-arcsecond precision of Gaia's astrometry will allow to refine the accuracy on the orbit of asteroids by several orders of magnitude. Such a precision will have a snowball effect on subsequent mass estimates from planetary ephemeris and orbit deflections. Close encounters between asteroids will also be observed during the mission and the mass of about 50 asteroids with an expected relative precision better than 10% will be determined (Mouret et al. 2007). Although most of these objects are most likely already listed in Appendix A, the mass estimates are expected to be less affected by biases, owing to the unprecedented completeness of Gaia catalog. The number of mass estimates and their level of accuracy is therefore expected to improve significantly at the 2020 horizon.

6.3. Accurate volume estimates

As described in Sect. 4, the contributions of the mass and diameter uncertainties to the density uncertainty are not even. The precision on the diameter is indeed the limiting factor of the most accurate density estimates (see also Fig. 3). Relative precision on the volume below 10–15% are required to take advantage of any mass determination. The accuracy on the diameter should therefore be of a few percent at most. Thanks to improved observing facilities and from improved methods

of analysis, our understanding of the physical properties of asteroids as seen a revolution in last decade, making such a goal achievable.

Many different observing techniques and methods of analysis can be used to evaluate the diameter of small bodies. In particular, multi-data approaches have been proven successful in determining the 3-D shape, size, and spin axis of small bodies (see Sect. 4.2). The recent flyby of asteroid (21) Lutetia by the ESA Rosetta mission showed that the diameter estimate derived before the flyby from optical lightcurves and disk-resolved images was accurate to 2% (using the KOALA 3-D shape modeling algorithm, see Kaasalainen 2011; Carry et al. 2010b, 2012). Besides, 3-D shape models offer the possibility to analyze thermal radiometry data with more advanced thermal models (e.g., Lagerros 1996, 1997; Müller et al. 2005; Mueller et al. 2006; Delbo and Tanga 2009; Rozitis and Green 2011; O'Rourke et al. 2012). Such models allow to derive several surface properties such as the albedo and thermal inertia. These quantities can in turn be used to help constraining the asteroid-meteorite links (Sect. 6.1). Large observing programs (e.g., lightcurves, adaptive-optics disk-resolved images on large telescopes, stellar occultation campaigns) to derive 3-D shape models of all the small bodies listed in Table 1 have therefore far-reaching implications.

7. Conclusion

An extensive review of current knowledge on the density and macroporosity of small bodies is presented. The density estimates of 287 small bodies are presented, computed from 994 mass estimates, 1454 volume-equivalent diameter estimates, and 24 indirect density estimates. All the dynamical classes are represented in the sample: 17 near-Earth asteroids, 230 Main-Belt and Trojan asteroids, 12 comets, and 28 transneptunian objects. The accuracy and biases affecting mass and diameter estimates are discussed and best-estimates are strictly selected. Bulk densities are computed and compared with meteorite density, allowing to estimate the macroporosity. Although the sample still suffers from large uncertainties and often biases (Sect. 4 and 5), several trends can be identified:

1. Dwarf-planets apparently have no macroporosity, contrary to small bodies which mass is inferior to $\approx 10^{20}$ kg.
2. Asteroids in the S-complex are more dense than those in the C-complex that in turn present a larger macroporosity.
3. There is a trend of increasing density with mass for asteroids in both S and C complexes. This trends is also visible from the lower density of NEAs with respect to MBAs.
4. B-types seem structurally different from other C-complex asteroids (albedo, reflectance spectra, density).
5. The X-complex encompasses many different compositions and should be revised using additional data (e.g., albedo).
6. Comets and TNOs have similar low density and high macroporosity, consistent with a structure of porous icy agglomerates.

Several lines of investigations to improve the number and accuracy of density estimates are discussed. The search for binary asteroids and subsequent orbital analysis, together with detailed 3-D shape modeling from multi-data inversion techniques stand out as key programs.

Acknowledgments

A big thank-you to P. Tanga and D. Hestroffer for poking me about coming to the Gaia GREAT meeting in Pisa, without them I wouldn't have started this painful (but fruitful!) task of compiling masses. Dankeschön, merci to T. Müller, F. Marchis and A. Fienga for sharing their results ahead of publication. Thanks to F. DeMeo for constructive discussions. Thank you to the two anonymous referees for their constructive comments. As a result, the present manuscript includes a significantly higher amount of material in the introductory sections. Gracias R. Soja and E. Treguier for all our discussions about this topic and for the fun in the office. This research made heavy use of NASA's Astrophysics Data System Abstract Service (ADS) and Data Archive, thanks to the developers and maintainers.

- A'Hearn, M.F., Belton, M.J.S., Delamere, W.A., Kissel, J., Klaasen, K.P., McFadden, L.A., Meech, K.J., Melosh, H.J., Schultz, P.H., Sunshine, J.M., Thomas, P.C., Veverka, J., Yeomans, D.K., Baca, M.W., Busko, I., Crockett, C.J., Collins, S.M., Desnoyer, M., Eberhardy, C.A., Ernst, C.M., Farnham, T.L., Feaga, L., Groussin, O., Hampton, D., Ipatov, S.I., Li, J.Y., Lindler, D., Lisse, C.M., Mastrodemos, N., Owen, W.M., Richardson, J.E., Wellnitz, D.D., White, R.L., 2005. Deep Impact: Excavating Comet Tempel 1. *Science* 310, 258–264.
- Altenhoff, W.J., Bertoldi, F., Menten, K.M., 2004. Size estimates of some optically bright KBOs. *Astronomy and Astrophysics* 415, 771–775.
- Archinal, B.A., A'Hearn, M.F., Bowell, E., Conrad, A., Consolmagno, G.J., Courtin, R., Fukushima, T., Hestroffer, D., Hilton, J.L., Krasinsky, G.A., Neumann, G., Oberst, J., Seidelmann, P.K., Stooke, P., Tholen, D.J., Thomas, P.C., Williams, I.P., 2011. Report of the IAU Working Group on Cartographic Coordinates and Rotational Elements: 2009. *Celestial Mechanics and Dynamical Astronomy* 109, 101–135.
- Aslan, Z., Gumerov, R., Hudkova, L., Ivantsov, A., Khamitov, I., Pinigin, G., 2007. Mass Determination of Small Solar System Bodies with Ground-based Observations, in: O. Demircan, S. O. Selam, & B. Albayrak (Ed.), *Solar and Stellar Physics Through Eclipses*, pp. 52–58.
- Baer, J., Chesley, S.R., 2008. Astrometric masses of 21 asteroids, and an integrated asteroid ephemeris. *Celestial Mechanics and Dynamical Astronomy* 100, 27–42.
- Baer, J., Chesley, S.R., Matson, R.D., 2011. Astrometric Masses of 26 Asteroids and Observations on Asteroid Porosity. *Astronomical Journal* 141, 143–155.
- Baer, J., Milani, A., Chesley, S.R., Matson, R.D., 2008. An Observational Error Model, and Application to Asteroid Mass Determination, in: *Bulletin of the American Astronomical Society*, p. 493.
- Bange, J., 1998. An estimation of the mass of asteroid 20-Massalia derived from the HIPPARCOS minor planets data. *Astronomy and Astrophysics* 340, L1–L4.
- Bange, J.F., Bec-Borsenberger, A., 1997. Determination of the Masses of Minor Planets, in: R. M. Bonnet, E. Høg, P. L. Bernacca, L. Emiliani, A. Blaauw, C. Turon, J. Kovalevsky, L. Lindgren, H. Hassan, M. Bouffard, B. Strim, D. Heger, M. A. C. Perryman, & L. Woltjer (Ed.), *Hipparcos - Venice '97*, pp. 169–172.
- Barucci, A., Belskaya, I., Fornasier, S., Fulchignoni, M., Clark, B.E., Coradini, A., Capaccioni, F., Dotto, E., Birlan, M., Leyrat, C., Sierks, H., Thomas, N., Vincent, J.B., 2012. Overview of Lutetia's surface composition. *Planetary and Space Science*.
- Barucci, M.A., Brown, M.E., Emery, J.P., Merlin, F., 2008. Composition and Surface Properties of Transneptunian Objects and Centaurs. *The Solar System Beyond Neptune*, 143–160.

- Barucci, M.A., Fulchignoni, M., Fornasier, S., Dotto, E., Vernazza, P., Birlan, M., Binzel, R.P., Carvano, J.M., Merlin, F., Barbieri, C., Belskaya, I.N., 2005. Asteroid target selection for the new Rosetta mission baseline. 21 Lutetia and 2867 Steins. *Astronomy and Astrophysics* 430, 313–317.
- Behrend, R., Bernasconi, L., Roy, R., Klotz, A., Colas, F., Antonini, P., Aoun, R., Augustesen, K., Barbotin, E., Berger, N., Berrouachdi, H., Brochard, E., Cazenave, A., Cavadore, C., Coloma, J., Cotrez, V., Deconihout, S., Demeautis, C., Dorseuil, J., Dubos, G., Durkee, R., Frappa, E., Hormuth, F., Itonen, T., Jacques, C., Kurtze, L., Laffont, A., Lavayssière, M., Lecacheux, J., Leroy, A., Manzini, F., Masi, G., Matter, D., Michelsen, R., Nomen, J., Oksanen, A., Pääkkönen, P., Peyrot, A., Pimentel, E., Pray, D.P., Rinner, C., Sanchez, S., Sonnenberg, K., Sposetti, S., Starkey, D., Stoss, R., Teng, J.P., Vignand, M., Waelchli, N., 2006. Four new binary minor planets: (854) Frostia, (1089) Tama, (1313) Berna, (4492) Debussy. *Astronomy and Astrophysics* 446, 1177–1184.
- Bell, J.F., Davis, D.R., Hartmann, W.K., Gaffey, M.J., 1989. Asteroids - The big picture. *Asteroids II*, 921–945.
- Benner, L.A.M., Margot, J., Nolan, M.C., Giorgini, J.D., Brozovic, M., Scheeres, D.J., Magri, C., Ostro, S.J., 2010. Radar Imaging and a Physical Model of Binary Asteroid 65803 Didymos, in: AAS/Division for Planetary Sciences Meeting Abstracts #42, p. 1056.
- Bertoldi, F., Altenhoff, W., Weiss, A., Menten, K.M., Thum, C., 2006. The trans-neptunian object UB₃₁₃ is larger than Pluto. *Nature* 439, 563–564.
- Binzel, R.P., Gaffey, M.J., Thomas, P.C., Zellner, B.H., Storrs, A.D., Wells, E.N., 1997. Geologic Mapping of Vesta from 1994 Hubble Space Telescope Images. *Icarus* 128, 95–103.
- Bottke, Jr., W.F., Cellino, A., Paolicchi, P., Binzel, R.P., 2002a. An Overview of the Asteroids: The Asteroids III Perspective. *Asteroids III*, 3–15.
- Bottke, Jr., W.F., Nesvorný, D., Grimm, R.E., Morbidelli, A., O'Brien, D.P., 2006. Iron meteorites as remnants of planetesimals formed in the terrestrial planet region. *Nature* 439, 821–824.
- Bottke, Jr., W.F., Vokrouhlický, D., Rubincam, D.P., Broz, M., 2002b. The Effect of Yarkovsky Thermal Forces on the Dynamical Evolution of Asteroids and Meteoroids. *Asteroids III*, 395–408.
- Britt, D.T., Bell, J.F., Haack, H., Scott, E.R.D., 1992. The Reflectance Spectrum of Troilite and the T-Type Asteroids. *Meteoritics* 27, 207.
- Britt, D.T., Consolmagno, G.J., 2003. Stony meteorite porosities and densities: A review of the data through 2001. *Meteoritics and Planetary Science* 38, 1161–1180.
- Britt, D.T., Yeomans, D.K., Housen, K.R., Consolmagno, G.J., 2002. Asteroid Density, Porosity, and Structure. *Asteroids III*, 485–500.
- Brooks, H.E., 2006. Orbits of Binary Near-Earth Asteroids from Radar Observations, in: AAS/Division for Planetary Sciences Meeting Abstracts #38, pp. 934–+.
- Brown, M.E., Bouchez, A.H., Rabinowitz, D.L., Sari, R., Trujillo, C.A., van Dam, M.A., Campbell, R.D., Chin, J.C.Y., Hartman, S.K., Johansson, E.M., Lafon, R.E., Le Mignant, D., Stomski Jr., P.J., Summers, D.M., Wizinowich, P.L., 2005. Keck Observatory Laser Guide Star Adaptive Optics Discovery and Characterization of a Satellite to the Large Kuiper Belt Object 2003 EL₆₁. *Astronomical Journal* 132, L45–L48.
- Brown, M.E., Ragozzine, D., Stansberry, J., Fraser, W.C., 2010. The Size, Density, and Formation of the Orcus-Vanth System in the Kuiper Belt. *Astronomical Journal* 139, 2700–2705.
- Brown, M.E., Schaller, E.L., 2007. The Mass of Dwarf Planet Eris. *Science* 316, 1585–.
- Brown, M.E., Schaller, E.L., Roe, H.G., Rabinowitz, D.L., Trujillo, C.A., 2006. Direct Measurement of the Size of 2003 UB₃₁₃ from the Hubble Space Telescope. *Astrophysical Journal* 643, L61–L63.
- Brown, M.E., Trujillo, C.A., 2004. Direct Measurement of the Size of the Large Kuiper Belt Object (50000) Quaoar. *Astronomical Journal* 127, 2413–2417.
- Brownlee, D.E., Horz, F., Newburn, R.L., Zolensky, M., Duxbury, T.C., Sandford, S., Sekanina, Z., Tsou, P., Hanner, M.S., Clark, B.C., Green, S.F., Kissel, J., 2004. Surface of Young Jupiter Family Comet 81 P/Wild 2: View from the Stardust Spacecraft. *Science* 304, 1764–1769.
- Brozović, M., Benner, L.A.M., Taylor, P.A., Nolan, M.C., Howell, E.S., Magri, C., Scheeres, D.J., Giorgini, J.D., Pollock, J.T., Pravec, P., Galád, A., Fang, J., Margot, J.L., Busch, M.W., Shepard, M.K., Reichart, D.E., Ivarsen, K.M., Haislip, J.B., Lacluyze, A.P., Jao, J., Slade, M.A., Lawrence, K.J., Hicks, M.D., 2011. Radar and optical observations and physical modeling of triple near-Earth Asteroid (136617) 1994 CC. *Icarus* 216, 241–256.
- Brucker, M.J., Grundy, W.M., Stansberry, J.A., Spencer, J.R., Sheppard, S.S., Chiang, E.I., Buie, M.W., 2009. High albedos of low inclination Classical Kuiper belt objects. *Icarus* 201, 284–294.
- Brunetto, R., de León, J., Licandro, J., 2007. Testing space weathering models on A-type asteroid (1951) Lick. *Astronomy and Astrophysics* 472, 653–656.
- Brunetto, R., Vernazza, P., Marchi, S., Birlan, M., Fulchignoni, M., Orofino, V., Strazzulla, G., 2006. Modeling asteroid surfaces from observations and irradiation experiments: The case of 832 Karin. *Icarus* 184, 327–337.
- Buie, M.W., Grundy, W.M., Young, E.F., Young, L.A., Stern, S.A., 2006. Orbits and Photometry of Pluto's Satellites: Charon, S/2005 P1, and S/2005 P2. *Astronomical Journal* 132, 290–298.
- Burbine, T.H., Duffard, R., Buchanan, P.C., Cloutis, E.A., Binzel, R.P., 2011. Spectroscopy of O-Type Asteroids, in: Lunar and Planetary Institute Science Conference Abstracts, p. 2483.
- Burbine, T.H., McCoy, T.J., Meibom, A., Gladman, B., Keil, K., 2002. Meteoritic Parent Bodies: Their Number and Identification. *Asteroids III*, 653–667.
- Burbine, T.H., Meibom, A., Binzel, R.P., 1996. Mantle material in the main belt: Battered to bits? *Meteoritics and Planetary Science* 31, 607–620.
- Bus, S.J., 1999. Compositional structure in the asteroid belt: Results of a spectroscopic survey. Ph.D. thesis. MASSACHUSETTS INSTITUTE OF TECHNOLOGY.
- Carpino, M., Knezevic, Z., 1996. Asteroid mass determination: (1) Ceres, in: S. Ferraz-Mello, B. Morando, & J.-E. Arlot (Ed.), Dynamics, Ephemerides, and Astrometry of the Solar System, pp. 203–+.
- Carry, B., Dumas, C., Fulchignoni, M., Merline, W.J., Berthier, J., Hestroffer, D., Fusco, T., Tamblyn, P., 2008. Near-Infrared Mapping and Physical Properties of the Dwarf-Planet Ceres. *Astronomy and Astrophysics* 478, 235–244.
- Carry, B., Dumas, C., Kaasalainen, M., Berthier, J., Merline, W.J., Erard, S., Conrad, A.R., Drummond, J.D., Hestroffer, D., Fulchignoni, M., Fusco, T., 2010a. Physical properties of (2) Pallas. *Icarus* 205, 460–472.
- Carry, B., Hestroffer, D., DeMeo, F.E., Thirouin, A., Berthier, J., Lacerda, P., Sicardy, B., Doressoundiram, A., Dumas, C., Farrelly, D., Müller, T.G., 2011. Integral-field spectroscopy of (90482) Orcus-Vanth. *Astronomy and Astrophysics* 534, A115.
- Carry, B., Kaasalainen, M., Leyrat, C., Merline, W.J., Drummond, J.D., Conrad, A.R., Weaver, H.A., Tamblyn, P.M., Chapman, C.R., Dumas, C., Colas, F., Christou, J.C., Dotto, E., Perna, D., Fornasier, S., Bernasconi, L., Behrend, R., Vachier, F., Kryszczyńska, A., Polinska, M., Fulchignoni, M., Roy, R., Naves, R., Poncy, R., Wiggins, P., 2010b. Physical properties of the ESA Rosetta target asteroid (21) Lutetia. II. Shape and flyby geometry. *Astronomy and Astrophysics* 523, A94.
- Carry, B., Kaasalainen, M., Merline, W.J., Müller, T.G., Jorda, L., Drummond, J.D., Berthier, J., O'Rourke, L., Durech, J., Küppers, M., Conrad, A.R., Dumas, C., Sierks, H., the OSIRIS Team, 2012. KOALA shape modeling technique validated at (21) Lutetia by ESA Rosetta mission. *Planetary and Space Science* in press.
- Castillo-Rogez, J.C., McCord, T.B., 2010. Ceres: evolution and present state constrained by shape data. *Icarus* 205, 443–459.
- Chapman, C.R., 1996. S-Type Asteroids, Ordinary Chondrites, and Space Weathering: The Evidence from Galileo's Fly-bys of Gaspra and Ida. *Meteoritics and Planetary Science* 31, 699–725.
- Chernetenko, Y.A., Kochetova, O.M., 2002. Masses of some large minor planets, in: B. Warmbein (Ed.), Asteroids, Comets, and Meteors: ACM 2002, pp. 437–440.
- Chesley, S.R., Owen, Jr., W.M., Hayne, E.W., Sullivan, A.M., Dumas, R.C., Giorgini, J.D., Chamberlin, A.B., Synnott, S.P., Vazquez, C.S., 2005. The Mass of Asteroid 10 Hygiea, in: AAS/Division of Dynamical Astronomy Meeting #36, p. 524.
- Clark, B.E., Bus, S.J., Rivkin, A.S., Shepard, M.K., Shah, S., 2004. Spectroscopy of X-Type Asteroids. *Astronomical Journal* 128, 3070–3081.
- Clark, B.E., Ockert-Bell, M.E., Cloutis, E.A., Nesvorný, D., Mothé-Diniz, T., Bus, S.J., 2009. Spectroscopy of K-complex asteroids: Parent bodies of carbonaceous meteorites? *Icarus* 202, 119–133.
- Clark, B.E., Ziffer, J., Nesvorný, D., Campins, H., Rivkin, A.S., Hiroi, T., Barucci, M.A., Fulchignoni, M., Binzel, R.P., Fornasier, S., DeMeo, F., Ockert-Bell, M.E., Licandro, J., Mothé-Diniz, T., 2010. Spectroscopy of B-type asteroids: Subgroups and meteorite analogs. *Journal of Geophysical Research (Planets)* 115, E06005.
- Cloutis, E.A., Hiroi, T., Gaffey, M.J., Alexander, C.M.O., Mann, P., 2011a. Spectral reflectance properties of carbonaceous chondrites: 1. CI chondrites.

- Icarus 212, 180–209.
- Cloutis, E.A., Hudon, P., Hiroi, T., Gaffey, M.J., Mann, P., 2011b. Spectral reflectance properties of carbonaceous chondrites: 2. CM chondrites. *Icarus* 216, 309–346.
- Conrad, A.R., Dumas, C., Merline, W.J., Drummond, J.D., Campbell, R.D., Goodrich, R.W., Le Mignant, D., Chaffee, F.H., Fusco, T., Kwok, S.H., Knight, R.I., 2007. Direct measurement of the size, shape, and pole of 511 Davida with Keck AO in a single night. *Icarus* 191, 616–627.
- Consolmagno, G., Britt, D., Macke, R., 2008. The significance of meteorite density and porosity. *Chemie der Erde / Geochemistry* 68, 1–29.
- Consolmagno, G.J., Britt, D.T., 1998. The density and porosity of meteorites from the Vatican collection. *Meteoritics and Planetary Science* 33, 1231–1241.
- Davidsson, B.J.R., Gutiérrez, P.J., 2004. Estimating the nucleus density of Comet 19P/Borrelly. *Icarus* 168, 392–408.
- Davidsson, B.J.R., Gutiérrez, P.J., 2005. Nucleus properties of Comet 67P/Churyumov Gerasimenko estimated from non-gravitational force modeling. *Icarus* 176, 453–477.
- Davidsson, B.J.R., Gutiérrez, P.J., 2006. Non-gravitational force modeling of Comet 81P/Wild 2. I. A nucleus bulk density estimate. *Icarus* 180, 224–242.
- Davidsson, B.J.R., Gutiérrez, P.J., Rickman, H., 2007. Nucleus properties of Comet 9P/Tempel 1 estimated from non-gravitational force modeling. *Icarus* 187, 306–320.
- de León, J., Duffard, R., Licandro, J., Lazzaro, D., 2004. Mineralogical characterization of A-type asteroid (1951) Lick. *Astronomy and Astrophysics* 422, L59–L62.
- Delbo, M., 2004. Thermal Infrared Asteroid Diameters and Albedo. NASA Planetary Data System. MSX-A-SPIRIT3-5-SBN0003-MIMPS-V1.0.
- Delbo, M., Liori, S., Matter, A., Cellino, A., Berthier, J., 2009. First VLTI-MIDI Direct Determinations of Asteroid Sizes. *Astrophysical Journal* 694, 1228–1236.
- Delbo, M., Tanga, P., 2009. Thermal inertia of main belt asteroids smaller than 100 km from IRAS data. *Planetary and Space Science* 57, 259–265.
- DeMeo, F.E., Binzel, R.P., Slivan, S.M., Bus, S.J., 2009. An extension of the Bus asteroid taxonomy into the near-infrared. *Icarus* 202, 160–180.
- Descamps, P., Marchis, F., Berthier, J.P., Emery, J.P., Duchêne, G., de Pater, I., Wong, M.H., Lim, L., Hammel, H.B., Vachier, F., Wiggins, P., Teng-Chuen-Yu, J.P., Peyrot, A., Pollock, J., Assafin, M., Vieira-Martins, R., Camargo, J.I.B., Braga-Ribas, F., Macomber, B., 2011. Triplicity and physical characteristics of Asteroid (216) Kleopatra. *Icarus* 211, 1022–1033.
- Descamps, P., Marchis, F., Durech, J., Emery, J.P., Harris, A.W., Kaasalainen, M., Berthier, J., Teng-Chuen-Yu, J.P., Peyrot, A., Hutton, L., Greene, J., Pollock, J., Assafin, M., Vieira-Martins, R., Camargo, J.I.B., Braga-Ribas, F., Vachier, F., Reichart, D.E., Ivarsen, K.M., Crain, J.A., Nysewander, M.C., Lacluyze, A.P., Haislip, J.B., Behrend, R., Colas, F., Lecacheux, J., Bernasconi, L., Roy, R., Baudouin, P., Brunetto, L., Sposetti, S., Manzini, F., 2009. New insights on the binary Asteroid 121 Hermione. *Icarus* 203, 88–101.
- Descamps, P., Marchis, F., Michalowski, T., Colas, F., Berthier, J., Vachier, F., Teng-Chuen-Yu, J.P., Peyrot, A., Payet, B., Dorseuil, J., Léonie, Y., Dijoux, T., Berrouachi, H., Chion Hock, C., Benard, F., 2007a. Nature of the small main belt Asteroid 3169 Ostro. *Icarus* 189, 362–369.
- Descamps, P., Marchis, F., Michalowski, T., Vachier, F., Colas, F., Berthier, J., Assafin, M., Dunckel, P.B., Polinska, M., Pych, W., Hestroffer, D., Miller, K.P.M., Vieira-Martins, R., Birlan, M., Teng-Chuen-Yu, J.P., Peyrot, A., Payet, B., Dorseuil, J., Léonie, Y., Dijoux, T., 2007b. Figure of the double Asteroid 90 Antiope from adaptive optics and lightcurve observations. *Icarus* 187, 482–499.
- Descamps, P., Marchis, F., Pollock, J., Berthier, J., Vachier, F., Birlan, M., Kaasalainen, M., Harris, A.W., Wong, M.H., Romanishin, W.J., Cooper, E.M., Kettner, K.A., Wiggins, P., Kryszczyńska, A., Polinska, M., Coliac, J.F., Devyatkin, A., Verestchagina, I., Gorshanov, D., 2008. New determination of the size and bulk density of the binary Asteroid 22 Kalliope from observations of mutual eclipses. *Icarus* 196, 578–600.
- Dorssoundiram, A., Barucci, M.A., Fulchignoni, M., Florczak, M., 1998. EOS Family: A Spectroscopic Study. *Icarus* 131, 15–31.
- Drummond, J.D., Christou, J.C., 2008. Triaxial ellipsoid dimensions and rotational poles of seven asteroids from Lick Observatory adaptive optics images, and of Ceres. *Icarus* 197, 480–496.
- Drummond, J.D., Christou, J.C., Nelson, J., 2009. Triaxial ellipsoid dimensions and poles of asteroids from AO observations at the Keck-II telescope. *Icarus* 202, 147–159.
- Drummond, J.D., Conrad, A., Merline, W.J., Carry, B., Chapman, C.R., Weaver, H.A., Tamblyn, P.M., Christou, J.C., Dumas, C., 2010. Physical properties of the ESA Rosetta target asteroid (21) Lutetia. I. The triaxial ellipsoid dimensions, rotational pole, and bulk density. *Astronomy and Astrophysics* 523, A93.
- Drummond, J.D., Merline, W.J., Conrad, A., Christou, J., Tamblyn, P., Carry, B., 2011. Asteroid (19) Fortuna: Triaxial Ellipsoid Dimensions and Rotational Pole with AO at Gemini North, in: AAS/Division for Planetary Sciences Meeting Abstracts #41, pp. –.
- Dumas, C., Carry, B., Hestroffer, D., Merlin, F., 2011. High-contrast observations of (136108) Haumea. A crystalline water-ice multiple system. *Astronomy and Astrophysics* 528, A105.
- Dunham, D.W., Herald, D., Frappa, E., Hayamizu, T., Talbot, J., Timerson, B., 2011. Asteroid Occultations. NASA Planetary Data System. EAR-A-3-RDR-OCULTATIONS-V9.0.
- Đurech, J., Kaasalainen, M., Herald, D., Dunham, D., Timerson, B., Hanuš, J., Frappa, E., Talbot, J., Hayamizu, T., Warner, B.D., Pilcher, F., Galád, A., 2011. Combining asteroid models derived by lightcurve inversion with asteroidal occultation silhouettes. *Icarus* 214, 652–670.
- Elkins-Tanton, L.T., Weiss, B.P., Zuber, M.T., 2011. Chondrites as samples of differentiated planetesimals. *Earth and Planetary Science Letters* 305, 1–10.
- Emery, J.P., Burr, D.M., Cruikshank, D.P., 2011. Near-infrared Spectroscopy of Trojan Asteroids: Evidence for Two Compositional Groups. *Astronomical Journal* 141, 25.
- Emery, J.P., Cruikshank, D.P., van Cleve, J., 2006. Thermal emission spectroscopy (5.2–38 μm) of three Trojan asteroids with the Spitzer Space Telescope: Detection of fine-grained silicates. *Icarus* 182, 496–512.
- Fang, J., Margot, J.L., Brozovic, M., Nolan, M.C., Benner, L.A.M., Taylor, P.A., 2011. Orbits of Near-Earth Asteroid Triples 2001 SN263 and 1994 CC: Properties, Origin, and Evolution. *Astronomical Journal* 141, 154–169.
- Fernández, Y.R., Sheppard, S.S., Jewitt, D.C., 2003. The Albedo Distribution of Jovian Trojan Asteroids. *Astronomical Journal* 126, 1563–1574.
- Fienga, A., Kuchynka, P., Laskar, J., Manche, H., Gastineau, M., 2011. Asteroid mass determinations with INPOP planetary ephemerides. EPSC-DPS Joint Meeting 2011, 1879.
- Fienga, A., Laskar, J., Morley, T., Manche, H., Kuchynka, P., Le Poncin-Lafitte, C., Budnik, F., Gastineau, M., Somenzi, L., 2009. INPOP08, a 4-D planetary ephemeris: from asteroid and time-scale computations to ESA Mars Express and Venus Express contributions. *Astronomy and Astrophysics* 507, 1675–1686.
- Fienga, A., Manche, H., Kuchynka, P., Laskar, J., Gastineau, M., 2010. INPOP10a. *Scientific Notes*.
- Fienga, A., Manche, H., Laskar, J., Gastineau, M., 2008. INPOP06: a new numerical planetary ephemeris. *Astronomy and Astrophysics* 477, 315–327.
- Folkner, W.M., Williams, J.G., Boggs, D.H., 2009. The planetary and lunar ephemeris de 421. *IPN Progress Report* 42, 1–34.
- Fornasier, S., Clark, B.E., Dotto, E., 2011. Spectroscopic survey of X-type asteroids. *Icarus* 214, 131–146.
- Fraser, W.C., Brown, M.E., 2010. Quaoar: A Rock in the Kuiper Belt. *Astrophysical Journal* 714, 1547–1550.
- Fujiwara, A., Kawaguchi, J., Yeomans, D.K., Abe, M., Mukai, T., Okada, T., Saito, J., Yano, H., Yoshikawa, M., Scheeres, D.J., Barnouin-Jha, O.S., Cheng, A.F., Demura, H., Gaskell, G.W., Hirata, N., Ikeda, H., Kominato, T., Miyamoto, H., Nakamura, R., Sasaki, S., Uesugi, K., 2006. The Rubble-Pile Asteroid Itokawa as Observed by Hayabusa. *Science* 312, 1330–1334.
- Fulvio, D., Brunetto, R., Vernazza, P., Strazzulla, G., 2012. Space weathering of Vesta and V-type asteroids: new irradiation experiments on HED meteorites. *Astronomy and Astrophysics* 537, L11.
- Goffin, E., 2001. New determination of the mass of Pallas. *Astronomy and Astrophysics* 365, 627–630.
- Gouelle, M., Morbidelli, A., Bland, P.A., Spurny, P., Young, E.D., Sephton, M., 2008. Meteorites from the Outer Solar System? The Solar System Beyond Neptune, 525–541.
- Grav, T., Mainzer, A.K., Bauer, J., Masiero, J., Spahr, T., McMillan, R.S., Walker, R., Cutri, R., Wright, E., Eisenhardt, P.R.M., Blauvelt, E., DeBaun, E., Elsbury, D., Gautier, IV, T., Gomillion, S., Hand, E., Wilkins, A., 2011. WISE/NEOWISE Observations of the Jovian Trojans: Preliminary Results. *Astrophysical Journal* 742, 40.
- Grundy, W.M., Noll, K.S., Buie, M.W., Benecchi, S.D., Stephens, D.C., Levison, H.F., 2009. Mutual orbits and masses of six transneptunian binaries.

- Icarus 200, 627–635.
- Grundy, W.M., Noll, K.S., Virtanen, J., Muinonen, K., Kern, S.D., Stephens, D.C., Stansberry, J.A., Levison, H.F., Spencer, J.R., 2008. (42355) Typhon Echidna: Scheduling observations for binary orbit determination. *Icarus* 197, 260–268.
- Grundy, W.M., Stansberry, J.A., Noll, K.S., Stephens, D.C., Trilling, D.E., Kern, S.D., Spencer, J.R., Cruikshank, D.P., Levison, H.F., 2007. The orbit, mass, size, albedo, and density of (65489) Ceto/Phorcys: A tidally-evolved binary Centaur. *Icarus* 191, 286–297.
- Halliday, A.N., Kleine, T., 2006. Meteorites and the Timing, Mechanisms, and Conditions of Terrestrial Planet Accretion and Early Differentiation. *Meteorites and the Early Solar System II*, 775–801.
- Harris, A.W., 1998. A Thermal Model for Near-Earth Asteroids. *Icarus* 131, 291–301.
- Harris, A.W., Davies, J.K., 1999. Physical Characteristics of Near-Earth Asteroids from Thermal Infrared Spectrophotometry. *Icarus* 142, 464–475.
- Hilton, J.L., 1999. US Naval Observatory Ephemerides of the Largest Asteroids. *Astronomical Journal* 117, 1077–1086.
- Hilton, J.L., 2002. Asteroid Masses and Densities. *Asteroids III*, 103–112.
- Ivantsov, A., 2008. Asteroid mass determination at Nikolaev Observatory. *Planetary and Space Science* 56, 1857–1861.
- Jenniskens, P., Shaddad, M.H., Numan, D., Elsir, S., Kudoda, A.M., Zolensky, M.E., Le, L., Robinson, G.A., Friedrich, J.M., Rumble, D., Steele, A., Chesley, S.R., Fitzsimmons, A., Duddy, S., Hsieh, H.H., Ramsay, G., Brown, P.G., Edwards, W.N., Tagliaferri, E., Boslough, M.B., Spalding, R.E., Dantowitz, R., Kozubal, M., Pravec, P., Borovicka, J., Charvat, Z., Vaubaillon, J., Kuiper, J., Albers, J., Bishop, J.L., Mancinelli, R.L., Sandford, S.A., Milam, S.N., Nuevo, M., P., W.S., 2009. The impact and recovery of asteroid 2008 TC₃. *Nature* 458, 485–488.
- Jewitt, D.C., 2004. From cradle to grave: the rise and demise of the comets, 659–676.
- Jones, T.D., Lebofsky, L.A., Lewis, J.S., Marley, M.S., 1990. The composition and Origin of the C,P and D Asteroids: Water as Tracer of Thermal Evolution in the Outer Belt. *Icarus* 88, 172–193.
- Kaasalainen, M., 2011. Maximum compatibility estimates and shape reconstruction with boundary curves and volumes of generalized projections. *Inverse Problems and Imaging* 5, 37–57.
- Kern, S.D., Elliot, J.L., 2005. Studies of Kuiper Belt Binaries, in: AAS/Division for Planetary Sciences Meeting Abstracts #37, p. 738.
- Kern, S.D., Elliot, J.L., 2006. Discovery and characteristics of the Kuiper belt binary 2003QY90. *Icarus* 183, 179–185.
- King, P.L., Izawa, M.R.M., Vernazza, P., McCutcheon, W.A., Berger, J.A., Dunn, T., 2011. Salt: A Critical Material to Consider when Exploring the Solar System. *Lunar and Planetary Institute Science Conference Abstracts* 42, 1985.
- Kochetova, O.M., 2004. Determination of Large Asteroid Masses by the Dynamical Method. *Solar System Research* 38, 66–75.
- Konopliv, A.S., Asmar, S.W., Folkner, W.M., Karatekin, Ö., Nunes, D.C., Smrekar, S.E., Yoder, C.F., Zuber, M.T., 2011. Mars high resolution gravity fields from MRO, Mars seasonal gravity, and other dynamical parameters. *Icarus* 211, 401–428.
- Konopliv, A.S., Miller, J.K., Owen, W.M., Yeomans, D.K., Giorgini, J.D., Garmier, R., Barriot, J.P., 2002. A Global Solution for the Gravity Field, Rotation, Landmarks, and Ephemeris of Eros. *Icarus* 160, 289–299.
- Konopliv, A.S., Yoder, C.F., Standish, E.M., Yuan, D.N., Sjogren, W.L., 2006. A global solution for the Mars static and seasonal gravity, Mars orientation, Phobos and Deimos masses, and Mars ephemeris. *Icarus* 182, 23–50.
- Kovačević, A., 2005. Determination of the mass of (4) Vesta based on new close approaches. *Astronomy and Astrophysics* 430, 319–325.
- Kovačević, A., Kuzmanoski, M., 2007. A New Determination of the Mass of (1) Ceres. *Earth Moon and Planets* 100, 117–123.
- Krasinsky, G.A., Pitjeva, E.V., Vasiliev, M.V., Yagudina, E.I., 2001. Estimating masses of asteroids, in: *Communications of IAA of RAS*.
- Kryszczyńska, A., Colas, F., Descamps, P., Bartczak, P., Polińska, M., Kwiatkowski, T., Lecacheux, J., Hirsch, R., Fagas, M., Kamiński, K., Michałowski, T., Marciniak, A., 2009. New binary asteroid 809 Lunda. I. Photometry and modelling. *Astronomy and Astrophysics* 501, 769–776.
- Kuzmanoski, M., 1996. A method for asteroid mass determination, in: S. Ferraz-Mello, B. Morando, & J.-E. Arlot (Ed.), *Dynamics, Ephemerides, and Astrometry of the Solar System*, pp. 207–+.
- Kuzmanoski, M., Apostolovska, G., Novaković, B., 2010. The Mass of (4) Vesta Derived from its Largest Gravitational Effects. *Astronomical Journal* 140, 880–886.
- Kuzmanoski, M., Kovačević, A., 2002. Motion of the asteroid (13206) 1997GC22 and the mass of (16) Psyche. *Astronomy and Astrophysics* 395, L17–L19.
- Lagerros, J.S.V., 1996. Thermal physics of asteroids. I. Effects of shape, heat conduction and beaming. *Astronomy and Astrophysics* 310, 1011–1020.
- Lagerros, J.S.V., 1997. Thermal physics of asteroids. III. Irregular shapes and albedo variegations. *Astronomy and Astrophysics* 325, 1226–1236.
- Lamy, P.L., Toth, I., Fernandez, Y.R., Weaver, H.A., 2004. The sizes, shapes, albedos, and colors of cometary nuclei. *Comets II*, 223–264.
- Lamy, P.L., Toth, I., Groussin, O., Jorda, L., Kelley, M.S., Stansberry, J.A., 2008. Spitzer Space Telescope observations of the nucleus of comet 67P/Churyumov-Gerasimenko. *Astronomy and Astrophysics* 489, 777–785.
- Lamy, P.L., Toth, I., Weaver, H.A., Jorda, L., Kaasalainen, M., Gutiérrez, P.J., 2006. Hubble Space Telescope observations of the nucleus and inner coma of comet 67P/Churyumov-Gerasimenko. *Astronomy and Astrophysics* 458, 669–678.
- Landgraf, W., 1992. A Determination of the Mass of (704) Interamnia from Observations of (993) Moultona, in: S. Ferraz-Mello (Ed.), *Chaos, Resonance, and Collective Dynamical Phenomena in the Solar System*, pp. 179–183.
- Lebofsky, L.A., 1978. Asteroid 1 Ceres - Evidence for water of hydration. *Monthly Notices of the Royal Astronomical Society* 182, 17–21.
- Lebofsky, L.A., Sykes, M.V., Tedesco, E.F., Veeder, G.J., Matson, D.L., Brown, R.H., Gradie, J.C., Feierberg, M.A., Rudy, R.J., 1986. A refined 'standard' thermal model for asteroids based on observations of 1 Ceres and 2 Pallas. *Icarus* 68, 239–251.
- Lellouch, E., Kiss, C., Santos-Sanz, P., Müller, T.G., Fornasier, S., Groussin, O., Lacerda, P., Ortiz, J.L., Thirouin, A., Delsanti, A., Duffard, R., Harris, A.W., Henry, F., Lim, T., Moreno, R., Mommert, M., Mueller, M., Protopapa, S., Stansberry, J., Trilling, D., Vilenius, E., Barucci, A., Crovisier, J., Doressoundiram, A., Dotto, E., Gutiérrez, P.J., Hainaut, O.R., Hartogh, P., Hestroffer, D., Horner, J., Jorda, L., Kidger, M., Lara, L.M., Rengel, M., Swinyard, B.M., Thomas, N., 2010. "TNOs are cool": A survey of the trans-Neptunian region. II. The thermal lightcurve of (136108) Haumea. *Astronomy and Astrophysics* 518, L147.
- Levison, H.F., Bottke, W.F., Gounelle, M., Morbidelli, A., Nesvorný, D., Tsiganis, K., 2009. Contamination of the asteroid belt by primordial trans-Neptunian objects. *Nature* 460, 364–366.
- Lim, T.L., Stansberry, J., Müller, T.G., Mueller, M., Lellouch, E., Kiss, C., Santos-Sanz, P., Vilenius, E., Protopapa, S., Moreno, R., Delsanti, A., Duffard, R., Fornasier, S., Groussin, O., Harris, A.W., Henry, F., Horner, J., Lacerda, P., Mommert, M., Ortiz, J.L., Rengel, M., Thirouin, A., Trilling, D., Barucci, A., Crovisier, J., Doressoundiram, A., Dotto, E., Gutiérrez Buenestado, P.J., Hainaut, O.R., Hartogh, P., Hestroffer, D., Kidger, M., Lara, L.M., Swinyard, B.M., Thomas, N., 2010. "TNOs are Cool": A survey of the trans-Neptunian region. III. Thermophysical properties of 90482 Orcus and 136472 Makemake. *Astronomy and Astrophysics* 518, L148.
- Lopez Garcia, A., Medvedev, Y.D., Morano Fernandez, J.A., 1997. Using Close Encounters of Minor Planets for the Improvement of their Masses, in: I. M. Wyrzyższczak, J. H. Lieske, & R. A. Feldman (Ed.), *IAU Colloq. 165: Dynamics and Astrometry of Natural and Artificial Celestial Bodies*, p. 199.
- Macke, R.J., Britt, D.T., Consolmagno, G.J., 2011. Density, porosity, and magnetic susceptibility of achondritic meteorites. *Meteoritics and Planetary Science* 46, 311–326.
- Macke, R.J., Consolmagno, G.J., Britt, D.T., Hutson, M.L., 2010. Enstatite chondrite density, magnetic susceptibility, and porosity. *Meteoritics and Planetary Science* 45, 1513–1526.
- Marchis, F., Descamps, P., Baek, M., Harris, A.W., Kaasalainen, M., Berthier, J., Hestroffer, D., Vachier, F., 2008a. Main belt binary asteroidal systems with circular mutual orbits. *Icarus* 196, 97–118.
- Marchis, F., Descamps, P., Berthier, J., Hestroffer, D., Vachier, F., Baek, M., Harris, A.W., Nesvorný, D., 2008b. Main belt binary asteroidal systems with eccentric mutual orbits. *Icarus* 195, 295–316.
- Marchis, F., Descamps, P., Dalba, P., Enriquez, J.E., Durech, J., Emery, J.P., Berthier, J., Vachier, F., Merlbourne, J., Stockton, A.N., Fassnacht, C.D., Dupuy, T.J., 2011. A Detailed Picture of the (93) Minerva Triple System, in: *EPSC-DPS Joint Meeting 2011*, p. 653.
- Marchis, F., Descamps, P., Hestroffer, D., Berthier, J., 2005a. Discovery of the triple asteroidal system 87 Sylvia. *Nature* 436, 822–824.

- Marchis, F., Hestroffer, D., Descamps, P., Berthier, J., Bouchez, A.H., Campbell, R.D., Chin, J.C.Y., van Dam, M.A., Hartman, S.K., Johansson, E.M., Lafon, R.E., Le Mignant, D., de Pater, I., Stomski Jr., P.J., Summers, D.M., Vachier, F., Wizinowich, P.L., Wong, M.H., 2006a. A low density of 0.8gcm⁻³ for the Trojan binary asteroid 617 Patroclus. *Nature* 439, 565–567.
- Marchis, F., Hestroffer, D., Descamps, P., Berthier, J., Laver, C., de Pater, I., 2005b. Mass and density of Asteroid 121 Hermione from an analysis of its companion orbit. *Icarus* 178, 450–464.
- Marchis, F., Kaasalainen, M., Hom, E.F.Y., Berthier, J., Enriquez, J., Hestroffer, D., Le Mignant, D., de Pater, I., 2006b. Shape, size and multiplicity of main-belt asteroids. *Icarus* 185, 39–63.
- Margot, J.L., Brown, M.E., 2001. Discovery and characterization of binary asteroids 22 Kalliope and 87 Sylvia, in: AAS/Division for Planetary Sciences Meeting Abstracts #33, p. 1133.
- Margot, J.L., Brown, M.E., 2003. A Low-Density M-type Asteroid in the Main Belt. *Science* 300, 1939–1942.
- Margot, J.L., Brown, M.E., Trujillo, C.A., Sari, R., 2004. HST observations of Kuiper Belt binaries, in: AAS/Division for Planetary Sciences Meeting Abstracts #36, p. 1081.
- Margot, J.L., Nolan, M.C., Benner, L.A.M., Ostro, S.J., Jurgens, R.F., Giorgini, J.D., Slade, M.A., Campbell, D.B., 2002. Binary Asteroids in the Near-Earth Object Population. *Science* 296, 1445–1448.
- Masiero, J.R., Mainzer, A.K., Grav, T., Bauer, J.M., Cutri, R.M., Daley, J., Eisenhardt, P.R.M., McMillan, R.S., Spahr, T.B., Skrutskie, M.F., Tholen, D., Walker, R.G., Wright, E.L., DeBaun, E., Elsbury, D., Gautier, IV, T., Gomillion, S., Wilkins, A., 2011. Main Belt Asteroids with WISE/NEOWISE. I. Preliminary Albedos and Diameters. *Astrophysical Journal* 741, 68.
- Matter, A., Delbo, M., Ligi, S., Crouzet, N., Tanga, P., 2011. Determination of physical properties of the asteroid (41) Daphne from interferometric observations in the thermal infrared. *Icarus* 215, 47–56.
- McCord, T.B., Adams, J.B., Johnson, T.V., 1970. Asteroid Vesta: Spectral Reflectivity and Compositional Implications. *Science* 168, 1445–1447.
- Merline, W.J., Close, L.M., Dumas, C., Chapman, C.R., Roddier, F., Ménard, F., Slater, D.C., Duvert, G., Shelton, C., Morgan, T., 1999. Discovery of a moon orbiting the asteroid 45 Eugenia. *Nature* 401, 565–568.
- Merline, W.J., Weidenschilling, S.J., Durda, D.D., Margot, J.L., Pravec, P., Storrs, A.D., 2002. Asteroids Do Have Satellites. *Asteroids III*, 289–312.
- Michalak, G., 2000. Determination of asteroid masses — I. (1) Ceres, (2) Pallas and (4) Vesta. *Astronomy and Astrophysics* 360, 363–374.
- Michalak, G., 2001. Determination of asteroid masses. II. (6) Hebe, (10) Hygiea, (15) Eunomia, (52) Europa, (88) Thisbe, (444) Typtis, (511) Davida and (704) Interamnia. *Astronomy and Astrophysics* 374, 703–711.
- Mignard, F., Cellino, A., Muinonen, K., Tanga, P., Delbo, M., Dell’Oro, A., Granvik, M., Hestroffer, D., Mouret, S., Thuillot, W., Virtanen, J., 2007. The Gaia Mission: Expected Applications to Asteroid Science. *Earth Moon and Planets* 101, 97–125.
- Mommert, M., Harris, A.W., Kiss, C., Pál, A., Santos Sanz, P., Stansberry, J., Delsanti, A., Vilenius, E., Müller, T., Peixinho, N., Lellouch, E., Szalai, N. and Henry, F., Böhnhardt, H., Duffard, R., Fornasier, S., Hartogh, P., Mueller, M., Ortiz, J.L., Protospapa, S., Rengel, M., Thirouin, A., 2012. TNOs are Cool: A survey of the trans-Neptunian region V. Physical characterization of 18 Plutinos using Herschel PACS observations. *Astronomy and Astrophysics* in press.
- Morbidelli, A., Bottke, W.F., Nesvorný, D., Levison, H.F., 2009. Asteroids were born big. *Icarus* 204, 558–573.
- Morbidelli, A., Levison, H.F., Tsiganis, K., Gomes, R., 2005. Chaotic capture of Jupiter’s Trojan asteroids in the early Solar System. *Nature* 435, 462–465.
- Mottola, S., Lahulla, F., 2000. Mutual Eclipse Events in Asteroidal Binary System 1996 FG₃: Observations and a Numerical Model. *Icarus* 146, 556–567.
- Mouret, S., Hestroffer, D., Mignard, F., 2007. Asteroid masses and improvement with GAIA. *Astronomy and Astrophysics* 472, 1017–1027.
- Mouret, S., Simon, J.L., Mignard, F., Hestroffer, D., 2009. The list of asteroids perturbing the Mars orbit to be seen during future space missions. *Astronomy and Astrophysics* 508, 479–489.
- Mueller, M., Delbo, M., Hora, J.L., Trilling, D.E., Bhattacharya, B., Bottke, W.F., Chesley, S., Emery, J.P., Fazio, G., Harris, A.W., Mainzer, A., Mommert, M., Penprase, B., Smith, H.A., Spahr, T.B., Stansberry, J.A., Thomas, C.A., 2011. ExploreNEOs. III. Physical Characterization of 65 Potential Spacecraft Target Asteroids. *Astronomical Journal* 141, 109.
- Mueller, M., Harris, A.W., Bus, S.J., Hora, J.L., Kassis, M., Adams, J.D., 2006. The size and albedo of Rosetta fly-by target 21 Lutetia from new IRTF measurements and thermal modeling. *Astronomy and Astrophysics* 447, 1153–1158.
- Mueller, M., Marchis, F., Emery, J.P., Harris, A.W., Mottola, S., Hestroffer, D., Berthier, J., di Martino, M., 2010. Eclipsing binary Trojan asteroid Patroclus: Thermal inertia from Spitzer observations. *Icarus* 205, 505–515. [0908.4198](https://doi.org/10.1016/j.icarus.2010.09.008).
- Müller, T.G., Blommaert, J.A.D.L., 2004. 65 Cybele in the thermal infrared: Multiple observations and thermophysical analysis. *Astronomy and Astrophysics* 418, 347–356.
- Müller, T.G., Lellouch, E., Böhnhardt, H., Stansberry, J., Barucci, A., Crovisier, J., Delsanti, A., Doressoundiram, A., Dotto, E., Duffard, R., Fornasier, S., Groussin, O., Gutiérrez, P.J., Hainaut, O.R., Harris, A.W., Hartogh, P., Hestroffer, D., Horner, J., Jewitt, D.C., Kidger, M., Kiss, C., Lacerda, P., Lara, L.M., Lim, T., Mueller, M., Moreno, R., Ortiz, J.L., Rengel, M., Santos-Sanz, P., Swinyard, B., Thomas, N., Thirouin, A., Trilling, D., 2009. TNOs are Cool: A Survey of the Transneptunian Region. *Earth Moon and Planets* 105, 209–219.
- Müller, T.G., Sekiguchi, T., Kaasalainen, M., Abe, M., Hasegawa, S., 2005. Thermal infrared observations of the Hayabusa spacecraft target asteroid 25143 Itokawa. *Astronomy and Astrophysics* 443, 347–355.
- Neish, C.D., Nolan, M.C., Howell, E.S., Rivkin, A.S., 2003. Radar Observations of Binary Asteroid 5381 Sekhmet, in: American Astronomical Society Meeting Abstracts, p. 134.02.
- Nolan, M.C., Howell, E.S., Miranda, G., 2004. Radar Images of Binary Asteroid 2003 YT₁, in: AAS/Division for Planetary Sciences Meeting Abstracts #36, p. 1132.
- Noll, K.S., Stephens, D.C., Grundy, W.M., Griffin, I., 2004a. The orbit, mass, and albedo of transneptunian binary (66652) 1999 RZ₂₅₃. *Icarus* 172, 402–407.
- Noll, K.S., Stephens, D.C., Grundy, W.M., Millis, R.L., Spencer, J., Buie, M.W., Tegler, S.C., Romanishin, W., Cruikshank, D.P., 2002. Detection of Two Binary Trans-Neptunian Objects, 1997 CQ₂₉ and 2000 CF₁₀₅, with the Hubble Space Telescope. *Astronomical Journal* 124, 3424–3429.
- Noll, K.S., Stephens, D.C., Grundy, W.M., Osip, D.J., Griffin, I., 2004b. The Orbit and Albedo of Trans-Neptunian Binary (58534) 1997 CQ₂₉. *Astronomical Journal* 128, 2547–2552.
- Ockert-Bell, M.E., Clark, B.E., Shepard, M.K., Isaacs, R.A., Cloutis, E.A., Fornasier, S., Bus, S.J., 2010. The composition of M-type asteroids: Synthesis of spectroscopic and radar observations. *Icarus* 210, 674–692.
- O’Rourke, L., Müller, T.G., Valtchanov, I., Altieri, B., González-García, B., Bhattacharya, B., Jorda, L., Carry, B., Küppers, M., Groussin, O., Altwegg, K., Barucci, A., Bockelée-Morvan, D., Crovisier, J., Dotto, E., Garcia-Lario, P., Kidger, M., Llorente, A., Llorente, R., Marston, A.P., Sanchez Portal, M., Schulz, R., Sierra, M., Teyssiera, D., Vavreka, R., 2012. Thermal & Shape properties of Asteroid (21) Lutetia from Herschel Observations around the Rosetta Flyby. *Planetary and Space Science* in press.
- Osip, D.J., Kern, S.D., Elliot, J.L., 2003. Physical Characterization of the Binary Edgeworth-Kuiper Belt Object 2001 QT₂₉₇. *Earth Moon and Planets* 92, 409–421.
- Ostro, S.J., Benner, L.A.M., Magri, C., Giorgini, J.D., Rose, R., Jurgens, R.F., Yeomans, D.K., Hine, A.A., Nolan, M.C., Scheeres, D.J., Broschart, S.B., Kaasalainen, M., Margot, J., 2005. Radar observations of Itokawa in 2004 and improved shape estimation. *Meteoritics and Planetary Science* 40, 1563–1574.
- Ostro, S.J., Hudson, R.S., Nolan, M.C., Margot, J.L., Scheeres, D.J., Campbell, D.B., Magri, C., Giorgini, J.D., Yeomans, D.K., 2000. Radar Observations of Asteroid 216 Kleopatra. *Science* 288, 836–839.
- Ostro, S.J., Magri, C., Benner, L.A.M., Giorgini, J.D., Nolan, M.C., Hine, A.A., Busch, M.W., Margot, J.L., 2010. Radar imaging of Asteroid 7 Iris. *Icarus* 207, 285–294.
- Ostro, S.J., Margot, J.L., Benner, L.A.M., Giorgini, J.D., Scheeres, D.J., Fahnestock, E.G., Broschart, S.B., Bellerose, J., Nolan, M.C., Magri, C., Pravec, P., Scheirich, P., Rose, R., Jurgens, R.F., De Jong, E.M., Suzuki, S., 2006. Radar Imaging of Binary Near-Earth Asteroid (66391) 1999 KW₄. *Science* 314, 1276–1280.
- Parker, A.H., Kavelaars, J.J., Petit, J.M., Jones, L., Gladman, B., Parker, J., 2011. Characterization of Seven Ultra-wide Trans-Neptunian Binaries. *Astrophysical Journal* 743, 1.
- Pätzold, M., Andert, T., Asmar, S.W., Anderson, J.D., Barriot, J.P., Bird, M.K.,

- Husler, B., Hahn, M., Tellmann, S., Sierks, H., Lamy, P., Weiss, B.P., 2011. Asteroid 21 Lutetia: Low Mass, High Density. *Science* 334, 491.
- Petit, J.M., Durda, D.D., Greenberg, R., Hurford, T.A., Geissler, P.E., 1997. The Long-Term Dynamics of Dactyl's Orbit. *Icarus* 130, 177–197.
- Pitjeva, E.V., 2001. Progress in the determination of some astronomical constants from radiometric observations of planets and spacecraft. *Astronomy and Astrophysics* 371, 760–765.
- Pitjeva, E.V., 2004. Estimations of masses of the largest asteroids and the main asteroid belt from ranging to planets, Mars orbiters and landers, in: J.-P. Paillé (Ed.), 35th COSPAR Scientific Assembly, p. 2014.
- Pitjeva, E.V., 2005. High-Precision Ephemerides of Planets - EPM and Determination of Some Astronomical Constants. *Solar System Research* 39, 176–186.
- Pravec, P., Harris, A.W., 2007. Binary asteroid population. 1. Angular momentum content. *Icarus* 190, 250–259.
- Pravec, P., Harris, A.W., Michalowski, T., 2002. Asteroid Rotations. *Asteroids III*, 113–122.
- Pravec, P., Scheirich, P., Kušnirák, P., Šarounová, L., Mottola, S., Hahn, G., Brown, P.G., Esquerdo, G.A., Kaiser, N., Krzeminski, Z., Pray, D.P., Warner, B.D., Harris, A.W., Nolan, M.C., Howell, E.S., Benner, L.A.M., Margot, J.L., Galád, A., Holliday, W., Hicks, M.D., Krugly, Y.N., Tholen, D.J., Whiteley, R.J., Marchis, F., Degraff, D.R., Grauer, A., Larson, S., Velichko, F.P., Cooney, W.R., Stephens, R., Zhu, J., Kirsch, K., Dyvig, R., Snyder, L., Reddy, V., Moore, S., Gajdoš, Š., Világi, J., Masi, G., Higgins, D., Funkhouser, G., Knight, B., Slivan, S.M., Behrend, R., Grenon, M., Burki, G., Roy, R., Demeautis, C., Matter, D., Waelchli, N., Revaz, Y., Klotz, A., Rieugné, M., Thierry, P., Cotrez, V., Brunetto, L., Kober, G., 2006. Photometric survey of binary near-Earth asteroids. *Icarus* 181, 63–93.
- Pravec, P., Vokrouhlický, D., Polishook, D., Scheeres, D.J., Harris, A.W., Galád, A., Vaduvescu, O., Pozo, F., Barr, A., Longa, P., Vachier, F., Colas, F., Pray, D.P., Pollock, J., Reichart, D., Ivarsen, K., Haislip, J., Lacluyze, A., Kušnirák, P., Henych, T., Marchis, F., Macomber, B., Jacobson, S.A., Krugly, Y.N., Sergeev, A.V., Leroy, A., 2010. Formation of asteroid pairs by rotational fission. *Nature* 466, 1085–1088.
- Rabinowitz, D.L., Barkume, K.M., Brown, M.E., Roe, H.G., Schwartz, M., Tourtellotte, S.W., Trujillo, C.A., 2006. Photometric Observations Constraining the Size, Shape, and Albedo of 2003 EL61, a Rapidly Rotating, Pluto-sized Object in the Kuiper Belt. *Astrophysical Journal* 639, 1238–1251.
- Ragozzine, D., Brown, M.E., 2009. Orbits and Masses of the Satellites of the Dwarf Planet Haumea (2003 EL61). *Astronomical Journal* 137, 4766–4776.
- Richardson, J.E., Melosh, H.J., Lisse, C.M., Carcich, B., 2007. A ballistics analysis of the Deep Impact ejecta plume: Determining Comet Tempel 1's gravity, mass, and density. *Icarus* 190, 357–390.
- Rivkin, A.S., Howell, E.S., Britt, D.T., Lebofsky, L.A., Nolan, M.C., Branston, D.D., 1995. Three-micron spectrometric survey of M- and E-class asteroids. *Icarus* 117, 90–100.
- Rivkin, A.S., Howell, E.S., Vilas, F., Lebofsky, L.A., 2002. Hydrated Minerals on Asteroids: The Astronomical Record. *Asteroids III*, 235–253.
- Rojo, P., Margot, J.L., 2011. Mass and Density of the B-type Asteroid (702) Alauda. *Astrophysical Journal* 727, 69–74.
- Rozitis, B., Green, S.F., 2011. Directional characteristics of thermal-infrared beaming from atmosphereless planetary surfaces - a new thermophysical model. *Monthly Notices of the Royal Astronomical Society* 415, 2042–2062.
- Ryan, E.L., Woodward, C.E., 2010. Rectified Asteroid Albedos and Diameters from IRAS and MSX Photometry Catalogs. *Astronomical Journal* 140, 933–943.
- Santos Sanz, P., Lellouch, E., Fornasier, S., Kiss, C., Pál, A., Müller, T., Vilenius, E., Stansberry, J., Mommert, M., Delsanti, A., Mueller, M., Böhnhardt, H., Peixinho, N., Henry, F., Ortiz, J.L., Thirouin, A., Protopapa, S., Duffard, R., Szalai, N., Lim, T., Ejeta, C., Hartogh, P., Harris, A.W., Rengel, M., 2012. TNOs are Cool: A Survey of the Transneptunian Region IV. Size/albedo characterization of 15 scattered disk and detached objects observed with Herschel Space Observatory-PACS. *Astronomy and Astrophysics* in press.
- Scheirich, P., Pravec, P., 2009. Modeling of lightcurves of binary asteroids. *Icarus* 200, 531–547.
- Schmidt, B.E., Thomas, P.C., Bauer, J.M., Li, J., McFadden, L.A., Mutchler, M.J., Radcliffe, S.C., Rivkin, A.S., Russell, C.T., Parker, J.W., Stern, S.A., 2009. The Shape and Surface Variation of 2 Pallas from the Hubble Space Telescope. *Science* 326, 275–278.
- Shepard, M.K., Clark, B.E., Nolan, M.C., Howell, E.S., Magri, C., Giorgini, J.D., Benner, L.A.M., Ostro, S.J., Harris, A.W., Warner, B.D., Pray, D.P., Pravec, P., Fauerbach, M., Bennett, T., Klotz, A., Behrend, R., Correia, H., Coloma, J., Casulli, S., Rivkin, A.S., 2008. A radar survey of M- and X-class asteroids. *Icarus* 195, 184–205.
- Shepard, M.K., Margot, J.L., Magri, C., Nolan, M.C., Schlieder, J., Estes, B., Bus, S.J., Volquardsen, E.L., Rivkin, A.S., Benner, L.A.M., Giorgini, J.D., Ostro, S.J., Busch, M.W., 2006. Radar and infrared observations of binary near-Earth Asteroid 2002 CE26. *Icarus* 184, 198–210.
- Sheppard, S.S., Ragozzine, D., Trujillo, C., 2011. 2007 TY430: A Cold Classical Kuiper Belt Type Binary in the Plutino Population. Accepted for publication in the *Astronomical Journal*.
- Sicardy, B., Ortiz, J.L., Assafin, M., Jehin, E., Maury, A., Lellouch, E., Hutton, R.G., Braga-Ribas, F., Colas, F., Hestroffer, D., Lecacheux, J., Roques, F., Santos-Sanz, P., Widemann, T., Morales, N., Duffard, R., Thirouin, A., Castro-Tirado, A.J., Jelínek, M., Kubánek, P., Sota, A., Sánchez-Ramírez, R., Andrei, A.H., Camargo, J.I.B., da Silva Neto, D.N., Gomes, A.R., Martins, R.V., Gillon, M., Manfroid, J., Tozzi, G.P., Harlinton, C., Saravia, S., Behrend, R., Mottola, S., Melendo, E.G., Peris, V., Fabregat, J., Madioso, J.M., Cuesta, L., Eibe, M.T., Ullán, A., Organero, F., Pastor, S., de Los Reyes, J.A., Pedraz, S., Castro, A., de La Cueva, I., Muler, G., Steele, I.A., Cebrián, M., Montañés-Rodríguez, P., Oscoz, A., Weaver, D., Jacques, C., Corradi, W.J.B., Santos, F.P., Reis, W., Milone, A., Emilio, M., Gutiérrez, L., Vázquez, R., Hernández-Toledo, H., 2011. A Pluto-like radius and a high albedo for the dwarf planet Eris from an occultation. *Nature* 478, 493–496.
- Sierks, H., Lamy, P., Barbieri, C., Koschny, D., Rickman, H., Rodrigo, R., A'Hearn, M.F., Angrilli, F., Barucci, A., Bertaux, J.L., Bertini, I., Besse, S., Carry, B., Cremonese, G., Da Deppo, V., Davidsson, B., Debei, S., De Cecco, M., De Leon, J., Ferri, F., Fornasier, S., Fulle, M., Hviid, S.F., Gaskell, G.W., Groussin, O., Gutierrez, P.J., Jorda, L., Kaasalainen, M., Keller, H.U., Knollenberg, J., Kramm, J.R., Kürt, E., Küppers, M., Lara, L.M., Lazzarin, M., Leyrat, C., Lopez Moreno, J.L., Magrin, S., Marchi, S., Marzari, F., Massironi, M., Michalik, H., Moissl, R., Naletto, G., Preusker, F., Sabau, L., Sabalo, W., Scholten, F., Snodgrass, C., Thomas, N., Tubiana, C., Vernazza, P., Vincent, J.B., Wenzel, K.P., Andert, T., Pätzold, M., Weiss, B.P., 2011. Images of asteroid (21) Lutetia: A remnant planetesimal from the early Solar System. *Science* 334, 487–490.
- Sitarski, G., Todorovic-Juchniewicz, B., 1992. Determination of the mass of (1) Ceres from perturbations on (203) Pompeja and (348) May. *Acta Astronomica* 42, 139–144.
- Sitarski, G., Todorovic-Juchniewicz, B., 1995. Determination of Masses of Ceres and Vesta from Their Perturbations on Four Asteroids. *Acta Astronomica* 45, 673–677.
- Snodgrass, C., Lowry, S.C., Fitzsimmons, A., 2006. Photometry of cometary nuclei: rotation rates, colours and a comparison with Kuiper Belt Objects. *Monthly Notices of the Royal Astronomical Society* 373, 1590–1602.
- Solem, J.C., 1994. Density and size of comet Shoemaker-Levy 9 deduced from a tidal breakup model. *Nature* 370, 349–351.
- Somenzi, L., Fienga, A., Laskar, J., Kuchynka, P., 2010. Determination of asteroid masses from their close encounters with Mars. *Planetary and Space Science* 58, 858–863.
- Sosa, A., Fernández, J.A., 2009. Cometary masses derived from non-gravitational forces. *Monthly Notices of the Royal Astronomical Society* 393, 192–214.
- Spencer, J.R., Stansberry, J.A., Grundy, W.M., Noll, K.S., 2006. A Low Density for Binary Kuiper Belt Object (26308) 1998 SM165, in: AAS/Division for Planetary Sciences Meeting Abstracts #38, pp. 546–.
- Standish, E.M., 2001. Suggested GM values for Ceres, Pallas, and Vesta. Technical Report. JPL Interoffice Memorandum.
- Stansberry, J., Grundy, W., Brown, M.E., Cruikshank, D.P., Spencer, J.R., Trilling, D., Margot, J.L., 2008. Physical Properties of Kuiper Belt and Centaur Objects: Constraints from the Spitzer Space Telescope. *The Solar System Beyond Neptune*, 161–179.
- Stansberry, J.A., Grundy, W.M., Margot, J.L., Cruikshank, D.P., Emery, J.P., Rieke, G.H., Trilling, D.E., 2006. The Albedo, Size, and Density of Binary Kuiper Belt Object (47171) 1999 TC₃₆. *Astrophysical Journal* 643, 556–566.
- Strazzulla, G., Dotto, E., Binzel, R.P., Brunetto, R., Barucci, M.A., Blanco, A., Orovino, V., 2005. Spectral alteration of the Meteorite Epinal (H5) induced

- by heavy ion irradiation: a simulation of space weathering effects on near-Earth asteroids. *Icarus* 174, 31–35.
- Sunshine, J.M., Connolly, H.C., McCoy, T.J., Bus, S.J., La Croix, L.M., 2008. Ancient Asteroids Enriched in Refractory Inclusions. *Science* 320, 514–.
- Tancredi, G., Fernández, J.A., Rickman, H., Licandro, J., 2006. Nuclear magnitudes and the size distribution of Jupiter family comets. *Icarus* 182, 527–549.
- Taylor, P.A., Margot, J.L., Nolan, M.C., Benner, L.A.M., Ostro, S.J., Giorgini, J.D., Magri, C., 2008. The Shape, Mutual Orbit, and Tidal Evolution of Binary Near-Earth Asteroid 2004 DC. *LPI Contributions* 1405, 8322.
- Tedesco, E.F., Egan, M.P., Price, S.D., 2004a. MSX Infrared Minor Planet Survey. NASA Planetary Data System. MSX-A-SPIRIT3-5-SBN0003-MIMPS-V1.0.
- Tedesco, E.F., Noah, P.V., Noah, M.C., Price, S.D., 2002. The Supplemental IRAS Minor Planet Survey. *Astronomical Journal* 123, 1056–1085.
- Tedesco, E.F., Noah, P.V., Noah, M.C., Price, S.D., 2004b. IRAS Minor Planet Survey. NASA Planetary Data System. IRAS-A-FPA-3-RDR-IMPS-V6.0.
- Tholen, D.J., Barucci, M.A., 1989. Asteroid taxonomy. *Asteroids II*, 298–315.
- Thomas, P.C., Binzel, R.P., Gaffey, M.J., Zellner, B.H., Storrs, A.D., Wells, E.N., 1997. Vesta: Spin Pole, Size, and Shape from HST Images. *Icarus* 128, 88–94.
- Thomas, P.C., Parker, J.W., McFadden, L.A., Russell, C.T., Stern, S.A., Sykes, M.V., Young, E.F., 2005. Differentiation of the asteroid Ceres as revealed by its shape. *Nature* 437, 224–226.
- Tsiganis, K., Gomes, R., Morbidelli, A., Levison, H.F., 2005. Origin of the orbital architecture of the giant planets of the Solar System. *Nature* 435, 459–461.
- Usui, F., Kuroda, D., Müller, T.G., Hasegawa, S., Ishiguro, M., Ootsubo, T., Ishihara, D., Kataza, H., Takita, S., Oyabu, S., Ueno, M., Matsuhara, H., Onaka, T., 2011. Asteroid Catalog Using Akari: AKARI/IRC Mid-Infrared Asteroid Survey. *Publications of the Astronomical Society of Japan* 63, 1117–1138.
- Vasiliev, M.V., Yagudina, E.I., 1999. Determination of masses for 26 selected minor planets from analysis of observations their mutual encounters with asteroids of lesser mass, in: *Communications of IAA of RAS*.
- Vernazza, P., Binzel, R.P., Rossi, A., Fulchignoni, M., Birlan, M., 2009a. Solar wind as the origin of rapid reddening of asteroid surfaces. *Nature* 458, 993–995.
- Vernazza, P., Binzel, R.P., Thomas, C.A., DeMeo, F.E., Bus, S.J., Rivkin, A.S., Tokunaga, A.T., 2008. Compositional differences between meteorites and near-Earth asteroids. *Nature* 454, 858–860.
- Vernazza, P., Brunetto, R., Binzel, R.P., Perron, C., Fulvio, D., Strazzulla, G., Fulchignoni, M., 2009b. Plausible parent bodies for enstatite chondrites and mesosiderites: Implications for Lutetia's fly-by. *Icarus* 202, 477–486.
- Vernazza, P., Brunetto, R., Strazzulla, G., Fulchignoni, M., Rochette, P., Meyer-Vernet, N., Zouganelis, I., 2006. Asteroid colors: a novel tool for magnetic field detection? The case of Vesta. *Astronomy and Astrophysics* 451, 43–46.
- Vernazza, P., Carry, B., Emery, J.P., Hora, J.L., Cruikshank, D.P., Binzel, R.P., Jackson, J., Helbert, J., Maturilli, A., 2010. Mid-infrared spectral variability for compositionally similar asteroids: Implications for asteroid particle size distributions. *Icarus* 207, 800–809.
- Vernazza, P., King, P.L., Izawa, M.R.M., Maturilli, A., Helbert, J., Cruikshank, D., Brunetto, R., Marchis, F., Binzel, R.P., Flemming, R.L., 2011a. Opening the Mid-IR Window on Asteroid Physical Properties. *Lunar and Planetary Institute Science Conference Abstracts* 42, 1344.
- Vernazza, P., Lamy, P., Groussin, O., Hiroi, T., Jorda, L., King, P.L., Izawa, M.R.M., Marchis, F., Birlan, M., Brunetto, R., 2011b. Asteroid (21) Lutetia as a remnant of Earth's precursor planetesimals. *Icarus* 216, 650–659.
- Veverka, J., Robinson, M., Thomas, P., Murchie, S., Bell, J.F., Izenberg, N., Chapman, C., Harch, A., Bell, M., Carcich, B., Cheng, A., Clark, B., Domingue, D., Dunham, D., Farquhar, R., Gaffey, M.J., Hawkins, E., Joseph, J., Kirk, R., Li, H., Lucey, P., Malin, M., Martin, P., McFadden, L., Merline, W.J., Miller, J.K., Owen, W.M., Peterson, C., Prockter, L., Warren, J., Wellnitz, D., Williams, B.G., Yeomans, D.K., 2000. NEAR at Eros: Imaging and Spectral Results. *Science* 289, 2088–2097.
- Viateau, B., 2000. Mass and density of asteroids (16) Psyche and (121) Hermione. *Astronomy and Astrophysics* 354, 725–731.
- Viateau, B., Rapaport, M., 1995. The orbit of (2) Pallas. *Astronomy and Astrophysics* 111, 305–+.
- Viateau, B., Rapaport, M., 1997a. Improvement of the Orbits of Asteroids and the Mass of (1) Ceres, in: R. M. Bonnet, E. Høg, P. L. Bernacca, L. Emiliani, A. Blaauw, C. Turon, J. Kovalevsky, L. Lindegren, H. Hassan, M. Bouffard, B. Strim, D. Heger, M. A. C. Perryman, & L. Woltjer (Ed.), *Hipparcos - Venice '97*, pp. 91–94.
- Viateau, B., Rapaport, M., 1997b. The Bordeaux meridian observations of asteroids. First determination of the mass of (11) Parthenope. *Astronomy* 320, 652–658.
- Viateau, B., Rapaport, M., 1998. The mass of (1) Ceres from its gravitational perturbations on the orbits of 9 asteroids. *Astronomy and Astrophysics* 334, 729–735.
- Viateau, B., Rapaport, M., 2001. Mass and density of asteroids (4) Vesta and (11) Parthenope. *Astronomy and Astrophysics* 370, 602–609.
- Vitagliano, A., Stoss, R.M., 2006. New mass determination of (15) Eunomia based on a very close encounter with (50278) 2000CZ12. *Astronomy and Astrophysics* 455, L29–L31.
- Walsh, K.J., Delbo, M., Mueller, M., Binzel, R.P., DeMeo, F., 2012. Physical characterization and origin of binary near-earth asteroid (175706) 1996 FG3. *Astrophysical Journal* 186, 498.
- Walsh, K.J., Morbidelli, A., Raymond, S.N., O'Brien, D.P., Mandell, A.M., 2011. A low mass for Mars from Jupiter's early gas-driven migration. *Nature* 475, 206–209.
- Walsh, K.J., Richardson, D.C., Michel, P., 2008. Rotational breakup as the origin of small binary asteroids. *Nature* 454, 188–191.
- Weisberg, M.K., McCoy, T.J., Krot, A.N., 2006. Systematics and Evaluation of Meteorite Classification. *Meteorites and the Early Solar System II*, 19–52.
- Weissman, P.R., Asphaug, E., Lowry, S.C., 2004. Structure and density of cometary nuclei. *Comets II*, 337–357.
- Williams, G.V., 1992. The mass of (1) Ceres from perturbations on (348) May, in: *Asteroids, Comets, Meteors 1991*, pp. 641–643.
- Wolters, S.D., Green, S.F., McBride, N., Davies, J.K., 2008. Thermal infrared and optical observations of four near-Earth asteroids. *Icarus* 193, 535–552.
- Wolters, S.D., Rozitis, B., Duddy, S.R., Lowry, S.C., Green, S.F., Snodgrass, C., Hainaut, O.R., Weissman, P., 2011. Physical characterization of low delta-V asteroid (175706) 1996 FG3. *Monthly Notices of the Royal Astronomical Society* 418, 1246–1257.
- Yeomans, D.K., Antreasian, P.G., Barriot, J.P., Chesley, S.R., Dunham, D.W., Farquhar, R.W., Giorgini, J.D., Helfrich, C.E., Konopliv, A.S., McAdams, J.V., Miller, J.K., Owen, W.M., Scheeres, D.J., Thomas, P.C., Veverka, J., Williams, B.G., 2000. Radio Science Results During the NEAR-Shoemaker Spacecraft Rendezvous with Eros. *Science* 289, 2085–2088.
- Yeomans, D.K., Barriot, J.P., Dunham, D.W., Farquhar, R.W., Giorgini, J.D., Helfrich, C.E., Konopliv, A.S., McAdams, J.V., Miller, J.K., Owen, Jr., W.M., Scheeres, D.J., Synnott, S.P., Williams, B.G., 1997. Estimating the Mass of Asteroid 253 Mathilde from Tracking Data During the NEAR Flyby. *Science* 278, 2106.
- Yurimoto, H., Abe, K.i., Abe, M., Ebihara, M., Fujimura, A., Hashiguchi, M., Hashizume, K., Ireland, T.R., Itoh, S., Katayama, J., Kato, C., Kawaguchi, J., Kawasaki, N., Kitajima, F., Kobayashi, S., Meike, T., Mukai, T., Nagao, K., Nakamura, T., Naraoka, H., Noguchi, T., Okazaki, R., Park, C., Sakamoto, N., Seto, Y., Takei, M., Tsuchiyama, A., Uesugi, M., Wakaki, S., Yada, T., Yamamoto, K., Yoshikawa, M., Zolensky, M.E., 2011. Oxygen Isotopic Compositions of Asteroidal Materials Returned from Itokawa by the Hayabusa Mission. *Science* 333, 1116–1118.
- Zielenbach, W., 2010. The Mass of (15) Eunomia from 923 Test Bodies. *Astronomical Journal* 139, 816–824.
- Zielenbach, W., 2011. Mass Determination Studies of 104 Large Asteroids. *Astronomical Journal* 142, 120–128.

Table 1: Compilation of the average mass (M) and volume-equivalent diameter (ϕ) estimates (see Appendix A, Appendix B, and Appendix C), and resulting bulk density (ρ) and macroporosity (\mathcal{P}) for 287 objects, with their associated uncertainties. For each object, the dynamical class is listed (Dyn.), together with the taxonomic class (Tax., for asteroids only) and associated meteorite (Met.). The density estimates are ranked A to E, owing to the level of confidence at which they are determined (see text). Unrealistic density estimates are marked with a cross (\times) and uncertainties on the macroporosity larger than 100% are listed as ∞ .
References: (1) Clark et al. (2010), (2) Ockert-Bell et al. (2010), and (3) Fornasier et al. (2011).

Designation		Classification			Masses (kg)			Diameter (km)			Density		Porosity		Rank
#	Name	Dyn.	Tax.	Met.	M	δM	Fig.	ϕ	$\delta\phi$	Fig.	ρ	$\delta\rho$	\mathcal{P}	$\delta\mathcal{P}$	
1	Ceres	MBA	C	CM	$9.44 \pm 0.06 \times 10^{20}$		A.1	944.79 ± 22.99		B.1	2.13 ± 0.15		4 ± 7		A
2	Pallas	MBA	B	CK ¹	$2.04 \pm 0.04 \times 10^{20}$		A.2	514.41 ± 19.12		B.2	2.86 ± 0.32		0 ± 11		A
3	Juno	MBA	Sq	OC	$2.73 \pm 0.29 \times 10^{19}$		A.3	241.79 ± 10.58		B.3	3.68 ± 0.62		0 ± 16		A
4	Vesta	MBA	V	HED	$2.63 \pm 0.05 \times 10^{20}$		A.4	519.33 ± 6.84		B.4	3.58 ± 0.15		0 ± 4		A
5	Astraea	MBA	S	OC	$2.64 \pm 0.44 \times 10^{18}$		A.5	113.41 ± 3.53		B.5	3.45 ± 0.66		0 ± 19		B
6	Hebe	MBA	S	OC	$1.39 \pm 0.10 \times 10^{19}$		A.6	190.92 ± 7.15		B.6	3.81 ± 0.50		0 ± 13		A
7	Iris	MBA	S	OC	$1.29 \pm 0.21 \times 10^{19}$		A.7	225.89 ± 25.94		B.7	2.14 ± 0.81		35 ± 38		C
8	Flora	MBA	S	OC	$9.17 \pm 1.75 \times 10^{18}$		A.8	139.12 ± 2.26		B.8	6.50 ± 1.28		0 ± 19		\times
9	Metis	MBA	S	OC	$8.39 \pm 1.67 \times 10^{18}$		A.9	164.46 ± 7.67		B.9	3.60 ± 0.87		0 ± 24		C
10	Hygiea	MBA	C	CM	$8.63 \pm 0.52 \times 10^{19}$		A.10	421.60 ± 25.69		B.10	2.19 ± 0.42		2 ± 19		A
11	Parthenope	MBA	Sq	OC	$5.91 \pm 0.45 \times 10^{18}$		A.11	151.07 ± 5.11		B.11	3.27 ± 0.41		1 ± 12		A
12	Victoria	MBA	L	CO	$2.45 \pm 0.46 \times 10^{18}$		A.12	124.09 ± 8.31		B.12	2.45 ± 0.67		19 ± 27		C
13	Egeria	MBA	Ch	CM	$8.82 \pm 4.25 \times 10^{18}$		A.13	214.73 ± 11.53		B.13	1.70 ± 0.86		24 ± 50		D
14	Irene	MBA	S	OC	$2.91 \pm 1.88 \times 10^{18}$		A.14	147.75 ± 5.03		B.14	1.72 ± 1.12		48 ± 65		D
15	Eunomia	MBA	K	CV	$3.14 \pm 0.18 \times 10^{19}$		A.15	256.63 ± 1.04		B.15	3.54 ± 0.20		0 ± 5		B
16	Psyche	MBA	Xk	Ata ²	$2.72 \pm 0.75 \times 10^{19}$		A.16	248.45 ± 17.13		B.16	3.38 ± 1.16		15 ± 34		C
17	Thetis	MBA	S	OC	$1.33 \pm 0.12 \times 10^{18}$		A.17	82.76 ± 8.79		B.17	4.48 ± 1.48		0 ± 33		C
18	Melpomene	MBA	S	OC	$3.22 \pm 1.28 \times 10^{18}$		A.18	141.72 ± 4.86		B.18	2.15 ± 0.88		35 ± 41		C
19	Fortuna	MBA	Ch	CM	$8.60 \pm 1.46 \times 10^{18}$		A.19	206.90 ± 6.49		B.19	1.85 ± 0.35		17 ± 19		A
20	Massalia	MBA	S	OC	$5.00 \pm 1.04 \times 10^{18}$		A.20	136.99 ± 8.82		B.20	3.71 ± 1.05		0 ± 28		C
21	Lutetia	MBA	Xk	EH ²	$1.70 \pm 0.01 \times 10^{18}$		A.21	98.00 ± 5.00		B.21	3.44 ± 0.52		0 ± 15		A
22	Kalliope	MBA	X	Ata ²	$7.96 \pm 0.31 \times 10^{18}$		A.22	170.23 ± 10.46		B.22	3.08 ± 0.58		23 ± 18		B
23	Thalia	MBA	S	OC	$1.96 \pm 0.09 \times 10^{18}$		A.23	106.81 ± 3.23		B.23	3.07 ± 0.31		7 ± 10		B
24	Themis	MBA	C	CM ¹	$5.89 \pm 1.91 \times 10^{18}$		A.24	183.84 ± 11.40		B.24	1.81 ± 0.67		19 ± 37		C
25	Phocaea	MBA	S	OC	$5.99 \pm 0.60 \times 10^{17}$		A.25	80.19 ± 4.66		B.25	2.21 ± 0.44		33 ± 20		C
26	Proserpina	MBA	S	OC	$7.48 \pm 8.95 \times 10^{17}$			89.63 ± 3.55		B.26	1.98 ± 2.38		$40 \pm \infty$		E
27	Euterpe	MBA	S	OC	$1.67 \pm 1.01 \times 10^{18}$		A.26	105.80 ± 7.23		B.27	2.69 ± 1.71		19 ± 63		D
28	Bellona	MBA	S	OC	$2.62 \pm 0.15 \times 10^{18}$		A.27	108.10 ± 11.49		B.28	3.95 ± 1.28		0 ± 32		C
29	Amphitrite	MBA	S	OC	$1.29 \pm 0.20 \times 10^{19}$		A.28	217.59 ± 10.71		B.29	2.38 ± 0.51		28 ± 21		C
30	Urania	MBA	S	OC	$1.74 \pm 0.49 \times 10^{18}$		A.29	94.48 ± 5.37		B.30	3.92 ± 1.29		0 ± 32		C
31	Euphrosyne	MBA	C	CM	$1.27 \pm 0.65 \times 10^{19}$		A.30	272.92 ± 8.85		B.31	1.18 ± 0.61		47 ± 52		D
33	Polyhymnia	MBA	S	OC	$6.20 \pm 0.74 \times 10^{18}$			53.98 ± 0.91			75.28 ± 9.71		0 ± 12		\times
34	Circe	MBA	Ch	CM	$3.66 \pm 0.03 \times 10^{18}$		A.31	113.02 ± 4.90		B.32	4.83 ± 0.63		0 ± 13		\times
36	Atalante	MBA	C	CM	$4.32 \pm 3.80 \times 10^{18}$			110.14 ± 4.38		B.33	6.17 ± 5.48		0 ± 88		E
38	Leda	MBA	Cgh	CM	$5.71 \pm 5.47 \times 10^{18}$			115.41 ± 1.33		B.34	7.09 ± 6.79		0 ± 95		E
39	Laetitia	MBA	S	OC	$4.72 \pm 1.14 \times 10^{18}$		A.32	153.80 ± 4.14		B.35	2.47 ± 0.63		25 ± 25		C
41	Daphne	MBA	Ch	CM	$6.31 \pm 0.11 \times 10^{18}$		A.33	181.05 ± 9.60		B.36	2.03 ± 0.32		9 ± 16		B
42	Isis	MBA	S	OC	$1.58 \pm 0.52 \times 10^{18}$		A.34	102.73 ± 2.73		B.37	2.78 ± 0.93		16 ± 33		C
43	Ariadne	MBA	Sq	OC	$1.21 \pm 0.22 \times 10^{18}$		A.35	63.61 ± 4.66		B.38	8.99 ± 2.57		0 ± 28		\times
45	Eugenia	MBA	C	CM	$5.79 \pm 0.14 \times 10^{18}$		A.36	201.81 ± 14.77		B.39	1.34 ± 0.29		40 ± 22		C
46	Hestia	MBA	Xc	Mes	$5.99 \pm 0.49 \times 10^{18}$		A.37	125.29 ± 5.21		B.40	5.81 ± 0.87		0 ± 14		E
47	Aglaja	MBA	B	CV	$3.25 \pm 1.68 \times 10^{18}$		A.38	141.90 ± 8.72		B.41	2.17 ± 1.19		22 ± 55		D
48	Doris	MBA	Ch	CM	$6.12 \pm 2.96 \times 10^{18}$		A.39	211.67 ± 10.85		B.42	1.23 ± 0.62		45 ± 50		D
49	Pales	MBA	Ch	CM	$4.22 \pm 2.15 \times 10^{18}$		A.40	150.82 ± 3.81		B.43	2.35 ± 1.21		0 ± 51		D
50	Virginia	MBA	Ch	CM ³	$2.31 \pm 0.70 \times 10^{18}$		A.41	99.42 ± 0.46		B.44	4.49 ± 1.35		0 ± 30		E
51	Nemausa	MBA	Ch	CM	$2.48 \pm 0.86 \times 10^{18}$		A.42	148.85 ± 3.56		B.45	1.43 ± 0.50		36 ± 35		C
52	Europa	MBA	C	CM	$2.38 \pm 0.58 \times 10^{19}$		A.43	310.21 ± 10.34		B.46	1.52 ± 0.39		32 ± 26		C
53	Kalypso	MBA	C	CM	$5.63 \pm 5.00 \times 10^{18}$			109.06 ± 7.27		B.47	8.28 ± 7.54		0 ± 91		\times
54	Alexandra	MBA	Cgh	CM	$6.16 \pm 3.50 \times 10^{18}$		A.44	149.68 ± 9.85		B.48	3.50 ± 2.11		0 ± 60		D
56	Melete	MBA	Xk	Mes	$4.61 \pm 0.00 \times 10^{18}$		A.45	113.63 ± 8.27		B.49	6.00 ± 1.31		0 ± 21		C
57	Mnemosyne	MBA	S	OC	$1.26 \pm 0.24 \times 10^{19}$		A.46	113.01 ± 4.46		B.50	16.62 ± 3.73		0 ± 22		\times

Table 1: Continued

Designation #	Name	Class			Masses (kg)			Diameter (km)			Density		Porosity		Rank
		Dyn.	Tax.	Met.	M	δM	Fig.	ϕ	$\delta\phi$	Fig.	ρ	$\delta\rho$	\mathcal{P}	$\delta\mathcal{P}$	
59	Elpis	MBA	B	CV	$3.00 \pm 0.50 \times 10^{18}$		A.47	163.61 ± 6.50		B.51	1.30 ± 0.26		53 ± 20	C	
60	Echo	MBA	S	OC	$3.15 \pm 0.32 \times 10^{17}$		A.48	60.00 ± 1.33		B.52	2.78 ± 0.33		16 ± 12	B	
61	Danae	MBA	S	OC	$2.89 \pm 2.78 \times 10^{18}$			82.52 ± 2.73		B.53	9.81 ± 9.49		0 ± 96	D	
63	Ausonia	MBA	S	OC	$1.53 \pm 0.15 \times 10^{18}$		A.49	94.45 ± 7.15		B.54	3.46 ± 0.86		0 ± 24	C	
65	Cybele	MBA	Xk	Mes	$1.36 \pm 0.31 \times 10^{19}$		A.50	248.29 ± 17.59		B.55	1.70 ± 0.52		59 ± 30	C	
67	Asia	MBA	S	OC	$1.03 \pm 0.10 \times 10^{18}$			60.99 ± 2.41		B.56	8.66 ± 1.32		0 ± 15	X	
68	Leto	MBA	S	OC	$3.28 \pm 1.90 \times 10^{18}$		A.51	124.96 ± 6.42		B.57	3.21 ± 1.92		3 ± 60	D	
69	Hesperia	MBA	Xk	Mes	$5.86 \pm 1.18 \times 10^{18}$		A.52	136.69 ± 4.71		B.58	4.38 ± 0.99		0 ± 22	C	
70	Panopaea	MBA	Cgh	CM	$4.33 \pm 1.09 \times 10^{18}$			133.43 ± 7.58		B.59	3.48 ± 1.05		0 ± 30	C	
72	Feronia	MBA	D	CM	$3.32 \pm 8.49 \times 10^{18}$			83.95 ± 4.02		B.60	10.71 ± 27.44		$0 \pm \infty$	X	
74	Galatea	MBA	C	CM	$6.13 \pm 5.36 \times 10^{18}$			120.67 ± 7.15		B.61	6.66 ± 5.94		0 ± 89	D	
76	Freia	MBA	C	CM	$1.97 \pm 4.20 \times 10^{18}$		A.53	167.87 ± 8.73		B.62	0.79 ± 1.69		$64 \pm \infty$	E	
77	Frigga	MBA	Xe	EH ²	$1.74 \pm 0.68 \times 10^{18}$			66.97 ± 1.28		B.63	11.05 ± 4.34		0 ± 39	X	
78	Diana	MBA	Ch	CM	$1.27 \pm 0.13 \times 10^{18}$		A.54	123.63 ± 4.57		B.64	1.28 ± 0.19		42 ± 14	B	
81	Terpsichore	MBA	Cb	CM	$6.19 \pm 5.31 \times 10^{18}$			121.77 ± 2.34		B.65	6.54 ± 5.62		0 ± 85	D	
84	Klio	MBA	Ch	CM	$5.47 \pm 4.06 \times 10^{17}$			79.40 ± 1.95		B.66	2.08 ± 1.55		7 ± 74	D	
85	Io	MBA	Cb	CM	$2.57 \pm 1.48 \times 10^{18}$		A.55	155.00 ± 6.00		B.67	1.31 ± 0.77		41 ± 58	D	
87	Sylvia	MBA	X	CV	$1.48 \pm 0.00 \times 10^{19}$		A.56	278.14 ± 10.75		B.68	1.31 ± 0.15		52 ± 11	B	
88	Thisbe	MBA	B	CV	$1.53 \pm 0.31 \times 10^{19}$		A.57	204.04 ± 9.12		B.69	3.44 ± 0.84		0 ± 24	C	
89	Julia	MBA	X	CV	$6.71 \pm 1.82 \times 10^{18}$		A.58	147.57 ± 8.32		B.70	3.98 ± 1.27		0 ± 31	C	
90	Antiope	MBA	C	CM	$8.30 \pm 0.20 \times 10^{17}$		A.59	122.15 ± 2.77		B.71	0.86 ± 0.06		61 ± 7	B	
92	Undina	MBA	Xk	Mes	$4.43 \pm 0.25 \times 10^{18}$		A.60	124.44 ± 3.25		B.72	4.39 ± 0.42		0 ± 9	B	
93	Minerva	MBA	C	CM	$3.50 \pm 0.40 \times 10^{18}$			149.79 ± 8.08		B.73	1.98 ± 0.39		11 ± 19	B	
94	Aurora	MBA	C	CM	$6.23 \pm 3.64 \times 10^{18}$		A.61	186.35 ± 8.84		B.74	1.83 ± 1.10		18 ± 60	D	
96	Aegle	MBA	T	Ata	$6.48 \pm 6.26 \times 10^{18}$		A.62	167.92 ± 5.49		B.75	2.61 ± 2.53		34 ± 97	D	
97	Klotho	MBA	Xc	Ata ²	$1.33 \pm 0.13 \times 10^{18}$			84.79 ± 3.13		B.76	4.16 ± 0.62		0 ± 14	B	
98	Ianthe	MBA	Ch	CM	$8.93 \pm 1.99 \times 10^{17}$		A.63	106.16 ± 3.76		B.77	1.42 ± 0.35		36 ± 24	C	
105	Artemis	MBA	Ch	CM	$1.53 \pm 0.54 \times 10^{18}$		A.64	119.10 ± 6.78		B.78	1.73 ± 0.67		23 ± 38	C	
106	Dione	MBA	Cgh	CM	$3.06 \pm 1.54 \times 10^{18}$		A.65	147.17 ± 3.34		B.79	1.83 ± 0.92		18 ± 50	D	
107	Camilla	MBA	X	CV	$1.12 \pm 0.03 \times 10^{19}$		A.66	210.68 ± 8.89		B.80	2.28 ± 0.29		18 ± 12	B	
111	Ate	MBA	Ch	CM	$1.76 \pm 0.44 \times 10^{18}$		A.67	142.85 ± 5.94		B.81	1.15 ± 0.32		48 ± 27	C	
112	Iphigenia	MBA	Ch	CM	$1.97 \pm 6.78 \times 10^{18}$			71.07 ± 0.52		B.82	10.48 ± 36.06		$0 \pm \infty$	X	
117	Lomia	MBA	X	CV	$6.08 \pm 0.63 \times 10^{18}$		A.68	146.78 ± 3.96		B.83	3.67 ± 0.48		0 ± 13	B	
121	Hermione	MBA	Ch	CM	$4.97 \pm 0.33 \times 10^{18}$		A.69	195.36 ± 10.62		B.84	1.27 ± 0.22		43 ± 17	B	
126	Velleda	MBA	S	OC	$0.47 \pm 5.79 \times 10^{18}$			44.79 ± 1.33		B.85	10.00 ± 123.00		$0 \pm \infty$	X	
127	Johanna	MBA	Ch	CM	$3.08 \pm 1.35 \times 10^{18}$		A.70	116.14 ± 3.93		B.86	3.75 ± 1.68		0 ± 44	C	
128	Nemesis	MBA	C	CM	$5.97 \pm 2.56 \times 10^{18}$		A.71	184.19 ± 5.19		B.87	1.82 ± 0.79		18 ± 43	C	
129	Antigone	MBA	X	Ste ²	$2.65 \pm 0.89 \times 10^{18}$		A.72	119.44 ± 3.91		B.88	2.96 ± 1.04		29 ± 35	C	
130	Elektra	MBA	Ch	CM	$6.60 \pm 0.40 \times 10^{18}$		A.73	189.62 ± 6.81		B.89	1.84 ± 0.22		17 ± 12	B	
132	Aethra	MBA	Xe	EH	$0.41 \pm 2.71 \times 10^{18}$			35.83 ± 6.59		B.90	17.09 ± 112.83		$0 \pm \infty$	X	
135	Hertha	MBA	Xk	Ata ²	$1.21 \pm 0.16 \times 10^{18}$		A.74	76.12 ± 3.29		B.91	5.23 ± 0.96		0 ± 18	B	
137	Meliboea	MBA	C	CM	$7.27 \pm 3.07 \times 10^{18}$		A.75	145.92 ± 3.58		B.92	4.46 ± 1.91		0 ± 42	E	
138	Tolosa	MBA	S	OC	$4.93 \pm 2.59 \times 10^{17}$			51.86 ± 3.07		B.93	6.74 ± 3.74		0 ± 55	E	
139	Juewa	MBA	X	CV	$5.54 \pm 2.20 \times 10^{18}$		A.76	161.43 ± 7.38		B.94	2.51 ± 1.05		9 ± 41	C	
141	Lumen	MBA	Ch	CM	$8.25 \pm 5.77 \times 10^{18}$			131.35 ± 5.21		B.95	6.95 ± 4.93		0 ± 70	X	
144	Vibilia	MBA	Ch	CM	$5.30 \pm 1.20 \times 10^{18}$		A.77	141.34 ± 2.76		B.96	3.58 ± 0.84		0 ± 23	C	
145	Adeona	MBA	Ch	CM	$2.08 \pm 0.57 \times 10^{18}$		A.78	149.50 ± 5.45		B.97	1.18 ± 0.34		47 ± 29	C	
147	Protogeneia	MBA	C	CM	$1.23 \pm 0.05 \times 10^{19}$			118.44 ± 10.45		B.98	14.13 ± 3.78		0 ± 26	X	
148	Gallia	MBA	S	OC	$4.89 \pm 1.67 \times 10^{18}$			83.45 ± 5.07		B.99	16.06 ± 6.22		0 ± 38	X	
150	Nuwa	MBA	C	CM	$1.62 \pm 0.20 \times 10^{18}$		A.79	146.54 ± 9.15		B.100	0.98 ± 0.22		56 ± 22	C	
152	Atala	MBA	S	OC	$5.43 \pm 1.24 \times 10^{18}$			60.03 ± 3.01		B.101	47.92 ± 13.10		0 ± 27	X	
154	Bertha	MBA	Cb	CM	$9.19 \pm 5.20 \times 10^{18}$		A.80	186.85 ± 1.83		B.102	2.69 ± 1.52		0 ± 56	D	
156	Xanthippe	MBA	Ch	CM	$6.49 \pm 3.71 \times 10^{18}$			116.34 ± 4.14		B.103	7.86 ± 4.57		0 ± 58	X	
163	Erigone	MBA	Ch	CM	$2.01 \pm 0.68 \times 10^{18}$			72.70 ± 1.95		B.104	9.99 ± 3.45		0 ± 34	X	

Table 1: Continued

Designation #	Name	Class			Masses (kg)			Diameter (km)			Density		Porosity		Rank
		Dyn.	Tax.	Met.	M	δM	Fig.	ϕ	$\delta\phi$	Fig.	ρ	$\delta\rho$	\mathcal{P}	$\delta\mathcal{P}$	
164	Eva	MBA	X	CV	$9.29 \pm 7.76 \times 10^{17}$			101.77	\pm 3.61	B.105	1.68	\pm 1.41	39	\pm 84	D
165	Loreley	MBA	C	CM	$1.91 \pm 0.19 \times 10^{19}$	A.81		164.92	\pm 8.14	B.106	8.14	\pm 1.46	0	\pm 17	X
168	Sibylla	MBA	Ch	CM	$3.92 \pm 1.80 \times 10^{18}$	A.82		149.06	\pm 4.29	B.107	2.26	\pm 1.05	0	\pm 46	C
173	Ino	MBA	X	CV	$4.79 \pm 3.11 \times 10^{18}$	A.83		160.07	\pm 6.04	B.108	2.23	\pm 1.47	20	\pm 65	D
179	Klytaemnestra	MBA	S	OC	$2.49 \pm 1.19 \times 10^{17}$			75.02	\pm 3.21	B.109	1.12	\pm 0.55	66	\pm 49	C
185	Eunike	MBA	C	CM	$3.56 \pm 2.61 \times 10^{18}$	A.84		160.61	\pm 5.00	B.110	1.64	\pm 1.21	27	\pm 74	D
187	Lamberta	MBA	Ch	CM	$1.80 \pm 0.85 \times 10^{18}$	A.85		131.31	\pm 1.08	B.111	1.51	\pm 0.71	32	\pm 47	C
189	Phthia	MBA	Sa	OC	$3.84 \pm 0.81 \times 10^{16}$			40.91	\pm 1.36	B.112	1.07	\pm 0.25	67	\pm 23	C
192	Nausikaa	MBA	S	OC	$1.79 \pm 0.42 \times 10^{18}$	A.86		90.18	\pm 2.80	B.113	4.64	\pm 1.17	0	\pm 25	C
194	Prokne	MBA	Ch	CM	$2.68 \pm 0.29 \times 10^{18}$	A.87		170.33	\pm 6.92	B.114	1.03	\pm 0.16	53	\pm 16	B
196	Philomela	MBA	S	OC	$4.00 \pm 1.53 \times 10^{18}$	A.88		145.29	\pm 7.71	B.115	2.48	\pm 1.02	25	\pm 41	C
200	Dynamene	MBA	Ch	CM	$1.07 \pm 0.16 \times 10^{19}$			130.71	\pm 3.01	B.116	9.14	\pm 1.51	0	\pm 16	X
204	Kallisto	MBA	S	OC	$0.60 \pm 1.81 \times 10^{18}$			50.36	\pm 1.69	B.117	8.98	\pm 27.07	0	\pm ∞	X
209	Dido	MBA	Xc	Mes	$4.59 \pm 7.42 \times 10^{18}$			140.35	\pm 10.12	B.118	3.17	\pm 5.17	25	\pm ∞	E
210	Isabella	MBA	Cb	CM	$3.41 \pm 1.09 \times 10^{18}$			73.70	\pm 8.47	B.119	16.26	\pm 7.65	0	\pm 47	X
211	Isolda	MBA	Ch	CM	$4.49 \pm 2.43 \times 10^{18}$	A.89		149.81	\pm 6.10	B.120	2.54	\pm 1.41	0	\pm 55	D
212	Medea	MBA	D	CM	$1.32 \pm 0.10 \times 10^{19}$			144.13	\pm 7.23	B.121	8.41	\pm 1.43	0	\pm 17	X
216	Kleopatra	MBA	Xe	Ata ²	$4.64 \pm 0.20 \times 10^{18}$	A.90		127.47	\pm 8.44	B.122	4.27	\pm 0.86	0	\pm 20	C
217	Eudora	MBA	X	CV	$1.52 \pm 0.06 \times 10^{18}$			68.62	\pm 1.41	B.123	8.98	\pm 0.65	0	\pm 7	X
221	Eos	MBA	K	CV	$5.87 \pm 0.34 \times 10^{18}$			103.52	\pm 5.60	B.124	10.10	\pm 1.74	0	\pm 17	X
230	Athamantis	MBA	S	OC	$1.89 \pm 0.19 \times 10^{18}$			110.17	\pm 4.57	B.125	2.69	\pm 0.43	19	\pm 15	B
234	Barbara	MBA	L	CO	$0.44 \pm 1.45 \times 10^{18}$			45.62	\pm 1.93	B.126	8.84	\pm 29.17	0	\pm ∞	X
238	Hypatia	MBA	Ch	CM	$4.90 \pm 1.70 \times 10^{18}$	A.91		146.13	\pm 2.66	B.127	2.99	\pm 1.05	0	\pm 35	C
240	Vanadis	MBA	C	CM	$1.10 \pm 0.92 \times 10^{18}$	A.92		94.03	\pm 5.37	B.128	2.53	\pm 2.15	0	\pm 84	D
241	Germania	MBA	Cb	CM	$0.86 \pm 5.00 \times 10^{18}$			178.60	\pm 7.84	B.129	0.28	\pm 1.67	87	\pm ∞	X
243	Ida	MBA	S	OC	$3.78 \pm 0.20 \times 10^{16}$			31.29	\pm 1.20	B.130	2.35	\pm 0.29	29	\pm 12	A
253	Mathilde	MBA	Cb	CM	$1.03 \pm 0.04 \times 10^{17}$	A.93		53.00	\pm 2.59	B.131	1.32	\pm 0.20	41	\pm 15	A
259	Aletheia	MBA	X	CV	$7.79 \pm 0.43 \times 10^{18}$	A.94		190.05	\pm 6.82	B.132	2.16	\pm 0.26	22	\pm 12	B
266	Aline	MBA	Ch	CM	$4.15 \pm 0.42 \times 10^{18}$			107.95	\pm 6.62	B.133	6.29	\pm 1.32	0	\pm 20	E
268	Adorea	MBA	X	CV	$3.25 \pm 2.26 \times 10^{18}$	A.95		140.31	\pm 3.34	B.134	2.24	\pm 1.56	19	\pm 69	D
283	Emma	MBA	C	CM ³	$1.38 \pm 0.03 \times 10^{18}$	A.96		132.74	\pm 10.13	B.135	1.12	\pm 0.25	49	\pm 23	C
304	Olga	MBA	Xc	Mes	$1.15 \pm 1.12 \times 10^{18}$			70.30	\pm 2.32	B.136	6.31	\pm 6.18	0	\pm 97	D
306	Unitas	MBA	S	OC	$5.33 \pm 5.77 \times 10^{17}$			52.88	\pm 3.48	B.137	6.88	\pm 7.57	0	\pm ∞	E
322	Phaeo	MBA	D	CM	$1.86 \pm 0.04 \times 10^{18}$			71.88	\pm 4.32	B.138	9.56	\pm 1.73	0	\pm 18	X
324	Bamberga	MBA	Cb	CM	$1.03 \pm 0.10 \times 10^{19}$	A.97		234.67	\pm 7.80	B.139	1.52	\pm 0.20	32	\pm 13	A
328	Gudrun	MBA	S	OC	$3.16 \pm 0.46 \times 10^{18}$	A.98		122.59	\pm 3.72	B.140	3.27	\pm 0.55	1	\pm 17	B
334	Chicago	MBA	C	CM	$5.06 \pm 5.63 \times 10^{18}$	A.99		167.26	\pm 7.27	B.141	2.06	\pm 2.31	8	\pm ∞	E
337	Devosa	MBA	Xk	Hex ³	$1.08 \pm 0.16 \times 10^{18}$	A.100		63.87	\pm 3.14	B.142	7.91	\pm 1.65	0	\pm 20	X
344	Desiderata	MBA	C	CM	$1.39 \pm 0.48 \times 10^{18}$	A.101		129.20	\pm 3.37	B.143	1.22	\pm 0.43	45	\pm 35	C
345	Tercidina	MBA	Ch	CM	$2.68 \pm 1.18 \times 10^{18}$	A.102		98.78	\pm 2.63	B.144	5.30	\pm 2.37	0	\pm 44	C
346	Hermentaria	MBA	S	OC	$6.33 \pm 0.18 \times 10^{18}$			93.27	\pm 3.05	B.145	14.89	\pm 1.52	0	\pm 10	X
349	Dembowska	MBA	R	OC	$3.58 \pm 1.03 \times 10^{18}$	A.103		145.23	\pm 17.21	B.146	2.23	\pm 1.01	33	\pm 45	C
354	Eleonora	MBA	A	Pal	$7.18 \pm 2.57 \times 10^{18}$	A.104		154.34	\pm 5.65	B.147	3.73	\pm 1.39	21	\pm 37	C
356	Liguria	MBA	Ch	CM	$7.83 \pm 1.50 \times 10^{18}$			134.76	\pm 5.17	B.148	6.10	\pm 1.36	0	\pm 22	X
365	Corduba	MBA	Ch	CM	$5.84 \pm 0.95 \times 10^{18}$			104.51	\pm 2.42	B.149	9.76	\pm 1.73	0	\pm 17	X
372	Palma	MBA	X	CV	$5.15 \pm 0.64 \times 10^{18}$	A.105		191.12	\pm 2.68	B.150	1.40	\pm 0.18	49	\pm 13	B
375	Ursula	MBA	Xc	Mes	$8.45 \pm 5.26 \times 10^{18}$	A.106		191.65	\pm 4.01	B.151	2.29	\pm 1.43	46	\pm 62	D
379	Huenna	MBA	C	CM ¹	$3.83 \pm 0.20 \times 10^{17}$			87.28	\pm 5.70	B.152	1.10	\pm 0.22	51	\pm 20	C
381	Myrrha	MBA	X	CV	$9.18 \pm 0.80 \times 10^{18}$			123.41	\pm 6.30	B.153	9.32	\pm 1.64	0	\pm 17	X
386	Siegena	MBA	Ch	CM	$8.14 \pm 1.58 \times 10^{18}$	A.107		170.35	\pm 8.40	B.154	3.14	\pm 0.76	0	\pm 24	C
387	Aquitania	MBA	L	CO	$1.90 \pm 0.64 \times 10^{18}$	A.108		103.51	\pm 2.23	B.155	3.27	\pm 1.11	0	\pm 34	C
404	Arsinoe	MBA	B	CV	$3.42 \pm 3.03 \times 10^{18}$			96.97	\pm 3.01	B.156	7.16	\pm 6.38	0	\pm 89	D
405	Thia	MBA	Ch	CM	$1.38 \pm 0.14 \times 10^{18}$			122.14	\pm 7.69	B.157	1.44	\pm 0.30	35	\pm 21	C
409	Aspasia	MBA	Xc	Mes	$1.18 \pm 0.23 \times 10^{19}$	A.109		176.33	\pm 4.50	B.158	4.10	\pm 0.84	3	\pm 20	C

Table 1: Continued

Designation #	Name	Class			Masses (kg)			Diameter (km)			Density		Porosity		Rank
		Dyn.	Tax.	Met.	M	δM	Fig.	ϕ	$\delta\phi$	Fig.	ρ	$\delta\rho$	\mathcal{P}	$\delta\mathcal{P}$	
410	Chloris	MBA	Ch	CM	$6.24 \pm 0.30 \times 10^{18}$		A.110	115.55 ±	8.22	B.159	7.72 ±	1.69	0 ±	21	✗
416	Vaticana	MBA	S	OC	$3.27 \pm 3.10 \times 10^{18}$			87.10 ±	2.57	B.160	9.44 ±	8.99	0 ±	95	D
419	Aurelia	MBA	Cb	CM ¹	$1.72 \pm 0.34 \times 10^{18}$		A.111	124.47 ±	3.08	B.161	1.70 ±	0.35	24 ±	21	C
420	Bertholda	MBA	X	CV	$1.48 \pm 0.09 \times 10^{19}$			141.54 ±	2.08	B.162	9.96 ±	0.75	0 ±	7	✗
423	Diotima	MBA	C	CM	$6.91 \pm 1.93 \times 10^{18}$		A.112	211.64 ±	16.02	B.163	1.39 ±	0.50	38 ±	35	C
433	Eros	NEA	S	OC	$6.69 \pm 0.00 \times 10^{15}$			16.20 ±	0.16	B.164	3.00 ±	0.08	9 ±	2	B
442	Eichsfeldia	MBA	Ch	CM	$1.95 \pm 0.20 \times 10^{17}$			65.58 ±	1.70	B.165	1.32 ±	0.16	41 ±	12	B
444	Gyptis	MBA	C	CM	$1.06 \pm 0.28 \times 10^{19}$		A.113	164.63 ±	2.60	B.166	4.55 ±	1.23	0 ±	27	C
445	Edna	MBA	Ch	CM	$3.47 \pm 0.78 \times 10^{18}$			88.60 ±	4.10	B.167	9.52 ±	2.50	0 ±	26	✗
449	Hamburga	MBA	C	CM	$1.57 \pm 1.40 \times 10^{18}$			66.76 ±	4.82	B.168	10.07 ±	9.24	0 ±	91	E
451	Patientia	MBA	Cb	CM	$1.09 \pm 0.53 \times 10^{19}$		A.114	234.42 ±	10.17	B.169	1.60 ±	0.80	28 ±	50	D
455	Bruchsalia	MBA	Xk	Mes	$1.19 \pm 0.12 \times 10^{18}$			88.13 ±	6.89	B.170	3.32 ±	0.84	21 ±	25	C
469	Argentina	MBA	Xk	Mes	$4.53 \pm 1.76 \times 10^{18}$		A.115	126.00 ±	4.91	B.171	4.32 ±	1.75	0 ±	40	C
471	Papagena	MBA	S	OC	$3.05 \pm 1.73 \times 10^{18}$		A.116	124.55 ±	8.77	B.172	3.01 ±	1.82	9 ±	60	D
481	Emita	MBA	Ch	CM	$5.78 \pm 1.45 \times 10^{18}$			107.23 ±	4.71	B.173	8.95 ±	2.53	0 ±	28	C
485	Genua	MBA	S	OC	$1.36 \pm 0.44 \times 10^{18}$			56.31 ±	4.15	B.174	14.53 ±	5.68	0 ±	39	✗
488	Kreusa	MBA	Ch	CM	$2.48 \pm 1.14 \times 10^{18}$		A.117	162.32 ±	9.54	B.175	1.10 ±	0.54	50 ±	49	C
490	Veritas	MBA	Ch	CM	$5.99 \pm 2.23 \times 10^{18}$		A.118	110.96 ±	3.80	B.176	8.37 ±	3.23	0 ±	38	C
491	Carina	MBA	X	CV	$4.82 \pm 1.95 \times 10^{18}$			97.36 ±	3.18	B.177	9.97 ±	4.15	0 ±	41	C
503	Evelyn	MBA	Ch	CM	$2.85 \pm 0.34 \times 10^{18}$			87.58 ±	3.58	B.178	8.10 ±	1.38	0 ±	17	✗
505	Cava	MBA	Xk	LL ¹	$3.99 \pm 3.84 \times 10^{18}$			101.51 ±	1.83	B.179	7.28 ±	7.02	0 ±	96	D
508	Princetonia	MBA	X	CV	$2.99 \pm 0.65 \times 10^{18}$		A.119	139.69 ±	3.40	B.180	2.09 ±	0.47	25 ±	22	C
511	Davida	MBA	C	CM	$3.38 \pm 1.02 \times 10^{19}$		A.120	298.28 ±	11.92	B.181	2.43 ±	0.79	0 ±	32	C
516	Amherstia	MBA	X	CV	$1.43 \pm 1.33 \times 10^{18}$			69.84 ±	4.38	B.182	8.01 ±	7.60	0 ±	94	D
532	Herculina	MBA	S	OC	$1.15 \pm 0.28 \times 10^{19}$		A.121	217.49 ±	5.10	B.183	2.12 ±	0.53	36 ±	25	C
536	Merapi	MBA	X	CV	$2.61 \pm 0.47 \times 10^{19}$		A.122	155.17 ±	3.53	B.184	13.36 ±	2.59	0 ±	19	✗
554	Peraga	MBA	Ch	CI ¹	$6.59 \pm 0.66 \times 10^{17}$		A.123	96.46 ±	1.68	B.185	1.40 ±	0.15	12 ±	11	B
582	Olympia	MBA	S	OC	$0.43 \pm 1.17 \times 10^{18}$			43.39 ±	1.49	B.186	10.00 ±	27.35	0 ±	∞	✗
584	Semiramis	MBA	S	OC	$8.23 \pm 5.77 \times 10^{17}$			51.78 ±	2.15	B.187	11.31 ±	8.06	0 ±	71	✗
602	Marianna	MBA	Ch	CM	$1.02 \pm 0.05 \times 10^{19}$			127.95 ±	2.86	B.188	9.29 ±	0.76	0 ±	8	✗
604	Tekmesssa	MBA	Xc	Mes	$1.45 \pm 0.28 \times 10^{18}$			64.42 ±	3.01	B.189	10.35 ±	2.46	0 ±	23	✗
617	Patroclus	MBA	X	CV	$1.36 \pm 0.11 \times 10^{18}$			143.14 ±	8.37	B.190	0.88 ±	0.17	68 ±	19	B
624	Hektor	MBA	X	CV	$9.95 \pm 0.12 \times 10^{18}$			226.68 ±	15.15	B.191	1.63 ±	0.32	41 ±	20	C
626	Notburga	MBA	Cb	CM	$3.24 \pm 1.30 \times 10^{18}$		A.124	96.84 ±	4.67	B.192	6.81 ±	2.90	0 ±	42	E
654	Zelinda	MBA	Ch	CM	$1.35 \pm 0.14 \times 10^{18}$			127.83 ±	5.23	B.193	1.23 ±	0.19	45 ±	15	B
665	Sabine	MBA	X	CV	$6.98 \pm 3.98 \times 10^{17}$			52.71 ±	0.72	B.194	9.10 ±	5.20	0 ±	57	E
675	Ludmilla	MBA	S	OC	$1.20 \pm 0.24 \times 10^{19}$			67.66 ±	0.94		73.99 ±	15.05	0 ±	20	✗
679	Pax	MBA	L	CO	$7.14 \pm 1.99 \times 10^{17}$			64.88 ±	3.64	B.195	4.99 ±	1.62	0 ±	32	C
680	Genoveva	MBA	X	CV	$2.69 \pm 0.04 \times 10^{18}$			84.69 ±	1.71	B.196	8.45 ±	0.52	0 ±	6	✗
690	Wratislavia	MBA	B	CV	$1.28 \pm 0.03 \times 10^{19}$			146.21 ±	11.02	B.197	7.81 ±	1.77	0 ±	22	✗
702	Alauda	MBA	B	CV	$6.06 \pm 3.60 \times 10^{18}$		A.125	191.65 ±	8.22	B.198	1.64 ±	0.99	41 ±	60	D
704	Interamnia	MBA	B	CI ¹	$3.28 \pm 0.45 \times 10^{19}$		A.126	317.19 ±	4.65	B.199	1.96 ±	0.28	0 ±	14	A
720	Bohlinia	MBA	Sq	OC	$5.97 \pm 0.80 \times 10^{16}$		A.127	34.64 ±	1.81	B.200	2.74 ±	0.56	17 ±	20	C
735	Marghanna	MBA	Ch	CM	$2.15 \pm 0.68 \times 10^{18}$			72.27 ±	2.22	B.201	10.87 ±	3.56	0 ±	32	✗
739	Mandeville	MBA	Xc	Mes	$1.16 \pm 1.07 \times 10^{18}$			105.53 ±	1.68	B.202	1.88 ±	1.74	55 ±	92	D
747	Winchester	MBA	B	CV	$3.81 \pm 2.22 \times 10^{18}$		A.128	170.07 ±	6.70	B.203	1.47 ±	0.87	47 ±	59	D
751	Faina	MBA	Ch	CM	$3.27 \pm 0.58 \times 10^{18}$		A.129	107.31 ±	1.48	B.204	5.05 ±	0.92	0 ±	18	B
758	Mancunia	MBA	X	CV	$9.31 \pm 0.80 \times 10^{17}$			87.08 ±	1.31	B.205	2.69 ±	0.26	3 ±	9	B
760	Massinga	MBA	S	OC	$1.33 \pm 1.32 \times 10^{18}$			70.82 ±	0.92	B.206	7.15 ±	7.10	0 ±	99	D
762	Pulcova	MBA	Cb	CM ¹	$1.40 \pm 0.10 \times 10^{18}$		A.130	138.40 ±	5.96	B.207	1.00 ±	0.14	55 ±	14	B
769	Tatjana	MBA		CM	$6.31 \pm 0.64 \times 10^{18}$			106.27 ±	4.02	B.208	10.03 ±	1.52	0 ±	15	✗
776	Berbericia	MBA	Cgh	CM	$2.20 \pm 2.71 \times 10^{18}$		A.131	152.29 ±	4.25	B.209	1.18 ±	1.46	47 ±	∞	E
784	Pickeringia	MBA	C	CM	$3.74 \pm 0.32 \times 10^{18}$			82.52 ±	7.18	B.210	12.70 ±	3.49	0 ±	27	✗
786	Bredichina	MBA	C	CM	$2.82 \pm 2.79 \times 10^{18}$			98.34 ±	6.00	B.211	5.66 ±	5.69	0 ±	∞	E

Table 1: Continued

Designation		Class			Masses (kg)			Diameter (km)			Density		Porosity		Rank
#	Name	Dyn.	Tax.	Met.	M	δM	Fig.	ϕ	$\delta\phi$	Fig.	ρ	$\delta\rho$	\mathcal{P}	$\delta\mathcal{P}$	
790	Pretoria	MBA	X	CV	$4.58 \pm 0.28 \times 10^{18}$		A.132	$160.98 \pm$	11.16	B.212	$2.09 \pm$	0.45	$24 \pm$	21	C
804	Hispania	MBA	C	CM	$5.00 \pm 1.78 \times 10^{18}$		A.133	$148.25 \pm$	4.08	B.213	$2.93 \pm$	1.06	$0 \pm$	36	C
809	Lundia	MBA	V	HED	$9.27 \pm 3.09 \times 10^{14}$			$10.26 \pm$	0.07		$1.64 \pm$	0.10	$49 \pm$	6	B
854	Frostia	MBA	V	HED	$1.06 \pm 0.95 \times 10^{15}$			$8.39 \pm$	1.27	B.214	$0.88 \pm$	0.13	$72 \pm$	14	B
895	Helio	MBA	B	CV	$9.87 \pm 6.05 \times 10^{18}$		A.134	$148.43 \pm$	5.02	B.215	$5.76 \pm$	3.58	$0 \pm$	62	D
914	Palisana	MBA	Ch	CM	$2.35 \pm 0.24 \times 10^{18}$			$81.27 \pm$	5.34	B.216	$8.36 \pm$	1.85	$0 \pm$	22	X
949	Hel	MBA	Xk	Mes	$1.73 \pm 0.62 \times 10^{18}$			$63.56 \pm$	4.01	B.217	$12.86 \pm$	5.19	$0 \pm$	40	X
1013	Tombecka	MBA	Xk	Mes	$0.17 \pm 1.43 \times 10^{18}$			$35.18 \pm$	2.24	B.218	$7.50 \pm$	62.74	$0 \pm$	∞	E
1015	Christa	MBA	Xc	Mes	$4.77 \pm 0.68 \times 10^{18}$			$99.77 \pm$	2.46	B.219	$9.17 \pm$	1.46	$0 \pm$	15	X
1021	Flammario	MBA	Cb	CM	$5.14 \pm 0.12 \times 10^{18}$			$99.27 \pm$	3.27	B.220	$10.03 \pm$	1.02	$0 \pm$	10	X
1036	Ganymed	NEA	S	OC	$1.67 \pm 3.18 \times 10^{17}$			$34.28 \pm$	1.38	B.221	$7.91 \pm$	15.10	$0 \pm$	∞	X
1089	Tama	MBA	S	OC	$8.90 \pm 3.20 \times 10^{14}$			$13.44 \pm$	0.61	B.222	$2.52 \pm$	0.29	$24 \pm$	11	B
1171	Rusthawelia	MBA	X	CV	$1.81 \pm 0.20 \times 10^{18}$			$70.98 \pm$	2.42	B.223	$9.66 \pm$	1.45	$0 \pm$	15	X
1313	Berna	MBA	S	OC	$2.25 \pm 2.00 \times 10^{15}$			$13.93 \pm$	0.64	B.224	$1.21 \pm$	0.14	$63 \pm$	11	B
1669	Dagmar	MBA	Cg	CM	$3.98 \pm 0.80 \times 10^{16}$		A.135	$42.99 \pm$	2.86	B.225	$0.95 \pm$	0.27	$57 \pm$	28	C
1686	De Sitter	MBA		CM	$6.76 \pm 3.18 \times 10^{18}$			$30.60 \pm$	1.41	B.226	$450.51 \pm$	220.97	$0 \pm$	49	X
3169	Ostro	MBA	Xe	EH	$1.86 \pm 0.62 \times 10^{14}$			$5.15 \pm$	0.08		$2.59 \pm$	0.20	$25 \pm$	7	B
3671	Dionysus	NEA	Cb	CM	$8.38 \pm 2.79 \times 10^{11}$			$0.92 \pm$	0.05	B.227	$1.60 \pm$	0.60	$28 \pm$	37	C
3749	Balam	MBA	S	OC	$5.09 \pm 0.20 \times 10^{14}$			$6.99 \pm$	3.00	B.228	$2.83 \pm$	3.64	$14 \pm$	∞	E
4492	Debussy	MBA		CM	$3.33 \pm 3.00 \times 10^{14}$			$15.78 \pm$	1.91	B.229	$0.90 \pm$	0.10	$60 \pm$	11	B
5381	Sekhmet	NEA	S	OC	$1.04 \pm 0.35 \times 10^{12}$			$1.00 \pm$	0.10		$1.98 \pm$	0.65	$40 \pm$	32	C
25143	Itokawa	NEA	S	OC	$3.50 \pm 0.10 \times 10^{10}$			$0.32 \pm$	0.01	B.230	$1.91 \pm$	0.21	$42 \pm$	11	A
26308	1998 SM165	TNO		Ice	$6.78 \pm 2.40 \times 10^{18}$			$284.37 \pm$	5.07	B.231	$0.56 \pm$	0.20	$43 \pm$	35	C
35107	1991 VH	NEA	Sq	OC	$1.40 \pm 0.14 \times 10^{12}$			$1.13 \pm$	0.01	B.232	$1.50 \pm$	0.50	$54 \pm$	33	C
42355	Typhon	TNO		Ice	$9.49 \pm 0.52 \times 10^{17}$			$181.70 \pm$	5.10	B.233	$0.30 \pm$	0.03	$69 \pm$	10	B
47171	1999 TC36	TNO		Ice	$1.42 \pm 0.02 \times 10^{19}$		A.136	$402.46 \pm$	9.40	B.234	$0.41 \pm$	0.03	$58 \pm$	7	B
50000	Quaoar	TNO		Ice	$1.60 \pm 0.30 \times 10^{21}$			$946.58 \pm$	137.26	B.235	$3.60 \pm$	1.70	$0 \pm$	47	C
58534	Logos	TNO		Ice	$2.70 \pm 0.30 \times 10^{17}$			$110.00 \pm$	40.00		$0.38 \pm$	0.42	$61 \pm$	∞	E
65489	Ceto	TNO		Ice	$5.41 \pm 0.42 \times 10^{18}$			$250.58 \pm$	28.70	B.236	$0.65 \pm$	0.23	$34 \pm$	35	C
65803	Didymos	NEA		CM	$5.24 \pm 0.52 \times 10^{11}$			$0.80 \pm$	0.08		$1.90 \pm$	0.53	$15 \pm$	28	C
66063	1998 RO1	NEA	S	OC	$3.60 \pm 1.80 \times 10^{11}$			$0.68 \pm$	0.11	B.237	$2.79 \pm$	1.47	$15 \pm$	52	D
66391	1999 KW4	NEA	S	OC	$2.35 \pm 0.10 \times 10^{12}$			$1.31 \pm$	0.03		$1.80 \pm$	0.29	$45 \pm$	16	B
66652	Borasisi	TNO		Ice	$3.75 \pm 0.40 \times 10^{18}$			$447.00 \pm$	90.00		$0.08 \pm$	0.04	$91 \pm$	61	D
88611	2001 QT297	TNO		Ice	$2.36 \pm 0.01 \times 10^{18}$		A.137	$225.00 \pm$	75.00		$0.39 \pm$	0.39	$60 \pm$	∞	E
90482	Orcus	TNO		Ice	$6.34 \pm 0.03 \times 10^{20}$		A.138	$915.50 \pm$	42.58	B.238	$1.57 \pm$	0.22	$0 \pm$	13	B
134340	Pluto	TNO		Ice	$1.30 \pm 0.01 \times 10^{22}$			$2390.00 \pm$	10.00		$1.81 \pm$	0.02	$0 \pm$	1	A
134860	2000 OJ67	TNO		Ice	$2.14 \pm 0.11 \times 10^{18}$			$190.00 \pm$	65.00		$0.59 \pm$	0.61	$40 \pm$	∞	E
136108	Haumea	TNO		Ice	$4.01 \pm 0.04 \times 10^{21}$		A.139	$1244.99 \pm$	92.39	B.239	$3.96 \pm$	0.88	$0 \pm$	22	C
136199	Eris	TNO		Ice	$1.66 \pm 0.02 \times 10^{22}$			$2357.83 \pm$	75.19	B.240	$2.41 \pm$	0.23	$0 \pm$	9	B
136617	1994 CC	NEA		CM	$2.59 \pm 0.13 \times 10^{11}$			$0.62 \pm$	0.06		$2.07 \pm$	0.61	$7 \pm$	29	C
153591	2001 SN263	NEA		CM	$9.17 \pm 0.02 \times 10^{12}$			$2.59 \pm$	0.20		$0.99 \pm$	0.22	$55 \pm$	23	C
164121	2003 YT1	NEA		CM	$1.27 \pm 0.39 \times 10^{12}$			$1.08 \pm$	0.01	B.241	$1.90 \pm$	0.59	$15 \pm$	31	C
175706	1996 FG3	NEA	C	CM	$4.27 \pm 1.42 \times 10^{12}$			$1.75 \pm$	0.06	B.242	$1.36 \pm$	0.65	$39 \pm$	47	C
185851	2000 DP107	NEA		CM	$4.60 \pm 0.50 \times 10^{11}$			$1.63 \pm$	0.35		$0.95 \pm$	1.04	$57 \pm$	∞	E
276049	2002 CE26	NEA	C	CM	$1.95 \pm 0.25 \times 10^{13}$			$3.46 \pm$	0.35		$0.89 \pm$	0.29	$60 \pm$	32	C
311066	2004 DC	NEA		CM	$3.57 \pm 0.36 \times 10^{10}$			$0.34 \pm$	0.03		$1.73 \pm$	0.49	$22 \pm$	28	C

Table 1: Continued

#	Designation Name	Class			Masses (kg)			Diameter (km)			Density		Porosity		Rank
		Dyn.	Tax.	Met.	M	δM	Fig.	ϕ	$\delta\phi$	Fig.	ρ	$\delta\rho$	\mathcal{P}	$\delta\mathcal{P}$	
1999 OJ4	TNO			Ice	$3.91 \pm 0.22 \times 10^{17}$			130.00 ± 45.00			0.33 ± 0.35	$66 \pm \infty$		E	
2000 CF105	TNO			Ice	$1.85 \pm 0.12 \times 10^{17}$			188.00 ± 38.00			0.05 ± 0.03	94 ± 60		X	
2000 QL251	TNO			Ice	$3.11 \pm 0.05 \times 10^{18}$			150.00 ± 50.00			1.75 ± 1.76	$0 \pm \infty$		E	
2000 UG11	NEA			CM	$9.35 \pm 1.59 \times 10^9$			0.30 ± 0.10			0.66 ± 0.67	$70 \pm \infty$		E	
2001 QC298	TNO			Ice	$1.08 \pm 0.07 \times 10^{19}$			244.00 ± 55.00			1.41 ± 0.96	0 ± 67		D	
2001 QW322	TNO			Ice	$2.15 \pm 0.18 \times 10^{18}$			128.00 ± 3.00			1.00 ± 1.00	$0 \pm \infty$		X	
2001 XR254	TNO			Ice	$4.00 \pm 0.17 \times 10^{18}$			225.00 ± 75.00			0.67 ± 0.67	$32 \pm \infty$		E	
2003 QY90	TNO			Ice	$1.01 \pm 0.78 \times 10^{18}$			150.00 ± 50.00			0.57 ± 0.72	$42 \pm \infty$		E	
2003 TJ58	TNO			Ice	$2.25 \pm 0.15 \times 10^{17}$			75.00 ± 25.00			1.01 ± 1.02	$0 \pm \infty$		E	
2003 UN284	TNO			Ice	$1.31 \pm 0.26 \times 10^{18}$			124.00 ± 8.00			1.00 ± 1.00	$0 \pm \infty$		X	
2004 PB108	TNO			Ice	$9.68 \pm 0.57 \times 10^{18}$			140.00 ± 50.00			6.73 ± 7.22	$0 \pm \infty$		E	
2005 EO304	TNO			Ice	$2.10 \pm 0.08 \times 10^{18}$			152.00 ± 2.00			1.00 ± 1.00	$0 \pm \infty$		X	
2006 BR284	TNO			Ice	$5.70 \pm 0.19 \times 10^{17}$			89.80 ± 0.90			1.00 ± 1.00	$0 \pm \infty$		X	
2006 JZ81	TNO			Ice	$1.18 \pm 0.51 \times 10^{18}$			122.00 ± 16.00			1.00 ± 1.00	$0 \pm \infty$		X	
2006 CH69	TNO			Ice	$8.30 \pm 2.75 \times 10^{17}$			99.99 ± 11.00			1.00 ± 1.00	$0 \pm \infty$		X	
2007 TY430	TNO			Ice	$7.90 \pm 2.10 \times 10^{17}$			50.00 ± 20.00			0.75 ± 1.00	$25 \pm \infty$		X	
1P/Halley	COM			Ice	$3.20 \pm 1.20 \times 10^{14}$			10.39 ± 2.00			0.54 ± 0.37	45 ± 68		D	
2P/Encke	COM			Ice	$9.20 \pm 5.80 \times 10^{13}$			4.71 ± 0.81		B.243	1.67 ± 1.36	0 ± 81		D	
6P/dArest	COM			Ice	$2.80 \pm 0.80 \times 10^{12}$			1.70 ± 0.20			1.08 ± 0.49	0 ± 45		C	
9P/Tempell	COM			Ice	$5.48 \pm 0.56 \times 10^{13}$	A.140		6.00 ± 0.20		B.244	0.48 ± 0.06	51 ± 14		B	
10P/Tempel2	COM			Ice	$3.50 \pm 1.50 \times 10^{14}$			9.60 ± 1.39			0.75 ± 0.46	24 ± 61		D	
19P/Borrelly	COM			Ice	$2.70 \pm 2.10 \times 10^{12}$			4.80 ± 0.40			0.12 ± 0.09	87 ± 77		X	
22P/Kopff	COM			Ice	$5.30 \pm 2.20 \times 10^{12}$			3.59 ± 0.40			0.21 ± 0.11	78 ± 53		D	
45P/H-M-P	COM			Ice	$1.90 \pm 3.50 \times 10^{11}$			0.66 ± 0.20			1.26 ± 2.59	$0 \pm \infty$		E	
46P/Wirtanen	COM			Ice	$3.30 \pm 2.30 \times 10^{11}$			1.15 ± 0.06			0.40 ± 0.28	59 ± 71		D	
67P/C-G	COM			Ice	$1.50 \pm 0.60 \times 10^{13}$			2.96 ± 0.10		B.245	0.43 ± 0.37	56 ± 85		D	
81P/Wild2	COM			Ice	$8.10 \pm 0.81 \times 10^{12}$			2.08 ± 0.06		B.246	0.70 ± 0.10	30 ± 14		B	
SL9	COM			Ice	$1.53 \pm 0.15 \times 10^{12}$			1.79 ± 0.18			0.50 ± 0.05	50 ± 10		B	

Table 3: Average density ρ_i for each asteroid taxonomic type (DeMeo et al. 2009), based on N_i estimates. The i indices stand for the level of accuracy considered: more accurate than 20%, 50%, and no restriction on precision (∞). For each class, the associated meteorite (Met., see Table 2) and number of asteroids observed by DeMeo et al. with the corresponding fraction represented by the class are reported. The average density for transneptunian objects and comets are also reported.

Type	Met.	Taxonomy		Average density for each class					
		(#)	(%)	N_∞	ρ_∞	N_{50}	ρ_{50}	N_{20}	ρ_{20}
S	OC	144	38	50	2.66 ± 1.29	28	2.70 ± 0.69	11	2.72 ± 0.54
Sa	OC	2	<1	1	1.07 ± 0.25	1	1.07 ± 0.25		–
Sq	OC	29	7	5	2.78 ± 0.85	4	2.78 ± 0.81	2	3.43 ± 0.20
Sr	OC	22	5		–		–		–
Sv	OC	2	<1		–		–		–
B	CV	4	1	10	2.19 ± 1.00	4	2.15 ± 0.74	2	2.38 ± 0.45
C	CM	13	3	33	1.57 ± 1.38	19	1.41 ± 0.69	5	1.33 ± 0.58
Cb	CM	3	<1	13	1.88 ± 2.09	6	1.43 ± 0.74	3	1.25 ± 0.21
Cg	CM	1	<1	1	0.96 ± 0.27	1	0.96 ± 0.27		–
Cgh	CM	10	2	5	2.64 ± 1.35	1	3.48 ± 1.06		–
Ch	CM	18	4	47	1.96 ± 1.65	27	1.70 ± 1.10	9	1.41 ± 0.29
X	CV	4	1	26	2.87 ± 2.59	15	1.99 ± 0.99	8	1.85 ± 0.81
Xc	Mes	3	<1	9	4.96 ± 2.39	3	4.63 ± 0.76	2	4.86 ± 0.81
Xe	EH	7	1	4	2.94 ± 0.85	2	2.91 ± 0.65	1	2.60 ± 0.20
Xk	Mes	18	4	13	3.85 ± 1.27	9	3.79 ± 1.18	3	4.22 ± 0.65
D	CM	16	4	3	9.56 ± 0.22		–		–
K	CV	16	4	2	4.25 ± 2.03	1	3.54 ± 0.21	1	3.54 ± 0.21
L	CO	22	5	4	3.24 ± 1.03	3	3.22 ± 0.97		–
T	Ata	4	1	1	2.61 ± 2.54		–		–
A	Pal	6	1	1	3.73 ± 1.40	1	3.73 ± 1.40		–
O	OC	1	<1		–		–		–
Q	OC	8	2		–		–		–
R	OC	1	<1	1	2.23 ± 1.02	1	2.23 ± 1.02		–
V	HED	17	4	3	1.93 ± 1.07	3	1.93 ± 1.07	3	1.93 ± 1.07
Transneptunian objects				22	0.77 ± 0.80	10	1.06 ± 0.80	6	1.06 ± 0.75
Comets				12	0.47 ± 0.25	4	0.56 ± 0.14	3	0.54 ± 0.09

Appendix A. Compilation of mass estimates

The 994 mass estimates gathered in the literature are listed in Table A.1. For objects with more than a single mass determination, Fig. A.1 to Fig. A.140 presents a comparison of the mass estimates, with additional information on discarded values. See Appendix D for the references, and Fig. A.140 for symbols key.

Table A.1: Compilation of mass estimates (M , in kg) for 287 objects, with their associated uncertainty (δM), bibliographic references (see Appendix D), and method of analysis: *Deflec*: orbital deflection, *Ephem*: planetary ephemeris, *PheMu*: mutual eclipsing phenomena in binary systems, *BinImg*: binary imaged at optical wavelength, *BinRad*: binary imaged with radar, *FlyBy*: radio experiment for spacecraft flyby or orbit, and, for comet nuclei *CNGF*: non-gravitational forces, and *BkUp*: break-up modeling. Estimates marked with a dagger (\dagger) were rejected from average mass computation.

#	Designation	M	δM	Method	Refs.
1	Ceres	9.55E+20	4.38E+19	Deflec	M ₁
1	Ceres	9.54E+20	1.69E+19	Deflec	M ₂
1	Ceres	9.94E+20	3.98E+19	Deflec	M ₅ [†]
1	Ceres	9.19E+20	1.41E+19	Deflec	M ₆
1	Ceres	9.29E+20	1.79E+19	Deflec	M ₇
1	Ceres	8.27E+20	3.78E+19	Deflec	M ₈ [†]
1	Ceres	9.52E+20	7.76E+18	Deflec	M ₁₁
1	Ceres	9.47E+20	4.57E+18	Deflec	M ₁₅
1	Ceres	8.73E+20	7.96E+18	Deflec	M ₁₇ [†]
1	Ceres	9.35E+20	7.96E+18	Deflec	M ₂₁
1	Ceres	9.35E+20	5.97E+19	Deflec	M ₂₃
1	Ceres	9.47E+20	2.98E+18	Deflec	M ₂₉
1	Ceres	9.57E+20	1.99E+18	Deflec	M ₂₅
1	Ceres	9.45E+20	3.98E+18	Deflec	M ₃₉
1	Ceres	9.45E+20	1.39E+18	Deflec	M ₄₉
1	Ceres	9.35E+20	5.57E+18	Deflec	M ₅₆
1	Ceres	9.42E+20	5.17E+18	Deflec	M ₆₃
1	Ceres	9.46E+20	1.59E+18	Deflec	M ₇₂
1	Ceres	9.46E+20	7.96E+17	Ephem	M ₇₀
1	Ceres	9.32E+20	9.32E+19	Ephem	M ₈₆
1	Ceres	9.46E+20	5.67E+18	Ephem	M ₉₃
1	Ceres	9.46E+20	1.43E+18	Deflec	M ₉₅
1	Ceres	9.31E+20	6.46E+18	Ephem	M ₁₀₃
2	Pallas	3.16E+20	9.94E+18	Deflec	M ₁₇ [†]
2	Pallas	2.41E+20	5.17E+19	Deflec	M ₂₁
2	Pallas	2.33E+20	5.97E+18	Deflec	M ₂₃ [†]
2	Pallas	2.14E+20	7.56E+18	Deflec	M ₂₉
2	Pallas	1.99E+20	1.99E+18	Deflec	M ₂₅
2	Pallas	2.06E+20	3.98E+18	Deflec	M ₃₉
2	Pallas	2.04E+20	5.97E+17	Deflec	M ₄₉
2	Pallas	2.04E+20	5.57E+18	Deflec	M ₅₆
2	Pallas	2.11E+20	7.96E+18	Deflec	M ₇₂
2	Pallas	2.04E+20	1.99E+17	Ephem	M ₇₀
2	Pallas	2.01E+20	2.01E+19	Ephem	M ₈₆
2	Pallas	2.22E+20	5.59E+18	Ephem	M ₉₃
2	Pallas	1.79E+20	8.95E+18	Deflec	M ₉₂ [†]
2	Pallas	2.01E+20	1.29E+19	Deflec	M ₉₅
2	Pallas	2.06E+20	5.07E+18	Ephem	M ₁₀₃
2	Pallas	2.07E+20	1.70E+19	Deflec	M ₉₇
2	Pallas	1.96E+20	1.52E+19	Deflec	M ₉₇
2	Pallas	2.06E+20	1.38E+19	Deflec	M ₉₇
2	Pallas	1.88E+20	2.38E+19	Deflec	M ₉₇
2	Pallas	2.06E+20	2.98E+18	Ephem	M ₁₀₀

# Designation	M	δM	Method	Refs.
3 Juno	4.16E+19	6.96E+18	Deflec	M_{31}^\dagger
3 Juno	4.16E+19	6.96E+18	Deflec	M_{42}^\dagger
3 Juno	2.82E+19	1.19E+18	Deflec	M_{39}
3 Juno	3.00E+19	5.97E+17	Deflec	M_{49}
3 Juno	2.96E+19	2.98E+18	Deflec	M_{56}
3 Juno	2.67E+19	4.57E+18	Deflec	M_{72}
3 Juno	2.30E+19	2.30E+18	Ephem	M_{86}
3 Juno	2.31E+19	2.61E+18	Ephem	M_{93}
3 Juno	1.38E+19	7.92E+18	Deflec	M_{92}^\dagger
3 Juno	2.86E+19	4.57E+18	Deflec	M_{95}
3 Juno	2.41E+19	1.81E+18	Ephem	M_{103}
3 Juno	2.68E+19	3.98E+18	Deflec	M_{97}
3 Juno	3.04E+19	3.30E+18	Deflec	M_{97}
3 Juno	3.10E+19	3.24E+18	Deflec	M_{97}
3 Juno	1.70E+19	5.17E+18	Deflec	M_{97}^\dagger
3 Juno	2.35E+19	1.19E+18	Ephem	M_{100}
4 Vesta	2.78E+20	8.55E+18	Deflec	M_6
4 Vesta	3.36E+20	9.94E+18	Deflec	M_{17}^\dagger
4 Vesta	2.70E+20	9.94E+18	Deflec	M_{21}
4 Vesta	2.60E+20	3.18E+18	Deflec	M_{24}
4 Vesta	2.67E+20	2.98E+18	Deflec	M_{29}
4 Vesta	2.70E+20	1.99E+18	Deflec	M_{25}
4 Vesta	2.74E+20	5.97E+18	Deflec	M_{33}
4 Vesta	2.70E+20	3.98E+18	Deflec	M_{39}
4 Vesta	2.67E+20	1.99E+17	Deflec	M_{49}
4 Vesta	2.57E+20	1.59E+19	Deflec	M_{43}
4 Vesta	2.61E+20	3.98E+18	Deflec	M_{43}
4 Vesta	2.23E+20	9.94E+18	Deflec	M_{43}^\dagger
4 Vesta	2.23E+20	3.38E+19	Deflec	M_{43}^\dagger
4 Vesta	2.70E+20	3.18E+18	Deflec	M_{56}
4 Vesta	2.62E+20	5.97E+17	Deflec	M_{72}
4 Vesta	2.68E+20	5.97E+17	Ephem	M_{70}
4 Vesta	2.64E+20	2.64E+19	Ephem	M_{86}
4 Vesta	2.65E+20	3.35E+18	Ephem	M_{93}
4 Vesta	2.58E+20	1.99E+17	Deflec	M_{89}
4 Vesta	2.59E+20	1.05E+18	Deflec	M_{95}
4 Vesta	2.61E+20	4.10E+18	Ephem	M_{103}
4 Vesta	2.65E+20	3.00E+18	Ephem	M_{103}
4 Vesta	2.61E+20	4.10E+18	Deflec	M_{97}
4 Vesta	2.59E+20	1.41E+18	Deflec	M_{97}
4 Vesta	2.59E+20	1.41E+18	Deflec	M_{97}
4 Vesta	2.65E+20	2.16E+18	Deflec	M_{97}
4 Vesta	2.59E+20	1.19E+18	Ephem	M_{100}
5 Astraea	2.38E+18	2.38E+17	Ephem	M_{86}
5 Astraea	8.50E+18	2.90E+18	Deflec	M_{97}^\dagger
5 Astraea	3.39E+18	6.92E+17	Deflec	M_{97}
5 Astraea	8.61E+18	2.26E+18	Deflec	M_{97}^\dagger
5 Astraea	1.26E+19	4.61E+18	Deflec	M_{97}^\dagger

# Designation	M	δM	Method	Refs.
6 Hebe	1.37E+19	4.38E+18	Deflec	M_{26}
6 Hebe	1.37E+19	1.79E+18	Deflec	M_{42}
6 Hebe	1.28E+19	6.36E+17	Deflec	M_{72}
6 Hebe	3.18E+17	2.19E+17	Ephem	M_{80}^\dagger
6 Hebe	9.07E+18	9.07E+17	Ephem	M_{86}^\dagger
6 Hebe	1.41E+19	2.41E+18	Ephem	M_{93}
6 Hebe	1.34E+19	3.26E+18	Ephem	M_{103}
6 Hebe	1.36E+19	2.86E+18	Deflec	M_{97}
6 Hebe	1.55E+19	1.82E+18	Deflec	M_{97}
6 Hebe	1.54E+19	2.42E+18	Deflec	M_{97}
6 Hebe	1.53E+19	3.39E+18	Deflec	M_{97}
6 Hebe	1.41E+19	1.39E+18	Ephem	M_{100}
7 Iris	3.98E+19	1.79E+19	Deflec	M_{18}^\dagger
7 Iris	1.19E+19	1.99E+18	Deflec	M_{28}
7 Iris	2.80E+19	2.78E+18	Deflec	M_{31}^\dagger
7 Iris	2.80E+19	2.78E+18	Deflec	M_{42}^\dagger
7 Iris	1.03E+19	1.59E+18	Deflec	M_{39}
7 Iris	1.25E+19	1.99E+17	Deflec	M_{49}
7 Iris	1.79E+19	1.99E+18	Ephem	M_{62}
7 Iris	1.36E+19	9.94E+17	Deflec	M_{72}
7 Iris	4.77E+19	5.97E+18	Deflec	M_{78}^\dagger
7 Iris	1.15E+19	1.99E+17	Ephem	M_{70}
7 Iris	1.19E+19	1.19E+18	Ephem	M_{86}
7 Iris	1.55E+19	2.27E+18	Ephem	M_{93}
7 Iris	1.62E+19	9.15E+17	Deflec	M_{95}
7 Iris	1.10E+19	2.63E+18	Ephem	M_{103}
7 Iris	1.75E+19	1.88E+18	Deflec	M_{97}
7 Iris	1.72E+19	1.60E+18	Deflec	M_{97}
7 Iris	1.68E+19	1.59E+18	Deflec	M_{97}
7 Iris	2.33E+19	3.12E+18	Deflec	M_{97}^\dagger
7 Iris	1.13E+19	7.96E+17	Ephem	M_{100}
8 Flora	8.47E+18	8.95E+17	Deflec	M_{72}
8 Flora	1.06E+19	9.95E+16	Ephem	M_{80}
8 Flora	3.54E+18	3.54E+17	Ephem	M_{86}^\dagger
8 Flora	8.10E+18	1.26E+18	Ephem	M_{93}
8 Flora	6.62E+18	8.35E+17	Deflec	M_{95}
8 Flora	4.00E+18	8.35E+17	Ephem	M_{103}^\dagger
8 Flora	8.44E+18	1.49E+18	Deflec	M_{97}
8 Flora	6.03E+18	1.29E+18	Deflec	M_{97}
8 Flora	7.35E+18	1.31E+18	Deflec	M_{97}
8 Flora	6.75E+18	2.06E+18	Deflec	M_{97}
8 Flora	6.66E+18	5.97E+17	Ephem	M_{100}
9 Metis	1.13E+19	2.78E+18	Deflec	M_{72}
9 Metis	2.29E+18	1.99E+18	Ephem	M_{80}^\dagger
9 Metis	8.50E+18	8.50E+17	Ephem	M_{86}
9 Metis	2.96E+19	1.66E+19	Deflec	M_{92}^\dagger
9 Metis	1.13E+19	2.19E+18	Deflec	M_{95}
9 Metis	6.52E+18	2.15E+18	Ephem	M_{103}
9 Metis	8.12E+18	2.05E+18	Deflec	M_{97}
9 Metis	9.08E+18	1.34E+18	Deflec	M_{97}
9 Metis	9.00E+18	1.33E+18	Deflec	M_{97}
9 Metis	1.60E+19	3.02E+18	Deflec	M_{97}^\dagger
9 Metis	5.95E+18	9.95E+17	Ephem	M_{100}

Table A.1: Continued

# Designation	M	δM	Method	Refs.
10 Hygiea	1.55E+20	4.97E+19	Deflec	M ₁₈ [†]
10 Hygiea	5.57E+19	1.99E+18	Deflec	M ₂₈ [†]
10 Hygiea	1.11E+20	1.39E+19	Deflec	M ₂₆ [†]
10 Hygiea	9.96E+19	8.15E+18	Deflec	M ₃₁
10 Hygiea	9.97E+19	8.16E+18	Deflec	M ₄₂
10 Hygiea	9.03E+19	2.59E+18	Deflec	M ₄₅
10 Hygiea	4.18E+19	5.97E+18	Ephem	M ₆₂ [†]
10 Hygiea	8.85E+19	1.39E+18	Deflec	M ₇₂
10 Hygiea	4.97E+19	7.96E+18	Deflec	M ₇₈ [†]
10 Hygiea	8.04E+19	8.04E+18	Ephem	M ₈₆
10 Hygiea	8.67E+19	1.47E+18	Deflec	M ₉₅
10 Hygiea	8.94E+19	1.54E+19	Ephem	M ₁₀₃
10 Hygiea	7.73E+19	3.88E+18	Deflec	M ₉₇
10 Hygiea	8.30E+19	2.94E+18	Deflec	M ₉₇
10 Hygiea	8.21E+19	2.92E+18	Deflec	M ₉₇
10 Hygiea	8.07E+19	4.19E+18	Deflec	M ₉₇
10 Hygiea	8.65E+19	5.57E+18	Ephem	M ₁₀₀
11 Parthenope	5.13E+18	1.99E+17	Deflec	M ₉
11 Parthenope	5.09E+18	1.39E+17	Deflec	M ₂₄ [†]
11 Parthenope	6.15E+18	3.98E+16	Deflec	M ₇₂
11 Parthenope	5.33E+18	5.33E+17	Ephem	M ₈₆
11 Parthenope	3.75E+18	2.05E+18	Ephem	M ₉₃
11 Parthenope	5.89E+18	2.53E+17	Deflec	M ₉₇
11 Parthenope	5.21E+18	1.57E+18	Deflec	M ₉₇
11 Parthenope	5.86E+18	2.51E+17	Deflec	M ₉₇
11 Parthenope	5.86E+18	2.55E+17	Deflec	M ₉₇
11 Parthenope	7.56E+18	1.79E+18	Ephem	M ₁₀₀
12 Victoria	2.33E+18	5.97E+16	Ephem	M ₈₀
12 Victoria	7.51E+18	3.34E+18	Ephem	M ₉₃ [†]
12 Victoria	4.49E+18	3.80E+18	Deflec	M ₉₇
12 Victoria	1.75E+18	2.37E+18	Deflec	M ₉₇
12 Victoria	1.64E+18	2.34E+18	Deflec	M ₉₇
12 Victoria	3.56E+18	5.13E+17	Ephem	M ₁₀₀
13 Egeria	1.63E+19	3.18E+18	Deflec	M ₇₂
13 Egeria	6.17E+18	6.17E+17	Ephem	M ₈₆
13 Egeria	2.22E+19	1.60E+19	Ephem	M ₉₃
13 Egeria	1.59E+19	4.38E+18	Deflec	M ₉₅
13 Egeria	1.29E+19	4.70E+18	Deflec	M ₉₇
13 Egeria	7.39E+18	3.24E+18	Deflec	M ₉₇
13 Egeria	6.07E+18	3.20E+18	Deflec	M ₉₇
13 Egeria	8.26E+18	6.10E+18	Deflec	M ₉₇
14 Irene	8.21E+18	1.45E+18	Deflec	M ₇₂ [†]
14 Irene	1.41E+18	1.99E+17	Ephem	M ₈₀
14 Irene	5.21E+18	5.21E+17	Ephem	M ₈₆
14 Irene	5.12E+19	1.59E+19	Deflec	M ₉₂ [†]
14 Irene	6.94E+18	1.63E+18	Deflec	M ₉₅
14 Irene	3.80E+18	1.61E+18	Ephem	M ₁₀₃
14 Irene	4.81E+18	2.85E+18	Deflec	M ₉₇
14 Irene	2.79E+18	2.02E+18	Deflec	M ₉₇
14 Irene	1.93E+18	2.00E+18	Deflec	M ₉₇
14 Irene	1.69E+19	5.28E+18	Deflec	M ₉₇ [†]

Table A.1: Continued

# Designation	M	δM	Method	Refs.
15 Eunomia	1.99E+19	7.96E+18	Deflec	M ₁₈
15 Eunomia	2.78E+19	3.98E+18	Deflec	M ₂₈
15 Eunomia	2.51E+19	5.97E+18	Deflec	M ₂₆
15 Eunomia	2.43E+19	3.18E+18	Deflec	M ₃₁ [†]
15 Eunomia	2.11E+19	3.18E+18	Deflec	M ₄₂ [†]
15 Eunomia	3.26E+19	1.19E+18	Deflec	M ₅₁
15 Eunomia	3.12E+19	3.98E+17	Deflec	M ₇₂
15 Eunomia	1.59E+19	5.97E+18	Deflec	M ₇₈ [†]
15 Eunomia	2.45E+19	2.45E+18	Ephem	M ₈₆ [†]
15 Eunomia	3.75E+19	3.22E+18	Ephem	M ₉₃ [†]
15 Eunomia	3.22E+19	9.94E+17	Deflec	M ₈₈
15 Eunomia	3.18E+19	2.98E+17	Deflec	M ₉₅
15 Eunomia	2.82E+19	2.96E+18	Ephem	M ₁₀₃
15 Eunomia	3.21E+19	7.94E+17	Deflec	M ₉₇
15 Eunomia	3.22E+19	7.88E+17	Deflec	M ₉₇
15 Eunomia	3.22E+19	7.88E+17	Deflec	M ₉₇
15 Eunomia	3.22E+19	8.10E+17	Deflec	M ₉₇
15 Eunomia	2.70E+19	1.71E+18	Ephem	M ₁₀₀
16 Psyche	2.53E+20	3.58E+19	Deflec	M ₁₈ [†]
16 Psyche	1.73E+19	5.17E+18	Deflec	M ₂₀
16 Psyche	4.97E+19	1.99E+18	Deflec	M ₂₈
16 Psyche	6.72E+19	5.57E+18	Deflec	M ₃₀ [†]
16 Psyche	2.67E+19	4.38E+18	Deflec	M ₄₂
16 Psyche	2.19E+19	7.96E+17	Deflec	M ₇₂
16 Psyche	7.96E+19	2.78E+19	Deflec	M ₇₈ [†]
16 Psyche	3.17E+19	6.37E+17	Ephem	M ₈₀
16 Psyche	3.35E+19	3.35E+18	Ephem	M ₈₆
16 Psyche	2.23E+19	1.03E+19	Ephem	M ₉₃
16 Psyche	4.59E+19	1.93E+19	Deflec	M ₉₂
16 Psyche	2.27E+19	8.35E+17	Deflec	M ₉₅
16 Psyche	2.47E+19	6.84E+18	Ephem	M ₁₀₃
16 Psyche	2.35E+19	3.94E+18	Deflec	M ₉₇
16 Psyche	2.46E+19	1.62E+18	Deflec	M ₉₇
16 Psyche	2.44E+19	1.61E+18	Deflec	M ₉₇
16 Psyche	2.02E+19	4.34E+18	Deflec	M ₉₇
16 Psyche	2.51E+19	3.64E+18	Ephem	M ₁₀₀
17 Thetis	1.18E+18	7.56E+16	Deflec	M ₇₂
17 Thetis	1.43E+18	4.97E+16	Deflec	M ₉₅
17 Thetis	4.04E+18	1.41E+18	Ephem	M ₁₀₀ [†]
18 Melpomene	3.00E+18	1.01E+18	Deflec	M ₇₂
18 Melpomene	1.81E+18	3.98E+17	Ephem	M ₈₀
18 Melpomene	4.00E+18	4.00E+17	Ephem	M ₈₆
18 Melpomene	3.96E+18	2.80E+18	Deflec	M ₉₇
18 Melpomene	5.69E+18	1.99E+18	Deflec	M ₉₇
18 Melpomene	4.94E+18	1.95E+18	Deflec	M ₉₇
18 Melpomene	1.19E+18	3.41E+18	Deflec	M ₉₇

Table A.1: Continued

# Designation	M	δM	Method	Refs.
19 Fortuna	1.27E+19	4.97E+17	Deflec	M ₇₂ [†]
19 Fortuna	4.02E+18	3.98E+17	Ephem	M ₈₀ [†]
19 Fortuna	6.94E+18	6.94E+17	Ephem	M ₈₆
19 Fortuna	6.37E+18	2.90E+18	Deflec	M ₉₂
19 Fortuna	8.31E+18	7.16E+17	Deflec	M ₉₅
19 Fortuna	6.37E+18	1.05E+18	Ephem	M ₁₀₃
19 Fortuna	1.00E+19	1.08E+18	Deflec	M ₉₇
19 Fortuna	1.02E+19	9.47E+17	Deflec	M ₉₇
19 Fortuna	1.01E+19	9.35E+17	Deflec	M ₉₇
19 Fortuna	1.05E+19	1.23E+18	Deflec	M ₉₇
19 Fortuna	8.35E+18	5.97E+17	Ephem	M ₁₀₀
20 Massalia	4.77E+18	7.96E+17	Deflec	M ₁₆
20 Massalia	5.67E+18	8.15E+17	Deflec	M ₇₂
20 Massalia	4.36E+18	4.36E+17	Ephem	M ₈₆
20 Massalia	3.34E+18	6.96E+17	Deflec	M ₉₅
20 Massalia	5.88E+18	1.46E+18	Deflec	M ₉₇
20 Massalia	5.67E+18	1.14E+18	Deflec	M ₉₇
20 Massalia	6.03E+18	1.13E+18	Deflec	M ₉₇
20 Massalia	7.07E+18	1.68E+18	Deflec	M ₉₇
21 Lutetia	2.57E+18	2.39E+17	Deflec	M ₇₂ [†]
21 Lutetia	2.06E+18	5.97E+17	Ephem	M ₈₀ [†]
21 Lutetia	2.08E+18	2.08E+17	Ephem	M ₈₆ [†]
21 Lutetia	2.54E+18	2.33E+18	Ephem	M ₉₃ [†]
21 Lutetia	2.61E+18	8.75E+17	Deflec	M ₇₂ [†]
21 Lutetia	1.70E+18	1.40E+16	FlyBy	M ₁₀₄
21 Lutetia	9.31E+17	2.56E+18	Deflec	M ₉₇ [†]
21 Lutetia	1.67E+18	1.23E+18	Ephem	M ₁₀₀ [†]
22 Kalliope	7.36E+18	4.42E+17	BinImg	M ₃₇
22 Kalliope	1.69E+19	5.57E+18	Deflec	M ₄₂ [†]
22 Kalliope	8.15E+18	2.59E+17	BinImg	M ₇₄
22 Kalliope	8.09E+18	1.99E+17	BinImg	M ₇₅
22 Kalliope	7.36E+18	7.36E+17	Ephem	M ₈₆ [†]
22 Kalliope	1.33E+19	5.18E+18	Deflec	M ₉₇ [†]
22 Kalliope	1.31E+19	3.76E+18	Deflec	M ₉₇ [†]
22 Kalliope	1.31E+19	3.84E+18	Deflec	M ₉₇ [†]
22 Kalliope	2.09E+19	7.06E+18	Deflec	M ₉₇ [†]
23 Thalia	5.97E+16	1.99E+16	Ephem	M ₈₀ [†]
23 Thalia	1.93E+18	1.93E+17	Ephem	M ₈₆
23 Thalia	2.21E+18	1.41E+18	Ephem	M ₁₀₃
24 Themis	5.75E+18	2.51E+18	Deflec	M ₁₂
24 Themis	1.99E+18	3.98E+18	Ephem	M ₆₂
24 Themis	1.13E+19	4.28E+18	Deflec	M ₇₁
24 Themis	6.04E+18	6.04E+17	Ephem	M ₈₆
24 Themis	5.62E+18	3.78E+18	Ephem	M ₉₃
24 Themis	3.96E+18	2.81E+18	Deflec	M ₉₇
24 Themis	4.78E+18	1.84E+18	Deflec	M ₉₇
24 Themis	6.16E+18	1.85E+18	Deflec	M ₉₇
24 Themis	5.25E+18	2.34E+18	Deflec	M ₉₇
24 Themis	1.06E+19	4.57E+18	Ephem	M ₁₀₀
25 Phocaea	5.99E+17	5.99E+16	Ephem	M ₈₆
25 Phocaea	3.98E+15	3.98E+15	Ephem	M ₉₃ [†]
26 Proserpina	7.48E+17	8.95E+17	Ephem	M ₉₃

Table A.1: Continued

# Designation	M	δM	Method	Refs.
27 Euterpe	1.26E+18	1.26E+17	Ephem	M ₈₆
27 Euterpe	4.35E+18	1.98E+18	Deflec	M ₉₇
27 Euterpe	2.09E+18	1.47E+18	Deflec	M ₉₇
27 Euterpe	2.20E+18	1.46E+18	Deflec	M ₉₇
27 Euterpe	5.59E+18	3.07E+18	Deflec	M ₉₇
28 Bellona	2.78E+18	2.78E+17	Deflec	M ₂₈
28 Bellona	1.39E+19	3.98E+18	Deflec	M ₇₈ [†]
28 Bellona	2.47E+18	2.47E+17	Ephem	M ₈₆
28 Bellona	9.25E+18	1.97E+18	Ephem	M ₉₃ [†]
29 Amphitrite	1.53E+19	2.39E+18	Deflec	M ₃₁
29 Amphitrite	1.53E+19	2.59E+18	Deflec	M ₄₂
29 Amphitrite	1.18E+19	5.97E+17	Deflec	M ₇₂
29 Amphitrite	9.77E+18	1.79E+18	Ephem	M ₈₀
29 Amphitrite	1.36E+19	1.36E+18	Ephem	M ₈₆
29 Amphitrite	1.18E+19	6.03E+18	Deflec	M ₉₂
29 Amphitrite	1.52E+19	6.17E+17	Deflec	M ₉₅
29 Amphitrite	1.48E+19	2.96E+18	Ephem	M ₁₀₃
29 Amphitrite	1.20E+19	1.91E+18	Deflec	M ₉₇
29 Amphitrite	1.06E+19	1.64E+18	Deflec	M ₉₇
29 Amphitrite	1.10E+19	1.63E+18	Deflec	M ₉₇
29 Amphitrite	9.77E+18	2.30E+18	Deflec	M ₉₇
29 Amphitrite	1.47E+19	1.69E+18	Ephem	M ₁₀₀
30 Urania	1.42E+18	1.42E+17	Ephem	M ₈₆
30 Urania	1.96E+18	6.46E+17	Deflec	M ₉₇
30 Urania	2.05E+18	6.21E+17	Deflec	M ₉₇
30 Urania	2.03E+18	6.21E+17	Deflec	M ₉₇
30 Urania	3.80E+18	2.31E+18	Deflec	M ₉₇
31 Euphrosyne	1.87E+19	1.03E+19	Deflec	M ₄₂
31 Euphrosyne	6.23E+18	1.17E+18	Deflec	M ₇₂
31 Euphrosyne	5.95E+19	1.35E+19	Ephem	M ₈₀ [†]
31 Euphrosyne	1.71E+19	1.71E+18	Ephem	M ₈₆
31 Euphrosyne	5.81E+19	1.97E+19	Deflec	M ₉₅ [†]
31 Euphrosyne	1.85E+19	1.13E+19	Deflec	M ₉₇
31 Euphrosyne	2.31E+19	9.44E+18	Deflec	M ₉₇
31 Euphrosyne	2.69E+19	9.10E+18	Deflec	M ₉₇
31 Euphrosyne	1.39E+19	1.27E+19	Deflec	M ₉₇
31 Euphrosyne	8.75E+18	3.98E+18	Ephem	M ₁₀₀
33 Polyhymnia	6.20E+18	7.36E+17	Ephem	M ₉₃
34 Circe	3.61E+18	3.39E+18	Ephem	M ₉₃
34 Circe	3.68E+18	1.51E+18	Ephem	M ₁₀₀
36 Atalante	4.32E+18	3.80E+18	Ephem	M ₉₃
38 Leda	5.71E+18	5.47E+18	Ephem	M ₉₃
39 Laetitia	1.75E+19	1.01E+18	Ephem	M ₉₃ [†]
39 Laetitia	5.63E+18	1.45E+18	Deflec	M ₉₅
39 Laetitia	2.28E+18	3.62E+18	Deflec	M ₉₇
39 Laetitia	3.95E+18	2.60E+18	Deflec	M ₉₇
39 Laetitia	4.45E+18	2.57E+18	Deflec	M ₉₇
39 Laetitia	5.66E+18	2.05E+18	Ephem	M ₁₀₀

Table A.1: Continued

Table A.1: Continued				
# Designation	M	δM	Method	Refs.
41 Daphne	1.05E+19	9.95E+17	Ephem	M ₈₀ [†]
41 Daphne	7.90E+18	7.90E+17	Ephem	M ₈₆ [†]
41 Daphne	1.83E+19	5.23E+18	Ephem	M ₉₃ [†]
41 Daphne	8.43E+18	3.52E+18	Ephem	M ₁₀₃ [†]
41 Daphne	6.31E+18	1.10E+17	BinImg	M ₁₀₇ [†]
41 Daphne	1.82E+19	7.20E+18	Deflec	M ₉₇ [†]
41 Daphne	3.02E+17	5.67E+18	Deflec	M ₉₇ [†]
41 Daphne	4.76E+18	5.50E+18	Deflec	M ₉₇ [†]
41 Daphne	1.21E+19	1.05E+19	Deflec	M ₉₇ [†]
41 Daphne	1.02E+19	1.19E+18	Ephem	M ₁₀₀ [†]
42 Isis	1.38E+18	1.38E+17	Ephem	M ₈₆
42 Isis	3.69E+18	2.13E+18	Ephem	M ₉₃
42 Isis	1.85E+18	5.93E+17	Ephem	M ₁₀₀
43 Ariadne	1.50E+18	8.55E+17	Ephem	M ₉₃
43 Ariadne	1.04E+18	5.11E+17	Ephem	M ₁₀₀
45 Eugenia	2.98E+18	2.98E+18	Deflec	M ₁₈ [†]
45 Eugenia	5.97E+18	1.99E+17	BinImg	M ₁₉
45 Eugenia	6.96E+18	3.98E+17	Deflec	M ₂₈ [†]
45 Eugenia	1.99E+18	5.97E+18	Ephem	M ₆₂ [†]
45 Eugenia	5.69E+18	1.19E+17	BinImg	M ₇₅
45 Eugenia	1.79E+19	5.97E+18	Deflec	M ₇₈ [†]
45 Eugenia	5.95E+18	5.95E+17	Ephem	M ₈₆ [†]
45 Eugenia	7.68E+18	2.81E+18	Deflec	M ₉₇ [†]
45 Eugenia	7.11E+18	1.63E+18	Deflec	M ₉₇ [†]
45 Eugenia	7.57E+18	1.62E+18	Deflec	M ₉₇ [†]
45 Eugenia	1.14E+19	1.97E+18	Deflec	M ₉₇ [†]
46 Hestia	2.17E+19	1.35E+19	Deflec	M ₁₀ [†]
46 Hestia	7.01E+18	5.23E+18	Ephem	M ₉₃
46 Hestia	5.75E+18	1.23E+18	Ephem	M ₁₀₀
47 Aglaja	2.17E+18	8.55E+17	Deflec	M ₇₂
47 Aglaja	1.07E+19	4.57E+17	Ephem	M ₉₃ [†]
47 Aglaja	5.88E+18	2.09E+18	Ephem	M ₁₀₀
48 Doris	1.21E+19	5.97E+18	Deflec	M ₄₂
48 Doris	4.00E+19	2.98E+19	Ephem	M ₉₃ [†]
48 Doris	5.89E+18	4.84E+18	Deflec	M ₉₇
48 Doris	3.78E+18	3.74E+18	Deflec	M ₉₇
48 Doris	3.84E+18	3.69E+18	Deflec	M ₉₇
48 Doris	7.94E+18	6.39E+18	Deflec	M ₉₇
48 Doris	2.40E+19	6.83E+18	Ephem	M ₁₀₀ [†]
49 Pales	2.69E+18	4.97E+17	Deflec	M ₇₂
49 Pales	5.07E+18	3.87E+18	Deflec	M ₉₇
49 Pales	8.11E+18	2.68E+18	Deflec	M ₉₇
49 Pales	7.61E+18	2.67E+18	Deflec	M ₉₇
49 Pales	4.93E+18	4.90E+18	Deflec	M ₉₇
50 Virginia	3.65E+18	2.67E+18	Ephem	M ₉₃
50 Virginia	1.95E+18	7.28E+17	Ephem	M ₁₀₀

Table A.1: Continued				
# Designation	M	δM	Method	Refs.
51 Nemausa	2.16E+18	2.16E+17	Ephem	M ₈₆
51 Nemausa	1.44E+18	8.37E+17	Ephem	M ₉₃
51 Nemausa	4.55E+18	2.72E+18	Deflec	M ₉₇
51 Nemausa	3.39E+18	1.62E+18	Deflec	M ₉₇
51 Nemausa	3.36E+18	1.62E+18	Deflec	M ₉₇
51 Nemausa	4.25E+18	2.08E+18	Deflec	M ₉₇
51 Nemausa	5.63E+18	1.30E+18	Ephem	M ₁₀₀ [†]
52 Europa	2.15E+19	1.19E+18	Deflec	M ₂₈
52 Europa	5.19E+19	1.75E+19	Deflec	M ₂₆
52 Europa	2.55E+19	4.97E+18	Deflec	M ₃₁
52 Europa	2.53E+19	4.97E+18	Deflec	M ₄₂
52 Europa	7.16E+19	7.96E+18	Ephem	M ₆₂ [†]
52 Europa	1.65E+19	1.61E+18	Deflec	M ₇₂
52 Europa	8.35E+19	2.19E+19	Deflec	M ₇₈ [†]
52 Europa	3.43E+19	1.99E+18	Ephem	M ₈₀
52 Europa	2.03E+19	2.03E+18	Ephem	M ₈₆
52 Europa	8.41E+19	1.60E+19	Ephem	M ₉₃ [†]
52 Europa	2.25E+19	9.57E+18	Deflec	M ₉₂
52 Europa	2.27E+19	1.57E+18	Deflec	M ₉₅
52 Europa	2.22E+19	1.67E+19	Ephem	M ₁₀₃
52 Europa	2.84E+19	3.86E+18	Deflec	M ₉₇
52 Europa	2.63E+19	3.29E+18	Deflec	M ₉₇
52 Europa	2.78E+19	3.25E+18	Deflec	M ₉₇
52 Europa	2.13E+19	4.90E+18	Deflec	M ₉₇
52 Europa	1.79E+19	4.77E+18	Ephem	M ₁₀₀
53 Kalypso	5.63E+18	5.00E+18	Ephem	M ₉₃
54 Alexandra	4.45E+18	2.21E+18	Ephem	M ₉₃
54 Alexandra	1.08E+19	6.11E+18	Deflec	M ₉₇
54 Alexandra	1.74E+18	3.19E+18	Deflec	M ₉₇
54 Alexandra	2.94E+18	3.15E+18	Deflec	M ₉₇
54 Alexandra	6.44E+18	6.95E+18	Deflec	M ₉₇
54 Alexandra	1.03E+19	1.74E+18	Ephem	M ₁₀₀
56 Melete	4.62E+18	3.60E+18	Ephem	M ₉₃
56 Melete	4.61E+18	9.65E+17	Ephem	M ₁₀₀
57 Mnemosyne	1.33E+19	7.96E+18	Deflec	M ₉₇
57 Mnemosyne	1.12E+19	5.68E+18	Deflec	M ₉₇
57 Mnemosyne	1.08E+19	5.58E+18	Deflec	M ₉₇
57 Mnemosyne	1.76E+19	1.08E+19	Deflec	M ₉₇
59 Elpis	5.15E+18	3.57E+18	Ephem	M ₉₃
59 Elpis	2.75E+18	3.76E+17	Deflec	M ₉₇
59 Elpis	2.88E+18	3.72E+17	Deflec	M ₉₇
59 Elpis	2.88E+18	3.72E+17	Deflec	M ₉₇
59 Elpis	3.05E+18	3.47E+18	Deflec	M ₉₇
59 Elpis	4.15E+18	1.75E+18	Ephem	M ₁₀₀
60 Echo	3.15E+17	3.15E+16	Ephem	M ₈₆
60 Echo	8.00E+17	7.46E+17	Ephem	M ₉₃ [†]
61 Danae	2.89E+18	2.78E+18	Ephem	M ₉₃
63 Ausonia	1.53E+18	1.53E+17	Ephem	M ₈₆
63 Ausonia	4.02E+18	3.35E+18	Ephem	M ₉₃ [†]

# Designation	M	δM	Method	Refs.
65 Cybele	1.15E+19	2.98E+18	Deflec	M ₃₁
65 Cybele	1.15E+19	2.98E+18	Deflec	M ₄₂
65 Cybele	1.78E+19	1.21E+18	Deflec	M ₇₂
65 Cybele	1.04E+19	1.04E+18	Ephem	M ₈₆
65 Cybele	1.43E+19	8.47E+18	Ephem	M ₉₃
65 Cybele	1.05E+19	1.91E+18	Deflec	M ₉₅
65 Cybele	1.62E+19	3.68E+18	Deflec	M ₉₇
65 Cybele	1.52E+19	3.46E+18	Deflec	M ₉₇
65 Cybele	1.52E+19	3.45E+18	Deflec	M ₉₇
65 Cybele	1.75E+19	1.16E+19	Deflec	M ₉₇
65 Cybele	1.75E+19	5.17E+18	Ephem	M ₁₀₀
67 Asia	1.03E+18	9.95E+16	Ephem	M ₉₃
68 Leto	1.39E+18	4.00E+18	Deflec	M ₉₇
68 Leto	2.60E+18	2.75E+18	Deflec	M ₉₇
68 Leto	3.03E+18	2.73E+18	Deflec	M ₉₇
68 Leto	7.23E+18	4.85E+18	Deflec	M ₉₇
69 Hesperia	6.20E+18	6.20E+17	Ephem	M ₈₆
69 Hesperia	1.99E+18	6.54E+18	Deflec	M ₉₇
69 Hesperia	4.98E+18	2.10E+18	Deflec	M ₉₇
69 Hesperia	6.56E+18	4.27E+18	Deflec	M ₉₇
69 Hesperia	8.12E+18	7.48E+18	Deflec	M ₉₇
70 Panopaea	4.33E+18	1.09E+18	Ephem	M ₁₀₀
72 Feronia	3.32E+18	8.49E+18	Ephem	M ₉₃
74 Galatea	6.13E+18	5.36E+18	Ephem	M ₉₃
76 Freia	4.12E+17	2.13E+18	Deflec	M ₉₇
76 Freia	6.72E+17	2.06E+18	Deflec	M ₉₇
76 Freia	1.43E+19	9.03E+18	Deflec	M ₉₇
77 Frigga	1.74E+18	6.76E+17	Ephem	M ₉₃
78 Diana	1.27E+18	1.27E+17	Ephem	M ₈₆
78 Diana	6.43E+18	4.61E+18	Ephem	M ₉₃ [†]
81 Terpsichore	6.19E+18	5.31E+18	Ephem	M ₉₃
84 Klio	5.47E+17	4.06E+17	Ephem	M ₉₃
85 Io	3.32E+17	3.45E+18	Deflec	M ₉₇
85 Io	3.87E+18	2.68E+18	Deflec	M ₉₇
85 Io	3.49E+18	2.64E+18	Deflec	M ₉₇
85 Io	1.40E+18	6.33E+18	Deflec	M ₉₇
87 Sylvia	5.37E+19	1.99E+19	Deflec	M ₁₈ [†]
87 Sylvia	1.39E+19	1.99E+18	Deflec	M ₂₈ [†]
87 Sylvia	1.46E+19	1.00E+18	BinImg	M ₂₇
87 Sylvia	3.58E+19	1.79E+19	Ephem	M ₆₂ [†]
87 Sylvia	1.48E+19	5.97E+16	BinImg	M ₄₈
87 Sylvia	5.17E+19	2.19E+19	Deflec	M ₇₈ [†]
87 Sylvia	1.17E+19	1.29E+19	Deflec	M ₉₇ [†]
87 Sylvia	1.36E+19	1.09E+19	Deflec	M ₉₇ [†]
87 Sylvia	1.18E+19	1.06E+19	Deflec	M ₉₇ [†]
87 Sylvia	5.98E+18	1.88E+19	Deflec	M ₉₇ [†]

# Designation	M	δM	Method	Refs.
88 Thisbe	1.47E+19	2.59E+18	Deflec	M ₂₆
88 Thisbe	1.17E+19	2.39E+18	Deflec	M ₄₂
88 Thisbe	1.05E+19	1.79E+18	Deflec	M ₇₂
88 Thisbe	1.72E+19	5.17E+17	Ephem	M ₈₀
88 Thisbe	1.83E+19	1.09E+18	Deflec	M ₉₅
88 Thisbe	9.53E+18	3.20E+18	Deflec	M ₉₇
88 Thisbe	7.61E+18	2.27E+18	Deflec	M ₉₇ [†]
88 Thisbe	7.63E+18	2.25E+18	Deflec	M ₉₇ [†]
89 Julia	7.14E+18	2.78E+17	Ephem	M ₈₀
89 Julia	8.32E+18	4.14E+18	Ephem	M ₉₃
89 Julia	3.72E+17	3.24E+18	Deflec	M ₉₇
90 Antiope	4.10E+17	1.19E+17	BinImg	M ₃₂ [†]
90 Antiope	8.30E+17	1.99E+16	BinImg	M ₆₅
92 Undina	4.19E+18	4.39E+18	Deflec	M ₉₇
92 Undina	4.31E+18	3.91E+18	Deflec	M ₉₇
92 Undina	4.77E+18	3.87E+18	Deflec	M ₉₇
93 Minerva	3.50E+18	4.00E+17	BinImg	M ₁₀₁
94 Aurora	6.20E+18	6.20E+17	Ephem	M ₈₆
94 Aurora	3.15E+19	2.29E+19	Ephem	M ₉₃ [†]
94 Aurora	1.51E+18	5.08E+18	Deflec	M ₉₇
94 Aurora	4.18E+16	4.17E+18	Deflec	M ₉₇
94 Aurora	1.57E+19	7.99E+18	Deflec	M ₉₇
94 Aurora	1.18E+19	4.36E+18	Ephem	M ₁₀₀
96 Aegle	1.74E+18	8.31E+18	Deflec	M ₉₇
96 Aegle	3.50E+17	4.69E+18	Deflec	M ₉₇
96 Aegle	1.34E+19	3.69E+18	Ephem	M ₁₀₀
97 Klotho	1.33E+18	1.33E+17	Ephem	M ₈₆
98 Ianthe	8.24E+17	8.24E+16	Ephem	M ₈₆
98 Ianthe	1.47E+18	6.90E+17	Ephem	M ₁₀₀
105 Artemis	1.32E+18	1.32E+17	Ephem	M ₈₆
105 Artemis	2.89E+18	8.43E+17	Ephem	M ₁₀₀
106 Dione	3.04E+17	3.59E+18	Deflec	M ₉₇
106 Dione	4.29E+18	2.64E+18	Deflec	M ₉₇
106 Dione	3.52E+18	2.62E+18	Deflec	M ₉₇
106 Dione	3.77E+18	5.80E+18	Deflec	M ₉₇
107 Camilla	1.12E+19	2.98E+17	BinImg	M ₇₅
107 Camilla	3.62E+19	9.24E+18	Ephem	M ₉₃ [†]
107 Camilla	3.88E+18	1.09E+19	Deflec	M ₉₇ [†]
107 Camilla	3.90E+19	1.06E+19	Deflec	M ₉₇ [†]
107 Camilla	1.76E+19	8.69E+18	Deflec	M ₉₇ [†]
107 Camilla	2.25E+18	1.80E+19	Deflec	M ₉₇ [†]
107 Camilla	2.71E+19	6.96E+18	Ephem	M ₁₀₀ [†]
111 Ate	1.99E+18	1.99E+17	Deflec	M ₂₈
111 Ate	1.67E+20	3.78E+19	Deflec	M ₇₈ [†]
111 Ate	1.74E+18	1.74E+17	Ephem	M ₈₆
111 Ate	2.71E+18	2.49E+18	Deflec	M ₉₇
111 Ate	3.42E+17	1.65E+18	Deflec	M ₉₇
111 Ate	8.16E+17	1.66E+18	Deflec	M ₉₇
112 Iphigenia	1.97E+18	6.78E+18	Ephem	M ₉₃

Table A.1: Continued

# Designation	M	δM	Method	Refs.
117 Lomia	1.72E+19	1.99E+17	Ephem	M ₉₃ [†]
117 Lomia	6.36E+18	4.35E+18	Deflec	M ₉₇
117 Lomia	5.85E+18	3.59E+18	Deflec	M ₉₇
117 Lomia	6.73E+18	3.55E+18	Deflec	M ₉₇
117 Lomia	4.88E+18	6.61E+18	Deflec	M ₉₇
121 Hermione	9.35E+18	1.59E+18	Deflec	M ₂₀ [†]
121 Hermione	5.38E+18	2.98E+17	BinImg	M ₄₇
121 Hermione	4.70E+18	2.00E+17	BinImg	M ₈₄
121 Hermione	5.12E+18	2.22E+18	Deflec	M ₉₇ [†]
121 Hermione	6.01E+18	1.70E+18	Deflec	M ₉₇ [†]
121 Hermione	4.58E+18	2.13E+18	Deflec	M ₉₇ [†]
121 Hermione	6.27E+18	2.28E+18	Deflec	M ₉₇ [†]
126 Velleda	4.71E+17	5.79E+18	Ephem	M ₉₃
127 Johanna	8.76E+18	8.75E+17	Ephem	M ₉₃ [†]
127 Johanna	3.08E+18	1.35E+18	Ephem	M ₁₀₀
128 Nemesis	3.36E+18	6.56E+17	Ephem	M ₈₀
128 Nemesis	9.12E+18	5.51E+18	Ephem	M ₉₃
128 Nemesis	9.94E+18	3.08E+18	Deflec	M ₉₇
128 Nemesis	8.40E+18	2.16E+18	Deflec	M ₉₇
128 Nemesis	8.38E+18	2.14E+18	Deflec	M ₉₇
128 Nemesis	3.89E+18	4.44E+18	Deflec	M ₉₇
128 Nemesis	6.69E+18	2.18E+18	Ephem	M ₁₀₀
129 Antigone	1.43E+19	2.78E+17	Ephem	M ₈₀ [†]
129 Antigone	8.62E+18	3.67E+18	Ephem	M ₉₃ [†]
129 Antigone	4.82E+18	5.48E+18	Deflec	M ₉₇
129 Antigone	1.97E+18	3.87E+18	Deflec	M ₉₇
129 Antigone	1.33E+18	3.79E+18	Deflec	M ₉₇
129 Antigone	2.76E+18	8.97E+17	Ephem	M ₁₀₀
130 Elektra	6.60E+18	3.98E+17	BinImg	M ₇₃
130 Elektra	2.22E+19	1.60E+19	Ephem	M ₉₃ [†]
130 Elektra	1.61E+19	8.35E+18	Deflec	M ₉₇ [†]
130 Elektra	1.00E+19	6.55E+18	Deflec	M ₉₇ [†]
130 Elektra	6.93E+18	6.42E+18	Deflec	M ₉₇ [†]
130 Elektra	1.34E+19	1.30E+19	Deflec	M ₉₇ [†]
130 Elektra	2.19E+17	1.19E+17	Ephem	M ₁₀₀ [†]
132 Aethra	4.12E+17	2.71E+18	Ephem	M ₉₃
135 Hertha	1.17E+18	1.17E+17	Ephem	M ₈₆
135 Hertha	1.82E+18	1.76E+18	Ephem	M ₉₃
137 Meliboea	5.03E+18	4.67E+18	Deflec	M ₉₇
137 Meliboea	5.80E+18	4.12E+18	Deflec	M ₉₇
137 Meliboea	6.37E+18	4.06E+18	Deflec	M ₉₇
137 Meliboea	1.34E+19	5.80E+18	Deflec	M ₉₇
138 Tolosa	4.93E+17	2.59E+17	Ephem	M ₉₃
139 Juewa	7.14E+18	1.99E+17	Ephem	M ₈₀
139 Juewa	2.82E+18	2.82E+17	Ephem	M ₈₆
139 Juewa	1.17E+19	6.59E+18	Ephem	M ₉₃
139 Juewa	7.32E+18	4.27E+18	Deflec	M ₉₇
139 Juewa	4.37E+18	3.25E+18	Deflec	M ₉₇
139 Juewa	6.00E+18	3.21E+18	Deflec	M ₉₇
139 Juewa	7.86E+18	4.83E+18	Deflec	M ₉₇
141 Lumen	8.25E+18	5.77E+18	Ephem	M ₉₃

Table A.1: Continued

# Designation	M	δM	Method	Refs.
144 Vibia	9.08E+18	5.92E+18	Ephem	M ₉₃
144 Vibia	4.63E+18	2.84E+18	Deflec	M ₉₇
144 Vibia	5.32E+18	1.86E+18	Deflec	M ₉₇
144 Vibia	4.95E+18	1.85E+18	Deflec	M ₉₇
144 Vibia	4.62E+18	3.06E+18	Deflec	M ₉₇
145 Adeona	2.26E+18	2.26E+17	Ephem	M ₈₆
145 Adeona	1.73E+17	2.39E+18	Deflec	M ₉₇
145 Adeona	2.10E+18	2.97E+18	Deflec	M ₉₇
147 Protogeneia	1.23E+19	4.77E+17	Ephem	M ₉₃
148 Gallia	4.89E+18	1.67E+18	Ephem	M ₉₃
150 Nuwa	1.81E+19	8.35E+17	Ephem	M ₉₃ [†]
150 Nuwa	2.04E+18	2.75E+18	Deflec	M ₉₇
150 Nuwa	1.52E+18	6.39E+17	Deflec	M ₉₇
152 Atala	5.43E+18	1.24E+18	Ephem	M ₁₀₀
154 Bertha	4.46E+17	1.40E+19	Deflec	M ₉₇
154 Bertha	1.18E+19	1.01E+19	Deflec	M ₉₇
154 Bertha	1.27E+19	9.57E+18	Deflec	M ₉₇
156 Xanthippe	6.49E+18	3.71E+18	Ephem	M ₉₃
163 Erigone	2.01E+18	6.76E+17	Ephem	M ₉₃
164 Eva	9.29E+17	7.76E+17	Ephem	M ₉₃
165 Loreley	3.18E+19	1.99E+19	Ephem	M ₆₂
165 Loreley	1.94E+19	1.99E+17	Ephem	M ₉₃
165 Loreley	1.08E+19	5.64E+18	Deflec	M ₉₇
165 Loreley	1.87E+19	4.30E+18	Deflec	M ₉₇
165 Loreley	1.71E+19	4.25E+18	Deflec	M ₉₇
165 Loreley	1.47E+18	6.86E+18	Deflec	M ₉₇ [†]
168 Sibylla	6.02E+18	7.82E+18	Deflec	M ₉₇
168 Sibylla	2.38E+18	5.74E+18	Deflec	M ₉₇
173 Ino	7.28E+18	5.97E+17	Ephem	M ₈₀
173 Ino	1.34E+19	1.13E+19	Ephem	M ₉₃
173 Ino	2.06E+18	1.30E+18	Deflec	M ₉₇
173 Ino	1.33E+18	1.22E+18	Deflec	M ₉₇
179 Klytaemnestra	2.49E+17	1.19E+17	Ephem	M ₁₀₀
185 Eunike	6.89E+18	6.23E+18	Deflec	M ₉₇
185 Eunike	1.97E+18	5.14E+18	Deflec	M ₉₇
185 Eunike	6.46E+17	5.03E+18	Deflec	M ₉₇
185 Eunike	5.94E+18	6.74E+18	Deflec	M ₉₇
187 Lamberta	1.57E+18	1.57E+17	Ephem	M ₈₆
187 Lamberta	4.94E+18	2.14E+18	Ephem	M ₉₃
189 Phthia	3.84E+16	8.15E+15	Deflec	M ₇₂
192 Nausikaa	2.73E+18	8.16E+17	Ephem	M ₈₀
192 Nausikaa	1.60E+18	1.60E+17	Ephem	M ₈₆
194 Prokne	2.73E+18	2.73E+17	Ephem	M ₈₆
194 Prokne	1.75E+19	5.81E+18	Ephem	M ₉₃ [†]
194 Prokne	2.84E+18	6.00E+18	Deflec	M ₉₇
194 Prokne	1.12E+18	7.68E+18	Deflec	M ₉₇
194 Prokne	1.60E+19	1.06E+18	Ephem	M ₁₀₀ [†]

Table A.1: Continued

# Designation	M	δM	Method	Refs.
196 Philomela	6.39E+18	5.54E+18	Deflec	M ₉₇
196 Philomela	3.16E+18	1.61E+18	Deflec	M ₉₇
196 Philomela	3.30E+18	1.61E+18	Deflec	M ₉₇
196 Philomela	7.59E+18	6.87E+18	Deflec	M ₉₇
200 Dynamene	1.07E+19	1.61E+18	Ephem	M ₉₃
204 Kallisto	6.01E+17	1.81E+18	Ephem	M ₉₃
209 Dido	4.59E+18	7.42E+18	Deflec	M ₉₇
210 Isabella	3.41E+18	1.09E+18	Ephem	M ₉₃
211 Isolda	7.56E+18	1.31E+18	Ephem	M ₉₃
211 Isolda	1.99E+18	2.28E+18	Deflec	M ₉₇
211 Isolda	2.67E+18	1.78E+18	Deflec	M ₉₇
211 Isolda	2.41E+18	1.78E+18	Deflec	M ₉₇
211 Isolda	4.16E+18	2.66E+18	Deflec	M ₉₇
211 Isolda	7.83E+18	3.13E+18	Ephem	M ₁₀₀
212 Medea	1.32E+19	1.05E+18	Ephem	M ₉₃
216 Kleopatra	7.02E+18	2.39E+17	Ephem	M ₈₀ [†]
216 Kleopatra	4.48E+18	4.48E+17	Ephem	M ₈₆ [†]
216 Kleopatra	1.12E+18	9.15E+17	Ephem	M ₉₃ [†]
216 Kleopatra	4.64E+18	2.00E+17	BinImg	M ₁₀₂
216 Kleopatra	7.31E+18	2.45E+18	Deflec	M ₉₇ [†]
216 Kleopatra	7.12E+18	3.95E+18	Deflec	M ₉₇ [†]
216 Kleopatra	7.64E+18	2.26E+18	Deflec	M ₉₇ [†]
216 Kleopatra	7.97E+18	2.54E+18	Deflec	M ₉₇ [†]
216 Kleopatra	5.69E+18	1.77E+18	Ephem	M ₁₀₀ [†]
217 Eudora	1.52E+18	5.97E+16	Ephem	M ₉₃
221 Eos	5.87E+18	3.38E+17	Ephem	M ₉₃
230 Athamantis	1.89E+18	1.89E+17	Ephem	M ₈₆
234 Barbara	4.40E+17	1.45E+18	Ephem	M ₉₃
238 Hypatia	4.86E+18	4.16E+18	Deflec	M ₉₇
238 Hypatia	5.44E+18	3.27E+18	Deflec	M ₉₇
238 Hypatia	6.20E+18	3.24E+18	Deflec	M ₉₇
238 Hypatia	8.63E+17	7.26E+18	Deflec	M ₉₇
240 Vanadis	4.11E+18	3.80E+18	Ephem	M ₉₃
240 Vanadis	8.25E+17	3.54E+17	Ephem	M ₁₀₀
241 Germania	8.61E+17	5.00E+18	Deflec	M ₉₇
243 Ida	3.78E+16	1.99E+15	BinImg	M ₁₃
253 Mathilde	1.03E+17	4.38E+15	FlyBy	M ₁₄
253 Mathilde	1.80E+18	1.29E+18	Ephem	M ₉₃ [†]
253 Mathilde	1.19E+18	5.97E+17	Ephem	M ₁₀₀ [†]
259 Aletheia	8.23E+18	4.66E+18	Deflec	M ₉₇
259 Aletheia	7.36E+18	4.58E+18	Deflec	M ₉₇
259 Aletheia	2.56E+19	9.38E+18	Deflec	M ₉₇ [†]
259 Aletheia	3.72E+17	1.69E+17	Ephem	M ₁₀₀ [†]
266 Aline	4.15E+18	4.18E+17	Ephem	M ₉₃
268 Adorea	1.56E+18	1.35E+18	Ephem	M ₉₃
268 Adorea	6.27E+18	2.42E+18	Ephem	M ₁₀₀

Table A.1: Continued

# Designation	M	δM	Method	Refs.
283 Emma	1.38E+18	3.00E+16	BinImg	M ₇₃
283 Emma	1.00E+19	5.16E+18	Deflec	M ₉₇ [†]
283 Emma	8.38E+18	3.68E+18	Deflec	M ₉₇ [†]
283 Emma	8.31E+18	3.65E+18	Deflec	M ₉₇ [†]
283 Emma	1.63E+19	6.03E+18	Deflec	M ₉₇ [†]
304 Olga	1.15E+18	1.12E+18	Ephem	M ₉₃
306 Unitas	5.33E+17	5.77E+17	Ephem	M ₉₃
322 Phaeo	1.86E+18	3.98E+16	Ephem	M ₉₃
324 Bamberga	4.56E+19	7.56E+18	Deflec	M ₄₂ [†]
324 Bamberga	1.01E+19	1.59E+18	Deflec	M ₃₉
324 Bamberga	1.09E+19	1.99E+17	Deflec	M ₄₉
324 Bamberga	9.35E+18	1.39E+18	Deflec	M ₅₆
324 Bamberga	9.15E+18	5.97E+17	Ephem	M ₇₀
324 Bamberga	9.90E+18	9.90E+17	Ephem	M ₈₆
324 Bamberga	9.33E+18	7.54E+17	Ephem	M ₉₃
324 Bamberga	1.06E+19	1.97E+18	Ephem	M ₁₀₃
324 Bamberga	5.61E+18	4.78E+18	Deflec	M ₉₇
324 Bamberga	1.13E+19	2.02E+18	Deflec	M ₉₇
324 Bamberga	1.08E+19	1.99E+18	Deflec	M ₉₇
324 Bamberga	1.09E+19	2.18E+18	Deflec	M ₉₇
324 Bamberga	1.13E+19	8.55E+17	Ephem	M ₁₀₀
328 Gudrun	9.72E+18	2.59E+17	Ephem	M ₉₃ [†]
328 Gudrun	3.74E+18	5.30E+18	Deflec	M ₉₇
328 Gudrun	1.86E+18	5.20E+18	Deflec	M ₉₇
328 Gudrun	3.25E+18	6.50E+17	Ephem	M ₁₀₀
334 Chicago	1.30E+19	3.22E+19	Deflec	M ₉₇
334 Chicago	1.06E+18	1.62E+19	Deflec	M ₉₇
337 Devosa	4.94E+17	4.94E+16	Ephem	M ₈₆ [†]
337 Devosa	1.08E+18	1.59E+17	Ephem	M ₉₃
344 Desiderata	1.71E+18	1.71E+17	Ephem	M ₈₆
344 Desiderata	6.80E+17	3.74E+17	Ephem	M ₉₃
344 Desiderata	4.05E+18	8.31E+17	Ephem	M ₁₀₀ [†]
345 Tercidina	4.37E+18	4.57E+17	Ephem	M ₉₃ [†]
345 Tercidina	2.68E+18	1.18E+18	Ephem	M ₁₀₀
346 Hermentaria	6.33E+18	1.79E+17	Ephem	M ₉₃
349 Dembowska	5.19E+18	3.23E+18	Deflec	M ₉₇
349 Dembowska	3.10E+18	2.51E+18	Deflec	M ₉₇
349 Dembowska	3.67E+18	2.50E+18	Deflec	M ₉₇
349 Dembowska	2.08E+18	4.34E+18	Deflec	M ₉₇
354 Eleonora	9.71E+18	6.96E+17	Ephem	M ₈₀
354 Eleonora	4.90E+18	4.90E+17	Ephem	M ₈₆
354 Eleonora	1.97E+19	7.63E+18	Deflec	M ₉₇ [†]
354 Eleonora	9.32E+18	5.00E+18	Deflec	M ₉₇
354 Eleonora	1.20E+19	4.90E+18	Deflec	M ₉₇
354 Eleonora	4.39E+18	7.18E+18	Deflec	M ₉₇
356 Liguria	7.83E+18	1.50E+18	Ephem	M ₁₀₀
365 Corduba	5.84E+18	9.55E+17	Ephem	M ₉₃
372 Palma	5.32E+18	5.32E+17	Ephem	M ₈₆
372 Palma	2.76E+18	7.48E+18	Deflec	M ₉₇

Table A.1: Continued

Table A.1: Continued

# Designation	M	δM	Method	Refs.	# Designation	M	δM	Method	Refs.
375 Ursula	2.64E+18	5.67E+18	Deflec	M ₉₇	455 Bruchsalia	1.19E+18	1.19E+17	Ephem	M ₉₃
375 Ursula	7.14E+18	3.93E+18	Deflec	M ₉₇	469 Argentina	7.25E+18	6.25E+18	Ephem	M ₉₃ [†]
375 Ursula	7.44E+18	3.89E+18	Deflec	M ₉₇	469 Argentina	4.53E+18	1.76E+18	Ephem	M ₁₀₀
375 Ursula	1.88E+19	6.40E+18	Ephem	M ₁₀₀	471 Papagena	1.26E+19	7.16E+17	Ephem	M ₉₃ [†]
379 Huenna	3.83E+17	1.99E+16	BinImg	M ₇₃	471 Papagena	2.31E+18	4.88E+18	Deflec	M ₉₇
381 Myrrha	9.18E+18	7.96E+17	Ephem	M ₉₃	471 Papagena	2.08E+18	4.78E+18	Deflec	M ₉₇
386 Siegena	2.35E+19	4.18E+17	Ephem	M ₉₃ [†]	471 Papagena	6.52E+18	9.75E+18	Deflec	M ₉₇
386 Siegena	6.30E+18	9.57E+18	Deflec	M ₉₇	481 Emita	5.78E+18	1.45E+18	Ephem	M ₉₃
386 Siegena	7.80E+18	4.21E+18	Deflec	M ₉₇	485 Genua	1.36E+18	4.38E+17	Ephem	M ₉₃
386 Siegena	7.70E+18	4.17E+18	Deflec	M ₉₇	488 Kreusa	2.46E+18	2.46E+17	Ephem	M ₈₆
386 Siegena	1.16E+19	9.19E+18	Deflec	M ₉₇	488 Kreusa	1.24E+19	1.10E+19	Ephem	M ₉₃
387 Aquitania	5.32E+18	6.17E+17	Ephem	M ₉₃ [†]	488 Kreusa	1.60E+19	6.15E+18	Deflec	M ₉₇ [†]
387 Aquitania	1.90E+18	6.37E+17	Ephem	M ₁₀₀	488 Kreusa	2.29E+18	6.62E+17	Deflec	M ₉₇
404 Arsinoe	3.42E+18	3.03E+18	Ephem	M ₉₃	488 Kreusa	2.19E+18	6.68E+17	Deflec	M ₉₇
405 Thia	1.38E+18	1.38E+17	Ephem	M ₈₆	488 Kreusa	8.25E+17	1.37E+19	Deflec	M ₉₇
409 Aspasia	2.09E+18	5.97E+16	Ephem	M ₈₀ [†]	488 Kreusa	9.77E+18	2.70E+18	Ephem	M ₁₀₀ [†]
409 Aspasia	3.24E+18	3.24E+17	Ephem	M ₈₆ [†]	490 Veritas	9.32E+18	4.37E+18	Deflec	M ₉₇
409 Aspasia	8.37E+18	4.89E+18	Deflec	M ₉₇	490 Veritas	4.48E+18	2.11E+18	Deflec	M ₉₇
409 Aspasia	1.12E+19	3.29E+18	Deflec	M ₉₇	490 Veritas	4.59E+18	2.10E+18	Deflec	M ₉₇
409 Aspasia	1.24E+19	3.24E+18	Deflec	M ₉₇	490 Veritas	9.51E+18	5.62E+18	Deflec	M ₉₇
409 Aspasia	1.55E+19	5.50E+18	Deflec	M ₉₇	491 Carina	4.82E+18	1.95E+18	Ephem	M ₉₃
410 Chloris	6.91E+18	4.73E+18	Ephem	M ₉₃	503 Evelyn	2.85E+18	3.38E+17	Ephem	M ₉₃
410 Chloris	6.11E+18	9.21E+17	Ephem	M ₁₀₀	505 Cava	3.99E+18	3.84E+18	Ephem	M ₉₃
416 Vaticana	3.27E+18	3.10E+18	Ephem	M ₉₃	508 Princetonia	1.18E+18	7.65E+18	Deflec	M ₉₇
419 Aurelia	1.53E+18	1.53E+17	Ephem	M ₈₆	508 Princetonia	3.16E+18	1.95E+18	Deflec	M ₉₇
419 Aurelia	1.98E+18	1.10E+18	Ephem	M ₉₃	508 Princetonia	3.27E+18	1.94E+18	Deflec	M ₉₇
419 Aurelia	2.45E+18	7.44E+17	Ephem	M ₁₀₀	511 Davida	6.64E+19	5.57E+18	Deflec	M ₂₆ [†]
420 Bertholda	1.48E+19	9.15E+17	Ephem	M ₉₃	511 Davida	4.77E+19	4.77E+18	Deflec	M ₃₁
423 Diotima	4.47E+18	5.75E+18	Deflec	M ₉₇	511 Davida	4.77E+19	4.77E+18	Deflec	M ₄₂
423 Diotima	5.76E+18	4.15E+18	Deflec	M ₉₇	511 Davida	4.38E+19	1.99E+18	Deflec	M ₇₂
423 Diotima	6.74E+18	4.11E+18	Deflec	M ₉₇	511 Davida	2.45E+19	2.45E+18	Ephem	M ₈₆
423 Diotima	1.14E+19	8.07E+18	Deflec	M ₉₇	511 Davida	3.96E+19	8.09E+18	Ephem	M ₉₃
423 Diotima	7.56E+18	3.48E+18	Ephem	M ₁₀₀	511 Davida	3.77E+19	1.97E+18	Deflec	M ₉₅
433 Eros	6.69E+15	2.98E+12	FlyBy	M ₂₂	511 Davida	1.71E+19	1.18E+19	Ephem	M ₁₀₃
442 Eichsfeldia	1.95E+17	1.99E+16	Ephem	M ₉₃	511 Davida	2.42E+19	7.49E+18	Deflec	M ₉₇
444 Gyptis	7.16E+18	3.18E+18	Deflec	M ₂₆	511 Davida	2.77E+19	5.20E+18	Deflec	M ₉₇
444 Gyptis	1.25E+19	2.39E+18	Deflec	M ₄₂	511 Davida	2.61E+19	6.03E+18	Deflec	M ₉₇
444 Gyptis	1.59E+19	1.11E+19	Ephem	M ₉₃	511 Davida	2.21E+19	9.21E+18	Deflec	M ₉₇
444 Gyptis	1.12E+19	4.54E+18	Deflec	M ₉₇	511 Davida	1.81E+19	4.77E+18	Ephem	M ₁₀₀
444 Gyptis	1.22E+19	2.70E+18	Deflec	M ₉₇	516 Amherstia	1.43E+18	1.33E+18	Ephem	M ₉₃
444 Gyptis	1.12E+19	2.67E+18	Deflec	M ₉₇	532 Herculina	3.34E+19	5.57E+18	Deflec	M ₄₂ [†]
444 Gyptis	4.09E+18	6.20E+18	Deflec	M ₉₇	532 Herculina	1.09E+19	1.99E+17	Ephem	M ₈₀
445 Edna	3.47E+18	7.76E+17	Ephem	M ₉₃	532 Herculina	1.33E+19	1.33E+18	Ephem	M ₈₆
449 Hamburga	1.57E+18	1.40E+18	Ephem	M ₉₃	532 Herculina	5.76E+18	1.51E+18	Ephem	M ₉₃ [†]
451 Patientia	9.14E+18	9.14E+17	Ephem	M ₈₆	532 Herculina	1.46E+19	6.92E+18	Deflec	M ₉₂
451 Patientia	4.17E+19	2.94E+19	Ephem	M ₉₃	532 Herculina	9.89E+18	5.59E+18	Ephem	M ₁₀₃
451 Patientia	1.78E+19	6.82E+18	Deflec	M ₉₇	532 Herculina	1.25E+19	6.31E+18	Deflec	M ₉₇
451 Patientia	1.11E+19	6.40E+18	Deflec	M ₉₇	532 Herculina	1.81E+19	4.46E+18	Deflec	M ₉₇
451 Patientia	8.99E+18	8.02E+18	Deflec	M ₉₇	532 Herculina	1.75E+19	4.33E+18	Deflec	M ₉₇
451 Patientia	2.98E+19	7.36E+18	Ephem	M ₁₀₀ [†]	532 Herculina	2.26E+19	8.76E+18	Deflec	M ₉₇
					532 Herculina	5.75E+18	1.91E+18	Ephem	M ₁₀₀

Table A.1: Continued				
# Designation	M	δM	Method	Refs.
536 Merapi	2.15E+19	2.44E+19	Deflec	M ₉₇
536 Merapi	3.10E+19	2.55E+19	Deflec	M ₉₇
554 Peraga	6.59E+17	6.59E+16	Ephem	M ₈₆
554 Peraga	3.13E+18	2.54E+18	Ephem	M ₉₃ [†]
582 Olympia	4.28E+17	1.17E+18	Ephem	M ₉₃
584 Semiramis	8.23E+17	5.77E+17	Ephem	M ₉₃
602 Marianna	1.02E+19	4.77E+17	Ephem	M ₉₃
604 Tekmessa	1.45E+18	2.78E+17	Ephem	M ₉₃
617 Patroclus	1.36E+18	1.09E+17	BinImg	M ₅₉
624 Hektor	9.95E+18	1.20E+17	BinImg	M ₁₀₆
626 Notburga	5.35E+18	6.52E+18	Ephem	M ₉₃ [†]
626 Notburga	3.24E+18	1.30E+18	Ephem	M ₁₀₀
654 Zelinda	1.35E+18	1.35E+17	Ephem	M ₈₆
665 Sabine	6.98E+17	3.98E+17	Ephem	M ₉₃
675 Ludmilla	1.20E+19	2.39E+18	Ephem	M ₉₃
679 Pax	7.14E+17	1.99E+17	Ephem	M ₉₃
680 Genoveva	2.69E+18	3.98E+16	Ephem	M ₉₃
690 Wratislavia	1.28E+19	2.78E+17	Ephem	M ₉₃
702 Alauda	1.36E+19	1.12E+19	Ephem	M ₉₃ [†]
702 Alauda	6.06E+18	3.60E+18	BinImg	M ₉₈
702 Alauda	3.45E+18	7.48E+18	Deflec	M ₉₇ [†]
702 Alauda	1.17E+18	7.44E+18	Deflec	M ₉₇ [†]
702 Alauda	2.46E+19	1.06E+19	Deflec	M ₉₇ [†]
702 Alauda	2.20E+19	4.95E+18	Ephem	M ₁₀₀ [†]
704 Interamnia	7.36E+19	3.38E+19	Deflec	M ₃ [†]
704 Interamnia	1.23E+20	1.31E+20	Deflec	M ₁₈
704 Interamnia	2.59E+19	1.39E+18	Deflec	M ₂₈
704 Interamnia	7.00E+19	1.85E+19	Deflec	M ₂₆ [†]
704 Interamnia	1.61E+19	8.35E+18	Deflec	M ₃₁ [†]
704 Interamnia	1.61E+19	8.35E+18	Deflec	M ₄₂ [†]
704 Interamnia	3.70E+19	2.19E+18	Deflec	M ₇₂
704 Interamnia	1.13E+20	3.18E+19	Deflec	M ₇₈ [†]
704 Interamnia	3.23E+19	1.99E+17	Ephem	M ₈₀
704 Interamnia	3.69E+19	3.69E+18	Ephem	M ₈₆
704 Interamnia	2.66E+19	1.09E+19	Deflec	M ₉₂
704 Interamnia	3.88E+19	1.77E+18	Deflec	M ₉₅
704 Interamnia	3.97E+19	1.31E+19	Ephem	M ₁₀₃
704 Interamnia	2.25E+19	6.62E+18	Deflec	M ₉₇
704 Interamnia	3.34E+19	5.16E+18	Deflec	M ₉₇
704 Interamnia	3.13E+19	5.19E+18	Deflec	M ₉₇
704 Interamnia	3.88E+19	7.50E+18	Deflec	M ₉₇
704 Interamnia	3.82E+19	3.58E+18	Ephem	M ₁₀₀
720 Bohlinia	1.19E+19	1.99E+18	Deflec	M ₁₈ [†]
720 Bohlinia	5.97E+16	7.96E+15	Deflec	M ₂₈
720 Bohlinia	2.78E+18	9.95E+17	Deflec	M ₇₈ [†]
735 Marghanna	2.15E+18	6.76E+17	Ephem	M ₉₃
739 Mandeville	1.16E+18	1.07E+18	Ephem	M ₉₃

Table A.1: Continued				
# Designation	M	δM	Method	Refs.
747 Winchester	7.96E+15	3.98E+15	Ephem	M ₈₀ [†]
747 Winchester	2.94E+18	2.94E+17	Ephem	M ₈₆
747 Winchester	1.20E+19	4.59E+18	Ephem	M ₉₃
747 Winchester	8.10E+18	5.86E+18	Deflec	M ₉₇
747 Winchester	4.31E+18	4.65E+18	Deflec	M ₉₇
747 Winchester	5.25E+18	4.47E+18	Deflec	M ₉₇
747 Winchester	1.33E+19	1.47E+18	Ephem	M ₁₀₀ [†]
751 Faina	7.07E+18	5.17E+17	Ephem	M ₉₃ [†]
751 Faina	3.27E+18	5.83E+17	Ephem	M ₁₀₀
758 Mancunia	9.31E+17	7.96E+16	Ephem	M ₉₃
760 Massinga	1.33E+18	1.32E+18	Ephem	M ₉₃
762 Pulcova	2.59E+18	3.98E+17	BinImg	M ₃₂ [†]
762 Pulcova	1.40E+18	9.94E+16	BinImg	M ₇₅
762 Pulcova	1.25E+19	7.46E+18	Deflec	M ₉₇ [†]
762 Pulcova	3.15E+19	7.45E+18	Deflec	M ₉₇ [†]
762 Pulcova	1.11E+18	4.42E+17	Ephem	M ₁₀₀ [†]
769 Tatjana	6.31E+18	6.37E+17	Ephem	M ₉₃
776 Berbericia	5.46E+18	4.70E+18	Deflec	M ₉₇
776 Berbericia	2.39E+16	3.26E+18	Deflec	M ₉₇
776 Berbericia	3.08E+17	3.24E+18	Deflec	M ₉₇
776 Berbericia	6.28E+18	7.31E+18	Deflec	M ₉₇
784 Pickeringia	3.74E+18	3.18E+17	Ephem	M ₉₃
786 Bredichina	2.82E+18	2.79E+18	Ephem	M ₉₃
790 Pretoria	4.86E+18	4.76E+18	Deflec	M ₉₇
790 Pretoria	4.30E+18	4.73E+18	Deflec	M ₉₇
804 Hispania	9.94E+18	7.96E+18	Deflec	M ₃
804 Hispania	4.02E+18	8.55E+17	Deflec	M ₇₂
804 Hispania	5.00E+18	3.62E+18	Ephem	M ₉₃
804 Hispania	3.48E+18	7.96E+17	Deflec	M ₉₅
804 Hispania	8.56E+18	4.71E+18	Deflec	M ₉₇
804 Hispania	5.03E+18	2.79E+18	Deflec	M ₉₇
804 Hispania	5.57E+18	2.77E+18	Deflec	M ₉₇
804 Hispania	8.65E+18	3.72E+18	Deflec	M ₉₇
804 Hispania	6.15E+18	2.39E+18	Ephem	M ₁₀₀
809 Lundia	9.27E+14	3.09E+14	PheMu	M ₇₉
854 Frostia	1.06E+15	9.50E+14	PheMu	M ₅₀
895 Helio	6.88E+18	1.39E+19	Deflec	M ₉₇
895 Helio	7.75E+18	3.43E+18	Deflec	M ₉₇
895 Helio	8.21E+18	3.41E+18	Deflec	M ₉₇
895 Helio	2.80E+19	1.37E+19	Deflec	M ₉₇
914 Palisana	2.35E+18	2.39E+17	Ephem	M ₉₃
949 Hel	1.73E+18	6.17E+17	Ephem	M ₉₃
1013 Tombecka	1.71E+17	1.43E+18	Ephem	M ₉₃
1015 Christa	4.77E+18	6.76E+17	Ephem	M ₉₃
1021 Flammario	5.14E+18	1.19E+17	Ephem	M ₉₃
1036 Ganymed	1.67E+17	3.18E+17	Ephem	M ₉₃
1089 Tama	8.90E+14	3.20E+14	PheMu	M ₅₀
1171 Rusthawelia	1.81E+18	1.99E+17	Ephem	M ₉₃
1313 Berna	2.25E+15	2.00E+15	PheMu	M ₅₀

Table A.1: Continued

# Designation	M	δM	Method	Refs.
1669 Dagmar	4.18E+19	3.18E+19	Deflec	M ₁₈ [†]
1669 Dagmar	3.98E+16	7.96E+15	Deflec	M ₂₈
1669 Dagmar	2.78E+19	3.98E+18	Deflec	M ₇₈ [†]
1686 De Sitter	6.76E+18	3.18E+18	Deflec	M ₇₈
3169 Ostro	1.86E+14	6.20E+13	PheMu	M ₆₆
3671 Dionysus	8.38E+11	2.79E+11	PheMu	M ₅₅
3749 Balam	5.09E+14	1.99E+13	BinImg	M ₇₃
4492 Debussy	3.33E+14	3.00E+14	PheMu	M ₅₀
5381 Sekhmet	1.04E+12	3.46E+11	BinRad	M ₃₅
25143 Itokawa	3.50E+10	1.05E+09	FlyBy	M ₆₀
26308 1998 SM165	6.78E+18	2.40E+18	BinImg	M ₄₀
35107 1991 VH	1.40E+12	1.40E+11	BinRad	M ₁₀₈
42355 Typhon	9.49E+17	5.20E+16	BinImg	M ₇₆
47171 1999 TC36	1.39E+19	2.50E+18	BinImg	M ₄₀
47171 1999 TC36	1.44E+19	2.20E+18	BinImg	M ₅₄
50000 Quaoar	1.60E+21	3.00E+20	BinImg	M ₉₀
58534 Logos	2.70E+17	3.00E+16	BinImg	M ₃₈
65489 Ceto	5.41E+18	4.20E+17	BinImg	M ₆₈
65803 Didymos	5.24E+11	5.24E+10	BinRad	M ₉₁
66063 1998 RO1	3.60E+11	1.80E+11	PheMu	M ₈₃
66391 1999 KW4	2.35E+12	9.94E+10	BinRad	M ₆₁
66652 Borasisi	3.75E+18	4.00E+17	BinImg	M ₄₁
88611 2001 QT297	3.30E+18	3.00E+18	BinImg	M ₃₆ [†]
88611 2001 QT297	2.36E+18	1.00E+16	BinImg	M ₄₆
90482 Orcus	6.32E+20	1.00E+18	BinImg	M ₈₇
90482 Orcus	6.41E+20	5.00E+18	BinImg	M ₉₄
134340 Pluto	1.30E+22	7.00E+19	BinImg	M ₅₃
134860 2000 OJ67	2.14E+18	1.10E+17	BinImg	M ₈₂
136108 Haumea	4.20E+21	1.00E+20	BinImg	M ₄₄ [†]
136108 Haumea	4.01E+21	4.00E+19	BinImg	M ₈₁
136199 Eris	1.66E+22	2.00E+20	BinImg	M ₆₉
136617 1994 CC	2.59E+11	1.30E+10	BinRad	M ₉₆
153591 2001 SN263	9.17E+12	2.24E+10	BinRad	M ₉₆
164121 2003 YT1	1.27E+12	3.90E+11	BinRad	M ₅₂
175706 1996 FG3	4.27E+12	1.42E+12	PheMu	M ₈₃
185851 2000 DP107	4.60E+11	5.00E+10	BinRad	M ₃₄
276049 2002 CE26	1.95E+13	2.50E+12	BinRad	M ₅₈
311066 2004 DC	3.57E+10	3.57E+09	BinRad	M ₇₇

Table A.1: Continued

# Designation	M	δM	Method	Refs.
1999 OJ4	3.91E+17	2.20E+16	BinImg	M ₈₂
2000 QL251	3.11E+18	5.10E+16	BinImg	M ₈₂
2000 UG11	9.35E+09	1.59E+09	BinRad	M ₃₂
2001 QC298	1.08E+19	7.00E+17	BinImg	M ₄₀
2001 XR254	4.00E+18	1.70E+17	BinImg	M ₈₂
2003 QY90	1.01E+18	7.85E+17	BinImg	M ₅₇
2003 TJ58	2.25E+17	1.50E+16	BinImg	M ₈₂
2004 PB108	9.68E+18	5.70E+17	BinImg	M ₈₂
1P/Halley	3.20E+14	1.20E+14	CNGF	M ₈₅
2P/Encke	9.20E+13	5.80E+13	CNGF	M ₈₅
6P/dArest	2.80E+12	8.00E+11	CNGF	M ₈₅
9P/Tempell	5.80E+13	1.60E+13	CNGF	M ₆₄ [†]
9P/Tempell	4.50E+13	4.85E+13	FlyBy	M ₆₇
9P/Tempell	2.30E+13	1.60E+13	CNGF	M ₈₅ [†]
10P/Tempel2	3.50E+14	1.50E+14	CNGF	M ₈₅
19P/Borrelly	2.70E+12	2.10E+12	CNGF	M ₈₅
22P/Kopff	5.30E+12	2.20E+12	CNGF	M ₈₅
45P/H-M-P	1.90E+11	3.50E+11	CNGF	M ₈₅
46P/Wirtanen	3.30E+11	2.30E+11	CNGF	M ₈₅
67P/C-G	1.50E+13	6.00E+12	CNGF	M ₈₅
81P/Wild2	8.10E+12	8.10E+11	CNGF	M ₈₅
SL9	1.53E+12	1.53E+11	BkUp	M ₄

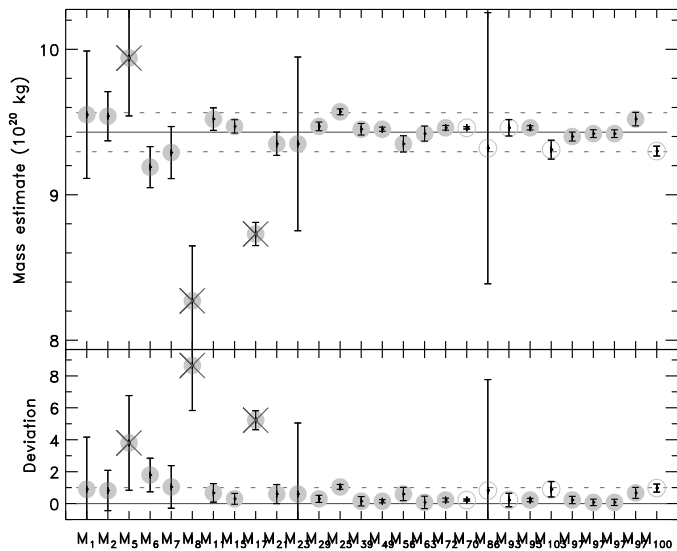


Figure A.1: Mass estimates for (1) Ceres.

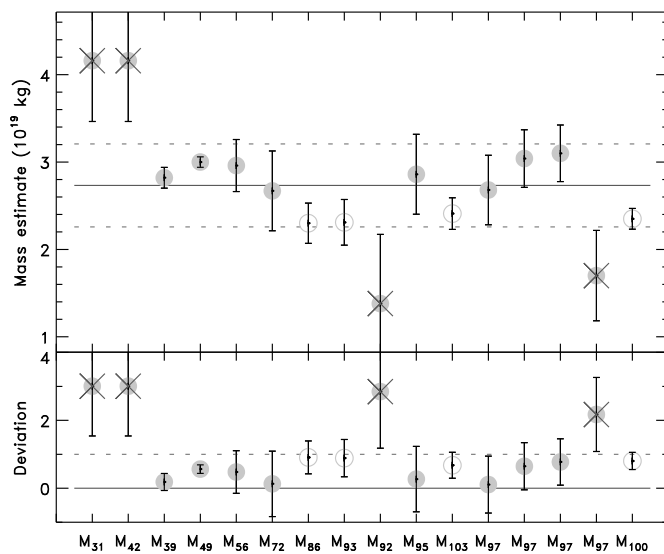


Figure A.3: Mass estimates for (3) Juno.

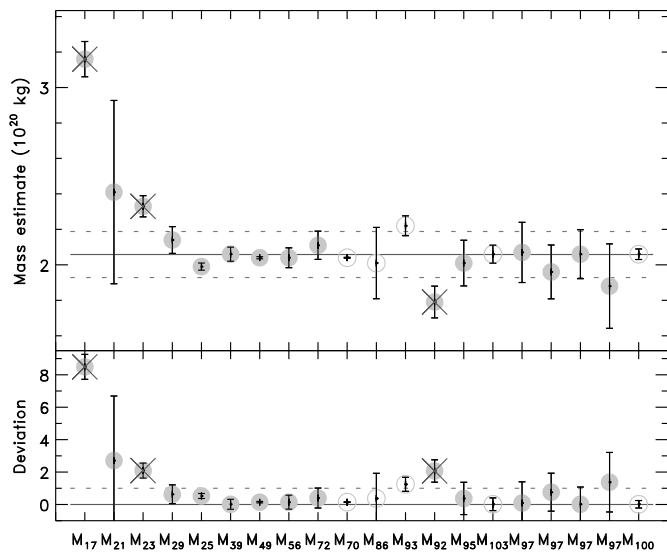


Figure A.2: Mass estimates for (2) Pallas.

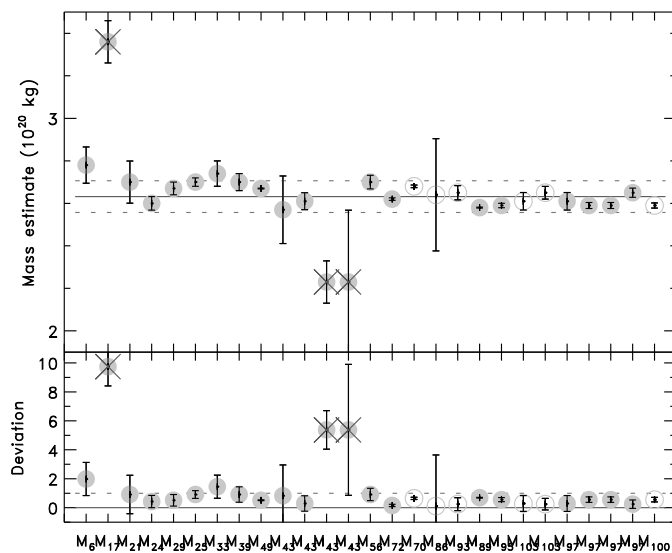


Figure A.4: Mass estimates for (4) Vesta.

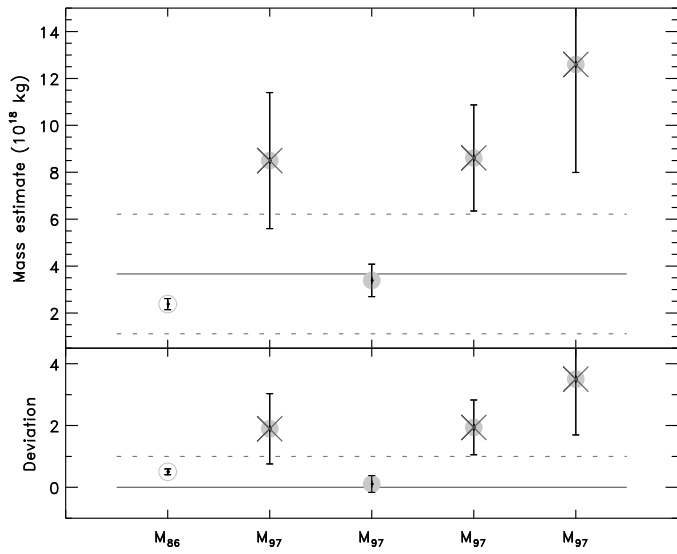


Figure A.5: Mass estimates for (5) Astraea.

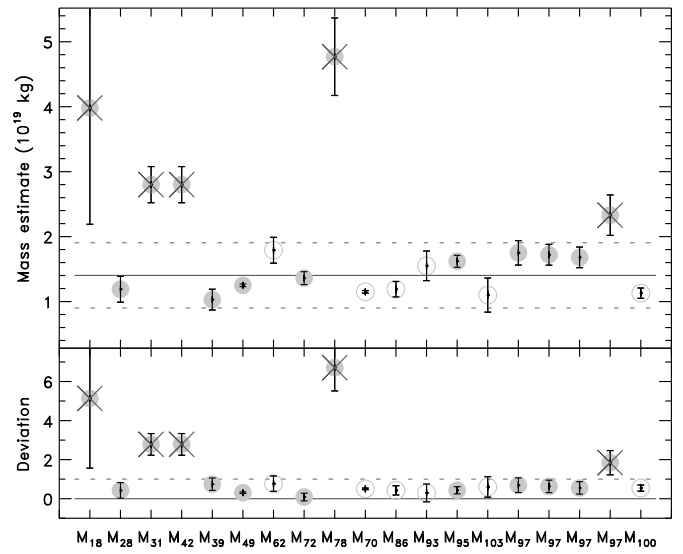


Figure A.7: Mass estimates for (7) Iris.

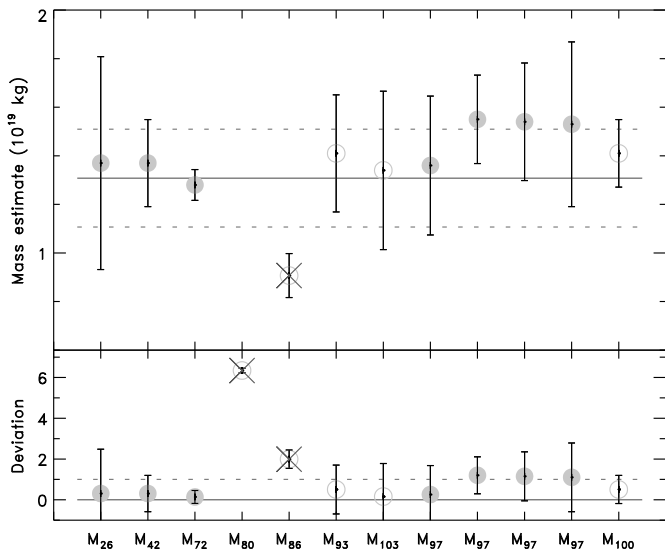


Figure A.6: Mass estimates for (6) Hebe.

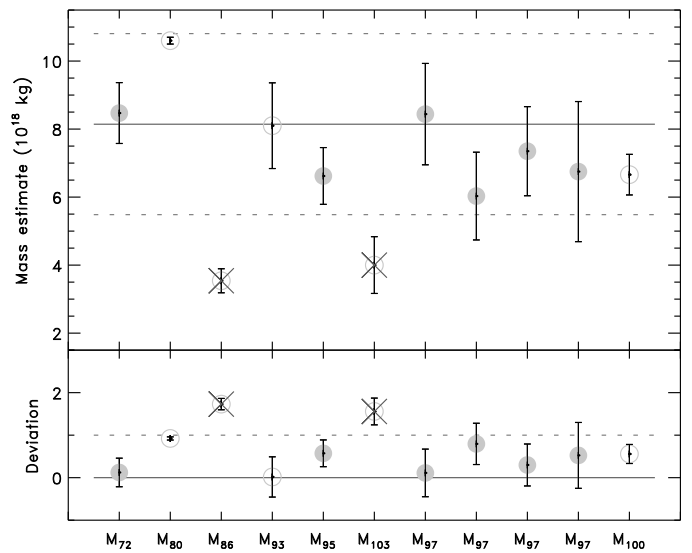


Figure A.8: Mass estimates for (8) Flora.

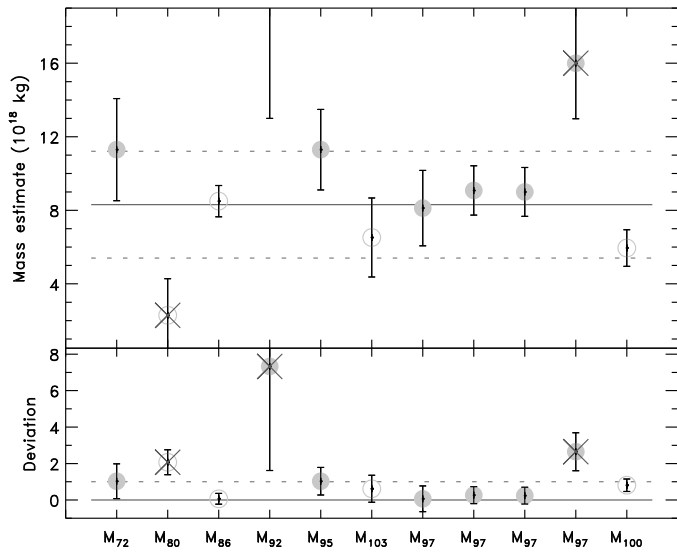


Figure A.9: Mass estimates for (9) Metis.

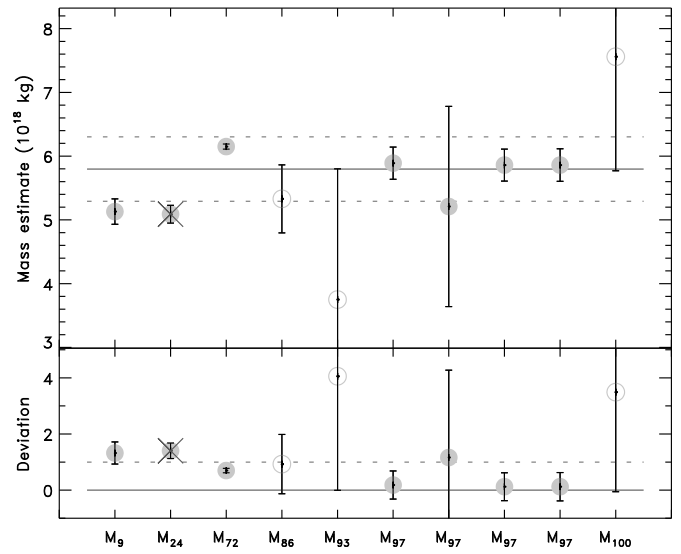


Figure A.11: Mass estimates for (11) Parthenope.

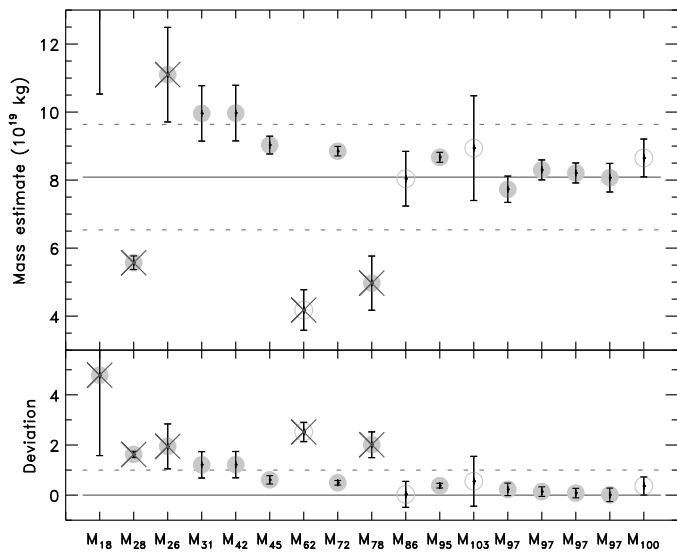


Figure A.10: Mass estimates for (10) Hygiea.

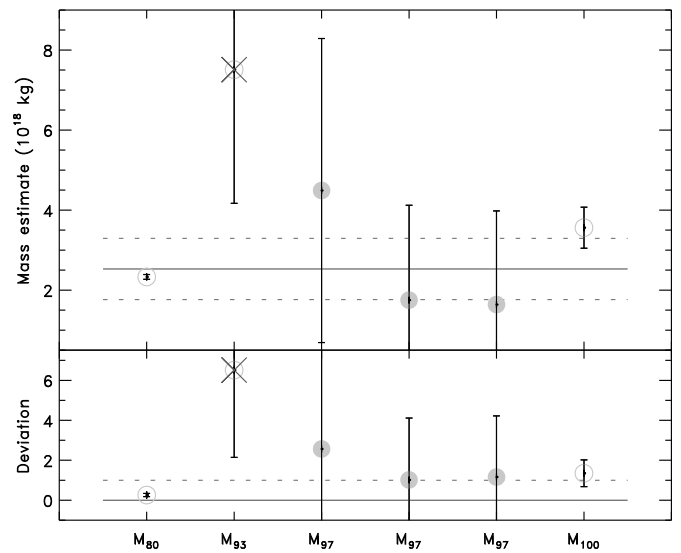


Figure A.12: Mass estimates for (12) Victoria.

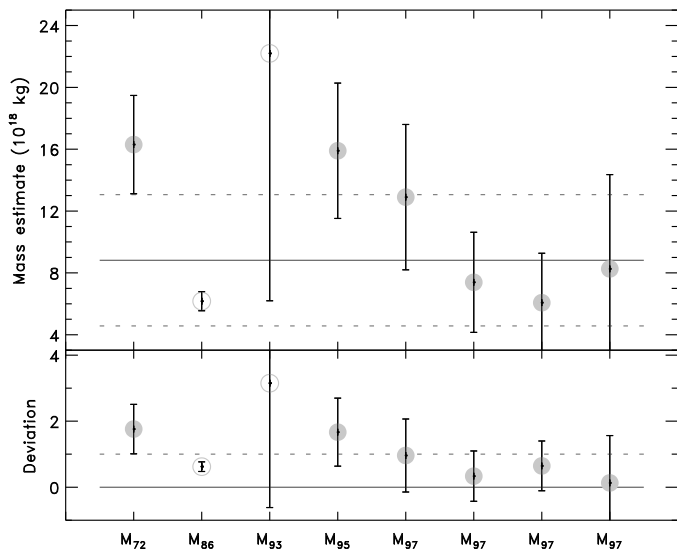


Figure A.13: Mass estimates for (13) Egeria.

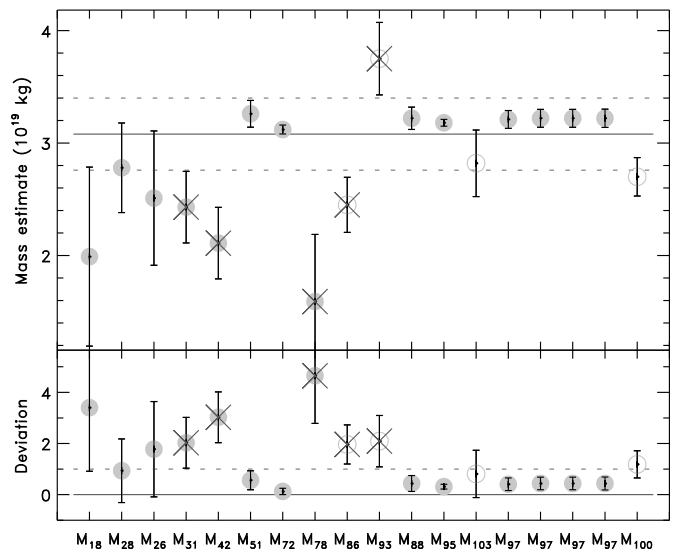


Figure A.15: Mass estimates for (15) Eunomia.

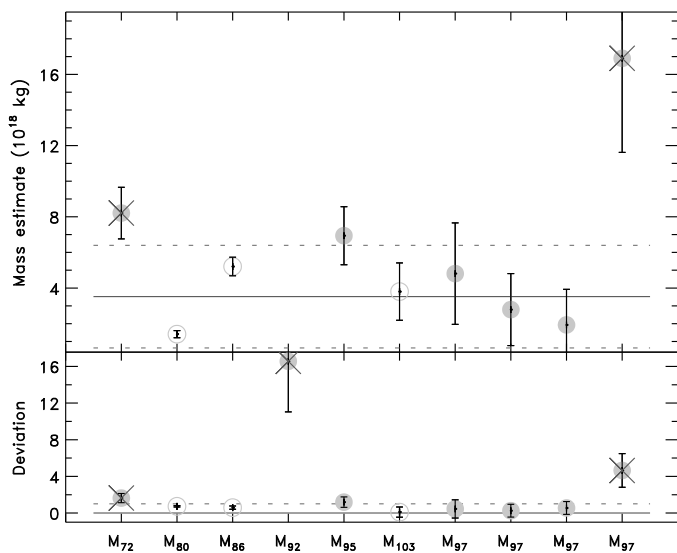


Figure A.14: Mass estimates for (14) Irene.

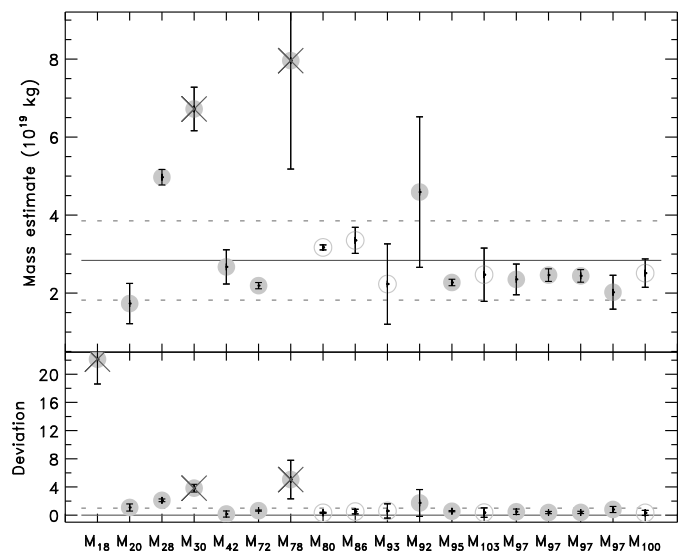


Figure A.16: Mass estimates for (16) Psyche.

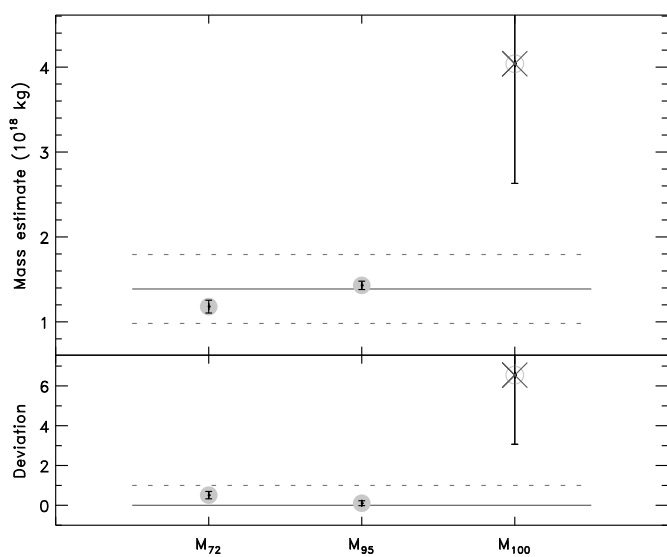


Figure A.17: Mass estimates for (17) Thetis.

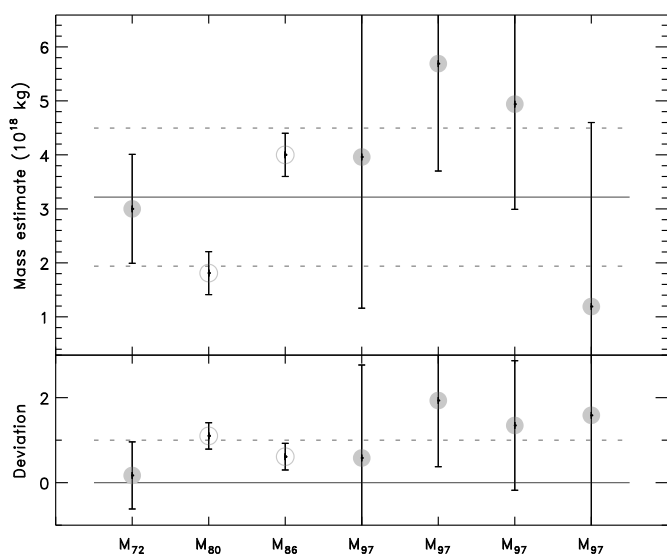


Figure A.18: Mass estimates for (18) Melpomene.

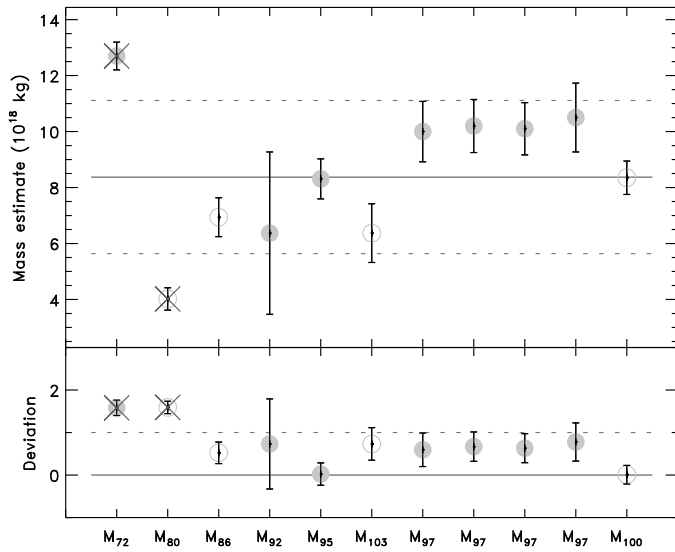


Figure A.19: Mass estimates for (19) Fortuna.

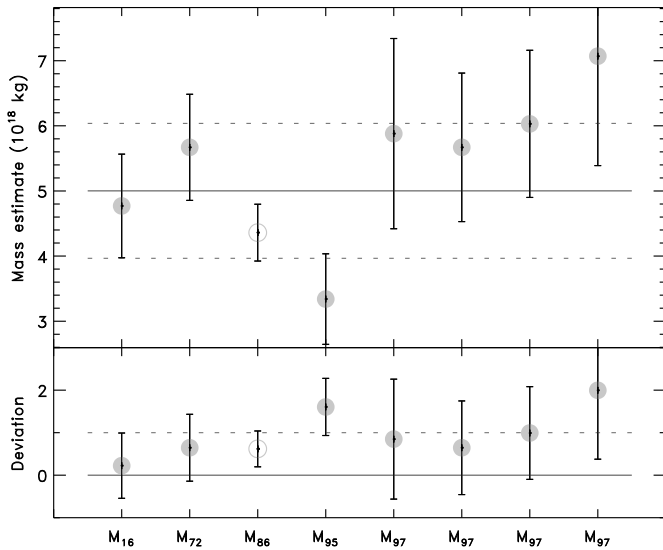


Figure A.20: Mass estimates for (20) Massalia.

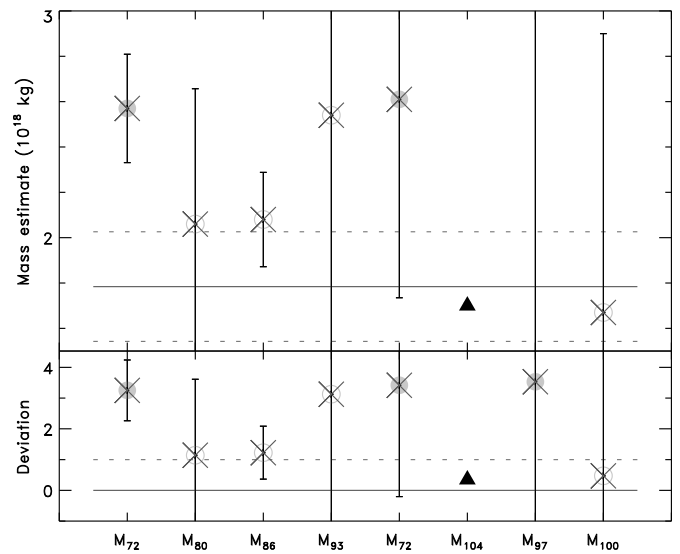


Figure A.21: Mass estimates for (21) Lutetia. Only the flyby estimate (M_{104}) is used here.

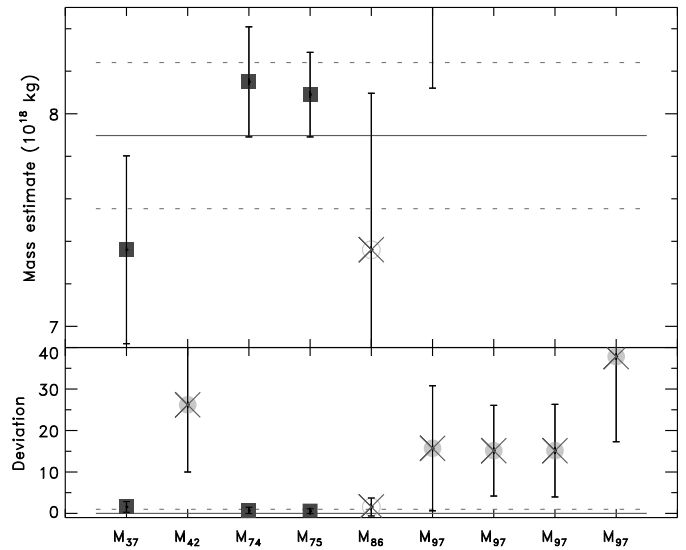


Figure A.22: Mass estimates for (22) Kalliope. Only the estimates based on direct imaging of the system are used here (M_{37} , M_{74} , and M_{75}). Apart from M_{86} , all the indirect determinations are far from the solution derived from the analysis of the satellite's orbit

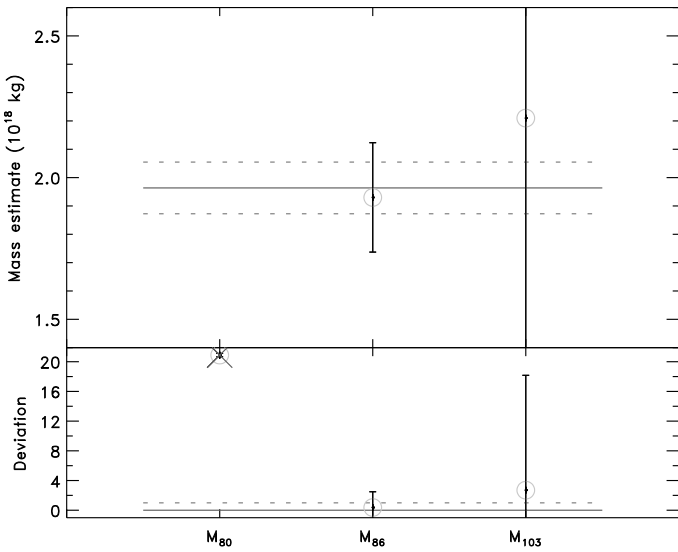


Figure A.23: Mass estimates for (23) Thalia. The mass estimate from M₈₀ gives an unrealistic density of 0.09 ± 0.03 if used alone, and is therefore discarded.

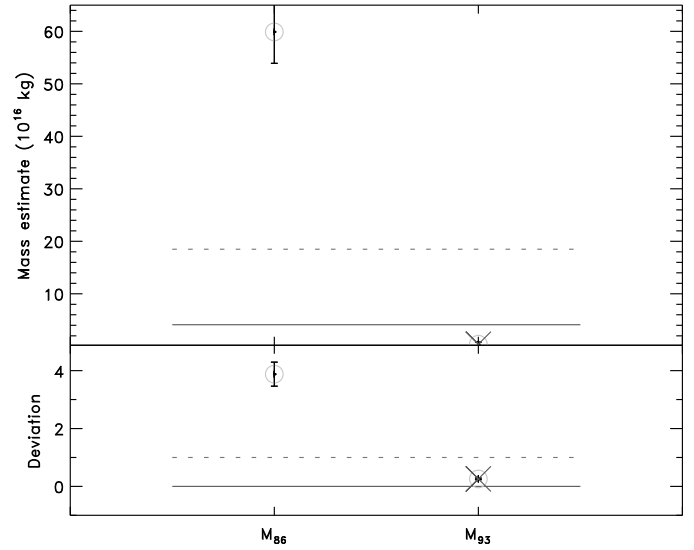


Figure A.25: Mass estimates for (25) Phocaea. Although the mass estimate from M₈₆ is outside the weighted average range, this is due to the very small uncertainty associated with the determination from M₉₃ which gives an unrealistic density of 0.02 ± 0.02 if used alone. M₉₃ estimate is therefore discarded.

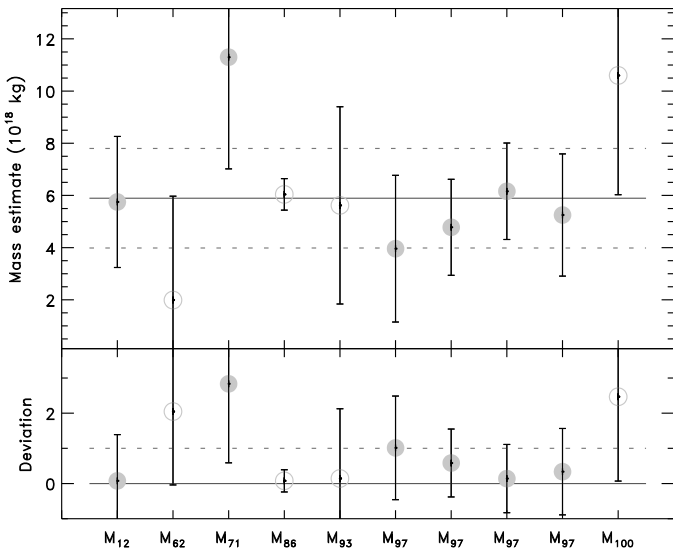


Figure A.24: Mass estimates for (24) Themis.

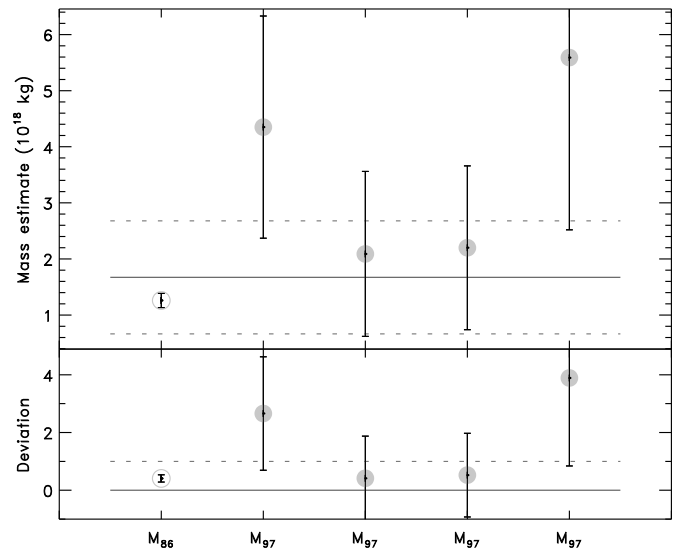


Figure A.26: Mass estimates for (27) Euterpe.

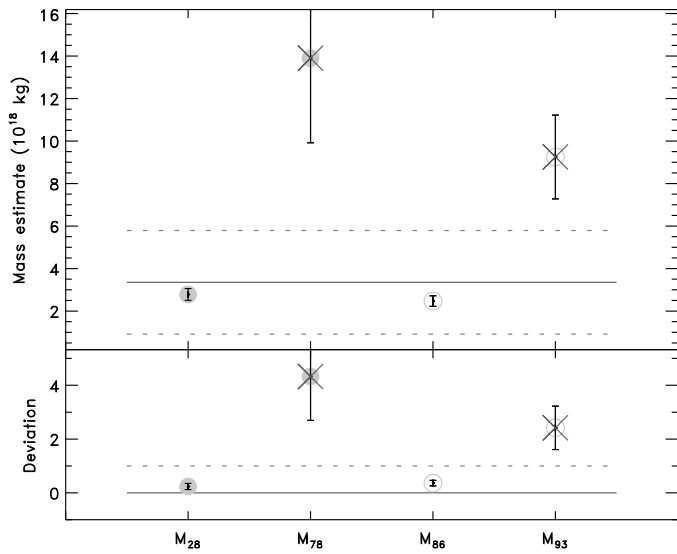


Figure A.27: Mass estimates for (28) Bellona. The mass estimates from M_{78} and M_{93} give unrealistic densities of 18 ± 7 and 12 ± 4 respectively, and are therefore discarded.

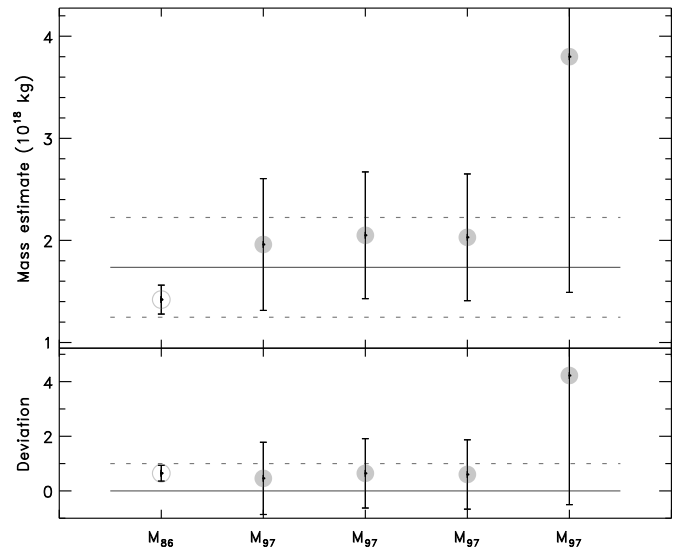


Figure A.29: Mass estimates for (30) Urania.

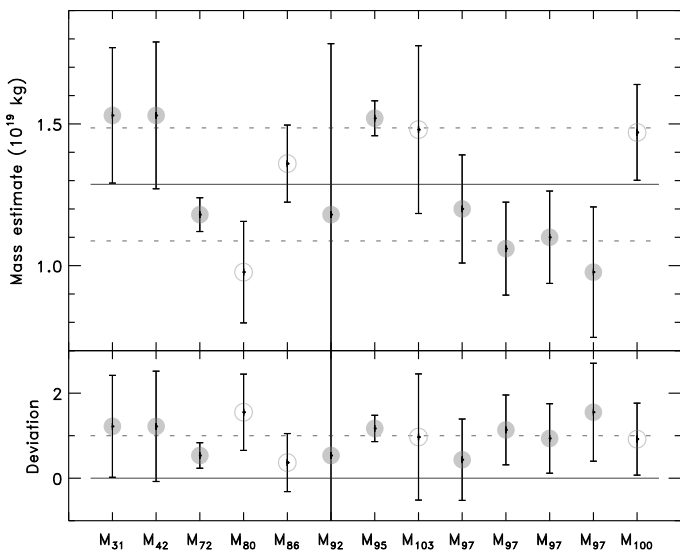


Figure A.28: Mass estimates for (29) Amphitrite.

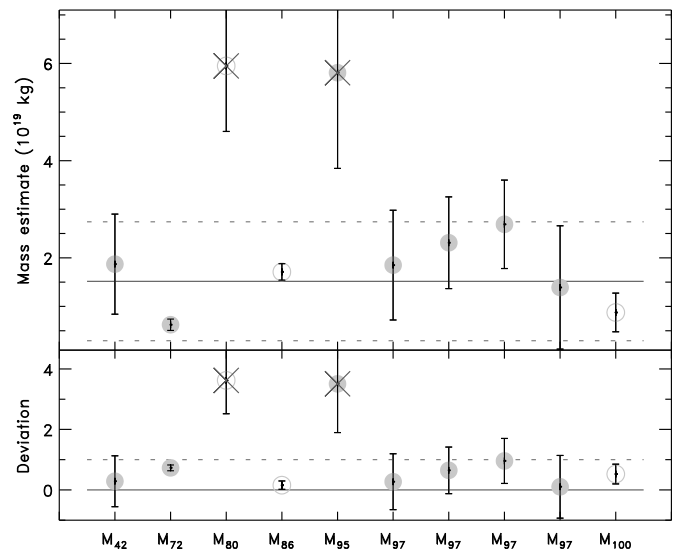


Figure A.30: Mass estimates for (31) Euphrosyne.

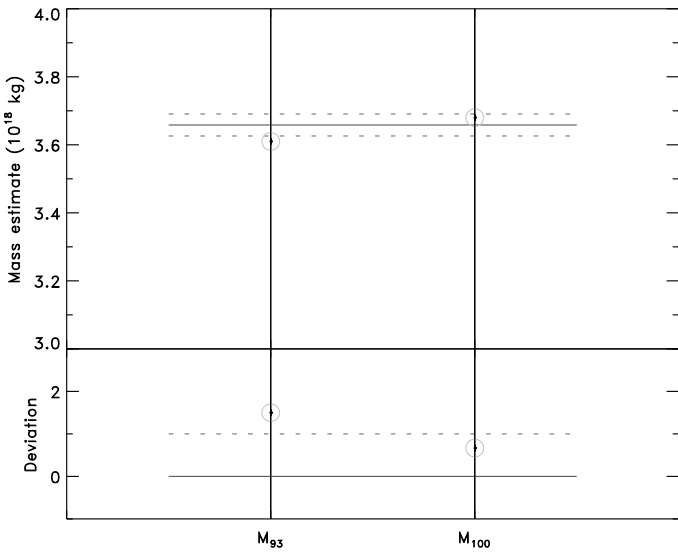


Figure A.31: Mass estimates for (34) Circe.

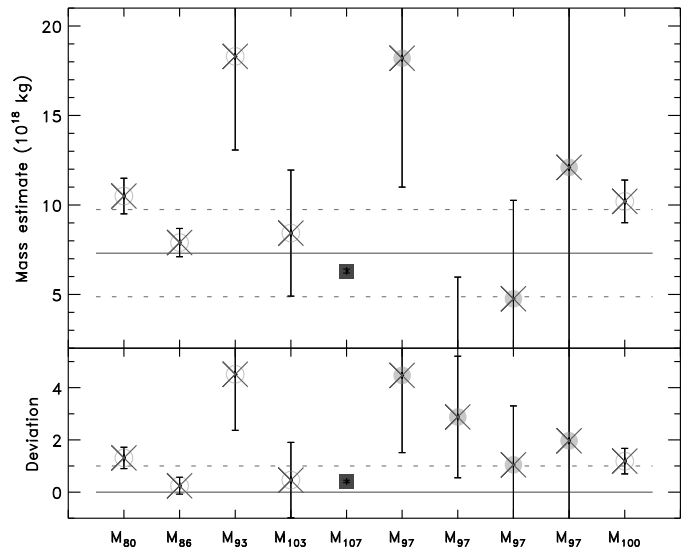


Figure A.33: Mass estimates for (41) Daphne.

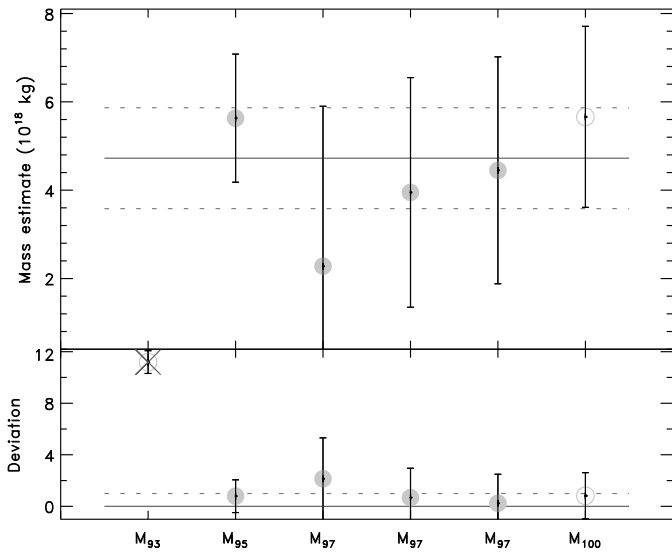


Figure A.32: Mass estimates for (39) Laetitia. The mass estimate from M₉₃ gives an unrealistic density of 8.9 ± 0.9 if used alone, and is therefore discarded.

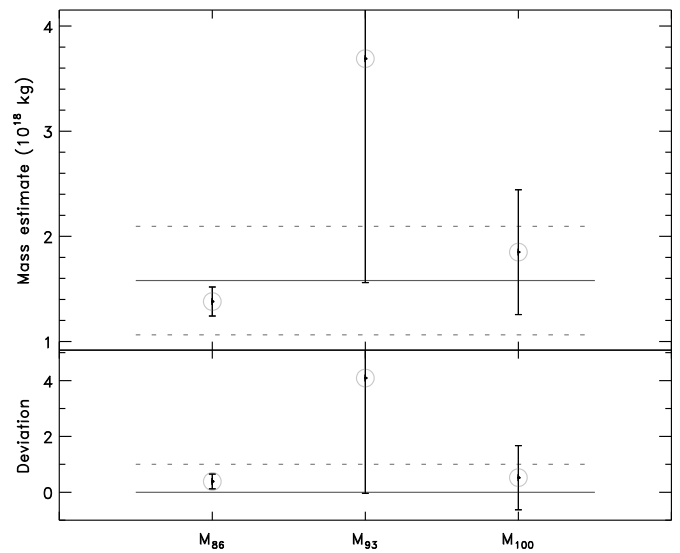


Figure A.34: Mass estimates for (42) Isis.

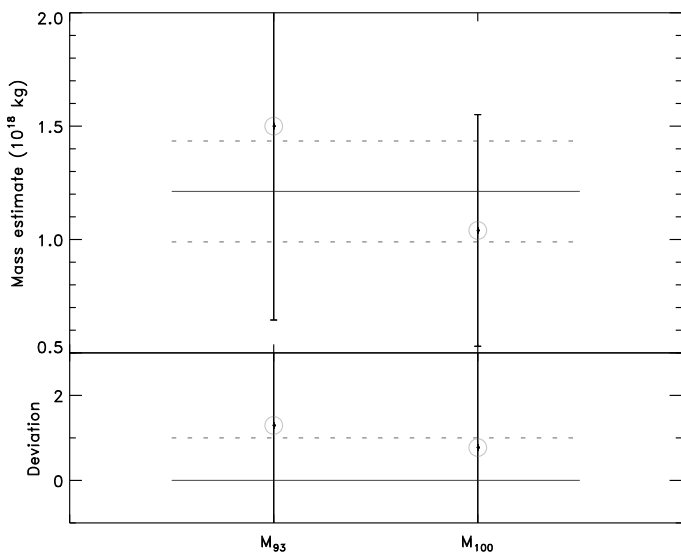


Figure A.35: Mass estimates for (43) Ariadne.

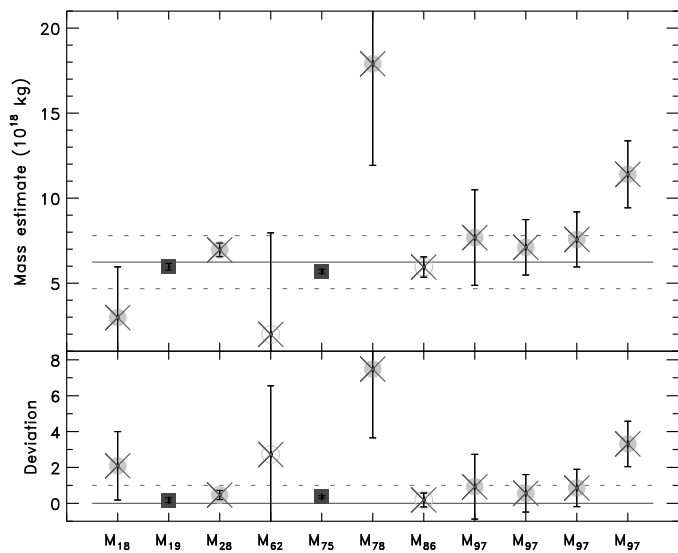


Figure A.36: Mass estimates for (45) Eugenia. Only the mass estimates based on direct imaging of the system are used here (M_{19} and M_{75}).

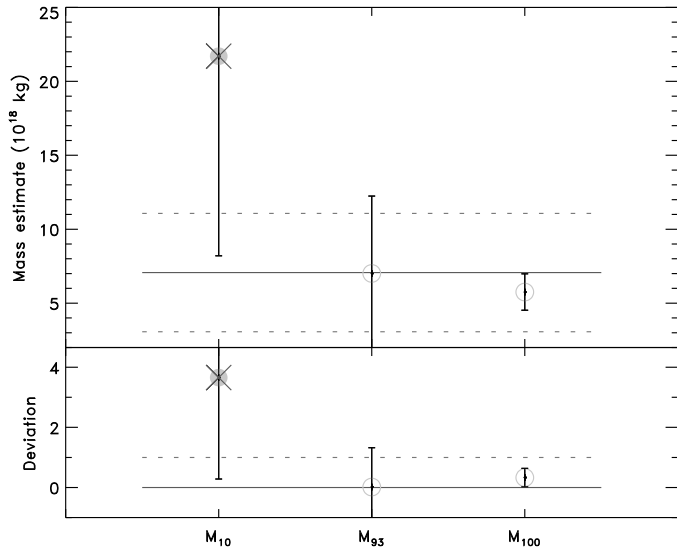


Figure A.37: Mass estimates for (46) Hestia. The mass estimate from M₁₀ gives an unrealistic density of 19 ± 12 if used alone, and is therefore discarded.

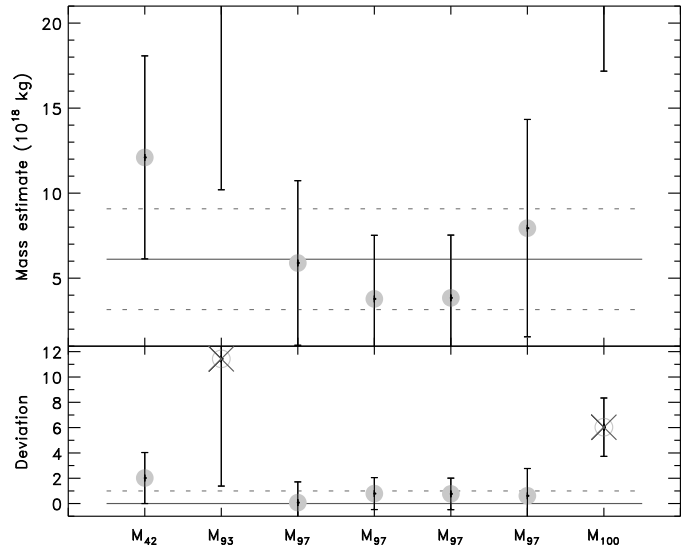


Figure A.39: Mass estimates for (48) Doris.

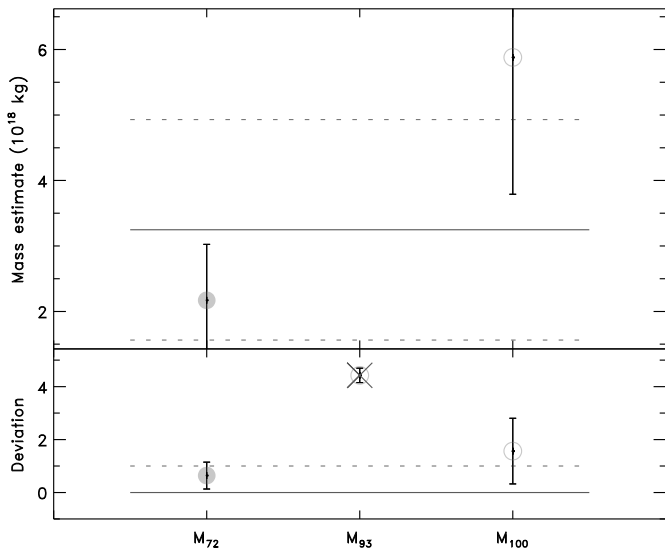


Figure A.38: Mass estimates for (47) Aglaja. The mass estimate from M₉₃ gives an unrealistic density of 10.3 ± 4.3 if used alone, and is therefore discarded.

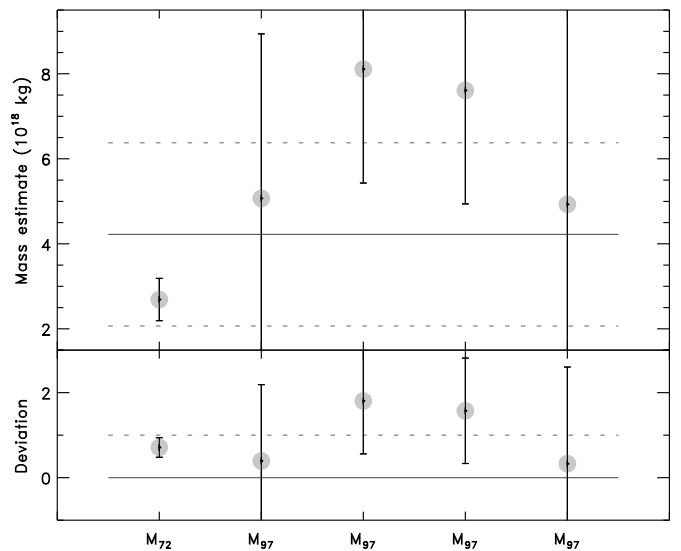


Figure A.40: Mass estimates for (49) Pales.

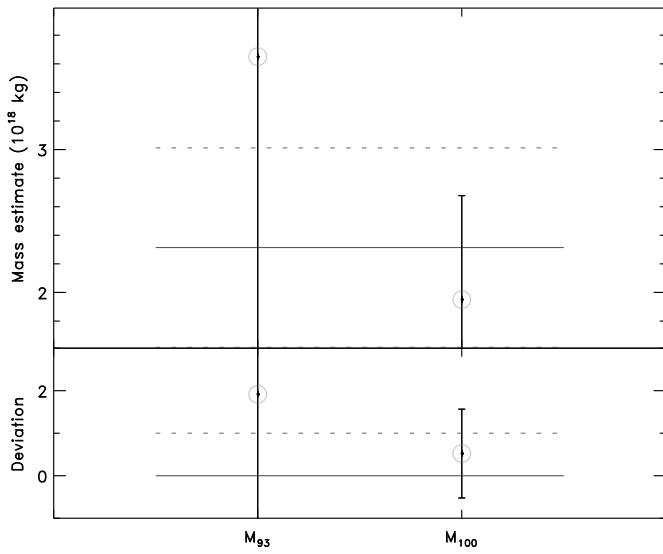


Figure A.41: Mass estimates for (50) Virginia.

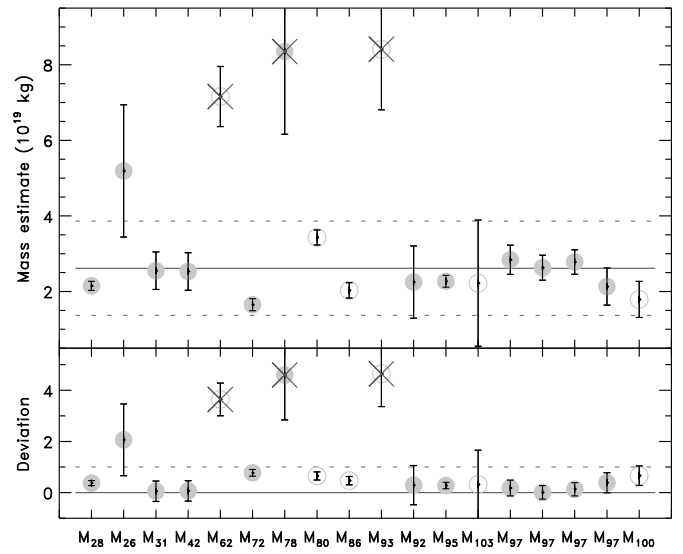


Figure A.43: Mass estimates for (52) Europa.

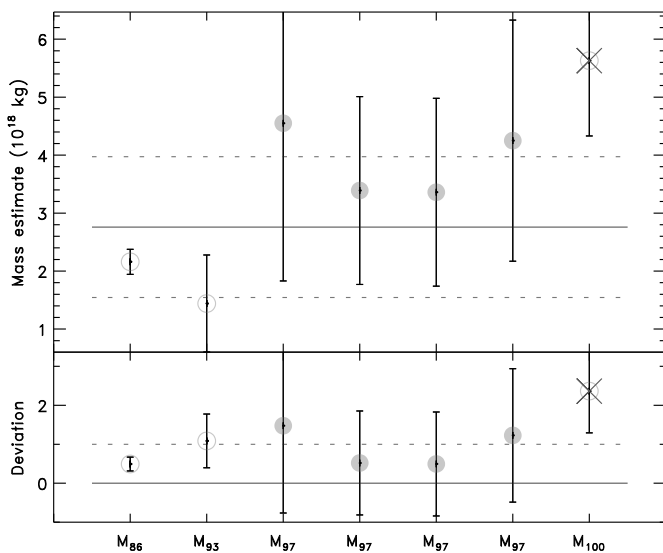


Figure A.42: Mass estimates for (51) Nemausa.

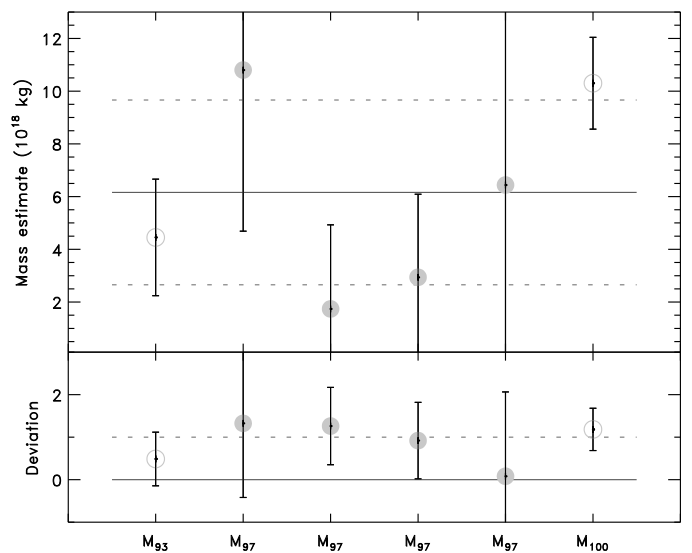


Figure A.44: Mass estimates for (54) Alexandra.

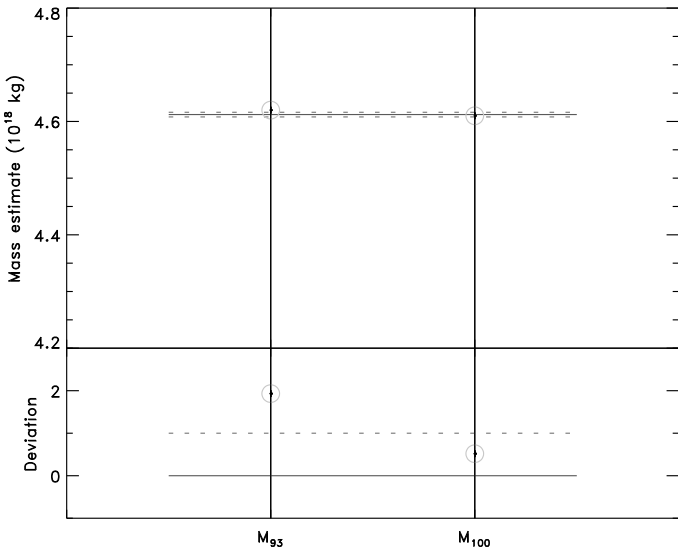


Figure A.45: Mass estimates for (56) Melete.

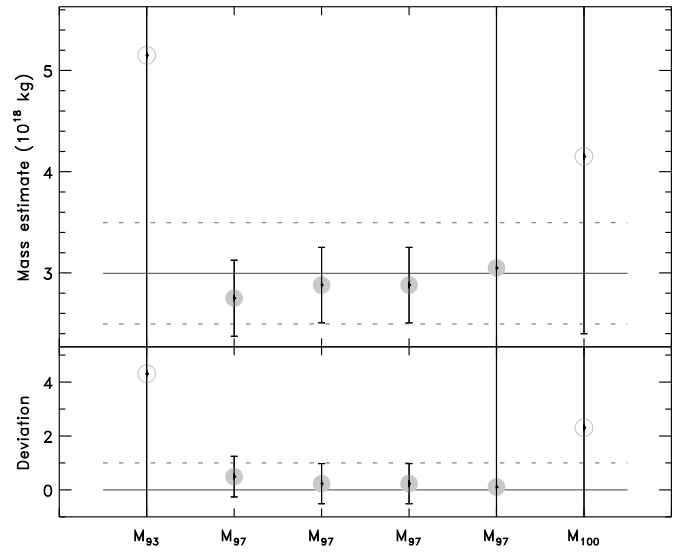


Figure A.47: Mass estimates for (59) Elpis.

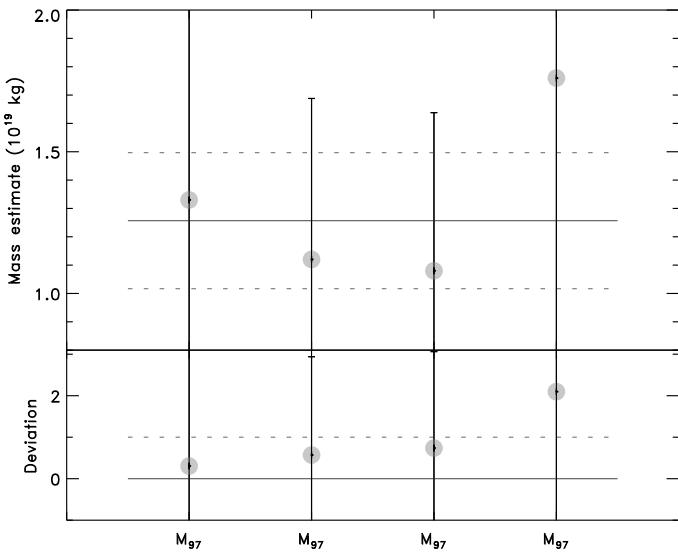


Figure A.46: Mass estimates for (57) Mnemosyne.

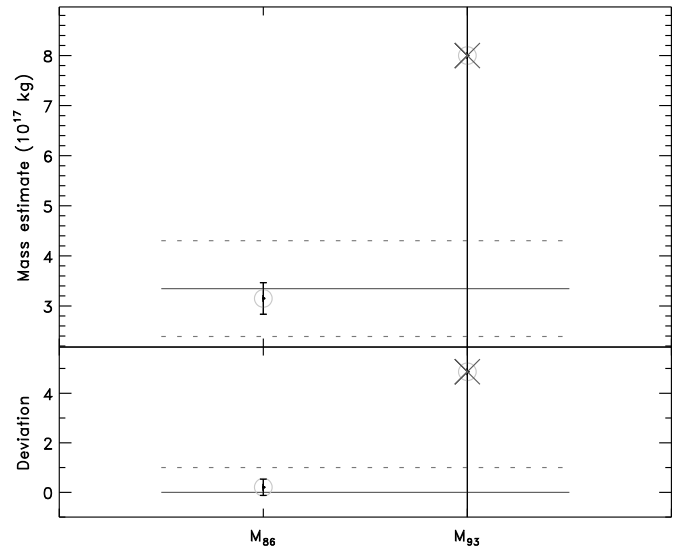


Figure A.48: Mass estimates for (60) Echo. The mass estimate from M_{93} gives a low-constrained density of 6.8 ± 6.4 if used alone. Only the estimate from M_{86} is used.

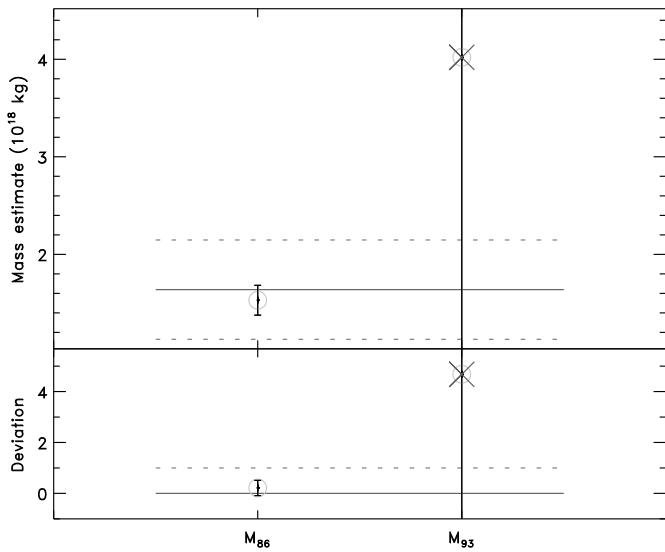


Figure A.49: Mass estimates for (63) Aousia. The mass estimate from M_{93} gives a low-constrained density of 9.7 ± 8.3 if used alone. Only the estimate from M_{86} is used.

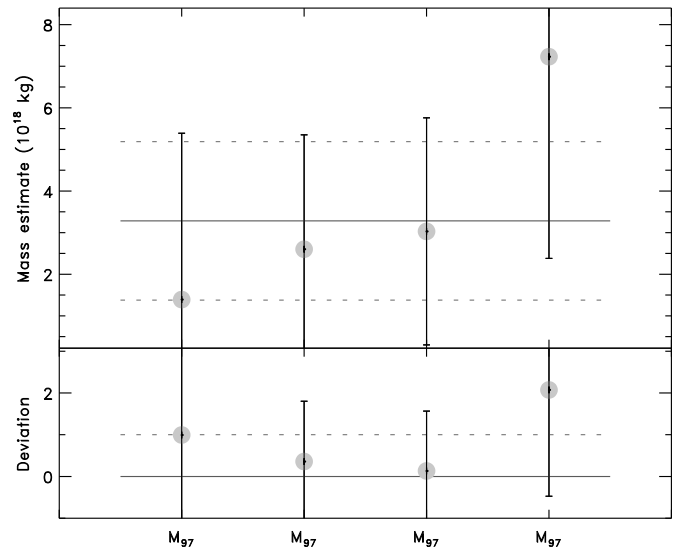


Figure A.51: Mass estimates for (68) Leto.

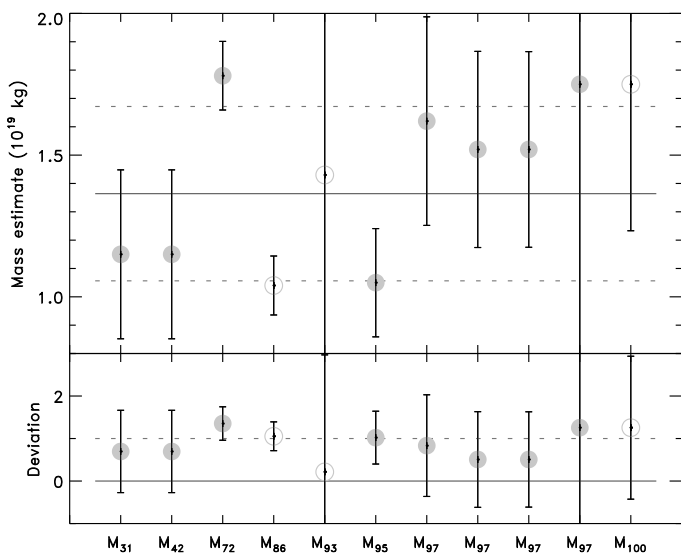


Figure A.50: Mass estimates for (65) Cybele.

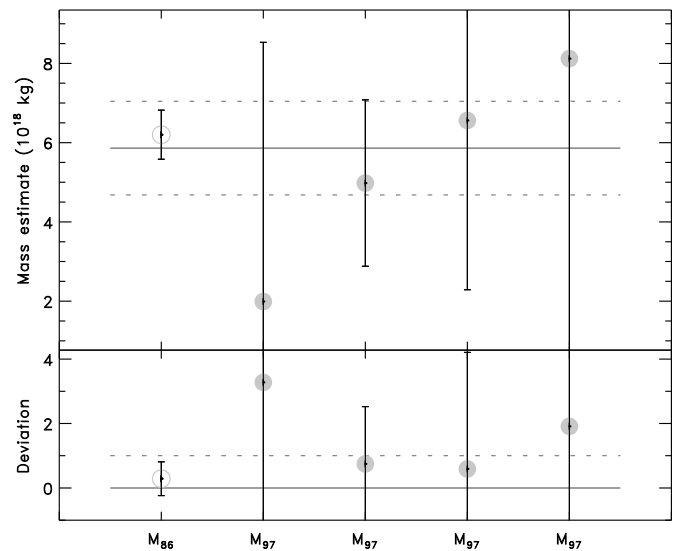


Figure A.52: Mass estimates for (69) Hesperia.

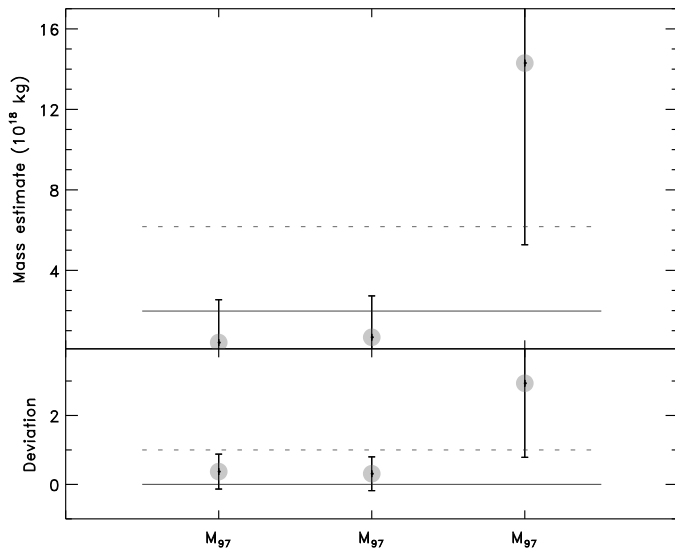


Figure A.53: Mass estimates for (76) Freia.

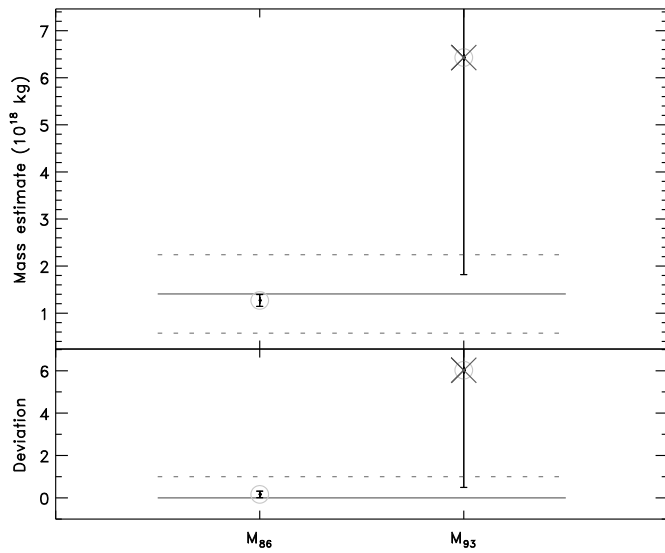


Figure A.54: Mass estimates for (78) Diana. The mass estimate from M_{93} gives a low-constrained density of 6.9 ± 5.0 if used alone. Only the estimate from M_{86} is used.

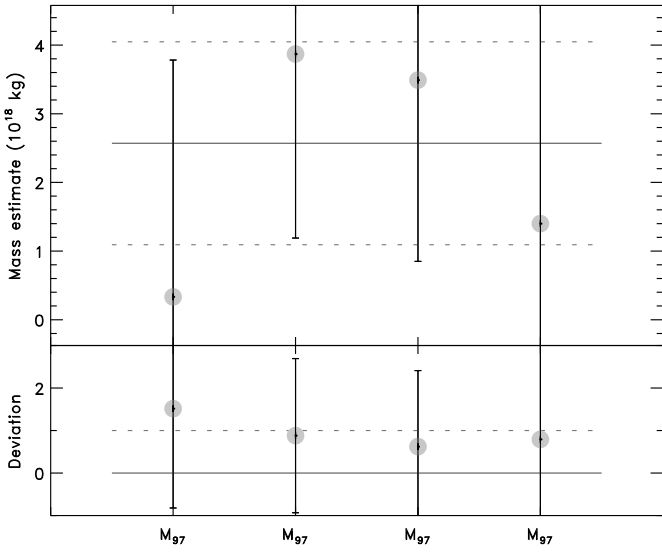


Figure A.55: Mass estimates for (85) Io.

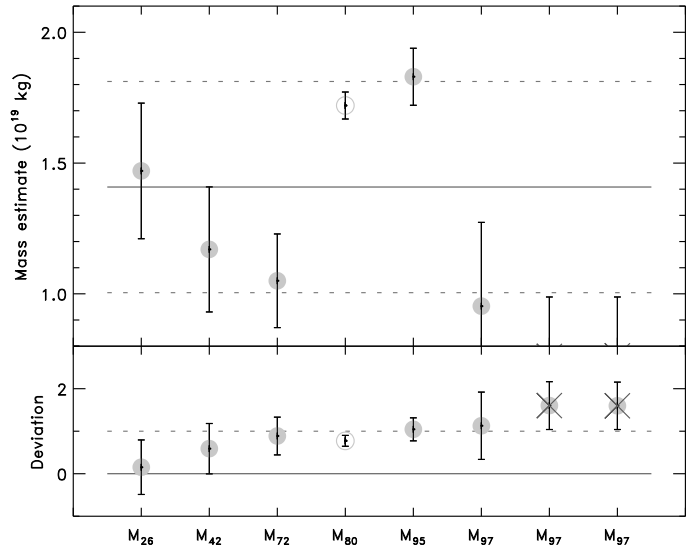


Figure A.57: Mass estimates for (88) Thisbe.

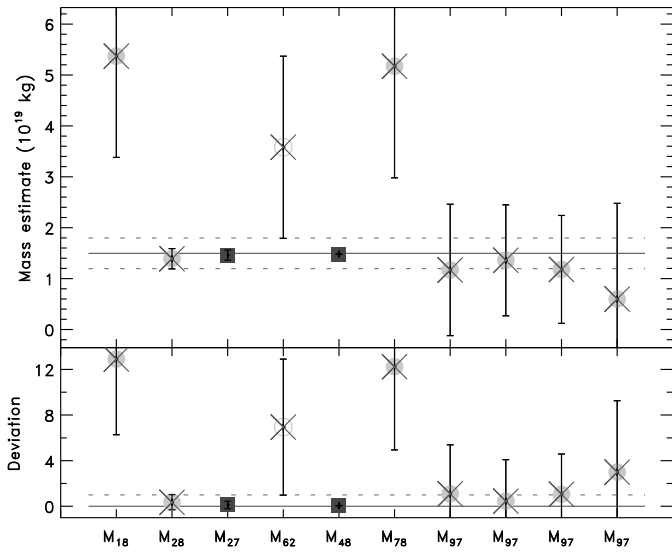


Figure A.56: Mass estimates for (87) Sylvia. Only the mass estimates based on direct imaging of the system are used here (M_{27} and M_{48}).

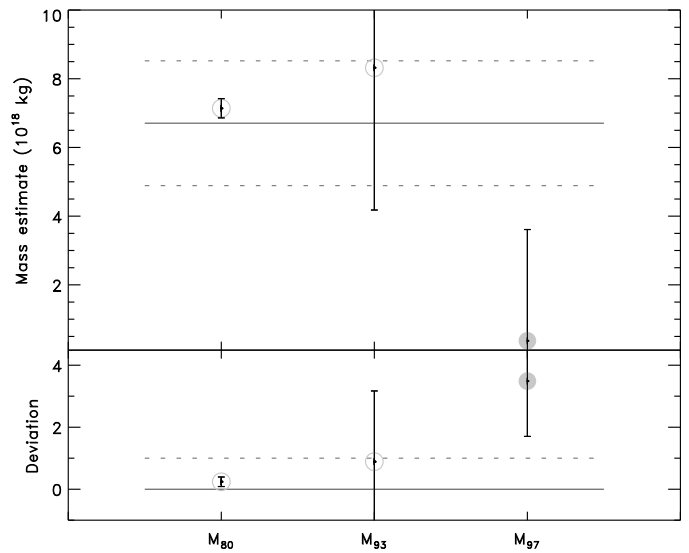


Figure A.58: Mass estimates for (89) Julia.

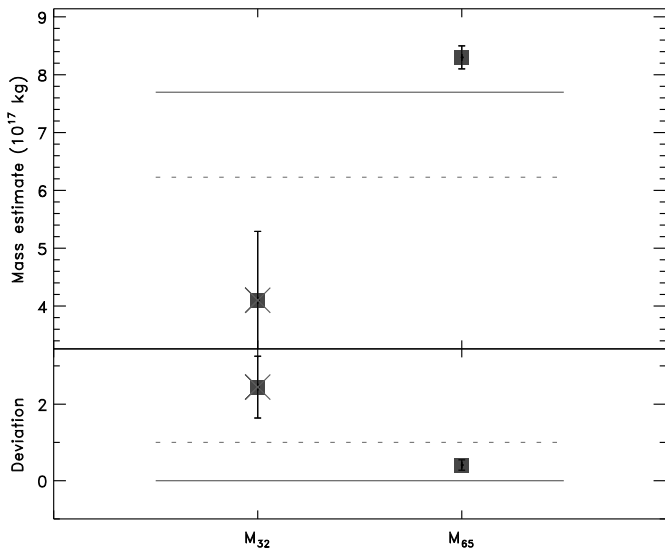


Figure A.59: Mass estimates for (90) Antiope. The mass estimate from M_{32} was based on few discovery images, and the estimate from M_{65} is preferred.

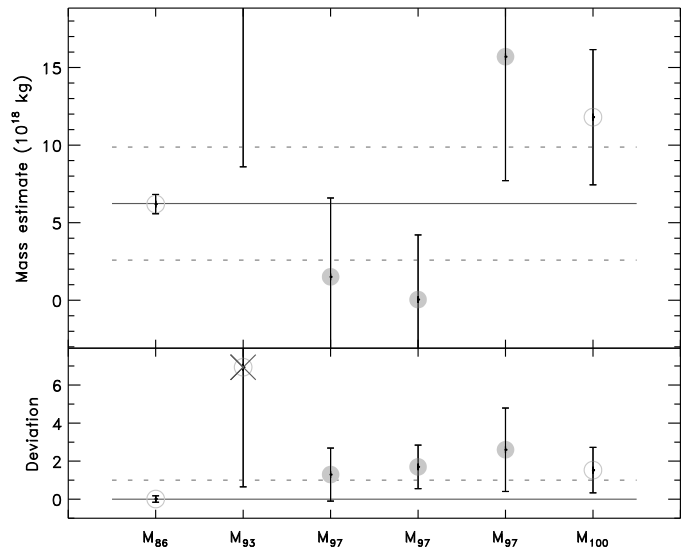


Figure A.61: Mass estimates for (94) Aurora.

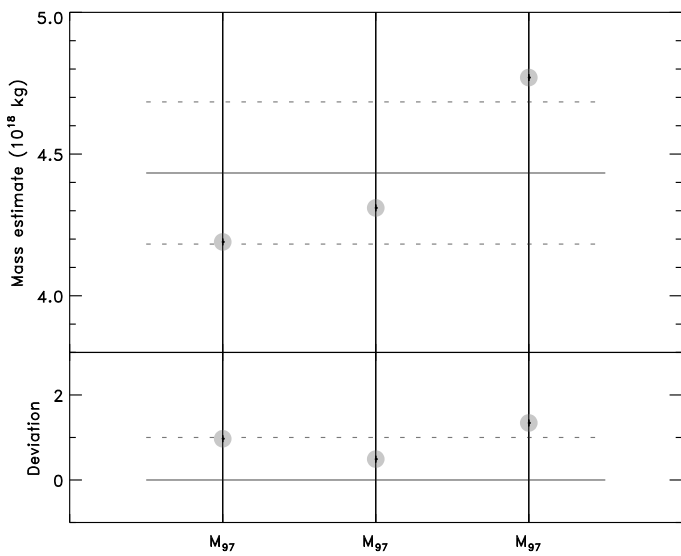


Figure A.60: Mass estimates for (92) Undina.

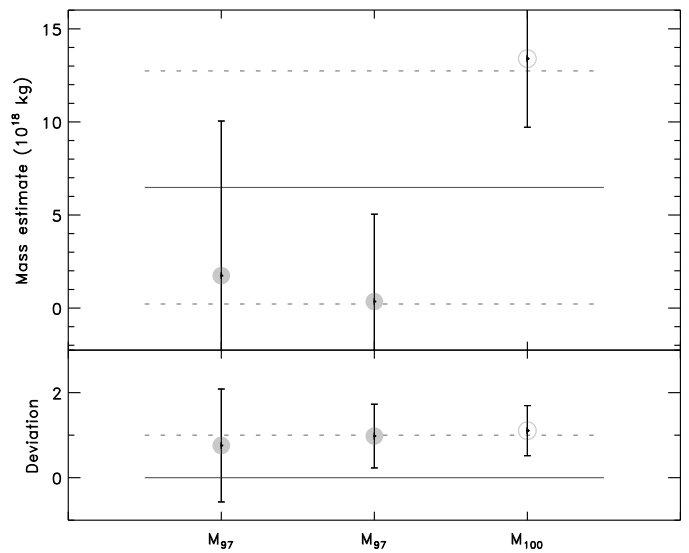


Figure A.62: Mass estimates for (96) Aegle.

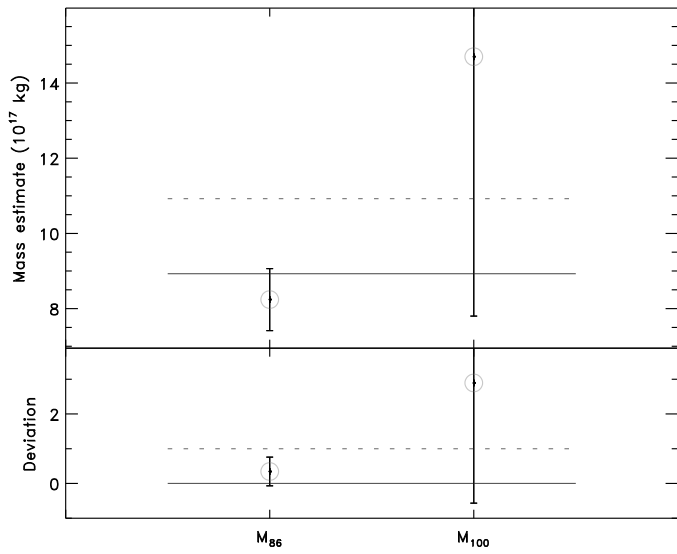


Figure A.63: Mass estimates for (98) Ianthe.

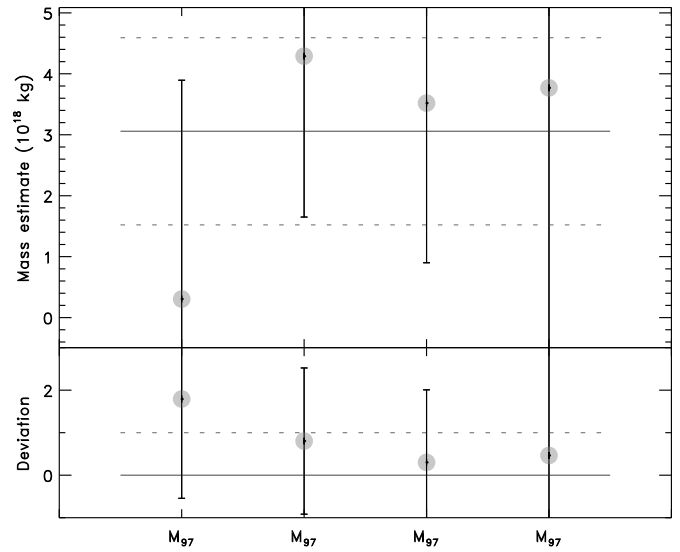


Figure A.65: Mass estimates for (106) Dione.

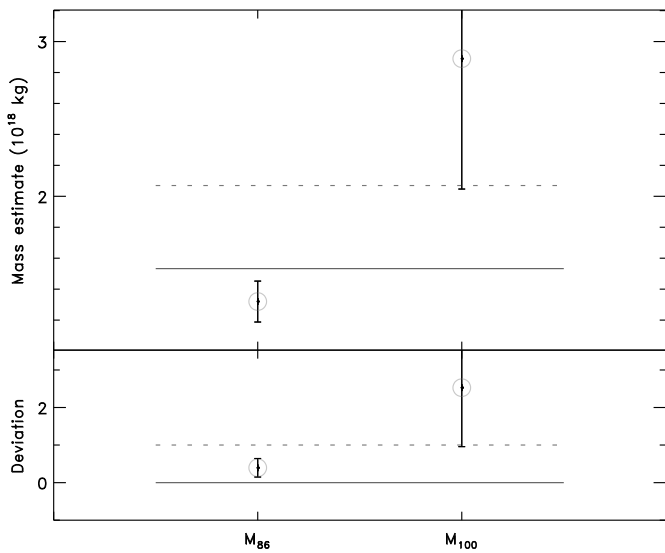


Figure A.64: Mass estimates for (105) Artemis.

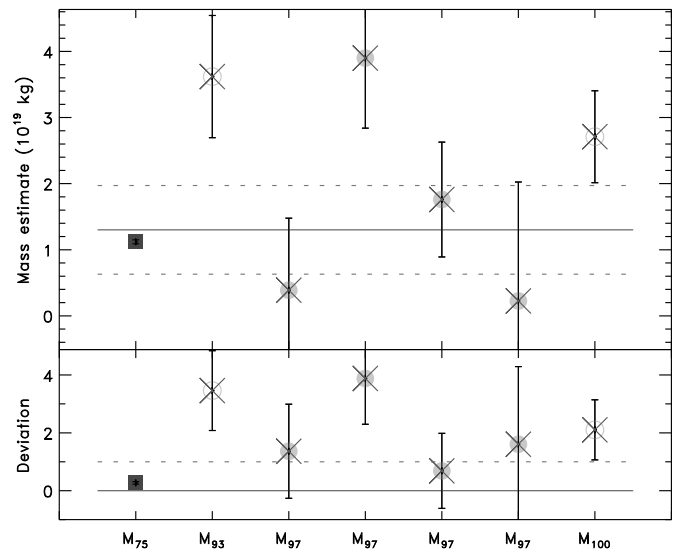


Figure A.66: Mass estimates for (107) Camilla. The mass estimate from M75 based on direct imaging of the binary system is preferred over the other estimates.

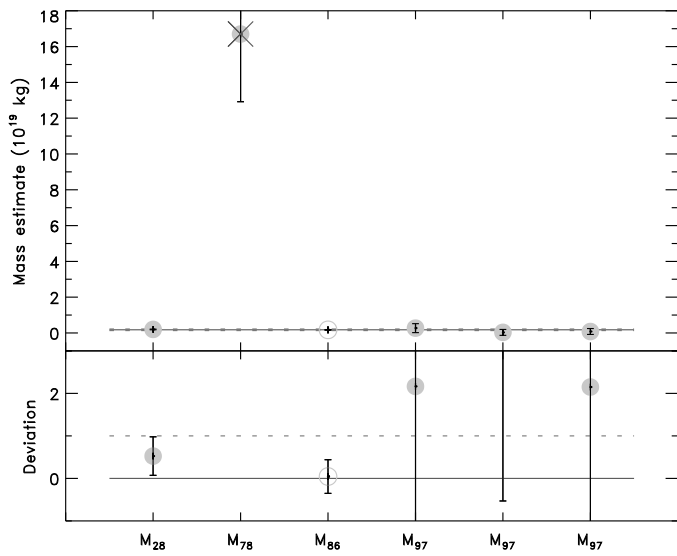


Figure A.67: Mass estimates for (111) Ate. The mass estimate from M₇₈ gives an unrealistic density of 113 ± 30 if used alone, and is therefore discarded.

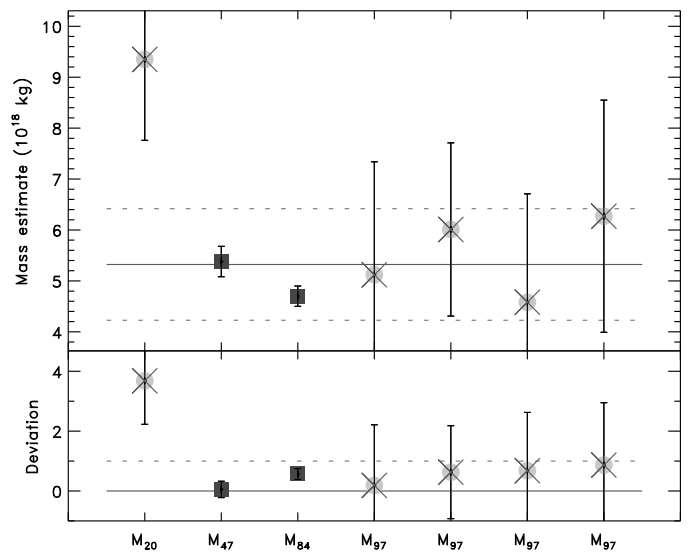


Figure A.69: Mass estimates for (121) Hermione. Only the mass estimates based on direct imaging of the system are used here (M₄₇ and M₈₄).

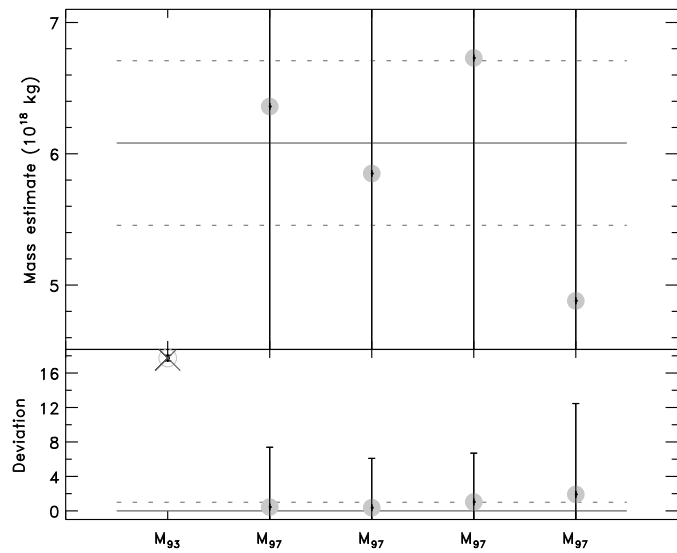


Figure A.68: Mass estimates for (117) Lomia.

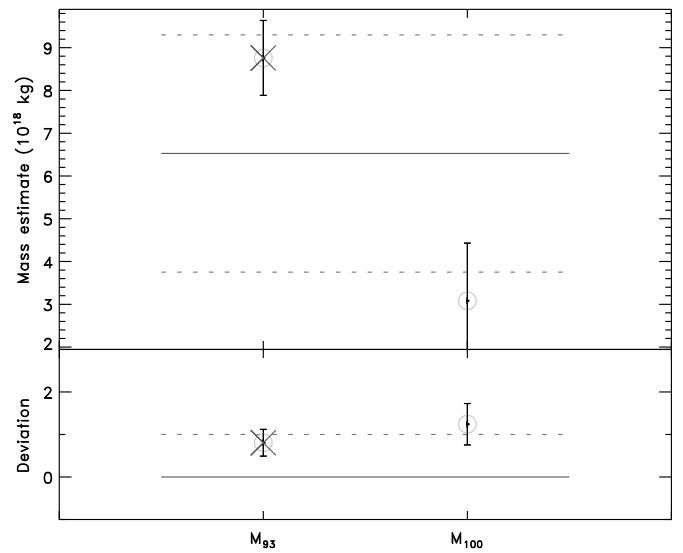


Figure A.70: Mass estimates for (127) Johanna.

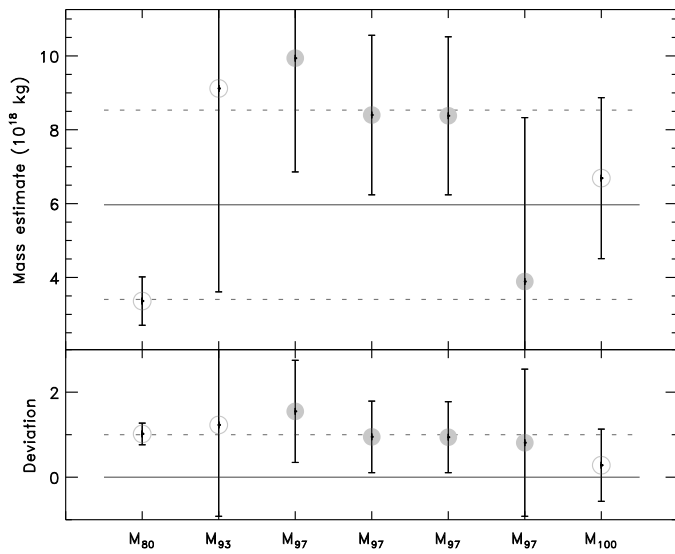


Figure A.71: Mass estimates for (128) Nemesis.

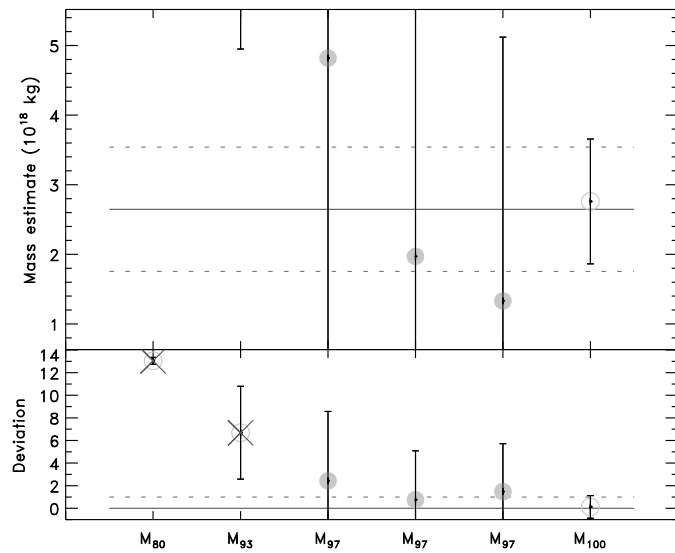


Figure A.72: Mass estimates for (129) Antigone. Both mass estimates from ephemeris (M_{80} and M_{93}) result in unrealistic high densities, and are thus discarded.

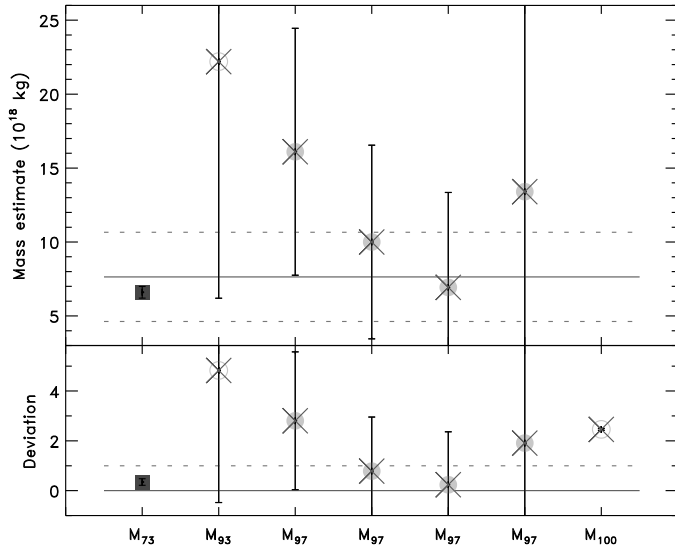


Figure A.73: Mass estimates for (130) Elektra. Only the estimate from M₇₃, based on direct imaging of the binary system is used.

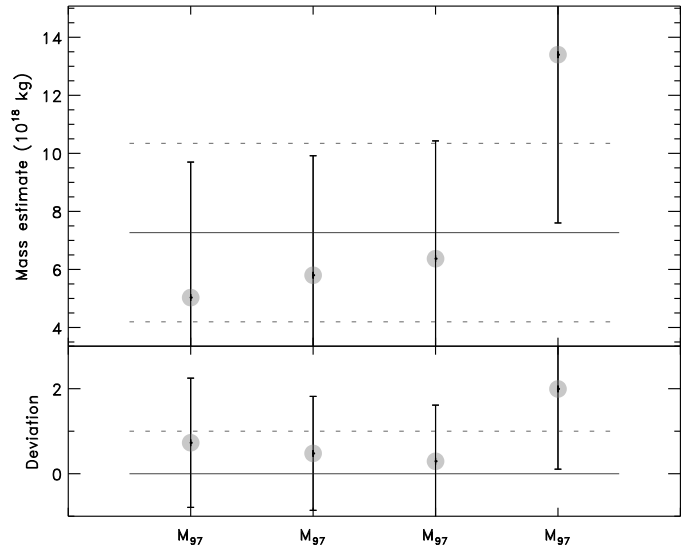


Figure A.75: Mass estimates for (137) Meliboea.

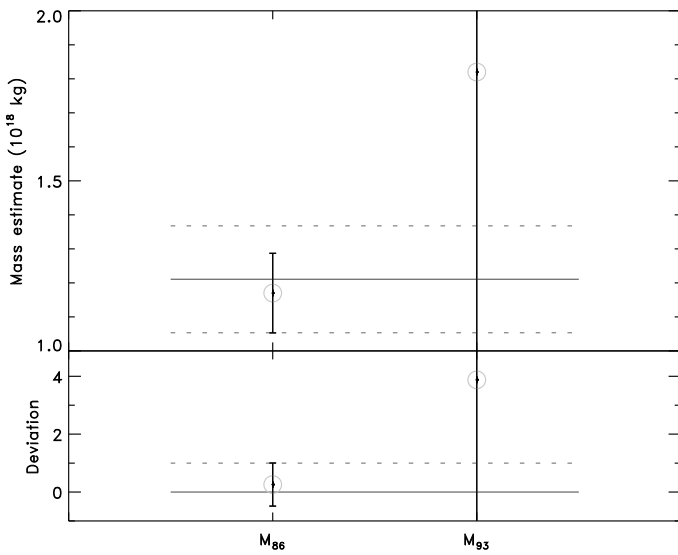


Figure A.74: Mass estimates for (135) Hertha.

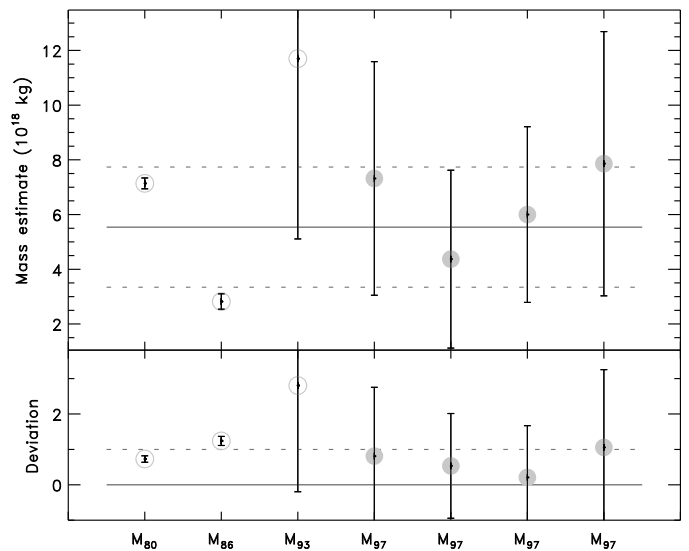


Figure A.76: Mass estimates for (139) Juwa.

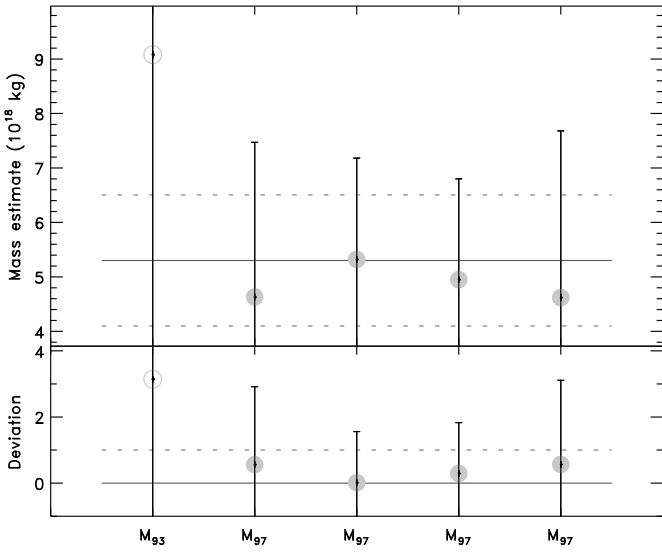


Figure A.77: Mass estimates for (144) Vibia.

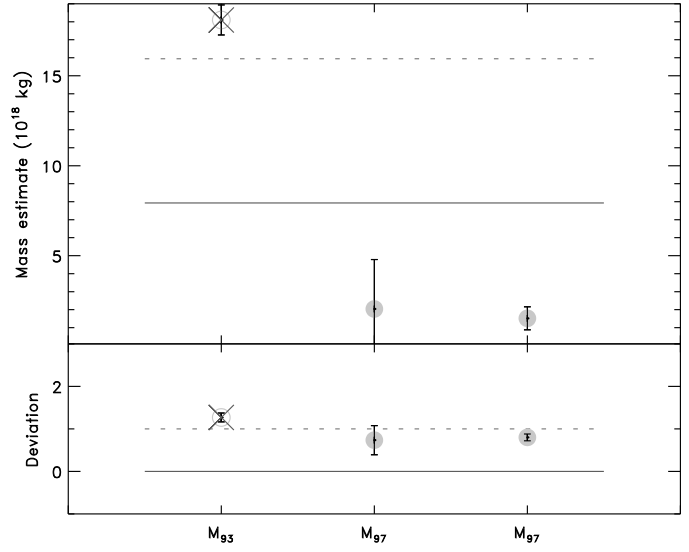


Figure A.79: Mass estimates for (150) Nuwa. The mass estimate M_{93} gives an unrealistic density of 10.4 ± 1.9 if used alone, and is therefore discarded.

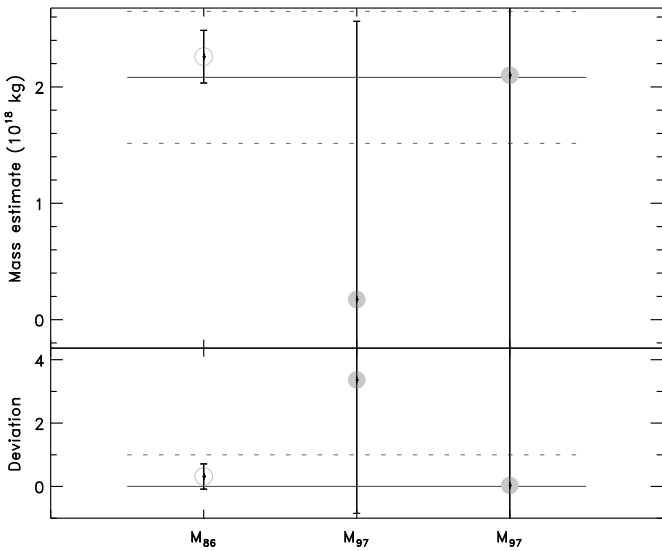


Figure A.78: Mass estimates for (145) Adeona.

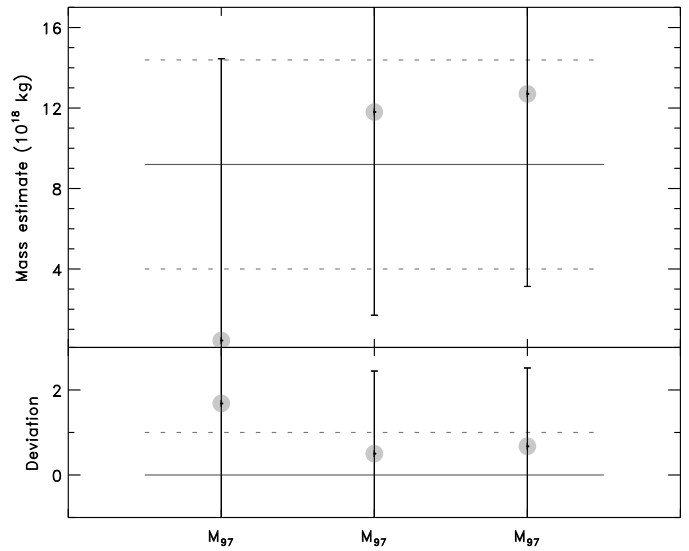


Figure A.80: Mass estimates for (154) Bertha.

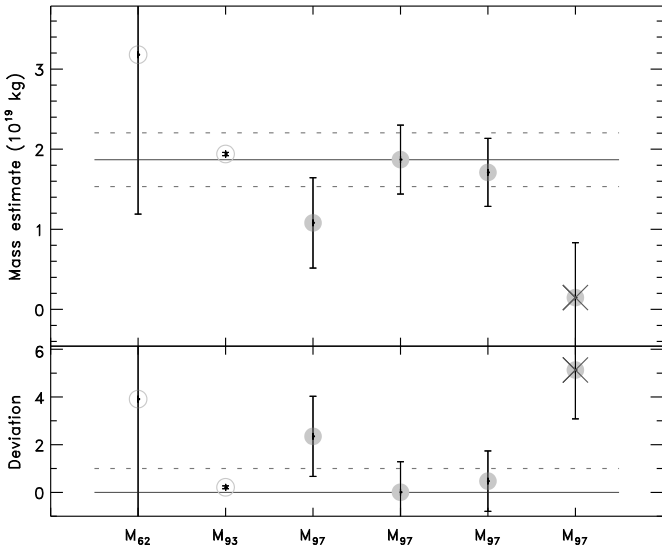


Figure A.81: Mass estimates for (165) Loreley.

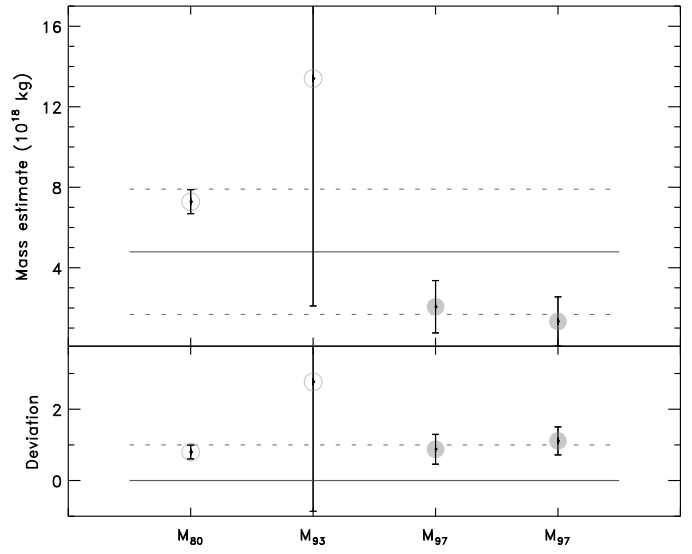


Figure A.83: Mass estimates for (173) Ino.

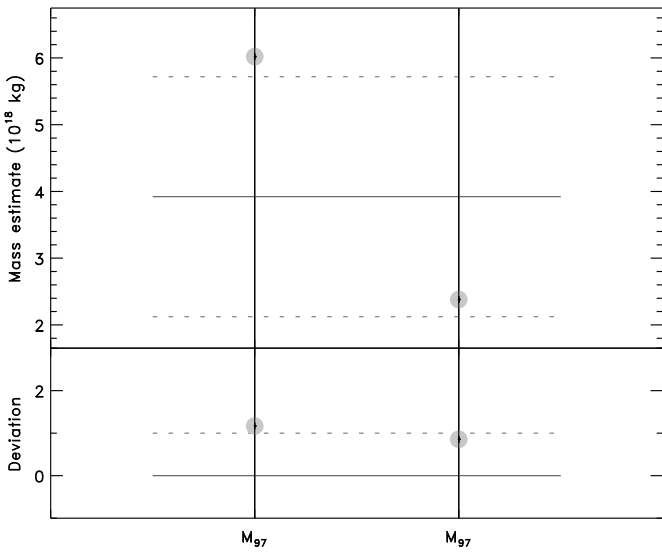


Figure A.82: Mass estimates for (168) Sibylla.

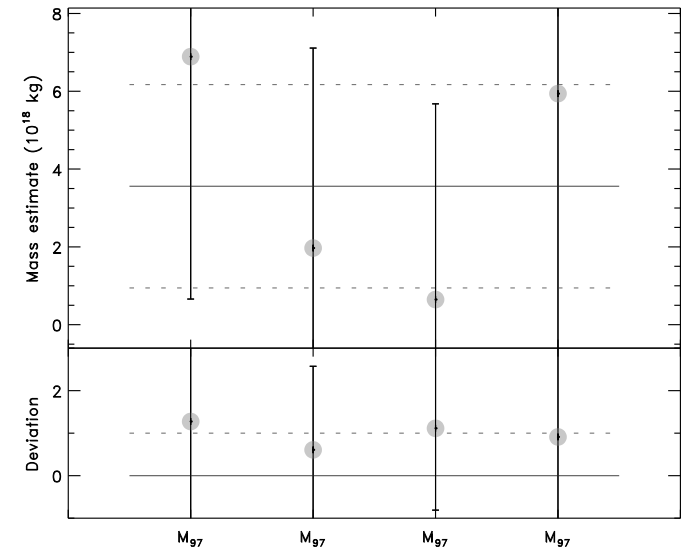


Figure A.84: Mass estimates for (185) Eunike.

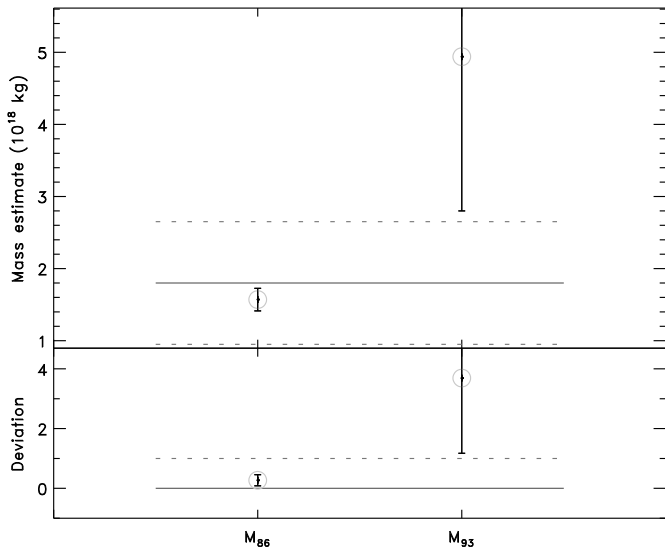


Figure A.85: Mass estimates for (187) Lamberta.

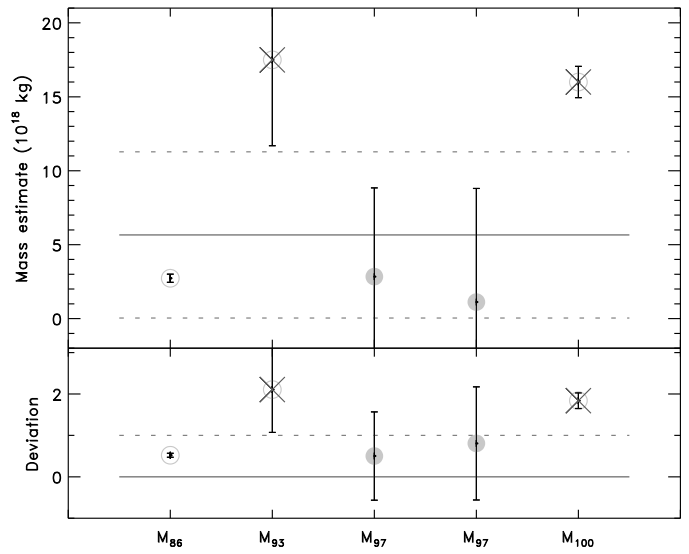


Figure A.87: Mass estimates for (194) Prokne.

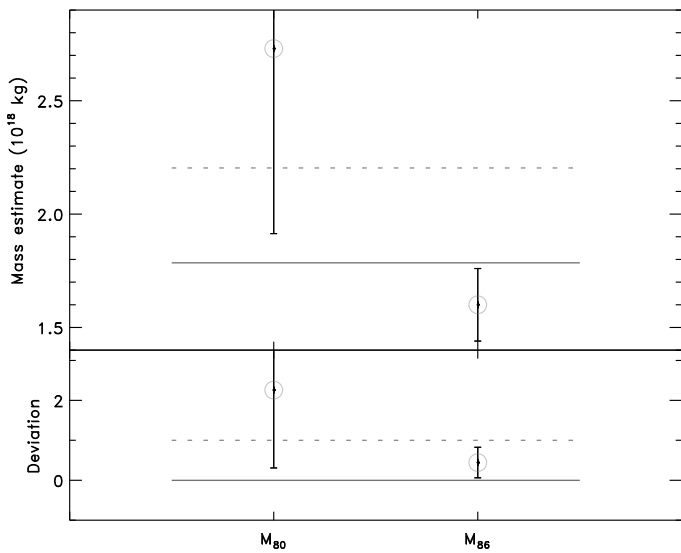


Figure A.86: Mass estimates for (192) Nausikaa.

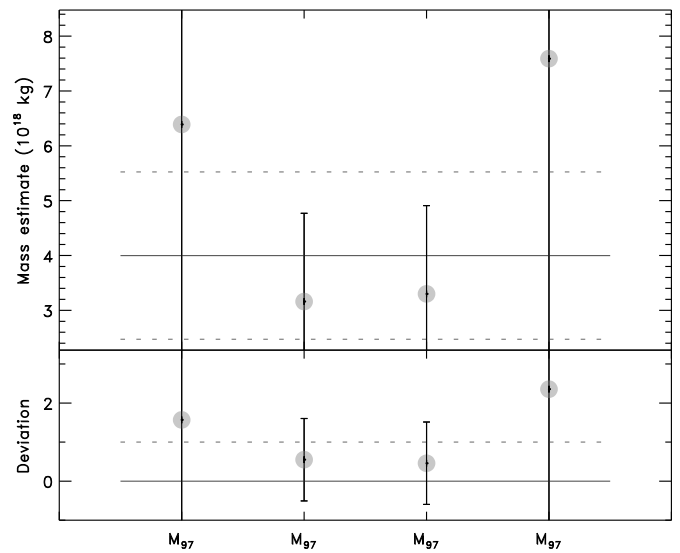


Figure A.88: Mass estimates for (196) Philomela.

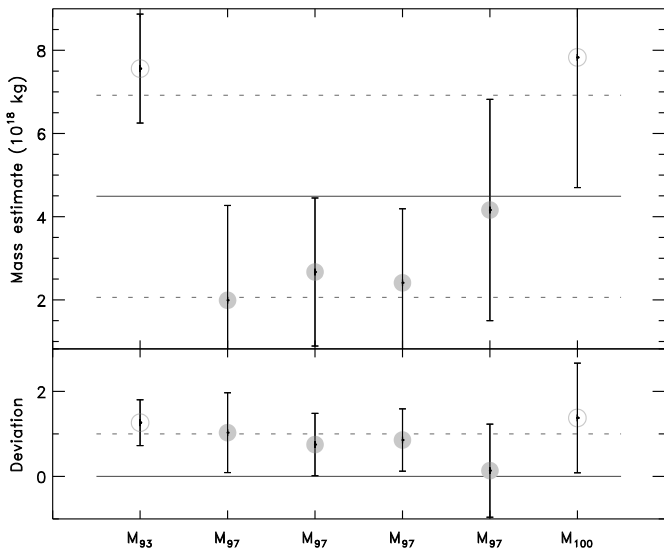


Figure A.89: Mass estimates for (211) Isolda.

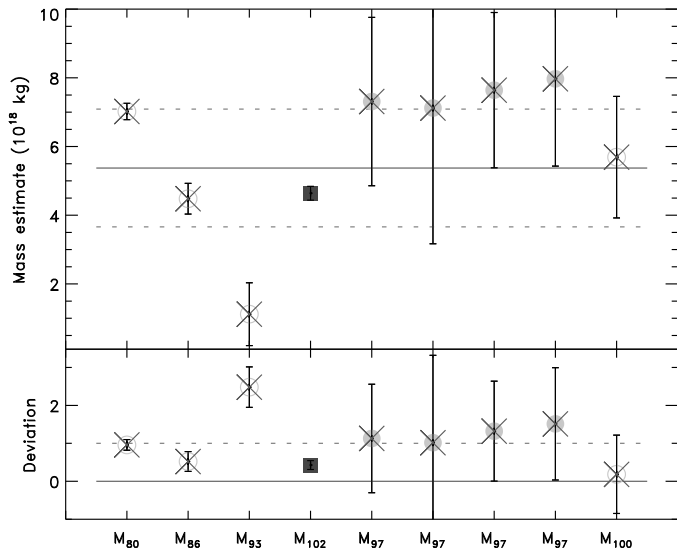


Figure A.90: Mass estimates for (216) Kleopatra. Only the mass estimate based on direct imaging of the system is used here (M_{102}).

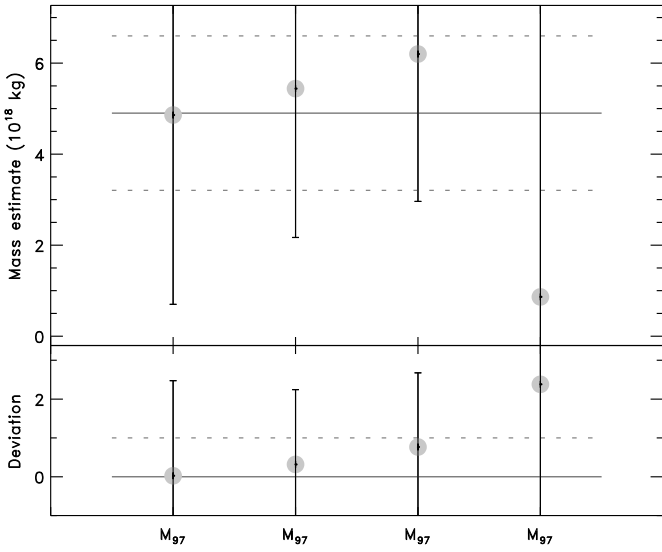


Figure A.91: Mass estimates for (238) Hypatia.

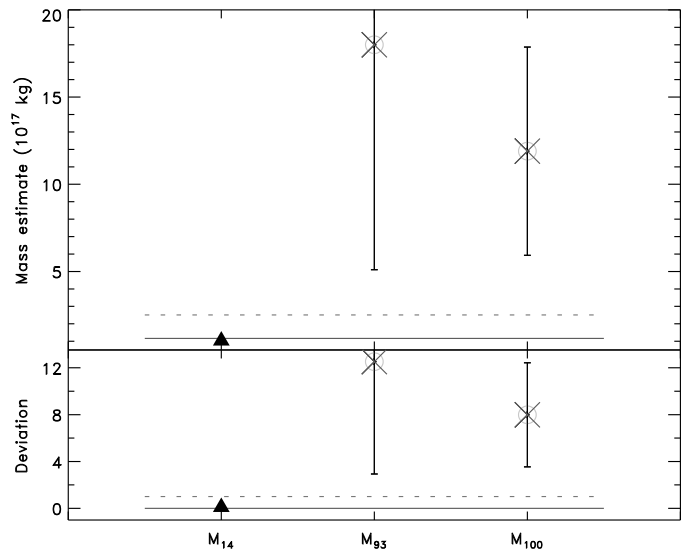


Figure A.93: Mass estimates for (253) Mathilde. Only the flyby estimate (M_{14}) is used here.

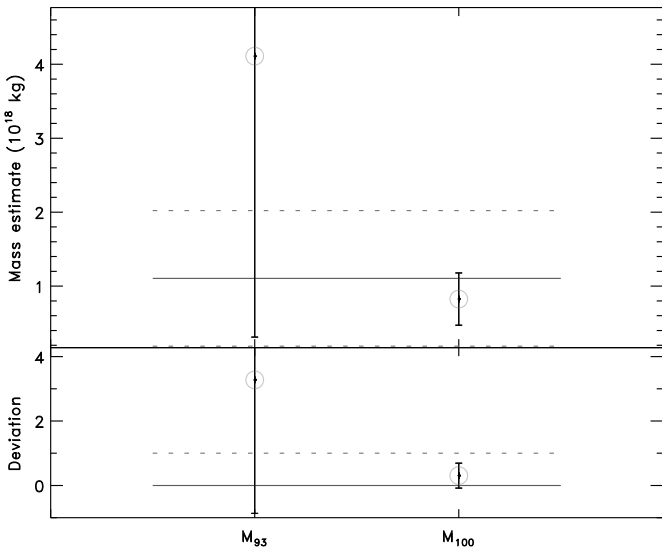


Figure A.92: Mass estimates for (240) Vanadis.

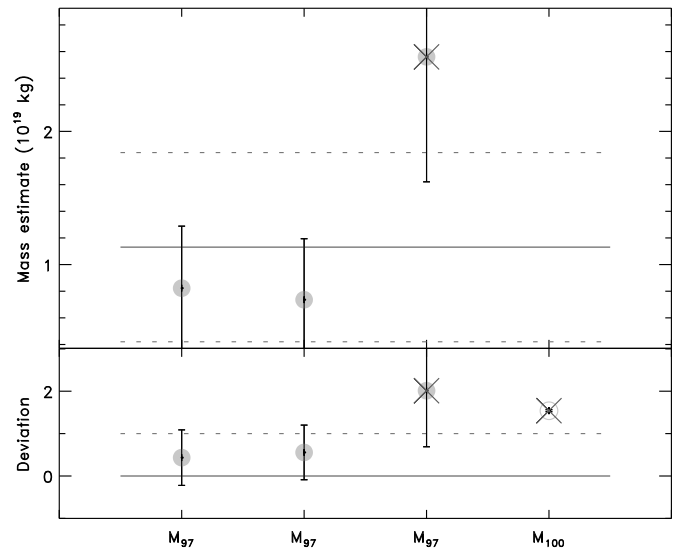


Figure A.94: Mass estimates for (259) Aletheia.

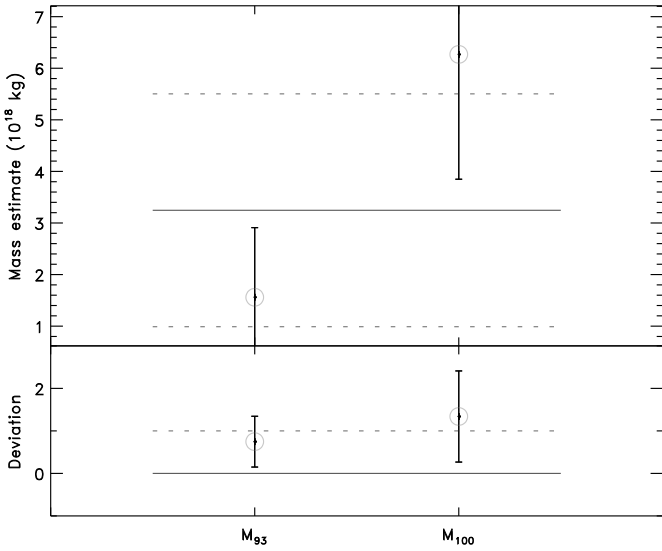


Figure A.95: Mass estimates for (268) Adorea.

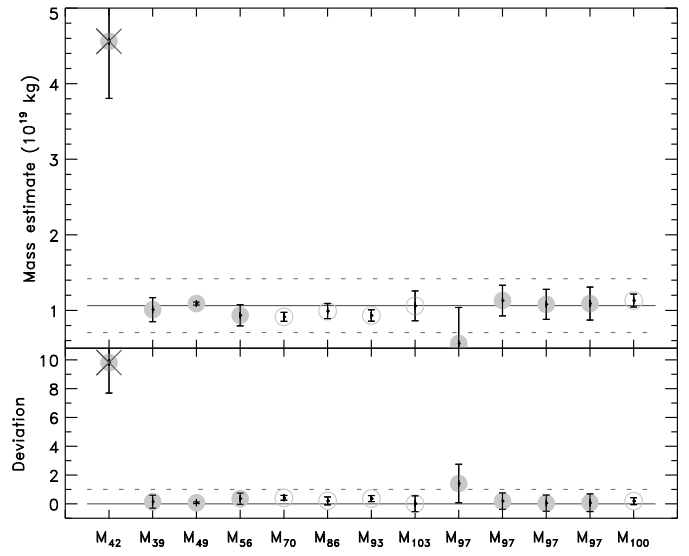


Figure A.97: Mass estimates for (324) Bamberga.

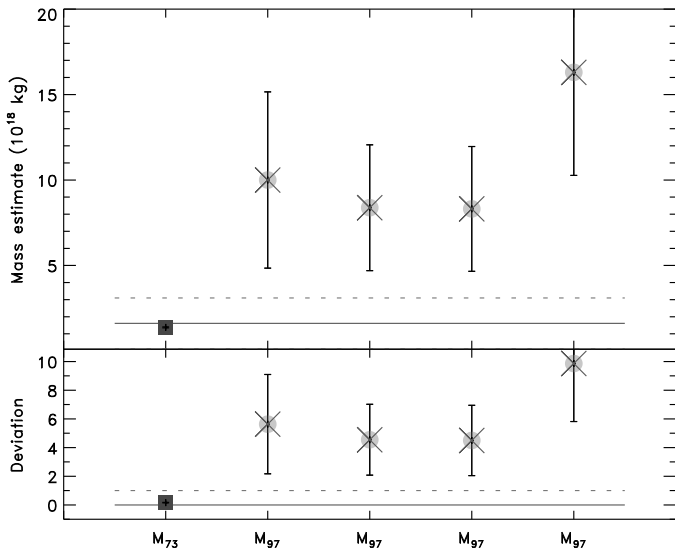


Figure A.96: Mass estimates for (283) Emma. Only the mass estimate based on direct imaging of the system is used here (M_{73}).

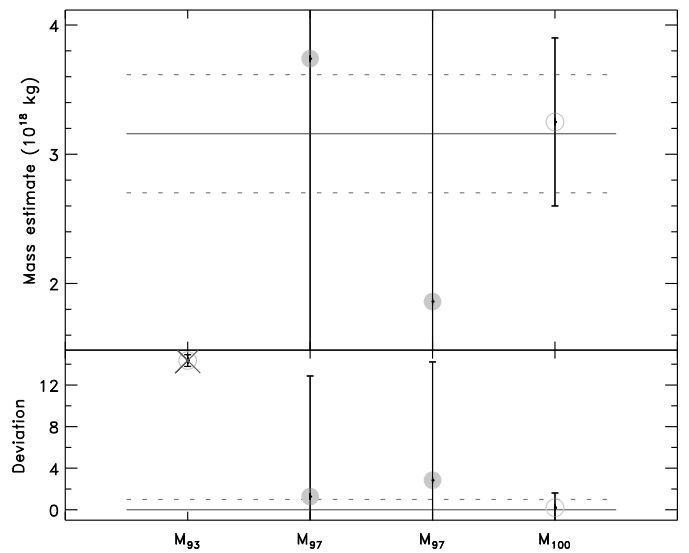


Figure A.98: Mass estimates for (328) Gudrun.

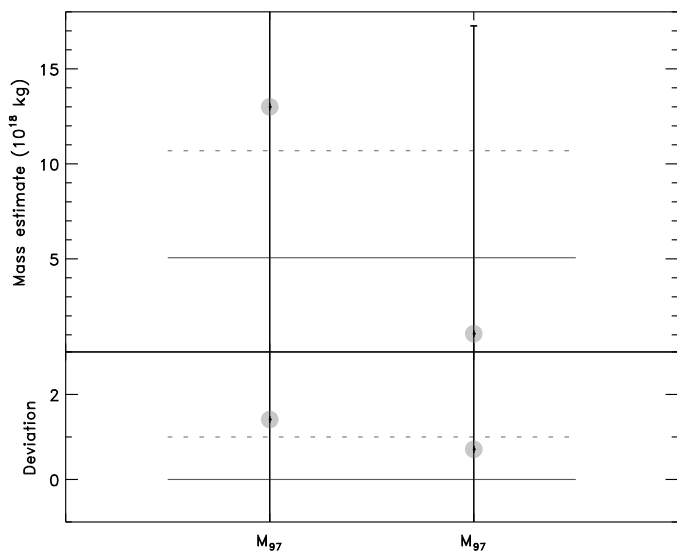


Figure A.99: Mass estimates for (334) Chicago.

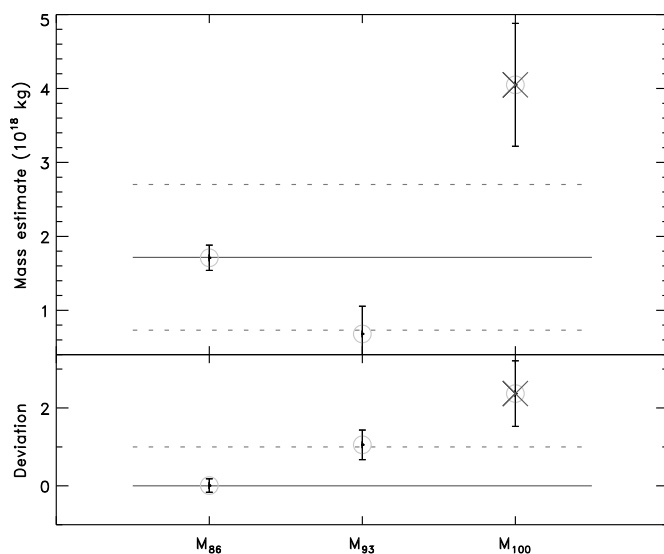


Figure A.101: Mass estimates for (344) Desiderata.

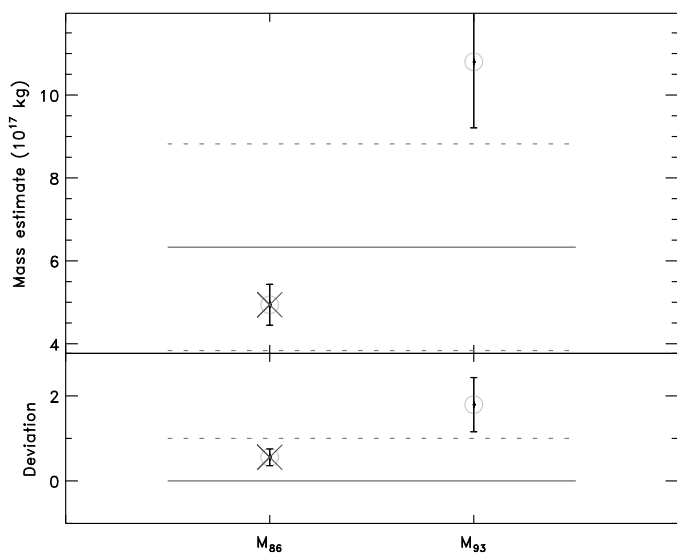


Figure A.100: Mass estimates for (337) Devosa. Fornasier et al. (2011) found that Hexahedrite iron meteorites provided the best match to (337) Devosa's reflectance spectrum. Mass estimate M_{86} leads to a density of 3.5 ± 1.4 if used alone, far from the density of these meteorites (~ 7.4). The estimate from M_{93} results in a density of 7.7 ± 3.2 , in better agreement with the meteorite.

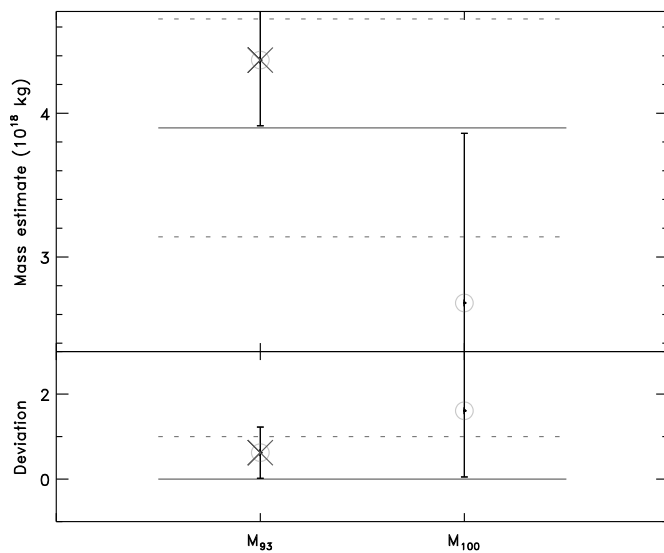


Figure A.102: Mass estimates for (345) Tercidina. The mass estimate from M_{93} gives a unrealistic high density of 8.6 ± 1.1 if used alone, and is therefore discarded.

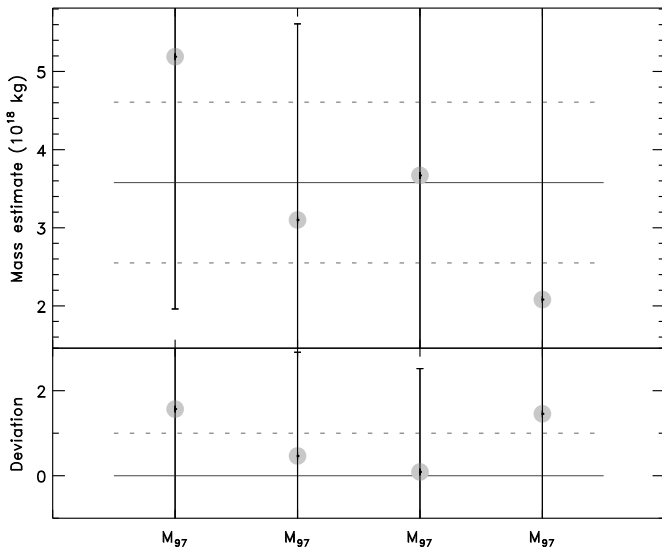


Figure A.103: Mass estimates for (349) Dembowska.

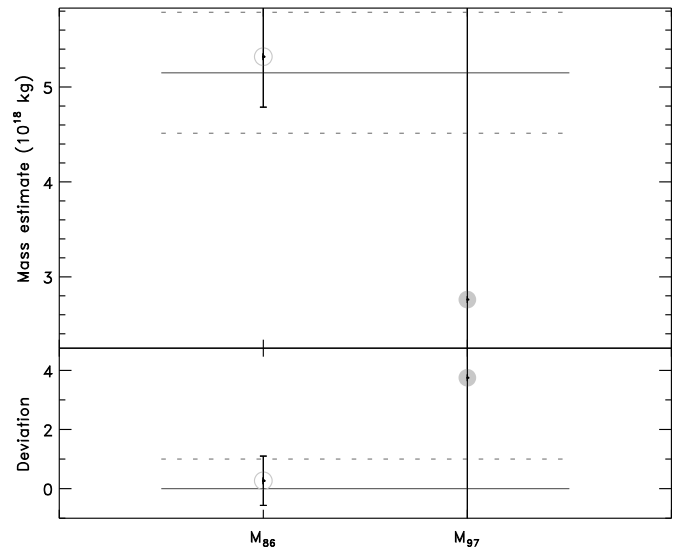


Figure A.105: Mass estimates for (372) Palma.

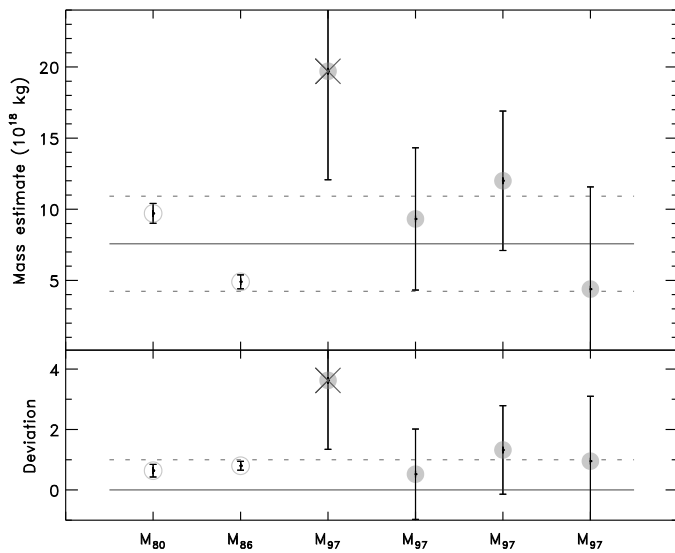


Figure A.104: Mass estimates for (354) Eleonora.

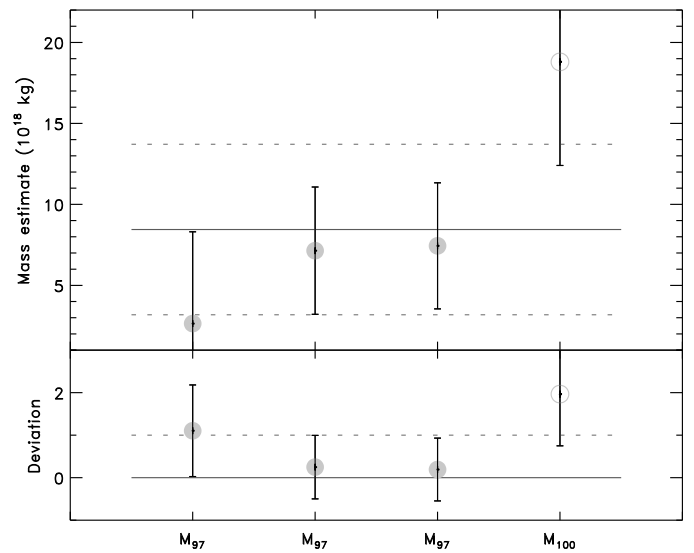


Figure A.106: Mass estimates for (375) Ursula.

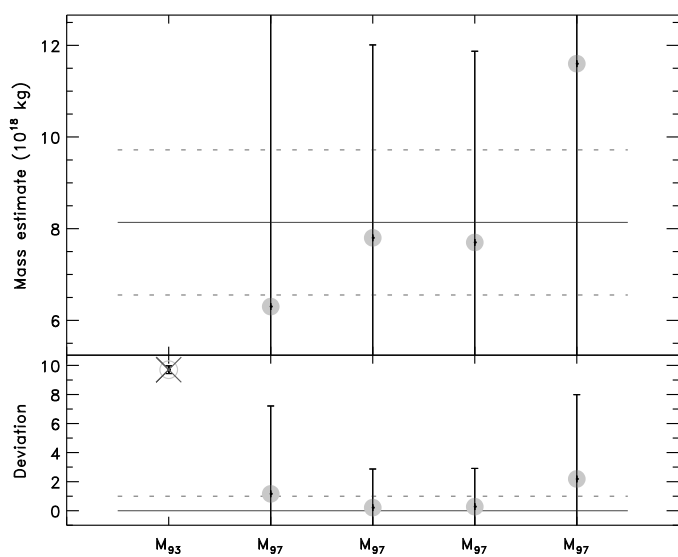


Figure A.107: Mass estimates for (386) Siegena.

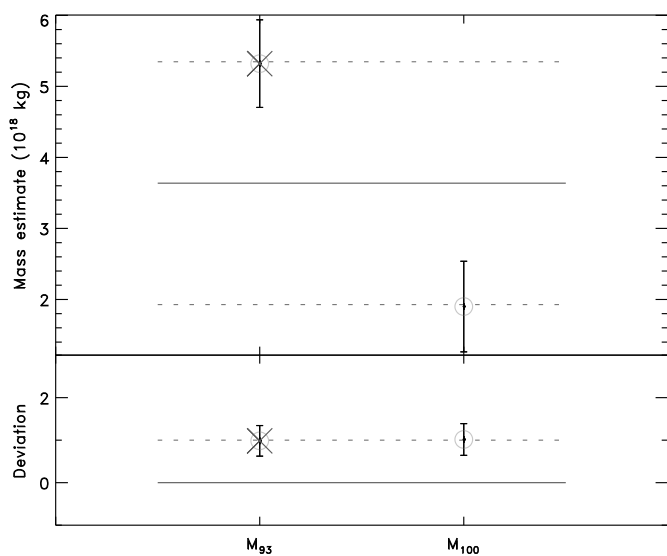


Figure A.108: Mass estimates for (387) Aquitania.

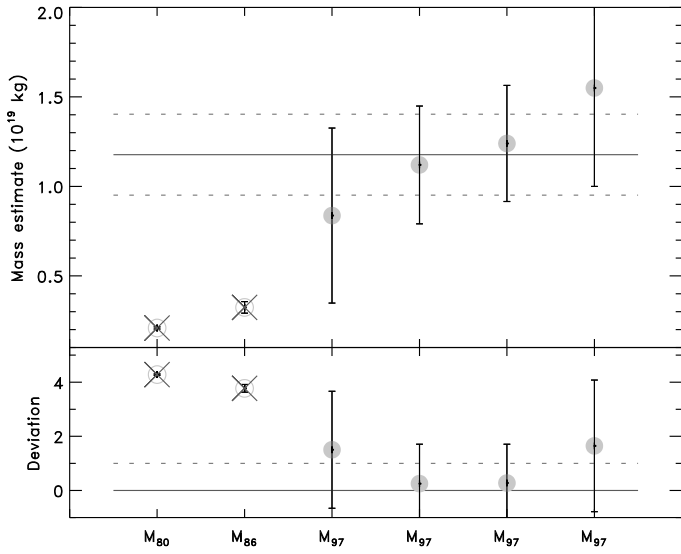


Figure A.109: Mass estimates for (409) Aspasia.

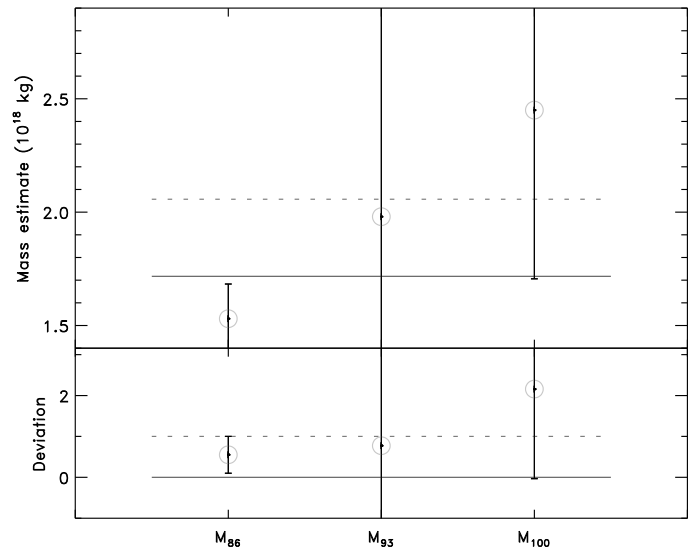


Figure A.111: Mass estimates for (419) Aurelia.

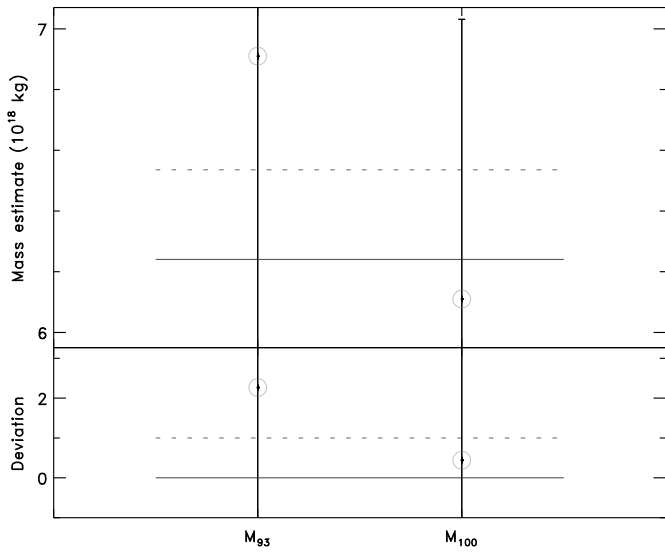


Figure A.110: Mass estimates for (410) Chloris.

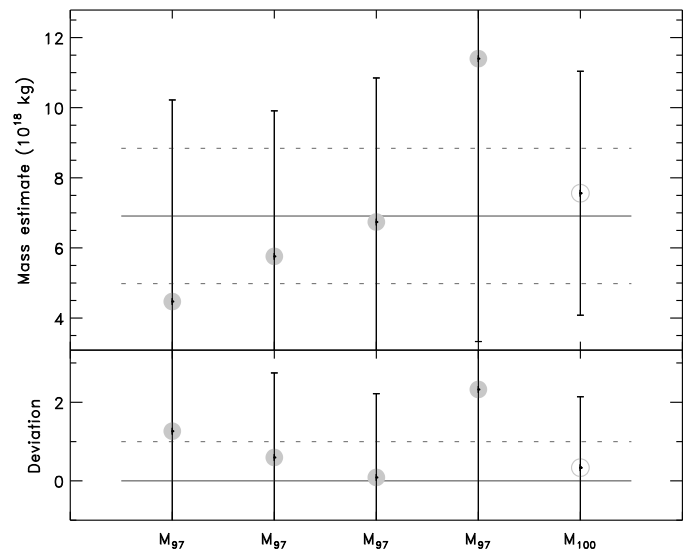


Figure A.112: Mass estimates for (423) Diotima.

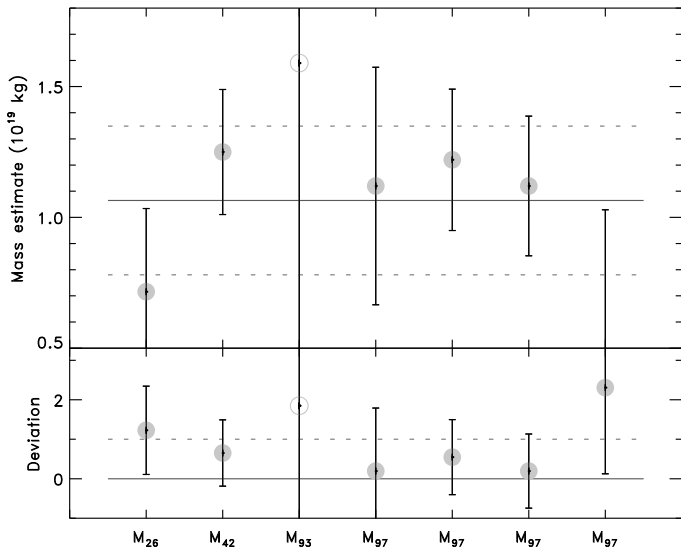


Figure A.113: Mass estimates for (444) Gyptis.

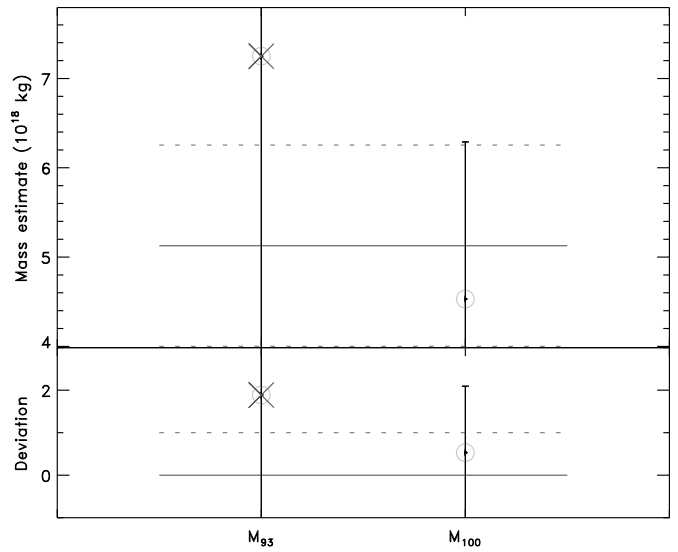


Figure A.115: Mass estimates for (469) Argentina.

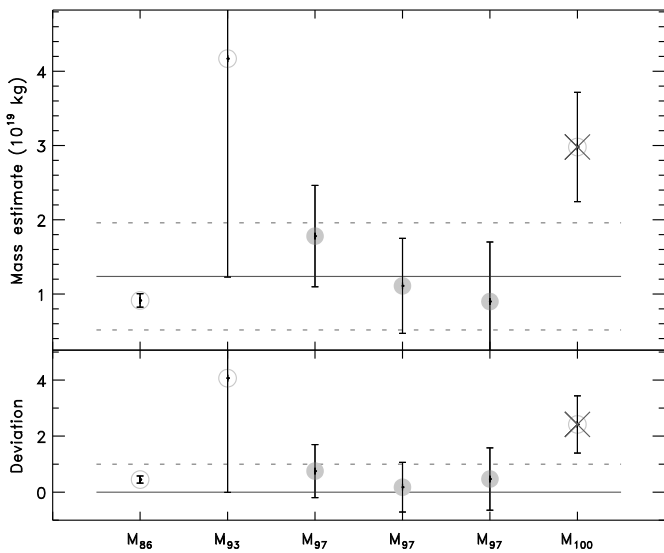


Figure A.114: Mass estimates for (451) Patientia.

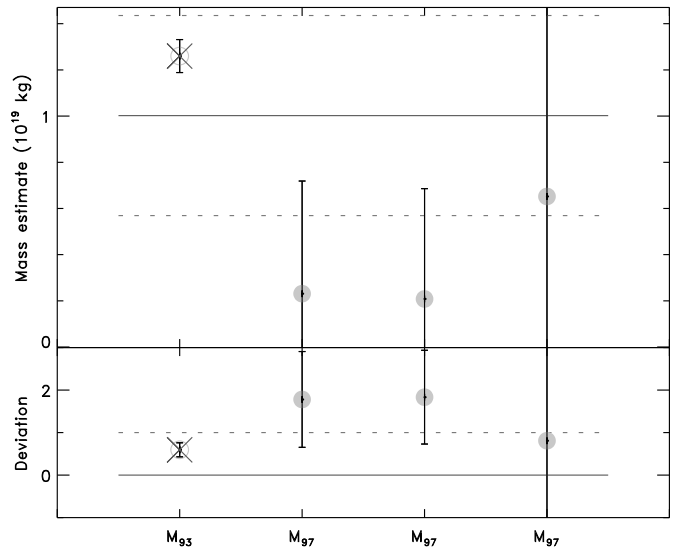


Figure A.116: Mass estimates for (471) Papagena. The mass estimate from M_{93} gives a unrealistic high density of 12.4 ± 2.5 if used alone, and is therefore discarded.

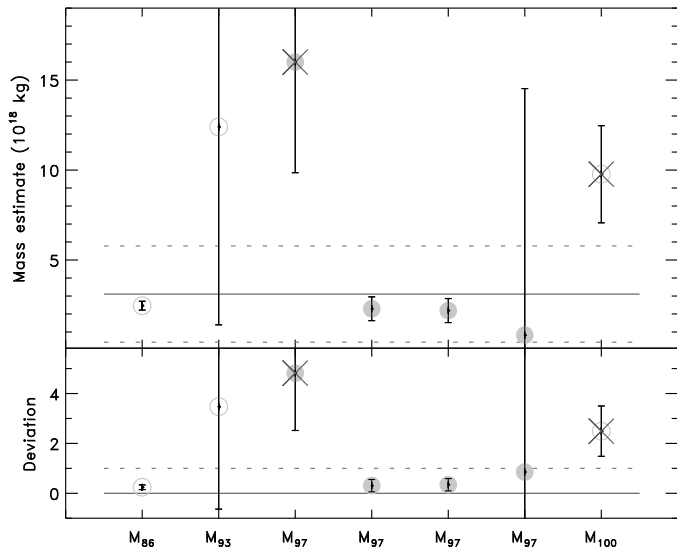


Figure A.117: Mass estimates for (488) Kreusa.

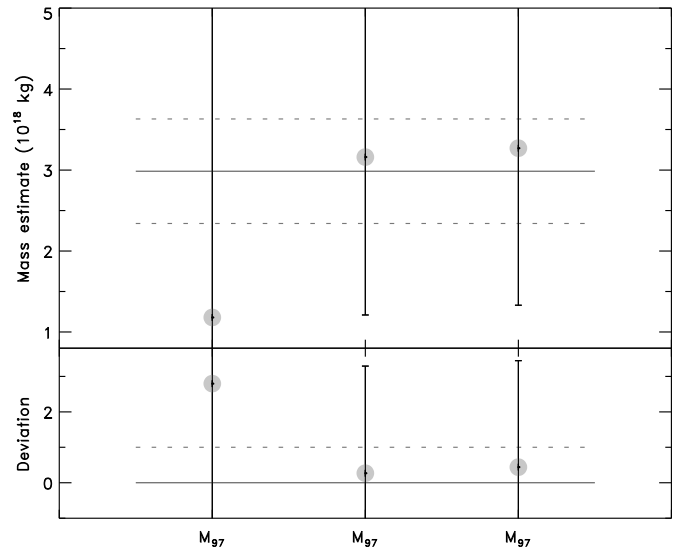


Figure A.119: Mass estimates for (508) Princetonia.

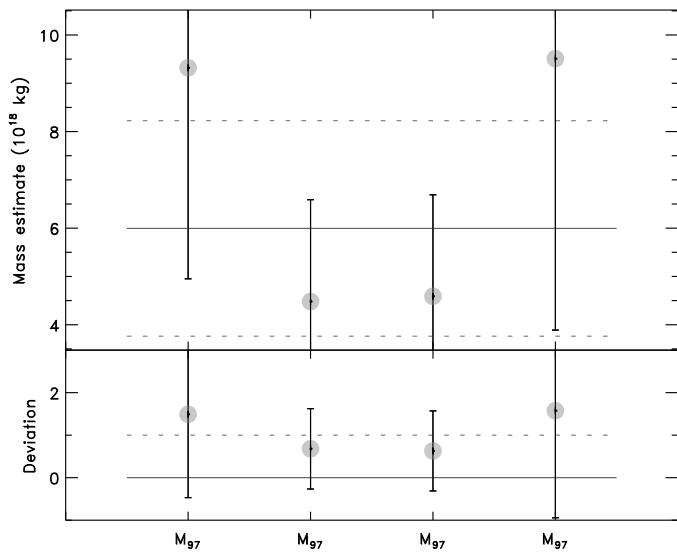


Figure A.118: Mass estimates for (490) Veritas.

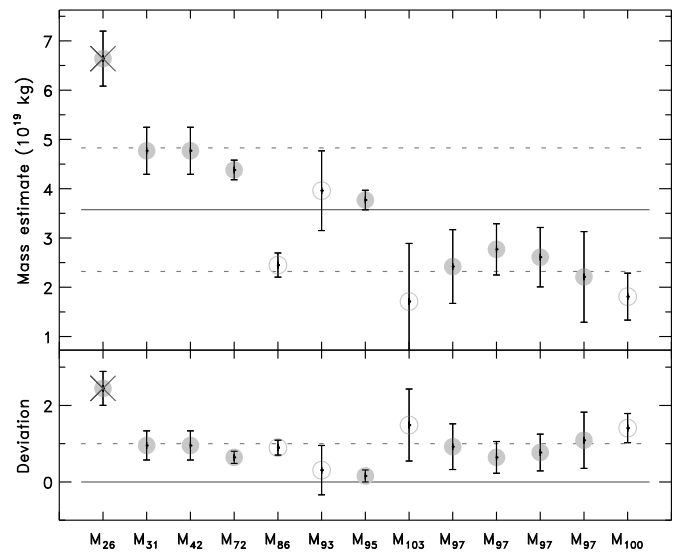


Figure A.120: Mass estimates for (511) Davida.

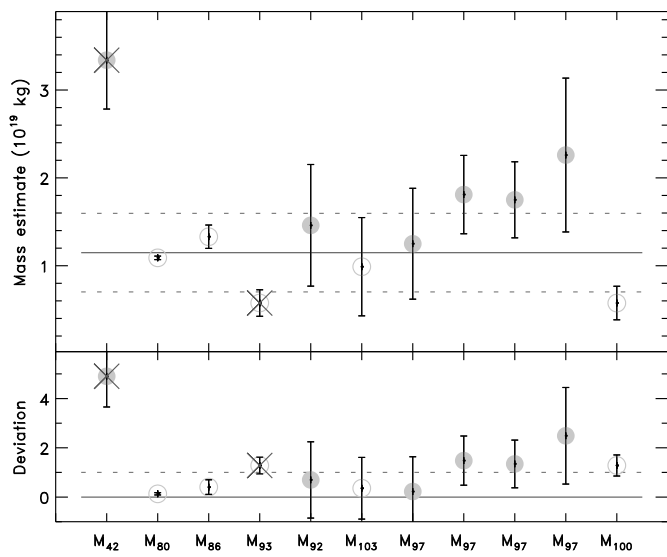


Figure A.121: Mass estimates for (532) Herculina.

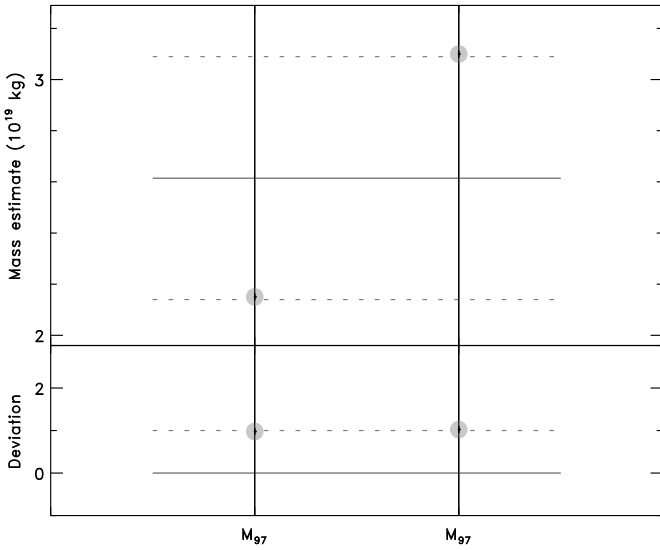


Figure A.122: Mass estimates for (536) Merapi.

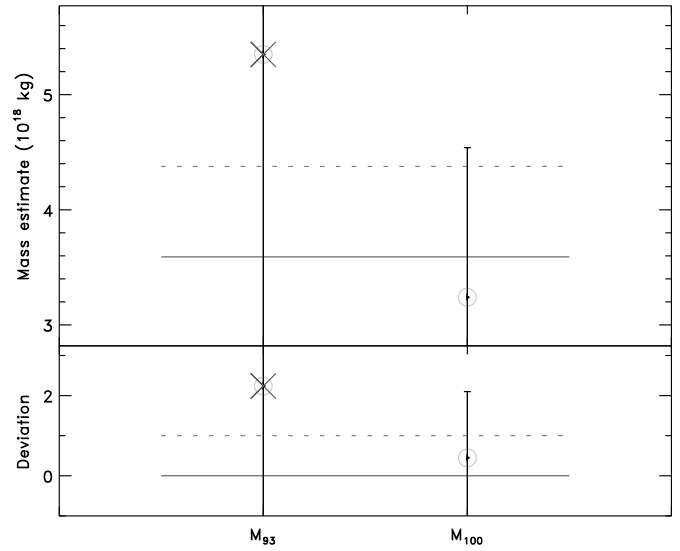


Figure A.124: Mass estimates for (626) Notburga.

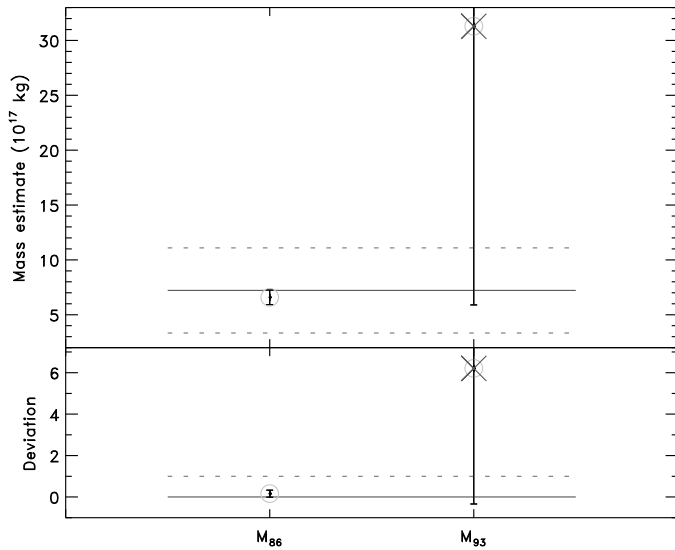


Figure A.123: Mass estimates for (554) Peraga. The mass estimate from M_{93} gives a low-constrained density of 6.2 ± 5.2 if used alone, far from the CI meteorite analogue. Only the estimate from M_{86} is used.

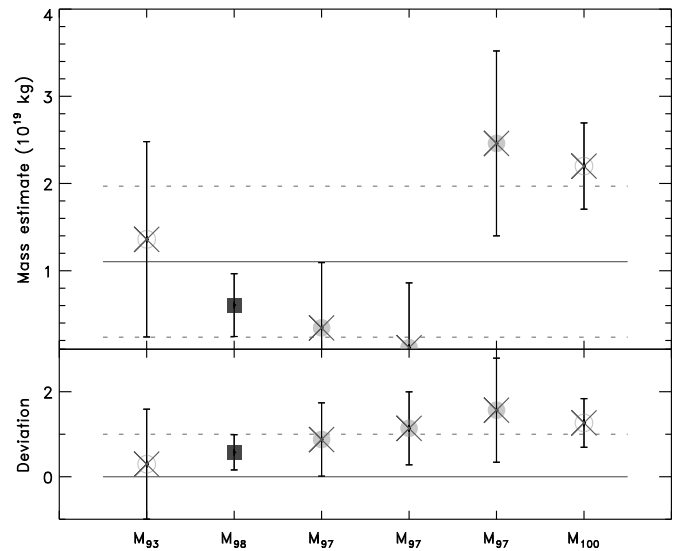


Figure A.125: Mass estimates for (702) Alauda. The estimate from M_{98} obtained by imaging the binary system is preferred.

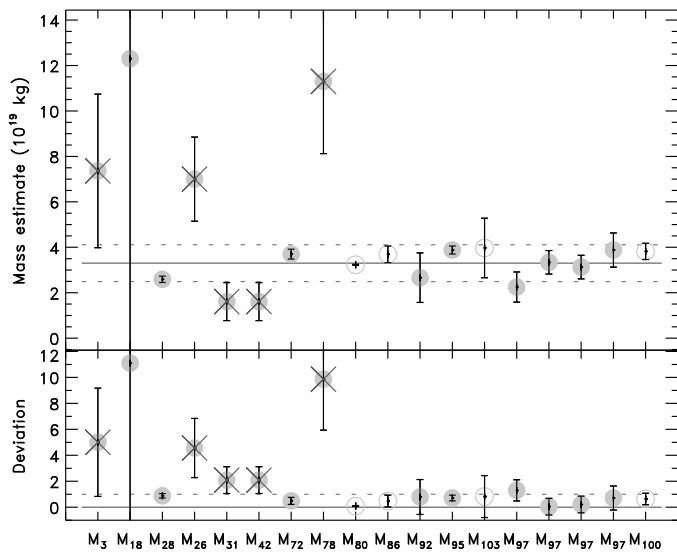


Figure A.126: Mass estimates for (704) Interamnia.

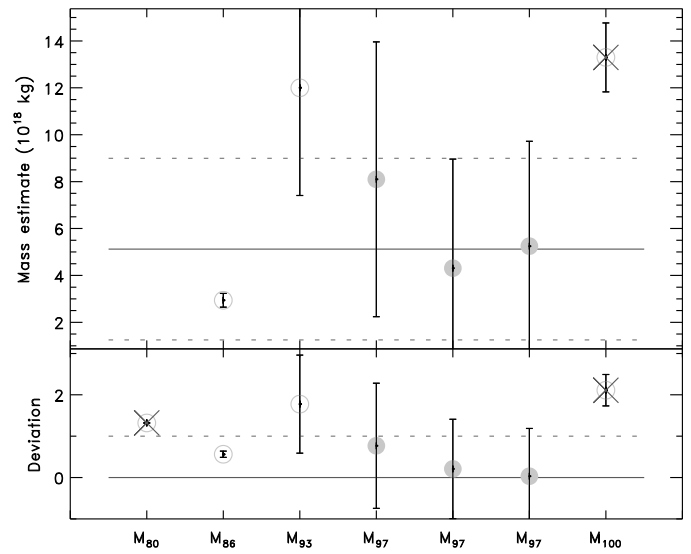


Figure A.128: Mass estimates for (747) Winchester. The mass estimate from M_{80} was listed as unrealistic by the authors, and is discarded here.

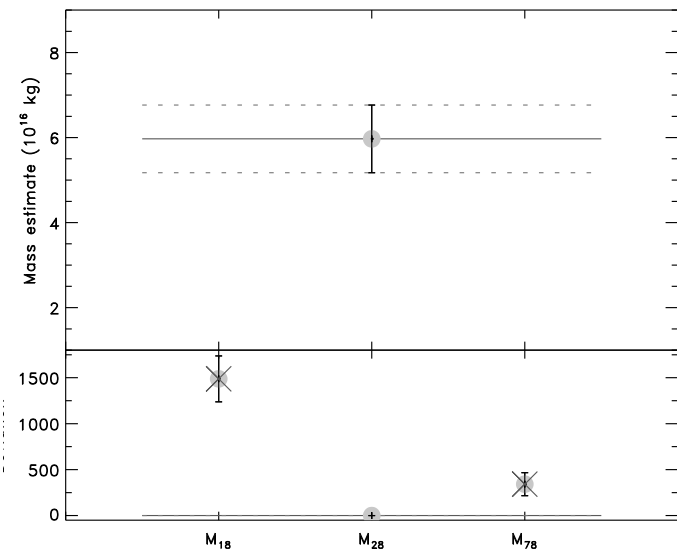


Figure A.127: Mass estimates for (720) Bohlinia.

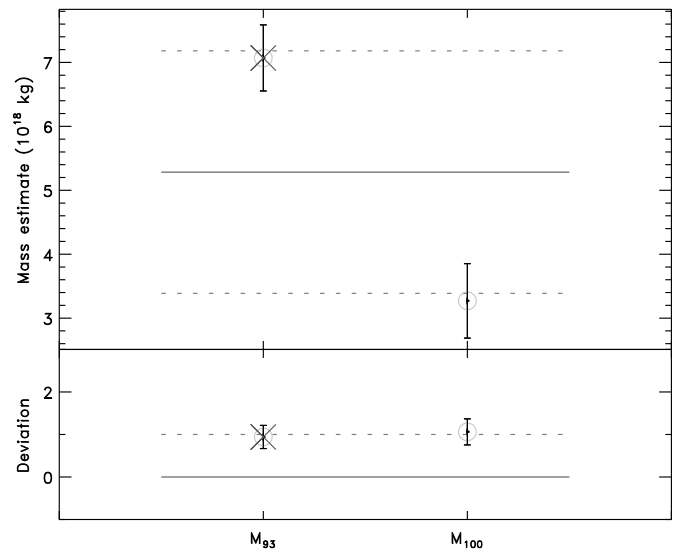


Figure A.129: Mass estimates for (751) Faina.

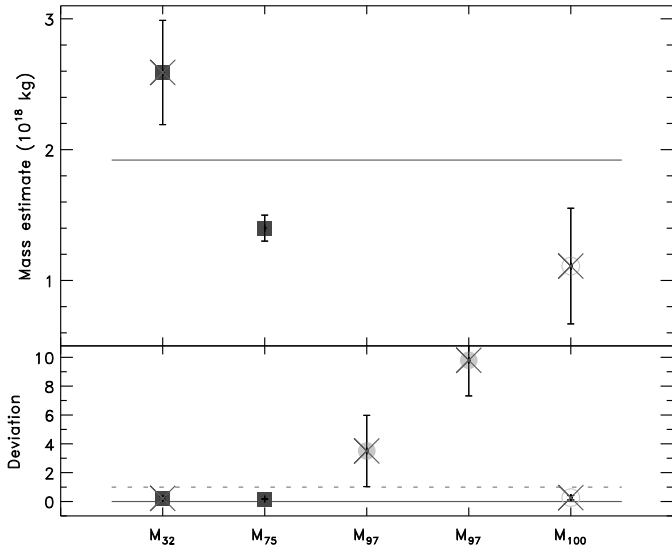


Figure A.130: Mass estimates for (762) Pulcova. The mass estimate from M_{32} was based on few discovery images, and the estimate from M_{75} is preferred.

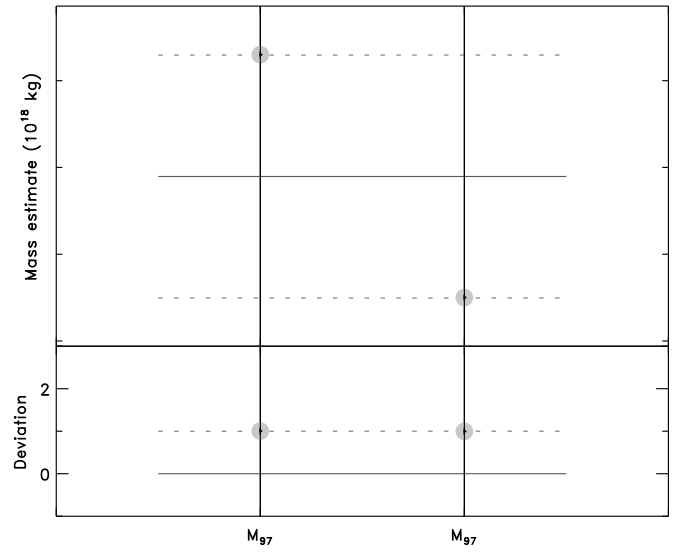


Figure A.132: Mass estimates for (790) Pretoria.

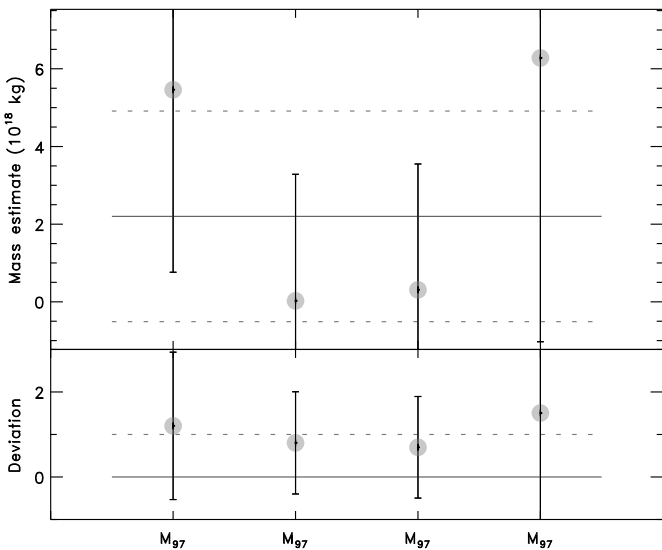


Figure A.131: Mass estimates for (776) Berbericia.

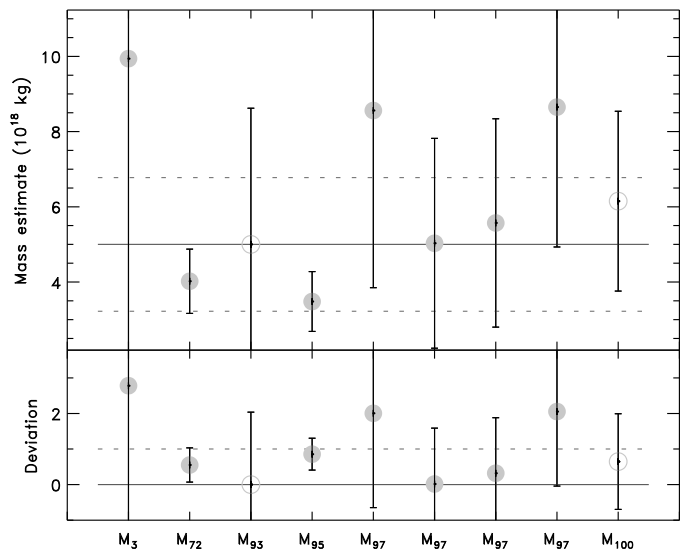


Figure A.133: Mass estimates for (804) Hispania.

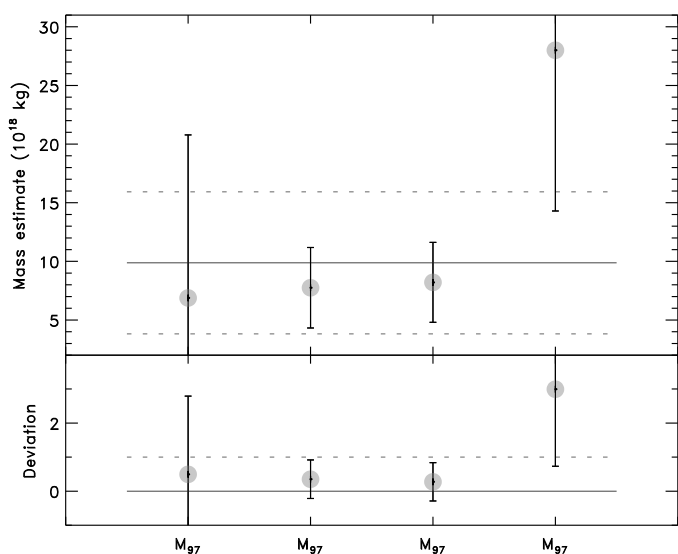


Figure A.134: Mass estimates for (895) Helio.

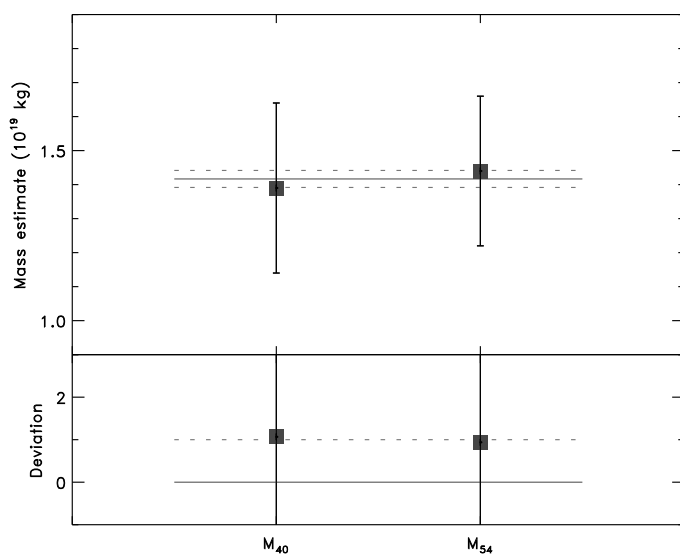


Figure A.136: Mass estimates for (47171) 1999 TC36.

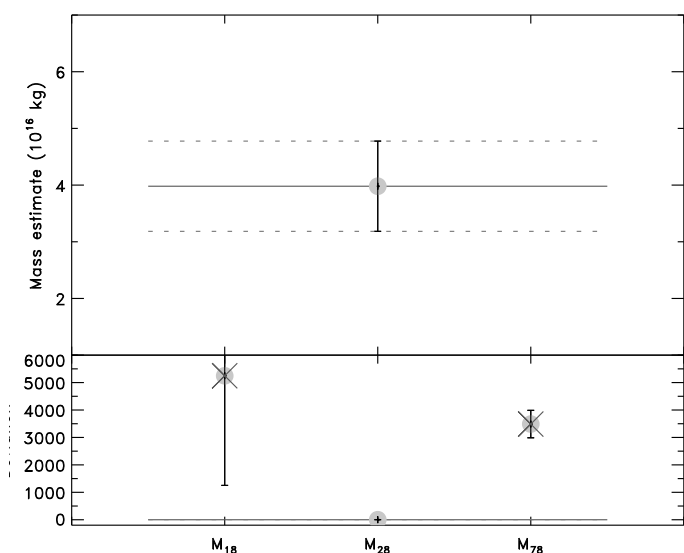


Figure A.135: Mass estimates for (1669) Dagmar.

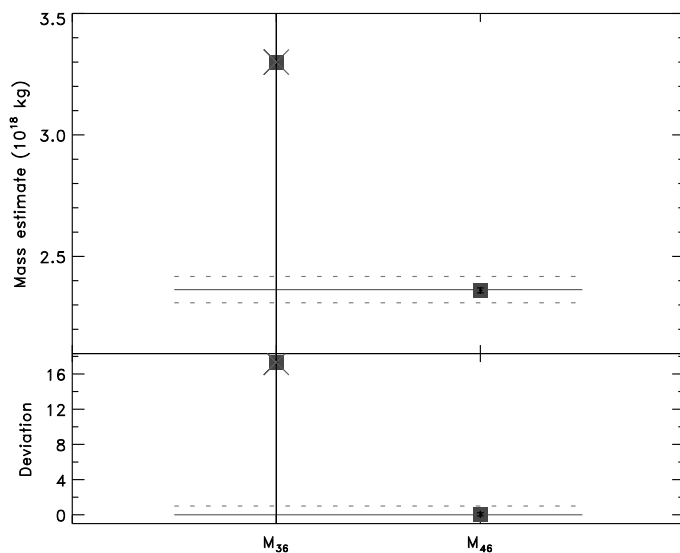


Figure A.137: Mass estimates for (88611) 2001 QT297. The mass estimate from M₃₆ has a crude relative precision (90%). The estimate from M₄₆ is preferred.

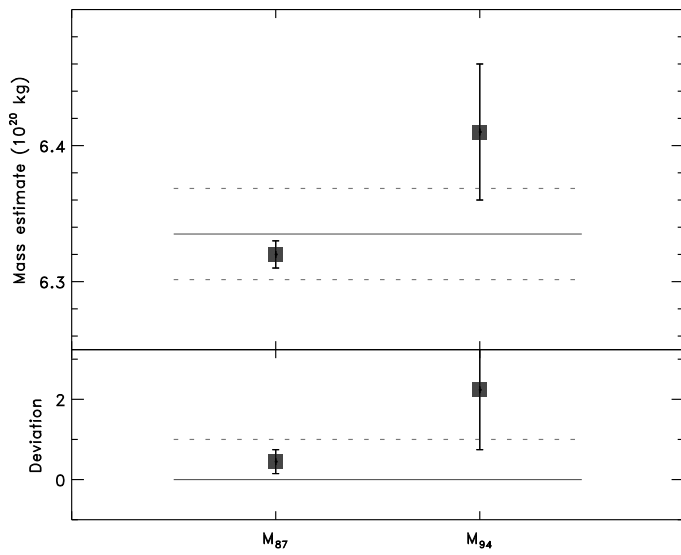


Figure A.138: Mass estimates for (90482) Orcus.

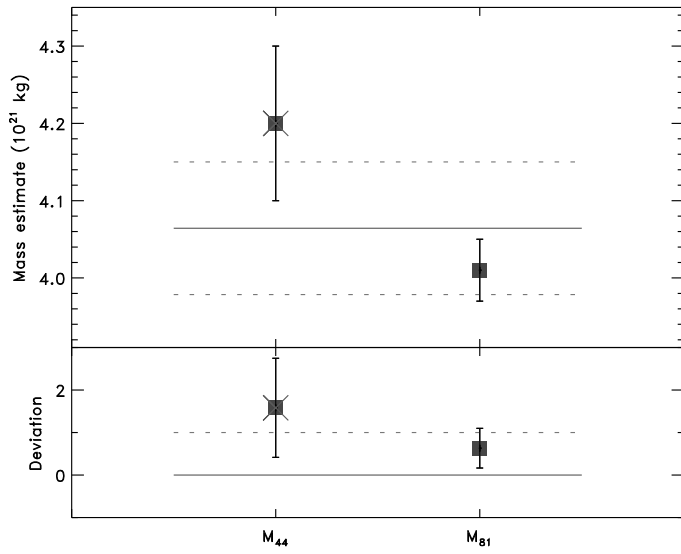


Figure A.139: Mass estimates for (136108) Haumea. The mass estimate from M₄₄ was based on few discovery images, and the estimate from M₈₁ is preferred.

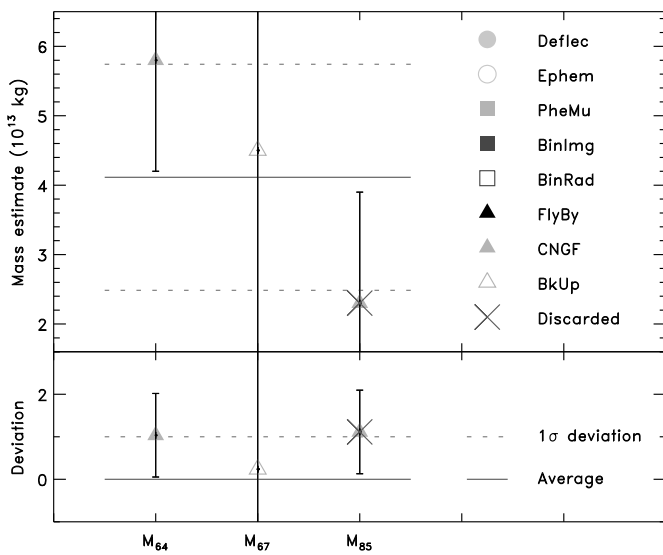


Figure A.140: Mass estimates for 9P/Tempell.

Appendix B. Compilation of volume estimates

The 1454 volume-equivalent diameter estimates gathered in the literature are listed in Table B.1. For objects with more than a single diameter determination, Fig. B.1 to Fig. B.246 presents a comparison of the diameter estimates, with additional information on discarded values. See Appendix D for the references, and Fig. B.246 for symbols key.

Table B.1: Compilation of volume-equivalent diameter estimates (ϕ , in km) for 232 objects, with their associated uncertainty ($\delta\phi$), bibliographic references (see Appendix D), and method of analysis: *H-mag*: crude estimate from absolute magnitude, *STM*: Standard Thermal Model, *NEATM*: Near-Earth Asteroid Thermal Model, *TPM*: Thermophysical Model, *Occ*: stellar occultation, *LC+Occ*: lightcurve 3-D model scaled using an occultation, *PheMu*: mutual eclipsing phenomena in binary systems, *Img-PSF*: profile deviation from a Point-Spread Function, *Img*: apparent size in disk-resolved imaging, *Img-TE*: triaxial ellipsoid model from images, *KOALA*: combined lightcurves, occultations, and disk-resolved images, *Radar*: radar imaging, *FlyBy*: images from spacecraft encounter, *IAU*: IAU WGCCR consensus value, and *BkUp*: break-up modeling of comet nucleus. Estimates marked with a dagger (\dagger) were rejected from average diameter computation.

#	Designation	ϕ	$\delta\phi$	Method	Refs.
1	Ceres	1014.00	101.40	STM	ϕ_{96}
1	Ceres	848.40	19.70	STM	ϕ_{93}^{\dagger}
1	Ceres	952.40	3.40	Img-TE	ϕ_{22}
1	Ceres	935.20	4.40	Img-TE	ϕ_{41}
1	Ceres	950.79	7.69	Img-TE	ϕ_{48}
1	Ceres	855.46	56.95	STM	ϕ_{64}
1	Ceres	886.47	27.29	NEATM	ϕ_{64}
1	Ceres	973.89	13.31	STM	ϕ_{83}
2	Pallas	589.00	58.90	STM	ϕ_{96}
2	Pallas	498.07	18.79	STM	ϕ_{93}
2	Pallas	502.00	6.00	Img-TE	ϕ_{54}
2	Pallas	544.00	18.00	Img-TE	ϕ_{58}
2	Pallas	512.00	6.00	KOALA	ϕ_{67}
2	Pallas	479.80	20.18	STM	ϕ_{64}
2	Pallas	523.97	20.82	NEATM	ϕ_{64}
2	Pallas	539.00	28.00	LC+Occ	ϕ_{78}
2	Pallas	512.59	4.98	STM	ϕ_{83}
2	Pallas	544.00	42.91	NEATM	ϕ_{72}
2	Pallas	544.00	60.70	NEATM	ϕ_{72}
3	Juno	247.00	24.70	STM	ϕ_{96}
3	Juno	233.91	11.19	STM	ϕ_{93}
3	Juno	250.30	5.30	Img-TE	ϕ_{48}
3	Juno	248.47	6.84	STM	ϕ_{64}
3	Juno	262.01	12.05	NEATM	ϕ_{64}
3	Juno	252.00	29.00	LC+Occ	ϕ_{78}
3	Juno	231.08	2.59	STM	ϕ_{83}
4	Vesta	530.00	53.00	STM	ϕ_{96}
4	Vesta	468.29	26.70	STM	ϕ_{93}^{\dagger}
4	Vesta	530.00	10.00	Img-TE	ϕ_2
4	Vesta	510.29	5.80	Img-TE	ϕ_{48}
4	Vesta	520.36	6.84	STM	ϕ_{64}
4	Vesta	515.85	19.25	NEATM	ϕ_{64}
4	Vesta	521.73	7.50	STM	ϕ_{83}
5	Astraea	121.00	12.10	STM	ϕ_{96}
5	Astraea	119.06	6.50	STM	ϕ_{93}
5	Astraea	97.96	3.61	STM	ϕ_{64}^{\dagger}
5	Astraea	133.72	6.46	NEATM	ϕ_{64}^{\dagger}
5	Astraea	115.00	6.00	LC+Occ	ϕ_{78}
5	Astraea	110.76	1.37	STM	ϕ_{83}
5	Astraea	115.00	9.35	NEATM	ϕ_{72}

Table B.1: Continued

# Designation	ϕ	$\delta\phi$	Method	Refs.
6 Hebe	204.00	20.39	STM	ϕ_{96}
6 Hebe	185.17	2.90	STM	ϕ_{93}
6 Hebe	180.42	8.50	STM	ϕ_{64}
6 Hebe	214.49	10.25	NEATM	ϕ_{64}^\dagger
6 Hebe	180.00	40.00	LC+Occ	ϕ_{78}
6 Hebe	197.14	1.83	STM	ϕ_{83}
6 Hebe	185.00	10.68	NEATM	ϕ_{72}
7 Iris	208.00	20.79	STM	ϕ_{96}
7 Iris	199.83	10.00	STM	ϕ_{93}
7 Iris	223.30	37.29	Radar	ϕ_{69}
7 Iris	190.46	11.44	STM	ϕ_{64}
7 Iris	226.36	10.93	NEATM	ϕ_{64}
7 Iris	198.00	27.00	LC+Occ	ϕ_{78}
7 Iris	199.00	26.00	LC+Occ	ϕ_{78}
7 Iris	254.19	3.26	STM	ϕ_{83}
8 Flora	162.00	16.20	STM	ϕ_{96}^\dagger
8 Flora	135.88	2.29	STM	ϕ_{93}
8 Flora	115.76	2.65	STM	ϕ_{64}^\dagger
8 Flora	145.75	7.05	NEATM	ϕ_{64}
8 Flora	141.00	10.00	LC+Occ	ϕ_{78}
8 Flora	140.00	7.00	LC+Occ	ϕ_{78}
8 Flora	138.30	1.37	STM	ϕ_{83}
8 Flora	140.00	1.15	NEATM	ϕ_{72}
9 Metis	185.00	18.50	STM	ϕ_{96}
9 Metis	154.66	4.25	STM	ϕ_{94}
9 Metis	181.00	1.50	Img	ϕ_{34}^\dagger
9 Metis	152.41	0.01	STM	ϕ_{64}^\dagger
9 Metis	178.11	0.02	NEATM	ϕ_{64}^\dagger
9 Metis	169.00	20.00	LC+Occ	ϕ_{78}
9 Metis	166.47	2.07	TPM	ϕ_{83}
9 Metis	204.52	3.67	NEATM	ϕ_{72}^\dagger
9 Metis	190.78	4.90	NEATM	ϕ_{72}^\dagger
10 Hygiea	430.00	43.00	STM	ϕ_{96}
10 Hygiea	407.11	6.80	STM	ϕ_{93}
10 Hygiea	357.26	8.59	STM	ϕ_{64}^\dagger
10 Hygiea	447.29	18.53	NEATM	ϕ_{64}
10 Hygiea	351.00	27.00	LC+Occ	ϕ_{78}
10 Hygiea	443.00	45.00	LC+Occ	ϕ_{78}
10 Hygiea	428.45	6.57	STM	ϕ_{83}
10 Hygiea	453.23	19.23	NEATM	ϕ_{72}
11 Parthenope	157.00	15.69	STM	ϕ_{96}
11 Parthenope	153.33	3.09	STM	ϕ_{93}
11 Parthenope	125.48	3.47	STM	ϕ_{64}^\dagger
11 Parthenope	142.36	4.01	NEATM	ϕ_{64}
11 Parthenope	150.47	2.05	STM	ϕ_{83}
11 Parthenope	159.11	5.94	NEATM	ϕ_{72}
12 Victoria	135.00	13.50	STM	ϕ_{96}
12 Victoria	112.76	3.09	STM	ϕ_{93}
12 Victoria	114.34	3.46	STM	ϕ_{64}
12 Victoria	131.02	6.15	NEATM	ϕ_{64}
12 Victoria	131.50	1.98	STM	ϕ_{83}
12 Victoria	126.63	3.20	NEATM	ϕ_{72}

Table B.1: Continued

# Designation	ϕ	$\delta\phi$	Method	Refs.
13 Egeria	244.00	24.39	STM	ϕ_{96}
13 Egeria	207.63	8.30	STM	ϕ_{93}
13 Egeria	223.08	3.46	STM	ϕ_{64}
13 Egeria	226.05	9.48	NEATM	ϕ_{64}
13 Egeria	203.36	2.56	STM	ϕ_{83}
13 Egeria	227.00	25.95	NEATM	ϕ_{72}
14 Irene	150.00	15.00	STM	ϕ_{96}
14 Irene	144.08	1.94	TPM	ϕ_{83}
14 Irene	155.39	4.38	NEATM	ϕ_{72}
15 Eunomia	259.00	25.89	STM	ϕ_{96}
15 Eunomia	255.33	15.00	STM	ϕ_{93}
15 Eunomia	225.75	6.84	STM	ϕ_{64}^\dagger
15 Eunomia	286.48	15.35	NEATM	ϕ_{64}^\dagger
15 Eunomia	256.41	3.08	STM	ϕ_{83}
15 Eunomia	259.00	35.50	NEATM	ϕ_{72}
16 Psyche	247.00	24.70	STM	ϕ_{96}
16 Psyche	253.16	4.00	STM	ϕ_{93}
16 Psyche	262.79	4.09	Img-TE	ϕ_{48}
16 Psyche	222.58	5.57	STM	ϕ_{64}
16 Psyche	269.69	11.50	NEATM	ϕ_{64}
16 Psyche	225.00	20.00	LC+Occ	ϕ_{78}
16 Psyche	225.00	36.00	LC+Occ	ϕ_{78}
16 Psyche	207.22	2.98	STM	ϕ_{83}^\dagger
17 Thetis	98.00	9.80	STM	ϕ_{96}
17 Thetis	90.04	3.70	STM	ϕ_{93}
17 Thetis	80.36	3.29	STM	ϕ_{64}
17 Thetis	95.84	6.01	NEATM	ϕ_{64}
17 Thetis	77.00	8.00	LC+Occ	ϕ_{78}
17 Thetis	74.58	0.99	STM	ϕ_{83}
17 Thetis	93.33	2.63	NEATM	ϕ_{72}
18 Melpomene	162.00	16.20	STM	ϕ_{96}
18 Melpomene	140.57	2.79	STM	ϕ_{93}
18 Melpomene	123.08	3.28	STM	ϕ_{64}^\dagger
18 Melpomene	142.85	6.80	NEATM	ϕ_{64}
18 Melpomene	139.94	1.85	STM	ϕ_{83}
18 Melpomene	141.00	14.71	NEATM	ϕ_{72}
19 Fortuna	221.00	22.10	STM	ϕ_{96}
19 Fortuna	210.10	3.77	Occ	ϕ_{95}
19 Fortuna	209.60	4.96	Img-TE	ϕ_{76}
19 Fortuna	199.66	3.01	TPM	ϕ_{83}
19 Fortuna	223.00	43.59	NEATM	ϕ_{72}
20 Massalia	134.00	13.39	STM	ϕ_{96}
20 Massalia	145.50	9.30	STM	ϕ_{93}
20 Massalia	152.27	7.19	STM	ϕ_{64}
20 Massalia	155.03	9.61	NEATM	ϕ_{64}
20 Massalia	131.55	1.15	STM	ϕ_{83}

# Designation	ϕ	$\delta\phi$	Method	Refs.
21 Lutetia	109.00	10.89	STM	ϕ_{96}^{\dagger}
21 Lutetia	95.76	4.09	STM	ϕ_{93}^{\dagger}
21 Lutetia	100.00	11.00	Radar	ϕ_{45}^{\dagger}
21 Lutetia	110.50	3.50	TPM	ϕ_{57}^{\dagger}
21 Lutetia	82.66	2.56	STM	ϕ_{64}^{\dagger}
21 Lutetia	104.20	7.11	NEATM	ϕ_{64}^{\dagger}
21 Lutetia	105.19	7.69	Img-TE	ϕ_{62}^{\dagger}
21 Lutetia	100.00	5.00	KOALA	ϕ_{61}^{\dagger}
21 Lutetia	98.00	5.00	FlyBy	ϕ_{84}
21 Lutetia	108.37	1.27	STM	ϕ_{83}^{\dagger}
22 Kalliope	174.00	17.39	STM	ϕ_{96}
22 Kalliope	181.00	4.59	STM	ϕ_{93}
22 Kalliope	166.19	2.79	PheMu	ϕ_{46}
22 Kalliope	177.00	4.00	NEATM	ϕ_{47}
22 Kalliope	162.66	5.00	STM	ϕ_{64}
22 Kalliope	183.11	7.84	NEATM	ϕ_{64}
22 Kalliope	143.00	10.00	LC+Occ	ϕ_{78}
22 Kalliope	139.77	2.14	STM	ϕ_{83}^{\dagger}
22 Kalliope	167.00	15.30	NEATM	ϕ_{72}
23 Thalia	117.00	11.69	STM	ϕ_{96}
23 Thalia	107.52	2.20	STM	ϕ_{93}
23 Thalia	105.98	3.51	STM	ϕ_{94}
23 Thalia	101.98	3.68	STM	ϕ_{64}
23 Thalia	111.04	6.26	NEATM	ϕ_{64}
23 Thalia	106.20	1.88	STM	ϕ_{83}
24 Themis	176.80	2.29	TPM	ϕ_{83}
24 Themis	202.33	6.05	NEATM	ϕ_{72}
25 Phocaea	72.00	7.19	STM	ϕ_{96}
25 Phocaea	75.12	3.59	STM	ϕ_{93}
25 Phocaea	71.00	8.00	Img	ϕ_{34}
25 Phocaea	61.61	2.01	STM	ϕ_{64}^{\dagger}
25 Phocaea	83.38	5.84	NEATM	ϕ_{64}
25 Phocaea	83.20	0.96	STM	ϕ_{83}
26 Proserpina	94.80	1.70	STM	ϕ_{93}
26 Proserpina	78.59	2.18	STM	ϕ_{64}^{\dagger}
26 Proserpina	95.91	5.46	NEATM	ϕ_{64}
26 Proserpina	87.44	0.95	STM	ϕ_{83}
26 Proserpina	87.12	1.32	NEATM	ϕ_{72}
27 Euterpe	117.00	11.69	STM	ϕ_{96}
27 Euterpe	96.80	2.20	Occ	ϕ_{95}
27 Euterpe	109.79	1.53	TPM	ϕ_{83}
27 Euterpe	118.00	22.30	NEATM	ϕ_{72}
28 Bellona	125.00	12.50	STM	ϕ_{96}
28 Bellona	120.90	3.40	STM	ϕ_{93}
28 Bellona	123.91	7.38	STM	ϕ_{94}
28 Bellona	104.25	2.64	STM	ϕ_{64}
28 Bellona	123.98	4.52	NEATM	ϕ_{64}
28 Bellona	97.00	11.00	LC+Occ	ϕ_{78}
28 Bellona	100.00	10.00	LC+Occ	ϕ_{78}
28 Bellona	97.40	1.42	STM	ϕ_{83}

# Designation	ϕ	$\delta\phi$	Method	Refs.
29 Amphitrite	200.00	20.00	STM	ϕ_{96}
29 Amphitrite	212.22	6.80	STM	ϕ_{93}
29 Amphitrite	231.21	6.55	STM	ϕ_{64}
29 Amphitrite	227.53	7.57	NEATM	ϕ_{64}
29 Amphitrite	206.86	2.59	STM	ϕ_{83}
29 Amphitrite	227.14	3.97	NEATM	ϕ_{72}
30 Urania	94.00	9.39	STM	ϕ_{96}
30 Urania	100.15	2.40	STM	ϕ_{93}
30 Urania	82.63	2.20	STM	ϕ_{64}^{\dagger}
30 Urania	102.01	4.69	NEATM	ϕ_{64}
30 Urania	88.91	0.97	STM	ϕ_{83}
30 Urania	98.41	2.14	NEATM	ϕ_{72}
31 Euphrosyne	255.89	11.50	STM	ϕ_{93}
31 Euphrosyne	265.94	7.00	STM	ϕ_{64}
31 Euphrosyne	286.91	12.53	NEATM	ϕ_{64}
31 Euphrosyne	276.48	2.85	STM	ϕ_{83}
31 Euphrosyne	280.00	60.77	NEATM	ϕ_{72}
33 Polyhymnia	53.97	0.91	STM	ϕ_{83}
34 Circe	111.00	11.10	STM	ϕ_{96}
34 Circe	113.54	3.29	STM	ϕ_{93}
34 Circe	109.50	1.79	Occ	ϕ_{95}
34 Circe	97.43	2.82	STM	ϕ_{64}^{\dagger}
34 Circe	121.54	7.09	NEATM	ϕ_{64}
34 Circe	96.00	10.00	LC+Occ	ϕ_{78}
34 Circe	107.00	10.00	LC+Occ	ϕ_{78}
34 Circe	116.45	1.13	STM	ϕ_{83}
34 Circe	113.23	2.89	NEATM	ϕ_{72}
36 Atalante	119.00	11.89	STM	ϕ_{96}
36 Atalante	105.61	4.00	STM	ϕ_{93}
36 Atalante	109.08	2.84	STM	ϕ_{64}
36 Atalante	121.06	9.59	NEATM	ϕ_{64}
36 Atalante	110.54	1.57	STM	ϕ_{83}
36 Atalante	103.00	11.44	NEATM	ϕ_{72}
38 Leda	115.93	2.09	STM	ϕ_{93}
38 Leda	97.31	2.69	STM	ϕ_{64}^{\dagger}
38 Leda	118.12	5.34	NEATM	ϕ_{64}
38 Leda	114.22	1.52	STM	ϕ_{83}
38 Leda	116.00	15.50	NEATM	ϕ_{72}
39 Laetitia	157.00	15.69	STM	ϕ_{96}
39 Laetitia	149.52	8.60	STM	ϕ_{93}
39 Laetitia	155.11	5.65	STM	ϕ_{64}
39 Laetitia	184.71	10.56	NEATM	ϕ_{64}^{\dagger}
39 Laetitia	163.00	12.00	LC+Occ	ϕ_{78}
39 Laetitia	151.57	1.65	STM	ϕ_{83}
39 Laetitia	163.00	14.02	NEATM	ϕ_{72}
41 Daphne	203.00	20.29	STM	ϕ_{96}
41 Daphne	174.00	11.69	STM	ϕ_{93}
41 Daphne	172.42	4.07	STM	ϕ_{64}
41 Daphne	207.86	10.52	NEATM	ϕ_{64}^{\dagger}
41 Daphne	187.00	20.00	LC+Occ	ϕ_{78}
41 Daphne	200.00	10.00	TPM	ϕ_{79}
41 Daphne	179.61	2.57	STM	ϕ_{83}

Table B.1: Continued

# Designation	ϕ	$\delta\phi$	Method	Refs.
42 Isis	94.00	9.39	STM	ϕ_{96}
42 Isis	100.19	3.40	STM	ϕ_{93}
42 Isis	102.90	2.28	STM	ϕ_{64}
42 Isis	104.69	6.11	NEATM	ϕ_{64}
42 Isis	104.50	1.37	STM	ϕ_{83}
43 Ariadne	85.00	8.50	STM	ϕ_{96}^\dagger
43 Ariadne	65.87	2.50	STM	ϕ_{93}
43 Ariadne	51.91	2.75	Occ	ϕ_{95}^\dagger
43 Ariadne	66.72	2.28	STM	ϕ_{64}
43 Ariadne	62.74	1.59	NEATM	ϕ_{64}
43 Ariadne	58.75	0.87	STM	ϕ_{83}
43 Ariadne	72.08	2.19	NEATM	ϕ_{72}
45 Eugenia	244.00	24.39	STM	ϕ_{96}
45 Eugenia	214.63	4.19	STM	ϕ_{93}
45 Eugenia	202.00	5.00	Img	ϕ_{34}
45 Eugenia	217.00	8.00	NEATM	ϕ_{47}
45 Eugenia	193.00	15.00	Img	ϕ_{47}
45 Eugenia	193.69	19.38	STM	ϕ_{64}
45 Eugenia	239.24	14.34	NEATM	ϕ_{64}^\dagger
45 Eugenia	183.57	2.84	STM	ϕ_{83}
45 Eugenia	206.13	6.21	NEATM	ϕ_{72}
46 Hestia	131.00	13.10	STM	ϕ_{96}
46 Hestia	124.13	3.59	STM	ϕ_{93}
46 Hestia	132.83	4.53	Occ	ϕ_{95}
46 Hestia	110.11	3.97	STM	ϕ_{64}^\dagger
46 Hestia	133.25	5.65	NEATM	ϕ_{64}
46 Hestia	120.62	1.52	STM	ϕ_{83}
46 Hestia	124.00	9.64	NEATM	ϕ_{72}
47 Aglaja	158.00	15.80	STM	ϕ_{96}
47 Aglaja	126.95	7.69	STM	ϕ_{93}
47 Aglaja	107.75	3.89	STM	ϕ_{64}^\dagger
47 Aglaja	140.80	6.57	NEATM	ϕ_{64}
47 Aglaja	147.05	3.57	STM	ϕ_{83}
47 Aglaja	138.00	11.10	NEATM	ϕ_{72}
48 Doris	221.80	7.50	STM	ϕ_{93}
48 Doris	211.30	16.01	STM	ϕ_{64}
48 Doris	238.78	9.21	NEATM	ϕ_{64}^\dagger
48 Doris	200.27	2.75	STM	ϕ_{83}
48 Doris	223.42	4.17	NEATM	ϕ_{72}
49 Pales	149.80	3.79	STM	ϕ_{93}
49 Pales	157.50	4.88	STM	ϕ_{64}
49 Pales	169.67	9.31	NEATM	ϕ_{64}^\dagger
49 Pales	148.02	2.55	STM	ϕ_{83}
50 Virginia	99.81	5.19	STM	ϕ_{93}
50 Virginia	98.96	3.04	NEATM	ϕ_{64}
50 Virginia	84.37	0.82	STM	ϕ_{83}^\dagger
50 Virginia	100.00	7.59	NEATM	ϕ_{72}
51 Nemausa	151.00	15.10	STM	ϕ_{96}
51 Nemausa	147.86	2.40	STM	ϕ_{93}
51 Nemausa	155.86	3.98	STM	ϕ_{64}
51 Nemausa	147.17	1.69	STM	ϕ_{83}
51 Nemausa	142.60	12.50	NEATM	ϕ_{72}

Table B.1: Continued

# Designation	ϕ	$\delta\phi$	Method	Refs.
52 Europa	292.00	29.20	STM	ϕ_{96}
52 Europa	302.50	5.40	STM	ϕ_{93}
52 Europa	308.00	1.50	Img	ϕ_{34}
52 Europa	264.32	6.96	STM	ϕ_{64}^\dagger
52 Europa	340.75	13.36	NEATM	ϕ_{64}
52 Europa	293.00	30.00	LC+Occ	ϕ_{78}
52 Europa	350.35	5.07	STM	ϕ_{83}^\dagger
52 Europa	334.55	20.94	NEATM	ϕ_{72}
52 Europa	314.00	8.00	Img-TE	ϕ_{91}
52 Europa	312.00	10.00	KOALA	ϕ_{91}
53 Kalypso	115.37	2.40	STM	ϕ_{93}
53 Kalypso	118.63	3.54	STM	ϕ_{64}
53 Kalypso	115.30	5.94	NEATM	ϕ_{64}
53 Kalypso	101.90	1.02	STM	ϕ_{83}
53 Kalypso	115.00	10.31	NEATM	ϕ_{72}
54 Alexandra	175.00	17.50	STM	ϕ_{96}
54 Alexandra	165.75	3.40	STM	ϕ_{93}
54 Alexandra	146.99	2.31	Occ	ϕ_{95}
54 Alexandra	177.41	4.55	STM	ϕ_{64}^\dagger
54 Alexandra	177.67	7.55	NEATM	ϕ_{64}^\dagger
54 Alexandra	135.00	20.00	LC+Occ	ϕ_{78}
54 Alexandra	142.00	9.00	LC+Occ	ϕ_{78}
54 Alexandra	144.46	1.79	STM	ϕ_{83}
54 Alexandra	142.00	14.76	NEATM	ϕ_{72}
56 Melete	144.00	14.39	STM	ϕ_{96}^\dagger
56 Melete	113.23	1.70	STM	ϕ_{93}
56 Melete	118.97	2.83	STM	ϕ_{64}
56 Melete	125.75	5.71	NEATM	ϕ_{64}
56 Melete	105.22	1.15	STM	ϕ_{83}
56 Melete	129.07	4.40	NEATM	ϕ_{72}
57 Mnemosyne	112.58	2.79	STM	ϕ_{93}
57 Mnemosyne	116.58	2.82	STM	ϕ_{64}
57 Mnemosyne	112.39	4.92	NEATM	ϕ_{64}
57 Mnemosyne	108.76	1.41	STM	ϕ_{83}
57 Mnemosyne	122.47	4.69	NEATM	ϕ_{72}
59 Elpis	164.80	6.00	STM	ϕ_{93}
59 Elpis	173.67	4.30	Occ	ϕ_{95}
59 Elpis	144.66	4.88	STM	ϕ_{64}^\dagger
59 Elpis	182.22	9.60	NEATM	ϕ_{64}^\dagger
59 Elpis	156.17	2.30	STM	ϕ_{83}
59 Elpis	165.69	3.03	NEATM	ϕ_{72}
60 Echo	51.00	5.09	STM	ϕ_{96}^\dagger
60 Echo	60.20	1.79	STM	ϕ_{93}
60 Echo	63.13	3.26	STM	ϕ_{64}
60 Echo	59.36	2.99	NEATM	ϕ_{64}
60 Echo	58.95	1.24	STM	ϕ_{83}
60 Echo	60.00	3.52	NEATM	ϕ_{72}

Table B.1: Continued

# Designation	ϕ	$\delta\phi$	Method	Refs.
61 Danae	76.76	4.26	STM	ϕ_{94}
61 Danae	82.04	4.30	STM	ϕ_{93}
61 Danae	78.12	5.11	STM	ϕ_{64}
61 Danae	93.01	4.32	NEATM	ϕ_{64}^\dagger
61 Danae	83.55	1.01	STM	ϕ_{83}
61 Danae	85.12	1.96	NEATM	ϕ_{72}
63 Ausonia	93.00	9.30	STM	ϕ_{96}
63 Ausonia	103.13	2.40	STM	ϕ_{93}
63 Ausonia	93.73	5.80	STM	ϕ_{64}
63 Ausonia	108.31	6.53	NEATM	ϕ_{64}^\dagger
63 Ausonia	90.00	18.00	LC+Occ	ϕ_{78}
63 Ausonia	87.47	1.13	STM	ϕ_{83}
63 Ausonia	102.97	2.75	NEATM	ϕ_{72}
65 Cybele	309.00	30.89	STM	ϕ_{96}^\dagger
65 Cybele	237.25	4.19	STM	ϕ_{93}
65 Cybele	272.70	10.89	TPM	ϕ_{12}
65 Cybele	231.86	9.43	STM	ϕ_{64}
65 Cybele	272.01	11.14	NEATM	ϕ_{64}
65 Cybele	300.54	4.82	STM	ϕ_{83}^\dagger
67 Asia	59.00	5.90	STM	ϕ_{96}
67 Asia	58.11	1.39	STM	ϕ_{93}
67 Asia	52.29	15.28	Occ	ϕ_{95}
67 Asia	60.18	1.90	STM	ϕ_{64}
67 Asia	66.69	3.95	NEATM	ϕ_{64}
67 Asia	61.63	0.65	STM	ϕ_{83}
67 Asia	62.70	1.76	NEATM	ϕ_{72}
68 Leto	127.00	12.69	STM	ϕ_{96}
68 Leto	116.33	4.82	STM	ϕ_{94}
68 Leto	122.56	5.30	STM	ϕ_{93}
68 Leto	128.05	4.03	STM	ϕ_{64}
68 Leto	130.90	6.32	NEATM	ϕ_{64}
68 Leto	148.00	25.00	LC+Occ	ϕ_{78}
68 Leto	151.00	25.00	LC+Occ	ϕ_{78}
68 Leto	121.95	1.19	STM	ϕ_{83}
68 Leto	128.85	4.17	NEATM	ϕ_{72}
69 Hesperia	108.00	10.80	STM	ϕ_{96}^\dagger
69 Hesperia	138.13	4.69	STM	ϕ_{93}
69 Hesperia	145.88	4.03	STM	ϕ_{64}
69 Hesperia	136.75	3.26	NEATM	ϕ_{64}
69 Hesperia	132.74	1.52	STM	ϕ_{83}
70 Panopaea	151.00	15.10	STM	ϕ_{96}
70 Panopaea	122.16	2.29	STM	ϕ_{93}
70 Panopaea	105.16	2.79	STM	ϕ_{64}^\dagger
70 Panopaea	130.88	6.53	NEATM	ϕ_{64}
70 Panopaea	131.19	1.49	Occ	ϕ_{95}
70 Panopaea	141.39	1.91	STM	ϕ_{83}
70 Panopaea	139.00	3.84	NEATM	ϕ_{72}
72 Feronia	95.00	9.50	STM	ϕ_{96}
72 Feronia	85.90	3.59	STM	ϕ_{93}
72 Feronia	74.13	2.25	STM	ϕ_{64}^\dagger
72 Feronia	90.83	4.59	NEATM	ϕ_{64}
72 Feronia	83.11	0.94	STM	ϕ_{83}
72 Feronia	79.48	1.94	NEATM	ϕ_{72}

Table B.1: Continued

# Designation	ϕ	$\delta\phi$	Method	Refs.
74 Galatea	118.70	2.79	STM	ϕ_{93}
74 Galatea	97.83	2.94	Occ	ϕ_{95}^\dagger
74 Galatea	127.66	3.33	STM	ϕ_{64}
74 Galatea	132.02	5.32	NEATM	ϕ_{64}
74 Galatea	113.08	2.15	STM	ϕ_{83}
76 Freia	117.00	11.69	STM	ϕ_{96}^\dagger
76 Freia	158.67	4.96	Occ	ϕ_{95}
76 Freia	183.66	4.00	STM	ϕ_{93}
76 Freia	161.67	5.23	STM	ϕ_{64}
76 Freia	192.41	8.56	NEATM	ϕ_{64}^\dagger
76 Freia	168.36	1.95	STM	ϕ_{83}
76 Freia	158.57	8.02	NEATM	ϕ_{72}
77 Frigga	66.00	6.59	STM	ϕ_{96}
77 Frigga	69.25	2.09	STM	ϕ_{93}
77 Frigga	65.69	3.18	STM	ϕ_{64}
77 Frigga	68.81	3.07	NEATM	ϕ_{64}
77 Frigga	65.81	0.86	STM	ϕ_{83}
77 Frigga	67.18	0.90	NEATM	ϕ_{72}
78 Diana	120.59	2.70	STM	ϕ_{93}
78 Diana	116.00	4.84	STM	ϕ_{64}
78 Diana	130.80	7.34	NEATM	ϕ_{64}
78 Diana	126.51	1.66	STM	ϕ_{83}
81 Terpsichore	119.08	2.09	STM	ϕ_{93}
81 Terpsichore	119.72	5.63	Occ	ϕ_{95}
81 Terpsichore	109.59	5.50	STM	ϕ_{64}^\dagger
81 Terpsichore	127.31	6.32	NEATM	ϕ_{64}
81 Terpsichore	122.95	1.41	STM	ϕ_{83}
81 Terpsichore	121.58	3.15	NEATM	ϕ_{72}
84 Klio	87.00	8.69	STM	ϕ_{96}
84 Klio	79.16	1.60	STM	ϕ_{93}
84 Klio	68.05	2.16	STM	ϕ_{64}^\dagger
84 Klio	81.06	3.42	NEATM	ϕ_{64}
84 Klio	78.31	0.96	STM	ϕ_{83}
84 Klio	79.00	4.86	NEATM	ϕ_{72}
85 Io	147.00	14.69	STM	ϕ_{96}
85 Io	169.63	23.00	Occ	ϕ_{95}
85 Io	154.78	3.79	STM	ϕ_{93}
85 Io	155.24	5.09	STM	ϕ_{64}
85 Io	168.00	10.56	NEATM	ϕ_{64}
85 Io	163.00	15.00	LC+Occ	ϕ_{78}
85 Io	150.66	1.91	STM	ϕ_{83}
85 Io	163.00	18.64	NEATM	ϕ_{72}
87 Sylvia	260.94	13.30	STM	ϕ_{93}^\dagger
87 Sylvia	286.50	11.50	Img-TE	ϕ_{21}
87 Sylvia	282.00	3.50	Img	ϕ_{34}
87 Sylvia	232.16	8.79	STM	ϕ_{64}^\dagger
87 Sylvia	290.30	14.46	NEATM	ϕ_{64}
87 Sylvia	262.67	3.85	STM	ϕ_{83}
87 Sylvia	288.38	7.61	NEATM	ϕ_{72}

Table B.1: Continued

# Designation	ϕ	$\delta\phi$	Method	Refs.
88 Thisbe	210.00	21.00	STM	ϕ_{96}
88 Thisbe	200.58	5.00	STM	ϕ_{93}
88 Thisbe	207.88	5.88	STM	ϕ_{64}
88 Thisbe	223.19	10.22	NEATM	ϕ_{64}
88 Thisbe	204.00	14.00	LC+Occ	ϕ_{78}
88 Thisbe	220.00	16.00	LC+Occ	ϕ_{78}
88 Thisbe	195.58	2.72	STM	ϕ_{83}
89 Julia	167.00	16.70	STM	ϕ_{96}
89 Julia	151.46	3.09	STM	ϕ_{93}
89 Julia	128.53	3.03	STM	ϕ_{94}^\dagger
89 Julia	134.27	4.00	STM	ϕ_{64}
89 Julia	160.83	6.53	NEATM	ϕ_{64}
89 Julia	140.00	10.00	LC+Occ	ϕ_{78}
89 Julia	146.77	1.90	STM	ϕ_{83}
89 Julia	148.08	10.07	NEATM	ϕ_{72}
90 Antiope	120.06	4.00	STM	ϕ_{93}
90 Antiope	111.50	5.00	LC+Occ	ϕ_{38}^\dagger
90 Antiope	127.01	5.09	NEATM	ϕ_{64}
90 Antiope	123.80	2.11	STM	ϕ_{83}
90 Antiope	123.55	2.91	NEATM	ϕ_{72}
90 Antiope	118.70	2.02	NEATM	ϕ_{72}
92 Undina	124.37	2.00	Occ	ϕ_{95}
92 Undina	126.41	3.40	STM	ϕ_{93}
92 Undina	125.18	2.61	STM	ϕ_{64}
92 Undina	133.66	7.38	NEATM	ϕ_{64}
92 Undina	120.93	1.70	STM	ϕ_{83}
93 Minerva	168.00	16.79	STM	ϕ_{96}
93 Minerva	141.55	4.00	STM	ϕ_{93}
93 Minerva	156.97	2.82	STM	ϕ_{94}
93 Minerva	142.69	3.29	STM	ϕ_{64}
93 Minerva	164.75	8.34	NEATM	ϕ_{64}
93 Minerva	147.10	2.24	STM	ϕ_{83}
94 Aurora	190.00	19.00	STM	ϕ_{96}
94 Aurora	204.88	3.59	STM	ϕ_{93}^\dagger
94 Aurora	169.00	6.50	Img	ϕ_{34}^\dagger
94 Aurora	183.16	4.61	STM	ϕ_{64}
94 Aurora	206.30	8.97	NEATM	ϕ_{64}
94 Aurora	179.14	3.82	STM	ϕ_{83}
94 Aurora	187.50	7.26	NEATM	ϕ_{72}
96 Aegle	167.41	36.86	Occ	ϕ_{95}
96 Aegle	170.02	3.40	STM	ϕ_{93}
96 Aegle	156.00	9.00	Img	ϕ_{34}
96 Aegle	173.11	5.15	STM	ϕ_{64}
96 Aegle	176.25	8.68	NEATM	ϕ_{64}
96 Aegle	164.77	2.53	STM	ϕ_{83}
97 Klotho	80.00	10.00	Occ	ϕ_{95}
97 Klotho	108.00	10.80	STM	ϕ_{96}^\dagger
97 Klotho	82.83	4.50	STM	ϕ_{93}
97 Klotho	80.44	4.50	STM	ϕ_{94}
97 Klotho	81.72	3.42	STM	ϕ_{64}
97 Klotho	102.48	6.59	NEATM	ϕ_{64}^\dagger
97 Klotho	87.83	0.97	STM	ϕ_{83}
97 Klotho	83.00	5.09	NEATM	ϕ_{72}

Table B.1: Continued

# Designation	ϕ	$\delta\phi$	Method	Refs.
98 Ianthe	104.44	1.79	STM	ϕ_{93}
98 Ianthe	101.97	3.67	STM	ϕ_{64}
98 Ianthe	114.30	5.23	NEATM	ϕ_{64}
98 Ianthe	104.23	1.28	STM	ϕ_{83}
98 Ianthe	110.87	2.31	NEATM	ϕ_{72}
105 Artemis	103.65	5.26	STM	ϕ_{93}
105 Artemis	119.08	2.79	STM	ϕ_{64}
105 Artemis	101.05	2.80	NEATM	ϕ_{64}^\dagger
105 Artemis	123.52	1.50	STM	ϕ_{83}
105 Artemis	119.00	17.34	NEATM	ϕ_{72}
106 Dione	140.00	14.00	STM	ϕ_{96}
106 Dione	145.61	0.82	Occ	ϕ_{95}
106 Dione	146.58	2.79	STM	ϕ_{93}
106 Dione	127.31	3.36	STM	ϕ_{64}^\dagger
106 Dione	162.91	7.86	NEATM	ϕ_{64}^\dagger
106 Dione	153.41	2.38	STM	ϕ_{83}
107 Camilla	213.00	21.29	STM	ϕ_{96}
107 Camilla	222.61	17.10	STM	ϕ_{93}
107 Camilla	185.00	9.00	Img	ϕ_{34}^\dagger
107 Camilla	249.00	18.00	NEATM	ϕ_{47}^\dagger
107 Camilla	246.00	13.00	Img	ϕ_{47}^\dagger
107 Camilla	208.85	10.79	STM	ϕ_{64}
107 Camilla	221.10	14.36	NEATM	ϕ_{64}
107 Camilla	214.00	28.00	LC+Occ	ϕ_{78}
107 Camilla	200.36	3.51	STM	ϕ_{83}
107 Camilla	219.36	5.94	NEATM	ϕ_{72}
111 Ate	134.55	4.59	STM	ϕ_{93}
111 Ate	140.16	2.40	STM	ϕ_{64}
111 Ate	153.16	5.79	NEATM	ϕ_{64}
111 Ate	146.55	2.34	STM	ϕ_{83}
111 Ate	135.00	18.57	NEATM	ϕ_{72}
112 Iphigenia	72.18	4.40	STM	ϕ_{93}
112 Iphigenia	59.84	2.07	STM	ϕ_{64}^\dagger
112 Iphigenia	80.62	4.21	NEATM	ϕ_{64}^\dagger
112 Iphigenia	71.05	0.94	STM	ϕ_{83}
112 Iphigenia	70.37	2.90	NEATM	ϕ_{72}
117 Lomia	144.61	5.57	STM	ϕ_{94}
117 Lomia	148.71	6.59	STM	ϕ_{93}
117 Lomia	164.10	3.30	Occ	ϕ_{95}^\dagger
117 Lomia	131.53	3.79	STM	ϕ_{64}^\dagger
117 Lomia	157.69	9.94	NEATM	ϕ_{64}
117 Lomia	144.91	1.86	STM	ϕ_{83}
117 Lomia	173.27	3.53	NEATM	ϕ_{72}^\dagger
121 Hermione	209.00	4.69	STM	ϕ_{93}
121 Hermione	178.89	7.19	Img	ϕ_{19}
121 Hermione	138.80	11.89	Img	ϕ_{19}^\dagger
121 Hermione	189.00	7.00	Img	ϕ_{34}
121 Hermione	187.00	6.00	KOALA	ϕ_{55}
121 Hermione	221.55	5.96	STM	ϕ_{64}^\dagger
121 Hermione	212.00	7.71	NEATM	ϕ_{64}
121 Hermione	194.11	2.69	STM	ϕ_{83}
121 Hermione	164.97	4.51	NEATM	ϕ_{72}^\dagger

Table B.1: Continued

# Designation	ϕ	$\delta\phi$	Method	Refs.
126 Velleda	44.81	1.29	STM	ϕ_{93}
126 Velleda	47.47	1.53	STM	ϕ_{64}
126 Velleda	49.66	2.33	NEATM	ϕ_{64}^\dagger
126 Velleda	43.93	0.49	STM	ϕ_{83}
127 Johanna	123.33	4.36	STM	ϕ_{94}
127 Johanna	112.98	8.79	Occ	ϕ_{95}
127 Johanna	109.62	0.01	STM	ϕ_{64}^\dagger
127 Johanna	120.04	0.01	NEATM	ϕ_{64}^\dagger
127 Johanna	114.19	1.52	TPM	ϕ_{83}
128 Nemesis	188.16	4.00	STM	ϕ_{93}
128 Nemesis	187.80	4.50	STM	ϕ_{94}
128 Nemesis	165.42	3.99	STM	ϕ_{64}^\dagger
128 Nemesis	190.33	7.67	NEATM	ϕ_{64}
128 Nemesis	177.94	2.06	STM	ϕ_{83}
128 Nemesis	188.00	9.00	NEATM	ϕ_{72}
129 Antigone	113.00	11.30	STM	ϕ_{96}
129 Antigone	113.00	12.00	Radar	ϕ_{45}
129 Antigone	125.00	13.00	Img-TE	ϕ_{54}
129 Antigone	118.00	19.00	LC+Occ	ϕ_{78}
129 Antigone	119.55	1.41	TPM	ϕ_{83}
129 Antigone	129.50	14.77	NEATM	ϕ_{72}
130 Elektra	174.00	17.39	STM	ϕ_{96}
130 Elektra	182.25	11.80	STM	ϕ_{93}
130 Elektra	191.00	2.00	Img	ϕ_{34}
130 Elektra	196.00	11.00	NEATM	ϕ_{44}
130 Elektra	215.00	15.00	Img	ϕ_{44}^\dagger
130 Elektra	158.82	6.09	STM	ϕ_{64}^\dagger
130 Elektra	200.50	13.31	NEATM	ϕ_{64}
130 Elektra	191.00	14.00	LC+Occ	ϕ_{78}
130 Elektra	183.02	2.26	STM	ϕ_{83}
130 Elektra	198.92	4.11	NEATM	ϕ_{72}
132 Aethra	42.86	1.60	STM	ϕ_{93}
132 Aethra	31.00	0.20	Occ	ϕ_{95}
132 Aethra	43.75	1.89	STM	ϕ_{64}
132 Aethra	50.20	3.64	NEATM	ϕ_{64}
132 Aethra	44.47	0.74	STM	ϕ_{83}
135 Hertha	77.58	2.69	Occ	ϕ_{95}
135 Hertha	79.23	2.00	STM	ϕ_{93}
135 Hertha	82.01	3.86	STM	ϕ_{94}
135 Hertha	67.29	1.88	STM	ϕ_{64}^\dagger
135 Hertha	92.12	5.55	NEATM	ϕ_{64}^\dagger
135 Hertha	77.00	7.00	LC+Occ	ϕ_{78}
135 Hertha	72.77	0.87	STM	ϕ_{83}
135 Hertha	77.00	7.82	NEATM	ϕ_{72}
137 Meliboea	150.00	15.00	STM	ϕ_{96}
137 Meliboea	145.41	3.29	STM	ϕ_{93}
137 Meliboea	129.27	4.25	STM	ϕ_{64}^\dagger
137 Meliboea	155.63	10.65	NEATM	ϕ_{64}
137 Meliboea	143.77	2.51	STM	ϕ_{83}
137 Meliboea	144.00	11.27	NEATM	ϕ_{72}

Table B.1: Continued

# Designation	ϕ	$\delta\phi$	Method	Refs.
138 Tolosa	45.50	2.09	STM	ϕ_{93}^\dagger
138 Tolosa	46.65	3.81	STM	ϕ_{64}
138 Tolosa	57.49	3.38	NEATM	ϕ_{64}
138 Tolosa	51.61	0.84	STM	ϕ_{83}
138 Tolosa	58.93	1.64	NEATM	ϕ_{72}^\dagger
139 Juewa	172.00	17.20	STM	ϕ_{96}
139 Juewa	156.60	2.79	STM	ϕ_{93}
139 Juewa	149.52	5.73	STM	ϕ_{94}
139 Juewa	132.27	3.55	STM	ϕ_{64}^\dagger
139 Juewa	170.78	7.88	NEATM	ϕ_{64}
139 Juewa	166.69	2.77	STM	ϕ_{83}
139 Juewa	164.00	25.20	NEATM	ϕ_{72}
141 Lumen	120.43	4.57	STM	ϕ_{94}
141 Lumen	131.02	2.90	STM	ϕ_{93}
141 Lumen	137.38	12.05	Occ	ϕ_{95}
141 Lumen	110.86	3.26	STM	ϕ_{64}^\dagger
141 Lumen	139.83	7.90	NEATM	ϕ_{64}
141 Lumen	132.16	1.51	STM	ϕ_{83}
141 Lumen	137.10	14.56	NEATM	ϕ_{72}
144 Vibilia	131.00	13.10	STM	ϕ_{96}
144 Vibilia	142.38	2.59	STM	ϕ_{93}
144 Vibilia	142.47	4.98	Occ	ϕ_{95}
144 Vibilia	138.39	9.11	STM	ϕ_{64}
144 Vibilia	161.19	9.02	NEATM	ϕ_{64}^\dagger
144 Vibilia	142.19	1.76	STM	ϕ_{83}
145 Adeona	151.13	3.20	STM	ϕ_{93}
145 Adeona	140.99	23.75	Occ	ϕ_{95}
145 Adeona	125.98	3.58	STM	ϕ_{64}^\dagger
145 Adeona	157.88	7.55	NEATM	ϕ_{64}
145 Adeona	141.38	5.17	STM	ϕ_{83}
145 Adeona	151.00	11.27	NEATM	ϕ_{72}
145 Adeona	151.00	8.56	NEATM	ϕ_{72}
147 Protogeneia	132.92	5.09	STM	ϕ_{93}
147 Protogeneia	122.31	2.85	STM	ϕ_{64}
147 Protogeneia	135.13	9.17	NEATM	ϕ_{64}
147 Protogeneia	108.41	1.66	STM	ϕ_{83}
148 Gallia	97.75	3.70	STM	ϕ_{93}^\dagger
148 Gallia	82.83	2.83	STM	ϕ_{64}
148 Gallia	95.65	4.52	NEATM	ϕ_{64}
148 Gallia	80.87	1.03	STM	ϕ_{83}
150 Nuwa	151.13	4.50	STM	ϕ_{93}
150 Nuwa	158.89	3.97	STM	ϕ_{64}
150 Nuwa	159.55	6.67	NEATM	ϕ_{64}
150 Nuwa	139.64	2.08	STM	ϕ_{83}
150 Nuwa	137.19	3.35	NEATM	ϕ_{72}
152 Atala	66.41	4.15	Occ	ϕ_{95}
152 Atala	65.00	8.00	LC+Occ	ϕ_{78}
152 Atala	57.11	0.97	STM	ϕ_{83}
152 Atala	60.83	0.94	NEATM	ϕ_{72}

Table B.1: Continued

# Designation	ϕ	$\delta\phi$	Method	Refs.
154 Bertha	184.92	3.59	STM	ϕ_{93}
154 Bertha	189.86	5.30	STM	ϕ_{64}
154 Bertha	186.35	8.97	NEATM	ϕ_{64}
154 Bertha	185.83	2.72	STM	ϕ_{83}
154 Bertha	188.75	4.76	NEATM	ϕ_{72}
156 Xanthippe	120.98	2.50	STM	ϕ_{93}
156 Xanthippe	122.04	3.51	STM	ϕ_{64}
156 Xanthippe	114.58	4.23	NEATM	ϕ_{64}
156 Xanthippe	115.48	1.74	STM	ϕ_{83}
156 Xanthippe	110.72	2.19	NEATM	ϕ_{72}
163 Erigone	72.62	5.69	STM	ϕ_{93}
163 Erigone	70.68	4.52	STM	ϕ_{64}
163 Erigone	77.58	4.65	NEATM	ϕ_{64}
163 Erigone	72.13	0.95	STM	ϕ_{83}
163 Erigone	81.58	3.05	NEATM	ϕ_{72}^{\dagger}
164 Eva	104.87	1.90	STM	ϕ_{93}
164 Eva	100.54	0.86	Occ	ϕ_{95}
164 Eva	85.58	2.26	STM	ϕ_{64}^{\dagger}
164 Eva	116.45	5.48	NEATM	ϕ_{64}^{\dagger}
164 Eva	97.69	1.55	STM	ϕ_{83}
164 Eva	108.95	2.97	NEATM	ϕ_{72}
165 Loreley	154.77	4.80	STM	ϕ_{93}
165 Loreley	166.00	5.50	Img	ϕ_{34}
165 Loreley	155.75	4.28	STM	ϕ_{64}^{\dagger}
165 Loreley	185.80	8.18	NEATM	ϕ_{64}^{\dagger}
165 Loreley	171.00	8.00	LC+Occ	ϕ_{78}
165 Loreley	173.66	2.65	STM	ϕ_{83}
168 Sibylla	148.38	4.00	STM	ϕ_{93}
168 Sibylla	154.61	2.00	STM	ϕ_{64}
168 Sibylla	155.83	10.60	NEATM	ϕ_{64}
168 Sibylla	146.47	1.74	STM	ϕ_{83}
168 Sibylla	144.00	2.86	NEATM	ϕ_{72}
173 Ino	154.10	3.50	STM	ϕ_{93}
173 Ino	131.39	3.33	STM	ϕ_{64}^{\dagger}
173 Ino	171.25	7.30	NEATM	ϕ_{64}
173 Ino	160.61	3.04	STM	ϕ_{83}
179 Klytaemnestra	77.69	1.39	STM	ϕ_{93}
179 Klytaemnestra	70.73	3.91	Occ	ϕ_{95}
179 Klytaemnestra	80.41	2.73	STM	ϕ_{64}
179 Klytaemnestra	84.94	3.93	NEATM	ϕ_{64}^{\dagger}
179 Klytaemnestra	64.25	0.79	STM	ϕ_{83}^{\dagger}
179 Klytaemnestra	72.79	0.80	NEATM	ϕ_{72}
185 Eunike	157.50	2.59	STM	ϕ_{93}
185 Eunike	138.00	3.81	STM	ϕ_{64}^{\dagger}
185 Eunike	179.80	8.07	NEATM	ϕ_{64}^{\dagger}
185 Eunike	167.72	2.82	STM	ϕ_{83}
185 Eunike	158.52	6.23	NEATM	ϕ_{72}
185 Eunike	155.46	5.26	NEATM	ϕ_{72}
187 Lamberta	130.39	2.70	STM	ϕ_{93}
187 Lamberta	131.41	4.65	STM	ϕ_{64}
187 Lamberta	132.07	7.75	NEATM	ϕ_{64}
187 Lamberta	130.44	1.89	STM	ϕ_{83}
187 Lamberta	133.00	2.50	NEATM	ϕ_{72}

Table B.1: Continued

# Designation	ϕ	$\delta\phi$	Method	Refs.
189 Phthia	42.00	4.19	STM	ϕ_{96}
189 Phthia	37.65	2.00	STM	ϕ_{93}
189 Phthia	32.38	1.48	STM	ϕ_{64}^{\dagger}
189 Phthia	40.84	3.22	NEATM	ϕ_{64}
189 Phthia	42.47	0.67	STM	ϕ_{83}
189 Phthia	40.56	0.39	NEATM	ϕ_{72}
192 Nausikaa	99.00	9.89	STM	ϕ_{96}
192 Nausikaa	103.26	1.90	STM	ϕ_{93}^{\dagger}
192 Nausikaa	86.00	4.00	Img	ϕ_{34}
192 Nausikaa	90.30	2.49	STM	ϕ_{64}
192 Nausikaa	106.87	4.96	NEATM	ϕ_{64}^{\dagger}
192 Nausikaa	89.44	1.14	STM	ϕ_{83}
192 Nausikaa	93.00	6.80	NEATM	ϕ_{72}
192 Nausikaa	93.00	8.36	NEATM	ϕ_{72}
194 Prokne	192.00	19.20	STM	ϕ_{96}
194 Prokne	168.41	4.09	STM	ϕ_{93}
194 Prokne	151.00	3.50	Img	ϕ_{34}^{\dagger}
194 Prokne	182.16	8.80	NEATM	ϕ_{64}
194 Prokne	166.72	1.89	STM	ϕ_{83}
194 Prokne	169.00	14.46	NEATM	ϕ_{72}
196 Philomela	161.00	16.10	STM	ϕ_{96}
196 Philomela	136.38	6.30	STM	ϕ_{93}
196 Philomela	118.55	3.72	STM	ϕ_{64}^{\dagger}
196 Philomela	146.64	7.55	NEATM	ϕ_{64}
196 Philomela	141.77	2.01	STM	ϕ_{83}
196 Philomela	158.05	6.36	NEATM	ϕ_{72}
200 Dynamene	128.36	2.09	STM	ϕ_{93}
200 Dynamene	125.11	5.90	STM	ϕ_{64}
200 Dynamene	135.86	6.90	NEATM	ϕ_{64}
200 Dynamene	129.19	3.64	Occ	ϕ_{95}
200 Dynamene	133.83	1.72	STM	ϕ_{83}
200 Dynamene	130.52	2.88	NEATM	ϕ_{72}
204 Kallisto	50.00	5.00	STM	ϕ_{96}
204 Kallisto	48.56	5.50	STM	ϕ_{94}
204 Kallisto	48.56	1.20	STM	ϕ_{93}
204 Kallisto	50.70	1.66	Occ	ϕ_{95}
204 Kallisto	47.99	2.40	STM	ϕ_{64}
204 Kallisto	54.15	2.41	NEATM	ϕ_{64}
204 Kallisto	51.02	0.60	STM	ϕ_{83}
204 Kallisto	54.88	1.74	NEATM	ϕ_{72}^{\dagger}
209 Dido	155.08	6.63	Occ	ϕ_{95}
209 Dido	159.94	3.09	STM	ϕ_{93}^{\dagger}
209 Dido	135.14	8.35	STM	ϕ_{64}
209 Dido	156.92	9.36	NEATM	ϕ_{64}
209 Dido	133.42	2.05	STM	ϕ_{83}
209 Dido	124.26	3.67	NEATM	ϕ_{72}^{\dagger}
210 Isabella	86.65	2.29	STM	ϕ_{93}
210 Isabella	66.83	1.11	Occ	ϕ_{95}
210 Isabella	89.04	8.35	STM	ϕ_{64}
210 Isabella	85.97	3.82	NEATM	ϕ_{64}
210 Isabella	69.58	0.92	STM	ϕ_{83}

Table B.1: Continued

# Designation	ϕ	$\delta\phi$	Method	Refs.
211 Isolda	166.00	16.60	STM	ϕ_{96}
211 Isolda	143.19	5.09	STM	ϕ_{93}
211 Isolda	142.57	4.36	STM	ϕ_{64}
211 Isolda	150.94	7.50	NEATM	ϕ_{64}
211 Isolda	153.49	1.71	STM	ϕ_{83}
211 Isolda	143.00	21.62	NEATM	ϕ_{72}
212 Medea	136.11	2.50	STM	ϕ_{93}
212 Medea	142.55	4.00	STM	ϕ_{64}
212 Medea	146.24	7.90	NEATM	ϕ_{64}
212 Medea	153.72	2.88	STM	ϕ_{83}
216 Kleopatra	135.07	2.09	STM	ϕ_{93}
216 Kleopatra	108.50	15.00	Radar	ϕ_4
216 Kleopatra	119.55	3.21	STM	ϕ_{64}
216 Kleopatra	140.74	7.78	NEATM	ϕ_{64}
216 Kleopatra	135.00	4.80	Img	ϕ_{77}
216 Kleopatra	121.55	1.60	STM	ϕ_{83}
216 Kleopatra	138.00	19.37	NEATM	ϕ_{72}
217 Eudora	66.23	2.29	STM	ϕ_{93}
217 Eudora	70.76	2.88	STM	ϕ_{64}
217 Eudora	68.83	2.54	NEATM	ϕ_{64}
217 Eudora	67.80	1.17	STM	ϕ_{83}
217 Eudora	69.73	1.21	NEATM	ϕ_{72}
221 Eos	95.00	9.50	STM	ϕ_{96}
221 Eos	103.87	3.59	STM	ϕ_{93}
221 Eos	100.84	4.13	STM	ϕ_{64}
221 Eos	113.26	7.00	NEATM	ϕ_{64}
221 Eos	107.73	1.51	STM	ϕ_{83}
221 Eos	95.77	2.82	NEATM	ϕ_{72}
230 Athamantis	125.00	12.50	STM	ϕ_{96}
230 Athamantis	108.98	2.00	STM	ϕ_{93}
230 Athamantis	105.04	10.00	Occ	ϕ_{95}
230 Athamantis	91.47	1.89	STM	ϕ_{64}^\dagger
230 Athamantis	118.59	5.23	NEATM	ϕ_{64}
230 Athamantis	108.27	1.17	STM	ϕ_{83}
230 Athamantis	109.00	13.02	NEATM	ϕ_{72}
234 Barbara	43.75	1.00	STM	ϕ_{93}
234 Barbara	46.36	5.23	Occ	ϕ_{95}
234 Barbara	44.59	0.30	NEATM	ϕ_{52}
234 Barbara	45.27	1.42	STM	ϕ_{64}
234 Barbara	51.20	2.52	NEATM	ϕ_{64}
234 Barbara	47.79	0.68	STM	ϕ_{83}
234 Barbara	53.81	1.12	NEATM	ϕ_{72}^\dagger
238 Hypatia	154.00	15.39	STM	ϕ_{96}
238 Hypatia	145.91	7.65	Occ	ϕ_{95}
238 Hypatia	148.49	3.59	STM	ϕ_{93}
238 Hypatia	149.21	14.17	STM	ϕ_{64}
238 Hypatia	163.64	7.15	NEATM	ϕ_{64}^\dagger
238 Hypatia	143.97	1.54	STM	ϕ_{83}
238 Hypatia	146.50	8.68	NEATM	ϕ_{72}

Table B.1: Continued

# Designation	ϕ	$\delta\phi$	Method	Refs.
240 Vanadis	103.90	2.50	STM	ϕ_{93}
240 Vanadis	93.08	3.57	Occ	ϕ_{95}
240 Vanadis	99.26	10.01	STM	ϕ_{64}
240 Vanadis	112.90	4.65	NEATM	ϕ_{64}^\dagger
240 Vanadis	90.12	1.22	STM	ϕ_{83}
240 Vanadis	91.37	2.65	NEATM	ϕ_{72}
241 Germania	200.00	20.00	STM	ϕ_{96}
241 Germania	183.80	112.59	Occ	ϕ_{95}
241 Germania	168.89	3.09	STM	ϕ_{93}
241 Germania	146.13	3.85	STM	ϕ_{64}^\dagger
241 Germania	171.42	7.30	NEATM	ϕ_{64}
241 Germania	181.57	2.93	STM	ϕ_{83}
241 Germania	179.96	5.98	NEATM	ϕ_{72}
241 Germania	186.27	4.34	NEATM	ϕ_{72}
243 Ida	27.98	3.20	STM	ϕ_{93}^\dagger
243 Ida	25.30	1.63	STM	ϕ_{64}^\dagger
243 Ida	36.22	6.25	NEATM	ϕ_{64}^\dagger
243 Ida	31.29	1.20	IAU	ϕ_{75}
243 Ida	29.00	0.43	STM	ϕ_{83}^\dagger
253 Mathilde	58.04	2.59	STM	ϕ_{93}^\dagger
253 Mathilde	49.61	1.94	STM	ϕ_{64}^\dagger
253 Mathilde	62.50	3.11	NEATM	ϕ_{64}^\dagger
253 Mathilde	53.00	2.59	IAU	ϕ_{75}
253 Mathilde	54.00	0.87	STM	ϕ_{83}^\dagger
259 Aletheia	178.60	6.80	STM	ϕ_{93}
259 Aletheia	190.50	6.00	Img	ϕ_{34}
259 Aletheia	195.74	1.83	STM	ϕ_{64}
259 Aletheia	198.47	14.97	NEATM	ϕ_{64}
259 Aletheia	174.66	2.36	STM	ϕ_{83}^\dagger
259 Aletheia	182.86	3.49	NEATM	ϕ_{72}
266 Aline	125.83	6.51	STM	ϕ_{94}^\dagger
266 Aline	109.08	2.90	STM	ϕ_{93}
266 Aline	112.86	2.78	STM	ϕ_{64}
266 Aline	125.19	8.40	NEATM	ϕ_{64}
266 Aline	101.98	1.39	STM	ϕ_{83}
266 Aline	109.00	18.32	NEATM	ϕ_{72}
268 Adorea	139.88	5.19	STM	ϕ_{93}
268 Adorea	145.55	5.03	Occ	ϕ_{95}
268 Adorea	143.58	2.70	STM	ϕ_{64}
268 Adorea	169.83	7.82	NEATM	ϕ_{64}^\dagger
268 Adorea	136.35	1.76	STM	ϕ_{83}
268 Adorea	140.58	3.18	NEATM	ϕ_{72}
283 Emma	148.05	4.59	STM	ϕ_{93}
283 Emma	141.00	6.00	NEATM	ϕ_{44}
283 Emma	160.00	10.00	Img	ϕ_{44}^\dagger
283 Emma	145.69	5.88	NEATM	ϕ_{64}
283 Emma	122.06	1.38	STM	ϕ_{83}
283 Emma	134.69	2.34	NEATM	ϕ_{72}

Table B.1: Continued

# Designation	ϕ	$\delta\phi$	Method	Refs.
304 Olga	67.86	2.09	STM	ϕ_{93}
304 Olga	69.19	1.79	Occ	ϕ_{95}
304 Olga	71.13	2.54	STM	ϕ_{64}
304 Olga	77.58	5.36	NEATM	ϕ_{64}
304 Olga	71.26	1.29	STM	ϕ_{83}
304 Olga	68.87	2.26	NEATM	ϕ_{72}
306 Unitas	46.70	2.29	STM	ϕ_{93}
306 Unitas	51.59	1.44	Occ	ϕ_{95}
306 Unitas	56.00	1.00	TPM	ϕ_{57}
306 Unitas	48.24	1.38	STM	ϕ_{64}
306 Unitas	55.47	2.80	NEATM	ϕ_{64}
306 Unitas	56.00	1.00	LC+Occ	ϕ_{78}
306 Unitas	53.00	5.00	LC+Occ	ϕ_{78}
306 Unitas	46.24	0.64	STM	ϕ_{83}^{\dagger}
306 Unitas	51.59	6.32	NEATM	ϕ_{72}
322 Phaeo	70.83	4.90	STM	ϕ_{93}
322 Phaeo	67.33	4.01	STM	ϕ_{64}
322 Phaeo	74.41	3.18	NEATM	ϕ_{64}
322 Phaeo	71.98	0.93	STM	ϕ_{83}
322 Phaeo	77.08	1.00	NEATM	ϕ_{72}
322 Phaeo	65.08	1.45	NEATM	ϕ_{72}
324 Bambergga	252.00	25.20	STM	ϕ_{96}
324 Bambergga	229.44	7.40	STM	ϕ_{93}
324 Bambergga	204.00	10.00	Img-TE	ϕ_{48}^{\dagger}
324 Bambergga	248.16	8.81	STM	ϕ_{64}
324 Bambergga	239.97	7.71	NEATM	ϕ_{64}
324 Bambergga	229.69	3.30	STM	ϕ_{83}
324 Bambergga	229.00	8.14	NEATM	ϕ_{72}
328 Gudrun	122.91	5.19	STM	ϕ_{93}
328 Gudrun	126.69	4.38	STM	ϕ_{64}
328 Gudrun	119.23	4.90	NEATM	ϕ_{64}
328 Gudrun	125.01	1.97	STM	ϕ_{83}
328 Gudrun	116.13	4.21	NEATM	ϕ_{72}
334 Chicago	174.02	7.11	Occ	ϕ_{95}
334 Chicago	158.55	8.89	STM	ϕ_{93}
334 Chicago	151.44	12.85	STM	ϕ_{64}
334 Chicago	182.25	19.87	NEATM	ϕ_{64}
334 Chicago	167.21	2.10	STM	ϕ_{83}
334 Chicago	174.10	12.79	NEATM	ϕ_{72}
337 Devosa	59.11	2.29	STM	ϕ_{93}
337 Devosa	62.22	2.23	STM	ϕ_{64}
337 Devosa	81.98	5.05	NEATM	ϕ_{64}^{\dagger}
337 Devosa	66.62	0.98	STM	ϕ_{83}
344 Desiderata	132.27	5.50	STM	ϕ_{93}
344 Desiderata	108.73	3.35	STM	ϕ_{64}^{\dagger}
344 Desiderata	142.85	5.30	NEATM	ϕ_{64}^{\dagger}
344 Desiderata	132.88	2.05	STM	ϕ_{83}
344 Desiderata	125.97	1.38	NEATM	ϕ_{72}

Table B.1: Continued

# Designation	ϕ	$\delta\phi$	Method	Refs.
345 Tercidina	94.12	4.90	STM	ϕ_{93}
345 Tercidina	99.30	1.39	Occ	ϕ_{95}
345 Tercidina	93.80	5.88	STM	ϕ_{64}
345 Tercidina	106.19	7.80	NEATM	ϕ_{64}
345 Tercidina	99.23	0.99	STM	ϕ_{83}
345 Tercidina	99.00	11.47	NEATM	ϕ_{72}
346 Hermentaria	106.51	2.20	STM	ϕ_{93}^\dagger
346 Hermentaria	90.62	2.45	STM	ϕ_{64}
346 Hermentaria	101.29	3.32	NEATM	ϕ_{64}
346 Hermentaria	93.01	0.89	STM	ϕ_{83}
346 Hermentaria	91.80	1.41	NEATM	ϕ_{72}
349 Dembowska	145.00	14.50	STM	ϕ_{96}
349 Dembowska	139.77	4.30	STM	ϕ_{93}
349 Dembowska	121.83	3.17	STM	ϕ_{64}
349 Dembowska	135.72	5.07	NEATM	ϕ_{64}
349 Dembowska	164.64	1.84	STM	ϕ_{83}
349 Dembowska	216.72	7.38	NEATM	ϕ_{72}^\dagger
349 Dembowska	228.91	8.22	NEATM	ϕ_{72}^\dagger
354 Eleonora	154.00	15.39	STM	ϕ_{96}
354 Eleonora	155.16	8.50	STM	ϕ_{93}
354 Eleonora	155.33	5.15	STM	ϕ_{64}
354 Eleonora	165.19	7.55	NEATM	ϕ_{64}
354 Eleonora	149.61	1.98	STM	ϕ_{83}
354 Eleonora	165.00	15.60	NEATM	ϕ_{72}
356 Liguria	155.00	15.50	STM	ϕ_{96}
356 Liguria	126.59	10.60	Occ	ϕ_{95}
356 Liguria	131.30	2.59	STM	ϕ_{93}
356 Liguria	135.69	5.07	STM	ϕ_{64}
356 Liguria	135.08	7.07	NEATM	ϕ_{64}
356 Liguria	136.55	1.88	STM	ϕ_{83}
356 Liguria	131.00	9.68	NEATM	ϕ_{72}
365 Corduba	105.91	3.00	STM	ϕ_{93}
365 Corduba	100.80	3.86	STM	ϕ_{64}
365 Corduba	109.44	4.98	NEATM	ϕ_{64}
365 Corduba	103.90	1.23	STM	ϕ_{83}
365 Corduba	91.50	2.91	NEATM	ϕ_{72}^\dagger
372 Palma	188.61	3.20	STM	ϕ_{93}
372 Palma	194.00	6.00	Occ	ϕ_{95}
372 Palma	192.82	4.73	STM	ϕ_{64}
372 Palma	210.11	9.50	NEATM	ϕ_{64}^\dagger
372 Palma	187.00	20.00	LC+Occ	ϕ_{78}
372 Palma	198.00	26.00	LC+Occ	ϕ_{78}
372 Palma	177.21	2.63	STM	ϕ_{83}^\dagger
372 Palma	190.36	6.63	NEATM	ϕ_{72}
375 Ursula	183.47	10.46	Occ	ϕ_{95}
375 Ursula	193.63	2.52	STM	ϕ_{83}
379 Huenna	92.33	1.70	STM	ϕ_{93}
379 Huenna	98.00	3.00	NEATM	ϕ_{44}
379 Huenna	82.01	2.55	STM	ϕ_{64}
379 Huenna	103.01	4.30	NEATM	ϕ_{64}^\dagger
379 Huenna	82.34	1.08	STM	ϕ_{83}
379 Huenna	87.47	2.35	NEATM	ϕ_{72}

Table B.1: Continued

# Designation	ϕ	$\delta\phi$	Method	Refs.
381 Myrrha	120.58	2.70	STM	ϕ_{93}
381 Myrrha	130.58	2.75	Occ	ϕ_{95}
381 Myrrha	120.30	3.45	STM	ϕ_{64}
381 Myrrha	136.57	7.13	NEATM	ϕ_{64}
381 Myrrha	117.12	1.58	STM	ϕ_{83}
381 Myrrha	129.00	9.94	NEATM	ϕ_{72}
381 Myrrha	129.00	6.01	NEATM	ϕ_{72}
386 Siegena	165.00	2.70	STM	ϕ_{93}
386 Siegena	173.99	12.89	Occ	ϕ_{95}
386 Siegena	145.66	3.77	STM	ϕ_{64}^\dagger
386 Siegena	186.50	9.51	NEATM	ϕ_{64}
386 Siegena	201.16	3.52	STM	ϕ_{83}^\dagger
387 Aquitania	100.51	2.90	STM	ϕ_{93}
387 Aquitania	101.48	5.59	STM	ϕ_{64}
387 Aquitania	107.59	16.76	NEATM	ϕ_{64}
387 Aquitania	105.05	1.34	STM	ϕ_{83}
404 Arsinoe	101.00	10.10	STM	ϕ_{96}
404 Arsinoe	97.70	1.50	STM	ϕ_{93}
404 Arsinoe	98.75	3.20	Occ	ϕ_{95}
404 Arsinoe	98.44	4.17	STM	ϕ_{64}
404 Arsinoe	102.30	4.53	NEATM	ϕ_{64}
404 Arsinoe	92.98	1.14	STM	ϕ_{83}
404 Arsinoe	98.69	3.45	NEATM	ϕ_{72}
405 Thia	124.90	2.29	STM	ϕ_{93}
405 Thia	129.60	3.97	STM	ϕ_{64}
405 Thia	134.89	6.73	NEATM	ϕ_{64}
405 Thia	113.31	1.72	STM	ϕ_{83}
405 Thia	125.00	17.43	NEATM	ϕ_{72}
409 Aspasia	161.61	6.80	STM	ϕ_{93}
409 Aspasia	180.00	2.00	Img-TE	ϕ_{54}
409 Aspasia	139.10	4.30	STM	ϕ_{64}^\dagger
409 Aspasia	174.52	7.40	NEATM	ϕ_{64}
409 Aspasia	173.00	17.00	LC+Occ	ϕ_{78}
409 Aspasia	197.25	3.72	STM	ϕ_{83}^\dagger
409 Aspasia	177.00	0.88	NEATM	ϕ_{72}
410 Chloris	135.00	13.50	STM	ϕ_{96}
410 Chloris	123.56	5.40	STM	ϕ_{93}
410 Chloris	118.01	5.23	STM	ϕ_{64}
410 Chloris	124.25	5.48	NEATM	ϕ_{64}
410 Chloris	106.68	1.44	STM	ϕ_{83}
410 Chloris	118.93	2.85	NEATM	ϕ_{72}
416 Vaticana	85.44	5.86	STM	ϕ_{94}
416 Vaticana	85.47	1.70	STM	ϕ_{93}
416 Vaticana	83.55	3.02	STM	ϕ_{64}
416 Vaticana	92.13	4.65	NEATM	ϕ_{64}
416 Vaticana	88.80	1.26	STM	ϕ_{83}
419 Aurelia	129.00	4.09	STM	ϕ_{93}
419 Aurelia	106.63	2.94	STM	ϕ_{64}^\dagger
419 Aurelia	139.94	5.96	NEATM	ϕ_{64}^\dagger
419 Aurelia	122.37	1.90	STM	ϕ_{83}

Table B.1: Continued

# Designation	ϕ	$\delta\phi$	Method	Refs.
420 Bertholda	138.85	2.41	STM	ϕ_{94}
420 Bertholda	141.25	6.90	STM	ϕ_{93}
420 Bertholda	143.97	2.51	Occ	ϕ_{95}
420 Bertholda	139.32	6.01	STM	ϕ_{64}
420 Bertholda	160.33	8.80	NEATM	ϕ_{64}^\dagger
420 Bertholda	141.89	2.58	STM	ϕ_{83}
420 Bertholda	144.00	5.67	NEATM	ϕ_{72}
423 Diotima	155.52	6.55	Occ	ϕ_{95}^\dagger
423 Diotima	208.77	4.90	STM	ϕ_{93}
423 Diotima	208.50	6.00	Img	ϕ_{34}
423 Diotima	211.02	4.76	STM	ϕ_{64}
423 Diotima	229.52	9.97	NEATM	ϕ_{64}
423 Diotima	226.91	3.10	STM	ϕ_{83}
423 Diotima	177.25	6.30	NEATM	ϕ_{72}
433 Eros	22.00	2.20	STM	ϕ_{96}^\dagger
433 Eros	16.20	0.16	FlyBy	ϕ_5
433 Eros	15.27	0.21	STM	ϕ_{83}^\dagger
433 Eros	30.70	9.00	NEATM	ϕ_{71}^\dagger
442 Eichsfeldia	66.73	1.39	STM	ϕ_{93}
442 Eichsfeldia	68.66	1.98	STM	ϕ_{64}
442 Eichsfeldia	65.91	2.56	NEATM	ϕ_{64}
442 Eichsfeldia	65.12	0.82	STM	ϕ_{83}
442 Eichsfeldia	63.20	1.22	NEATM	ϕ_{72}
444 Gyptis	166.00	16.60	STM	ϕ_{96}
444 Gyptis	163.08	10.00	STM	ϕ_{93}
444 Gyptis	129.00	7.50	Img	ϕ_{34}^\dagger
444 Gyptis	159.33	13.67	STM	ϕ_{64}
444 Gyptis	167.72	6.77	NEATM	ϕ_{64}
444 Gyptis	166.02	6.65	STM	ϕ_{83}
444 Gyptis	163.00	12.60	NEATM	ϕ_{72}
444 Gyptis	163.00	22.13	NEATM	ϕ_{72}
445 Edna	89.30	4.53	STM	ϕ_{94}
445 Edna	87.16	2.09	STM	ϕ_{93}
445 Edna	81.40	4.34	STM	ϕ_{64}
445 Edna	98.18	5.30	NEATM	ϕ_{64}
445 Edna	89.16	1.42	STM	ϕ_{83}
445 Edna	105.50	1.51	NEATM	ϕ_{72}^\dagger
449 Hamburga	85.58	1.90	STM	ϕ_{93}^\dagger
449 Hamburga	68.75	2.52	Occ	ϕ_{95}
449 Hamburga	76.58	2.86	STM	ϕ_{64}
449 Hamburga	89.27	3.63	NEATM	ϕ_{64}^\dagger
449 Hamburga	63.61	0.75	STM	ϕ_{83}
451 Patientia	279.00	27.89	STM	ϕ_{96}^\dagger
451 Patientia	224.96	4.40	STM	ϕ_{93}
451 Patientia	221.52	7.28	STM	ϕ_{64}
451 Patientia	242.08	14.11	NEATM	ϕ_{64}
451 Patientia	234.91	2.66	STM	ϕ_{83}
451 Patientia	251.80	5.44	NEATM	ϕ_{72}

Table B.1: Continued

# Designation	ϕ	$\delta\phi$	Method	Refs.
455 Bruchsalia	105.00	10.50	STM	ϕ_{96}
455 Bruchsalia	84.41	5.00	STM	ϕ_{93}
455 Bruchsalia	92.08	3.36	STM	ϕ_{64}
455 Bruchsalia	99.65	4.44	NEATM	ϕ_{64}
455 Bruchsalia	83.45	1.00	STM	ϕ_{83}
455 Bruchsalia	112.37	4.36	NEATM	ϕ_{72}^\dagger
469 Argentina	125.56	5.59	STM	ϕ_{93}
469 Argentina	131.52	4.00	STM	ϕ_{64}
469 Argentina	137.50	8.15	NEATM	ϕ_{64}
469 Argentina	123.11	1.65	STM	ϕ_{83}
469 Argentina	121.59	4.61	NEATM	ϕ_{72}
471 Papagena	144.00	14.39	STM	ϕ_{96}
471 Papagena	134.19	5.19	STM	ϕ_{93}
471 Papagena	121.45	5.03	Occ	ϕ_{95}
471 Papagena	121.83	4.63	STM	ϕ_{64}
471 Papagena	138.53	6.23	NEATM	ϕ_{64}
471 Papagena	137.00	25.00	LC+Occ	ϕ_{78}
471 Papagena	117.44	1.50	STM	ϕ_{83}
481 Emita	113.23	3.07	STM	ϕ_{93}
481 Emita	102.04	0.01	STM	ϕ_{64}^\dagger
481 Emita	108.41	0.01	NEATM	ϕ_{64}^\dagger
481 Emita	103.52	1.90	STM	ϕ_{83}
485 Genua	63.88	2.90	STM	ϕ_{93}
485 Genua	70.76	13.10	Occ	ϕ_{95}
485 Genua	54.09	1.52	STM	ϕ_{64}
485 Genua	70.50	3.76	NEATM	ϕ_{64}^\dagger
485 Genua	54.70	0.72	STM	ϕ_{83}
488 Kreusa	150.13	6.40	STM	ϕ_{93}
488 Kreusa	155.99	6.94	STM	ϕ_{64}
488 Kreusa	161.58	7.38	NEATM	ϕ_{64}
488 Kreusa	172.55	2.54	STM	ϕ_{83}
488 Kreusa	150.00	11.32	NEATM	ϕ_{72}
490 Veritas	108.09	4.59	Occ	ϕ_{95}
490 Veritas	115.55	5.50	STM	ϕ_{93}
490 Veritas	131.50	4.00	Img	ϕ_{34}^\dagger
490 Veritas	102.93	5.26	STM	ϕ_{64}
490 Veritas	111.98	5.07	NEATM	ϕ_{64}
490 Veritas	112.81	1.66	STM	ϕ_{83}
491 Carina	97.29	3.79	STM	ϕ_{93}
491 Carina	106.05	5.90	NEATM	ϕ_{64}
491 Carina	97.15	1.13	STM	ϕ_{83}
491 Carina	94.00	2.68	NEATM	ϕ_{72}
503 Evelyn	81.68	4.90	STM	ϕ_{93}
503 Evelyn	83.36	4.90	STM	ϕ_{64}
503 Evelyn	83.56	9.89	NEATM	ϕ_{64}
503 Evelyn	90.18	1.04	STM	ϕ_{83}
505 Cava	100.55	1.24	TPM	ϕ_{83}
505 Cava	105.00	4.48	NEATM	ϕ_{72}

Table B.1: Continued

# Designation	ϕ	$\delta\phi$	Method	Refs.
508 Princesonia	129.38	0.20	Occ	ϕ_{95}^\dagger
508 Princesonia	136.14	5.44	STM	ϕ_{94}
508 Princesonia	142.35	2.59	STM	ϕ_{93}
508 Princesonia	133.75	5.71	STM	ϕ_{64}
508 Princesonia	144.99	6.77	NEATM	ϕ_{64}
508 Princesonia	139.42	2.30	STM	ϕ_{83}
508 Princesonia	120.26	2.92	NEATM	ϕ_{72}^\dagger
511 Davida	323.00	32.29	STM	ϕ_{96}
511 Davida	326.05	5.30	STM	ϕ_{93}^\dagger
511 Davida	316.00	5.00	Img	ϕ_{34}
511 Davida	289.00	21.00	Img-TE	ϕ_{39}
511 Davida	314.73	12.30	STM	ϕ_{64}
511 Davida	335.32	14.35	NEATM	ϕ_{64}^\dagger
511 Davida	290.98	4.19	STM	ϕ_{83}
511 Davida	276.23	3.27	NEATM	ϕ_{72}^\dagger
511 Davida	290.44	2.26	NEATM	ϕ_{72}
516 Amherstia	64.00	6.40	STM	ϕ_{96}
516 Amherstia	73.09	1.70	STM	ϕ_{93}
516 Amherstia	76.86	2.32	STM	ϕ_{64}
516 Amherstia	83.08	4.38	NEATM	ϕ_{64}^\dagger
516 Amherstia	66.26	0.62	STM	ϕ_{83}
516 Amherstia	74.27	2.49	NEATM	ϕ_{72}
532 Herculina	220.00	22.00	STM	ϕ_{96}
532 Herculina	222.38	4.19	STM	ϕ_{93}
532 Herculina	217.33	9.10	STM	ϕ_{64}
532 Herculina	241.25	8.50	NEATM	ϕ_{64}^\dagger
532 Herculina	216.77	2.96	STM	ϕ_{83}
532 Herculina	203.00	14.23	NEATM	ϕ_{72}
536 Merapi	153.77	2.98	Occ	ϕ_{95}
536 Merapi	154.50	2.20	STM	ϕ_{94}
536 Merapi	151.41	9.00	STM	ϕ_{93}
536 Merapi	157.80	8.10	STM	ϕ_{64}
536 Merapi	167.21	13.92	NEATM	ϕ_{64}^\dagger
536 Merapi	146.33	2.56	STM	ϕ_{83}^\dagger
536 Merapi	164.91	2.86	NEATM	ϕ_{72}^\dagger
554 Peraga	101.00	10.10	STM	ϕ_{96}
554 Peraga	95.87	4.09	STM	ϕ_{93}
554 Peraga	93.93	3.41	STM	ϕ_{64}
554 Peraga	109.06	5.67	NEATM	ϕ_{64}^\dagger
554 Peraga	96.98	1.16	STM	ϕ_{83}
582 Olympia	48.93	5.05	STM	ϕ_{94}
582 Olympia	43.40	2.59	STM	ϕ_{93}
582 Olympia	42.06	2.26	STM	ϕ_{64}
582 Olympia	47.36	3.13	NEATM	ϕ_{64}
582 Olympia	42.65	0.38	STM	ϕ_{83}
582 Olympia	43.49	0.50	NEATM	ϕ_{72}
584 Semiramis	51.00	5.09	STM	ϕ_{96}
584 Semiramis	54.00	1.39	STM	ϕ_{93}
584 Semiramis	47.72	1.76	STM	ϕ_{64}
584 Semiramis	65.26	3.82	NEATM	ϕ_{64}^\dagger
584 Semiramis	52.63	0.52	STM	ϕ_{83}
584 Semiramis	48.68	4.26	NEATM	ϕ_{72}

Table B.1: Continued

# Designation	ϕ	$\delta\phi$	Method	Refs.
602 Marianna	137.00	13.69	STM	ϕ_{96}
602 Marianna	124.72	2.20	STM	ϕ_{93}
602 Marianna	111.06	3.49	STM	ϕ_{64}^\dagger
602 Marianna	130.05	5.52	NEATM	ϕ_{64}
602 Marianna	129.86	1.92	STM	ϕ_{83}
602 Marianna	126.81	2.05	NEATM	ϕ_{72}
604 Tekmessa	65.16	4.09	STM	ϕ_{93}
604 Tekmessa	64.26	4.01	STM	ϕ_{64}
604 Tekmessa	66.19	4.61	NEATM	ϕ_{64}
604 Tekmessa	59.75	1.86	STM	ϕ_{83}
604 Tekmessa	67.16	1.38	NEATM	ϕ_{72}
617 Patroclus	158.00	15.80	STM	ϕ_{96}
617 Patroclus	140.91	4.69	STM	ϕ_{93}
617 Patroclus	140.60	4.00	NEATM	ϕ_9
617 Patroclus	166.60	4.80	NEATM	ϕ_9^\dagger
617 Patroclus	137.60	1.90	STM	ϕ_{64}
617 Patroclus	164.22	5.77	NEATM	ϕ_{64}
617 Patroclus	145.00	15.00	NEATM	ϕ_{68}
617 Patroclus	140.85	3.36	STM	ϕ_{83}
617 Patroclus	185.10	13.10	NEATM	ϕ_{73}^\dagger
624 Hektor	233.00	23.29	STM	ϕ_{96}
624 Hektor	203.00	3.59	NEATM	ϕ_9
624 Hektor	239.19	2.40	NEATM	ϕ_9
624 Hektor	230.99	3.94	TPM	ϕ_{83}
624 Hektor	163.89	7.19	NEATM	ϕ_{73}^\dagger
626 Notburga	100.73	2.00	STM	ϕ_{93}
626 Notburga	95.98	4.15	STM	ϕ_{64}
626 Notburga	101.41	3.89	NEATM	ϕ_{64}
626 Notburga	76.55	1.49	STM	ϕ_{83}^\dagger
626 Notburga	90.44	2.20	NEATM	ϕ_{72}
654 Zelinda	127.40	3.90	STM	ϕ_{93}
654 Zelinda	129.05	3.79	STM	ϕ_{94}
654 Zelinda	119.27	17.53	Occ	ϕ_{95}
654 Zelinda	112.50	4.00	Img	ϕ_{34}^\dagger
654 Zelinda	138.03	4.63	STM	ϕ_{64}
654 Zelinda	134.27	6.28	NEATM	ϕ_{64}
654 Zelinda	123.58	1.46	STM	ϕ_{83}
654 Zelinda	127.00	20.46	NEATM	ϕ_{72}
665 Sabine	51.09	2.40	STM	ϕ_{93}
665 Sabine	52.95	1.92	STM	ϕ_{64}
665 Sabine	53.25	3.30	NEATM	ϕ_{64}
665 Sabine	53.00	0.77	STM	ϕ_{83}
675 Ludmilla	67.66	0.94	STM	ϕ_{83}
679 Pax	71.00	7.09	STM	ϕ_{96}
679 Pax	51.47	2.40	STM	ϕ_{93}^\dagger
679 Pax	62.00	4.00	Img	ϕ_{34}
679 Pax	50.63	1.66	STM	ϕ_{64}^\dagger
679 Pax	68.23	2.86	NEATM	ϕ_{64}
679 Pax	60.65	0.64	STM	ϕ_{83}
679 Pax	64.77	1.14	NEATM	ϕ_{72}
679 Pax	68.81	0.73	NEATM	ϕ_{72}

Table B.1: Continued

# Designation	ϕ	$\delta\phi$	Method	Refs.
680 Genoveva	83.91	1.39	STM	ϕ_{93}
680 Genoveva	87.51	2.58	STM	ϕ_{64}
680 Genoveva	96.29	4.53	NEATM	ϕ_{64}^{\dagger}
680 Genoveva	82.63	1.58	STM	ϕ_{83}
680 Genoveva	85.86	1.51	NEATM	ϕ_{72}
690 Wratislavia	134.64	3.79	STM	ϕ_{93}
690 Wratislavia	137.08	3.03	STM	ϕ_{64}
690 Wratislavia	157.74	9.19	NEATM	ϕ_{64}
690 Wratislavia	158.11	2.48	STM	ϕ_{83}
702 Alauda	194.72	3.20	STM	ϕ_{93}
702 Alauda	175.00	6.00	Img	ϕ_{34}
702 Alauda	169.08	4.34	STM	ϕ_{64}^{\dagger}
702 Alauda	215.63	9.22	NEATM	ϕ_{64}^{\dagger}
702 Alauda	190.58	2.65	STM	ϕ_{83}
702 Alauda	201.96	4.63	NEATM	ϕ_{72}
704 Interamnia	338.00	33.79	STM	ϕ_{96}
704 Interamnia	316.61	5.19	STM	ϕ_{93}
704 Interamnia	319.00	9.00	Img-TE	ϕ_{54}
704 Interamnia	285.20	7.00	STM	ϕ_{64}^{\dagger}
704 Interamnia	358.47	14.73	NEATM	ϕ_{64}^{\dagger}
704 Interamnia	316.25	3.24	STM	ϕ_{83}
704 Interamnia	312.00	34.52	NEATM	ϕ_{72}
704 Interamnia	312.00	19.72	NEATM	ϕ_{72}
720 Bohlinia	34.00	3.40	STM	ϕ_{96}
720 Bohlinia	33.72	1.39	STM	ϕ_{93}
720 Bohlinia	41.00	1.00	TPM	ϕ_{57}^{\dagger}
720 Bohlinia	28.61	0.98	STM	ϕ_{64}^{\dagger}
720 Bohlinia	40.20	3.13	NEATM	ϕ_{64}
720 Bohlinia	34.18	0.49	STM	ϕ_{83}
735 Marghanna	74.31	1.60	STM	ϕ_{93}
735 Marghanna	65.05	1.96	STM	ϕ_{64}^{\dagger}
735 Marghanna	76.90	3.72	NEATM	ϕ_{64}
735 Marghanna	78.69	1.62	STM	ϕ_{83}^{\dagger}
735 Marghanna	70.63	1.23	NEATM	ϕ_{72}
735 Marghanna	70.76	1.26	NEATM	ϕ_{72}
739 Mandeville	107.52	2.50	STM	ϕ_{93}
739 Mandeville	104.87	4.28	STM	ϕ_{64}
739 Mandeville	106.87	8.97	NEATM	ϕ_{64}
739 Mandeville	123.13	1.83	STM	ϕ_{83}^{\dagger}
739 Mandeville	103.70	2.28	NEATM	ϕ_{72}
747 Winchester	204.00	20.39	STM	ϕ_{96}^{\dagger}
747 Winchester	171.71	3.09	STM	ϕ_{93}
747 Winchester	159.13	5.15	STM	ϕ_{64}
747 Winchester	185.97	10.40	NEATM	ϕ_{64}
747 Winchester	171.00	15.00	LC+Occ	ϕ_{78}
747 Winchester	170.08	2.51	STM	ϕ_{83}
751 Faina	110.50	4.30	STM	ϕ_{93}
751 Faina	109.58	7.90	STM	ϕ_{64}
751 Faina	122.51	6.23	NEATM	ϕ_{64}^{\dagger}
751 Faina	106.80	1.27	STM	ϕ_{83}
751 Faina	106.29	1.63	NEATM	ϕ_{72}

Table B.1: Continued

# Designation	ϕ	$\delta\phi$	Method	Refs.
758 Mancunia	85.48	6.69	STM	ϕ_{93}
758 Mancunia	85.45	3.44	STM	ϕ_{64}
758 Mancunia	102.23	7.92	NEATM	ϕ_{64}^{\dagger}
758 Mancunia	88.08	1.07	STM	ϕ_{83}
758 Mancunia	85.00	9.35	NEATM	ϕ_{72}
760 Massinga	71.29	1.90	STM	ϕ_{93}
760 Massinga	60.27	2.30	STM	ϕ_{64}^{\dagger}
760 Massinga	72.65	4.73	NEATM	ϕ_{64}
760 Massinga	70.02	1.25	STM	ϕ_{83}
762 Pulcova	137.08	3.20	STM	ϕ_{93}
762 Pulcova	143.00	2.00	NEATM	ϕ_{47}
762 Pulcova	118.69	3.29	STM	ϕ_{64}^{\dagger}
762 Pulcova	147.75	8.35	NEATM	ϕ_{64}
762 Pulcova	129.21	1.78	STM	ϕ_{83}
762 Pulcova	141.72	1.53	NEATM	ϕ_{72}
769 Tatjana	106.44	2.59	STM	ϕ_{93}
769 Tatjana	110.22	1.36	STM	ϕ_{64}
769 Tatjana	113.80	4.42	NEATM	ϕ_{64}
769 Tatjana	102.30	1.40	STM	ϕ_{83}
769 Tatjana	102.79	1.89	NEATM	ϕ_{72}
776 Berbericia	151.16	4.00	STM	ϕ_{93}
776 Berbericia	155.80	5.13	STM	ϕ_{64}
776 Berbericia	165.86	10.38	NEATM	ϕ_{64}
776 Berbericia	149.75	1.78	STM	ϕ_{83}
776 Berbericia	151.11	4.09	NEATM	ϕ_{72}
784 Pickeringia	89.41	3.40	STM	ϕ_{93}
784 Pickeringia	84.41	8.64	STM	ϕ_{64}
784 Pickeringia	104.55	8.55	NEATM	ϕ_{64}^{\dagger}
784 Pickeringia	89.66	1.17	NEATM	ϕ_{72}
784 Pickeringia	74.88	0.92	STM	ϕ_{83}
786 Bredichina	91.59	6.19	STM	ϕ_{93}
786 Bredichina	86.33	3.31	STM	ϕ_{64}^{\dagger}
786 Bredichina	88.48	4.46	NEATM	ϕ_{64}
786 Bredichina	111.47	1.29	STM	ϕ_{83}^{\dagger}
786 Bredichina	98.72	1.00	NEATM	ϕ_{72}
786 Bredichina	108.86	3.58	NEATM	ϕ_{72}
790 Pretoria	176.00	17.60	STM	ϕ_{96}
790 Pretoria	151.47	2.82	Occ	ϕ_{95}
790 Pretoria	170.36	2.59	STM	ϕ_{93}
790 Pretoria	165.44	9.32	STM	ϕ_{64}
790 Pretoria	173.41	7.38	NEATM	ϕ_{64}
790 Pretoria	144.85	4.94	STM	ϕ_{83}
804 Hispania	141.00	14.10	STM	ϕ_{96}
804 Hispania	157.58	5.80	STM	ϕ_{93}
804 Hispania	122.00	6.50	Img	ϕ_{34}^{\dagger}
804 Hispania	147.72	6.80	STM	ϕ_{64}
804 Hispania	182.36	10.39	NEATM	ϕ_{64}^{\dagger}
804 Hispania	147.00	1.92	STM	ϕ_{83}
804 Hispania	146.97	3.40	NEATM	ϕ_{72}
809 Lundia	10.26	0.07	NEATM	ϕ_{72}

Table B.1: Continued

# Designation	ϕ	$\delta\phi$	Method	Refs.
854 Frostia	15.19	6.19	PheMu	ϕ_{24}
854 Frostia	9.48	0.65	STM	ϕ_{83}
854 Frostia	7.84	0.20	NEATM	ϕ_{72}
895 Helio	141.89	3.50	STM	ϕ_{93}
895 Helio	150.92	2.52	STM	ϕ_{64}
895 Helio	155.11	7.63	NEATM	ϕ_{64}
895 Helio	128.16	1.78	STM	ϕ_{83}^{\dagger}
895 Helio	119.31	1.54	NEATM	ϕ_{72}^{\dagger}
914 Palisana	80.45	1.91	STM	ϕ_{94}
914 Palisana	76.61	1.70	STM	ϕ_{93}
914 Palisana	91.15	2.58	Occ	ϕ_{95}
914 Palisana	76.50	5.00	Img	ϕ_{34}
914 Palisana	66.95	2.09	STM	ϕ_{64}^{\dagger}
914 Palisana	83.63	3.76	NEATM	ϕ_{64}
914 Palisana	97.33	1.49	STM	ϕ_{83}^{\dagger}
914 Palisana	77.00	13.13	NEATM	ϕ_{72}
949 Hel	69.16	1.39	STM	ϕ_{93}
949 Hel	58.31	1.70	STM	ϕ_{64}
949 Hel	75.06	4.21	NEATM	ϕ_{64}^{\dagger}
949 Hel	60.97	0.74	STM	ϕ_{83}
949 Hel	66.73	1.23	NEATM	ϕ_{72}
1013 Tombecka	31.93	1.50	STM	ϕ_{93}
1013 Tombecka	37.29	1.78	STM	ϕ_{64}
1013 Tombecka	45.20	9.13	NEATM	ϕ_{64}
1013 Tombecka	36.61	0.58	STM	ϕ_{83}
1013 Tombecka	34.06	0.43	NEATM	ϕ_{72}
1015 Christa	96.94	3.59	STM	ϕ_{93}
1015 Christa	99.70	3.92	STM	ϕ_{64}
1015 Christa	104.06	4.34	NEATM	ϕ_{64}
1015 Christa	101.04	1.37	STM	ϕ_{83}
1015 Christa	96.58	2.90	NEATM	ϕ_{72}
1021 Flammario	99.38	2.29	STM	ϕ_{93}
1021 Flammario	84.98	2.85	STM	ϕ_{64}^{\dagger}
1021 Flammario	107.58	5.05	NEATM	ϕ_{64}
1021 Flammario	97.37	1.23	STM	ϕ_{83}
1021 Flammario	98.01	8.38	NEATM	ϕ_{72}
1036 Ganymed	31.65	2.79	STM	ϕ_{93}
1036 Ganymed	35.00	0.78	STM	ϕ_{83}
1089 Tama	12.92	0.60	STM	ϕ_{93}
1089 Tama	12.10	1.00	PheMu	ϕ_{24}
1089 Tama	14.35	0.44	STM	ϕ_{64}
1089 Tama	13.85	0.51	NEATM	ϕ_{64}
1089 Tama	13.31	0.19	STM	ϕ_{83}
1171 Rusthawelia	66.88	3.60	STM	ϕ_{94}
1171 Rusthawelia	70.12	2.29	STM	ϕ_{93}
1171 Rusthawelia	59.77	2.43	STM	ϕ_{64}^{\dagger}
1171 Rusthawelia	77.88	6.40	NEATM	ϕ_{64}
1171 Rusthawelia	72.08	1.19	STM	ϕ_{83}
1171 Rusthawelia	70.22	1.55	NEATM	ϕ_{72}
1313 Berna	17.29	7.09	PheMu	ϕ_{24}
1313 Berna	14.27	0.36	STM	ϕ_{83}
1313 Berna	13.50	0.31	NEATM	ϕ_{72}

Table B.1: Continued

# Designation	ϕ	$\delta\phi$	Method	Refs.
1669 Dagmar	35.77	2.40	STM	ϕ_{93}
1669 Dagmar	35.68	1.34	STM	ϕ_{64}^{\dagger}
1669 Dagmar	41.47	2.85	NEATM	ϕ_{64}
1669 Dagmar	43.00	0.77	STM	ϕ_{83}
1669 Dagmar	45.18	0.62	NEATM	ϕ_{72}
1686 De Sitter	33.09	4.32	STM	ϕ_{94}
1686 De Sitter	32.65	0.77	STM	ϕ_{83}
1686 De Sitter	29.65	0.29	NEATM	ϕ_{72}
3169 Ostro	5.15	0.08	NEATM	ϕ_{72}
3671 Dionysus	1.00	0.20	STM	ϕ_3
3671 Dionysus	0.89	0.11	NEATM	ϕ_{71}
3749 Balam	7.00	3.00	H-mag	ϕ_7
3749 Balam	4.65	0.21	NEATM	ϕ_{72}^{\dagger}
4492 Debussy	10.89	4.40	PheMu	ϕ_{24}
4492 Debussy	14.75	0.91	STM	ϕ_{83}
4492 Debussy	17.36	0.70	NEATM	ϕ_{72}
5381 Sekhmet	1.00	0.10	Radar	ϕ_{10}
25143 Itokawa	0.83	0.01	STM	ϕ_{92}^{\dagger}
25143 Itokawa	0.91	0.01	NEATM	ϕ_{92}^{\dagger}
25143 Itokawa	0.32	0.03	TPM	ϕ_{18}^{\dagger}
25143 Itokawa	0.36	0.03	Radar	ϕ_{20}^{\dagger}
25143 Itokawa	0.32	0.01	FlyBy	ϕ_{36}
25143 Itokawa	0.31	0.04	NEATM	ϕ_{71}^{\dagger}
26308 1998 SM165	290.00	36.00	NEATM	ϕ_{30}
26308 1998 SM165	279.79	29.29	NEATM	ϕ_{51}
35107 1991 VH	1.14	0.11	PheMu	ϕ_{31}
35107 1991 VH	1.12	0.21	NEATM	ϕ_{71}
42355 Typhon	173.80	16.79	NEATM	ϕ_{51}
42355 Typhon	175.00	17.00	STM	ϕ_{87}^{\dagger}
42355 Typhon	185.00	7.00	STM	ϕ_{87}
47171 1999 TC36	609.00	70.00	STM	ϕ_{11}^{\dagger}
47171 1999 TC36	405.00	55.00	NEATM	ϕ_{29}
47171 1999 TC36	414.60	38.59	NEATM	ϕ_{51}
47171 1999 TC36	393.10	26.00	STM	ϕ_{86}
50000 Quaoar	1260.00	190.00	Img-PSF	ϕ_{13}
50000 Quaoar	844.40	198.14	NEATM	ϕ_{51}
50000 Quaoar	908.00	115.00	NEATM	ϕ_{53}
50000 Quaoar	890.70	70.00	Img-PSF	ϕ_{65}
58534 Logos	110.00	40.00	H-mag	ϕ_{14}
65489 Ceto	218.00	20.00	NEATM	ϕ_{40}
65489 Ceto	229.69	18.39	NEATM	ϕ_{51}
65489 Ceto	300.00	39.00	STM	ϕ_{87}^{\dagger}
65489 Ceto	281.00	11.00	STM	ϕ_{87}
65803 Didymos	0.80	0.08	Radar	ϕ_{66}
66063 1998 RO1	0.80	0.15	Radar	ϕ_{89}
66063 1998 RO1	0.56	0.16	NEATM	ϕ_{43}
66391 1999 KW4	1.32	0.03	Radar	ϕ_{37}
66652 Borasisi	447.00	90.00	H-mag	ϕ_{16}
88611 2001 QT297	225.00	75.00	H-mag	ϕ_{90}
90482 Orcus	946.29	73.19	NEATM	ϕ_{51}
90482 Orcus	940.00	70.00	NEATM	ϕ_{63}
90482 Orcus	850.00	85.00	TPM	ϕ_{60}
134340 Pluto	2390.00	10.00	IAU	ϕ_{75}
134860 2000 OJ67	190.00	65.00	H-mag	ϕ_{90}

Table B.1: Continued

# Designation	ϕ	$\delta\phi$	Method	Refs.
136108 Haumea	1350.00	100.00	H-mag	ϕ_{27}
136108 Haumea	1151.00	59.90	NEATM	ϕ_{51}
136108 Haumea	1313.00	131.00	NEATM	ϕ_{59}
136199 Eris	3000.00	200.00	STM	ϕ_{35}^{\dagger}
136199 Eris	2400.00	100.00	Img-PSF	ϕ_{28}
136199 Eris	2657.00	212.35	NEATM	ϕ_{51}
136199 Eris	2326.00	12.00	Occ	ϕ_{82}
136199 Eris	2420.00	109.00	STM	ϕ_{87}^{\dagger}
136199 Eris	2454.00	117.00	STM	ϕ_{87}
136617 1994 CC	0.62	0.06	Radar	ϕ_{80}
153591 2001 SN263	2.59	0.20	H-mag	ϕ_{70}
164121 2003 YT1	1.10	0.20	Radar	ϕ_{15}
164121 2003 YT1	1.05	0.30	Radar	ϕ_{26}
175706 1996 FG3	1.69	0.15	TPM	ϕ_{81}
175706 1996 FG3	1.83	0.50	NEATM	ϕ_{71}
175706 1996 FG3	1.83	0.28	NEATM	ϕ_{88}
185851 2000 DP107	1.63	0.35	Radar	ϕ_8
276049 2002 CE26	3.46	0.35	Radar	ϕ_{33}
311066 2004 DC	0.34	0.03	Radar	ϕ_{50}
1999 OJ4	130.00	45.00	H-mag	ϕ_{90}
2000 CF105	188.00	38.00	Img-PSF	ϕ_6
2000 QL251	150.00	50.00	H-mag	ϕ_{90}
2000 UG11	0.30	0.10	H-mag	ϕ_{90}
2001 QC298	244.00	55.00	H-mag	ϕ_{49}
2001 XR254	225.00	75.00	H-mag	ϕ_{90}
2001 QW322	128.00	3.00	H-mag	ϕ_{74}
2003 QY90	150.00	50.00	H-mag	ϕ_{90}
2003 TJ58	75.00	25.00	H-mag	ϕ_{90}
2003 UN284	124.00	8.00	H-mag	ϕ_{74}
2004 PB108	140.00	50.00	H-mag	ϕ_{90}
2005 EO304	152.00	2.00	H-mag	ϕ_{74}
2006 BR284	89.80	0.90	H-mag	ϕ_{74}
2006 JZ81	122.00	16.00	H-mag	ϕ_{74}
2006 CH69	100.00	11.00	H-mag	ϕ_{74}
2007 TY430	50.00	20.00	H-mag	ϕ_{85}
1P/Halley	10.39	2.00	FlyBy	ϕ_{56}
2P/Encke	6.00	2.00	H-mag	ϕ_{56}
2P/Encke	4.19	0.80	H-mag	ϕ_{56}
6P/dArest	1.70	0.20	H-mag	ϕ_{32}
9P/Tempel1	6.00	0.20	FlyBy	ϕ_{23}
9P/Tempel1	5.03	0.30	H-mag	ϕ_{32}^{\dagger}
10P/Tempel2	9.60	1.39	H-mag	ϕ_{56}
19P/Borrelly	4.80	0.40	FlyBy	ϕ_{56}
22P/Kopff	3.59	0.40	H-mag	ϕ_{32}
45P/H-M-P	0.66	0.20	H-mag	ϕ_{32}
46P/Wirtanen	1.15	0.06	H-mag	ϕ_{32}
67P/C-G	4.19	0.25	H-mag	ϕ_{32}^{\dagger}
67P/C-G	2.96	0.04	H-mag	ϕ_{25}^{\dagger}
67P/C-G	2.96	0.10	TPM	ϕ_{42}
81P/Wild2	3.81	0.76	H-mag	ϕ_{32}^{\dagger}
81P/Wild2	2.08	0.06	FlyBy	ϕ_{17}
SL9	1.79	0.18	BkUp	ϕ_1

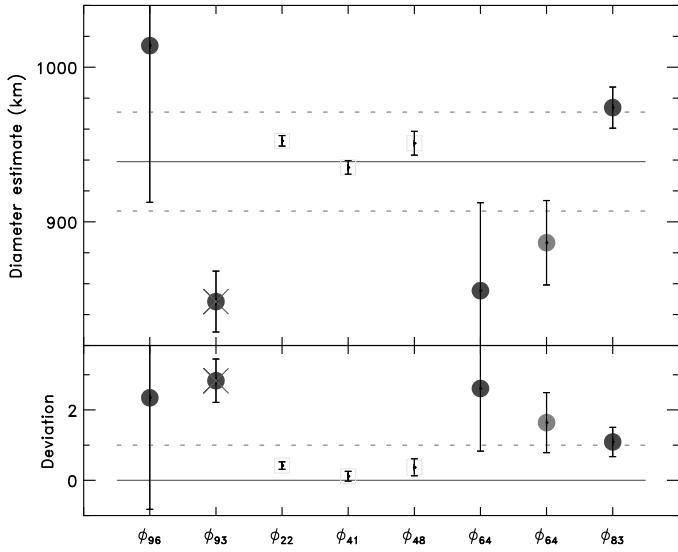


Figure B.1: Diameter estimates for (1) Ceres.

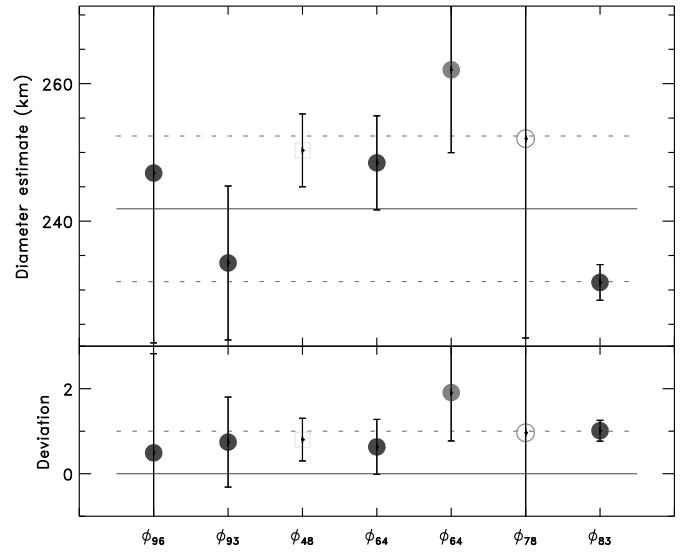


Figure B.3: Diameter estimates for (3) Juno.

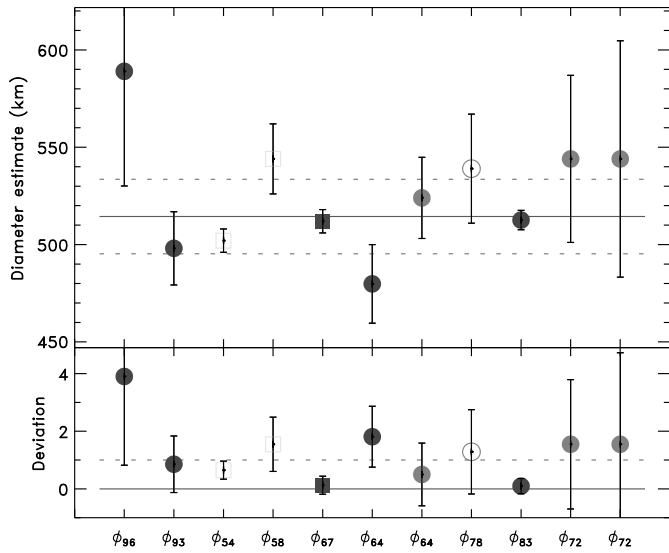


Figure B.2: Diameter estimates for (2) Pallas.

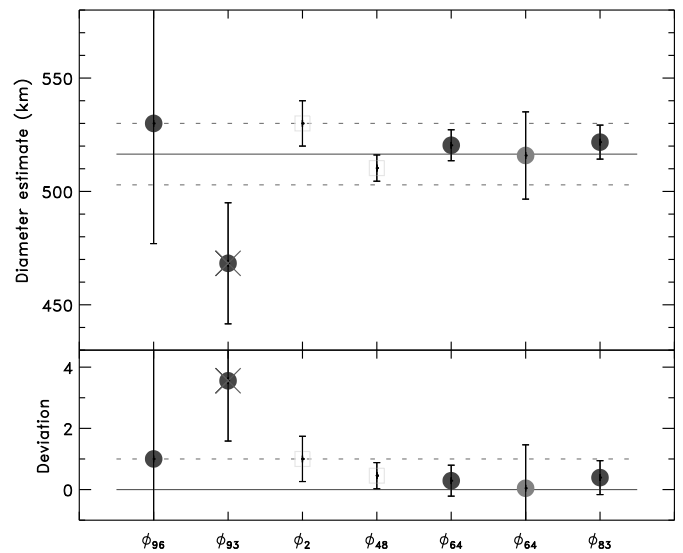


Figure B.4: Diameter estimates for (4) Vesta.

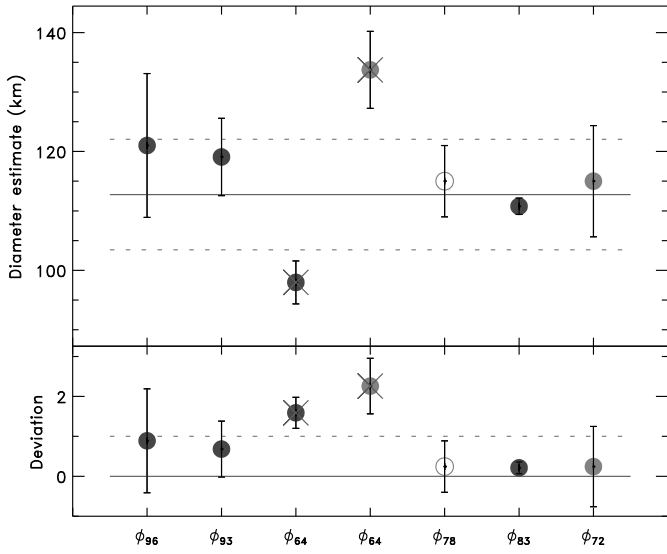


Figure B.5: Diameter estimates for (5) Astraea.

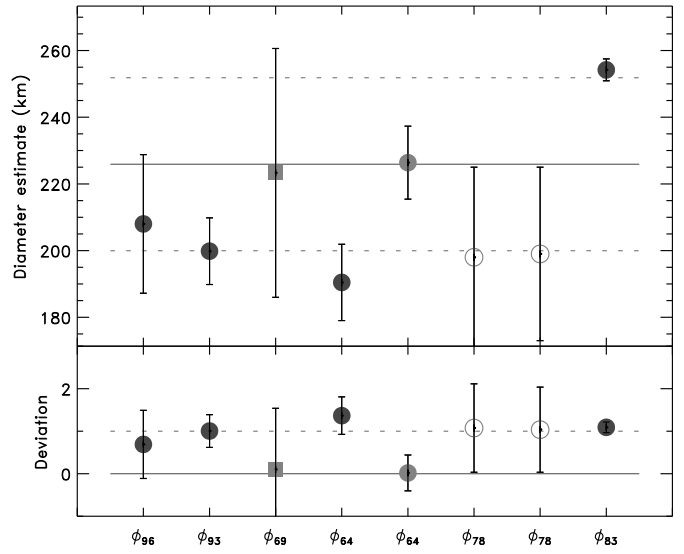


Figure B.7: Diameter estimates for (7) Iris.

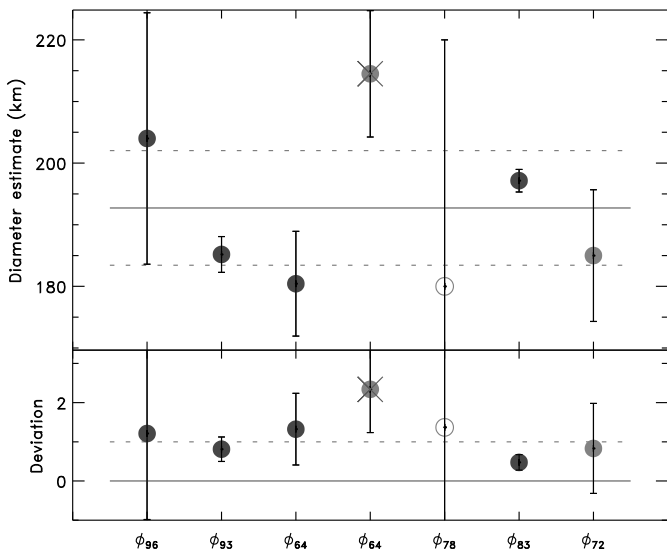


Figure B.6: Diameter estimates for (6) Hebe.

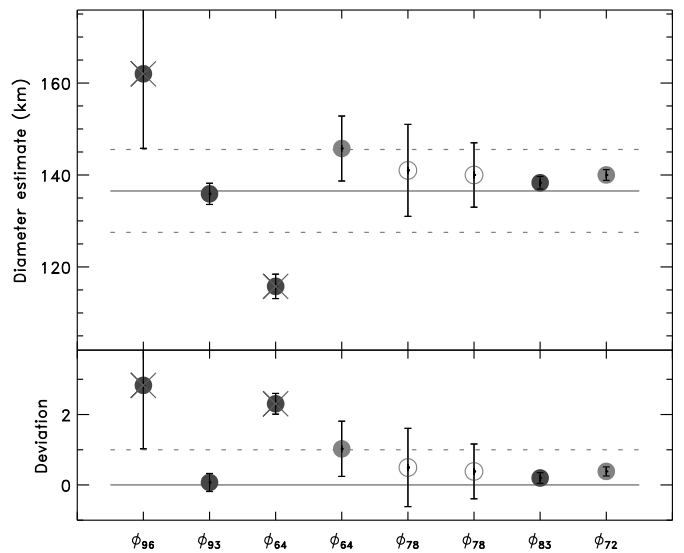


Figure B.8: Diameter estimates for (8) Flora.

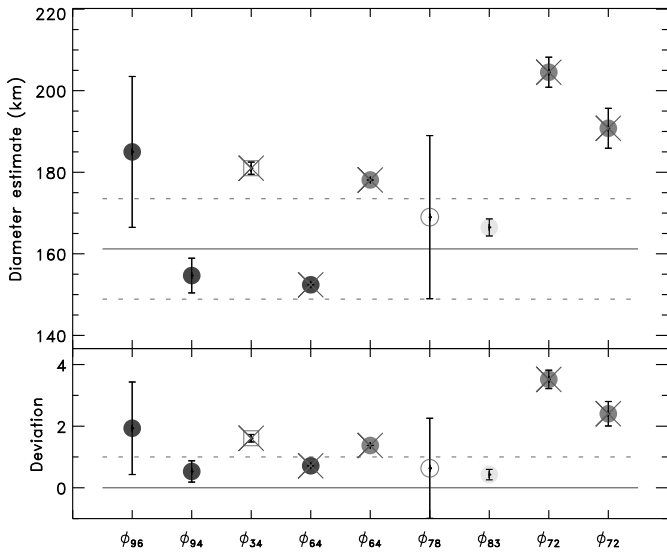


Figure B.9: Diameter estimates for (9) Metis. The diameter estimates from ϕ_{64} have unrealistic small uncertainties of 0.02 km. Using these values strongly biases the average.

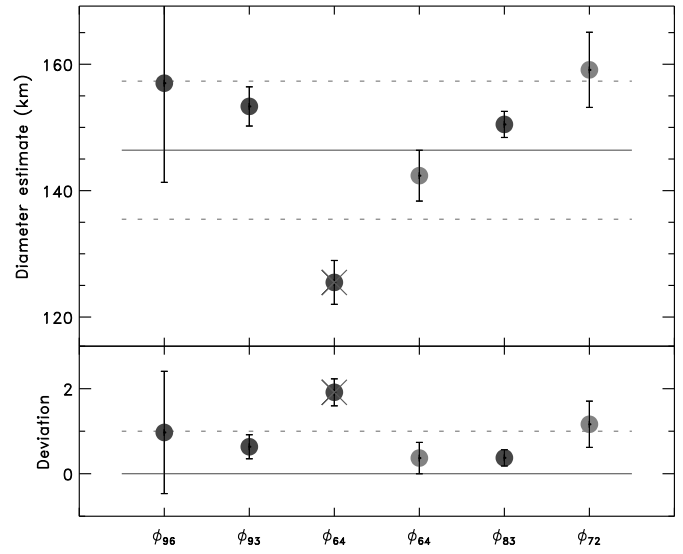


Figure B.11: Diameter estimates for (11) Parthenope.

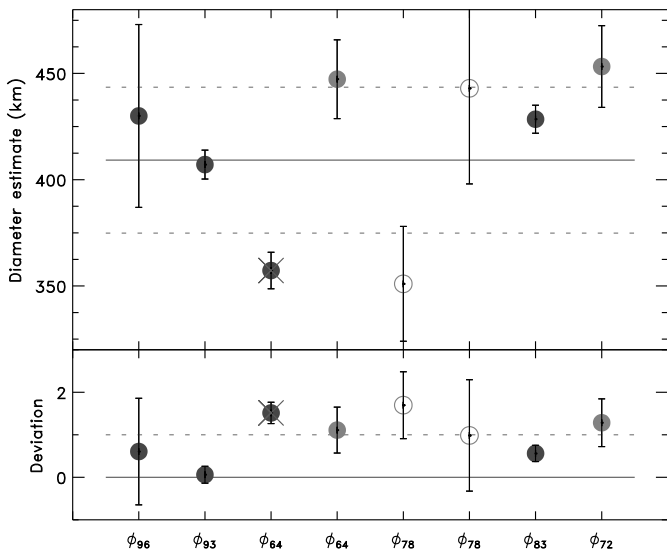


Figure B.10: Diameter estimates for (10) Hygiea.

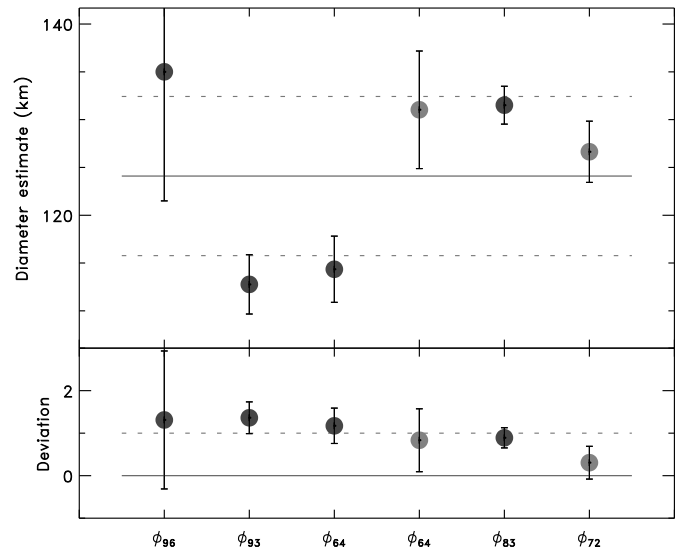


Figure B.12: Diameter estimates for (12) Victoria.

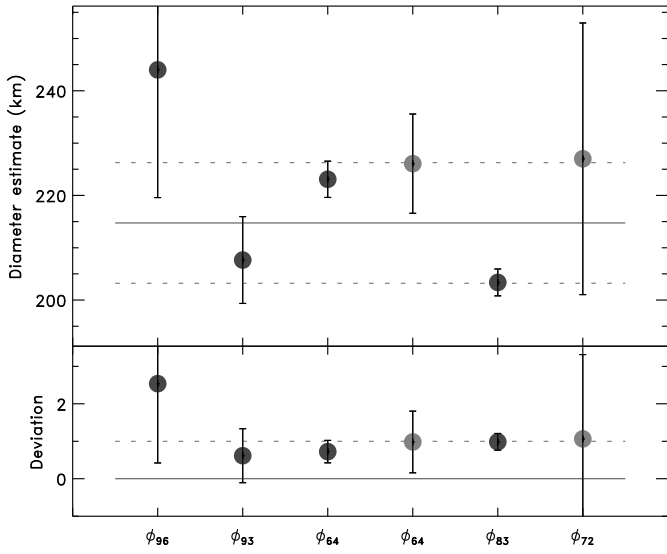


Figure B.13: Diameter estimates for (13) Egeria.

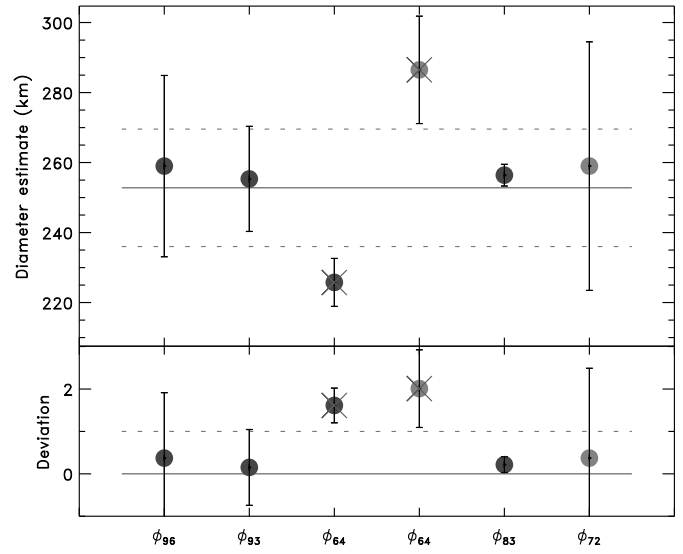


Figure B.15: Diameter estimates for (15) Eunomia.

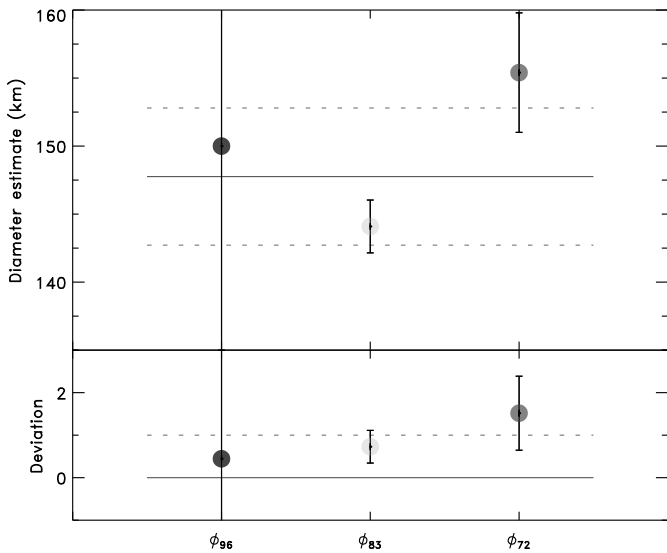


Figure B.14: Diameter estimates for (14) Irene.

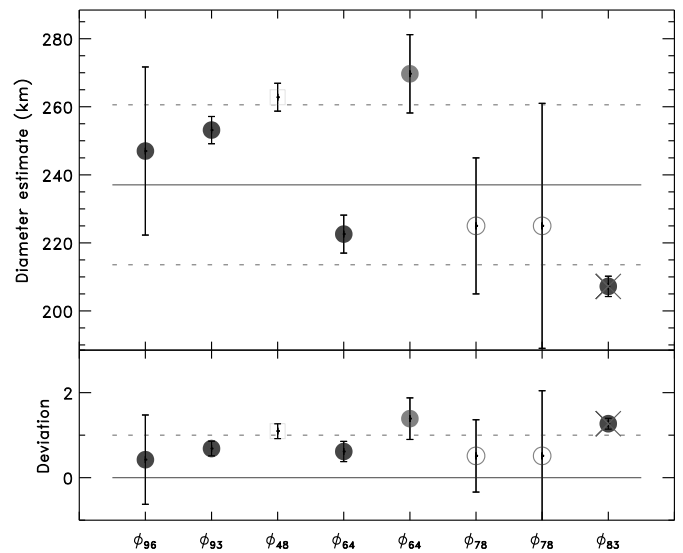


Figure B.16: Diameter estimates for (16) Psyche.

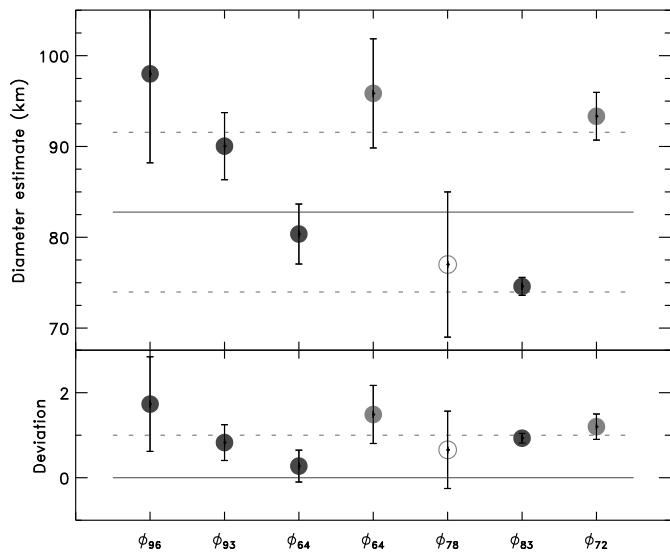


Figure B.17: Diameter estimates for (17) Thetis.

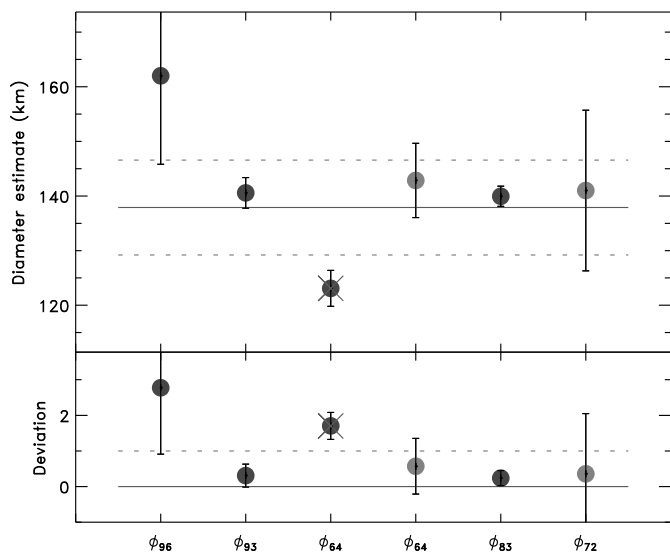


Figure B.18: Diameter estimates for (18) Melpomene.

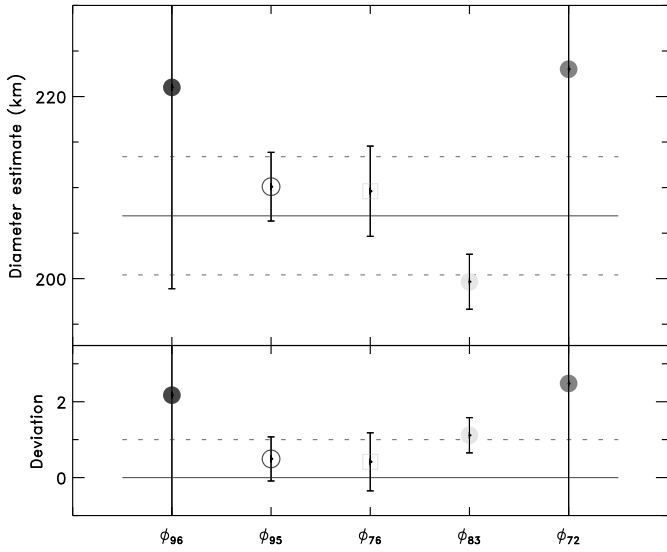


Figure B.19: Diameter estimates for (19) Fortuna.

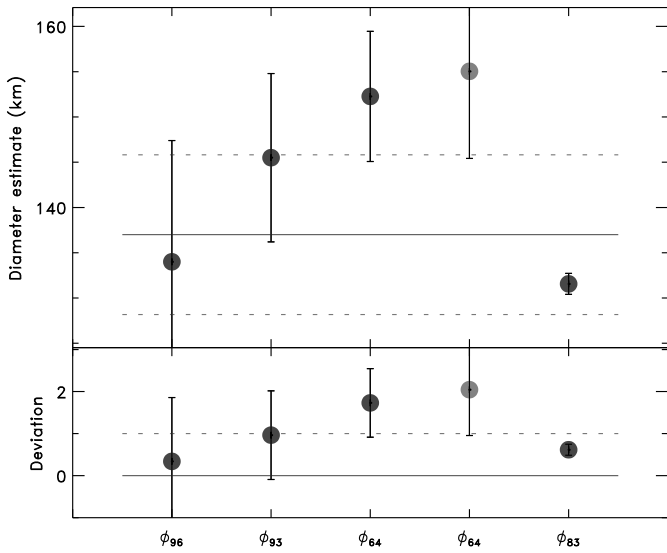


Figure B.20: Diameter estimates for (20) Massalia.

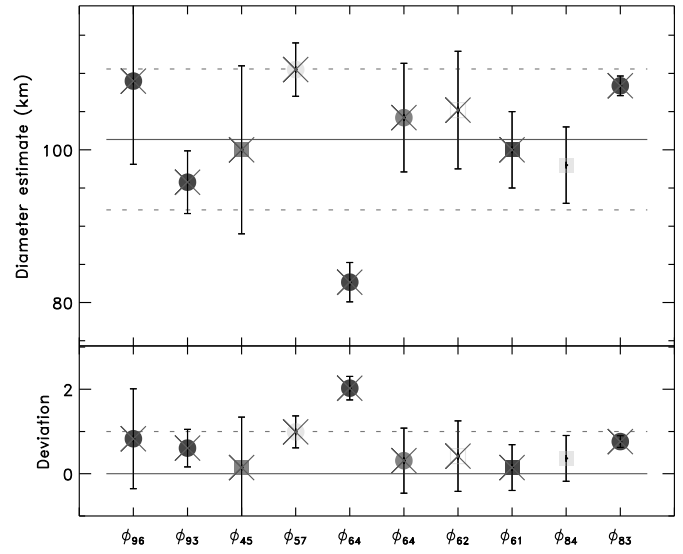


Figure B.21: Diameter estimates for (21) Lutetia. Only the flyby estimate from ϕ_{61}^\dagger is used here.

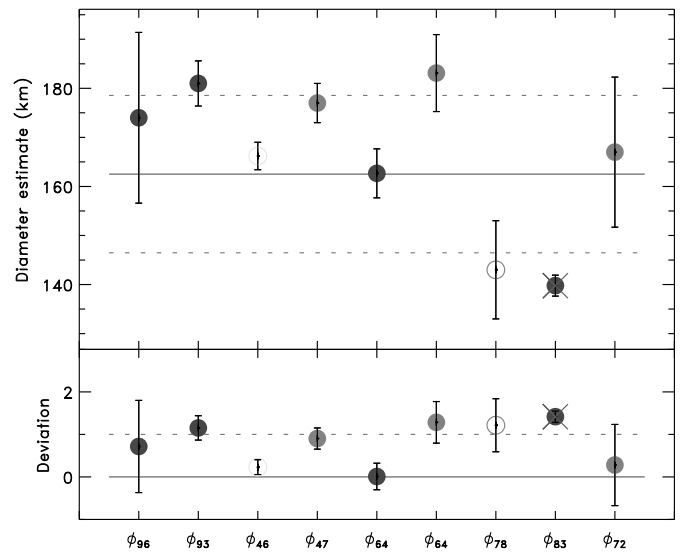


Figure B.22: Diameter estimates for (22) Kalliope.

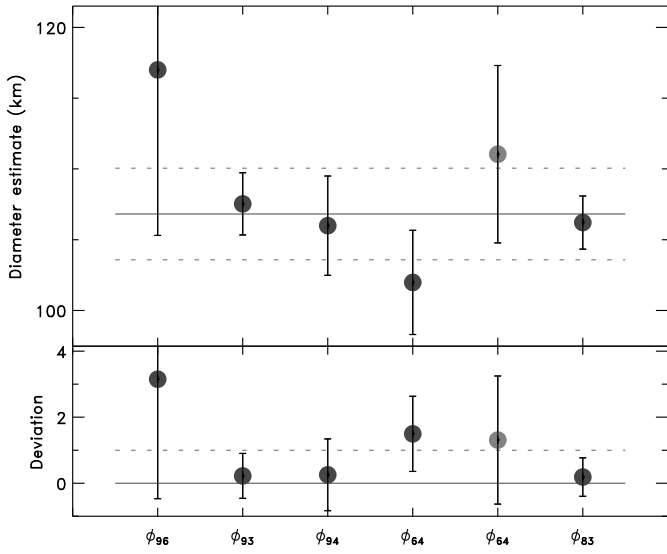


Figure B.23: Diameter estimates for (23) Thalia.

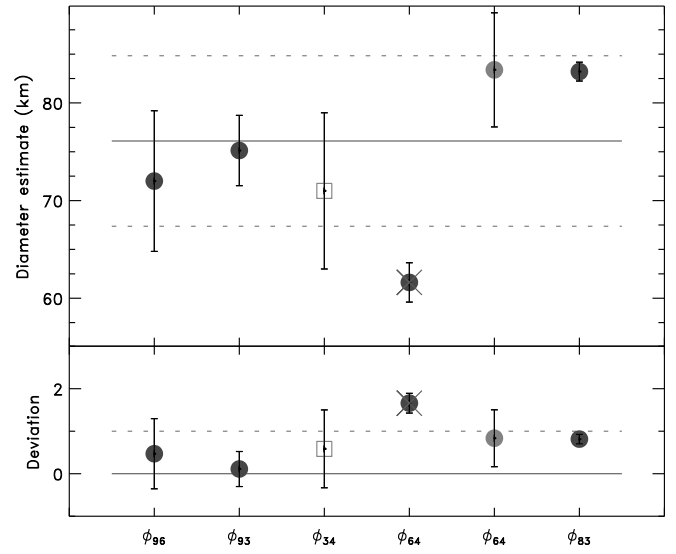


Figure B.25: Diameter estimates for (25) Phocaea.

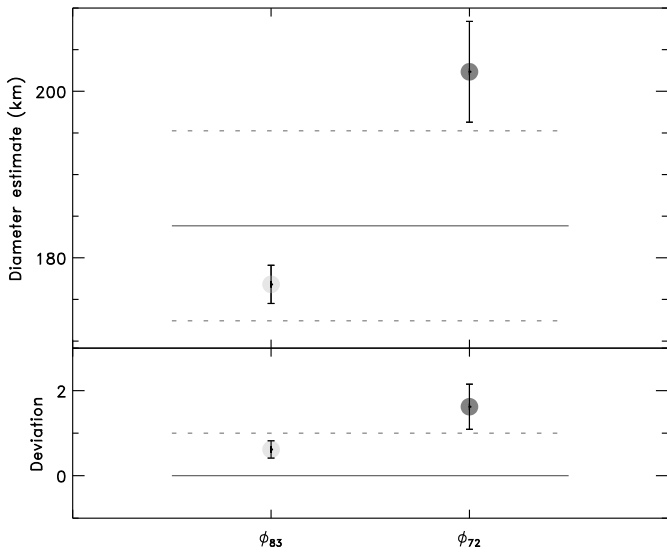


Figure B.24: Diameter estimates for (24) Themis.

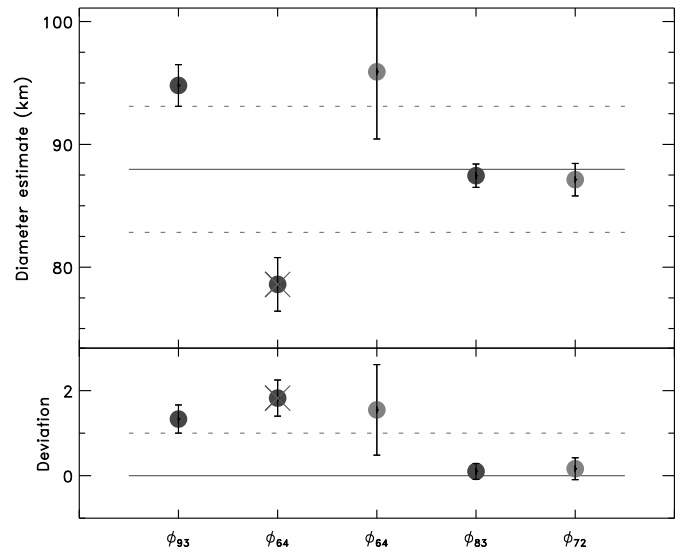


Figure B.26: Diameter estimates for (26) Proserpina.

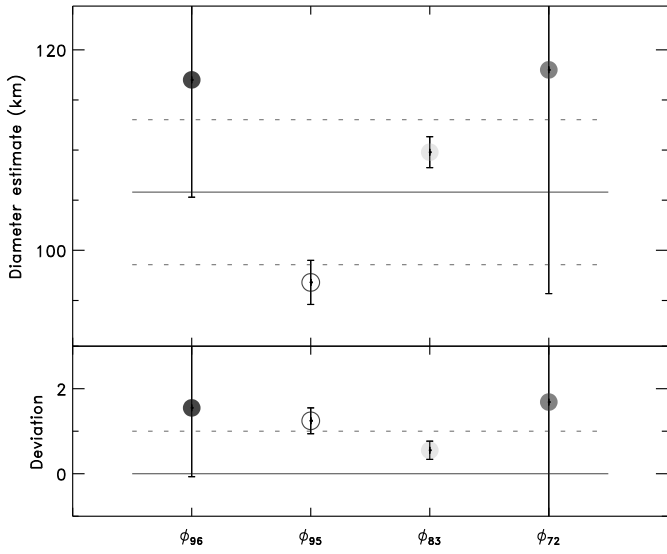


Figure B.27: Diameter estimates for (27) Euterpe.

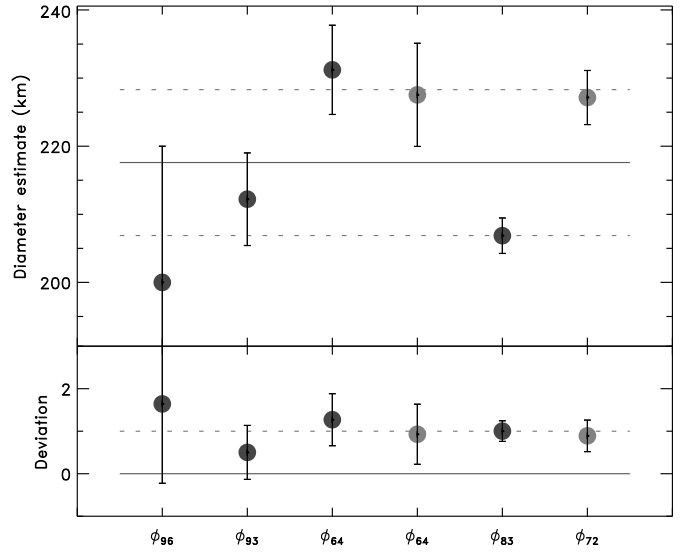


Figure B.29: Diameter estimates for (29) Amphitrite.

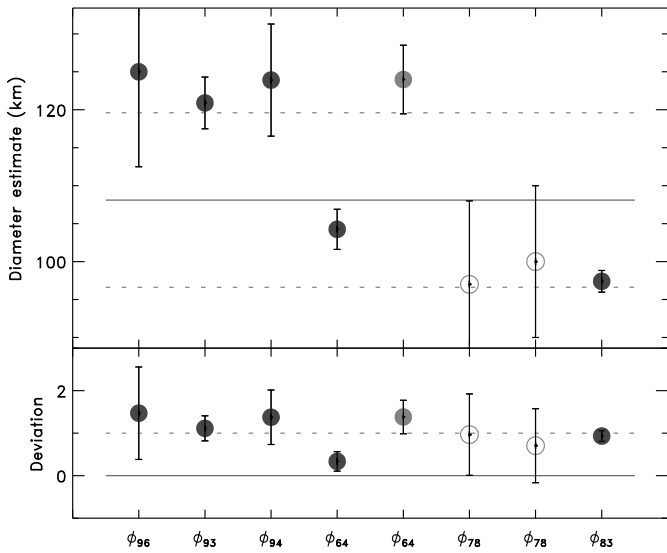


Figure B.28: Diameter estimates for (28) Bellona.

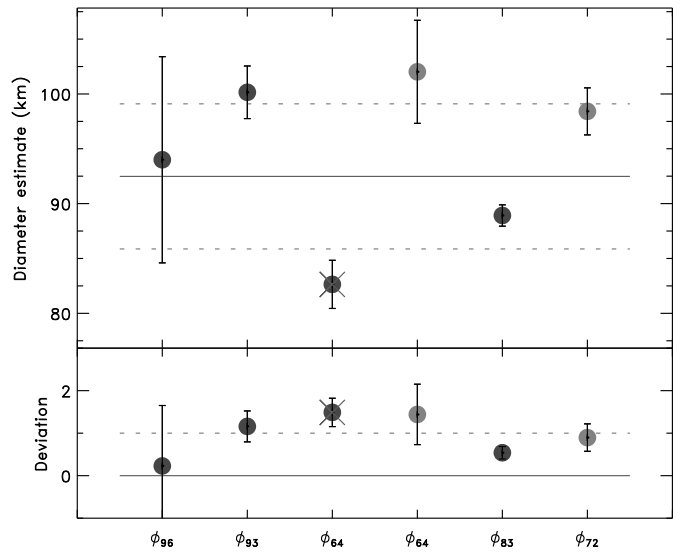


Figure B.30: Diameter estimates for (30) Urania.

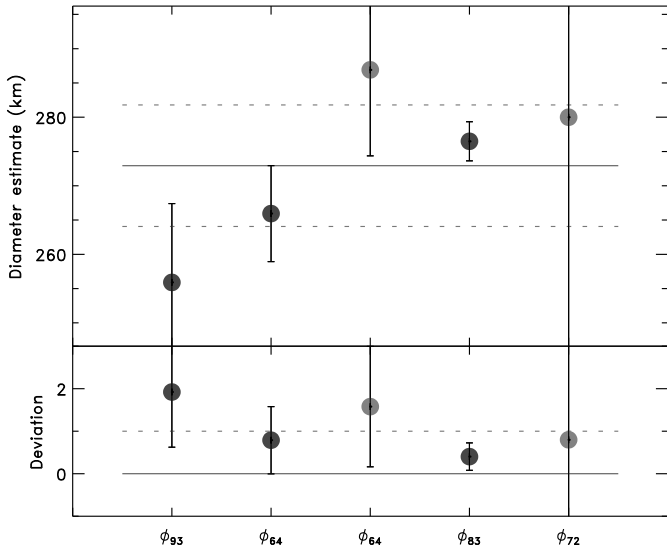


Figure B.31: Diameter estimates for (31) Euphrosyne.

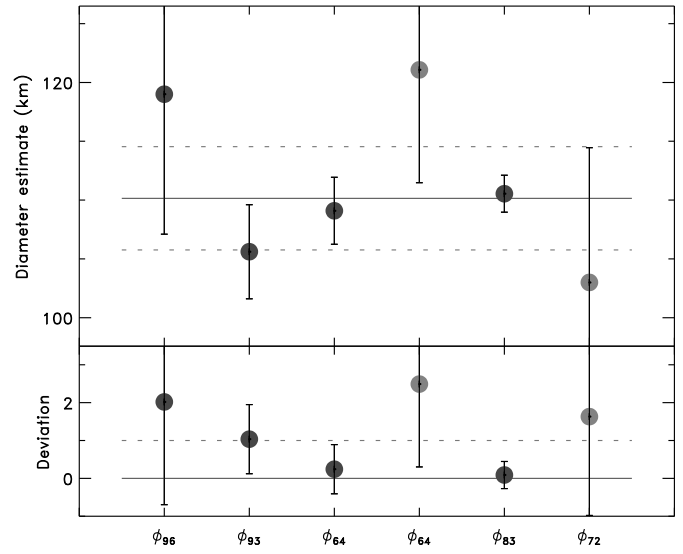


Figure B.33: Diameter estimates for (36) Atalante.

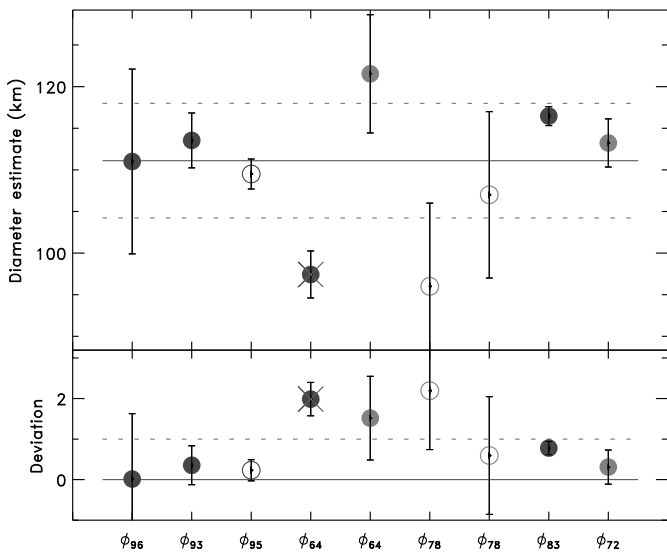


Figure B.32: Diameter estimates for (34) Circe.

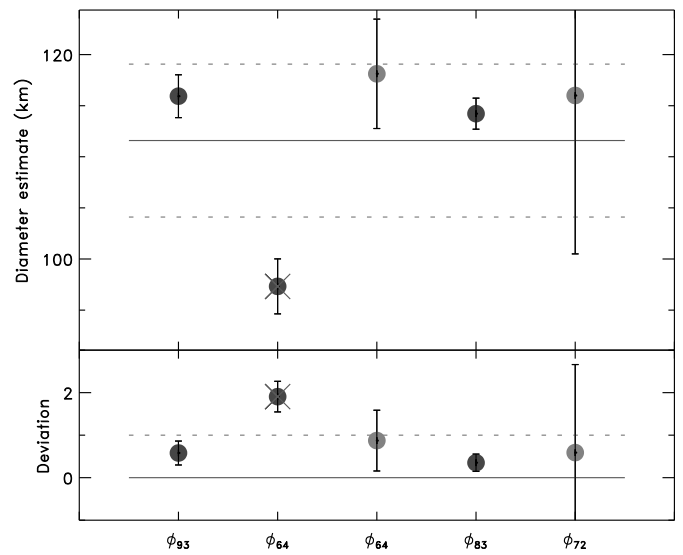


Figure B.34: Diameter estimates for (38) Leda.

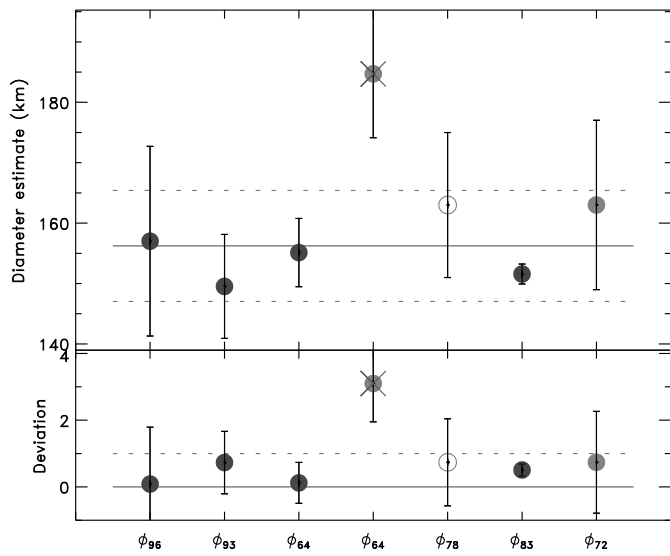


Figure B.35: Diameter estimates for (39) Laetitia.

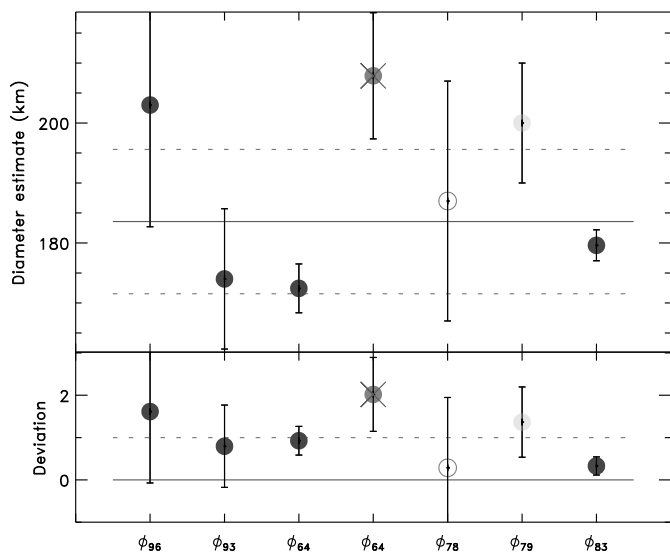


Figure B.36: Diameter estimates for (41) Daphne.

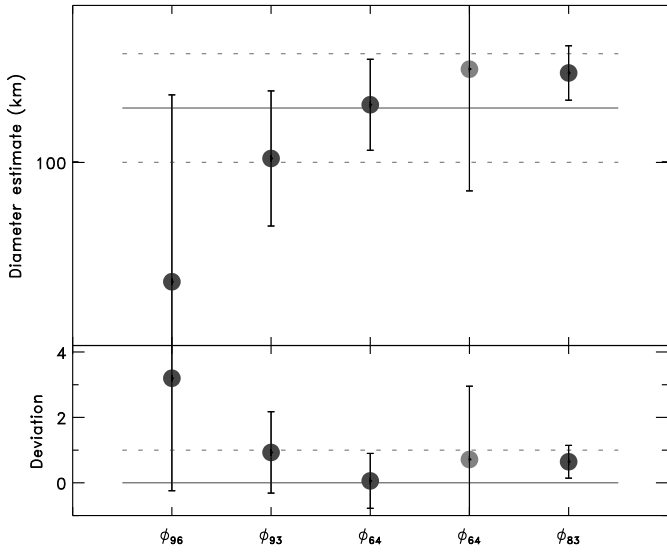


Figure B.37: Diameter estimates for (42) Isis.

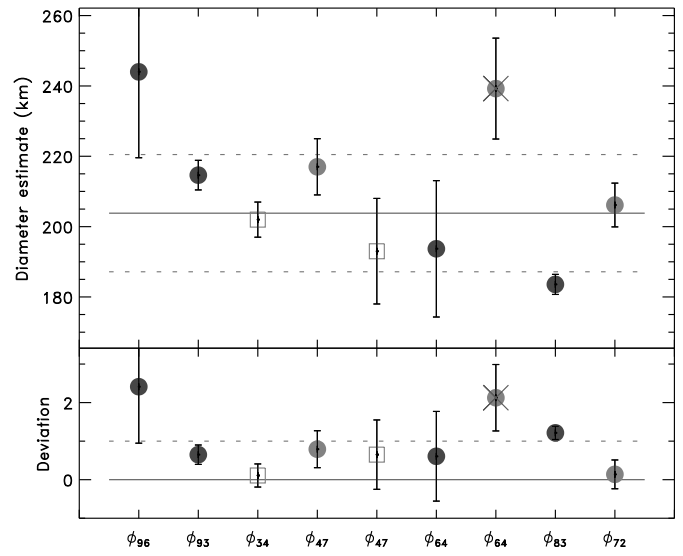


Figure B.39: Diameter estimates for (45) Eugenia.

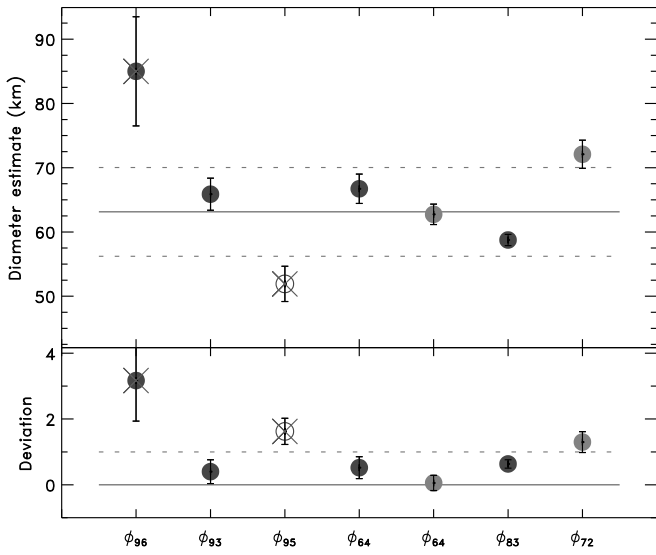


Figure B.38: Diameter estimates for (43) Ariadne.

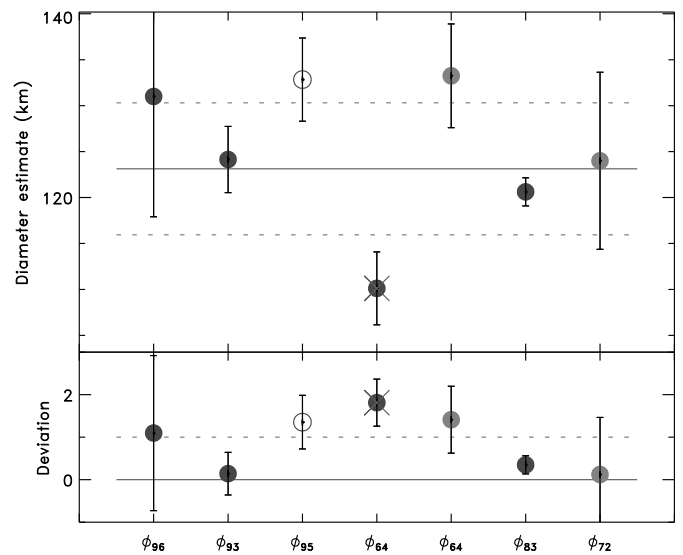


Figure B.40: Diameter estimates for (46) Hestia.

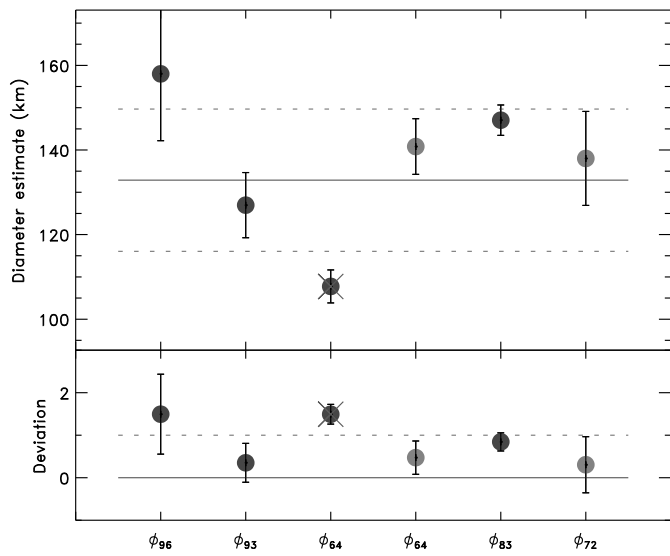


Figure B.41: Diameter estimates for (47) Aglaja.

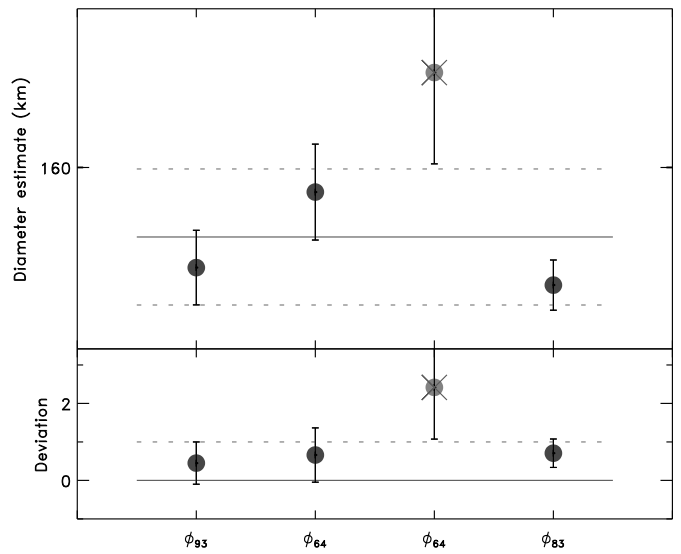


Figure B.43: Diameter estimates for (49) Pales.

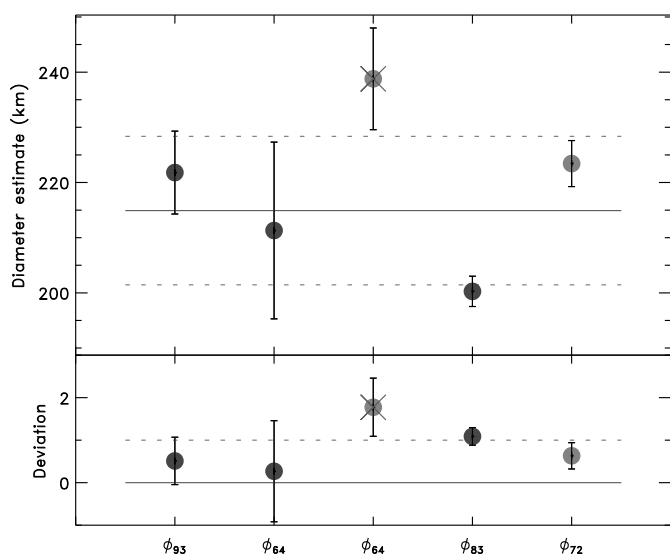


Figure B.42: Diameter estimates for (48) Doris.

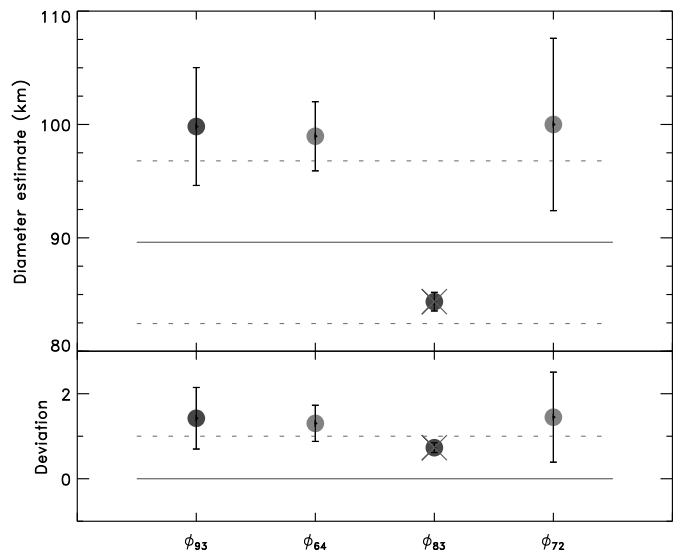


Figure B.44: Diameter estimates for (50) Virginia. The diameter estimate from ϕ_{83} raises the density from 7.1 ± 5.2 to 9.9 ± 7.6 and is therefore discarded.

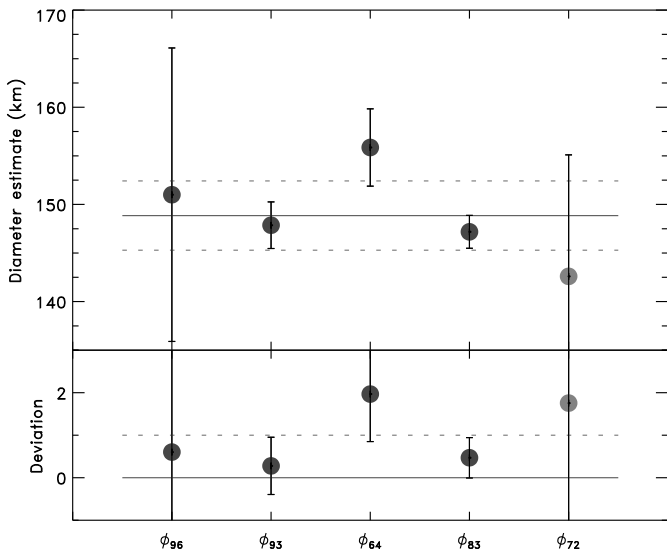


Figure B.45: Diameter estimates for (51) Nemausa.

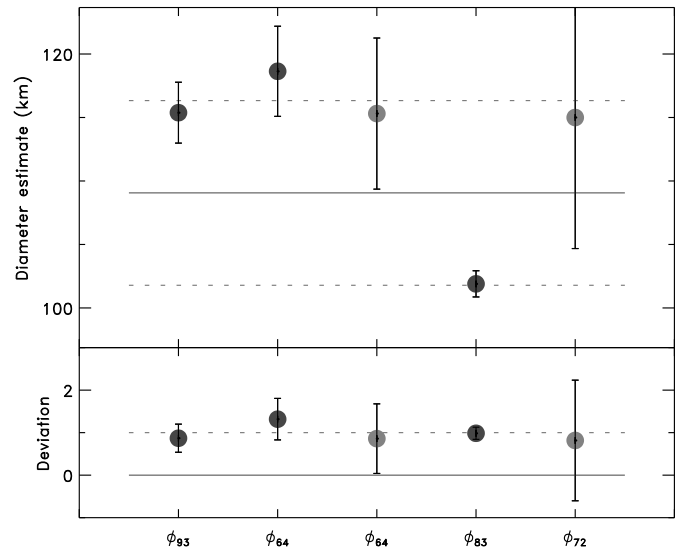


Figure B.47: Diameter estimates for (53) Kalypso. The large uncertainty on the mass determination forbid to sort between the diameter estimates. Values from ϕ_{93} , ϕ_{64} , and ϕ_{64} were obtained using IRAS data (Tedesco et al. 2002; Ryan and Woodward 2010), and ϕ_{83} with AKARI data (Usui et al. 2011). Discrepancy could likely result from different observing geometries (e.g., polar vs equatorial) not taken into account.

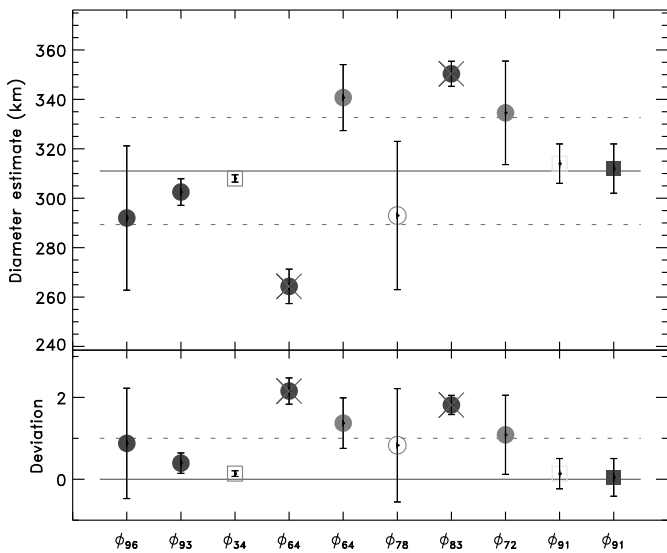


Figure B.46: Diameter estimates for (52) Europa.

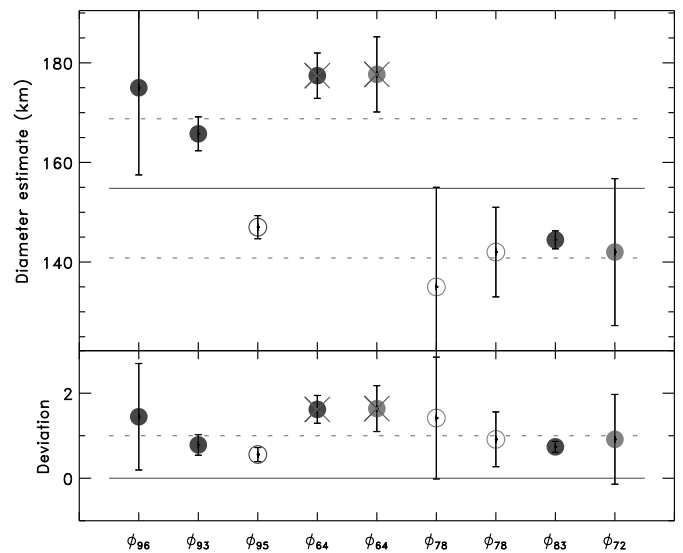


Figure B.48: Diameter estimates for (54) Alexandra.

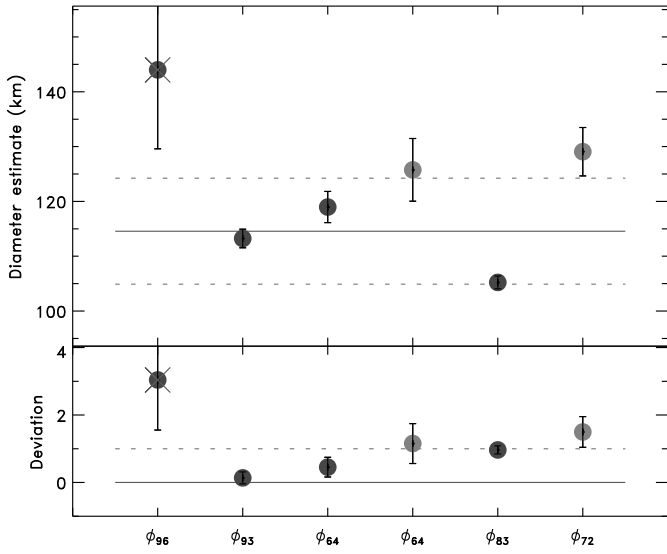


Figure B.49: Diameter estimates for (56) Melete.

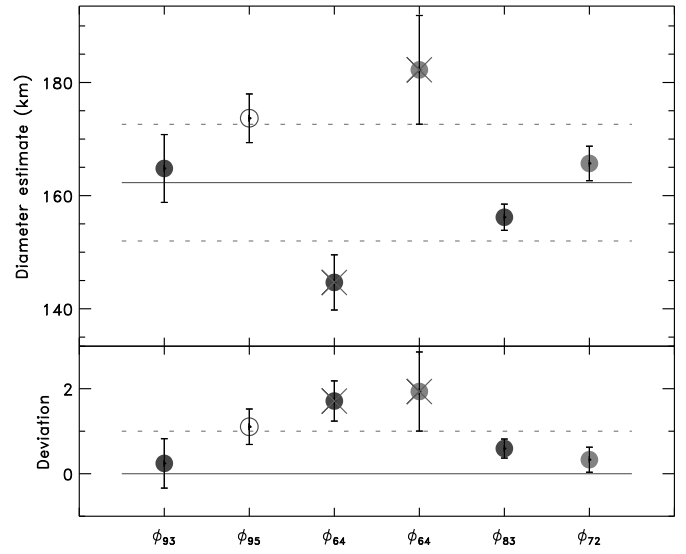


Figure B.51: Diameter estimates for (59) Elpis.

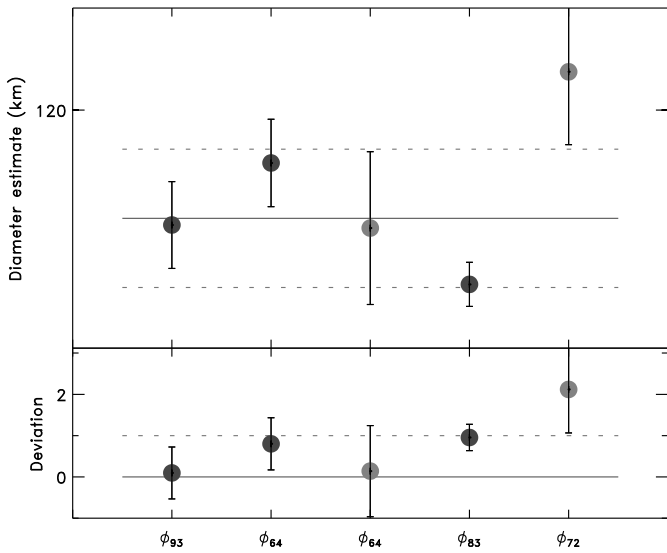


Figure B.50: Diameter estimates for (57) Mnemosyne.

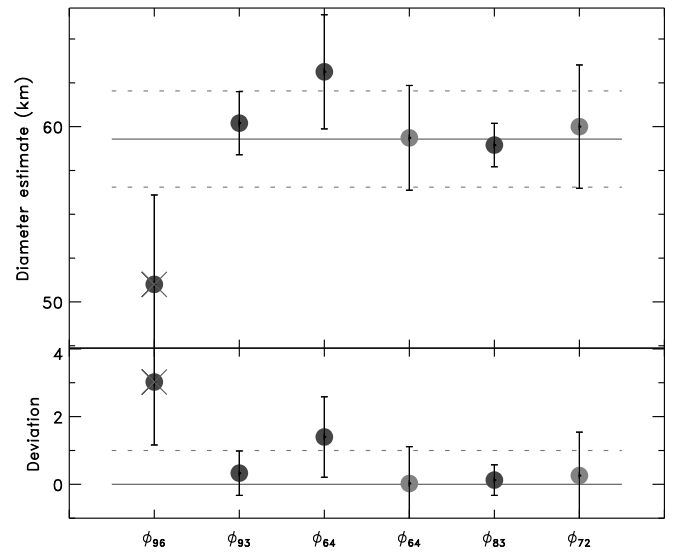


Figure B.52: Diameter estimates for (60) Echo.

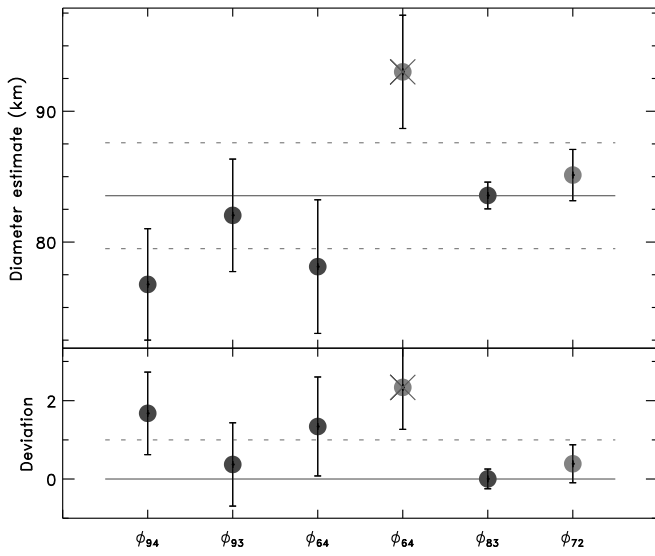


Figure B.53: Diameter estimates for (61) Danae.

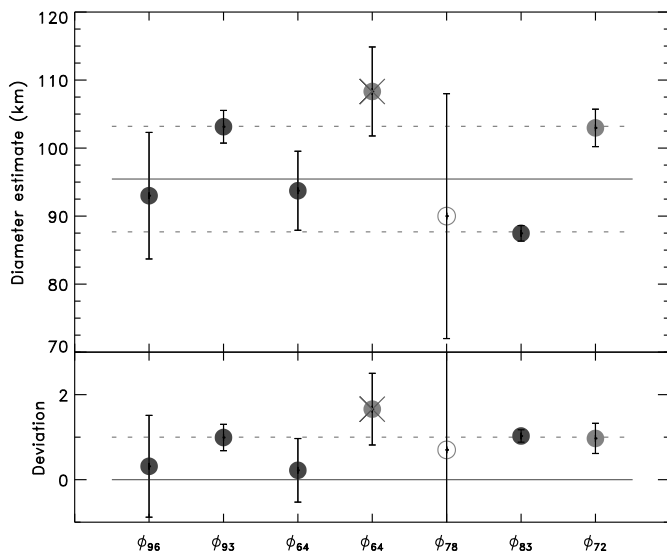


Figure B.54: Diameter estimates for (63) Ausonia.

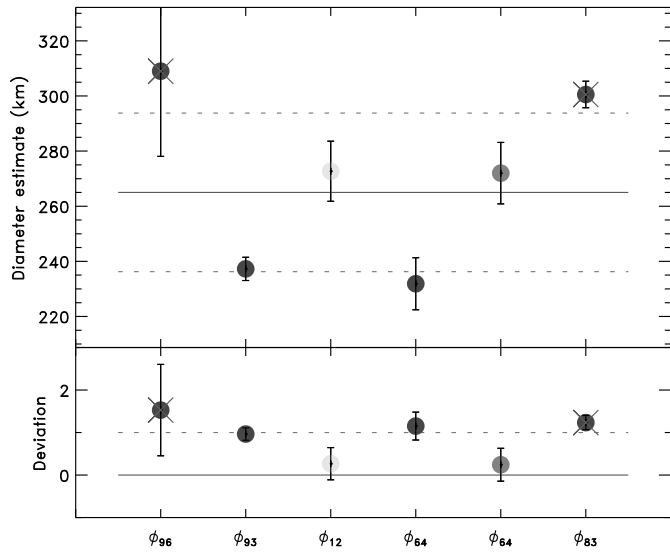


Figure B.55: Diameter estimates for (65) Cybele.

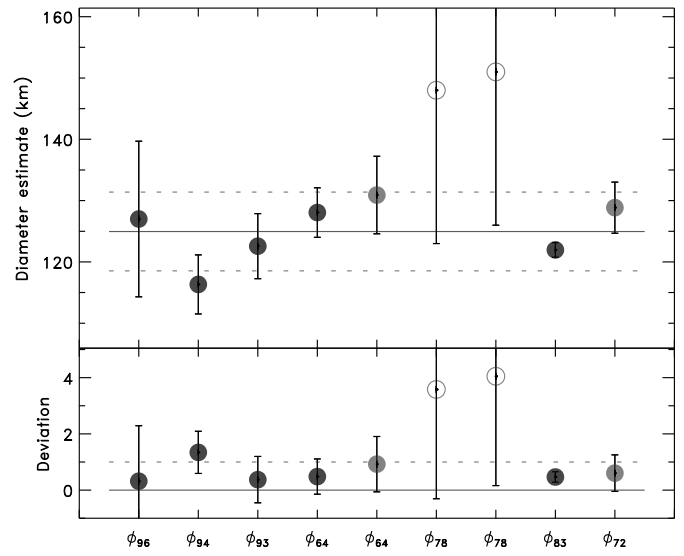


Figure B.57: Diameter estimates for (68) Leto.

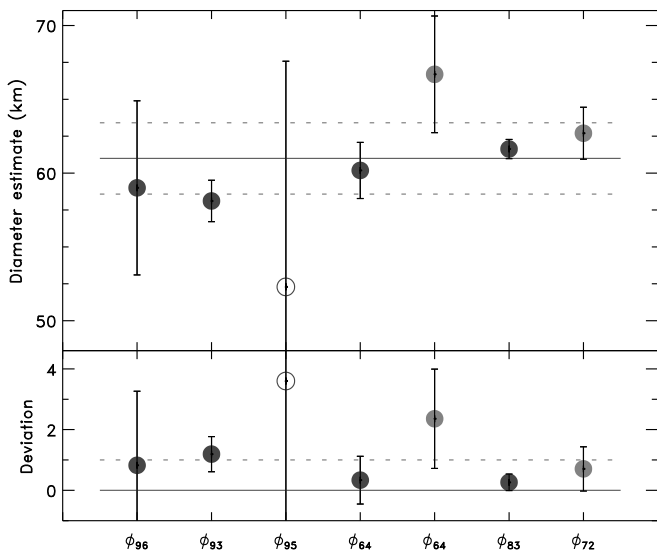


Figure B.56: Diameter estimates for (67) Asia.

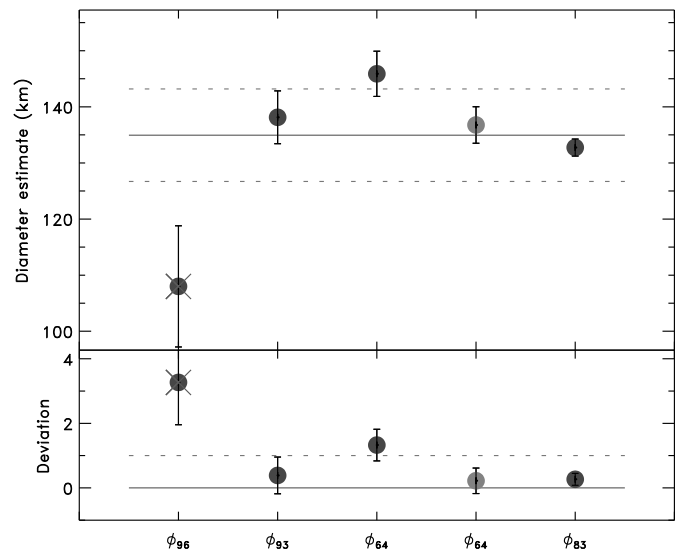


Figure B.58: Diameter estimates for (69) Hesperia.

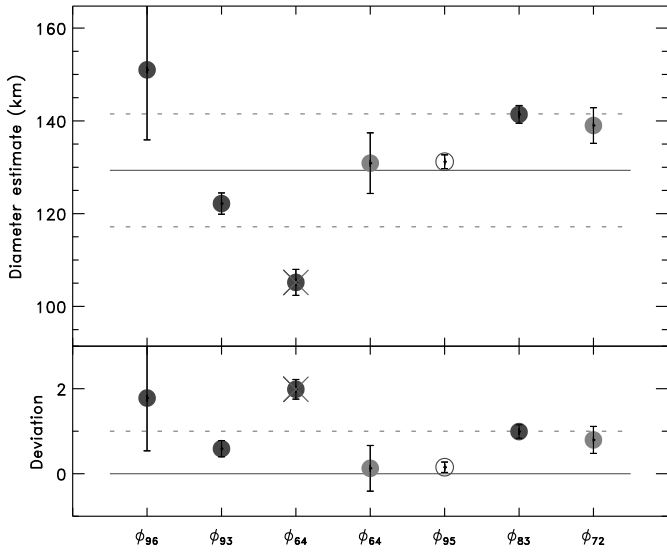


Figure B.59: Diameter estimates for (70) Panopaea.

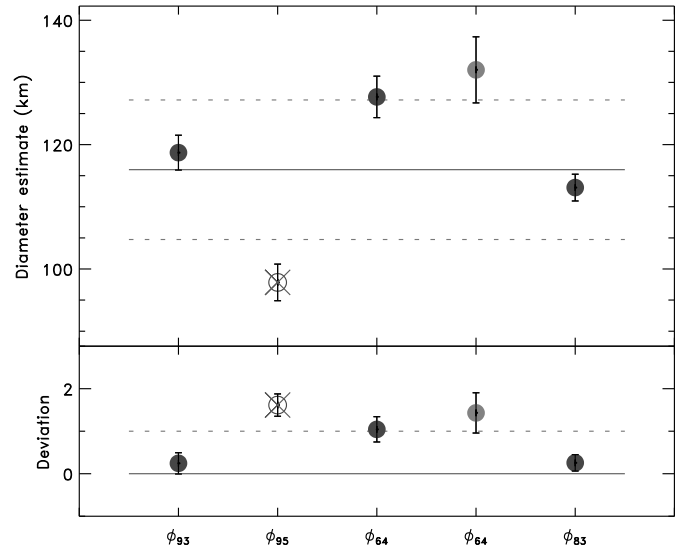


Figure B.61: Diameter estimates for (74) Galatea.

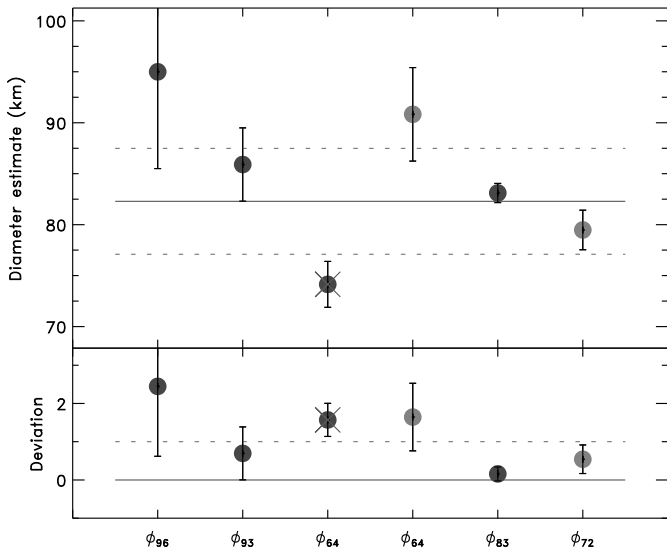


Figure B.60: Diameter estimates for (72) Feronia.

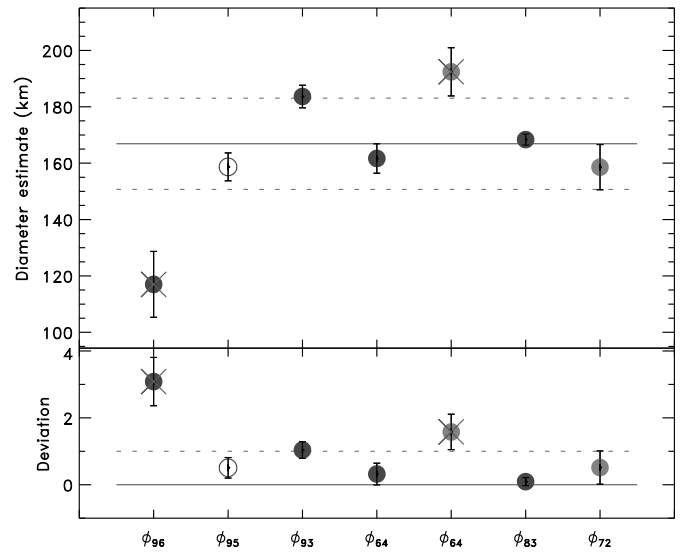


Figure B.62: Diameter estimates for (76) Freia.

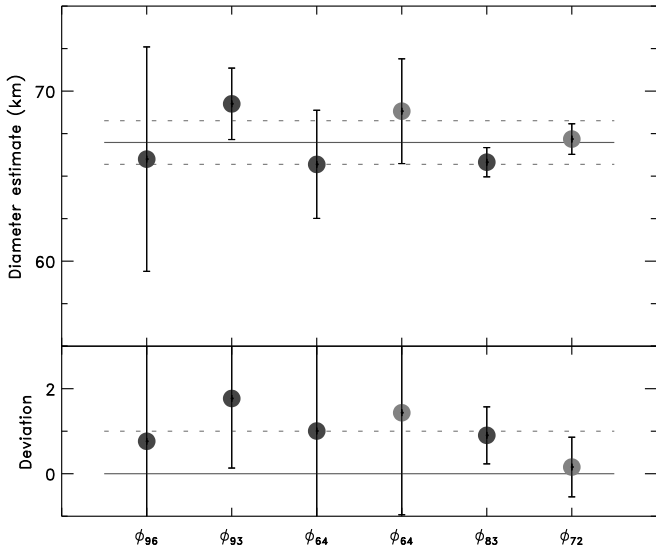


Figure B.63: Diameter estimates for (77) Frigga.

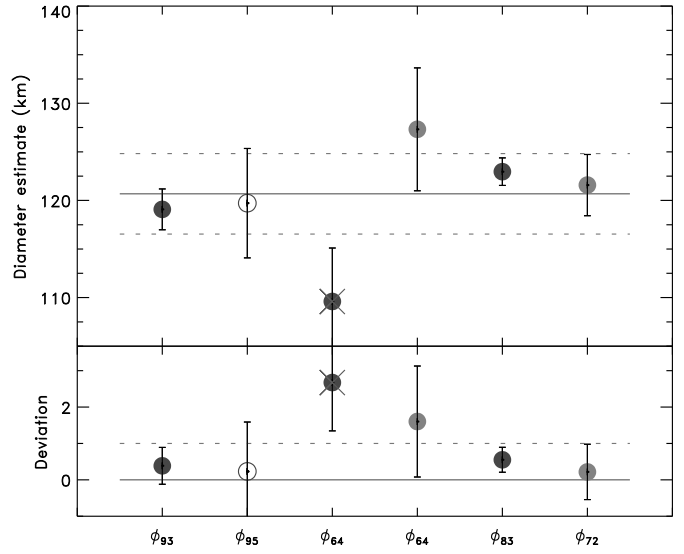


Figure B.65: Diameter estimates for (81) Terpsichore.

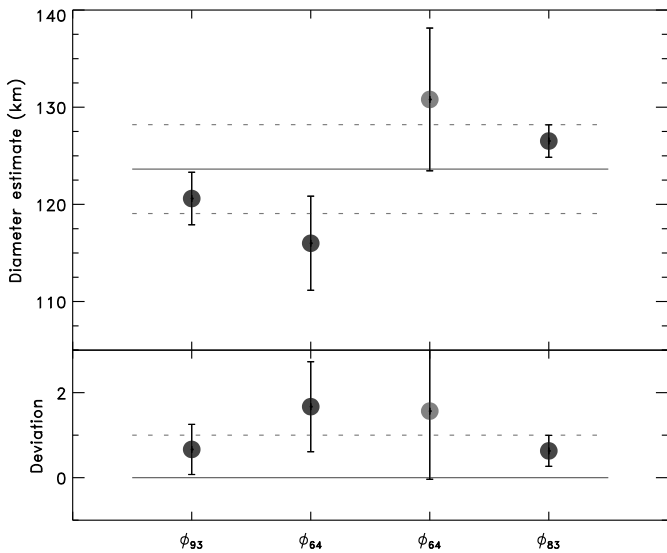


Figure B.64: Diameter estimates for (78) Diana.

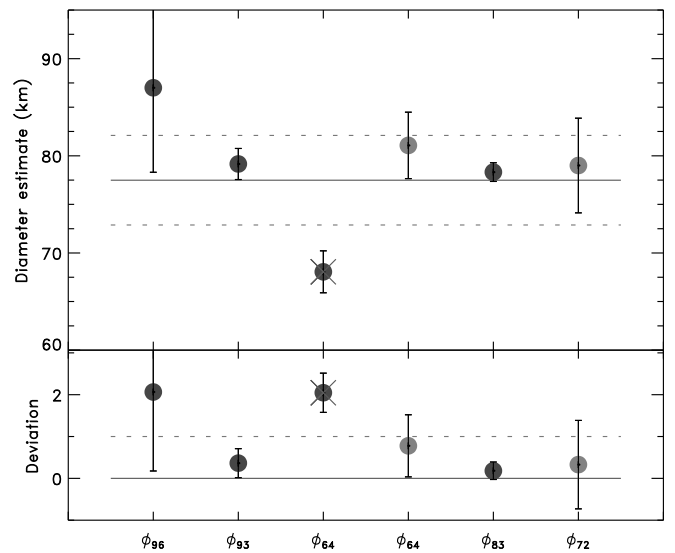


Figure B.66: Diameter estimates for (84) Klio.

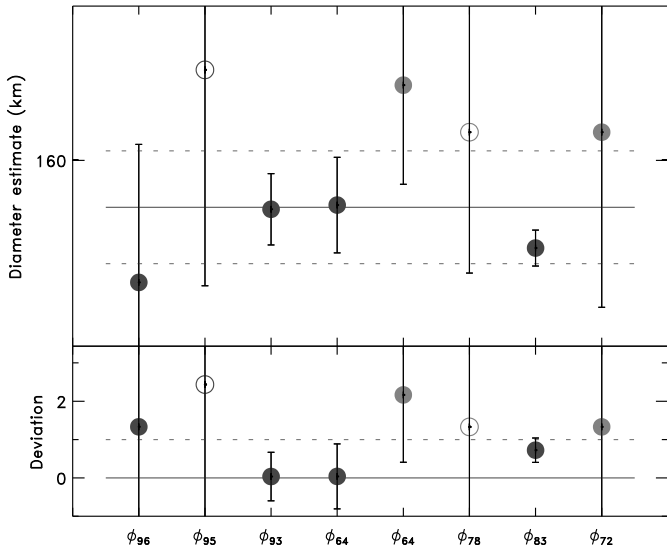


Figure B.67: Diameter estimates for (85) Io.

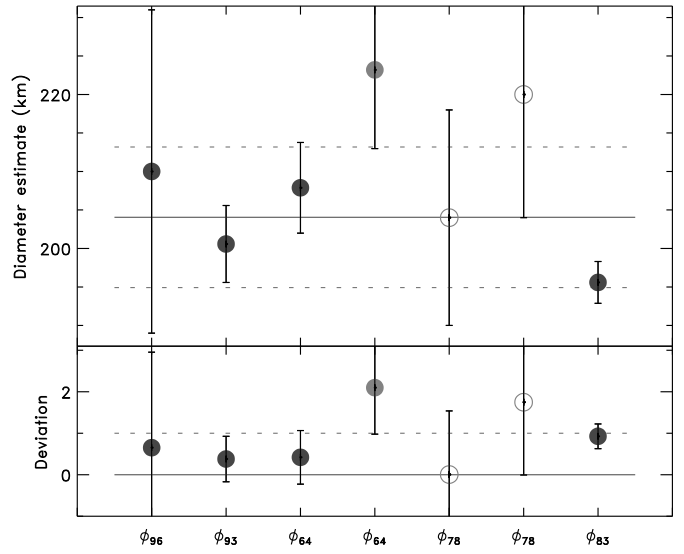


Figure B.69: Diameter estimates for (88) Thisbe.

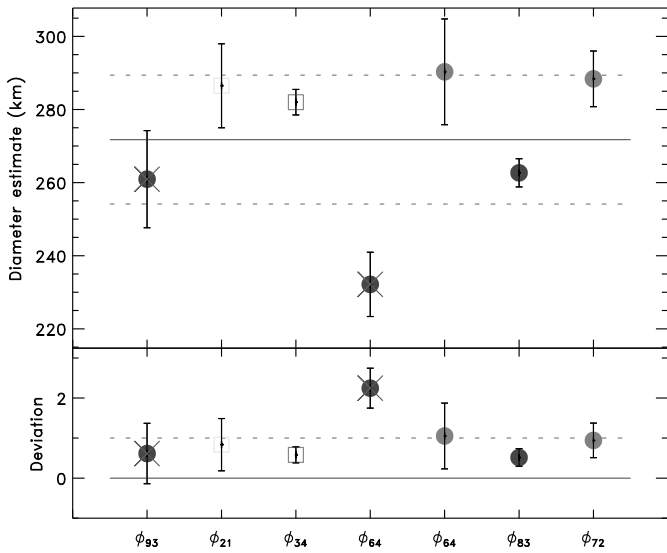


Figure B.68: Diameter estimates for (87) Sylvia.

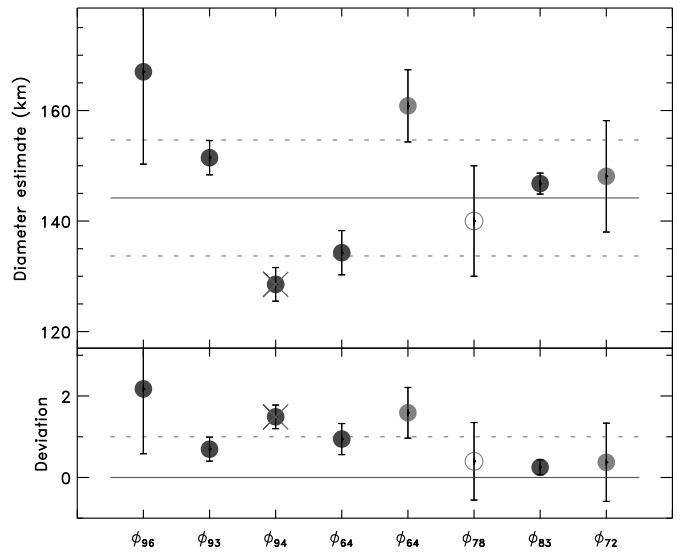


Figure B.70: Diameter estimates for (89) Julia.

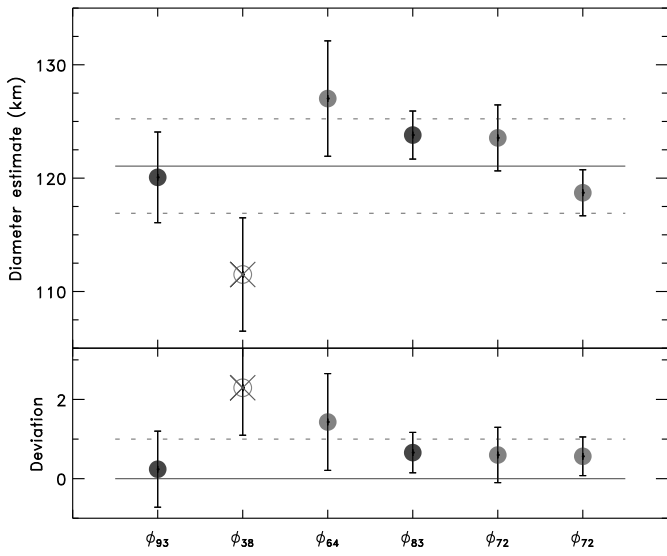


Figure B.71: Diameter estimates for (90) Antiope.

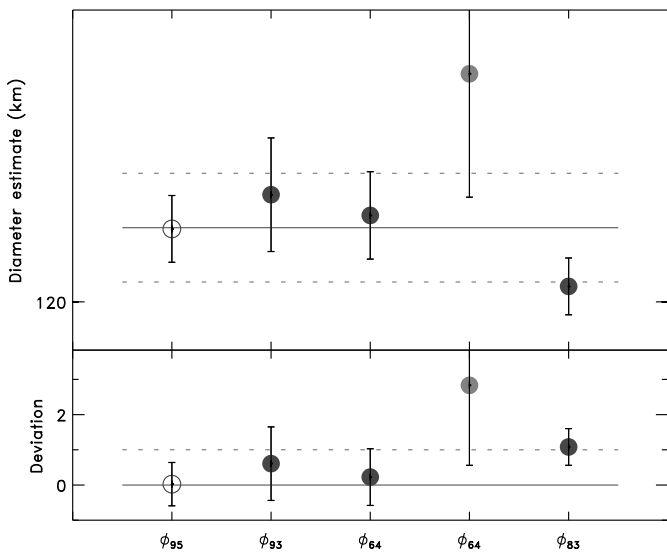


Figure B.72: Diameter estimates for (92) Undina.

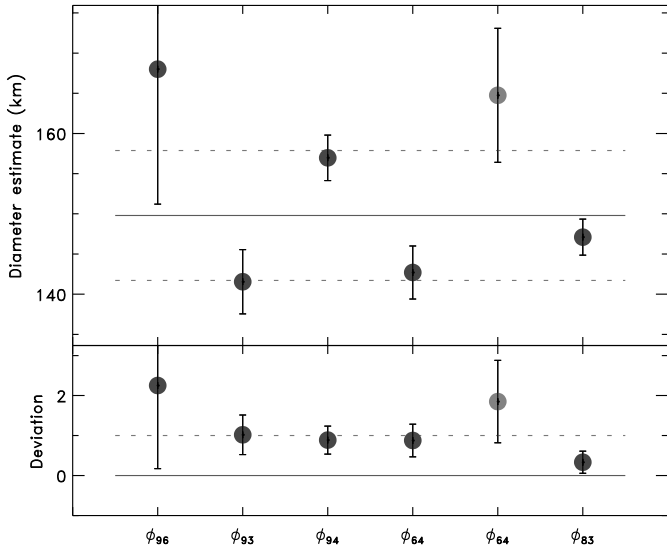


Figure B.73: Diameter estimates for (93) Minerva.

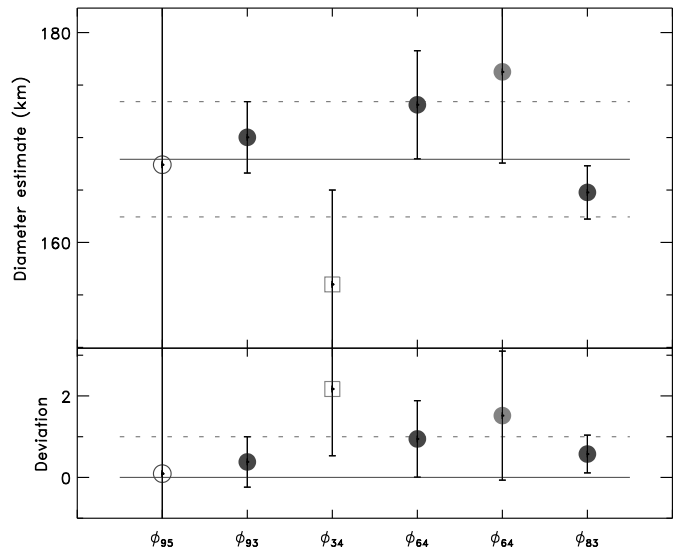


Figure B.75: Diameter estimates for (96) Aegle.

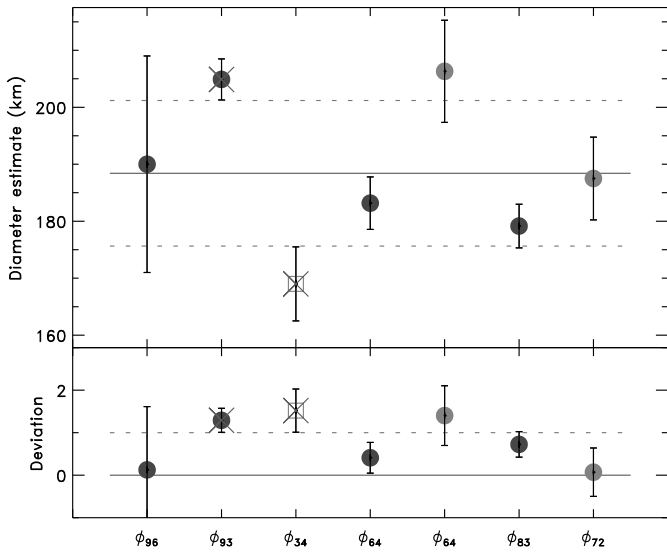


Figure B.74: Diameter estimates for (94) Aurora.

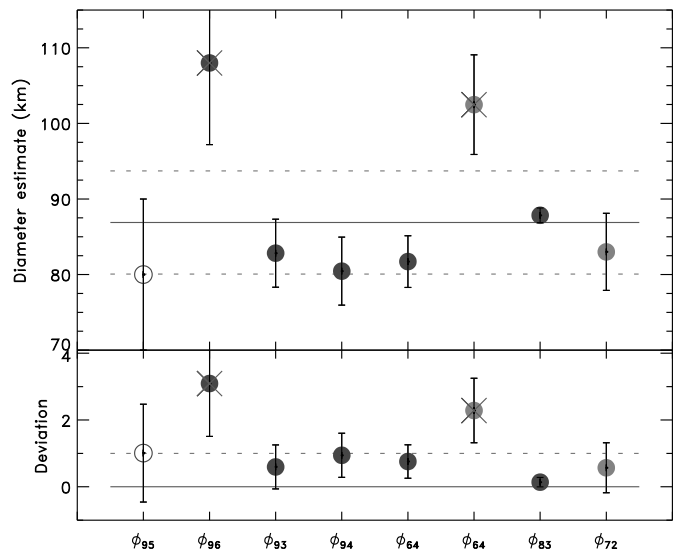


Figure B.76: Diameter estimates for (97) Klotho.

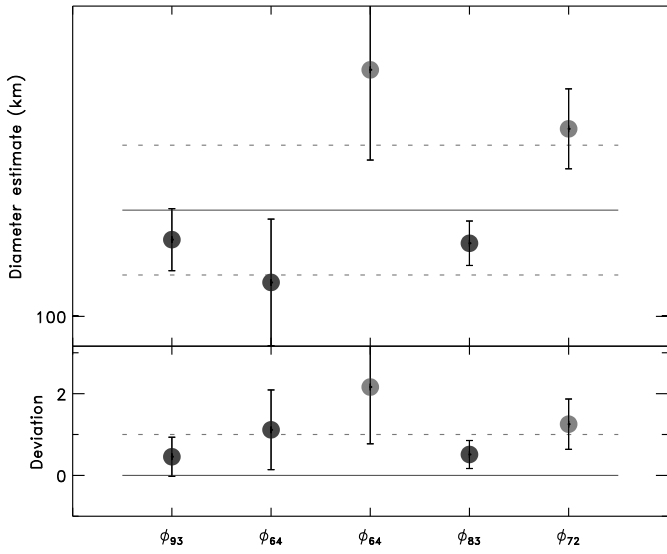


Figure B.77: Diameter estimates for (98) Ianthe.

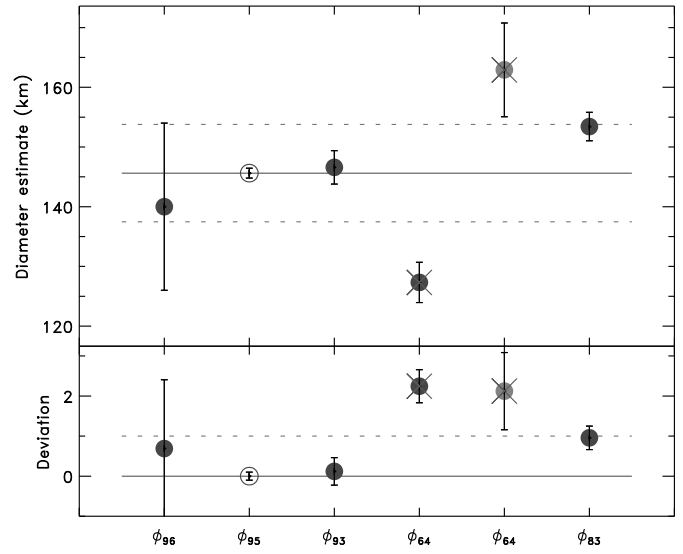


Figure B.79: Diameter estimates for (106) Dione.

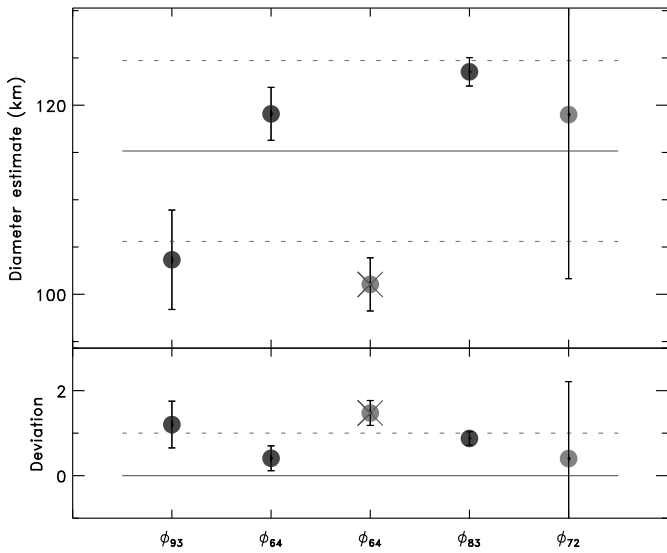


Figure B.78: Diameter estimates for (105) Artemis.

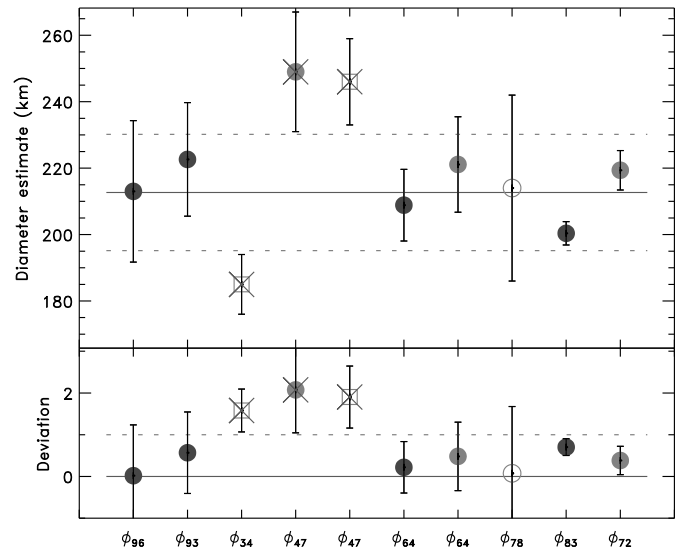


Figure B.80: Diameter estimates for (107) Camilla.

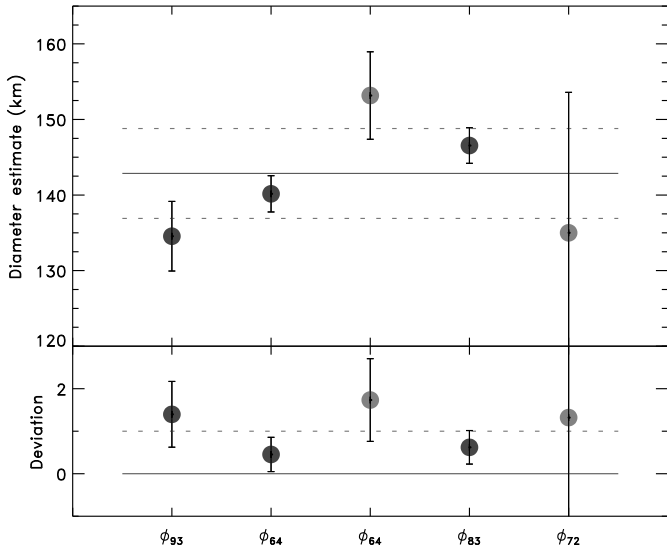


Figure B.81: Diameter estimates for (111) Ate.

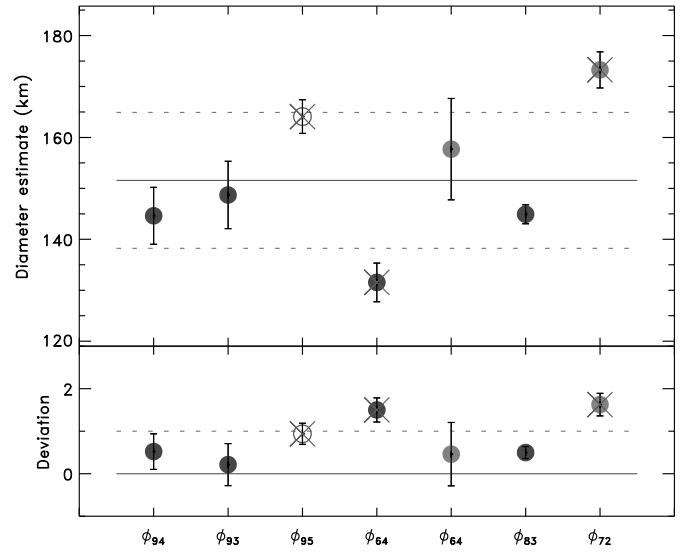


Figure B.83: Diameter estimates for (117) Lomia.

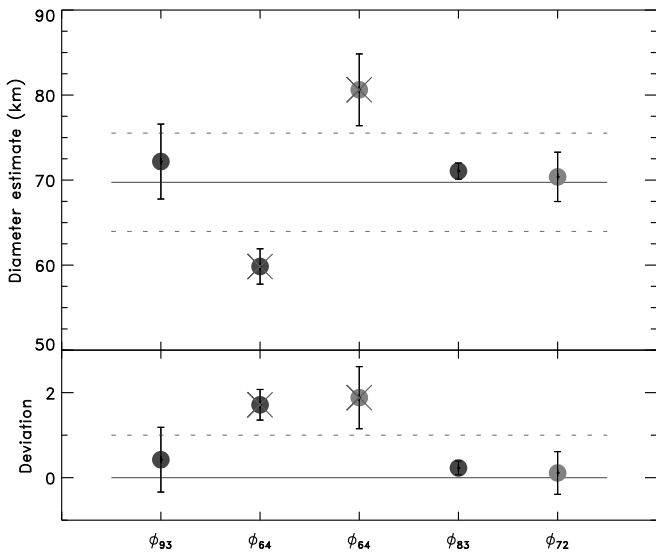


Figure B.82: Diameter estimates for (112) Iphigenia.

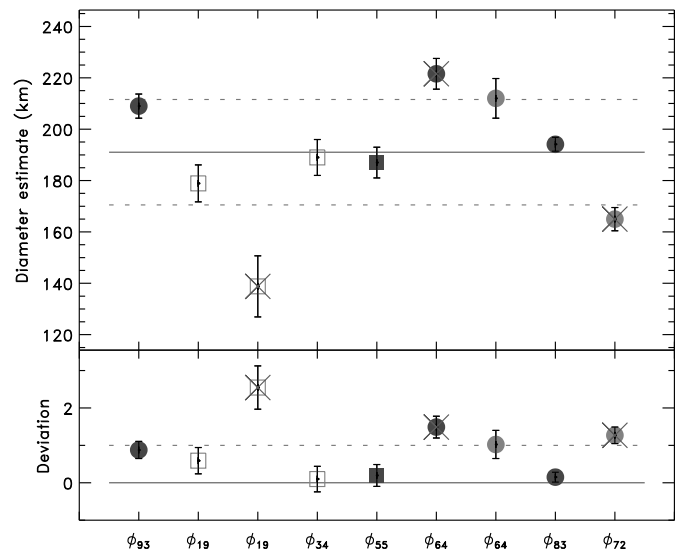


Figure B.84: Diameter estimates for (121) Hermione.

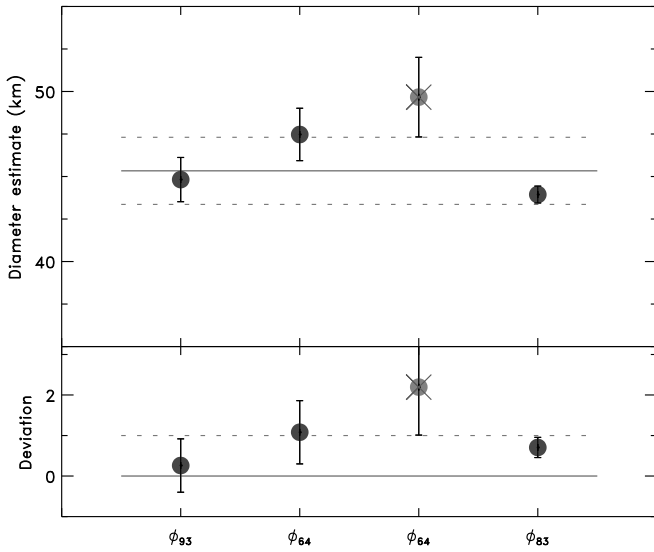


Figure B.85: Diameter estimates for (126) Velleda.

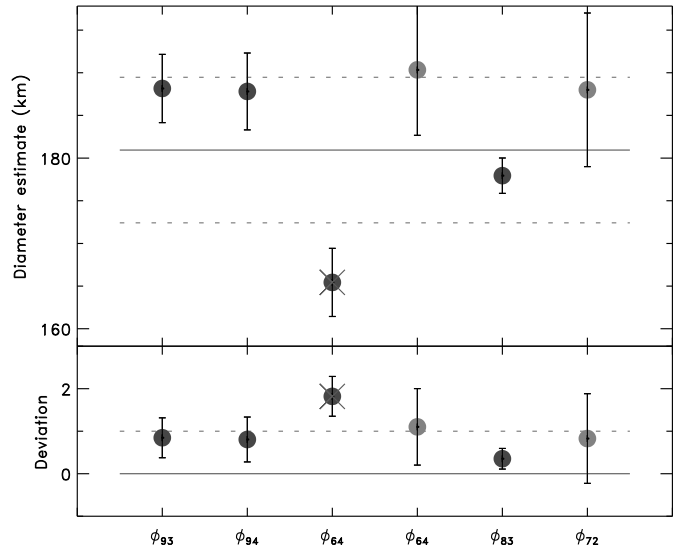


Figure B.87: Diameter estimates for (128) Nemesis.

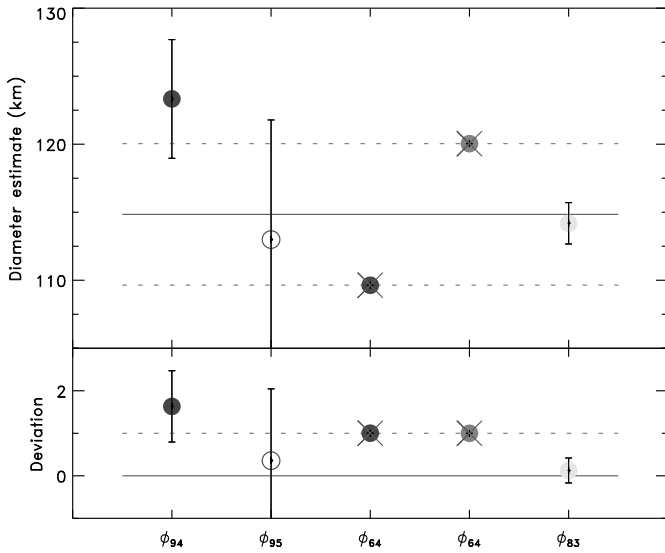


Figure B.86: Diameter estimates for (127) Johanna. The diameter estimates from ϕ_{64} have unrealistic small uncertainties of 0.02 km. Using these values strongly biases the average.

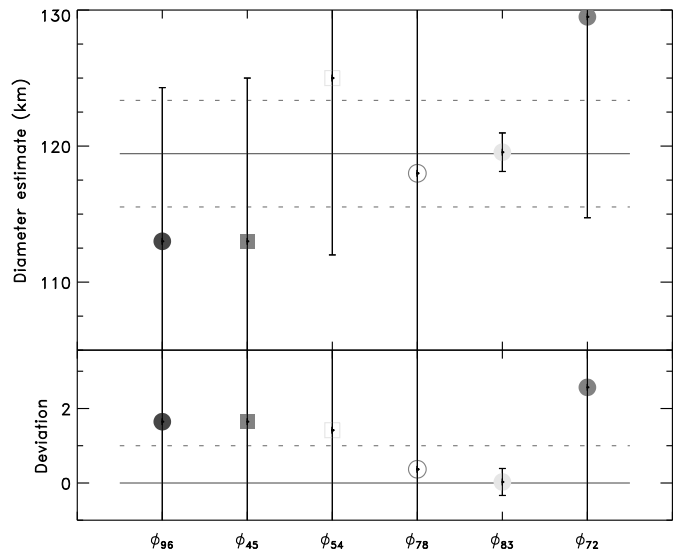


Figure B.88: Diameter estimates for (129) Antigone.

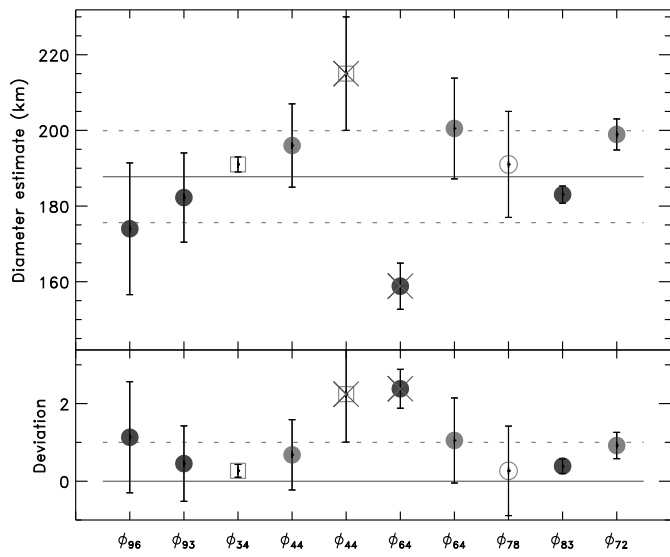


Figure B.89: Diameter estimates for (130) Elektra.

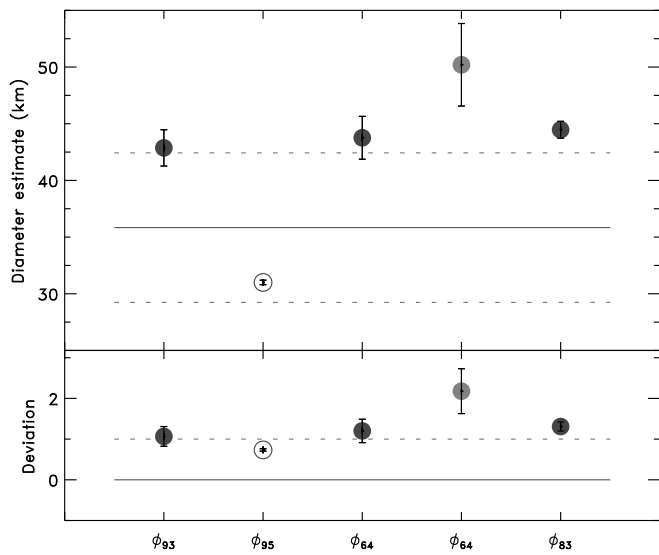


Figure B.90: Diameter estimates for (132) Aethra. The large uncertainty on the mass determination forbid to sort between the diameter estimates.

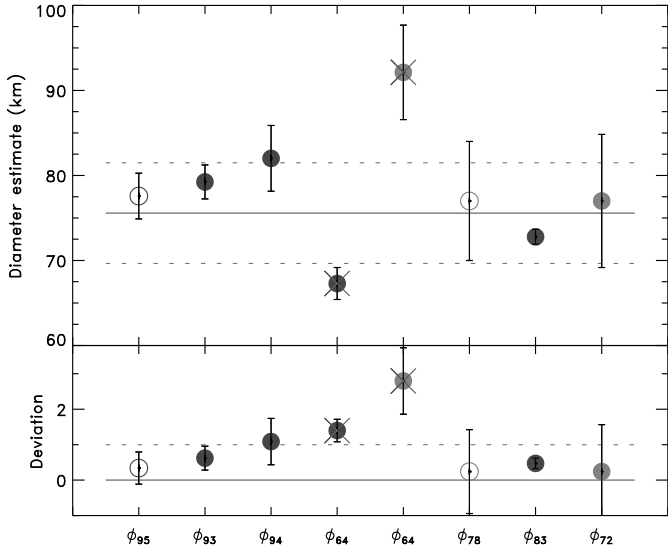


Figure B.91: Diameter estimates for (135) Hertha.

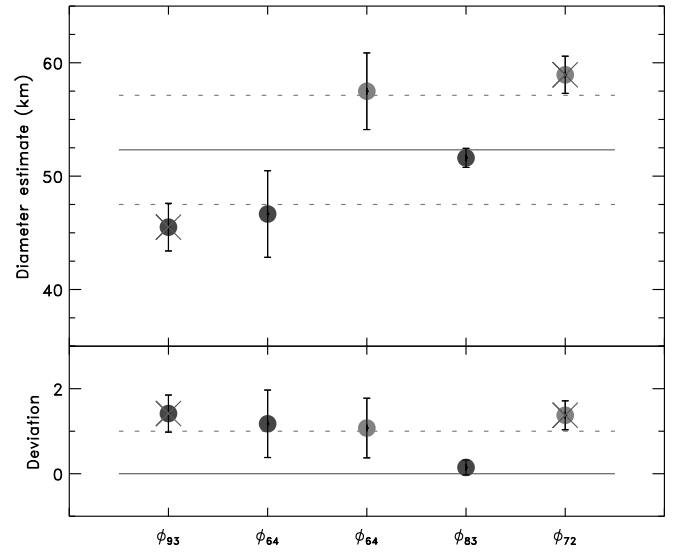


Figure B.93: Diameter estimates for (138) Tolosa.

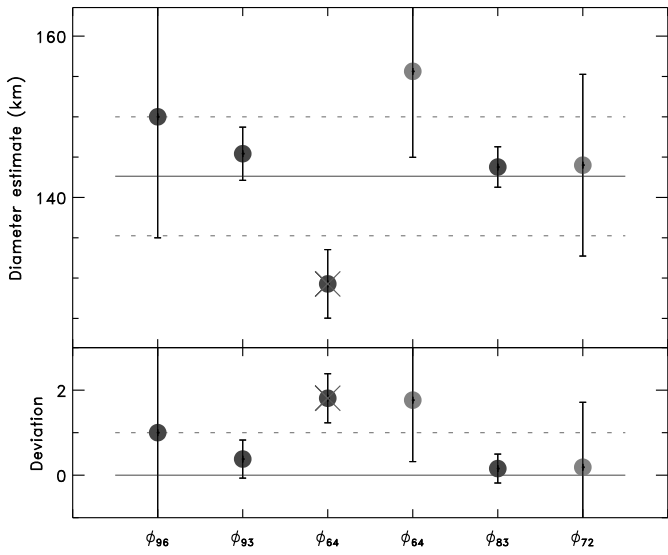


Figure B.92: Diameter estimates for (137) Meliboea.

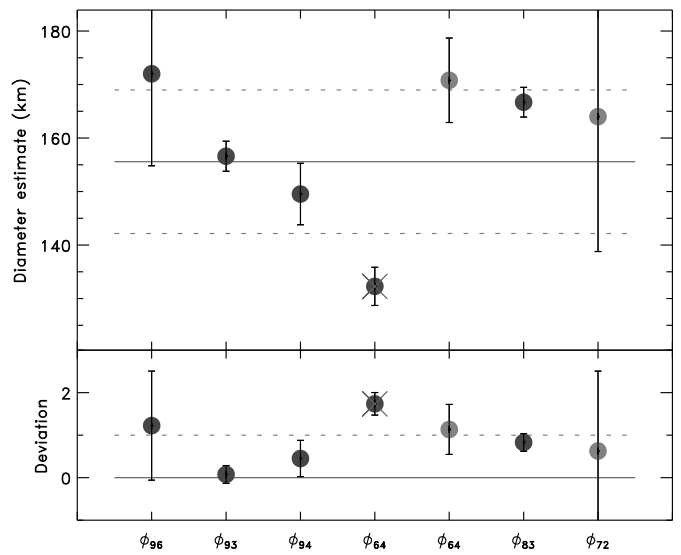


Figure B.94: Diameter estimates for (139) Juewa.

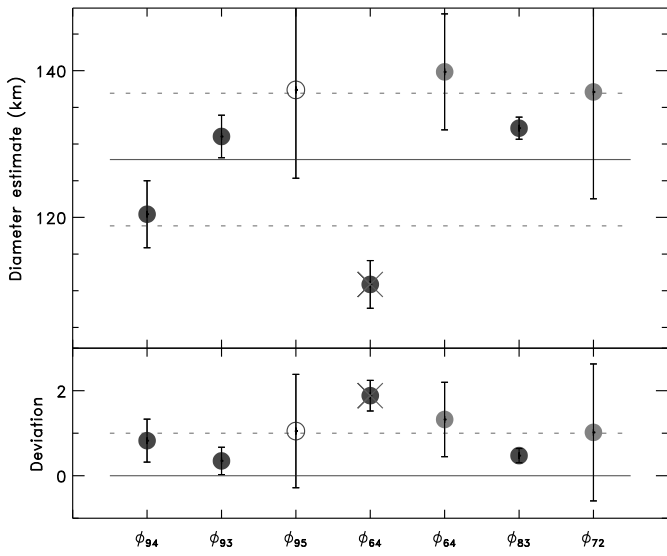


Figure B.95: Diameter estimates for (141) Lumen.

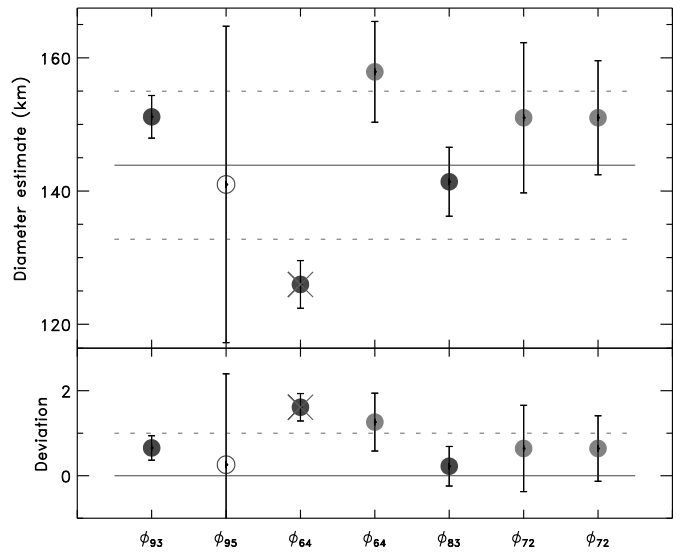


Figure B.97: Diameter estimates for (145) Adeona.

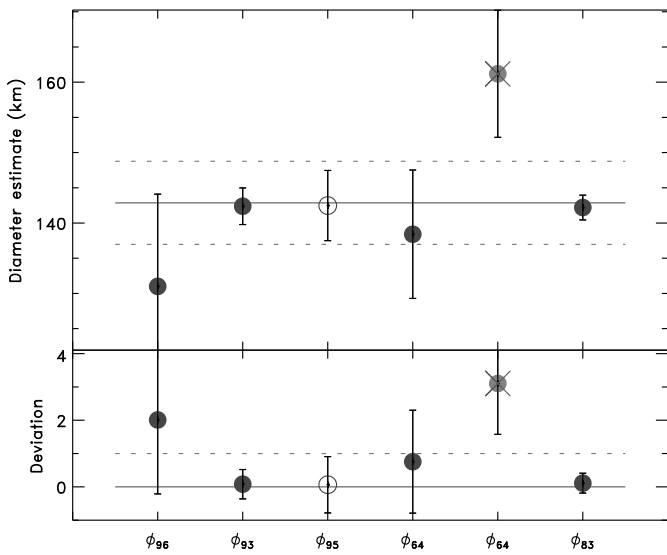


Figure B.96: Diameter estimates for (144) Vibia.

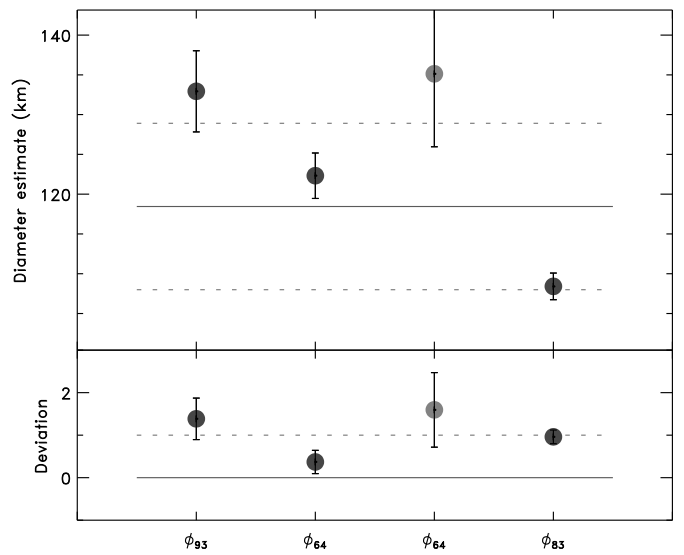


Figure B.98: Diameter estimates for (147) Protogeneia.

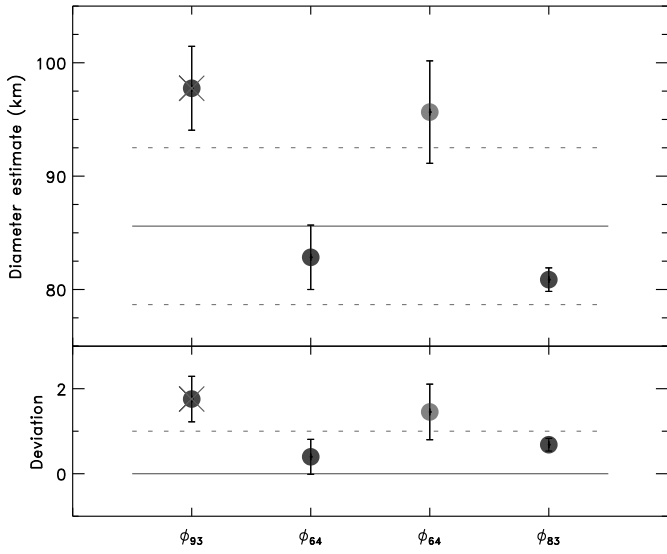


Figure B.99: Diameter estimates for (148) Gallia.

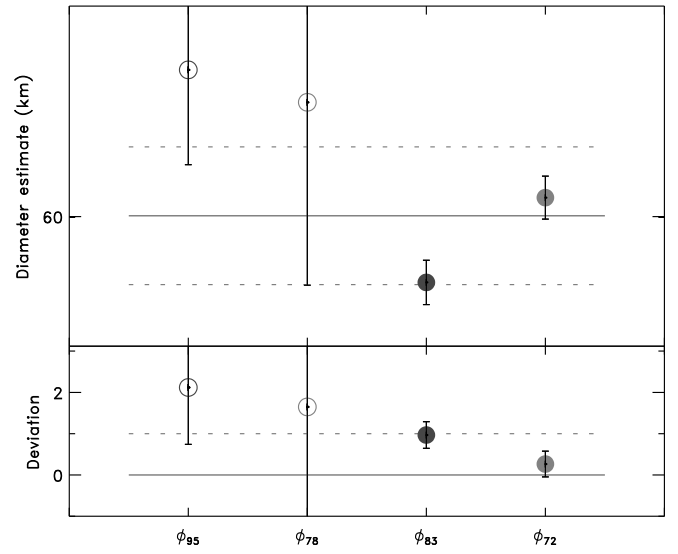


Figure B.101: Diameter estimates for (152) Atala.

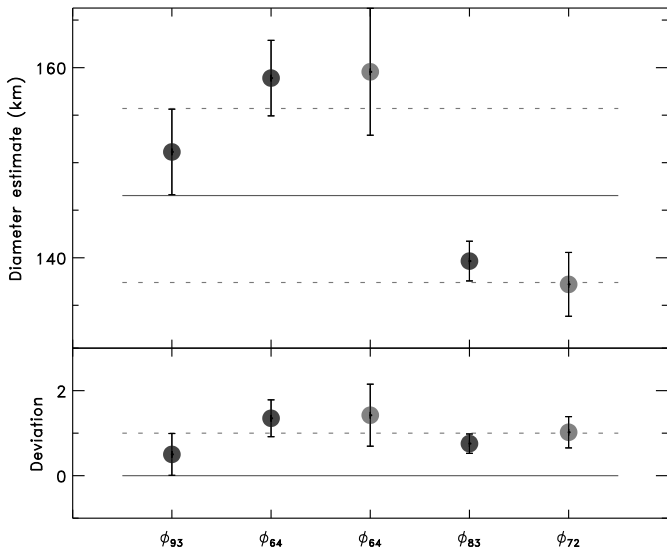


Figure B.100: Diameter estimates for (150) Nuwa.

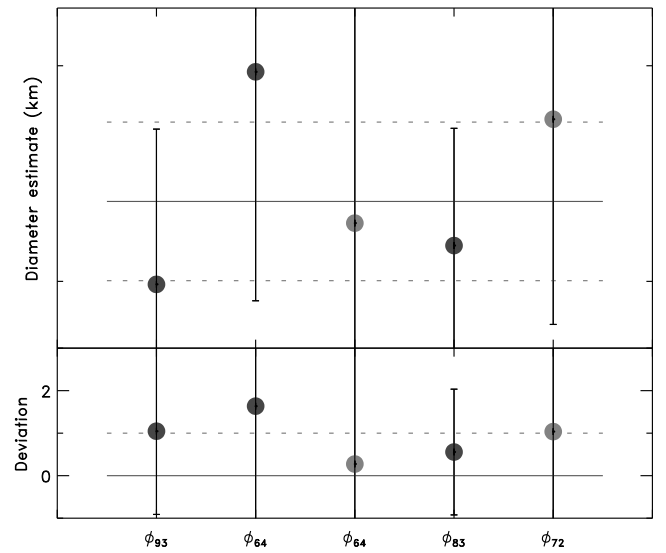


Figure B.102: Diameter estimates for (154) Bertha.

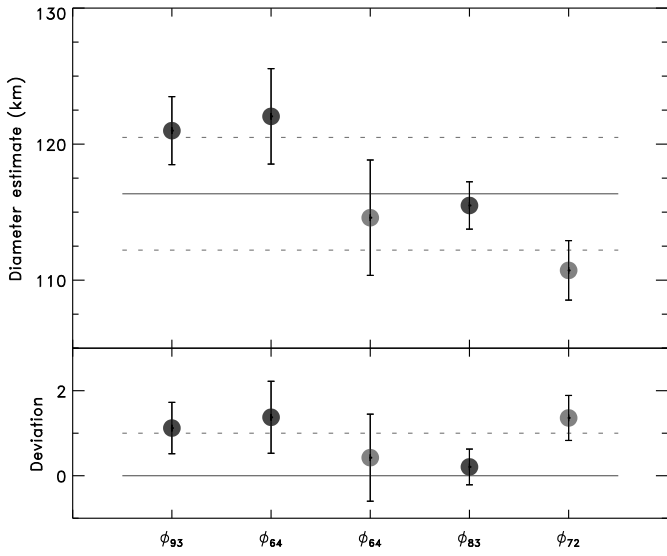


Figure B.103: Diameter estimates for (156) Xanthippe.

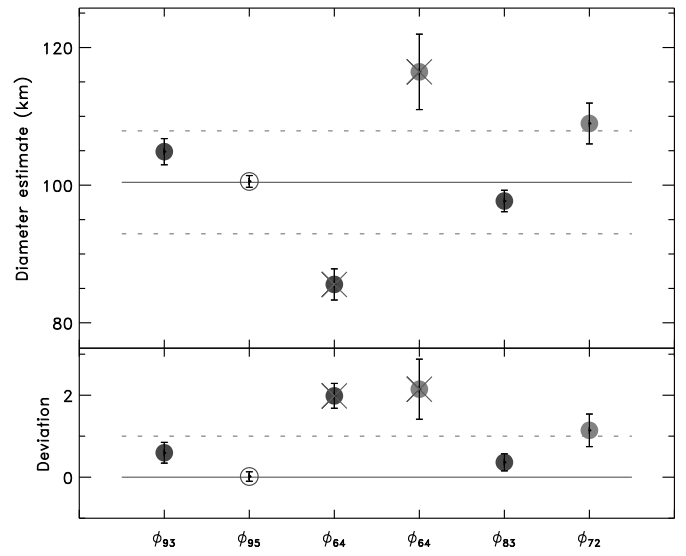


Figure B.105: Diameter estimates for (164) Eva.

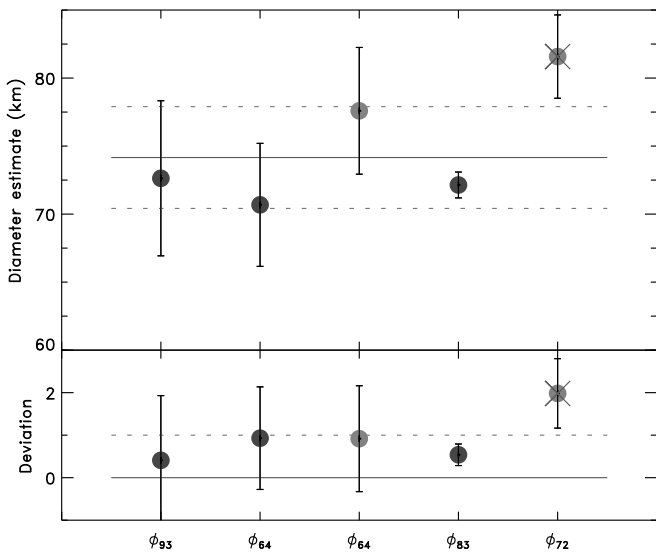


Figure B.104: Diameter estimates for (163) Erigone.

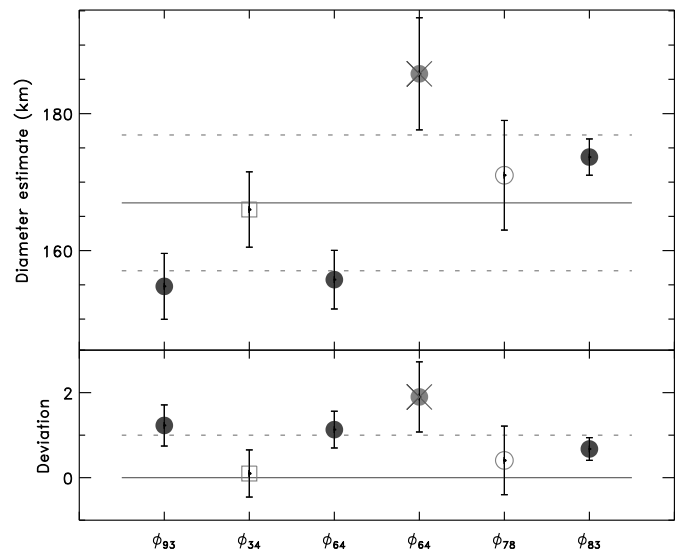


Figure B.106: Diameter estimates for (165) Loreley.

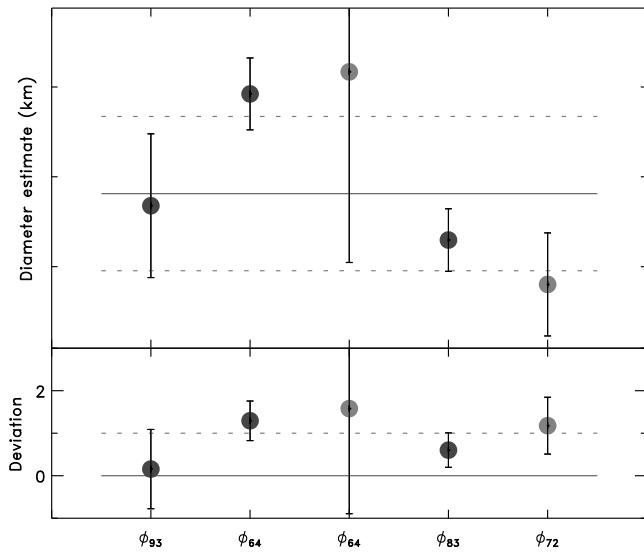


Figure B.107: Diameter estimates for (168) Sibylla.

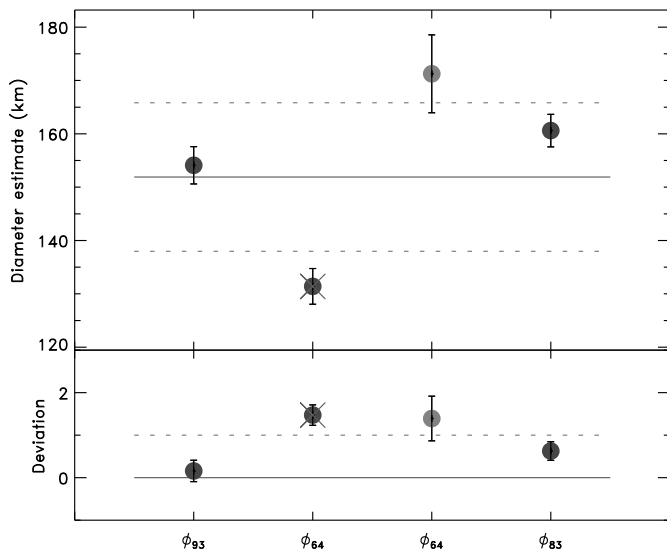


Figure B.108: Diameter estimates for (173) Ino.

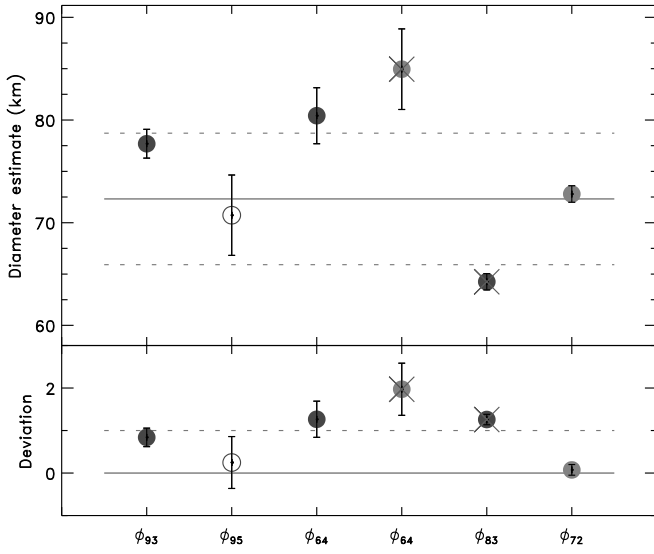


Figure B.109: Diameter estimates for (179) Klytaemnestra.

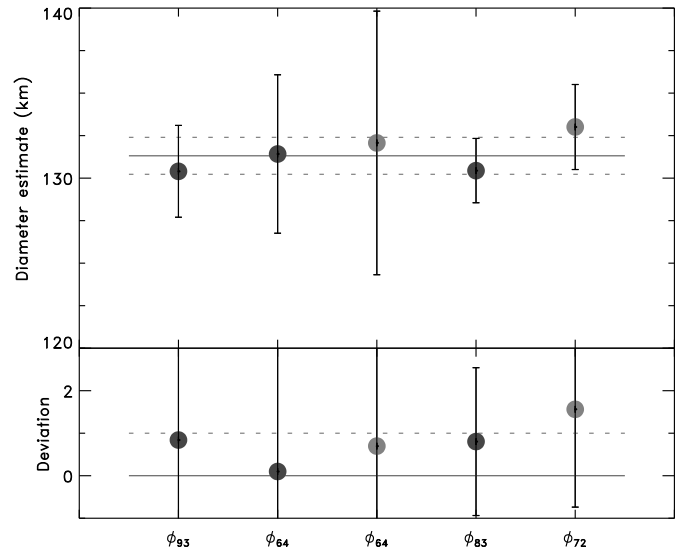


Figure B.111: Diameter estimates for (187) Lamberta.

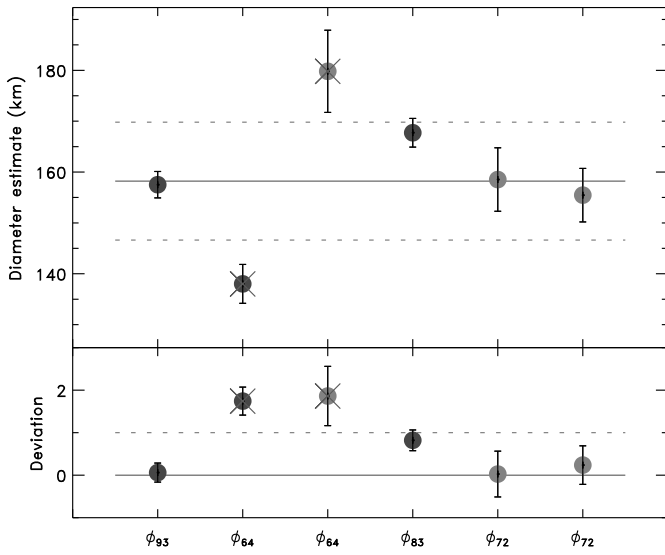


Figure B.110: Diameter estimates for (185) Eunike.

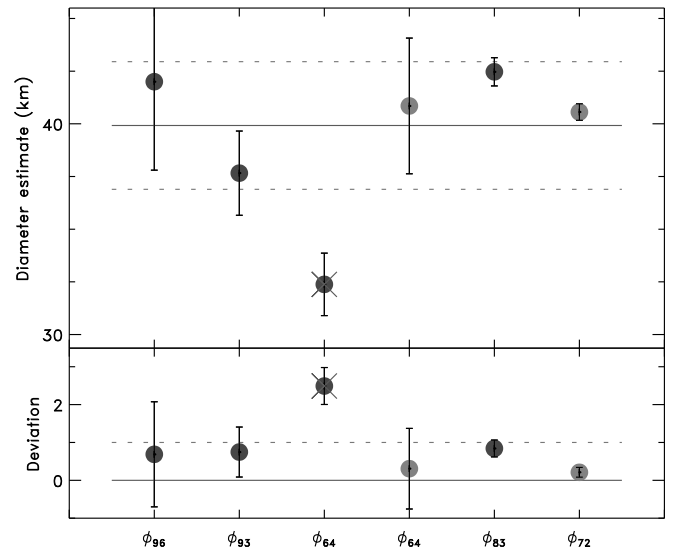


Figure B.112: Diameter estimates for (189) Phthia.

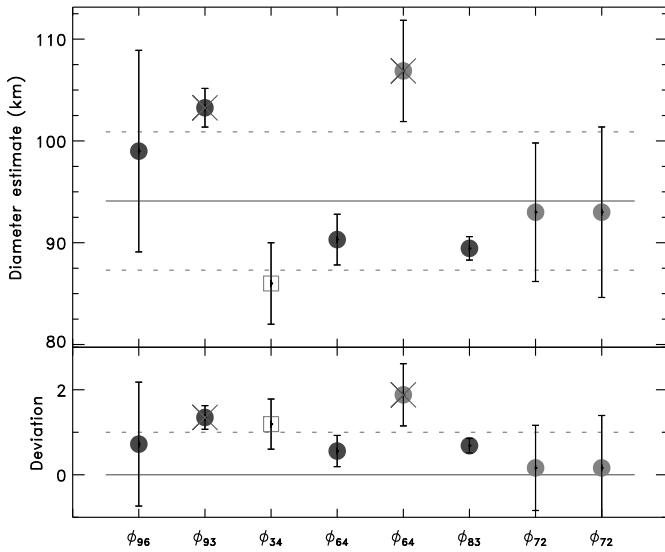


Figure B.113: Diameter estimates for (192) Nausikaa.

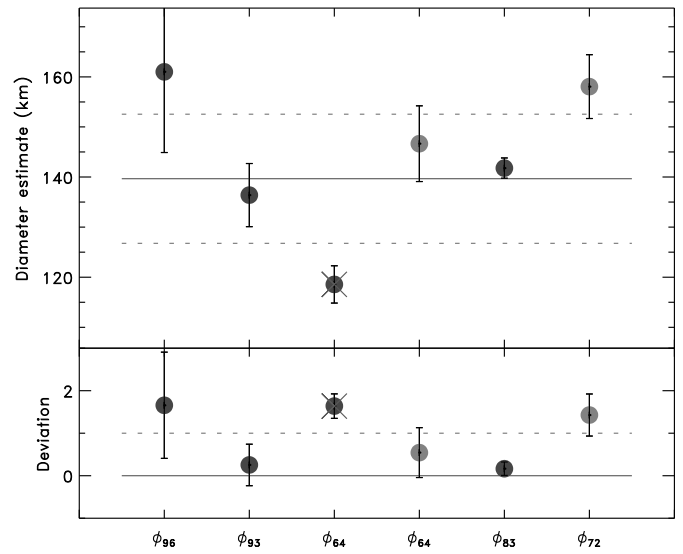


Figure B.115: Diameter estimates for (196) Philomela.

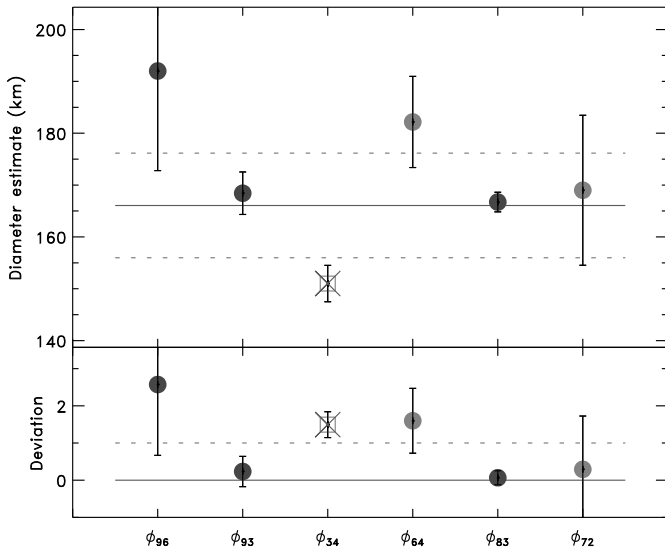


Figure B.114: Diameter estimates for (194) Prokne. The diameter estimated by ϕ_{34}^\dagger falls outside the range drawn by the weighted average. It is, however, the unique direct measurement of Prokne's diameter (although limited to a single geometry).

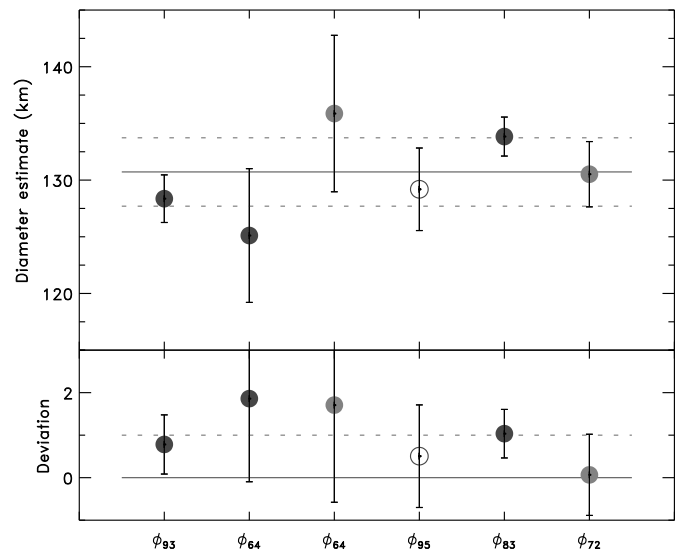


Figure B.116: Diameter estimates for (200) Dynamene.

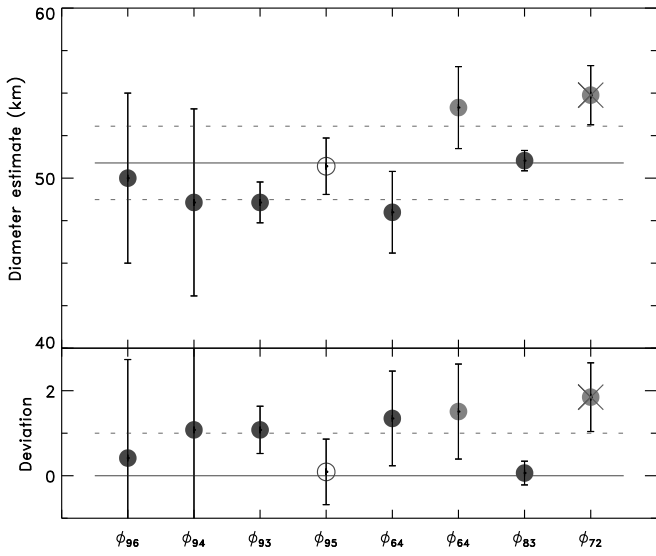


Figure B.117: Diameter estimates for (204) Kallisto.

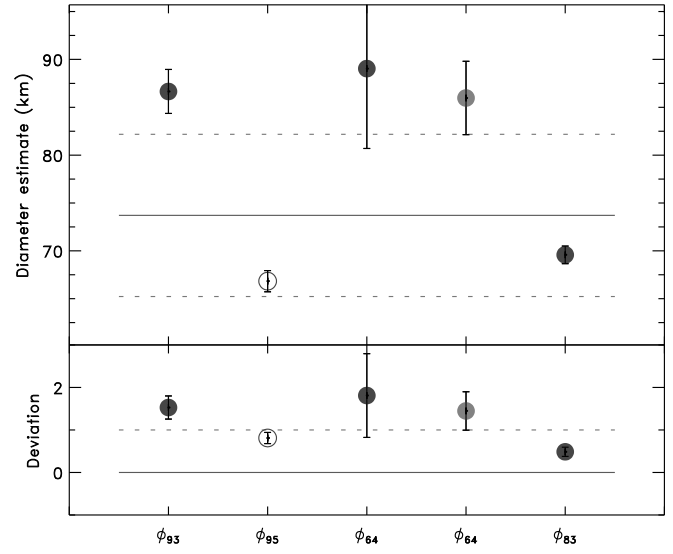


Figure B.119: Diameter estimates for (210) Isabella. The large uncertainty on the mass determination forbid to sort between the diameter estimates. However, diameter estimates are all independantly based on single-geometry (e.g., ϕ_{93} and ϕ_{64} with IRAS, ϕ_{95} by occultation) and their differences most likely result from these different geometries, not properly taken into account.

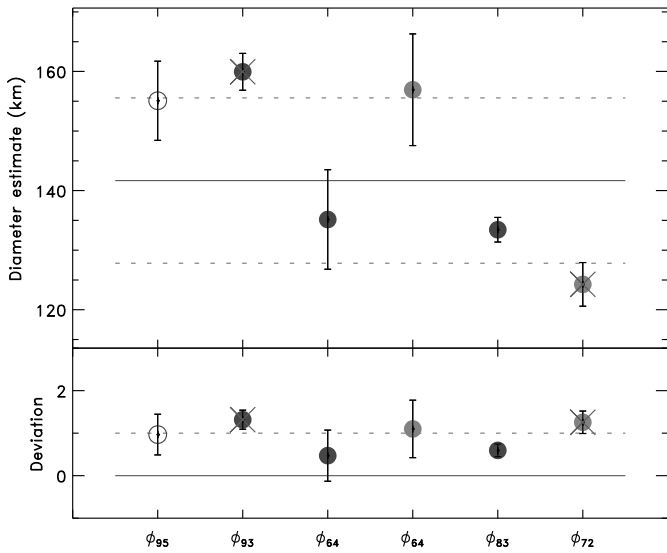


Figure B.118: Diameter estimates for (209) Dido.

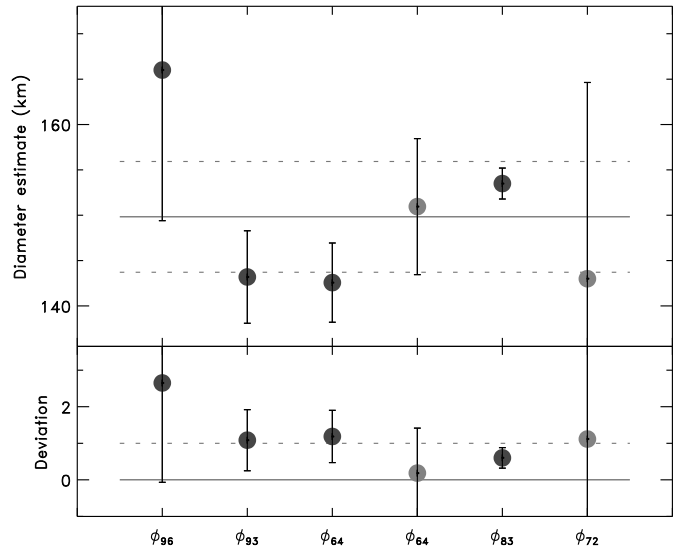


Figure B.120: Diameter estimates for (211) Isolda.

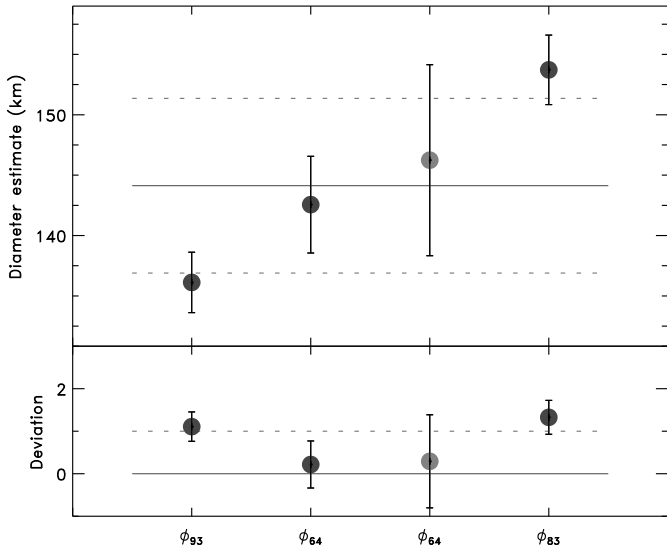


Figure B.121: Diameter estimates for (212) Medea.

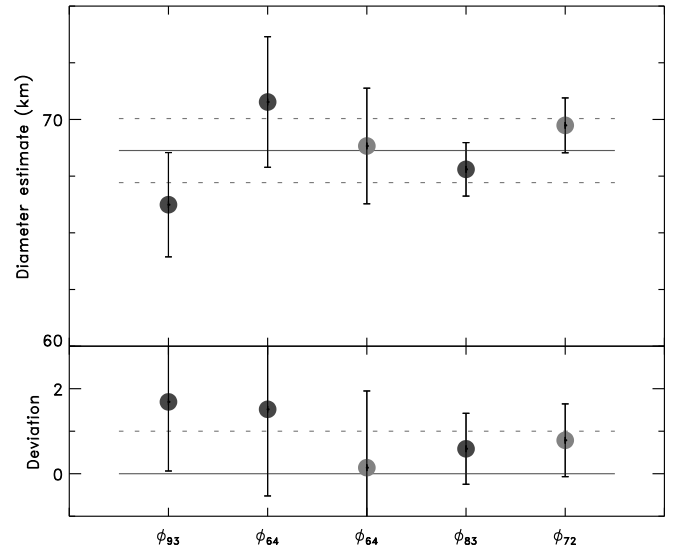


Figure B.123: Diameter estimates for (217) Eudora.

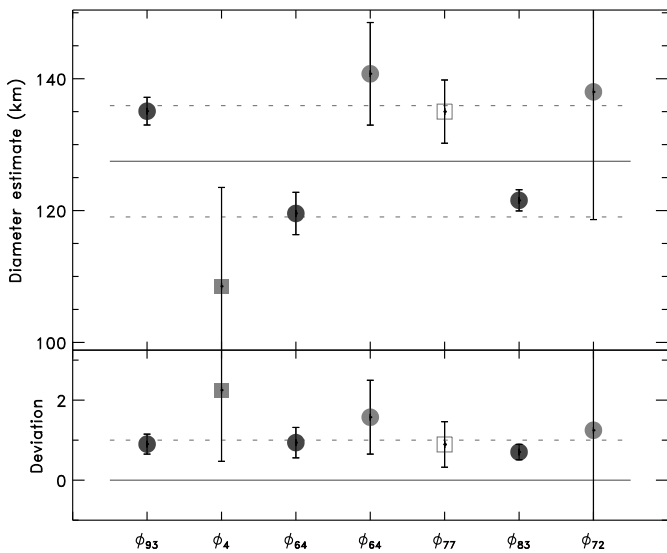


Figure B.122: Diameter estimates for (216) Kleopatra.

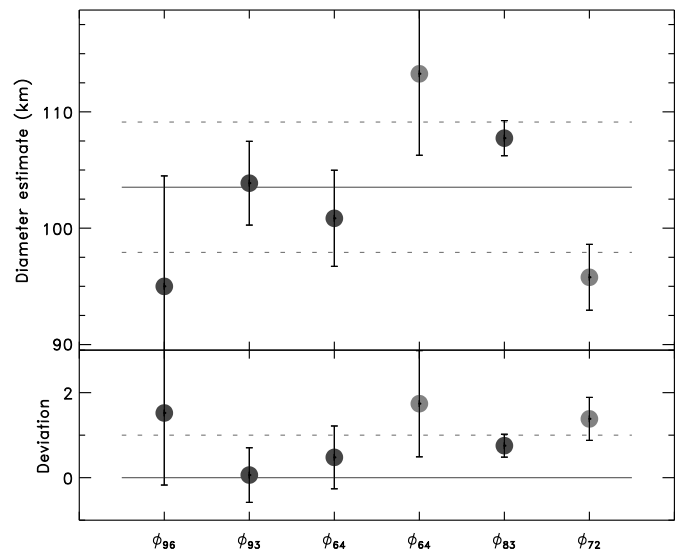


Figure B.124: Diameter estimates for (221) Eos.

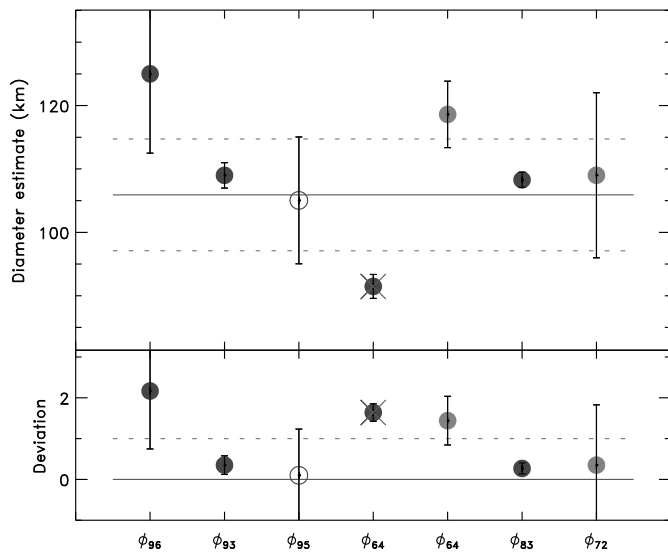


Figure B.125: Diameter estimates for (230) Athamantis.

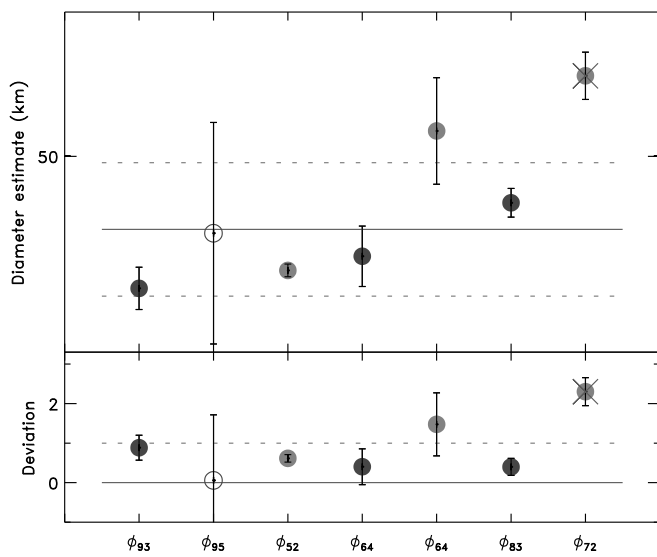


Figure B.126: Diameter estimates for (234) Barbara.

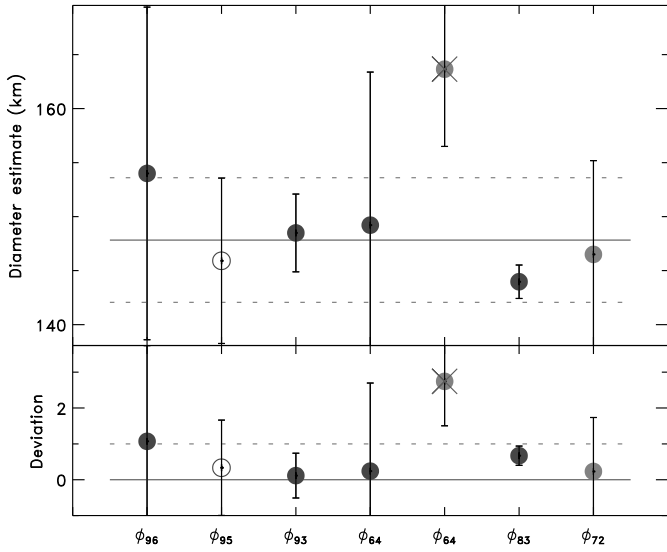


Figure B.127: Diameter estimates for (238) Hypatia.

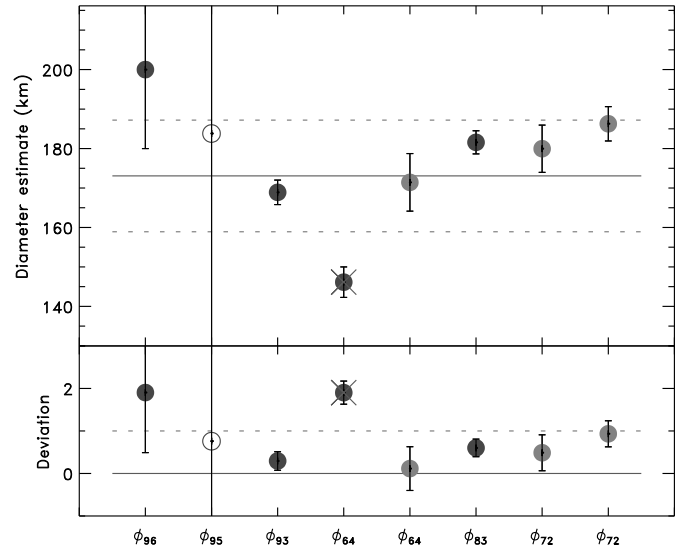


Figure B.129: Diameter estimates for (241) Germania.

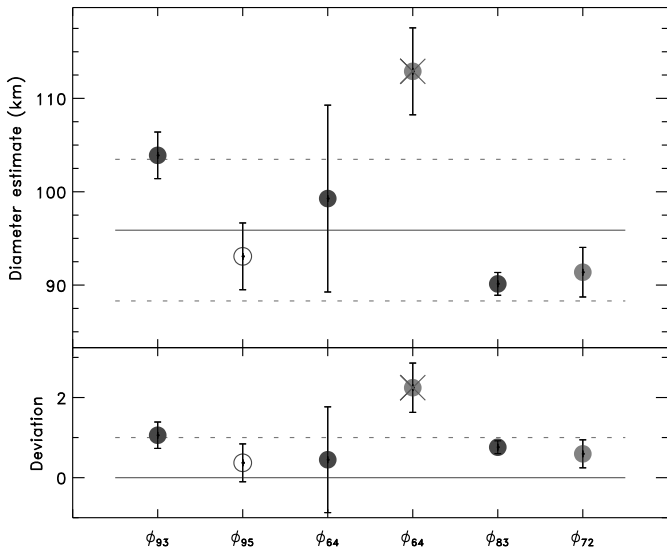


Figure B.128: Diameter estimates for (240) Vanadis.

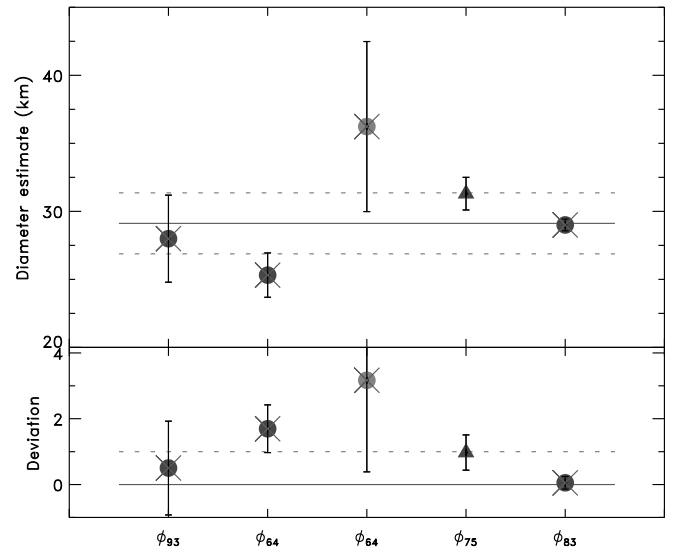


Figure B.130: Diameter estimates for (243) Ida. Only the flyby estimate from ϕ_{75} is used here.

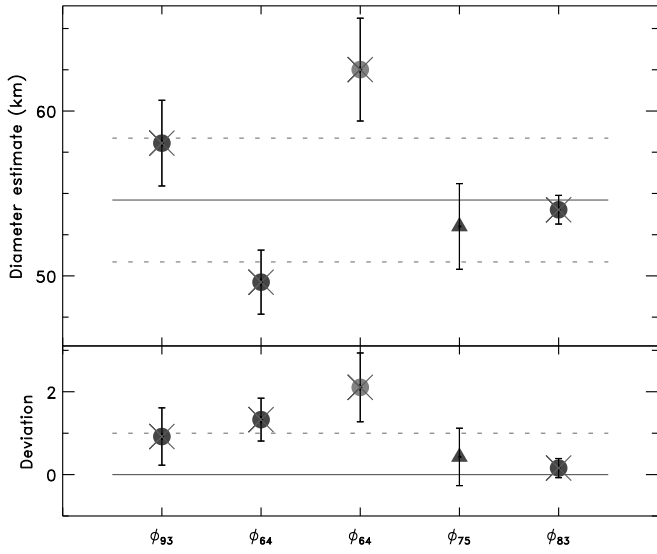


Figure B.131: Diameter estimates for (253) Mathilde. Only the flyby estimate from ϕ_{75} is used here.

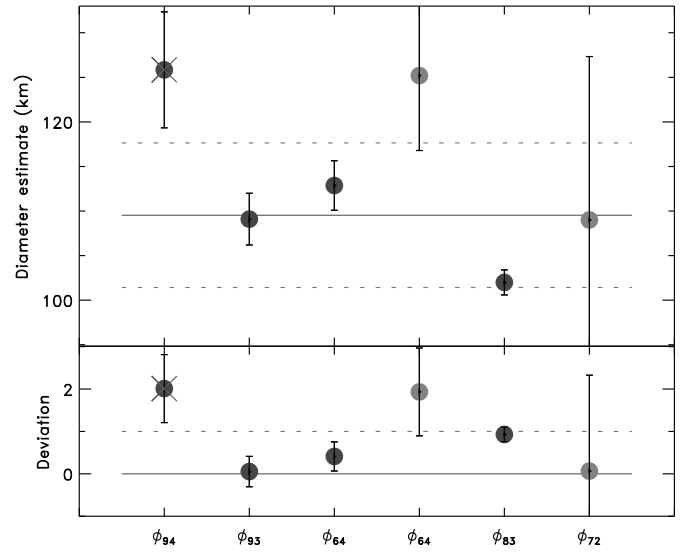


Figure B.133: Diameter estimates for (266) Aline.

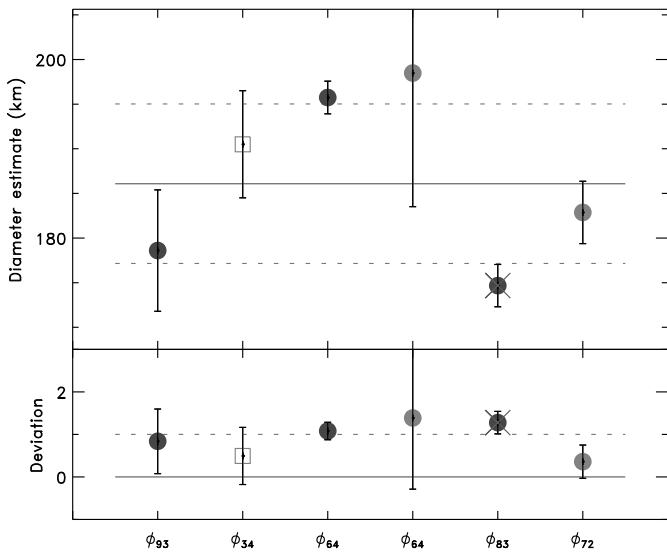


Figure B.132: Diameter estimates for (259) Aletheia.

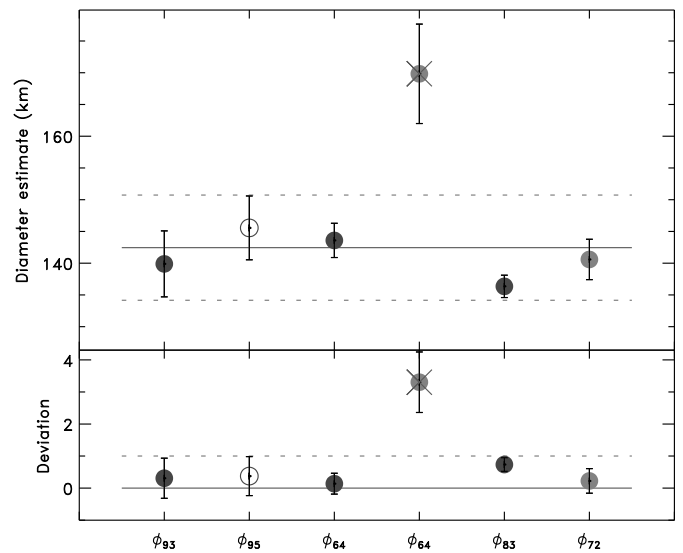


Figure B.134: Diameter estimates for (268) Adorea.

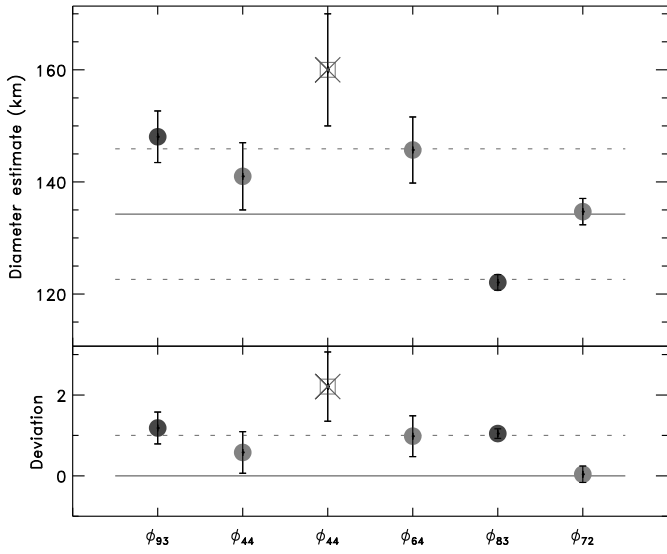


Figure B.135: Diameter estimates for (283) Emma.

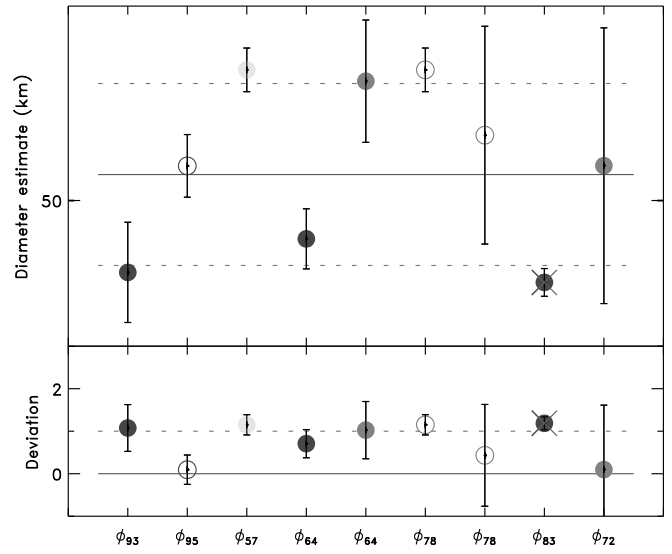


Figure B.137: Diameter estimates for (306) Unitas.

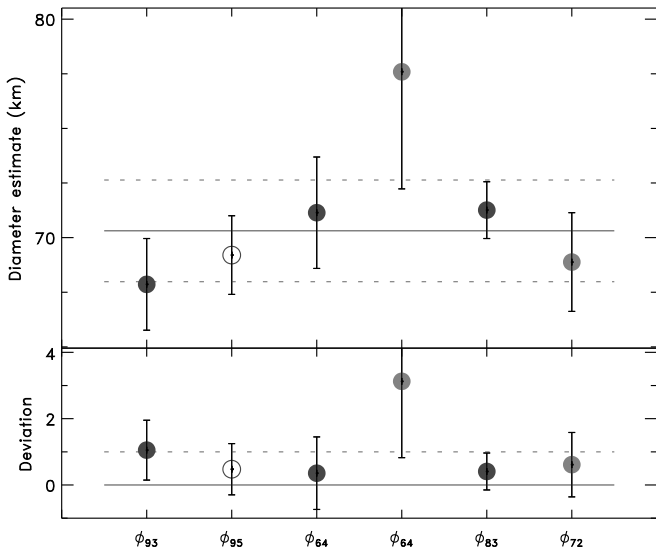


Figure B.136: Diameter estimates for (304) Olga.

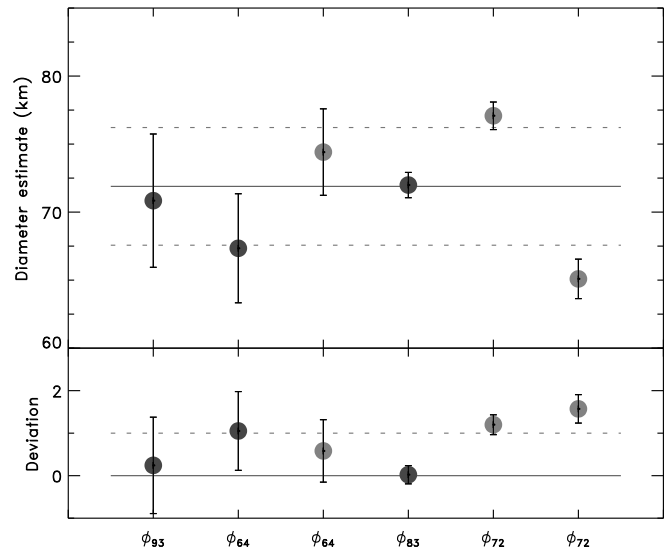


Figure B.138: Diameter estimates for (322) Phaeo.

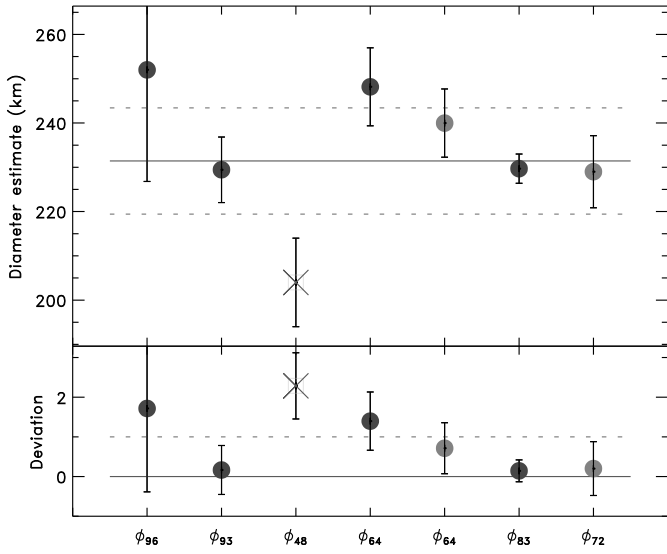


Figure B.139: Diameter estimates for (324) Bamberga.

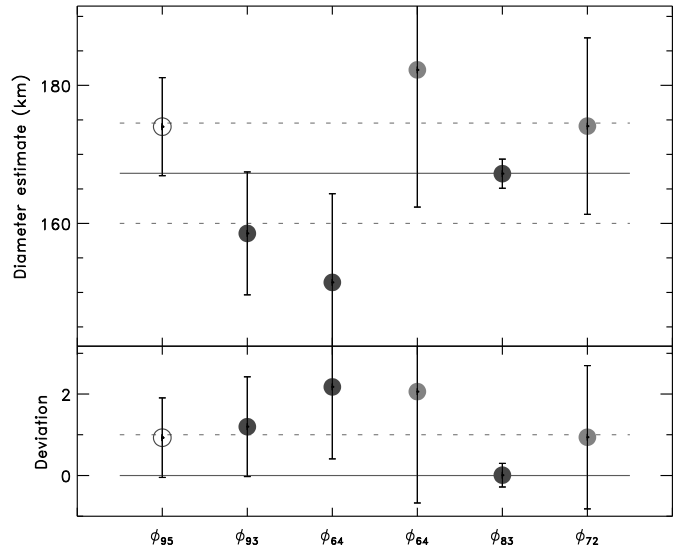


Figure B.141: Diameter estimates for (334) Chicago.

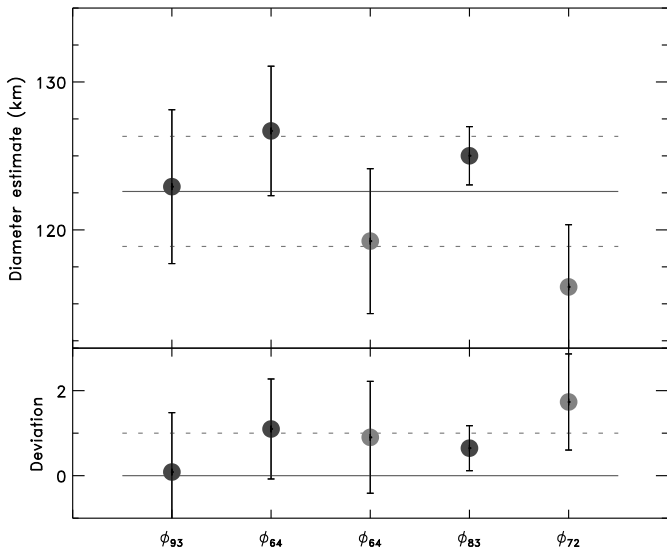


Figure B.140: Diameter estimates for (328) Gudrun.

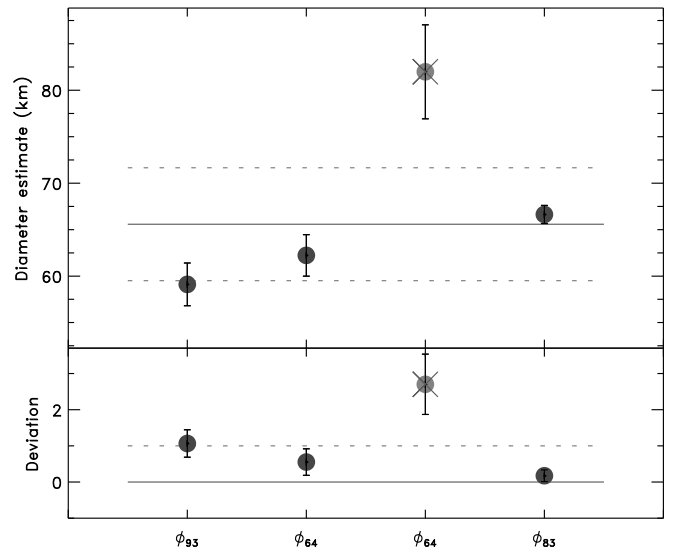


Figure B.142: Diameter estimates for (337) Devosa.

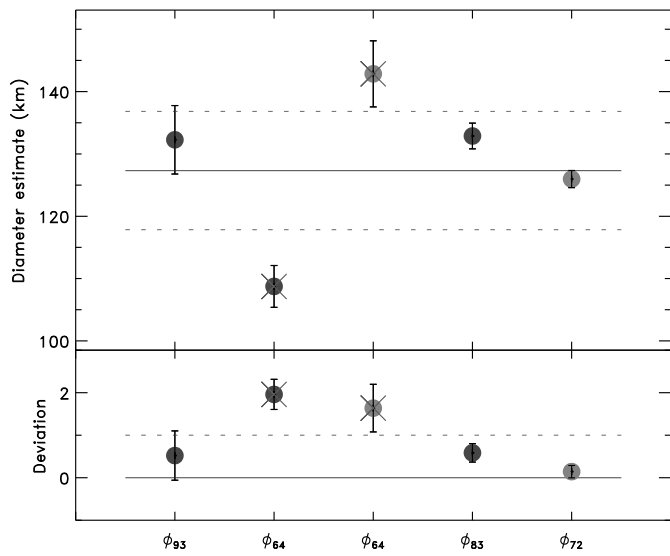


Figure B.143: Diameter estimates for (344) Desiderata.

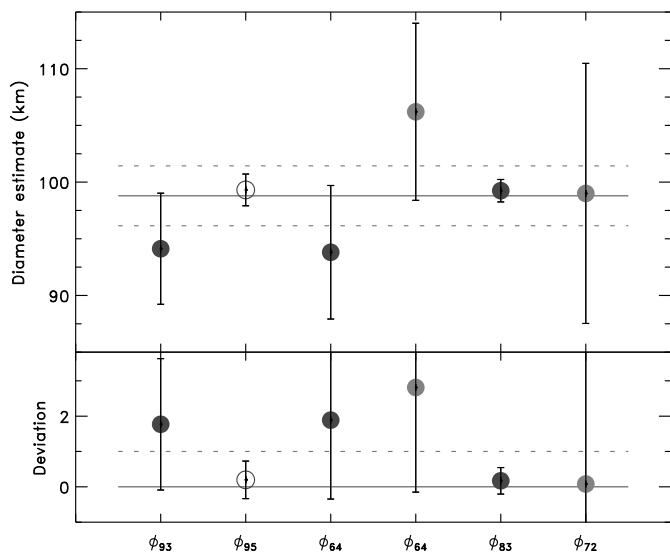


Figure B.144: Diameter estimates for (345) Tercidina.

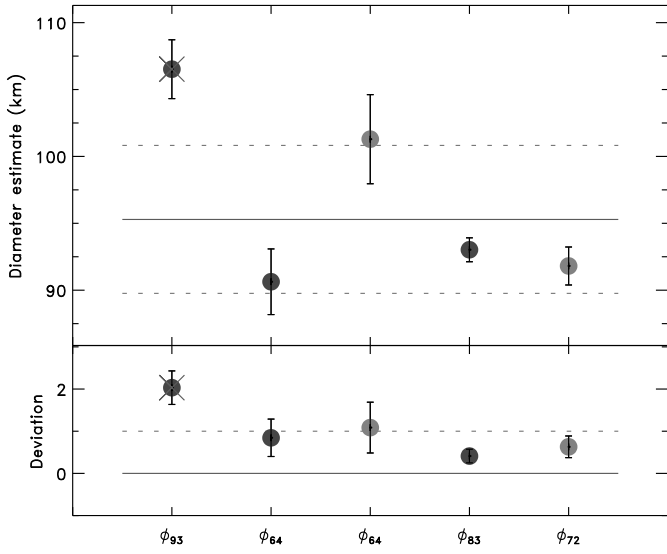


Figure B.145: Diameter estimates for (346) Hermentaria.

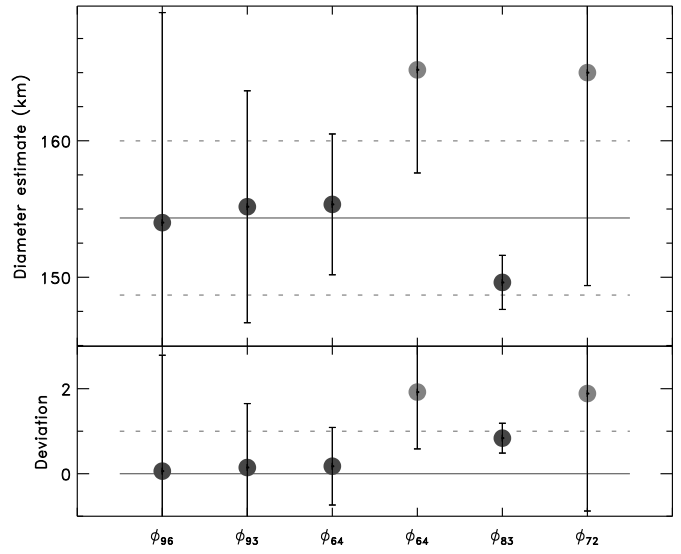


Figure B.147: Diameter estimates for (354) Eleonora.

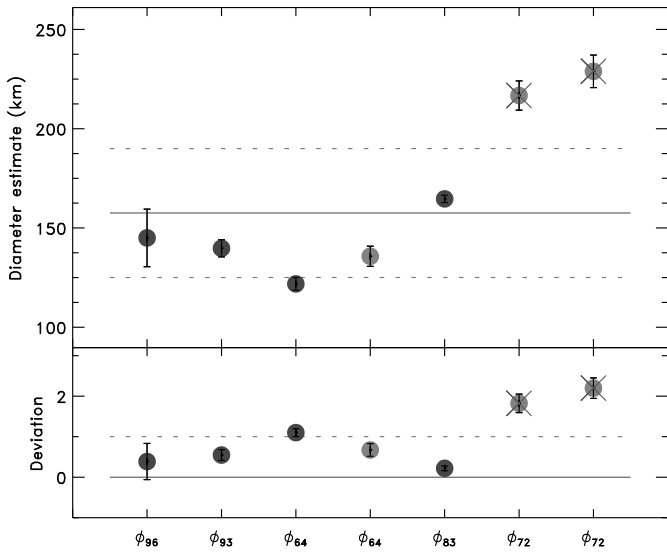


Figure B.146: Diameter estimates for (349) Dembowska.

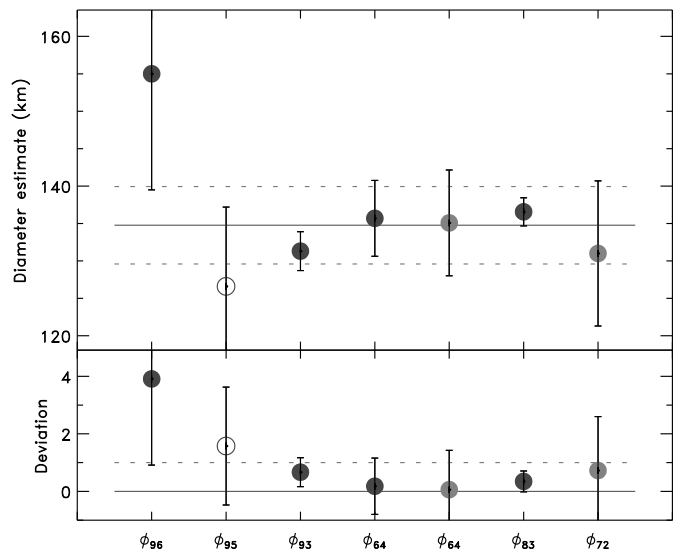


Figure B.148: Diameter estimates for (356) Liguria.

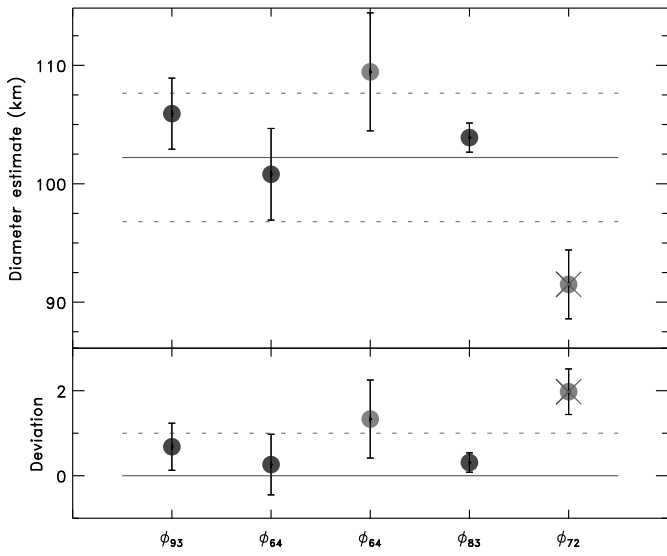


Figure B.149: Diameter estimates for (365) Corduba.

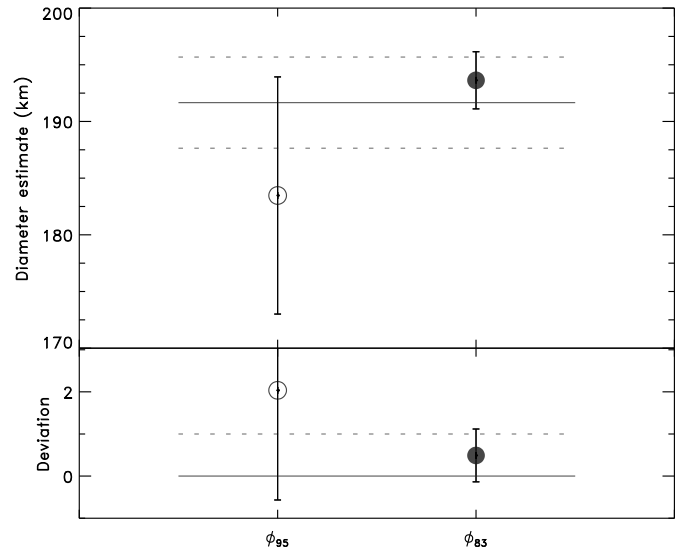


Figure B.151: Diameter estimates for (375) Ursula.

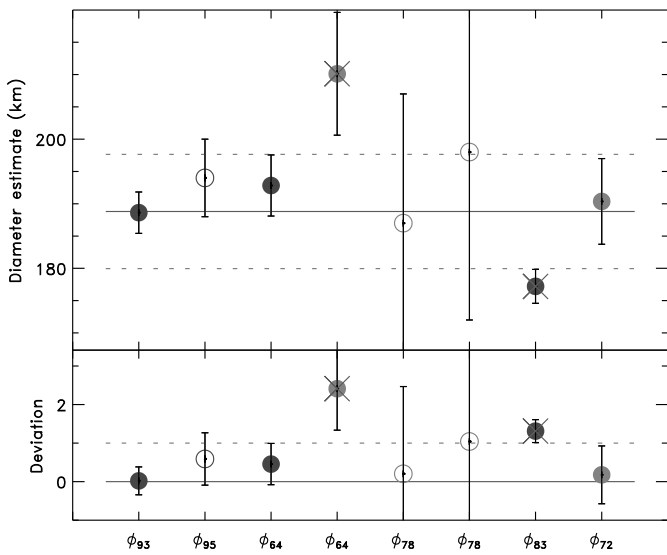


Figure B.150: Diameter estimates for (372) Palma.

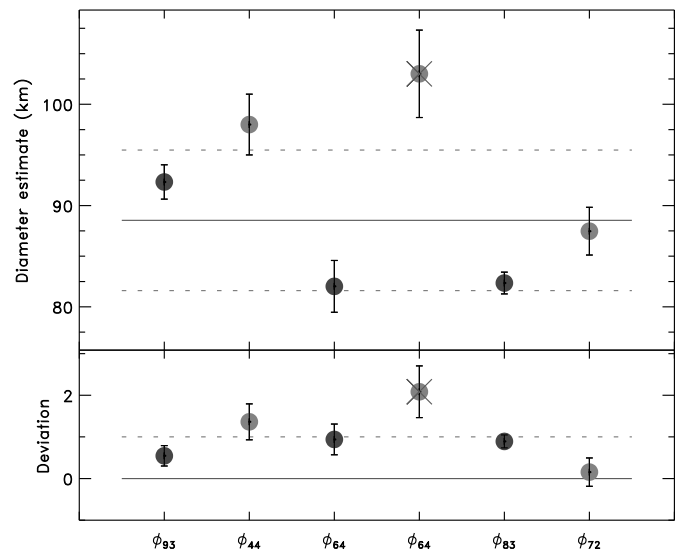


Figure B.152: Diameter estimates for (379) Huenna.

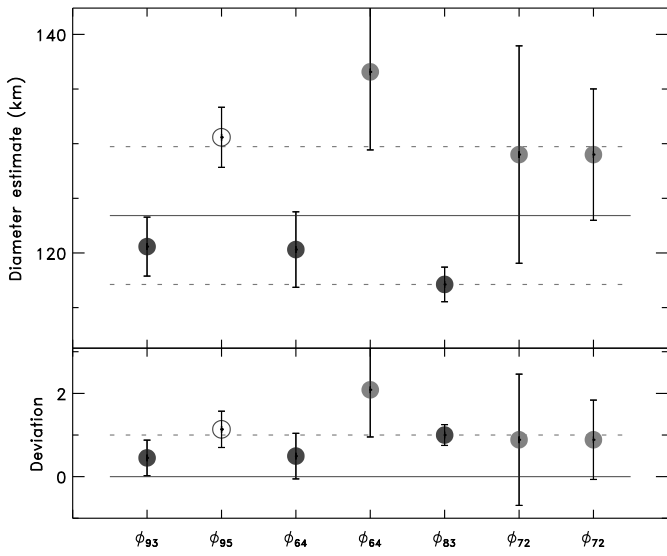


Figure B.153: Diameter estimates for (381) Myrrha.

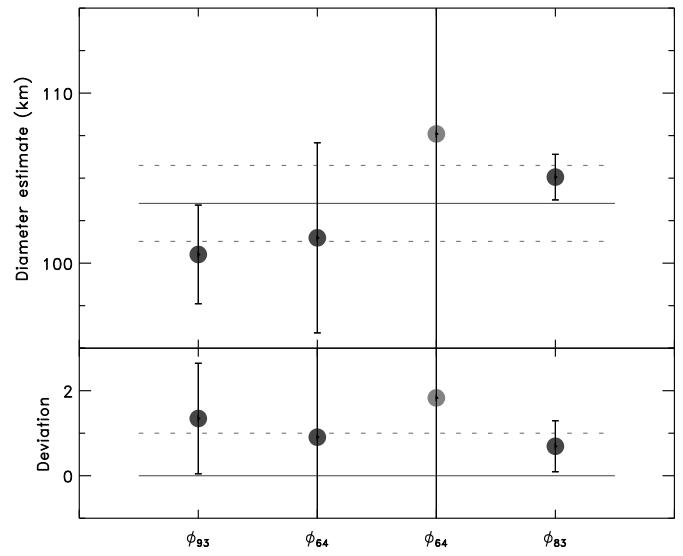


Figure B.155: Diameter estimates for (387) Aquitania.

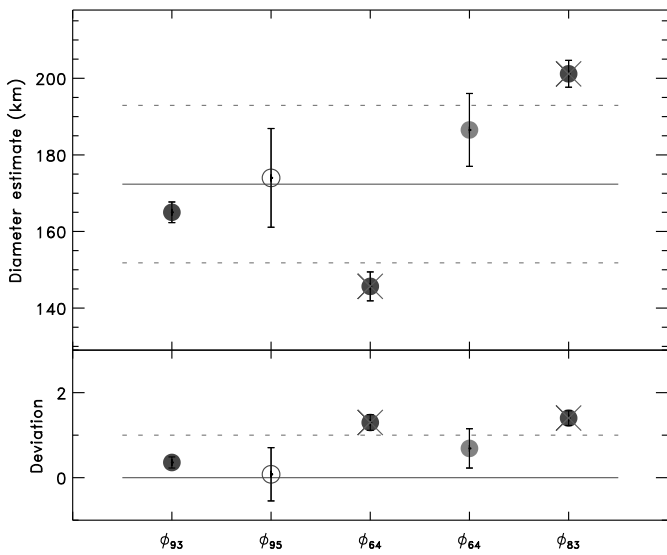


Figure B.154: Diameter estimates for (386) Siegena.

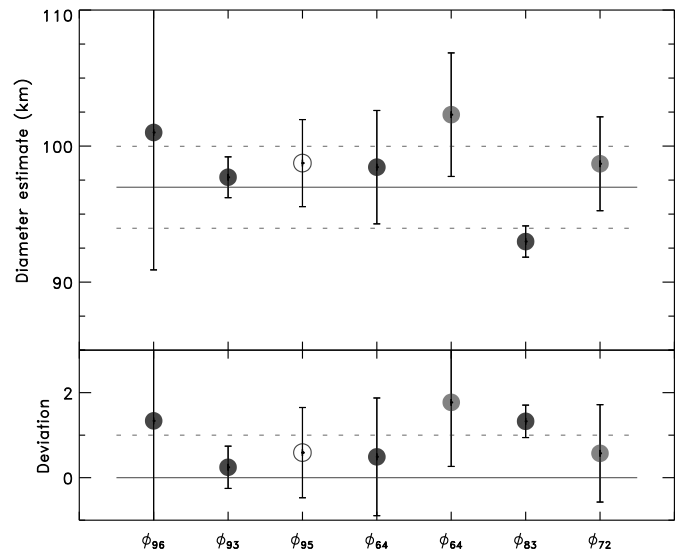


Figure B.156: Diameter estimates for (404) Arsinoe.

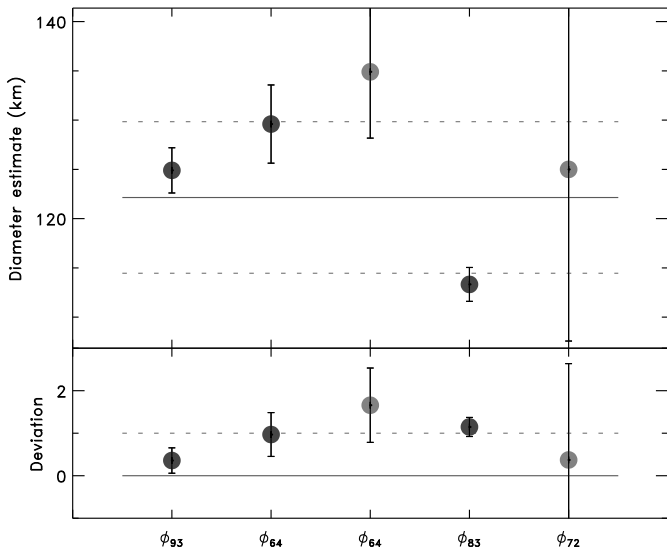


Figure B.157: Diameter estimates for (405) Thia.

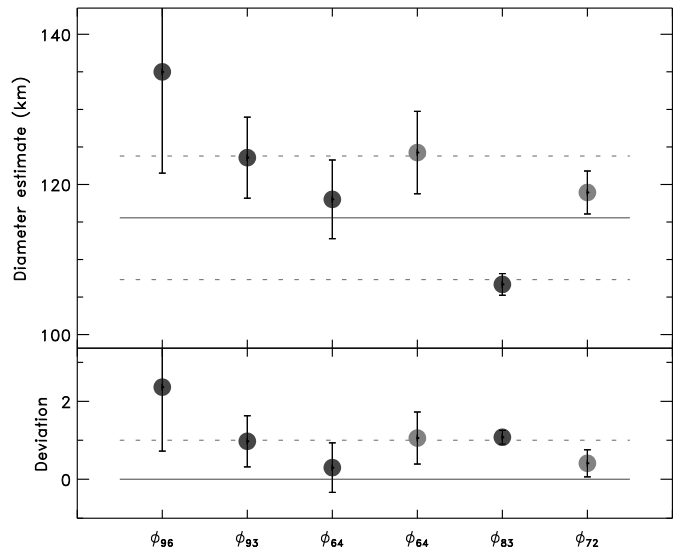


Figure B.159: Diameter estimates for (410) Chloris.

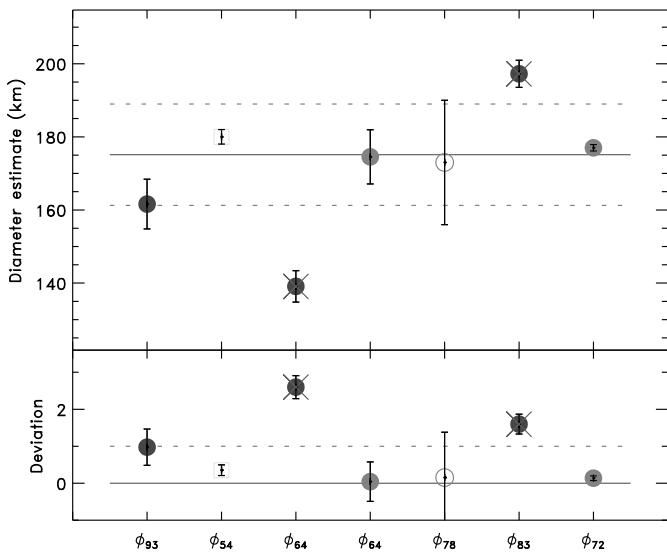


Figure B.158: Diameter estimates for (409) Aspasia.

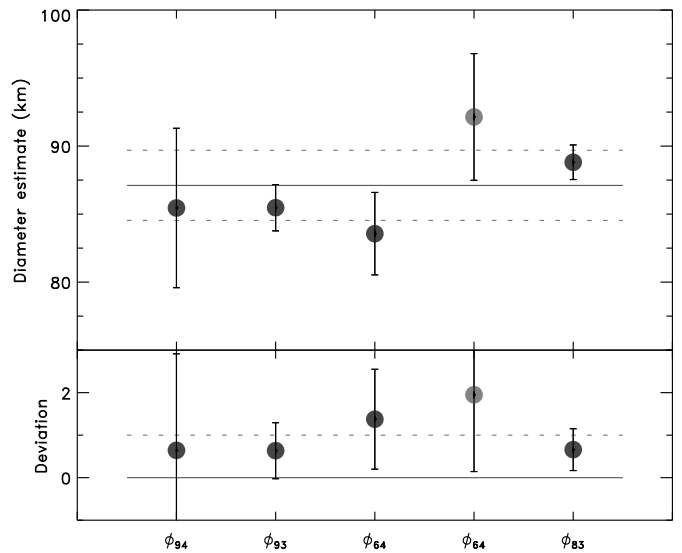


Figure B.160: Diameter estimates for (416) Vaticana.

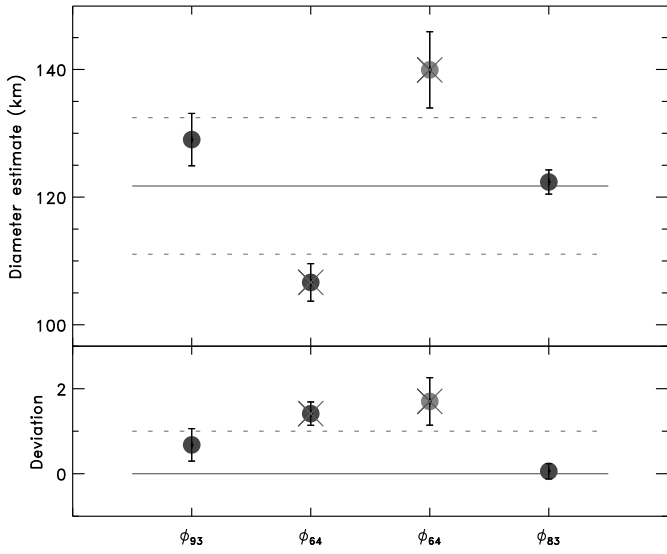


Figure B.161: Diameter estimates for (419) Aurelia.

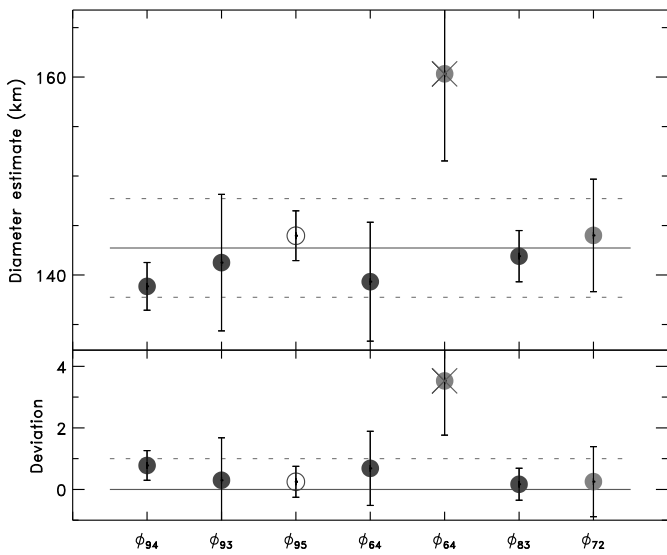


Figure B.162: Diameter estimates for (420) Bertholda.

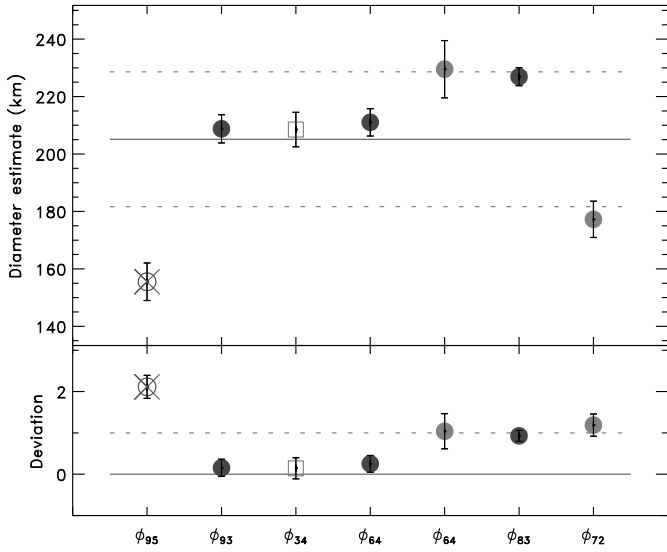


Figure B.163: Diameter estimates for (423) Diotima.

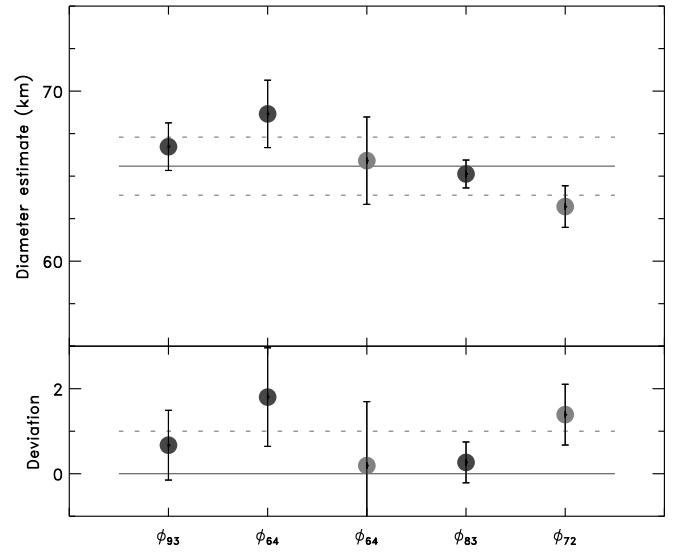


Figure B.165: Diameter estimates for (442) Eichsfeldia.

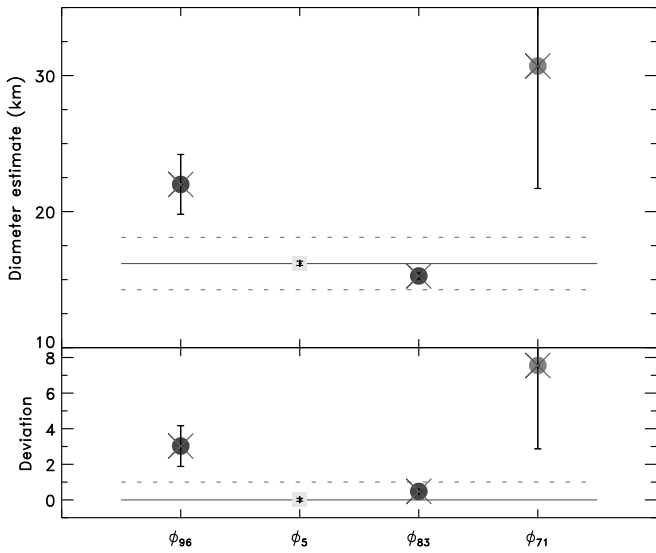


Figure B.164: Diameter estimates for (433) Eros. Only the flyby estimate from ϕ_5 is used here.

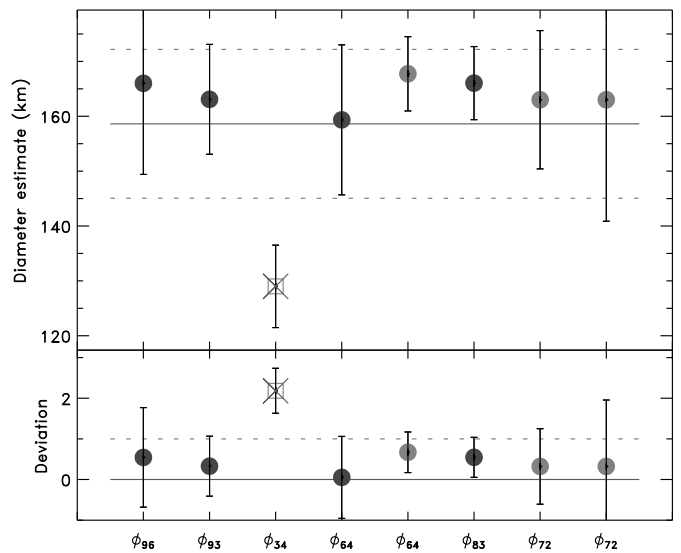


Figure B.166: Diameter estimates for (444) Gyptis.

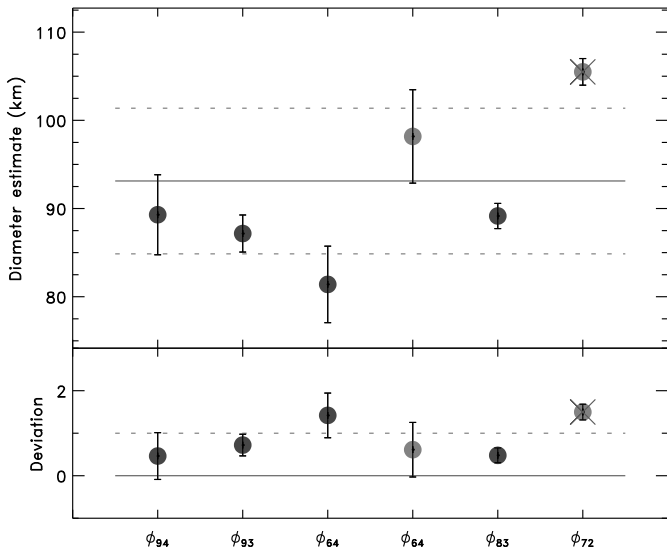


Figure B.167: Diameter estimates for (445) Edna.

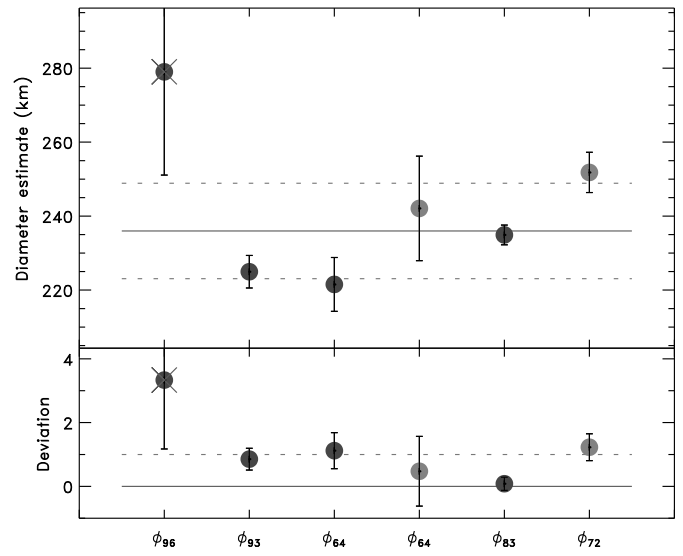


Figure B.169: Diameter estimates for (451) Patientia.

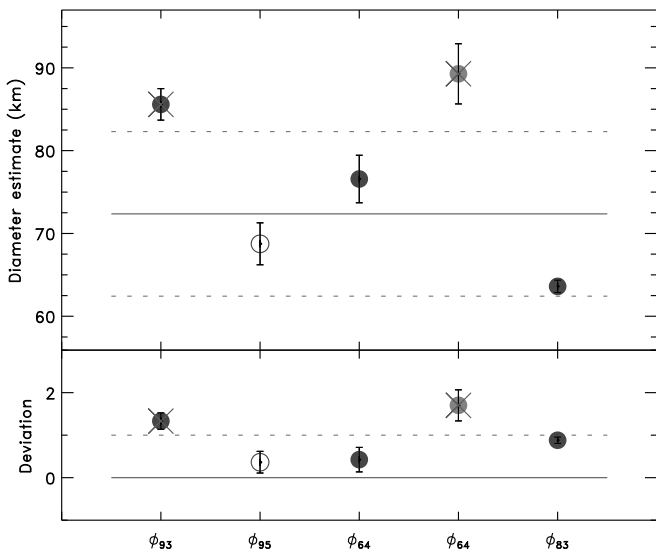


Figure B.168: Diameter estimates for (449) Hamburga.

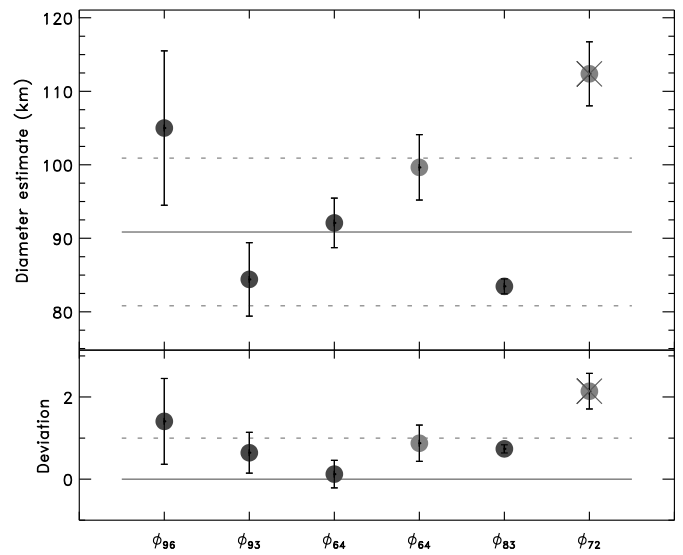


Figure B.170: Diameter estimates for (455) Bruchsalia.

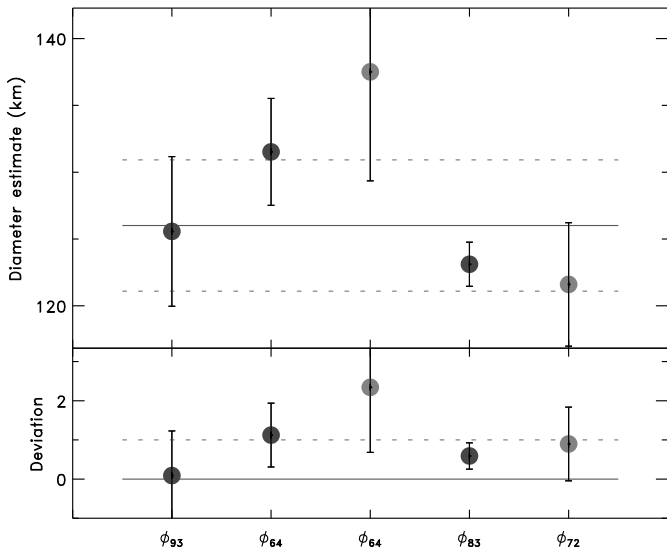


Figure B.171: Diameter estimates for (469) Argentina.

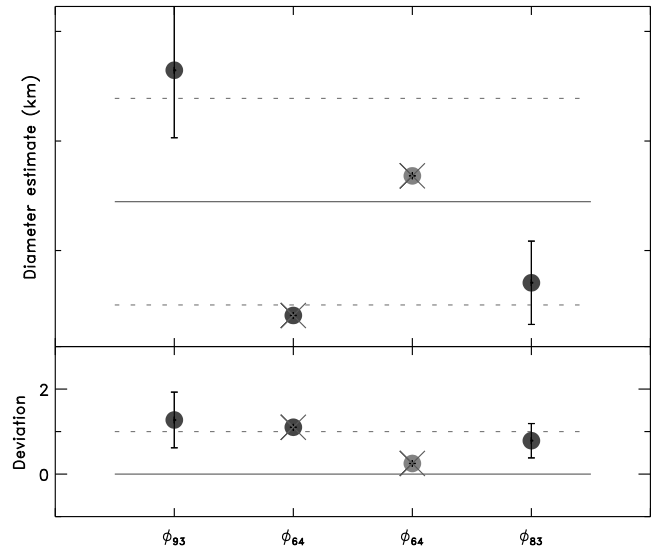


Figure B.173: Diameter estimates for (481) Erita. The diameter estimates from ϕ_{64} have unrealistic small uncertainties of 0.01 km. Using these values strongly biases the average.

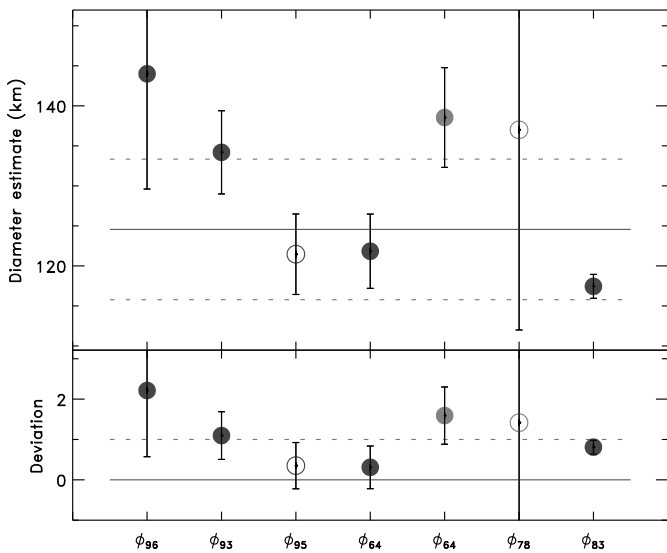


Figure B.172: Diameter estimates for (471) Papagena.

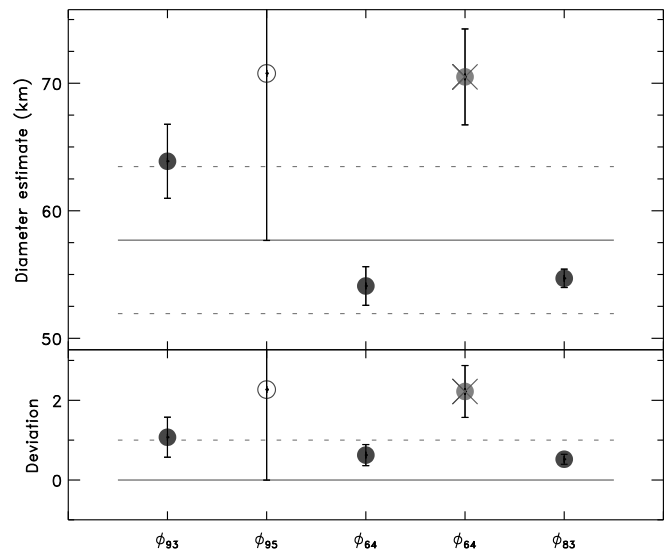


Figure B.174: Diameter estimates for (485) Genua.

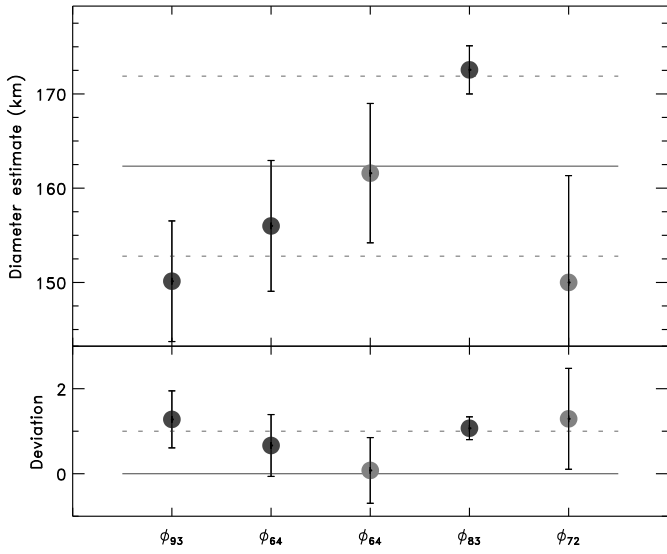


Figure B.175: Diameter estimates for (488) Kreusa.

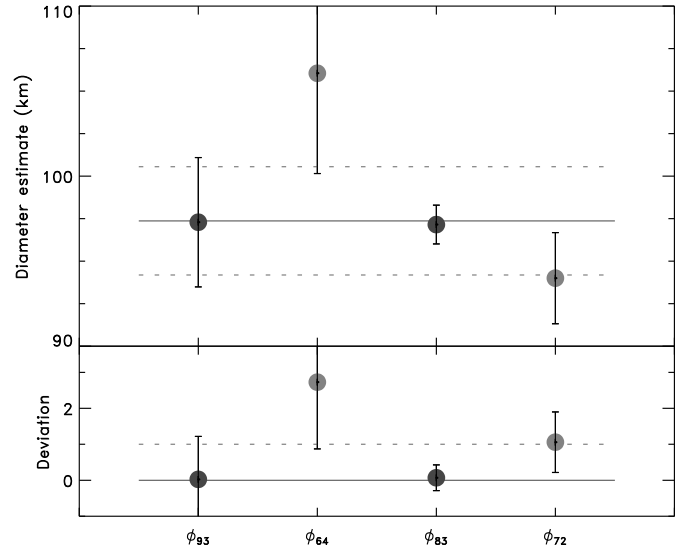


Figure B.177: Diameter estimates for (491) Carina.

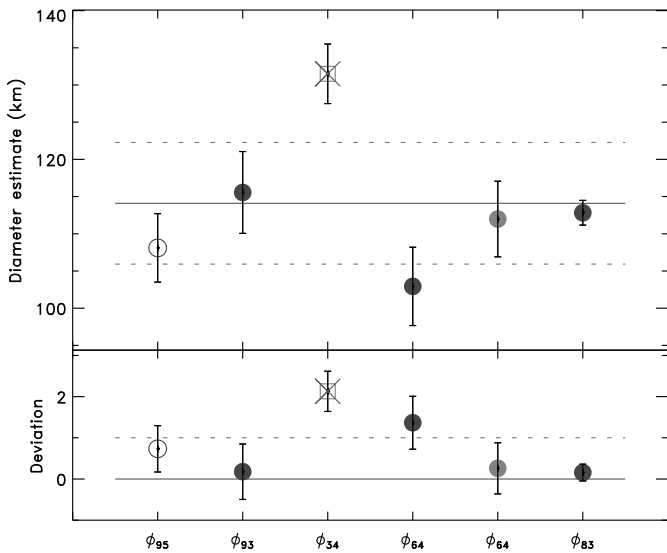


Figure B.176: Diameter estimates for (490) Veritas.

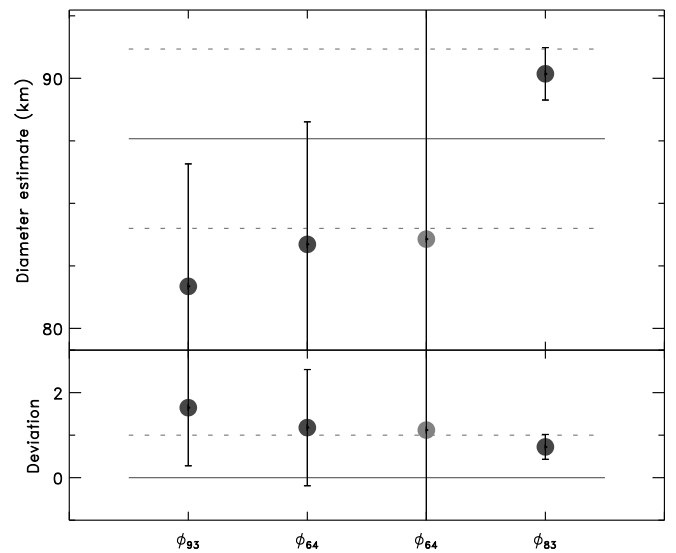


Figure B.178: Diameter estimates for (503) Evelyne.

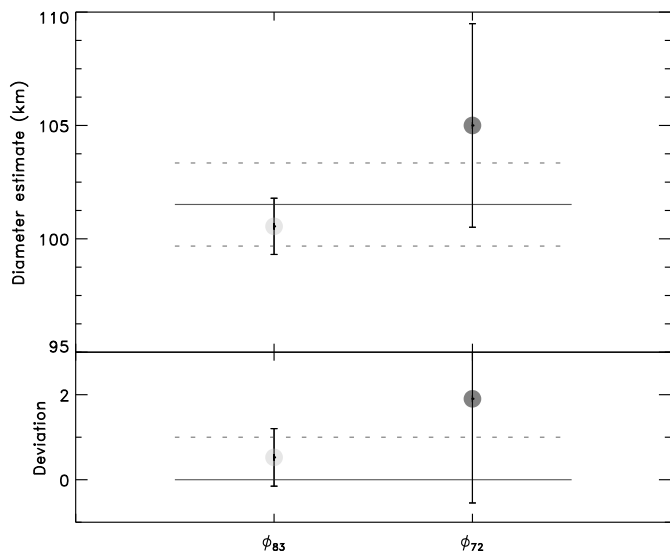


Figure B.179: Diameter estimates for (505) Cava.

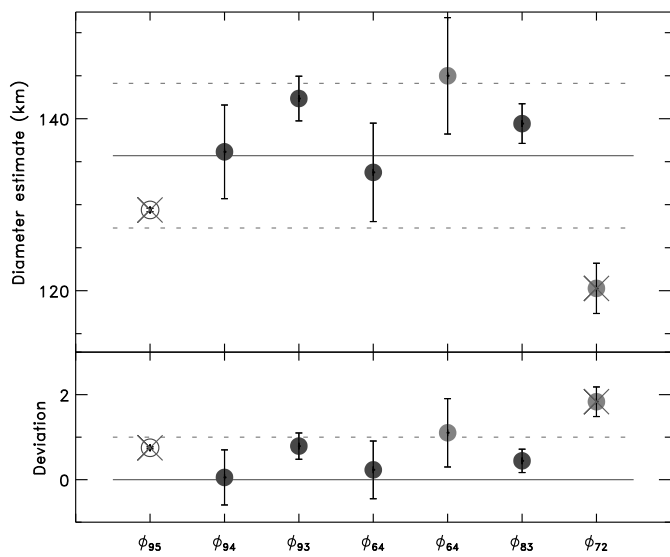


Figure B.180: Diameter estimates for (508) Princetonia.

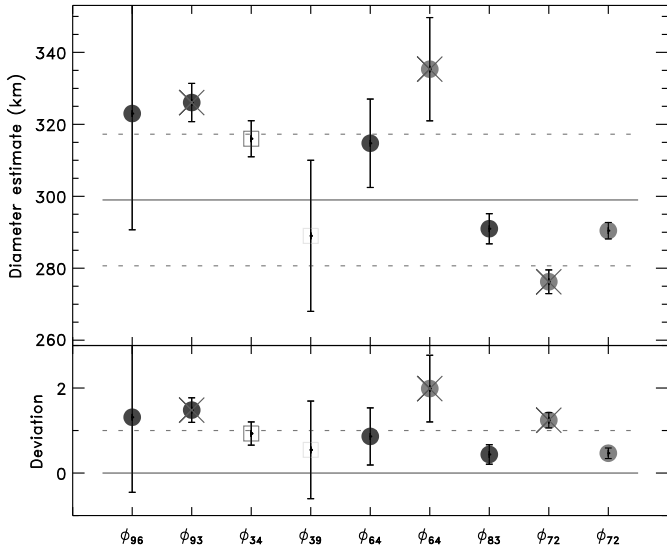


Figure B.181: Diameter estimates for (511) Davida.

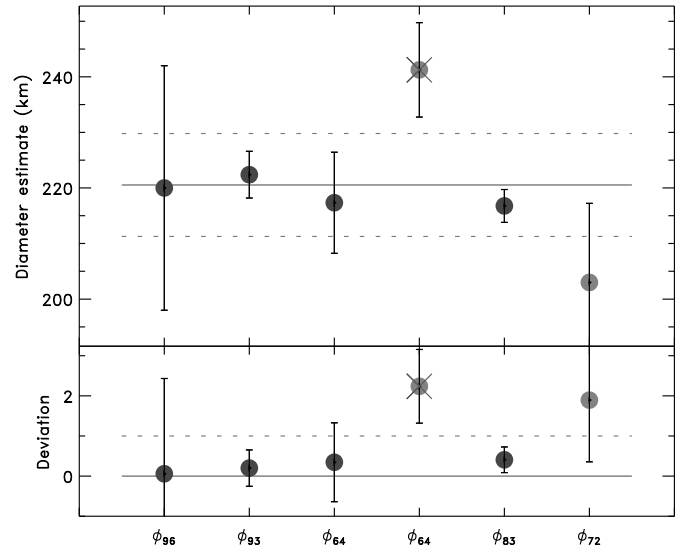


Figure B.183: Diameter estimates for (532) Herculina.

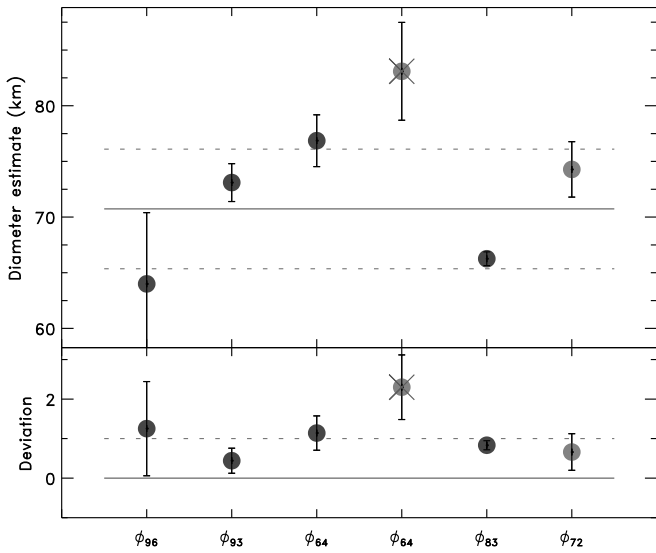


Figure B.182: Diameter estimates for (516) Amherstia.

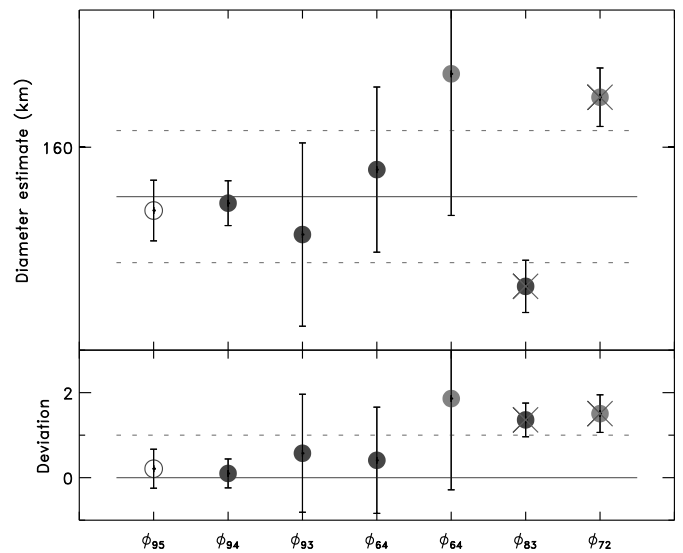


Figure B.184: Diameter estimates for (536) Merapi.

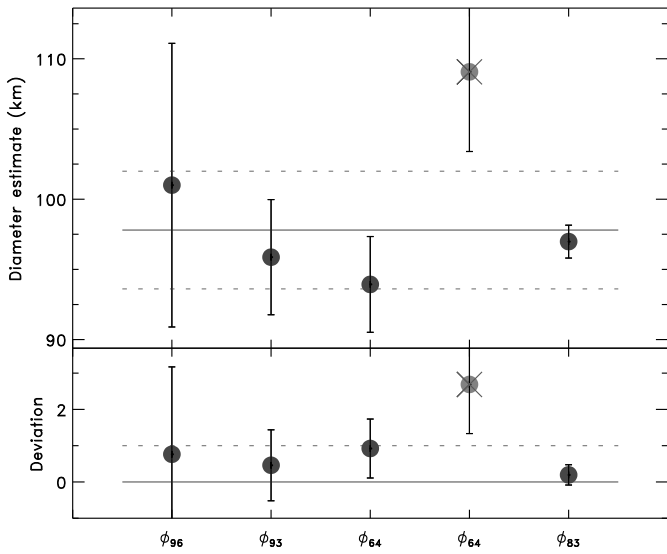


Figure B.185: Diameter estimates for (554) Peraga.

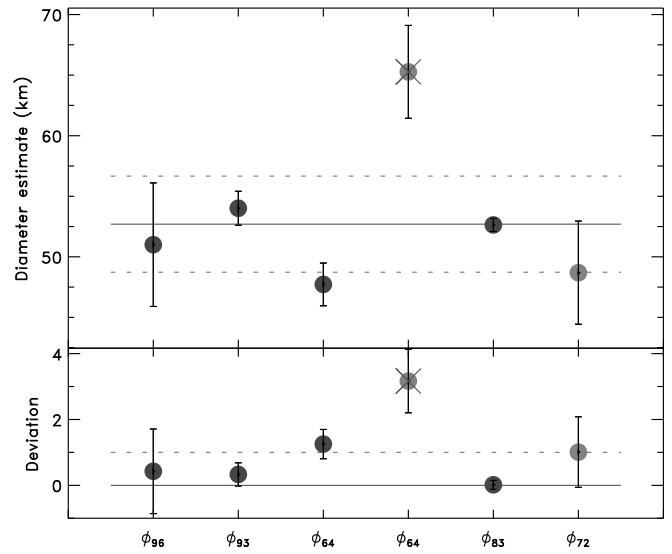


Figure B.187: Diameter estimates for (584) Semiramis.

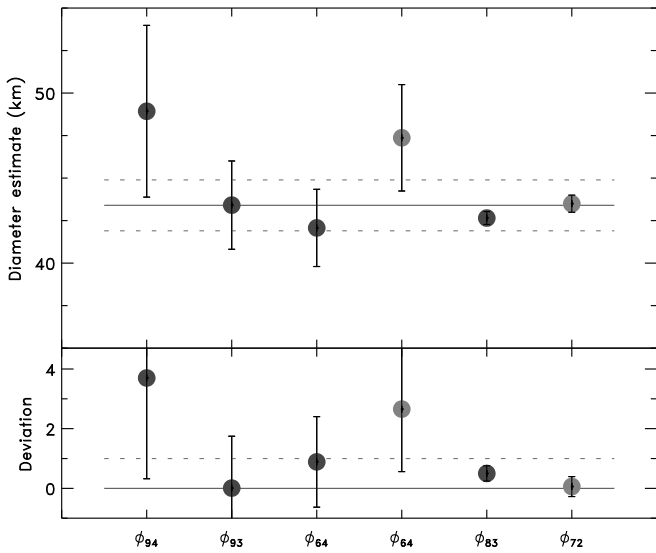


Figure B.186: Diameter estimates for (582) Olympia.

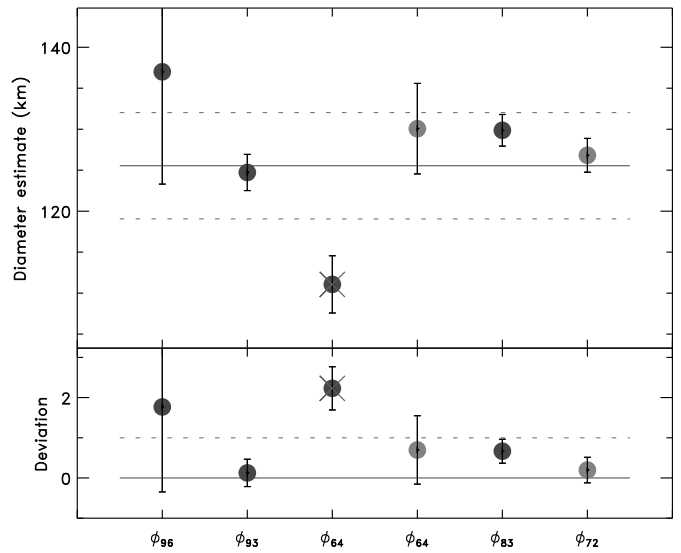


Figure B.188: Diameter estimates for (602) Marianna.

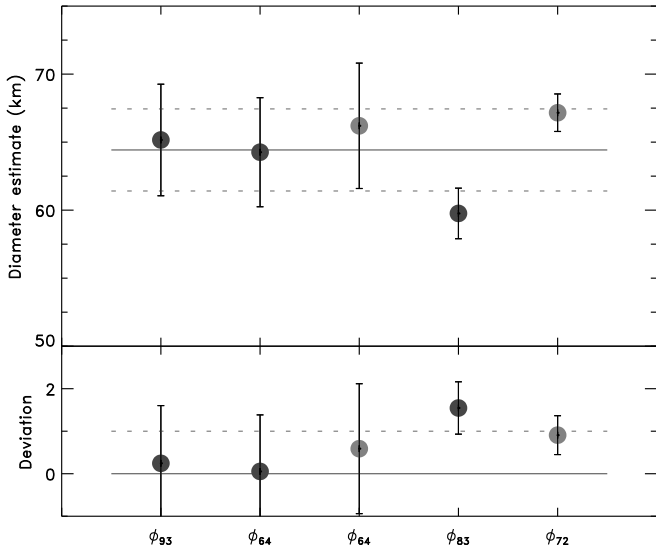


Figure B.189: Diameter estimates for (604) Tekmessia.

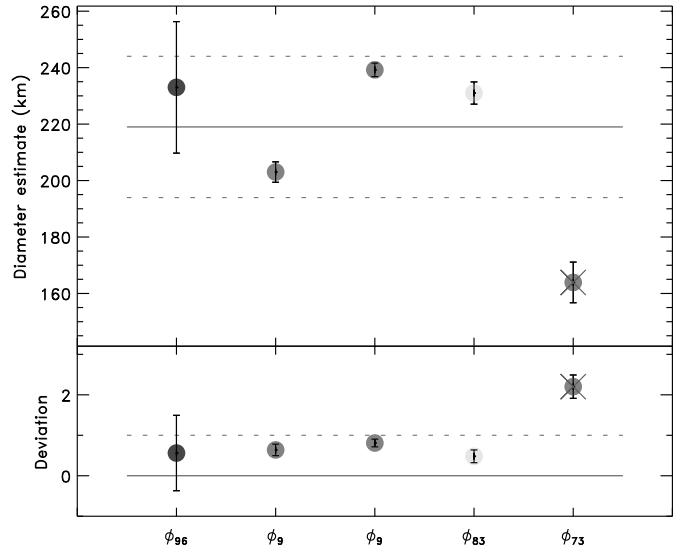


Figure B.191: Diameter estimates for (624) Hektor.

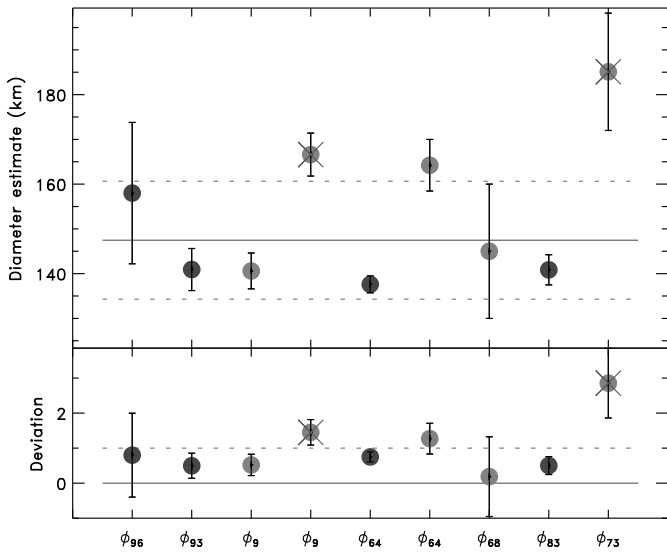


Figure B.190: Diameter estimates for (617) Patroclus.

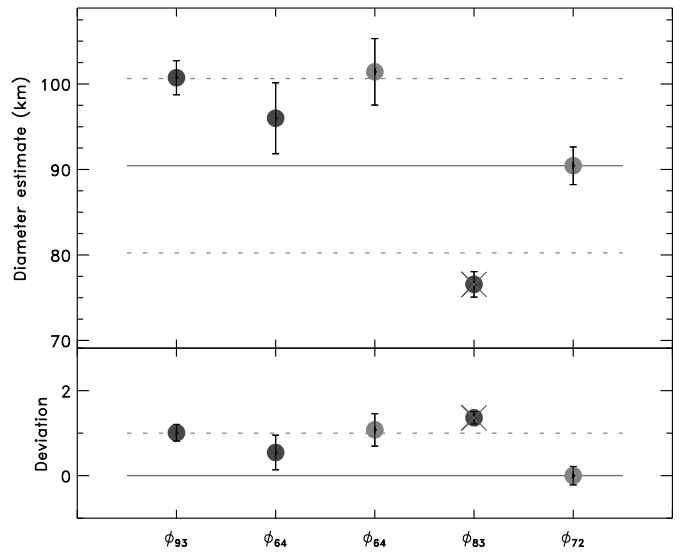


Figure B.192: Diameter estimates for (626) Notburga.

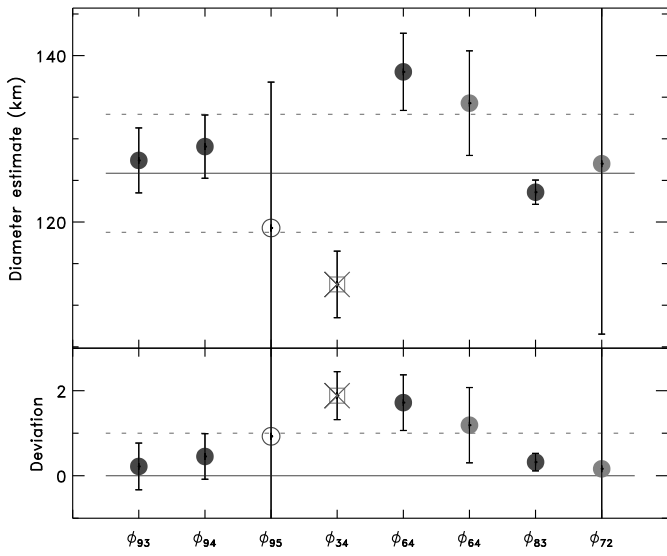


Figure B.193: Diameter estimates for (654) Zelinda.

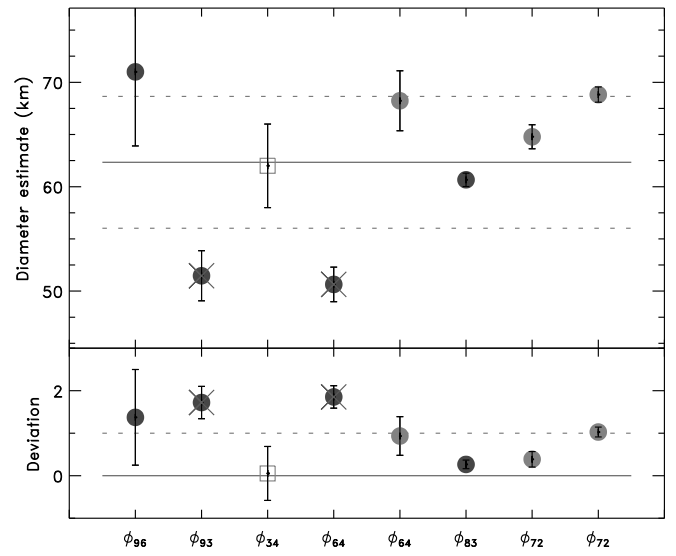


Figure B.195: Diameter estimates for (679) Pax.

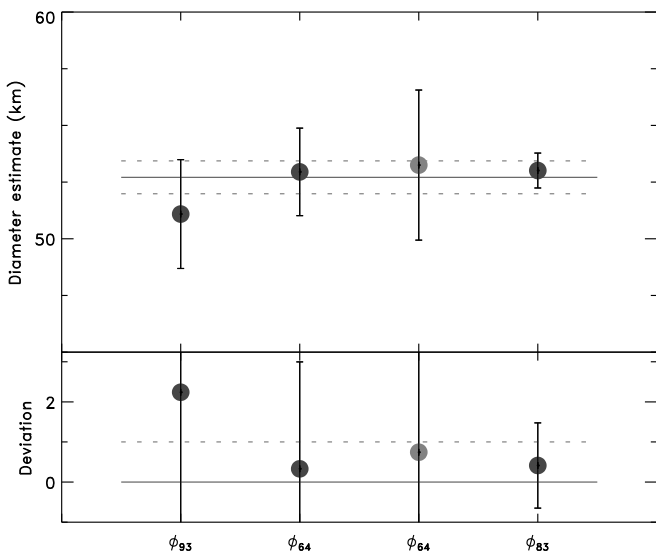


Figure B.194: Diameter estimates for (665) Sabine.

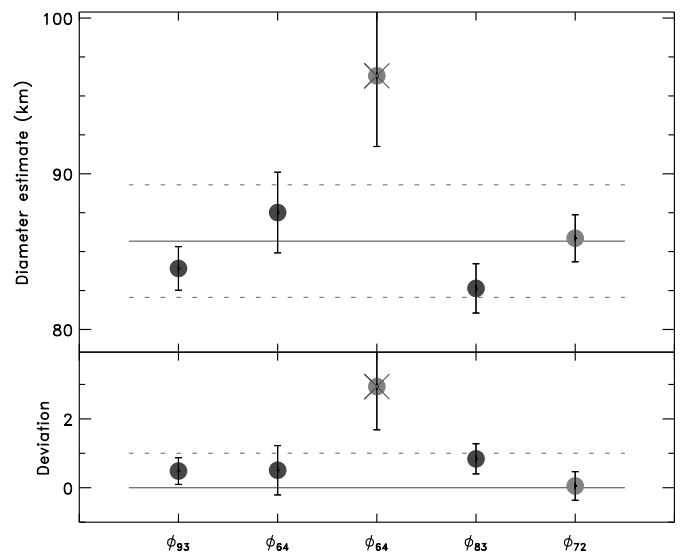


Figure B.196: Diameter estimates for (680) Genova.

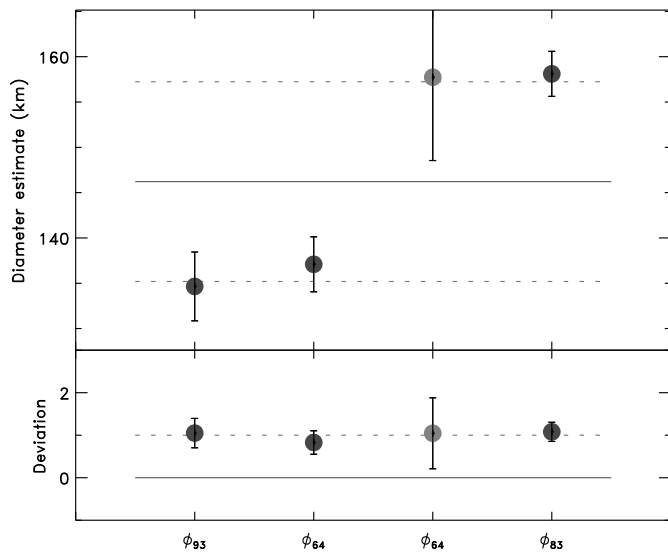


Figure B.197: Diameter estimates for (690) Wratislavia.

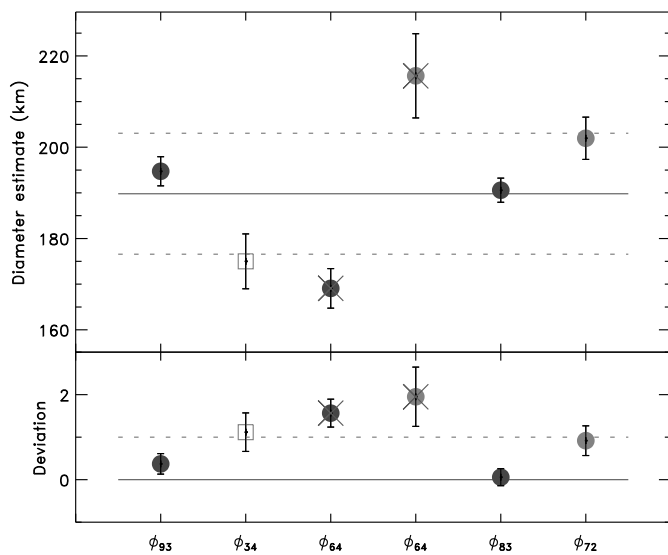


Figure B.198: Diameter estimates for (702) Alauda.

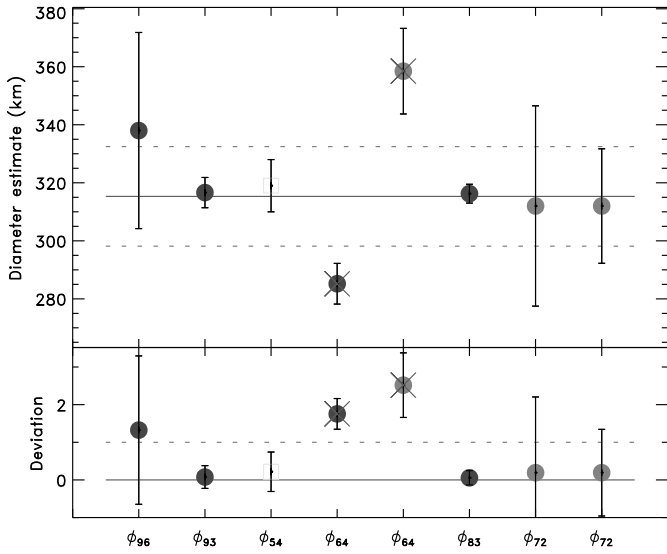


Figure B.199: Diameter estimates for (704) Interamnia.

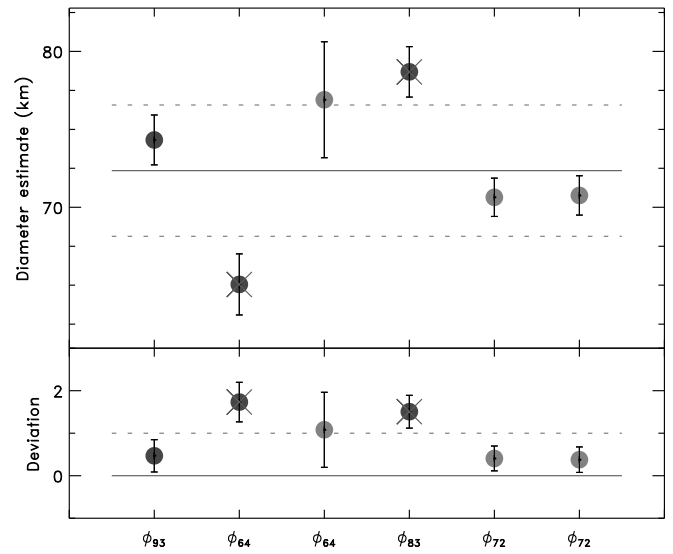


Figure B.201: Diameter estimates for (735) Marghanna.

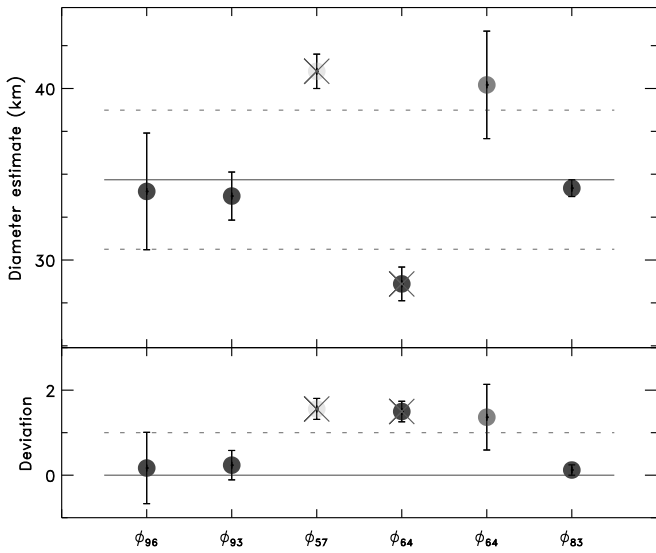


Figure B.200: Diameter estimates for (720) Bohlinia.

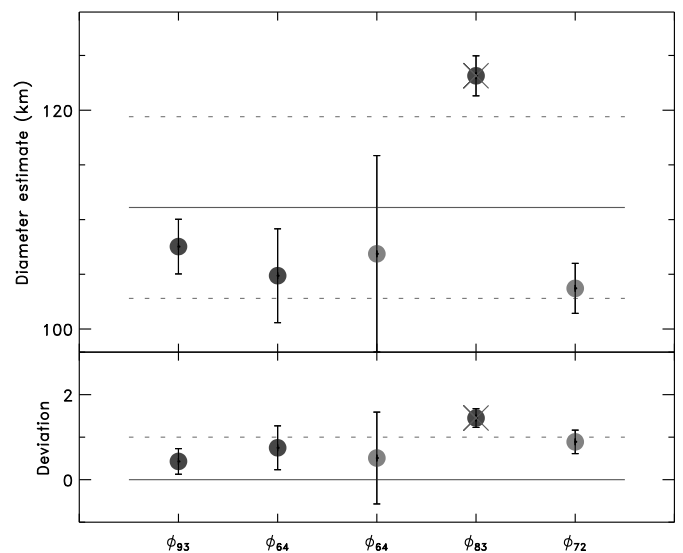


Figure B.202: Diameter estimates for (739) Mandeville.

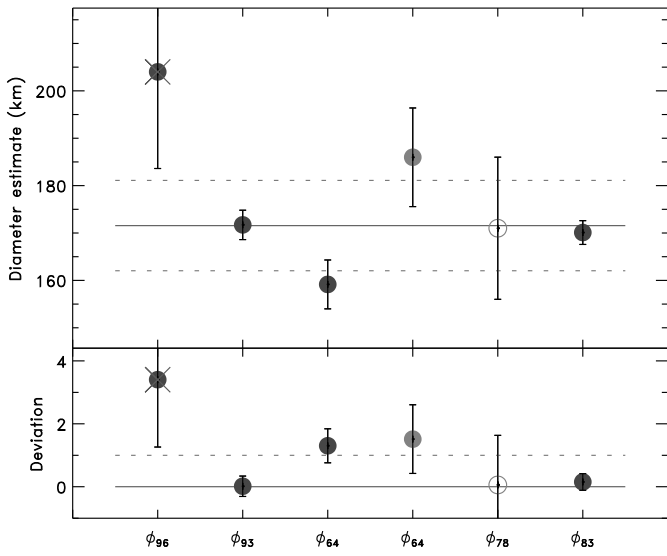


Figure B.203: Diameter estimates for (747) Winchester.

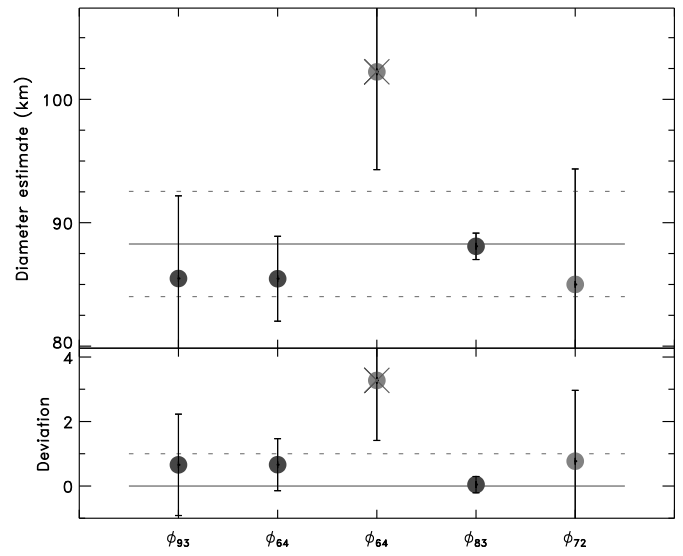


Figure B.205: Diameter estimates for (758) Mancunia.

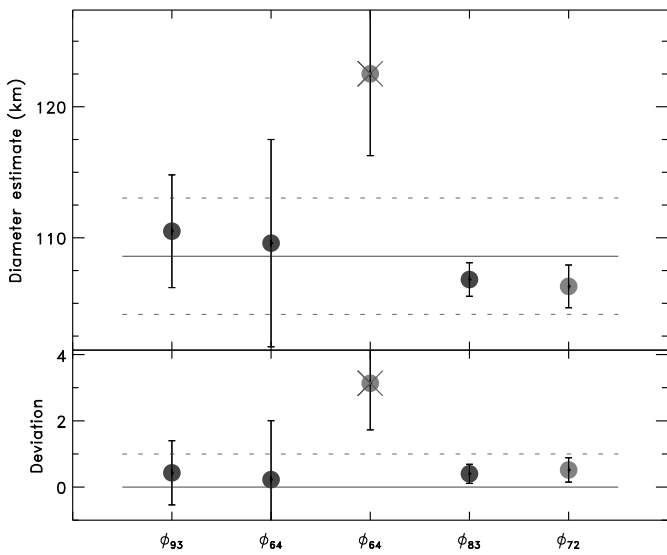


Figure B.204: Diameter estimates for (751) Faina.

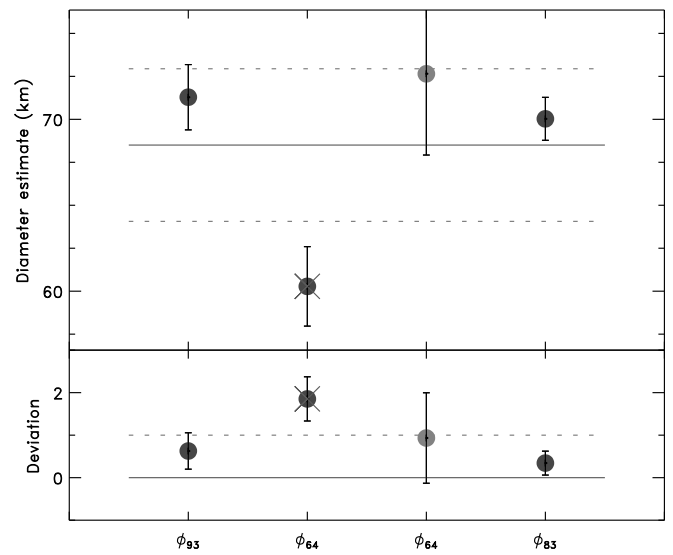


Figure B.206: Diameter estimates for (760) Massinga.

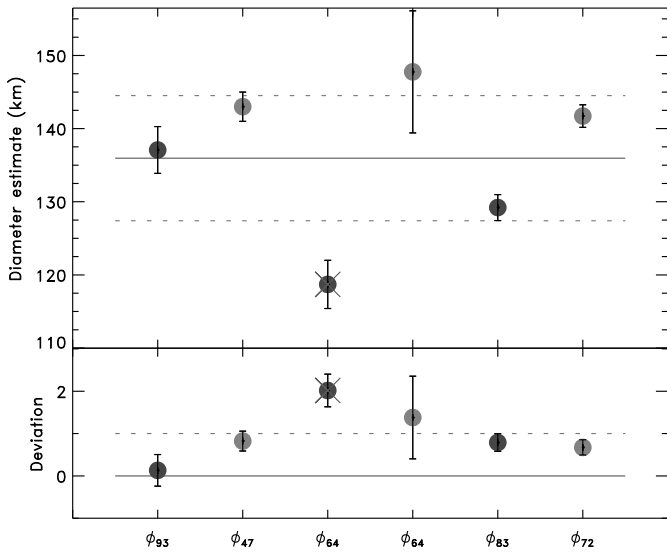


Figure B.207: Diameter estimates for (762) Pulcova.

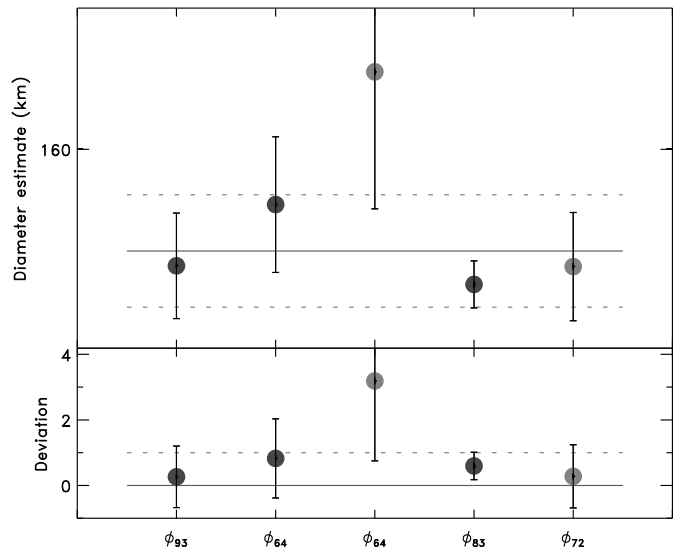


Figure B.209: Diameter estimates for (776) Berbericia.

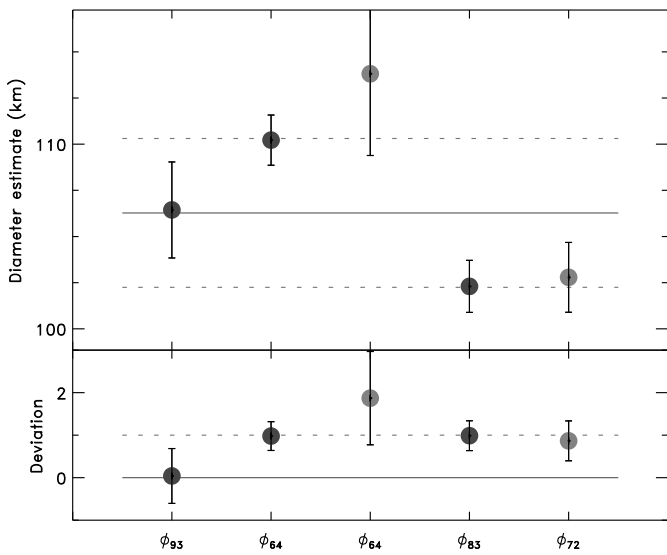


Figure B.208: Diameter estimates for (769) Tatjana.

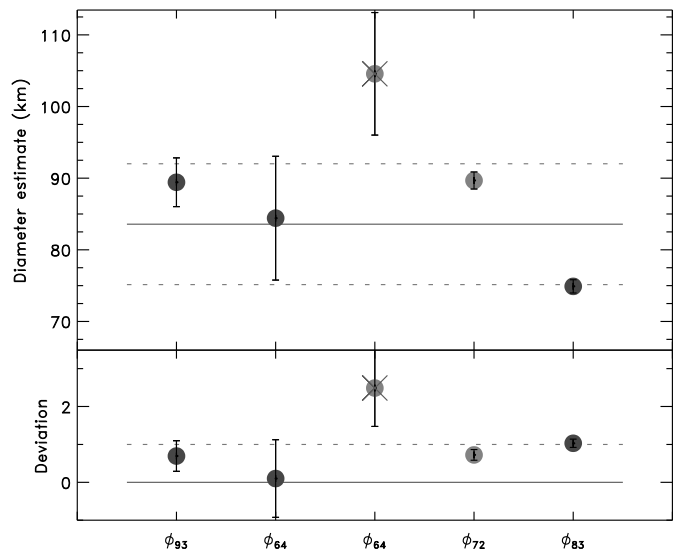


Figure B.210: Diameter estimates for (784) Pickeringia.

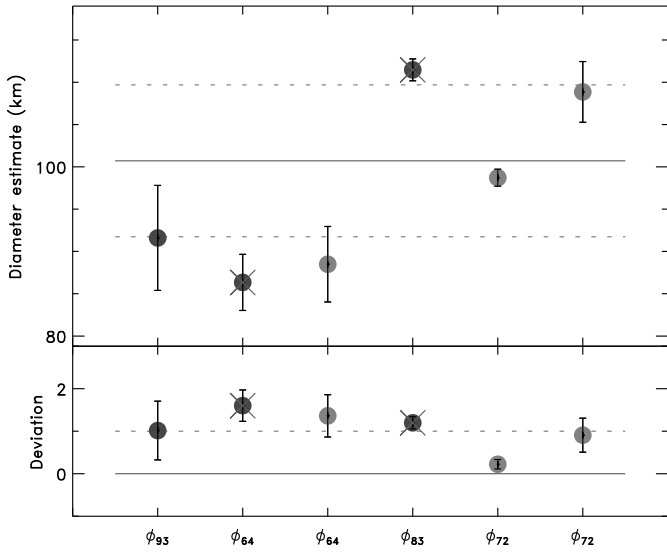


Figure B.211: Diameter estimates for (786) Bredichina.

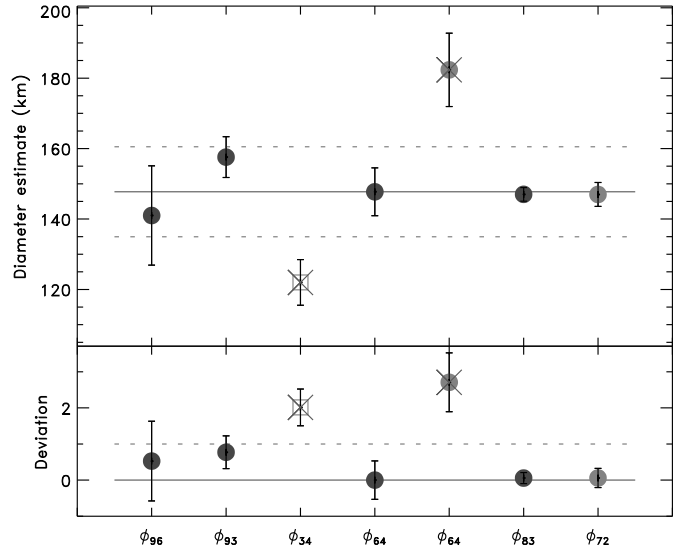


Figure B.213: Diameter estimates for (804) Hispania.

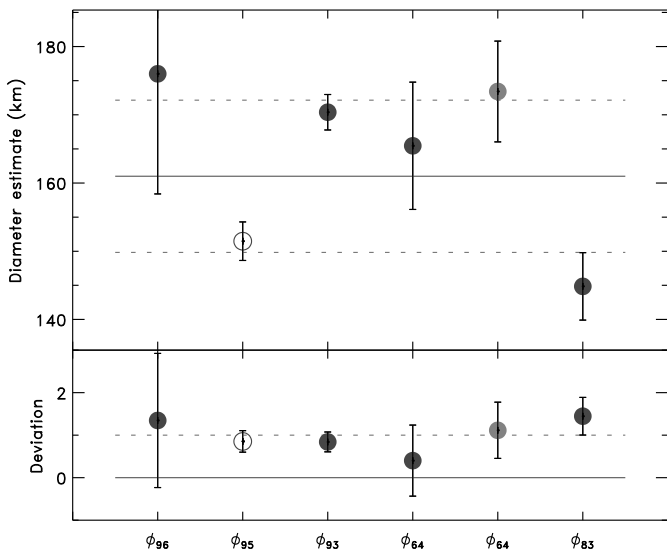


Figure B.212: Diameter estimates for (790) Pretoria.

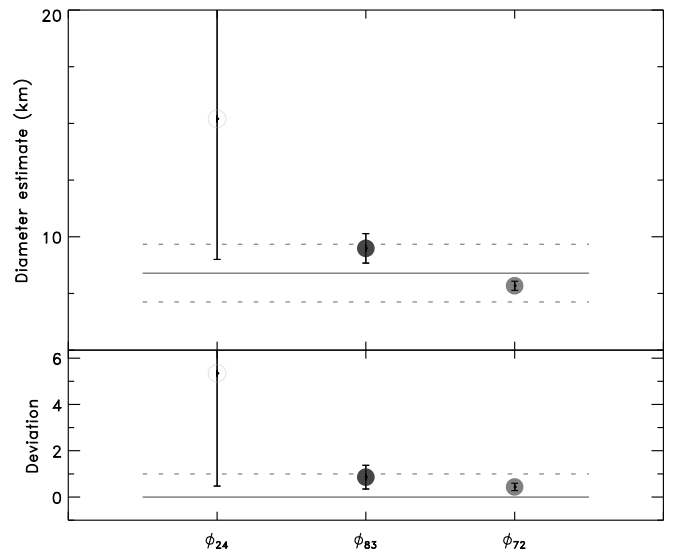


Figure B.214: Diameter estimates for (854) Frostia.

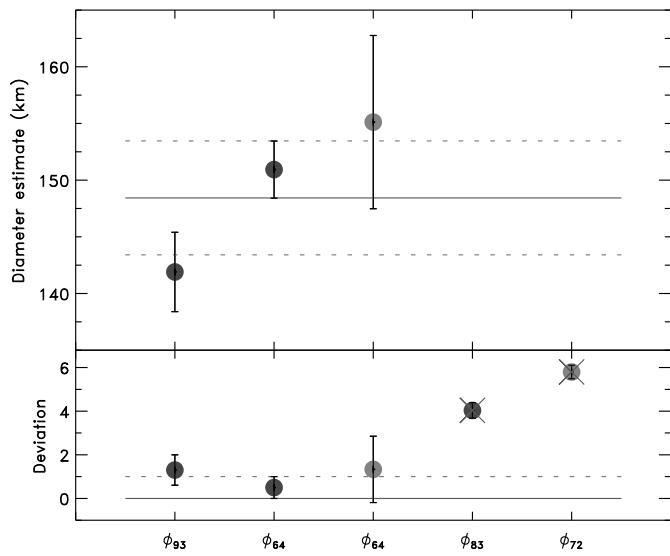


Figure B.215: Diameter estimates for (895) Helio.

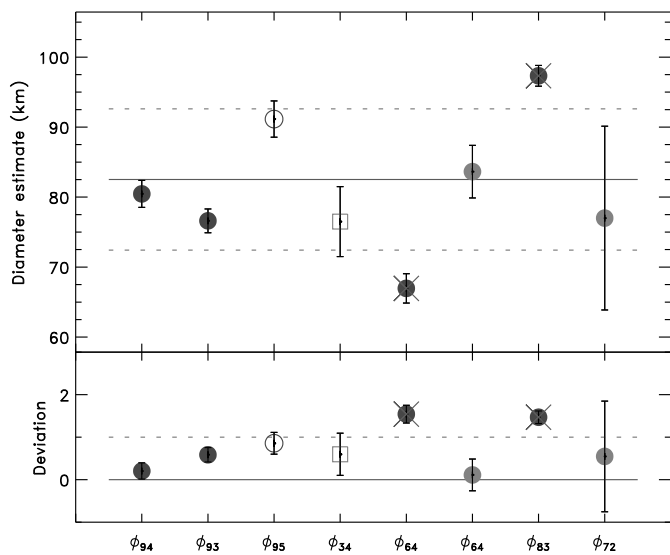


Figure B.216: Diameter estimates for (914) Palisana.

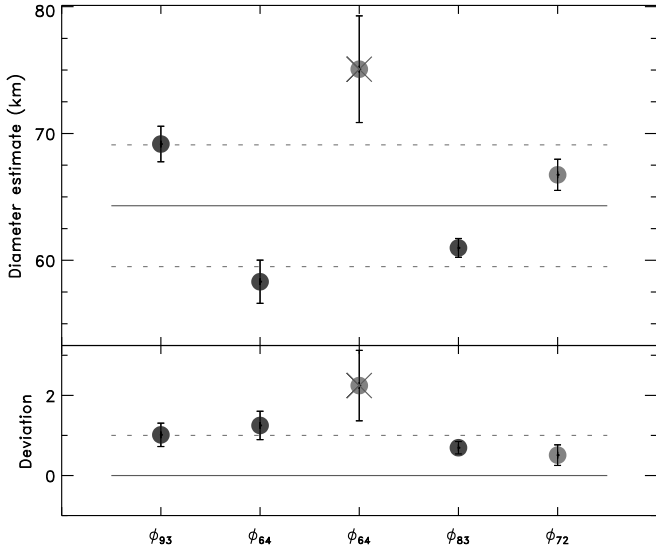


Figure B.217: Diameter estimates for (949) Hel.

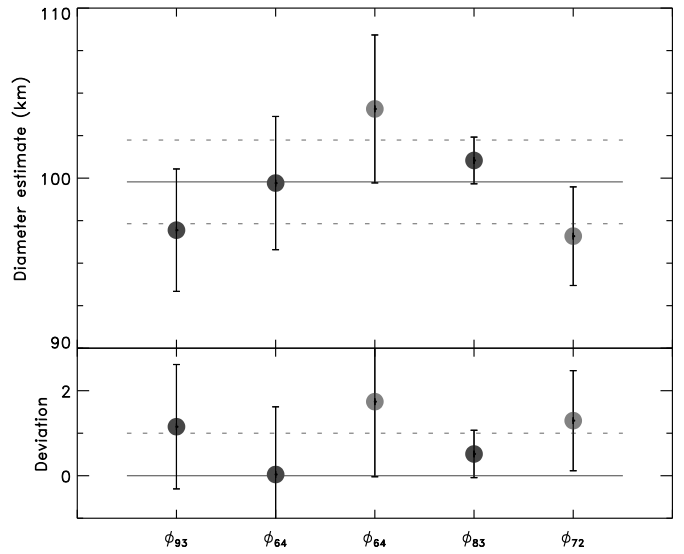


Figure B.219: Diameter estimates for (1015) Christa.

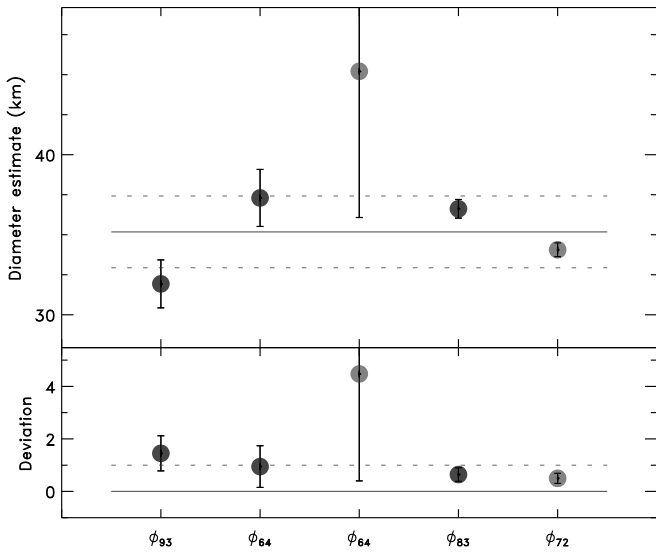


Figure B.218: Diameter estimates for (1013) Tombecka.

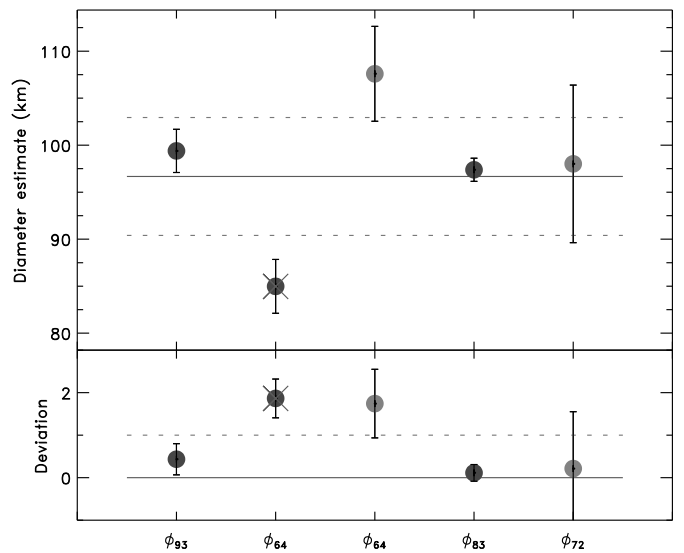


Figure B.220: Diameter estimates for (1021) Flammario.

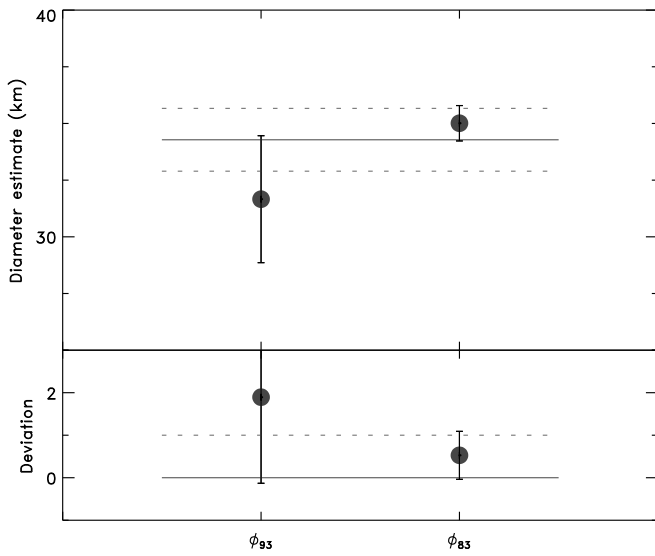


Figure B.221: Diameter estimates for (1036) Ganymed.

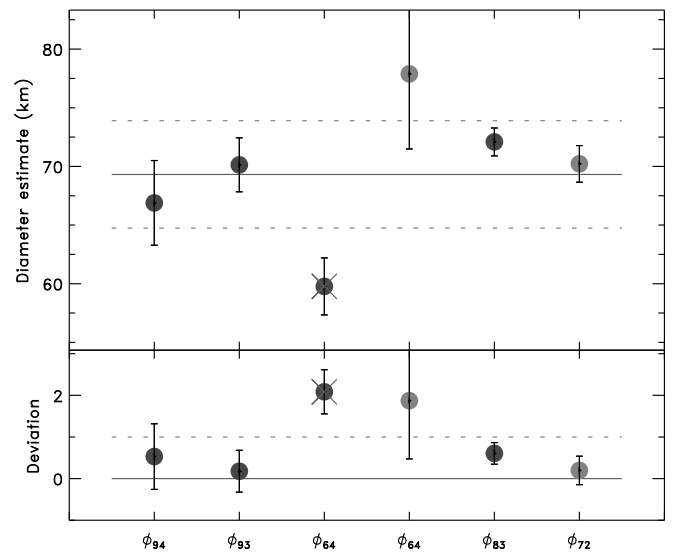


Figure B.223: Diameter estimates for (1171) Rusthawelia.

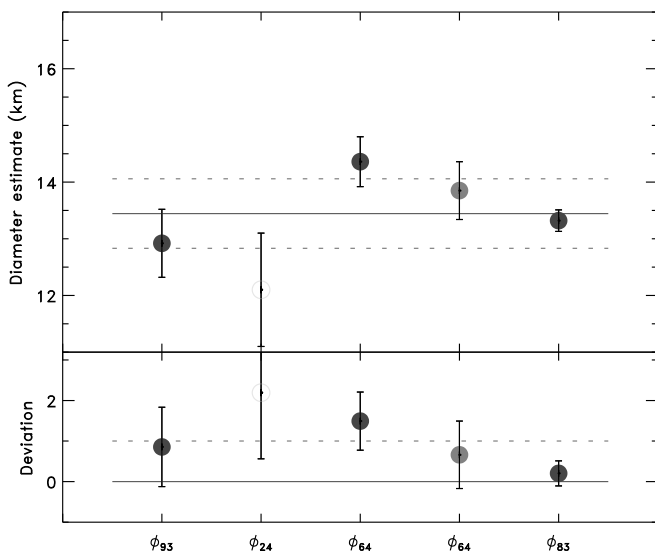


Figure B.222: Diameter estimates for (1089) Tama.

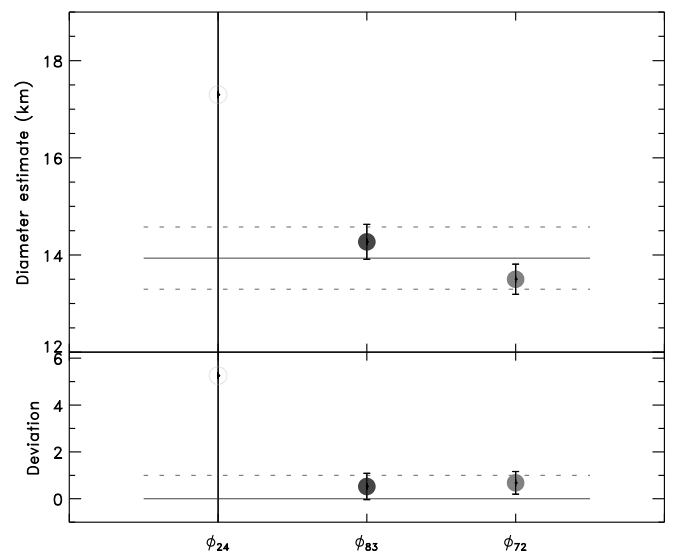


Figure B.224: Diameter estimates for (1313) Berna.

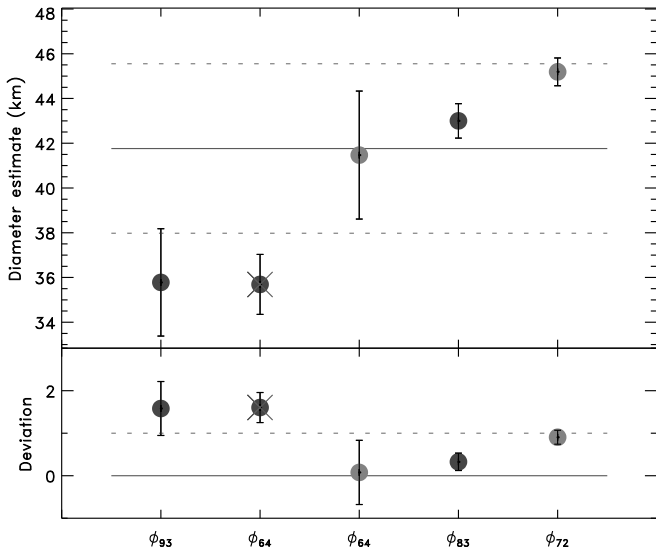


Figure B.225: Diameter estimates for (1669) Dagmar.

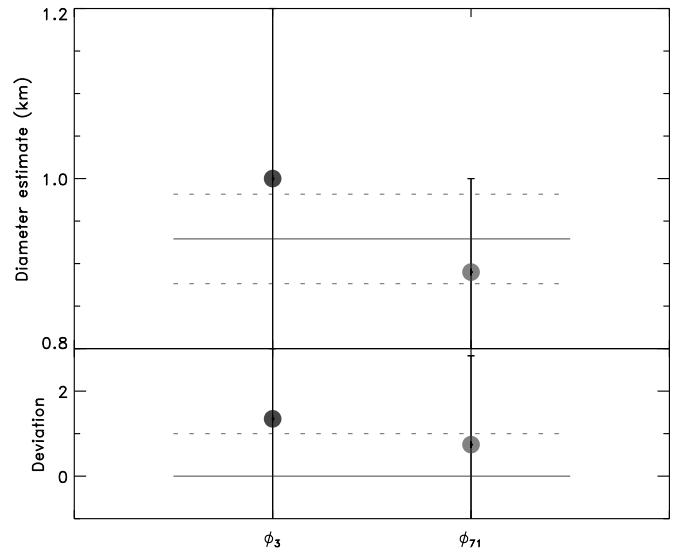


Figure B.227: Diameter estimates for (3671) Dionysus.

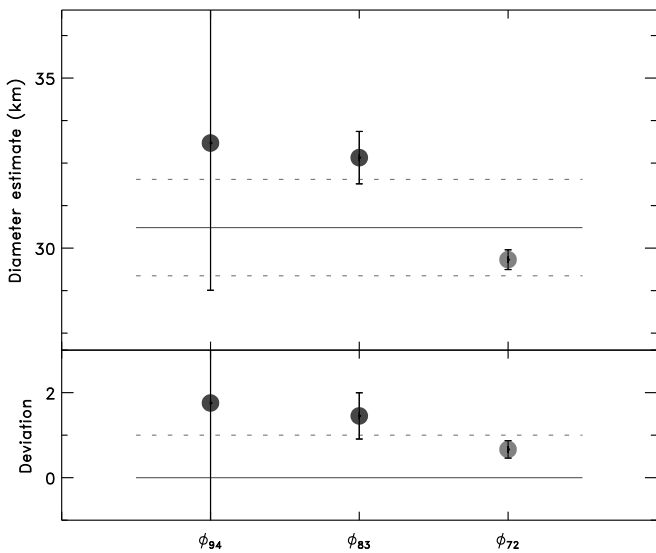


Figure B.226: Diameter estimates for (1686) De Sitter.

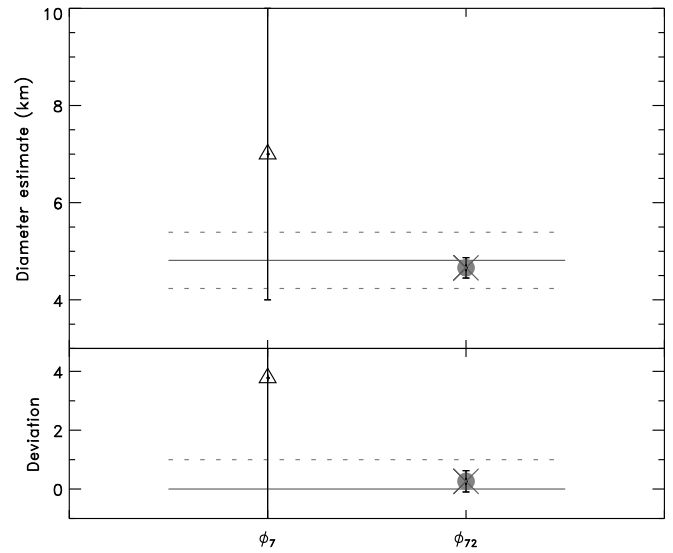


Figure B.228: Diameter estimates for (3749) Balam. The diameter estimate from ϕ_{72} give an unrealistic high density of 9.6 ± 1.3 if used alone. Only the estimate from ϕ_7 is used.

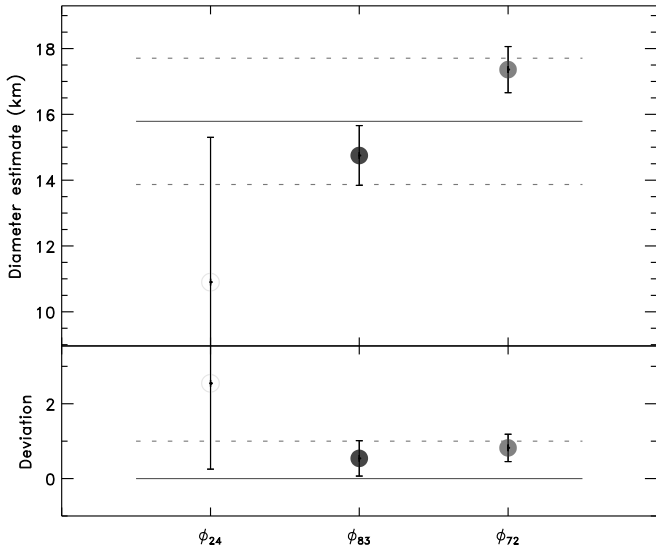


Figure B.229: Diameter estimates for (4492) Debussy.

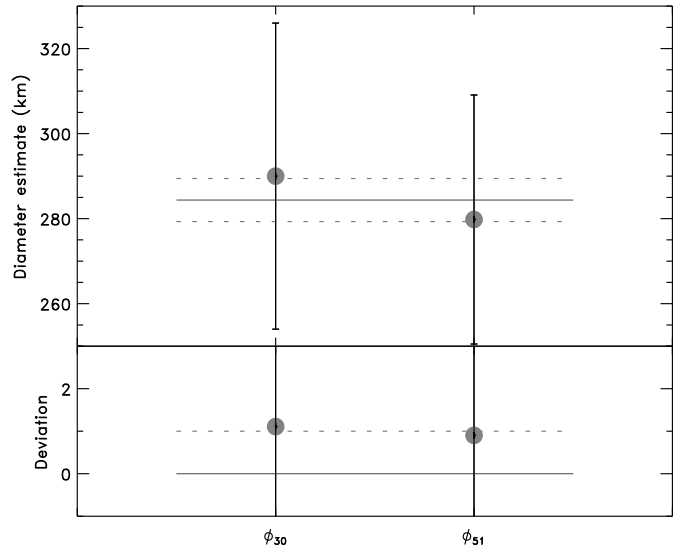


Figure B.231: Diameter estimates for (26308) 1998 SM165.

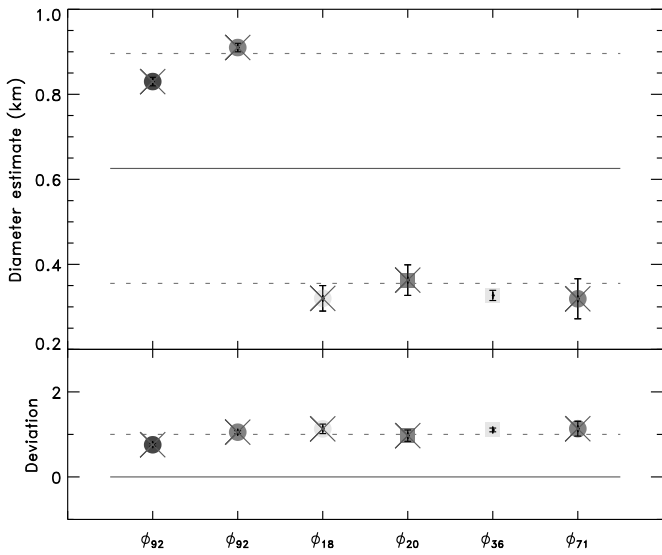


Figure B.230: Diameter estimates for (25143) Itokawa. Only the flyby estimate from ϕ_{36} is used here.

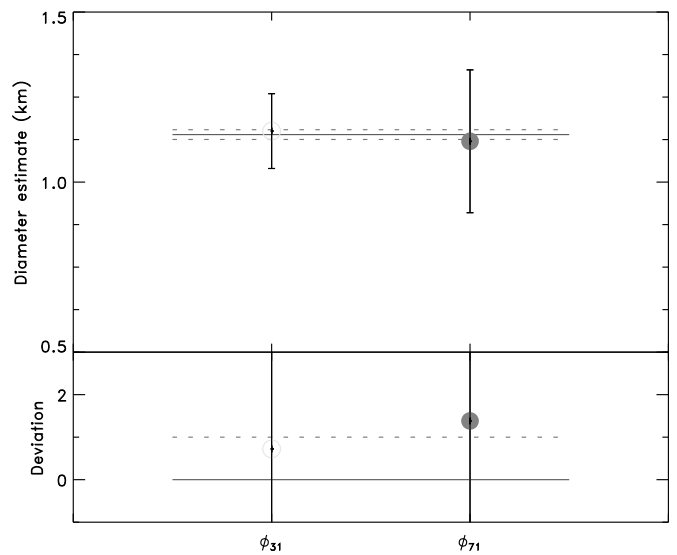


Figure B.232: Diameter estimates for (35107) 1991 VH.

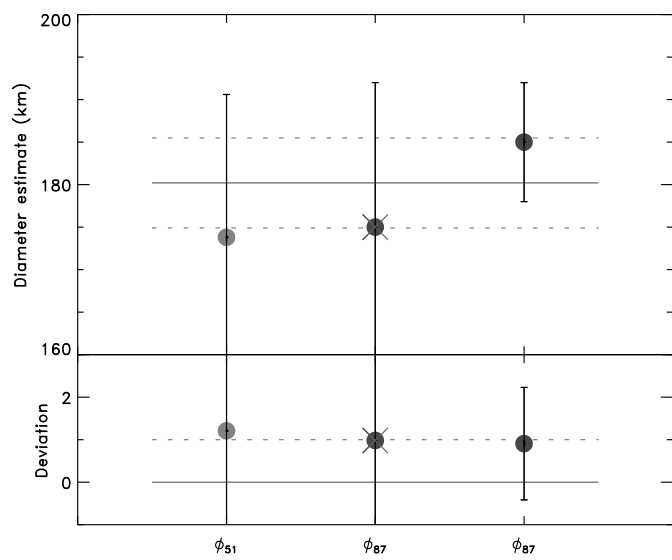


Figure B.233: Diameter estimates for (42355) Typhon.

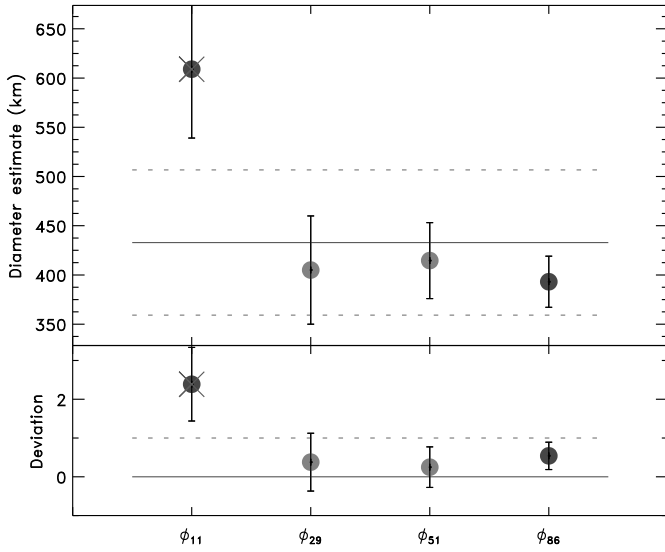


Figure B.234: Diameter estimates for (47171) 1999 TC36.

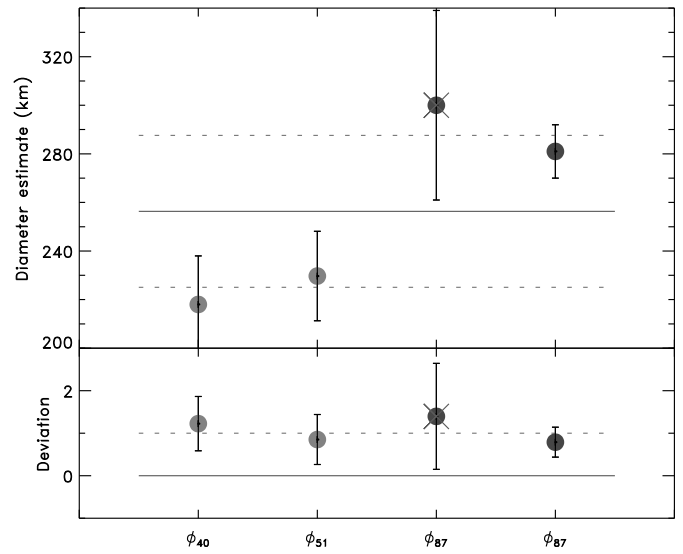


Figure B.236: Diameter estimates for (65489) Ceto.

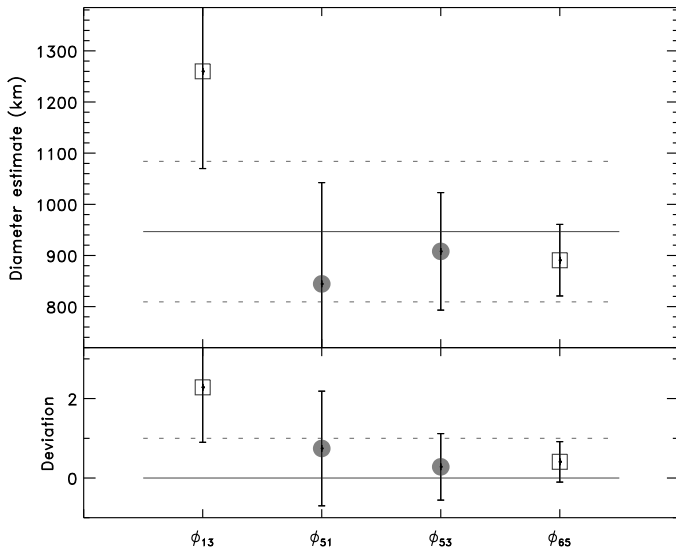


Figure B.235: Diameter estimates for (50000) Quaoar.

Appendix C. Compilation of indirect density estimates

The 24 indirect density estimates gathered in the literature are listed in Table C.1. See Appendix D for the references.

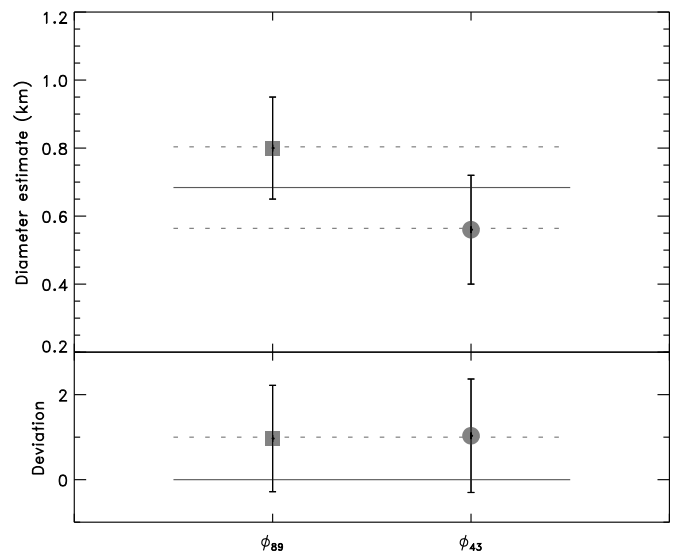


Figure B.237: Diameter estimates for (66063) 1998 RO1.

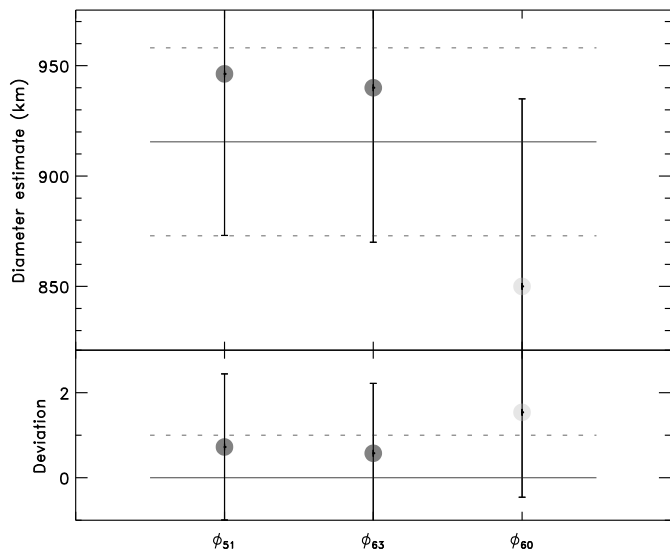


Figure B.238: Diameter estimates for (90482) Orcus.

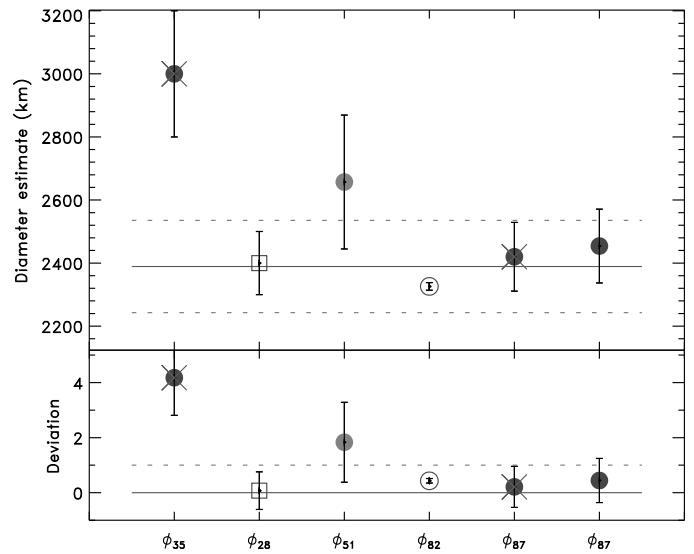


Figure B.240: Diameter estimates for (136199) Eris.

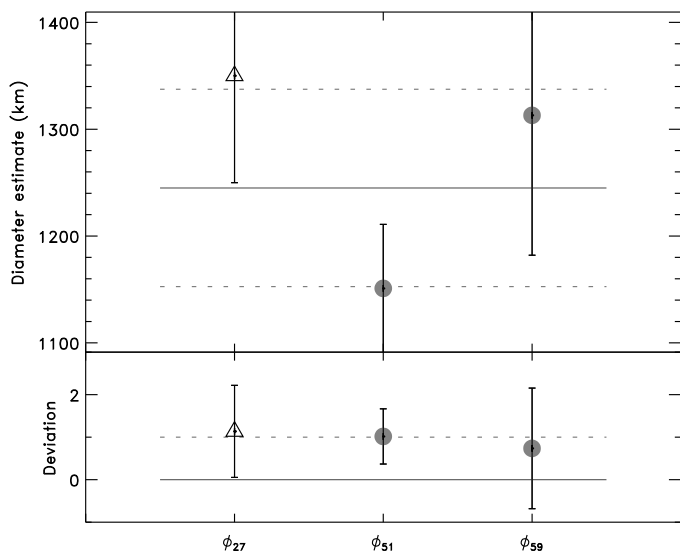


Figure B.239: Diameter estimates for (136108) Haumea.

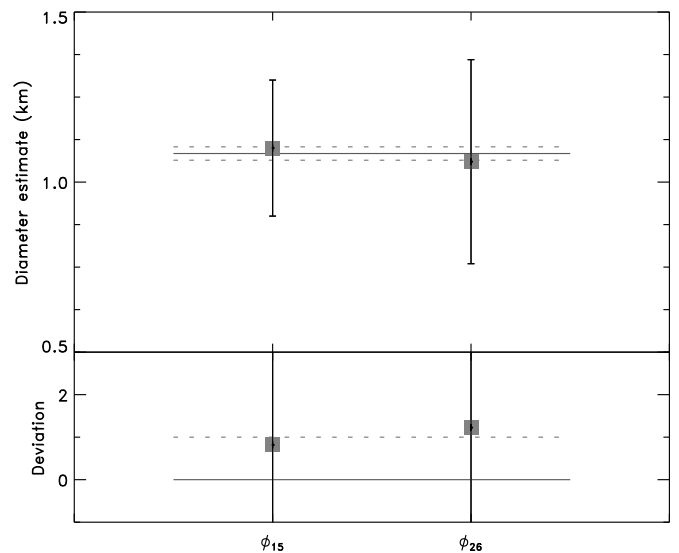


Figure B.241: Diameter estimates for (164121) 2003 YF1.

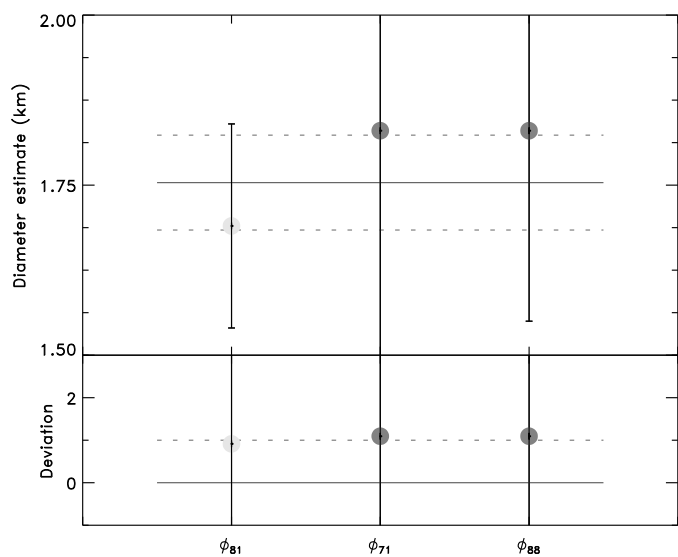


Figure B.242: Diameter estimates for (175706) 1996 FG3.

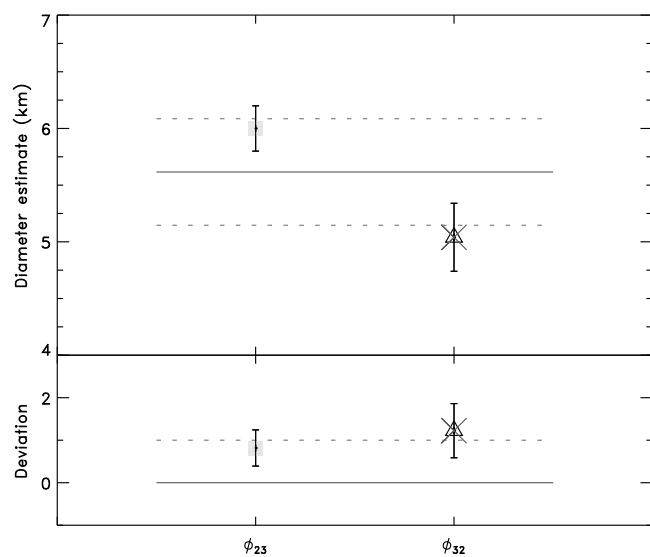


Figure B.244: Diameter estimates for 9P/Tempel1.

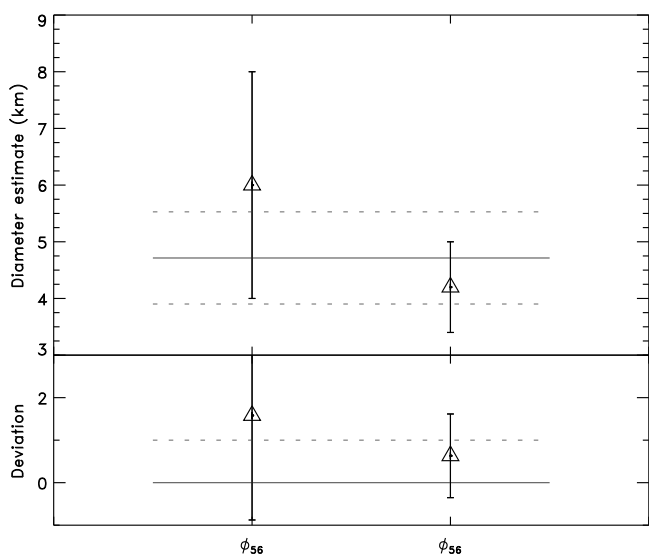


Figure B.243: Diameter estimates for 2P/Encke.

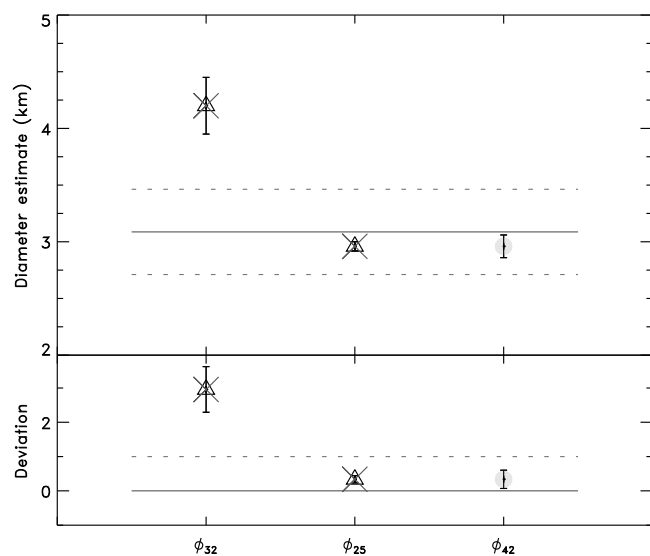


Figure B.245: Diameter estimates for 67P/C-G.

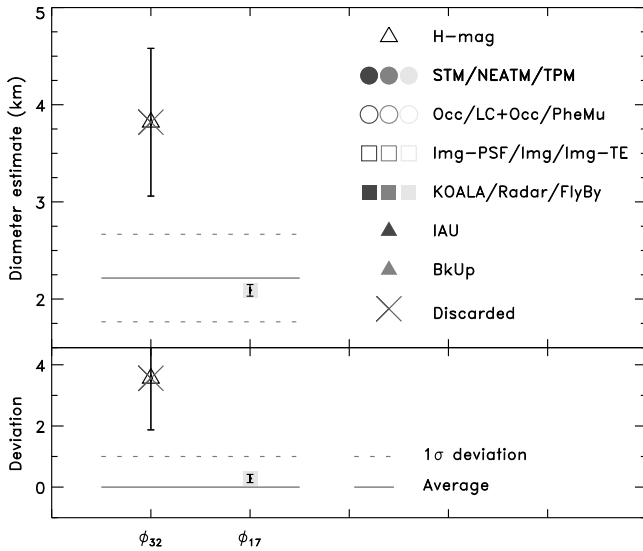


Figure B.246: Diameter estimates for 81P/Wild2.

Table C.1: Compilation of indirect estimates of density (ρ) for 24 objects, with their associated uncertainty ($\delta\rho$), bibliographic references (see Appendix D), and method of analysis: *PheMu*: mutual eclipsing phenomena in binary systems, *BinRad*: radar imaging, *Assum*: assumed, and, for comet nuclei, *CNGF*: non-gravitational forces, and *BkUp*: break-up modeling. Estimates marked with a dagger (\dagger) were used in the computation of the average density with other estimates derived from the mass and volume measurements. Other estimates are the only density estimates available for these targets.

#	Designation	ρ	$\delta\rho$	Method	Refs.
809	Lundia	1.64	0.1	PheMu	D ₁₀
854	Frostia	0.88	0.13	PheMu	D ₈
1089	Tama	2.52	0.29	PheMu	D ₈
1313	Berna	1.21	0.14	PheMu	D ₈
3169	Ostro	2.6	0.2	PheMu	D ₉
3671	Dionysus	1.60	0.60	PheMu	D ₇
4492	Debussy	0.90	0.10	PheMu	D ₈
5381	Sekhmet	1.98	0.65	BinRad	D ₃
35107	1991 VH	1.40	0.50	PheMu	D ₇
35107	1991 VH	1.60	0.50	PheMu	D ₇
65803	Didymos	1.70	0.40	PheMu	D ₇
65803	Didymos	2.10	0.60	PheMu	D ₇
65803	Didymos	1.70	0.50	PheMu	D ₁₁
65803	Didymos	2.10	0.65	PheMu	D ₁₁
66063	1998 RO1	1.5	1.15	PheMu	D ₁₁
66063	1998 RO1	4.1	1.8	PheMu	D ₁₁
66391	1999 KW4	1.20	0.80	PheMu	D ₁₁ [†]
175706	1996 FG3	1.40	0.30	PheMu	D ₂
175706	1996 FG3	1.30	0.60	PheMu	D ₇
175706	1996 FG3	1.4	1.05	PheMu	D ₁₁
185851	2000 DP107	0.8	0.6	PheMu	D ₁₁
185851	2000 DP107	1.1	1.5	PheMu	D ₁₁
	2001 QW322	1.0	1.0	Assum	D ₁₁
	2003 UN284	1.0	1.0	Assum	D ₁₂
	2005 EO304	1.0	1.0	Assum	D ₁₂
	2006 BR284	1.0	1.0	Assum	D ₁₂
	2006 JZ81	1.0	1.0	Assum	D ₁₂
	2006 CH69	1.0	1.0	Assum	D ₁₂
	2007 TY430	0.75	1.0	Assum	D ₁₃
	19P/Borrelly	0.24	0.06	CNGF	D ₄ [†]
	67P/C-G	0.23	0.14	CNGF	D ₅ [†]
	81P/Wild2	0.70	0.10	CNGF	D ₆
	SL9	0.50	0.05	BkUp	D ₁

Appendix D. Bibliographic references

References for mass estimates:

- (M₁) Williams (1992) (M₂) Sitarski and Todorovic-Juchniewicz (1992) (M₄) Solem (1994) (M₆) Sitarski and Todorovic-Juchniewicz (1995) (M₈) Kuzmanoski (1996) (M₁₀) Bange and Bec-Borsenberger (1997) (M₁₂) Lopez Garcia et al. (1997) (M₁₄) Yeomans et al. (1997) (M₁₆) Bange (1998) (M₁₈) Vasiliev and Yagudina (1999) (M₂₀) Viateau (2000) (M₂₂) Yeomans et al. (2000) (M₂₄) Viateau and Rapaport (2001) (M₂₆) Michalak (2001) (M₂₈) Krasinsky et al. (2001) (M₃₀) Kuzmanoski and Kovačević (2002) (M₃₂) Merline et al. (2002) (M₃₄) Margot et al. (2002) (M₃₆) Osip et al. (2003) (M₃₈) Noll et al. (2004b) (M₄₀) Margot et al. (2004) (M₄₂) Kochetova (2004) (M₄₄) Brown et al. (2005) (M₄₆) Kern and Elliot (2005) (M₄₈) Marchis et al. (2005a) (M₅₀) Behrend et al. (2006) (M₅₂) Brooks (2006) (M₅₄) Stansberry et al. (2006) (M₅₆) Konopliv et al. (2006) (M₅₈) Shepard et al. (2006) (M₆₀) Fujiwara et al. (2006) (M₆₂) Aslan et al. (2007) (M₆₄) Davidsson et al. (2007) (M₆₆) Descamps et al. (2007a) (M₆₈) Grundy et al. (2007) (M₇₀) Fienga et al. (2008) (M₇₂) Baer et al. (2008) (M₇₄) Descamps et al. (2008) (M₇₆) Grundy et al. (2008) (M₇₈) Ivantsov (2008) (M₈₀) Fienga et al. (2009) (M₈₂) Grundy et al. (2009) (M₈₄) Descamps et al. (2009) (M₈₆) Folkner et al. (2009) (M₈₈) Zielenbach (2010) (M₉₀) Fraser and Brown (2010) (M₉₂) Somenzi et al. (2010) (M₉₄) Carry et al. (2011) (M₉₆) Fang et al. (2011) (M₉₈) Rojo and Margot (2011) (M₁₀₀) Fienga et al. (2011) (M₁₀₂) Descamps et al. (2011) (M₁₀₄) Pätzold et al. (2011) (M₁₀₆) Descamps et al. (pers. com.)
- (M₃) Landgraf (1992) (M₅) Viateau and Rapaport (1995) (M₇) Carpio and Knezevic (1996) (M₉) Viateau and Rapaport (1997b) (M₁₁) Viateau and Rapaport (1997a) (M₁₃) Petit et al. (1997) (M₁₅) Viateau and Rapaport (1998) (M₁₇) Hilton (1999) (M₁₉) Merline et al. (1999) (M₂₁) Michalak (2000) (M₂₃) Goffin (2001) (M₂₅) Pitjeva (2001) (M₂₇) Margot and Brown (2001) (M₂₉) Standish (2001) (M₃₁) Chernetenko and Kochetova (2002) (M₃₃) Konopliv et al. (2002) (M₃₅) Neish et al. (2003) (M₃₇) Margot and Brown (2003) (M₃₉) Pitjeva (2004) (M₄₁) Noll et al. (2004a) (M₄₃) Kovačević (2005) (M₄₅) Chesley et al. (2005) (M₄₇) Marchis et al. (2005b) (M₄₉) Pitjeva (2005) (M₅₁) Vitagliano and Stoss (2006) (M₅₃) Buie et al. (2006) (M₅₅) Pravec et al. (2006) (M₅₇) Kern and Elliot (2006) (M₅₉) Marchis et al. (2006a) (M₆₁) Ostro et al. (2006) (M₆₃) Kovačević and Kuzmanoski (2007) (M₆₅) Descamps et al. (2007b) (M₆₇) Richardson et al. (2007) (M₆₉) Brown and Schaller (2007) (M₇₁) Baer and Chesley (2008) (M₇₃) Marchis et al. (2008b) (M₇₅) Marchis et al. (2008a) (M₇₇) Taylor et al. (2008) (M₇₉) Kryszczyńska et al. (2009) (M₈₁) Ragozzine and Brown (2009) (M₈₃) Scheirich and Pravec (2009) (M₈₅) Sosa and Fernández (2009) (M₈₇) Brown et al. (2010) (M₈₉) Kuzmanoski et al. (2010) (M₉₁) Benner et al. (2010) (M₉₃) Fienga et al. (2010) (M₉₅) Baer et al. (2011) (M₉₇) Zielenbach (2011) (M₉₉) Parker et al. (2011) (M₁₀₁) Marchis et al. (2011) (M₁₀₃) Konopliv et al. (2011) (M₁₀₅) Sheppard et al. (2011) (M₁₀₇) Merline et al. (pers. com.)
- (M₁) Solem (1994) (M₃) Harris and Davies (1999) (M₅) Veverka et al. (2000) (M₇) Merline et al. (2002) (M₉) Fernández et al. (2003) (M₁₁) Altenhoff et al. (2004) (M₁₃) Brown and Trujillo (2004) (M₁₅) Nolan et al. (2004) (M₁₇) Brownlee et al. (2004) (M₁₉) Marchis et al. (2005b) (M₂₁) Marchis et al. (2005a) (M₂₃) A'Hearn et al. (2005) (M₂₅) Lamy et al. (2006) (M₂₇) Rabinowitz et al. (2006) (M₂₉) Stansberry et al. (2006) (M₃₁) Pravec et al. (2006) (M₃₃) Shepard et al. (2006) (M₃₅) Bertoldi et al. (2006) (M₃₇) Ostro et al. (2006) (M₃₉) Conrad et al. (2007) (M₄₁) Carry et al. (2008) (M₄₃) Wolters et al. (2008) (M₄₅) Shepard et al. (2008) (M₄₇) Marchis et al. (2008a) (M₄₉) Grundy et al. (2008) (M₅₁) Stansberry et al. (2008) (M₅₃) Brucker et al. (2009) (M₅₅) Descamps et al. (2009) (M₅₇) Delbo and Tanga (2009) (M₅₉) Lellouch et al. (2010) (M₆₁) Carry et al. (2010b) (M₆₃) Brown et al. (2010) (M₆₅) Fraser and Brown (2010) (M₆₇) Carry et al. (2010a) (M₆₉) Ostro et al. (2010) (M₇₁) Mueller et al. (2011) (M₇₃) Grav et al. (2011) (M₇₅) Archinal et al. (2011) (M₇₇) Descamps et al. (2011) (M₇₉) Matter et al. (2011) (M₈₁) Wolters et al. (2011) (M₈₃) Usui et al. (2011) (M₈₅) Sheppard et al. (2011) (M₈₇) Santos Sanz et al. (2012) (M₈₉) Benner (pers. com.) (M₉₁) Merline et al. (pers. com.) (M₉₃) Tedesco et al. (2004b) (M₉₅) Dunham et al. (2011)
- (M₂) Thomas et al. (1997) (M₄) Ostro et al. (2000) (M₆) Noll et al. (2002) (M₈) Margot et al. (2002) (M₁₀) Neish et al. (2003) (M₁₂) Müller and Blommaert (2004) (M₁₄) Noll et al. (2004b) (M₁₆) Noll et al. (2004a) (M₁₈) Müller et al. (2005) (M₂₀) Ostro et al. (2005) (M₂₂) Thomas et al. (2005) (M₂₄) Behrend et al. (2006) (M₂₆) Brooks (2006) (M₂₈) Brown et al. (2006) (M₃₀) Spencer et al. (2006) (M₃₂) Tancredi et al. (2006) (M₃₄) Marchis et al. (2006b) (M₃₆) Fujiwara et al. (2006) (M₃₈) Descamps et al. (2007b) (M₄₀) Grundy et al. (2007) (M₄₂) Lamy et al. (2008) (M₄₄) Marchis et al. (2008b) (M₄₆) Descamps et al. (2008) (M₄₈) Drummond and Christou (2008) (M₅₀) Taylor et al. (2008) (M₅₂) Delbo et al. (2009) (M₅₄) Drummond et al. (2009) (M₅₆) Sosa and Fernández (2009) (M₅₈) Schmidt et al. (2009) (M₆₀) Lim et al. (2010) (M₆₂) Drummond et al. (2010) (M₆₄) Ryan and Woodward (2010) (M₆₆) Benner et al. (2010) (M₆₈) Mueller et al. (2010) (M₇₀) Fang et al. (2011) (M₇₂) Masiero et al. (2011) (M₇₄) Parker et al. (2011) (M₇₆) Drummond et al. (2011) (M₇₈) Āurech et al. (2011) (M₈₀) Brozović et al. (2011) (M₈₂) Sicardy et al. (2011) (M₈₄) Sierks et al. (2011) (M₈₆) Mommert et al. (2012) (M₈₈) Walsh et al. (2012) (M₉₀) MPEC (M₉₂) Delbo (2004) (M₉₄) Tedesco et al. (2004a)

Ref-

References for indirect density estimates:

- (D₁) Solem (1994) (D₂) Mottola and Lahulla (2000) (D₃) Neish et al. (2003) (D₄) Davidsson and Gutiérrez (2004) (D₅) Davidsson and Gutiérrez (2005) (D₆) Davidsson and Gutiérrez (2006) (D₇) Pravec et al. (2006) (D₈) Behrend et al. (2006) (D₉) Descamps et al. (2007a) (D₁₀) Kryszczyńska et al. (2009) (D₁₁) Scheirich and Pravec (2009) (D₁₂) Parker et al. (2011) (D₁₃) Sheppard et al. (2011)

References for diameter estimates: